Charles University

Faculty of Science

Department of Zoology

PhD study program: Zoology

Matthias Seidel, MSc.

Evolutionary history, systematics and biogeography of Southern Hemisphere hydrophilid beetles (Coleoptera)

Evoluce, systematika a biogeografie vodomilovitých brouků (Coleoptera: Hydrophilidae) jižní polokoule

Doctoral thesis

Supervisor: Martin Fikáček, PhD.

Prague, 2019

I declare that this thesis has not been submitted for the purpose of obtaining of the same or another academic degree earlier or at another institution. My involvement in the research presented in this thesis is expressed through the authorship order of the included publications and manuscripts. All literature sources I used when writing this thesis have been properly cited.

Prague, 2019 Matthias Seidel

This is to declare that Matthias Seidel contributed to the papers co-authored by us and included in his PhD thesis. We hereby agree that these papers may be included in his PhD thesis.

MSc. Emmanuel Arriaga-Varela

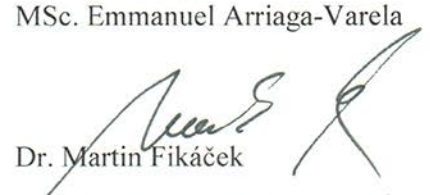

Dr. Martin Fikáček

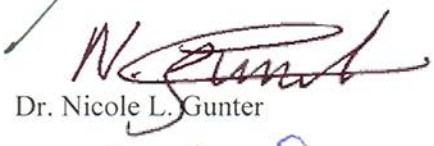

Dr. Nicole L. Gunter

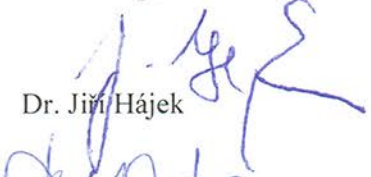

Dr. Jiří Hájek

Dr. David Král

Dr. Richard A. B. Leschen

Dr. Yūsuke N. Minoshima

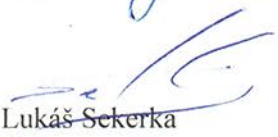

Dr. Lukáš Sekerka

Dr. Andrew E. Z. Short

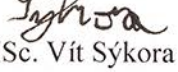

MSc. Vít Sýkora

Dr. Emmanuel F. A. Toussaint

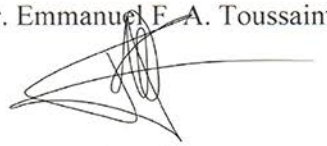

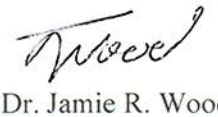

Dr. Jamie R. Wood

CONTENTS

LIST OF ATTACHED PUBLICATIONS AND MANUSCRIPTS

1. Toussaint, E. A. F., **Seidel, M.**, Arriaga-Varela, E., Hájek, J., Král, D., Sekerka, L., Short, A. E. Z. & Fikáček, M. (2017) The peril of dating beetles. *Systematic Entomology,* 42(1): 1-10.

2. Seidel, M., Sýkora, V., Leschen, R. A. B., & Fikáček, M. Systematics and biogeography of the Southern Hemisphere endemic Cylominae beetles (Coleoptera: Hydrophilidae) (manuscript draft).

3. Seidel, M., Arriaga-Varela, E. & Fikáček, M. (2016). Establishment of Cylominae Zaitzev, 1908 as a valid name for the subfamily Rygmodinae Orchymont, 1916 with an updated list of genera (Coleoptera: Hydrophilidae). *Acta Entomologica Musei Nationalis Pragae,* 56(1): 159-165.

4. Seidel, M., Minoshima, Y. N., Arriaga-Varela, E., & Fikáček, M. (2018). Breaking a disjunct distribution: a review of the Southern Hemisphere genera *Cylorygmus* and *Relictorygmus* gen. nov. (Hydrophilidae: Cylominae). *Annales zoologici,* 68(2): 375-403.

5. Seidel, M., Minoshima, Y. N., Leschen, R. A. B., & Fikáček, M. Phylogeny, systematics and rarity assessment of New Zealand endemic *Saphydrus* beetles and related enigmatic larvae (Coleoptera: Hydrophilidae: Cylominae) (manuscript draft).

6. Minoshima, Y. N., **Seidel, M.**, Wood, J. R., Leschen, R. A., Gunter, N. L., & Fikáček, M. (2018). Morphology and biology of the flower-visiting water scavenger beetle genus *Rygmodus* (Coleoptera: Hydrophilidae). *Entomological Science*, 21(4): 363-384.

ACKNOWLEDGEMENTS

My sincere and deep gratitude goes first and foremost to my supervisor Martin Fikáček for his support, advice and friendship over the last 4 years. I am furthermore grateful to Alexey Solodovnikov and everyone involved or enrolled in BIG4. I would also like to acknowledge Richard Leschen and Elena Hilario for their support and hospitality in New Zealand. I would like to thank the colleagues of the Entomology Department of the National Museum, Prague and the Department of Zoology, Faculty of Science, Charles University for always being supportive in my studies. Thanks to Vít Sýkora, Emmanuel Arriaga-Varela, Dominik Vondráček, Albert Deler-Hernández, Lukáš Sekerka and Jiří Hájek (= the National Museum beetle team) for their support in expeditions and science. Thanks to Richard Leschen, Christiane Ehrt, Max Barclay, Nicole Gunter and Josh Jenkins Shaw for their helpful comments on my thesis.
Thanks to my parents for their support through my Bachelor and Master studies, that paved the way to my PhD. I am very grateful to Emmanuel Arriaga-Varela and Ana Molgora for their friendship and the two years of sharing a flat together.

Finally, I must express my very profound gratitude to Axel González for the awesome last years together and the massive support in life and my PhD studies.

This work was supported by the European Union's Horizon 2020 research and innovation program under the Marie Skłodowska-Curie grant agreement No. 642241 to M. Seidel and by the Ministry of Culture of the Czech Republic (DKRVO 2019-2023/5.I.a, National Museum, 00023272). The work at the Department of Zoology, Charles University, Prague was partly supported by grant SVV 260 434 /2019.

ABSTRACT

The research presented in my PhD thesis consists of phylogenetic, biogeographic, taxonomic and ecological research of Southern Hemisphere water scavenger beetles (Coleoptera: Hydrophilidae) with a special emphasis on New Zealand. The introductory chapter provides a brief outline on the break-up of Gondwana and geological processes that shaped New Zealand and its fauna. Furthermore, the diversity of New Zealand Hydrophilidae and worldwide diversity of the hydrophilid subfamily Cylominae and its taxonomic history are illustrated. The scientific part of the thesis contains 4 published papers and 2 manuscripts. The first study recalibrates the Coleoptera time tree, providing new age estimates for the Hydrophiloidea, among others. The new age estimate is implemented in the second study, a phylogenetic study that reconstructs the biogeography of the 'Gondwanan' Cylominae beetles. The Cylominae, whose name was reinstated through nomenclatural priority over Rygmodinae in a separate paper, are found to consist of two tribes, Andotypini and Cylomini. The disjunct distribution of Cylominae is shown to be partly the result of vicariance and partly of long-distance oversea dispersal. The most remarkable long-distance dispersal is that of the only African representative of the subfamily which reached Africa from Australia about 50 million years after Africa diverged from the remaining Gondwanan land masses. Based on morphological evidence, a new genus *Relictorygmus* is established for the two African species and is diagnosed from the Chilean *Cylorygmus*. The morphological and molecular studies of New Zealand cylomine beetles revealed a total of 13 genera and 61 species of which 3 genera and 25 species remain undescribed. The New Zealand genus *Saphydrus* is revised, revealing two new species, *S. moeldnerae* and *S. tanemahuta*, known from very few specimens indicating the extreme rarity of the genus. Furthermore, immature stages were associated with *Saphydrus* adults by DNA sequences and described. Another lineage genetically and morphologically distant to *Saphydrus*, is described as *Enigmahydrus larvalis*. It is the first hydrophilid genus and species described from immature stages only. Lastly, the ecology of *Rygmodus*, the enigmatic New Zealand hydrophilid with flower-visiting pollen-feeding adults and aquatic larvae, is studied and summarized. The genus is found to be unique within the Hydrophilidae in inhabiting different habitats as adult and larvae. The larvae of *Rygmodus* are described for the first time.

ABSTRAKT

Výzkum prezentovaný v mé dizertační práci je složen z výsledků studia fylogeneze, biogeografie, taxonomie a ekologie vodomilovitých brouků (Coleptera: Hydrophilidae) jižní polokoule se zaměřením na Nový Zéland. Úvodní kapitola stručně shrnuje rozpad Gondwany a geologické procesy, které ovlivnily Nový Zéland a jeho faunu. Je charakterizována fauna vodomilovitých brouků Nového Zélandu a divezita podčeledi Cylominae na Novém Zélandu a celosvětově. Výzkumná část zahrnuje čtyři publikované práce a dva rukopisy. První práce rekalibruje datovanou fylogenezi brouků a poskytuje tak mimo jiné nový odhad stáří nadčeledi Hydrophiloidea. Tento odhad je následně využit v druhé studii týkající se fylogeneze a biogeografie gondwanských Cylominae. Tato podčeleď, jejíž jméno bylo obnoveno díky prioritě před jménem Rygmodinae, se skládá ze dvou tribů: Andotypini a Cylomini. Disjunktní rozšíření podčeledi Cylominae je z části výsledkem vikariance a z části disperze na dlouhou vzdálenost mezi kontinenty. Nejpozoruhodnějším příkladem disperze je případ jediného afrického zástupce podčeledi, který kolonizoval Afriku z Austrálie ca před 50 miliony let, tj. dlouho po oddělení Afriky od zbytku Gondwany. Na základě morfologie je popsán nový rod *Relictorygmus* se dvěma africkými druhy a oddělen od chilského rodu *Cylorygmus*. Morfologické a molekulární studie novozélandských Cylominae odhalily existenci celkem 13 rodů a 61 druhů, z nichž tři rody a 25 druhů zůstává nepopsáno. Revidován je novozélandský rod *Saphydrus*, se dvěma novými druhy, *S. moeldnerae* a *S. tanemahuta*, známými pouze z několika jedinců. To ukazuje na extrémní vzácnost celého rodu. Pomocí sekvencí DNA byly k dospělcům tohoto rodu přiřazeny larvy, která jsou následně popsány. Další linie, která je geneticky i morfologicky vzdálená od rodu *Saphydrus*, je popsána jako *Enigmahydrus larvalis*. Jedná se o první rod vodomila popsaný pouze na základě larvy. Nakonec je studována a shrnuta ekologie rodu *Rygmodus*, zvláštní novozélandské skupiny, jejíž dospělci navštěvují květy a živí se pylem, zatímco larvy žijí ve vodním prostředí. Dospělec a larva tedy obývají zcela různé habitaty, což je v rámci vodomilů unikátní. Součástí práce je rovněž první popis larev tohoto rodu.

INTRODUCTION

1. Break-up of southern Gondwana and its biogeographic implications

To understand the disjunct distributions of Southern Hemisphere biota it is crucial to understand the geological history of continents, from Gondwana to today's configuration. Many geological and paleontological studies of the southern supercontinent exist, sometimes reporting incongruent evidence. The most tested and accepted synthesis of the break-up of southern Gondwana is the sequence of events presented by Sanmartín & Ronquist (2004) (Fig. 1). The supercontinent Pangea (Fig. 2) that existed until the early Mesozoic consisted of a northern part, Laurasia, and the southern part most commonly known as Gondwana. The initial break-up of Gondwana into West and East Gondwana started through sea floor spreading in the Somali basin approximately 165 million years ago (Mya) (McLoughlin 2001, Rabinowitz et al. 1983). According to the Eurogondwanan hypothesis of Ezcurra & Agnolín (2012), the European areas (part of Laurasia) maintained a close biogeographical affinity with Gondwana until 145-130 Mya. The separation of West Gondwana was initiated at about 135 Mya with sea floor spreading, opening the South Atlantic leading to the separation of Southern South America and Africa (Scotese et al. 1988, Goodland et al. 1982). Finally, Africa was isolated from Northern South America through a transform fault opening between Brazil and Guinea (110-95 Mya, Sanmartín & Ronquist 2004) with final separation at ca. 90 Mya (Thomaz Filho et al. 2000). The remaining Southern Gondwanan landmasses containing Australia, Zealandia, Antarctica and South America, remained connected until the late Cretaceous. Zealandia, containing today's New Zealand, New Caledonia, Norfolk and Lord Howe Islands, was separated from East Gondwana through sea floor spreading, opening the Tasman Sea that lasted from ca. 80 Mya to 55.5 Mya (McLoughlin 2001). New Zealand and New Caledonia were separated between 40 to 30 Mya through the opening of the New Caledonian Basin (Sanmartín & Ronquist 2004). At about 90 Mya Australia began to separate from Antarctica but the continents remained partially connected via a Tasmanian land bridge. From about 50 Mya the biotic separation between mainland Australia and Antarctica started when a shallow seaway appeared between them (Woodburne & Case 1996) and complete separation of the continents, including Tasmania, occurred approximately 35 Mya (Torsvik et al., 2008). Concurrently, South America and West Antarctica began to disconnect through the drowning of the

Weddelian Isthmus that previously allowed biotic exchange via land starting from, ca. 55 Mya (Reguero et al. 2014) and by 34 to 30 Mya, they were completely separated through the opening of the Drake passage (e.g. Livermore et al. 2006). From 34 Mya, glaciation of Antarctica prohibited any further dispersal through the continent (Pross et al. 2012, Houben et al. 2019).

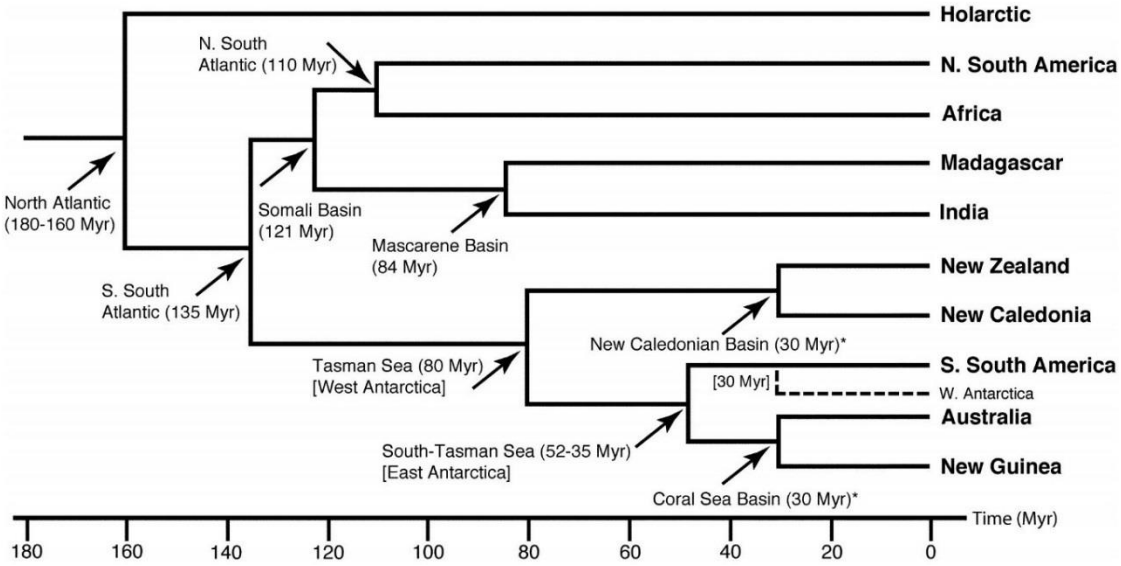

Figure 1. Geological cladogram indicating the sequence of the break-up of Gondwana adopted from Sanmartín & Ronquist (2004) - times of vicariance are assumed to be of primary fragmentation (∗70–60 Mya in alternative reconstructions).

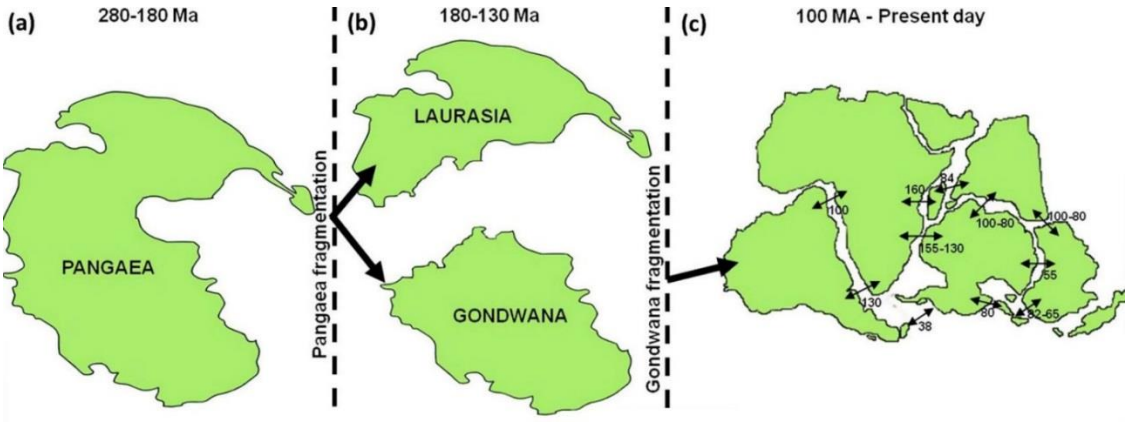

Figure 2. Schematic map of continental configuration at different times (modified from McCulloch et al. 2016). (a) Supercontinent Pangea. (b) Fragmentation of Pangea into Laurasia and Gondwana. (c) Break-up of Gondwana (numbers indicate splitting times in million of years ago).

2. Geological history of New Zealand and its effect on its fauna

Zealandia separated from the East Gondwana during the Late Cretaceous about 80 Mya and by 60 Mya, all links between New Zealand and Australia were broken (Giribet & Boyer 2010). New Zealand has since then undergone drastic geological changes. Its area was reduced to ca. 15% during the Oligocene (Fleming 1979; Cooper & Cooper 1995; Landis et al. 2008) causing severe population bottlenecks (Cooper & Cooper 1995). Previous research suggested an almost complete submergence of New Zealand (e.g. Wallis & Trewick 2009) - a theory that has been refuted (e.g. Giribet & Boyer 2010, Krosch & Cranston 2013). However, some authors argue that the Oligocene bottleneck only had little effect on insects as the total area of the islands exceeded that of modern New Caledonia (Lee et al. 2001). Over the past 23 Mya the New Zealand islands were subject to a 500 km displacement along the alpine fault (Bunce et al. 2009). About 5 to 4 Mya, the uplift of Southern Alps (Tippett & Kamp 1995) resulted in a barrier of gene flow and an extreme gradient in rainfall leading to big differences in forest cover between the opposite sides especially of the South Island. The most recent process with a strong impact on fauna was the Last Glacial Maximum between 34 and 18 thousand of years ago. Due to the decrease of sea level, land bridges between individual islands of New Zealand were formed, allowing for dispersal. The severe glaciation in the South Island and great reduction of forest cover in the North Island also pushed most taxa to refugia (Burrows 1965; Wardle 1988; Leschen et al. 2008; Marske et al. 2009; Marra & Thackray 2010; McGlone et al. 2010) and left large areas open for a subsequent recolonization.

The complexity of New Zealand geology and changing climatic conditions is underlined by the complexity of the origins and composition of New Zealand's fauna. New Zealand has lineages assumed to be ancient Gondwanan survivors such as tuatara or leiopelmatid frogs (Pyron & Wiens 2011; Zheng & Wiens 2016) and, on the other hand, later colonizers that often evolved into unusual forms like moa, kiwi or alpine cicadas (Marshall et al. 2015; Yonezawa et al. 2017). Radiations in some insect groups (e.g. Chinn & Gemmell 2004; Marshall et al. 2008; Pratt et al. 2008) including freshwater ones, e.g. Plecoptera (McLellan 2006) or Hydraenidae (Delgado & Palma 1999; 2010) as well as cylomine beetles (*Adolopus*, *Cyloma*, *Rygmodus,* Seidel & Fikáček, unpubl.) have been recorded. Available studies indicate that the groups with higher species diversity arrived to New Zealand prior to the Oligocene bottleneck, while the species-poor ones either arrived more recently or are ancient relic lineages that were pruned by extinction

(Buckley et al. 2015). However, the insufficient number of dated phylogenetic studies, which are crucial for the explanation of diversity patterns in New Zealand, renders the New Zealand biogeography a topic of major interest.

3. Southern Hemisphere water scavenger beetles

3.1 Hydrophilidae (excl. Cylominae) of New Zealand

All genera, species and distribution of non-cylomine Hydrophilidae are summarized in Table 1 and one species of each genus is illustrated in Figure 3.

Hydrophilinae. Hydrophilinae is the largest aquatic lineage of water scavenger beetles occurring in New Zealand, represented by three tribes: Berosini, Laccobiini and Hydrophilini. *Berosus pallidipennis* (Sharp, 1884) is the only currently valid species of *Berosus*, placed in its own monotypic subgenus *Phelerosus* Sharp, 1884. This species is distributed over the North and South Island and can be commonly collected in side pools of rivers or submerged vegetation. A recent study (Seidel et al. unpubl.) discovered three more undescribed species (one in the North Island, two in the South Island) that belong to the same subgenus. The New Zealand *Berosus* are estimated to have colonized New Zealand from Australia at the beginning of the Paleocene and may be regarded as New Zealand paleoendemics (Seidel et al. unpubl.). The tribe Laccobiini is represented by three genera, *Tormus* Sharp, 1884, *Laccobius* Erichson, 1837 and *Paracymus* Thomson, 1867. *Tormus* is a moss-inhabiting terrestrial genus, previously thought to be a member of Cylominae and moved to the Laccobiini by Short & Fikáček (2013) based on molecular phylogenetics. It has been shown that the genus contains two morphologically similar and apterous species; one of them, *Tormus helmsi* Sharp, 1884, shows deep genetic structure between populations (Fikáček et al. 2013). The genus is found from the south of the South Island (Fiordland) along the west of the Southern Alps to the west of the North Island (Fikáček et al. 2013). *Paracymus* is represented by a single species, currently considered to the conspecific with *Paracymus pygmaeus* (MacLeay, 1871) described from Australia; preliminary studies (Fikáček, pers. comm.) indicate that the New Zealand specimens may in fact be of a separate species. *Laccobius* is currently represented by two described species: *Laccobius arrowi* Orchymont, 1925 and *Laccobius mineralis* Winterbourn, 1970, both endemic to New Zealand; a third undescribed species occurs in the region of Auckland in the North Island (Seidel & Fikáček, unpubl.). All *Laccobius* species can be collected on gravel banks of slowly flowing rivers (Seidel, pers.

observ.). *Limnoxenus zealandicus* (Broun 1880) is the only representative of Hydrophilini in New Zealand; the species also occurs in Australia and New Caledonia (Short 2010).

Chaetarthriinae. *Horelophus walkeri* Orchymont, 1913 is the only member of the monotypic genus *Horelophus*. It attracted the attention of hydrophilid researchers because of its unusual morphology and its occurrence in New Zealand; moreover, for a long time, it was only known from historical type specimens. Hansen (1991) proposed a separate subfamily Horelophinae Hansen, 1991 for the genus, based on a morphological phylogenetic analysis. Later Fikáček et al. (2012) rediscovered the taxon, collecting it in hygropetric habitats in the north-west of the South Island. Based on molecular analyses, Short & Fikáček (2013) later synonymized the Horelophinae with Chaetarthriinae moving *Horelophus* into the Anacaenini group of genera. Our fieldwork after 2012 added few localities for the genus in the South Island. Moreover, morphological data seem to indicate that *Horelophus* is closely related to some species currently classified in *Crenitis* Bedel, 1881 (Fikáček, unpubl.).

Enochrinae. In New Zealand, the subfamily is only represented by *Enochrus*. Three species are recorded, with only *Enochrus abditus* (Sharp, 1884) being endemic to the country. *E. tritus* (Broun, 1880) was originally described from New Zealand, but is also found in the Cook and Society Islands; therefore, its original distribution range is not clear and Kuschel (1990) suggested that it was introduced to New Zealand. *E. maculipes* (MacLeay, 1871) is reported widely from the Australian region (Australia, New Caledonia, Vanuatu and Western Samoa) (Hansen 1999) and was recently reported by Thorpe (2011) from New Zealand. It can be commonly collected in the North Island of New Zealand (Seidel & Fikáček, pers. observ.). Currently, it is unknown whether New Zealand is its natural range or if the species was introduced from other parts of the Australian region. Based on our fieldwork and museum collection research, we do not expect more species in New Zealand, but we will provide further faunistic records in the future (Seidel & Fikáček, unpubl.).

Sphaeridiinae. *Cercyodes laevigatus* Broun, 1886 is the only New Zealand native sphaeridiine. It lives in rotten sea weed habitat (Broun 1886, Fikáček, pers. observ.). It was described from Mokohinau Island (North Island) but occurs almost all across the North Island, South Island and in the Chatham Islands (Hansen, unpubl.). Its closest relative and the only other species in the genus, *Cercyodes kingensis* (Blackburn, 1907), is found in a similar habitat at the coast of Tasmania (Hansen 1990a). All other

Sphaeridiinae, i.e. two *Dactylosternum* Wollaston, 1854 species, five *Cercyon* Leach, 1817 species and one *Sphaeridium* Fabricius, 1775 species have been introduced to New Zealand and are mainly found in anthropogenic habitats (Table 1).

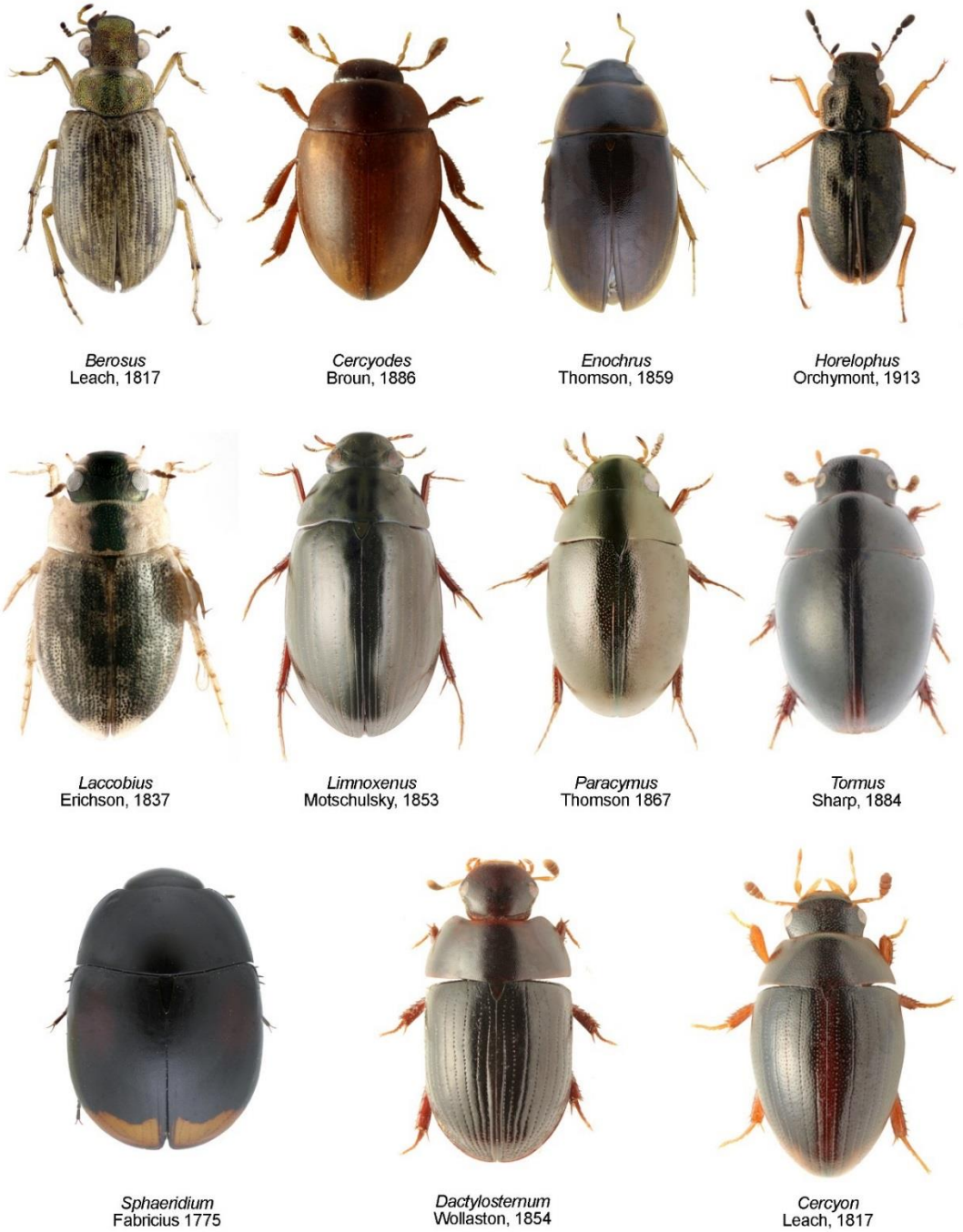

Figure 3. Dorsal habitus of non-Cyclominae hydrophilid genera. Image sources: Fikáček 2019 (*Limnoxenus, Paracymus, Dactylosternum, Cercyon*), Fikáček et al. 2013 (*Tormus*), Fikáček et al. 2012 (*Horelophus*).

Table 1. Overview of non-Cylominae species and their distribution. *most recent references on distribution.

Species	Distribution in New Zealand	References*
Cercyodes Broun, 1886		
C. laevigatus Broun, 1886	North Is., South Is., Chatham Is.	Hansen 1990, Hansen unpubl.
Dactylosternum Wollaston, 1854		
D. abdominale (Fabricius, 1792)	North Is., South Is. (introduced)	Newton 1989
D. marginale (Sharp, 1876)	North Is. (introduced from Australia)	Newton 1989
Sphaeridium Fabricius, 1775		
S. lunatum Fabricius, 1792	North Is. (introduced from Palaeactic)	Hansen unpubl.
Cercyon Leach, 1817		
C. analis (Paykull, 1798)	North Is. (introduced from Palearctic)	Kuschel 1990, Hansen unpubl.
C. haemorrhoidalis (Fabricius, 1775)	North Is., South Is., Chatham Is. (introduced from Palearctic)	Hansen unpubl.
C. depressus Stephens, 1829	North Is., South Is. (introduced from Palearctic)	Kuschel 1990, Hansen unpubl.
C. nigriceps (Marsham, 1802)	North Is. (introduced from Palearctic)	Kuschel 1990, Hansen unpubl.
C. terminatus (Marsham, 1802)	North Is., South Is. (introduced from Palaearctic)	Kuschel 1990, Hansen unpubl.
Horelophus Orchymont, 1913		
H. walkeri Orchymont, 1913	South Is.	Fikáček et al. 2012
Berosus Leach, 1817		
B. pallidipennis (Sharp, 1884)	North Is., South Is.	Seidel et al. unpubl.
+3 undescribed species		
Paracymus Thomson, 1867		
P. pygmaeus (MacLeay, 1871)	North Is., South Is.	Hansen unpubl., Winterbourn 1970
Laccobius Erichson, 1837		
Laccobius arrowi Orchymont, 1925	South Is.	Gentili 1981
Laccobius mineralis Winterbourn, 1970	North Is.	Winterbourn 1970
+1 undescribed species		
Enochrus Thomson, 1859		
E. abditus (Sharp, 1884)	North Is.	Orchymont 1937
E. tritus (Broun, 1880)	North Is., South Is. (possibly introduced from Australian region)	Hansen unpubl., Winterbourn 1970
E. maculiceps (MacLeay, 1871)	North Is. (possibly introduced from Australian region)	Thorpe unpubl.
Limnoxenus Motschulsky, 1853		
L. zealandicus (Broun, 1880)	North Is., South Is.	Hansen unpubl.
Tormus Sharp, 1844		
T. helmsi Sharp, 1884	North Is., South Is.	Fikáček et al. 2013
T. posticalis (Broun, 1917)	South Is.	Fikáček et al. 2013

3.2 Cylominae

All genera, species and distribution of Cylominae are summarized in Table 2 and one species of each genus is illustrated in Figure 5.

3.2.1 Taxonomic history of the subfamily

The subfamily Cylominae has a complicated taxonomic history that was only recently resolved by means of molecular tools. The first family-group name proposed for members of the subfamily was established by Zaitzev (1908) as a hydrophilid tribe 'Cylomina' to encompass three genera that he was unable to accommodate in other tribes: *Cyloma* Sharp, 1872, *Psephoboragus* Broun, 1893 (= *Cyloma*) and *Cylomissus* Broun, 1903. His new tribe was basically ignored by Orchymont (1916) who himself established a tribe Rygmodini, based on the enigmatic flower-visiting genus *Rygmodus* White, 1846. Rygmodini contained the three genera grouped in Zaitzev's Cylomina plus further New Zealand, Chilean and Australian genera: *Adolopus* Sharp, 1884, *Gitocyloma* Broun, 1915 (= *Cyloma*), *Namostygnus* Broun, 1909 (= *Cyloma*), *Exydrus* Broun, 1886, *Hydrostygnus* Sharp, 1884, *Rygmodus*, *Saphydrus* Sharp, 1884, *Tormissus* Broun, 1893, *Thomosis* Broun, 1904, *Tormus*, *Stygnohydrus* Broun, 1893 (=*Tormus*), *Cylorygmus* Orchymont, 1933, *Rygmostralia* Orchymont, 1933 and *Pseudohydrobius* Blackburn, 1898 (Orchymont 1916, 1919, 1933).

The priority of Cylomina over Rygmodini was ignored until Hansen (1991) treated the group and synonymized Cylomina with Coelostomatini based on the transfer of the genera *Cyloma* and *Adolopus* to the latter tribe. Furthermore, Hansen's phylogenetic analysis based on morphological characters (Fig. 4) transferred the genera assigned to Rygmodini by Orchymont (1916) to other tribes (Hansen 1991, 1999): *Cylomissus* and *Anticura* Spangler, 1979 were transferred to Sperchopsini; *Tormus*, *Afrotormus* Hansen, 1999, *Exydrus*, *Hydrostygnus* and *Tormissus* to Tormissini. Hansen (1991, 1999) redefined Rygmodini and added new genera to the tribe: *Pseudohydrobius*, *Rygmostralia*, *Saphydrus*, *Rygmodus*, *Eurygmus* Hansen, 1990, and *Pseudorygmodus* Hansen, 1999.

The first comprehensive phylogeny and currently accepted classification of Hydrophilidae was published by Short & Fikáček (2013). They found strong support to erect the subfamily Rygmodinae and synonymized the tribes Andotypini Hansen, 1990, Borborophorini Hansen, 1990 and Tormissini Hansen, 1990 with it since the known adult characters did not allow for a subdivision of the subfamily into tribes. *Adolopus, Cyloma*, *Cylomissus* and *Anticura* were transferred back to Rygmodinae. *Tormus* and *Afrotormus* were moved to Laccobiini (Short & Fikáček 2013). Later, *Pseudorygmodus* was found to

be a member of Anacaenini (Fikáček & Vondráček 2014). Seidel et al. (2016) established Cylominae for the subfamily based on the priority of Zaitzev's name (1908) over Rygmodinae, not considered by Short & Fikáček (2013).

As a part of my thesis, I performed the phylogenetic analysis focused on the Cylominae and provide evidence to re-instate two tribes: Cylomini and Andotypini (Seidel et al., in prep., Chapter 2).

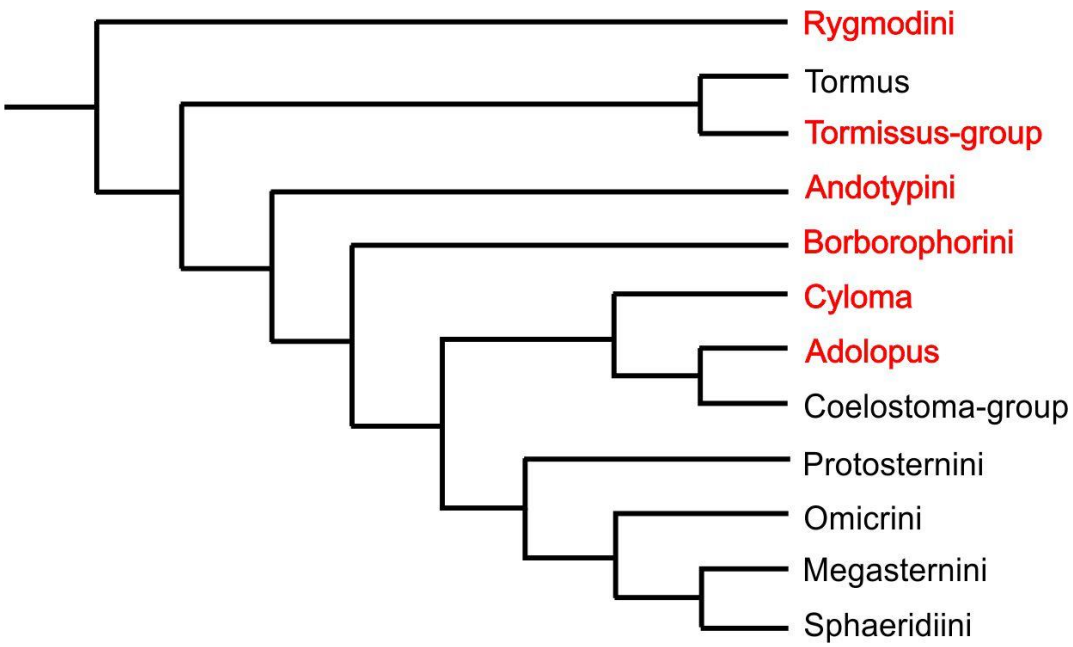

Figure 4. Preferred cladogram of Sphaeridiinae from Hansen (1991) (actual Cylominae in red; figure modified from Hansen (1991))

3.2.2 Generic overview

Adolopus Sharp, 1884 is endemic to New Zealand but is not reported from the sub-Antarctic islands. Currently, five valid species are recognized, with further four names considered as synonyms (Hansen 1997). Species of the genus look very similar and can be collected in mushrooms, in rotten/wet wood and mold, and are frequently sifted from leaf litter (Seidel & Fikáček, pers. observ.). Based on our phylogenetic analyses, we recognize nine species (Seidel et al. in prep., Chapter 2). However, this number might increase since the historical types have not yet been compared with our DNA grade material. Furthermore, Hansen intended to describe new species from areas that we were not able to sample (e.g. Three Kings Islands). Two further genera, which are morphologically closely allied to *Adolopus* (New Genus 1 and New Genus 2 in Seidel et al., in prep., Chapter 2) including three new species, remain to be described. Immature

stages of *Adolopus* and allied New Zealand genera remain undescribed but are available to us.

Andotypus Spangler, 1979 is endemic to Chile and was recently revised by Fikáček et al. (2014). It is the type genus of the tribe Andotypini Hansen, 1990, reinstated by Seidel et al. (in prep., Chapter 2). It contains two species that can be collected in pitfall traps (baited with dung or carrion) and in flight intercept traps in rainforests of Central and Southern Chile (Fikáček et al. 2014). Immature stages of *A. ashworthi* Spangler, 1979 have been described in detail (Fikáček et al. 2014).

Anticura Spangler, 1979 is endemic to Chile and the Andean part of Argentina, and is known from a single species *A. flinti* Spangler, 1979. Spangler (1979) described the adult, and the morphology of larvae and pupa. Later, Minoshima et al. (2015) redescribed the immature stages in more detail and provided the first molecular evidence for *Anticura* being related to the cylomine genus *Cylomissus*. *Anticura* can be collected in water-soaked plant matter and debris along rivers and from wet mosses at the sides of these rivers (Minoshima et al. 2015).

Austrotypus Fikáček, Minoshima & Newton, 2014 is the only genus of Cylominae with a disjunct distribution. The Australian *Austrotypus nothofagi* Fikáček et al., 2014 and Peruvian *Austrotypus peruanus* Fikáček et al., 2014, share the same morphology of the mouthparts and mesoventrite and were therefore considered conspecific by Fikáček et al. (2014). The larva of the Australian species has been described (Fikáček et al. 2014). We were able to generate DNA data for the species (Seidel et al., in prep., Chapter 2). The Peruvian species lives in similar climatic conditions as *A. nothofagi* but its immature stages remain unknown and DNA-grade specimens are unavailable. Both species can be collected using pitfall traps baited with carrion, or using flight intercept traps. *Austrotypus nothofagi* was also found in fermenting malt, dung and rotten fruits (Fikáček et al. 2014). The monophyly of the genus requires molecular testing.

Borborophorus Hansen, 1990 is the type species of the Borborophorini, at present synonymized with Cylomini (Seidel et al. 2016). It is endemic to Australia and contains three species that can be collected in rainforest leaf litter, dung, carrion or by fogging from dead wood (Fikáček 2019) A larva associated with adults of *Borborophorus* has been diagnosed and illustrated by Fikáček (2019) and compared to other cylomine larvae by Minoshima et al. (2018, Chapter 6).

Coelostomopsis Hansen, 1990 contains two species and is endemic to Australia. Little is known about the biology of the species. They can be collected in leaf litter or with flight intercept traps (Fikáček 2019). Immature stages have not been discovered yet.

Cyloma Sharp, 1872 is the largest genus of Cylominae currently containing eight valid species (Hansen 1997) and thirteen undescribed ones revealed by the combination of morphological and molecular characters (Seidel et al., in prep., Chapter 2, Seidel & Fikáček, unpubl.). It is endemic to New Zealand with two species, *C. flemingi* (Ordish, 1974) and *C. pictus* (Kirsch, 1877), being described from sub-Antarctic islands. Phylogenetically, species group into two main clades corresponding to *Psephoboragus* Broun, 1893 and *Cyloma* s. str. The synonymy of *Psephoboragus*, *Namostygnus* Broun, 1909 and *Gitocyloma* Broun, 1915 with *Cyloma* is confirmed. *Cyloma* can be easily collected in leaf litter, in pit fall traps baited with carrion or in flight intercept traps in native New Zealand forests.

Cylomissus Broun, 1903 is endemic to New Zealand and consists of one described and up to three undescribed species (Seidel et al., in prep., Chapter 2). Adults and larvae can be collected through floating moss growing on stones in the spray zone of forest streams. The larvae have been recently described by Minoshima et al. (2015). A new genus and species closely related to *Cylomissus* with a similar life style awaits description (Seidel et al., in prep., Chapter 2).

Cylorygmus Orchymont, 1933 is a monotypic genus endemic to Chile, containing a single species *C. lineatopunctatus* Orchymont, 1933. Seidel et al. (2018) recently redescribed its adult and larval morphology. The adults and immature stages can be collected in humid to wet debris, leaf litter and moss, along streams in sclerophyll or *Nothofagus* forests (Seidel et al. 2018, Chapter 4). The potential distribution of *Cylorygmus* was modeled by Fikáček & Vondráček (2014) and seems to be restricted in the region of Santiago de Chile.

Enigmahydrus Seidel, Minoshima, Leschen & Fikáček (in prep.) is the first hydrophilid genus and species are described based on immature stages only. Its larvae were collected from moist leaf litter in lowland forests of New Zealand. The adults remain unknown. For diagnosis of the genus see Chapter 5.

Eurygmus Hansen, 1990 is endemic to Australia and contains a single species *E. helocharoides* Hansen, 1990. The species exhibits strong sexual dimorphism, with expanded male pro- and mesotarsi and expanded and upturned anterolateral margin of the clypeus in males (Fikáček, 2019). The species ecology is unknown, but the genus is

terrestrial and was so far only collected in flight intercept traps in rainforest habitat (Hansen 1990, Fikáček 2019).

Exydrus Broun, 1886 is a monotypic genus, endemic to New Zealand. It is easily recognizable by the asymmetrical labrum which is a unique character within Hydrophilidae. Specimens can be collected in pit-fall traps baited with carrion, or can be sifted from leaf litter in subtropical forests of the northern North Island (Seidel & Fikáček, pers. observ.). Its immature stages remain unknown.

Hydrostygnus Sharp, 1884 is a monotypic New Zealand genus with the similar distribution range and collecting circumstances as *Exydrus* (Seidel & Fikáček, pers. observ.). Its immature stages remain unknown.

Petasopsis Hansen, 1990 is a monotypic Australian genus known from a few specimens only. Its only species, *Petasopsis brevitarsis* Hansen, 1990, has a very derived morphology, with characters fitting both Cylominae and Coelostomatini (Fikáček 2019). It is the only cylomine genus not available in DNA-grade preservation, and therefore still awaits molecular confirmation for being a true cylomine. Its immature stages remain unknown.

Pseudohydrobius Blackburn, 1898 is endemic to Australia and currently consists of three valid species and ca. three species awaiting description (Fikáček 2019). It is the only reported Australian hydrophilid collected from flowers and it is possibly exhibiting pollen-feeding habit as the closely related New Zealand *Rygmodus*. Immature stages remain unknown but might have the same aquatic lifestyle as found in *Rygmodus* (Fikáček 2019).

Relictorygmus Seidel, Minoshima, Arriaga-Varela & Fikáček, 2018 represents the only cylomine representative from Africa. Its significance for understanding the biogeography and systematics of Cylominae became clear after Hebauer (2002) described a species resembling the Chilean *Cylorygmus lineatopunctatus* from Africa. Seidel et al. (2018) established *Relictorygmus* for that species and described a second one. Both species can be collected in Western Cape of the Republic of South Africa through sifting litter of reed stands or by flooding drying muddy pools at lake shores or wet meadows. Immature stages remain unknown (Seidel et al. 2018, Chapter 4).

Rygmodus White, 1846 is an endemic genus from New Zealand. After *Cyloma*, it is the second largest genus of Cylominae. It is composed of eleven species (Hansen 1997); the molecular study I performed indicates that some of the currently accepted species may be species complexes (Seidel, unpubl.). Some species exhibit sexual dimorphism with

males having an expanded and upturned anterolateral margin of the clypeus. The life history of *Rygmodus* is the most unusual one when compared to other Cylominae: adults are flower-visiting and pollen-feeding, whereas larvae inhabit the sides of streams. Larvae have been recently described by Minoshima et al. (2018, Chapter 6).

Rygmostralia Orchymont, 1933 is a currently monotypic genus endemic to Australia. At least one species awaits description (Fig. 5). An undescribed *Rygmostralia* species is the only cylomine species ever collected at light. Otherwise biology and immature stages remain unknown (Fikáček 2019).

Saphydrus Sharp, 1884 is endemic to New Zealand and contains five species. The genus is unusually rare in collections and hard to collect. Four of the five species are known from a few specimens only (Seidel et al., in prep., Chapter 5). *Saphydrus suffusus* can be collected in large numbers using flight intercept traps, but specimens of other species and larvae are known to us mainly from leaf litter. Larvae of the genus have been described recently and can be easily distinguished from its closely allied genus *Enigmahydrus* (Seidel et al., in prep., Chapter 5).

Thomosis Broun, 1904 is the only cylomine genus endemic to the sub-Antarctic islands of New Zealand (Antipodes and Bounty Islands). It was previously synonymized with *Tormissus*, (Hansen 1991) but the results of the molecular phylogeny described herein (Seidel et al., in prep., Chapter 2) indicate that it is a separate early-branching lineage of the New Zealand Andotypini. The genus contains one species, *Thomosis guanicola* Broun, 1904, that has been collected in penguin guano or from carrion. Its larvae have been illustrated by Ordish (1974) but need a more detailed redescription.

Tormissus Broun, 1893 is currently a monotypic genus, after Hansen (1997) synonymized the other two species under *Tormissus linsi* Sharp, 1884. The phylogenetic study by Seidel et al. (in prep., Chapter 2) showed that *T. magnulus* is a valid species and one further species seems to be undescribed. Adult beetles can be collected in pit-fall traps baited with carrion or through sifting leaf litter. Immature stages remain undescribed but are available to me.

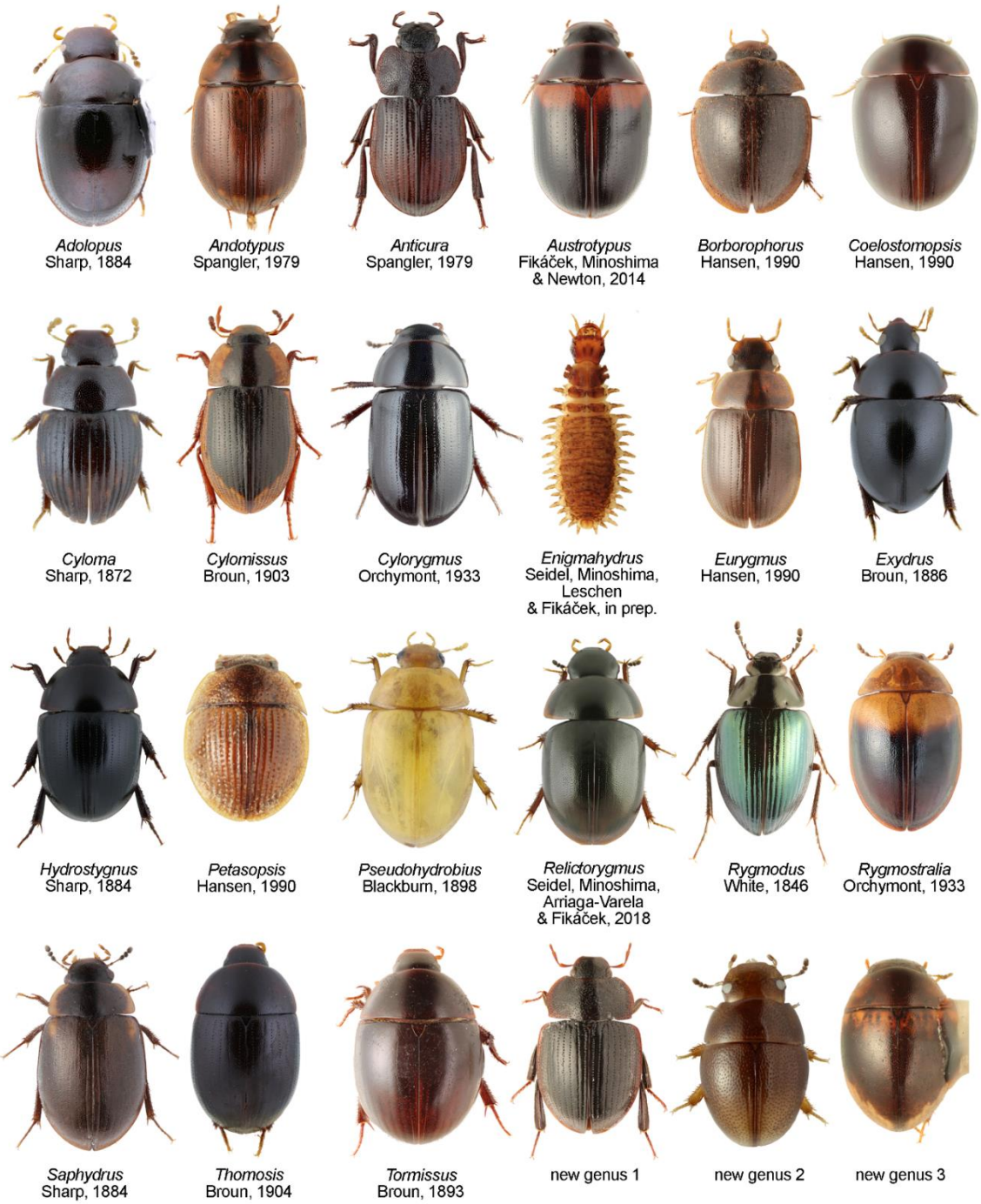

Figure 5. Dorsal habitus of Cyclominae genera. Image sources: Fikáček 2019 (*Borborophorus, Coelostomopsis, Eurygmus, Petasopsis, Rygmostralia*), Fikáček et al. 2014 (*Andotypus, Austrotypus*), Seidel et al. 2018 (*Cylorygmus, Relictorygmus*), Minoshima et al. 2015 (*Anticura, Cylomissus*), Minoshima et al. 2018 (*Rygmodus*).

Table 2. Overview of Cylominae species and their distribution (ARG - Argentina, AUS - Australia, CH - Chile, NZ - New Zealand, PE - Peru, RSA - Republic of South Africa) *most recent references on distribution.

Species	Distribution	References*
Adolopus Sharp, 1884		
A. altulus (Broun, 1909)	NZ: North Is.	Hansen 1997
A. badius (Broun, 1880)	NZ: North Is.	Hansen 1997
A. convexus Broun, 1893	NZ: South Is.	Hansen 1997
A. helmsi Sharp, 1884	NZ: North Is., South Is.	Hansen 1997
A. rugipennis Broun, 1886	NZ: North Is.	Hansen 1997
+4 undescribed species		
Andotypus Spangler, 1979		
A. araucariae Fikáček, Minoshima & Newton, 2014	CH: La Araucanía	Fikáček et al. 2014
A. ashworthi Spangler, 1979	CH: Aisén, Viobío, Los Rios, Los Lagos, Magallanes	Fikáček et al. 2014
Anticura Spangler, 1979		
A. flinti Spangler, 1979	ARG: Neuquén; CH: Los Lagos, La Araucanía	Fikáček & Vondráček 2014
Austrotypus Fikáček, Minoshima & Newton, 2014		
A. nothofagi Fikáček, Minoshima & Newton, 2014	AUS: New South Wales, Queensland	Fikáček et al. 2014
A. peruanus Fikáček, Minoshima & Newton, 2014	PE: Huánuco	Fikáček et al. 2014
Borborophorus Hansen 1990		
B. pubescens Hansen, 1990	AUS: New South Wales, Queensland	Hansen 1990
B. punctatus Hansen, 1990	AUS: New South Wales	Hansen 1990
B. tuberculus Hansen, 1990	AUS: Queensland	Hansen 1990
Coelostomopsis Hansen, 1990		
C. major Hansen, 1990	AUS: Queensland	Hansen 1990
C. picea Hansen, 1990	AUS: Queensland	Hansen 1990
Cyloma Sharp, 1872		
C. flemingi (Ordish, 1974)	NZ: Snares Is.	Hansen 1997
C. guttulatus Sharp, 1884	NZ: North Is., South Is., Stewart Is.	Hansen 1997, Seidel unpubl.
C. lawsonus Sharp, 1872	NZ: North Is.	Hansen 1997
C. lineatus (Broun, 1893)	NZ: North Is., South Is.	Hansen 1997
C. nigratus (Broun, 1915)	NZ: Soutrh Is.	Hansen 1997
C. pictus (Kirsch, 1877)	NZ: Auckland Is.	Hansen 1997
C. stewarti Broun, 1894	NZ: North Is.	Hansen 1997
C. thomsonus Sharp, 1884	NZ: South Is., Stewart Is.	Hansen 1997, Seidel unpubl.
+13 undescribed species		
Cylomissus Broun, 1903		
C. glabratus Broun, 1903	NZ: North Is., South Is.	Minoshima et al. 2015, Seidel unpubl.
+2 undescribed species		
Cylorygmus Orchymont, 1933		
C. lineatopunctatus Orchymont, 1933	CH: Región Metropolitana de Santiago, Valparaíso	Seidel et al. 2018 (Chapter 4)
Enigmahydrus Seidel, Minoshima, Leschen & Fikáček, in prep.		
E. larvalis Seidel, Minoshima, Leschen & Fikáček, in prep.	NZ: North Is., South Is.	Seidel et al., in prep. (Chapter 5)
Eurygmus Hansen, 1990		
E. helocharoides Hansen, 1990	AUS: Queensland	Hansen 1990
Exydrus Broun, 1886		
E. gibbosus (Broun, 1880)	NZ: North Is.	Hansen 1997
Hydrostygnus Sharp, 1884		
H. frontalis (Broun, 1880)	NZ: North Is.	Hansen 1997
Petasopsis Hansen, 1990		
P. brevitarsis Hansen, 1990	AUS: Queensland	Hansen 1990

Continuation of Table 2. Overview of Cylominae species and their distribution (ARG - Argentina, AUS - Australia, CH - Chile, NZ - New Zealand, PE - Peru, RSA - Republic of South Africa) *most recent references on distribution.

Pseudohydrobius Blackburn, 1898		
P. flavus Lea, 1919	AUS: New South Wales, Queensland	Hansen 1999
P. floricola Blackburn, 1898	AUS: Victoria	Hansen 1999
P. neogallicus (Gentili, 1996)	AUS: New South Wales	Fikáček & Watts 2015
+4 undescribed species		
Relictorygmus Seidel, Minoshima, Arriaga-Varela & Fikáček, 2018		
R. repentinus (Hebauer, 2002)	RSA: Western Cape	Seidel et al. 2018 (Chapter 4)
R. trevornoahi Seidel, Minoshima, Arriaga-Varela & Fikáček, 2018	RSA: Western Cape	Seidel et al. 2018 (Chapter 4)
Rygmodus White, 1846		
R. alienus Broun, 1893	NZ: South Is.	Hansen 1997
R. antennatus (Sharp, 1884)	NZ: South Is.	Hansen 1997
R. cyaneus Broun, 1881	NZ: North Is., South Is.	Hansen 1997, Hansen unpublished
R. femoratus Sharp, 1884	NZ: North Is., South Is.	Hansen 1997, Hansen unpublished
R. incertus Broun, 1880	NZ: North Is.	Hansen 1997
R. longulus (Sharp, 1884)	NZ: South Is.	Hansen 1997
R. modestus White, 1846	NZ: North Is., South Is.	Hansen 1997
R. oblongus Broun, 1880	NZ: North Is.	Hansen 1997
R. opimus Broun, 1880	NZ: South Is.	Hansen 1997
R. pedinoides White, 1846	NZ: no detailed locality	Hansen 1997
R. tibialis Broun, 1893	NZ: South Is.	Hansen 1997
Rygmostralia Orchymont, 1933		
R. brunnea Orchymont, 1933	AUS: New South Wales	Hansen 1990
+1 undescribed species		
Saphydrus Sharp, 1884		
S. moeldnerae Seidel, Minoshima, Leschen & Fikáček, in prep.	NZ: North Is.	Seidel et al., in prep. (Chapter 5)
S. monticola Broun, 1893	NZ: North Is.	Seidel et al., in prep. (Chapter 5)
S. obesus Sharp, 1884	NZ: North Is., South Is.	Seidel et al., in prep. (Chapter 5)
S. suffusus Sharp, 1884	NZ: North Is., South Is.	Seidel et al., in prep. (Chapter 5)
S. tanemahuta Seidel, Minoshima, Leschen & Fikáček in prep.	NZ: South Is.	Seidel et al., in prep. (Chapter 5)
Thomosis Broun, 1904		
Thomosis guanicola Broun, 1904	NZ: Antipodes Is., Bounty Is.	Hansen 1997, Hansen unpubl.
Tormissus Broun, 1893		
T. linsi (Sharp, 1884)	NZ: North Is., South Is.	Hansen 1997
T. magnulus	NZ: South Is.	Hansen 1997
+1 undescribed species		

References

Broun, T. (1886). Manual of the New Zealand Coleoptera. Part IV. *Colonial Museum and Geological Survey Department, Wellington*, 817–973.

Buckley, T. R., Krosch, M., & Leschen, R. A. B. (2015). Evolution of New Zealand insects: summary and prospectus for future research. *Austral Entomology*, 54(1), 1-27.

Bunce, M., Worthy, T. H., Phillips, M. J., Holdaway, R. N., Willerslev, E., Haile, J., Shapiro, B., Scofield, R. P., Drummond, A., Kamp, P. J. J, & Cooper, A. (2009). The evolutionary history of the extinct ratite moa and New Zealand Neogene paleogeography. *Proceedings of the National Academy of Sciences*, 106(49), 20646-20651.

Burrows, C. J. (1965). *Some discontinuous distributions of plants within New Zealand and their ecological significance. Part II: Disjunctions between Otago-Southland and Nelson-Marlborough and related distribution patterns*. Timaru Herald Print.

Chinn, W. G., & Gemmell, N. J. (2004). Adaptive radiation within New Zealand endemic species of the cockroach genus Celatoblatta Johns (Blattidae): a response to Plio-Pleistocene mountain building and climate change. *Molecular Ecology*, 13(6), 1507-1518.

Cooper, A., & Cooper, R. A. (1995). The Oligocene bottleneck and New Zealand biota: genetic record of a past environmental crisis. *Proceedings of the Royal Society of London. Series B: Biological Sciences*, 261(1362), 293-302.

Delgado, J. A., & Palma, R. L. (1999). Taxonomic review of the genus Orchymontia (Coleoptera: Hydraenidae). *New Zealand Entomologist*, 22(1), 23-32.

Delgado, J. A., & Palma, R. L. (2010). A revision of the genus Podaena Ordish (Insecta: Coleoptera: Hydraenidae). *Zootaxa*, 2678(1), 1-47.

Ezcurra, M. D., & Agnolín, F. L. (2012). A new global palaeobiogeographical model for the late Mesozoic and early Tertiary. *Systematic Biology*, 61(4), 553-566.

Fikáček, M. (2019). 20. Hydrophilidae Leach, 1815. pp. 271–337. *In*: Slipinski, A., and Lawrence, J. (eds). Australian Beetles. Volume 2. Archostemata, Myxophaga, Adephaga, Polyphaga (part). CSIRO Publishing, Clayton South, 765 pp.

Fikáček, M., & Watts, C. H. (2015). Notes on the Australian Anacaenini (Coleoptera: Hydrophilidae): description of male of Phelea breviceps Hansen and unravelling the identity of Crenitis neogallica Gentili. *Zootaxa*, 3980(3), 427-434.

Fikáček, M., Leschen, R. A., Newton, A. F., & Gunter, N. (2012). Horelophus walkeri rediscovered: adult morphology and notes on biology (Coleoptera: Hydrophilidae). *Acta Entomologica Musei Nationalis Pragae*, 52(1), 129–146.

Fikáček, M., Minoshima, Y. N., Vondráček, D., Gunter, N., & Leschen, R. A. B. (2013). Morphology of adults and larvae and integrative taxonomy of southern hemisphere genera Tormus and Afrotormus (Coleoptera: Hydrophilidae). *Acta Entomologica Musei Nationalis Pragae*, 53(1) 75–126.

Fikáček, M., Minoshima, Y. N., & Newton, A. F. (2014). A review of Andotypus and Austrotypus gen. nov., rygmodine genera with an austral disjunction (Hydrophilidae: Rygmodinae). *Annales Zoologici.* 64(4), 557-596.

Fikáček, M., & Vondráček, D. (2014). A review of Pseudorygmodus (Coleoptera: Hydrophilidae), with notes on the classification of the Anacaenini and on distribution of genera endemic to southern South America. *Acta Entomologica Musei Nationalis Pragae*, 54(2), 479-514.

Fleming, C. A. (1979). *The geological history of New Zealand and its life*. Auckland University Press.

Gentili, E. (1981). The genera Laccobius and Nothydrus (Coleoptera, Hydrophilidae) in Australia and New Zealand. *South Australian Museum.* 18(7), 143-154.

Giribet, G., & Boyer, S. L. (2010). 'Moa's Ark' or 'Goodbye Gondwana': is the origin of New Zealand's terrestrial invertebrate fauna ancient, recent, or both?. *Invertebrate Systematics*, 24(1), 1-8.

Goodlad, S. W., Martin, A. K., & Hartnady, C. J. H. (1982). Mesozoic magnetic anomalies in the southern Natal Valley. *Nature*, 295(5851), 686.

Hansen, M. (1990). Australian Sphaeridiinae (Coleoptera: Hydrophilidae): A taxonomic outline with descriptions of new genera and species. *Invertebrate Taxonomy*, 4, 317–395.

Hansen, M. (1991). The hydrophiloid beetles. Phylogeny, classification and a revision of the genera (Coleoptera, Hydrophiloidea*). Biologiske Skrifter,* 40, 1–367.

Hansen M (1997). Synopsis of the endemic New Zealand genera of the beetle subfamily Sphaeridiinae (Coleoptera: Hydrophilidae). *New Zealand Journal of Zoology*, 24, 351–370.

Hansen, M. (1999). Hydrophiloidea (s. str.)(Coleoptera). *World catalogue of insects*. 416 pp.

Hebauer, F. (2002). New Hydrophilidae of the Old World (Coleoptera, Hydrophilidae). *Acta Coleopterologica*, 18(3), 3-24.

Houben, A. J., Bijl, P. K., Sluijs, A., Schouten, S., & Brinkhuis, H. (2019). Late Eocene Southern Ocean cooling and invigoration of circulation preconditioned Antarctica for full-scale glaciation. *Geochemistry, Geophysics, Geosystems,* 20(5), 2214-2234.

Krosch, M., & Cranston, P. S. (2013). Not drowning,(hand) waving? Molecular phylogenetics, biogeography and evolutionary tempo of the 'Gondwanan'midge Stictocladius Edwards (Diptera: Chironomidae). *Molecular Phylogenetics and Evolution*, 68(3), 595-603.

Kuschel, G. (1990). Beetles in a suburban environment: a New Zealand case study. The identity and status of Coleoptera in the natural and modified habitats of Lynfield, Auckland (1974-1989), *DSIR Plant Protection Report,* 3, 1-118.

Lee, D. E., Lee, W. G., & Mortimer, N. (2001). Where and why have all the flowers gone? Depletion and turnover in the New Zealand Cenozoic angiosperm flora in relation to palaeogeography and climate. *Australian Journal of Botany*, 49(3), 341-356.

Landis, C. A., Campbell, H. J., Begg, J. G., Mildenhall, D. C., Paterson, A. M., & Trewick, S. A. (2008). The Waipounamu Erosion Surface: questioning the antiquity of the New Zealand land surface and terrestrial fauna and flora. *Geological Magazine*, 145(2), 173-197.

Leschen, R. A., Buckley, T. R., Harman, H. M., & Shulmeister, J. (2008). Determining the origin and age of the Westland beech (Nothofagus) gap, New Zealand, using fungus beetle genetics. *Molecular Ecology*, 17(5), 1256-1276.

Livermore, R., Nankivell, A., Eagles, G., & Morris, P. (2005). Paleogene opening of Drake passage. *Earth and Planetary Science Letters*, 236(1-2), 459-470.

Marra, M. J., & Thackray, G. D. (2010). Glacial forest refugium in Howard Valley, South Island, New Zealand. *Journal of Quaternary Science: Published for the Quaternary Research Association*, 25(3), 309-319.

Marshall, D. C., Slon, K., Cooley, J. R., Hill, K. B., & Simon, C. (2008). Steady Plio-Pleistocene diversification and a 2-million-year sympatry threshold in a New Zealand cicada radiation. *Molecular Phylogenetics and Evolution*, 48(3), 1054-1066.

Marshall, D. C., Hill, K. B., Moulds, M., Vanderpool, D., Cooley, J. R., Mohagan, A. B., & Simon, C. (2015). Inflation of molecular clock rates and dates: molecular phylogenetics, biogeography, and diversification of a global cicada radiation from Australasia (Hemiptera: Cicadidae: Cicadettini). *Systematic Biology*, 65(1), 16-34.

Marske, K. A., Leschen, R. A., Barker, G. M., & Buckley, T. R. (2009). Phylogeography and ecological niche modelling implicate coastal refugia and trans-alpine dispersal of a New Zealand fungus beetle. *Molecular Ecology*, 18(24), 5126-5142.

McCulloch, G. A., Wallis, G. P., & Waters, J. M. (2016). A time-calibrated phylogeny of Southern Hemisphere stoneflies: Testing for Gondwanan origins. *Molecular Phylogenetics and Evolution*, 96, 150-160.

McGlone, M. S., Newnham, R. M., & Moar, N. T. (2010). The vegetation cover of New Zealand during the Last Glacial Maximum: do pollen records under-represent woody vegetation. *Terra Australis*, 32, 49-68.

McLellan, I. (2006). Endemism and biogeography of New Zealand Plecoptera (Insecta). *Illiesia*, 2(2), 15-23.

McLoughlin, S. (2001). The breakup history of Gondwana and its impact on pre-Cenozoic floristic provincialism. *Australian Journal of Botany*, 49(3), 271-300.

Minoshima, Y. N., Fikáček, M., Gunter, N., & Leschen, R. A. (2015). Larval Morphology and Biology of the New Zealand-Chilean Genera Cylomissus Broun and Anticura Spangler (Coleoptera: Hydrophilidae: Rygmodinae). *The Coleopterists Bulletin*, 69(4), 687-713.

Minoshima, Y. N., Seidel, M., Wood, J. R., Leschen, R. A., Gunter, N. L., & Fikáček, M. (2018). Morphology and biology of the flower-visiting water scavenger beetle genus Rygmodus (Coleoptera: Hydrophilidae). *Entomological Science*, 21(4), 363-384.

Newton, A. F. (1989). Review of Dactylosternum Wollaston species of Australia and New Zealand (Coleoptera: Hydrophilidae). *The Australian Entomologist,* 16(3), 49.

Orchymont, A. d'. (1916). De la place que doivent occuper dans la classification les sous-familles des Sphaeridiinae et des Hydrophilinae [Col. Hydrophilidae]. *Bulletin de la Societe entomologique de France*, 21(15), 235-240.

Orchymont, A. d'. (1919). Contribution a l'étude des sous-familles des Sphaeridiinae et des Hydrophilinae (Col. Hydrophilidae). *Annales de la Société entomologique de France,* 88, 105-168.

Orchymont, A. d'. (1933). Contribution a l'etude des Palpicornia. VIII. *Bulletin et Annales de la Societe entomologique de Belgique*, 73, 271-314.

Orchymont, A. d'. (1937). Check List of the Palpicornia of Oceania (Coleoptera, Polyphaga). *Occasional Papers of the Bernice P. Bishop Museum*, 13, 147-160.

Ordish, R. G. (1974). Arthropoda of the subantarctic islands of New Zealand (3) Coleoptera: Hydrophilidae. *Journal of the Royal Society of New Zealand*, 4(3), 307-314.

Pratt, R. C., Morgan-Richards, M., & Trewick, S. A. (2008). Diversification of New Zealand weta (Orthoptera: Ensifera: Anostostomatidae) and their relationships in Australasia. *Philosophical Transactions of the Royal Society B: Biological Sciences*, 363(1508), 3427-3437.

Pross, J., Contreras, L., Bijl, P.K., Greenwood, D.R., Bohaty, S.M., Schouten, S., Bendle, J.A., Röhl, U., Tauxe, L., Raine, J.I., Huck, C.E., Flierdt, T. van de, Jamieson, S.S.R., Stickley, C.E., Schootbrugge, B. van de, Escutia, C., Brinkhuis, H., Scientists, I.O.D.P.E. 318, Brinkhuis, H., Dotti, C.E., Klaus, A., Fehr, A., Williams, T., Bendle, J.A.P., Bijl, P.K., Bohaty, S.M., Carr, S.A., Dunbar, R.B., Gonzàlez, J.J., Hayden, T.G., Iwai, M., Jimenez-Espejo, F.J., Katsuki, K., Kong, G.S., McKay, R.M., Nakai, M., Olney, M.P., Passchier, S., Pekar, S.F., Pross, J., Riesselman, C.R., Röhl, U., Sakai, T., Shrivastava, P.K., Stickley, C.E., Sugisaki, S., Tauxe, L., Tuo, S., Flierdt, T. van de, Welsh, K., Yamane, M., (2012). Persistent near-tropical warmth on the Antarctic continent during the early Eocene epoch. *Nature*, 488(7409), 73.

Pyron, R. A., & Wiens, J. J. (2011). A large-scale phylogeny of Amphibia including over 2800 species, and a revised classification of extant frogs, salamanders, and caecilians. *Molecular Phylogenetics and Evolution*, 61(2), 543-583.

Rabinowitz, P. D., Coffin, M. F., & Falvey, D. (1983). The separation of Madagascar and Africa. *Science*, 220(4592), 67-69.

Reguero, M. A., Gelfo, J. N., López, G. M., Bond, M., Abello, A., Santillana, S. N., & Marenssi, S. A. (2014). Final Gondwana breakup: the Paleogene South American native ungulates and the demise of the South America–Antarctica land connection. *Global and Planetary Change*, 123, 400-413.

Sanmartín, I., & Ronquist, F. (2004). Southern Hemisphere biogeography inferred by event-based models: plant versus animal patterns. *Systematic Biology*, 53(2).

Scotese, C. R., Gahagan, L. M., & Larson, R. L. (1988). Plate tectonic reconstructions of the Cretaceous and Cenozoic ocean basins. *Tectonophysics*, 155(1-4), 27-48.

Seidel, M., Arriaga-Varela, E., & Fikáček, M. (2016). Establishment of Cylominae Zaitzev, 1908 as a valid name for the subfamily Rygmodinae Orchymont, 1916 with an updated list of genera (Coleoptera: Hydrophilidae). *Acta Entomologica Musei Nationalis Pragae*, 56(1), 159-165.

Seidel, M., Minoshima, Y. N., Arriaga-Varela, E., & Fikáček, M. (2018). Breaking a disjunct distribution: a review of the Southern hemisphere genera Cylorygmus and Relictorygmus gen. nov. (Hydrophilidae: Cylominae). *Annales Zoologici,* 68(2), 375-403.

Seidel, M., Minoshima, Y. N., Leschen, R, & Fikáček, M. (in prep.). Phylogeny, systematics and rarity assessment of New Zealand endemic Saphydrus beetles and related enigmatic larvae (Coleoptera: Hydrophilidae: Cylominae).

Seidel, M., Sýkora, V., Leschen, R. A. B., & Fikáček, M. (in prep.). Systematics and biogeography of the Southern Hemisphere endemic Cylominae beetles (Coleoptera: Hydrophilidae).

Short, A. E. Z. (2010). Hydrophilidae: Hydrobiusina (Coleoptera). *Water Beetles of New Caledonia*, 1, 319-322.

Short, A. E. Z., & Fikáček, M. (2013). Molecular phylogeny, evolution and classification of the Hydrophilidae (Coleoptera). *Systematic Entomology*, 38(4), 723-752.

Spangler, P. J. (1979). A new genus of water beetle from austral South America (Coleoptera: Hydrophilidae). *Proceedings of the Biological Society of Washington,* 92(4), 697–718.

Thomaz Filho, A., Mizusaki, A. M. P., Milani, E. J., & De Cesero, P. (2000). Rifting and magmatism associated with the South America and Africa break up. *Revista Brasileira de Geociências*, 30(1), 017-019.

Thorpe, S. (2011). (2011, January 16). *Enochrus maculiceps*. Retrieved (16 July 2019) from https://species-id.net/wiki/Enochrus_maculiceps

Tippett, J. M., and Kamp, P. J. J. (1995). Geomorphic evolution of the Southern Alps, New Zealand. *Earth Surface Processes and Landforms*, 20, 177–192.

Torsvik, T. H., Gaina, C., & Redfield, T. F. (2008). Antarctica and global paleogeography: from Rodinia, through Gondwanaland and Pangea, to the birth of the Southern Ocean and the opening of gateways. *Antarctica: A keystone in a changing world*, 125-141.

Wallis, G. P., and Trewick, S. A. (2009). New Zealand phylogeography: evolution on a small continent. *Molecular Ecology*, 18, 3548-3580.

Wardle, P. (1988). Effects of glacial climates on floristic distribution in New Zealand 1. A review of the evidence. *New Zealand Journal of Botany*, 26(4), 541-555.

Winterbourn, M. J. (1970). The Hydrophilidae (Coleoptera) of New Zealand's thermal waters. *Transactions of the Royal Society of New Zealand. Biological Science*, 12, 21–28.

Woodburne, M. O., & Case, J. A. (1996). Dispersal, vicariance, and the Late Cretaceous to early Tertiary land mammal biogeography from South America to Australia. *Journal of Mammalian Evolution*, 3(2), 121-161.

Yonezawa, T., Segawa, T., Mori, H., Campos, P. F., Hongoh, Y., Endo, H., Akiyoshi, A., Kohno, N., Nishida, S., Wu, J., Jin, H., Adachi, J., Kishino, H., Kurokawa, K., Nogi, Y., Tanabe, H., Mukoyama, H., Yoshida, K., Rasoamiaramanana, A., Yamagishi, S., Hayashi, Y., Yoshida, A., Koike, H., Akishinonomiya, F., Willerslev, E. & Hasegawa, M. (2017). Phylogenomics and morphology of extinct paleognaths reveal the origin and evolution of the ratites. *Current Biology*, 27(1), 68-77.

Zaitzev, F. A. (1908). Catalogue des Coléoptères aquatiques des familles Dryopidae, Georyssidae, Cyathoceridae, Heteroceridae et Hydrophilidae. *Horae Societatis Entomologicae Rossicae*, 38, 283–420.

Zheng, Y., & Wiens, J. J. (2016). Combining phylogenomic and supermatrix approaches, and a time-calibrated phylogeny for squamate reptiles (lizards and snakes) based on 52 genes and 4162 species. *Molecular Phylogenetics and Evolution*, 94, 537-547.

ATTACHED PUBLICATIONS AND MANUSCRIPTS

CHAPTER 1

Toussaint, E. A. F., **Seidel, M.**, Arriaga-Varela, E., Hájek, J., Král, D., Sekerka, L., Short, A. E. Z. & Fikáček, M. (2017). The peril of dating beetles. *Systematic Entomology*, 42(1): 1-10.

Author contributions: ET run the phylogenetic analyses; MS, EAV, JH, DK, LS & MF performed the literature review and fossil selection; ET drafted the manuscript and ET, MF, MS, EAV and AS contributed to the writing.

Systematic Entomology

Systematic Entomology (2017), **42**, 1–10 DOI: 10.1111/syen.12198

OPINION

The peril of dating beetles

EMMANUEL F. A. TOUSSAINT[1], MATTHIAS SEIDEL[2,3], EMMANUEL ARRIAGA-VARELA[2,3], JIŘÍ HÁJEK[3], DAVID KRÁL[2], LUKAŠ SEKERKA[3], ANDREW E. Z. SHORT[1] and MARTIN FIKÁČEK[2,3]

[1]Department of Ecology & Evolutionary Biology & Division of Entomology, Biodiversity Institute, University of Kansas, Lawrence, KS, U.S.A., [2]Department of Zoology, Faculty of Science, Charles University in Prague, Prague, Czech Republic and [3]Department of Entomology, National Museum, Prague, Czech Republic

Introduction

Recently, McKenna *et al.*, 2015 (MCK15 hereafter) investigated the higher level phylogenetic relationships of beetles (Insecta, Coleoptera) using the most comprehensive molecular dataset to date, and inferred the absolute ages of major groups using multiple fossil calibrations across the beetle tree of life. Based on the result of their dating analysis, beetles diverged from Strepsiptera in the Early Permian *c.* 278.33 Ma with a 95% credibility interval (95% CI) of 288.28 to 271.89 Ma, and the crown age of Coleoptera was estimated for the Late Permian *c.* 252.89 Ma (95% CI: 267.68 to 238.78 Ma), supporting the view that beetles originated before and survived through the End-Permian Mass Extinction that occurred *c.* 252 Ma (Shen *et al.*, 2011). However, some of the age estimates found in MCK15 are in conflict with current knowledge of the beetle fossil record (e.g. Nikolajev & Ren, 2010; Pan *et al.*, 2011, Prokin & Ren, 2011; Fikáček *et al.*, 2012a; Wang *et al.*, 2013, 2014; Cai *et al.*, 2014b, 2015a; Kirejtshuk *et al.*, 2014; Boucher *et al.*, 2016) and with other recently published molecular age estimates for some major beetle clades (e.g. Zhang & Zhou, 2013; Ahrens *et al.*, 2014; Bloom *et al.*, 2014; Kergoat *et al.*, 2014; Kim & Farrell, 2015; Bocák *et al.*, 2016; Gunter *et al.*, 2016). In some cases, the difference in age estimates is significant and might change our understanding of the mode and tempo of diversification dynamics of these groups.

Based on a careful examination of the data and analyses performed in MCK15, we propose that the divergence time estimates which they found are likely to underestimate clade ages. We believe this is due to the subset of fossil Coleoptera that MCK15 selected as calibration points, as well as the methodological approach used in their analyses. To explore the impact of fossil selection on the age of Coleoptera, we derived an alternative set of fossil calibration points based on best-practice recommendations (e.g. Parham *et al.*, 2012), and performed new molecular dating analyses to investigate the effect of fossil selection and maximum ages, on posterior estimates of divergence times.

Correspondence: Emmanuel F. A. Toussaint, Department of Ecology & Evolutionary Biology & Division of Entomology, Biodiversity Institute, University of Kansas, Lawrence, KS, U.S.A. E-mail: Toussaint@ku.edu

Materials and methods

Analyses based on the original set of fossils

We first replicated the results of MCK15 using the same dataset (File S2 in MCK15) and settings. To do so, we recovered the molecular matrix from MCK15 comprising eight gene fragments for a total of ~9000 bp (see MCK15 for more details). We then specified the same fossil constraints as in MCK15 following the procedure described in the original paper. Calibrated nodes as well as some suprafamilial nodes were constrained to be monophyletic. The Tree Model was set to a Yule: speciation prior in BEAUti 1.8.2 (Drummond *et al.*, 2012). All fossil calibrations were specified using a lognormal prior (mean = 30, log-SD = 0.75) on the stem of the targeted clades except for the root that received a normal prior density (mean = 302, SD = 30). The prior distribution of the root was then truncated to the interval 270–396 Ma as in MCK15. The partitions (one partition for the ribosomal gene fragments, one partition for first and second positions of protein-coding gene fragment codons, and one partition for third positions of protein-coding gene fragment codons) and substitution models (GTR + Γ + I for all partitions) were the same as in MCK15. Preliminary analyses revealed that most parameters were critically undersampled and their associated ESS values <100 when using only a 100 million generations sampled every 1000 generations, as described in MCK15. Therefore, we ran two independent analyses with a Markov chain Monte Carlo (MCMC) running for 300 million generations and a parameter sampling every 3000 generations. The posterior trees and log files were resampled at a frequency of 30 000 then combined in LogCombiner 1.8.2 (Drummond *et al.*, 2012) before applying a conservative burn-in of 50%.

Second, we replicated these analyses but instead of using monophyletic constraints, we used a fixed topology the same

as the time tree of MCK15 (provided by Duane McKenna) as a starting tree, and unchecked the parameters allowing topology changes in BEAUti 1.8.2. The objective of this analysis was to show that by enforcing a fixed topology we would recover similar ages as in the analysis using monophyletic constraints.

We found very similar ages between the original chronogram from MCK15 and our analyses with or without fixing the tree topology (see Files S1 and S2). Therefore, we conducted the rest of the analyses with a fixed topology.

Analyses based on the new set of fossils

In order to calibrate the tree from MCK15, we carefully checked the fossil record of Coleoptera. We selected beetle fossils known as the most ancient representatives of clades recovered in MCK15. We checked fossils for the presence of synapomorphies or relevant diagnostic characters, based partly on consultations with specialists on particular groups (see File S3 and Acknowledgements). The selection was not solely based on published data because in some instances, original descriptions had incomplete or even lacked reliable justification for the systematic placement of the fossils. Fossils were selected on the basis of shared apomorphies with a specific clade of the tree to allow their confident placement on the stem of each focal clade. Our search targeted all beetle clades and selected all available oldest representatives that we could possibly fit in the tree using the same stringent criteria. Our final fossil set consisted of 34 fossils listed in detail in Table 1. Justification for their placement in the tree is provided following the recommendation of Parham *et al.* (2012) when possible. It is noteworthy that Table 1 lists only the specimens that were ultimately retained to provide a minimum age; however, in many cases additional fossils of nearly the same age were available and reliably assigned to the same or sister clades, thereby providing even more evidence for the calibration of particular stems (see File S3 for more details).

We chose not to use the fossil calibrations used to enforce minimum ages for Hymenoptera and Neuroptera in MCK15 for several reasons. First, the taxon sampling in these two clades is extremely reduced and most major branching events are missing. Second, multiple orders of insects closely related to Coleoptera were not included in the dataset. In order to use such fossil calibrations, it would have been advisable to sample representatives of the other megadiverse orders Diptera and Lepidoptera that are representatives of the sister group of beetles and their closest relatives (e.g. Misof *et al.*, 2014). Third, the fact that all fossil calibrations from MCK15 were originally enforced at the stem of focal clades means that the fossil calibration used to constrain Hymenoptera actually enforced a minimum age on the root of the tree. This is problematic because it means that the root has in fact two different constraints that are not enforcing the same age prior. If the root was constrained with the Hymenoptera fossil calibration, then 95% of the age distribution would be found between 240 and 330 Ma. These ages are far younger than the original root calibration in MCK15 where the truncated normal distribution encompassed an older interval (270–396 Ma). A similar issue was found for the Chrysomeloidea and Curculionoidea calibrations where the stems of both clades were constrained with different fossil taxa. However, because both calibrations were on the stem of sister lineages, the only node being constrained was the crown of Chrysomeloidea + Curculionoidea (=Phytophaga). Fortunately, in that case, both calibrations encapsulate the same information because the chrysomeloid and curculionoid fossils are from the same geological stratum in Kazakhstan. Nonetheless, these imprecisions lowered the number of informative fossil calibrations from 15 to 13 in MCK15.

Although MCK15 would not have been able to know at the time of their analyses, the root calibration they used (270–396 Ma) has proven to be problematic in light of contemporary studies. The minimum bound of the root prior in MCK15 conflicts with the most recent reviews of the beetle fossil record (e.g. Kirejtshuk *et al.*, 2014) and also with the most recent phylogenomic studies of insect evolution. In Misof *et al.* (2014) and Tong *et al.* (2015), the lower bound of the age credibility interval for the Holometabola node was estimated at 320 and 350 Ma, respectively. For future studies, a more justifiable way to place an interval on the age of the root is to use the age estimates of the recent dating studies of Misof *et al.* (2014) and Tong *et al.* (2015) in which the age of the crown Holometabola was found to be ∼345 Ma (CI: ∼320–370 Ma) and ∼370 Ma (CI: ∼350–400 Ma), respectively. These studies are based on the same phylogenomic dataset. Tong *et al.* (2015) only revisited the ages of Misof *et al.* (2014) using additional fossil evidence and different parametrisation of the Bayesian molecular dating analyses. We therefore chose to use an interval encompassing both estimates (320–400 Ma).

The new fossil calibrations were enforced in BEAUti 1.8.2 (Drummond *et al.*, 2012) using the same priors used in MCK15, a lognormal density with mean = 30 and log (SD) = 0.75 was assigned to every fossil calibration. All other settings were left identical as in MCK15. As for the previous runs, we conducted two independent analyses of 300 million generations with a sampling every 3000 cycles. The .xml file generated in BEAUti to perform this analysis is provided in File S4. The resulting log and tree files were then resampled at a lower frequency (30 000) and combined in LogCombiner 1.8.2 with a conservative burn-in of 50% (Drummond *et al.*, 2012).

Results

All BEAST analyses performed with 300 million generations converged, with all parameters properly sampled as indicated by ESS values >200. The chronograms recovered in the preliminary tests (monophyletic constraints vs fixed topology) are presented in Files S1 and S2. Using the same settings as specified in MCK15, we recovered very similar age estimates, as indicated in File S1. Likewise, when constraining the topology to the time tree of MCK15 as presented in File S4 of the original paper, we did not recover major differences in divergence time estimates in comparison to the unconstrained analysis (File S2). The median age estimates from these two analyses are very similar to the ones of MCK15 presented in Table 2.

Table 1. List of the fossil calibrations used in the present study to infer beetle absolute divergence times.

FC	Taxon	Node (stem)	Deposit	Age	Ref.	CR1	CR2	CR3	CR4	CR5
1	*Coleopsis archaica*	Coleoptera	Grügelborn, Germany	295.5	1	✓	✓	✓	✓	✓
2	*Omma liassicum*	Ommatidae	Hasfield, United Kingdon	201.3	2	✓	✓	✓	✓	✓
3	*Priacma tuberculosa*	Priacminae	Huangbanjigou, Yixian Formation, China	125.5	3	✓	✓	✓	✓	✓
4	*Haplochelus georissoides*	Lepiceridae	Burmese amber, Myanmar	93.5	4,5	✓	✓	✓	✓	✓
5	*Protonectes germanicus*	Hydradephaga	Schönbachsmühle, Hassberge Formation, Germany	221.5	6	✓	✓	✓	✓	✓
6	*Oxycheilopsis cretacicus*	Cicindelinae	Crato Formation, Brazil	112.0	7	✓	✓	✓	✓	✓
7	*Juropeltastica sinica*	Derodontidae	Daohugou, Nei Mongol, China	157.3	8	✓	✓	✓	✓	✓
8	Undescribed species	Silphidae	Daohugou, Nei Mongol, China	157.3	9	✓	✓	✓	✓	✓
9	Undescribed species	Nicrophorinae	Hunagbanjigou, Yixian Formation, China	125.5	9	✓	✓	✓	✓	✓
10	*Protochares brevipalpis*	Hydrophilidae	Talbragar Fossil Fish Beds, Australia	152.1	10	✓	✓	✓	✓	✓
11	*Mesochodaeus daohugouensis*	Ochodaeidae	Daohugou, Nei Mongol, China	157.3	11	✓	✓	✓	✓	✓
12	*Sinaesalus longipes*	Lucanidae	Yangshuwanzi, Yixian Formation, China	122.5	12	✓	✓	✓	✓	✓
13	*Glaresis tridentata*	Glaresidae	Chaomidian, Yixian Formation, China	125.5	13	✓	✓	✓	✓	✓
14	*Cretodascillus sinensis*	Dascillidae	Liutiaogou, Yixian Formation, China	122.5	14	✓	✓	✓	✓	✓
15	*Sinoparathyrea bimaculata*	Schizopodidae	Daohugou, Nei Mongol, China	157.3	15, 16	✓	✓	✓	✓	✓
16	*Elmadulescens rugosus*	Elmidae	El Soplao amber, Las Peñosas Formation, Spain	109.0	17	✓	✓	✓	✓	✓
17	*Heterocerites magnus*	Heteroceridae	Chaomidian, Yixian Formation, China	125.5	18	✓	✓	✓	✓	✓
18	*Sinobrevipogon jurassicus*	Artematopodidae	Daohugou, Nei Mongol, China	157.3	19	✓	✓	✓	✓	✓
19	*Stephanopachys vetus*	Dinoderinae	Font-de-Benon Quarry, Charentese amber, France	99.6	20	✓	✓	✓	✓	✓
20	*Actenobius magneoculus*	Anobiinae	San Just amber, Spain	105.3	21	✓	✓	✓	✓	✓
21	*Rhyzobius antiquus*	Coccidulinae	Oise amber, France	47.8	22	✓	✓	✓	✓	✓
22	*Archelatrius marinae*	Latridiinae	Lebanese amber, Lebanon	122.5	23	✓	✓	?	✓	✓
23	*Paleoripiphorus deploegi*	Ripidiinae	Archingeay/Les Nouillers amber, France	99.6	24, 25, 26	✓	✓	✓	✓	✓
24	*Vetuprostomis consimilis*	Prostomidae	Burmese amber, Myanmar	93.5	27	✓	✓	✓	✓	✓
25	*Mirimordella gracilicruralis*	Mordellidae	Huangbanjigou, Yixian Formation, China	125.5	28	✓	✓	✓	✓	✓
26	Undescribed species	Aderidae	Lebanese amber, Lebanon	122.5	29	✓	✓	✓	✓	✓
27	*Alphitopsis initialis*	Tenebrioninae	Beipiao City, Yixian Formation, China	125.5	30	✓	✓	✓	✓	✓
28	*Idgiaites jurassicus*	Prionoceridae	Daohugou, Nei Mongol, China	157.3	31	✓	✓	✓	✓	✓
29	*Paracretocateres bellus*	Lophocaterinae	Huangbanjigou, Yixian Formation, China	125.5	32	✓	✓	✓	✓	✓
30	*Jurorhizophagus alienus*	Monotomidae	Daohugou, Nei Mongol, China	157.3	33	✓	✓	✓	✓	✓
31	*Cretoprionus liutiaogouensis*	Prioninae + Parandrinae	Liutiaogou, Yixian Formation, China	122.5	34	✓	✓	✓	✓	✓
32	*Mesopachymerus antiquus*	Bruchinae	Canadian amber, Grassy Lake, Canada	70.6	35	✓	✓	✓	✓	✓
33	Multiple fossils	Nemonychidae	Karatau-Mikhailovka, Kazakhstan	157.3	36	✓	✓	✓	✓	✓
34	*Cylindrobrotus pectinatus*	Scolytinae	Lebanese amber, Lebanon	122.5	37	✓	✓	✓	✓	✓

FC, fossil calibration number; CR, Parham *et al.* (2012) criteria; CR1, single/multiple operational taxonomic units (OTUs) with museum numbers; CR2, apomorphy-based or phylogenetic analysis; CR3, agreement of morphology and molecular data; CR4, detailed locality and stratigraphy data provided; CR5, radioisotopic age or numeric age references given. A more detailed justification after Parham *et al.*'s (2012) criteria is provided in File S3. References: 1, Kirejtshuk *et al.* (2014); 2, Crowson (1962); 3, Tan *et al.* (2006); 4, Kirejtshuk & Poinar (2006); 5, Ge *et al.* (2010); 6, Prokin *et al.* (2013a); 7, Cassola & Werner, (2004); 8, Cai *et al.* (2014a); 9, Cai *et al.* (2014b); 10, Fikáček *et al.* (2014); 11, Nikolajev & Ren (2010); 12, Nikolajev & Ren (2011); 13, Bai *et al.* (2014); 14, Jin *et al.* (2013); 15, Pan *et al.* (2011); 16, Cai *et al.* (2015a); 17, Peris *et al.* (2015a); 18, Prokin & Ren, (2011); 19, Cai *et al.* (2015b); 20, Peris *et al.* (2014); 21, Peris *et al.* (2015b); 22, Kirejtshuk & Nel (2012); 23, Kirejtshuk *et al.* (2009a); 24, Perrichot *et al.* (2004); 25, Batelka *et al.* (2006); 26, Falin & Engel (2010); 27, Engel & Grimaldi (2008); 28, Liu *et al.* (2007); 29, Grimaldi & Engel (2005); 30, Kirejtshuk *et al.* (2012); 31, Liu *et al.* (2015); 32, Yu *et al.* (2015); 33, Cai *et al.* (2015c); 34, Wang *et al.* (2014); 35, Poinar (2005); 36, Legalov (2013); 37, Kirejtshuk *et al.* (2009b).

The chronogram derived from the new fossil calibration set is available with full annotations in File S5 and summarised in Fig. 1. We recovered large differences between our estimates and the estimates of MCK15 (Figs 1, 2 and Table 2). The root of the tree (crown Holometabola) was found at 385.27 Ma with a 95% credibility interval (CI) of 365.49–400.00 Ma. We recovered the split between Strepsiptera and Coleoptera at 356 Ma (95% CI: 336–375 Ma) in the Early Carboniferous. The estimated origin

Table 2. Median crown age estimates and 95% credibility intervals recovered in the present study and McKenna *et al.* (2015) (MCK15).

Crown group taxon	Median age (Ma) in the present study (95% CI)	Median age (Ma) in MCK15 (95% CI)
Holometabola (Neuropteroidea + Hymenoptera)	385.27 (400.00 to 365.49)	297.97 (318.95 to 281.96)
Neuropteroidea (Coleoptera + Neuropterida + Strepsiptera)	375.56 (394.27 to 355.87)	289.77 (304.06 to 278.31)
Coleopterida (Coleoptera + Strepsiptera)	356.04 (375.03 to 336.81)	278.33 (288.28 to 271.89)
Coleoptera	332.85 (349.21 to 317.12)	252.89 (267.68 to 238.78)
Archostemata + Adephaga + Myxophaga	317.75 (335.42 to 300.34)	242.01 (256.67 to 230.37)
Archostemata + Myxophaga	300.43 (319.60 to 281.69)	219.55 (237.45 to 204.51)
Archostemata	249.30 (267.80 to 231.87)	157.82 (192.43 to 122.62)
Myxophaga	272.99 (295.37 to 247.29)	197.18 (221.87 to 170.13)
Adephaga	248.32 (267.96 to 231.33)	196.58 (217.84 to 174.74)
Geadephaga	220.26 (239.62 to 199.75)	172.50 (196.99 to 148.61)
Hydradephaga	237.29 (257.73 to 220.28)	183.89 (208.15 to 160.58)
Polyphaga	313.87 (328.95 to 299.69)	229.2 (246.57 to 213.49)
Scirtoidea + Derodontoidea s.s.	300.04 (317.56 to 281.63)	219.72 (237.74 to 199.33)
Core Polyphaga	298.07 (311.27 to 284.81)	212.21 (227.13 to 199.0)
Derodontoidea s.s.	223.31 (255.37 to 191.82)	172.13 (200.19 to 139.36)
Staphyliniformia	288.34 (302.28 to 274.09)	200.23 (216.96 to 182.84)
Staphylinoidea (+Jacobsoniidae)	280.42 (294.88 to 265.46)	193.16 (210.26 to 175.26)
Staphylinidae (+Silphidae and *Colon*)	245.58 (261.04 to 230.71)	165.03 (∼180 to 150)
Scarabaeoidea	221.22 (241.76 to 201.90)	141.11 (161.0 to 116.87)
Hydrophiloidea s.l.	253.49 (272.86 to 233.15)	168.31 (187.52 to 151.09)
Hydrophiloidea s.s.	190.35 (214.68 to 168.95)	123.93 (151.66 to 88.34)
Histeroidea	203.60 (226.50 to 179.36)	131.60 (156.60 to 106.09)
Elateriformia (+*Nosodendron*)	273.07 (287.43 to 258.61)	189.45 (205.74 to 175.0)
Elateroidea	246.02 (260.12 to 231.35)	166.18 (181.57 to 151.83)
Dascilloidea	179.92 (212.39 to 149.25)	120.47 (155.79 to 82.36)
Buprestoidea	184.06 (206.24 to 164.18)	111.76 (141.94 to 74.96)
Byrrhoidea	238.65 (254.67 to 222.21)	160.03 (176.96 to 142.85)
Bostrichoidea (here = Bostrichiformia)	263.46 (281.83 to 241.72)	181.65 (200.53 to 161.39)
Cucujiformia	274.64 (287.21 to 262.29)	189.76 (202.06 to 179.03)
Coccinelloidea	252.57 (267.14 to 238.60)	171.18 (187.0 to 157.09)
Tenebrionoidea + Lymexyloidea	259.18 (272.03 to 246.86)	175.15 (187.75 to 163.74)
Tenebrionidae	165.74 (178.80 to 153.83)	105.14 (∼120 to 80)
Cleroidea (+Biphyllidae and Byturidae)	252.07 (266.63 to 237.31)	169.02 (184.68 to 152.9)
Cucujoidea s.s. (−Biphyllidae and Byturidae)	244.79 (258.67 to 231.66)	167.08 (178.4 to 156.24)
Phytophaga (Chrysomeloidea + Curculionoidea)	239.87 (252.13 to 227.58)	161.66 (169.54 to 155.56)
Chrysomeloidea	218.46 (234.63 to 203.25)	145.14 (159.47 to 124.55)
Chrysomelidae	206.18 (222.82 to 187.56)	132.38 (∼160 to 110)
Cerambycidae (+Disteniidae and *Vesperus*)	162.03 (176.56 to 148.93)	90.66 (∼110 to 70)
Curculionoidea	226.88 (239.70 to 215.30)	149.64 (160.70 to 138.46)
Curculionidae	160.29 (170.21 to 150.76)	93.45 (∼110 to 80)

of extant beetle clades was found to be as old as 332 Ma (95% CI: 317–349 Ma) in the Mid Carboniferous. Most superfamilies were found to have originated in the Permian or Triassic (Fig. 2). In a substantial number of clades, the credibility intervals we recovered do not overlap with the ones estimates in MCK15, as highlighted in Fig. 2.

Discussion

Evolutionary history of beetles in the light of a new molecular timeframe

Our recalibrated time tree of Coleoptera based on MCK15 sequence data and topology, and a revised set of fossil calibrations resulted in node ages significantly older than in MCK15 and in other dated phylogenies focusing on the whole beetle tree of life (e.g. Hunt *et al.*, 2007; McKenna & Farrell, 2009; Misof *et al.*, 2014). However, our estimates are more in agreement with the few recent studies that looked at divergence times of major beetle clades (e.g. Zhang & Zhou, 2013; Ahrens *et al.*, 2014; Bloom *et al.*, 2014; Kergoat *et al.*, 2014; Kim & Farrell, 2015; Bocák *et al.*, 2016; Gunter *et al.*, 2016). Our estimates place the origin of Coleoptera during the Mid Carboniferous. We also infer an origin of the four extant beetle suborders in the Late Carboniferous to Early Permian, and an origin of many principal clades (series and superfamilies) predating the End-Permian Mass Extinction. Finally, our results support an origin of the large phytophagan families Curculionidae, Cerambycidae and Chrysomelidae during the Late Triassic to Mid Jurassic. These new age estimates and derived credibility

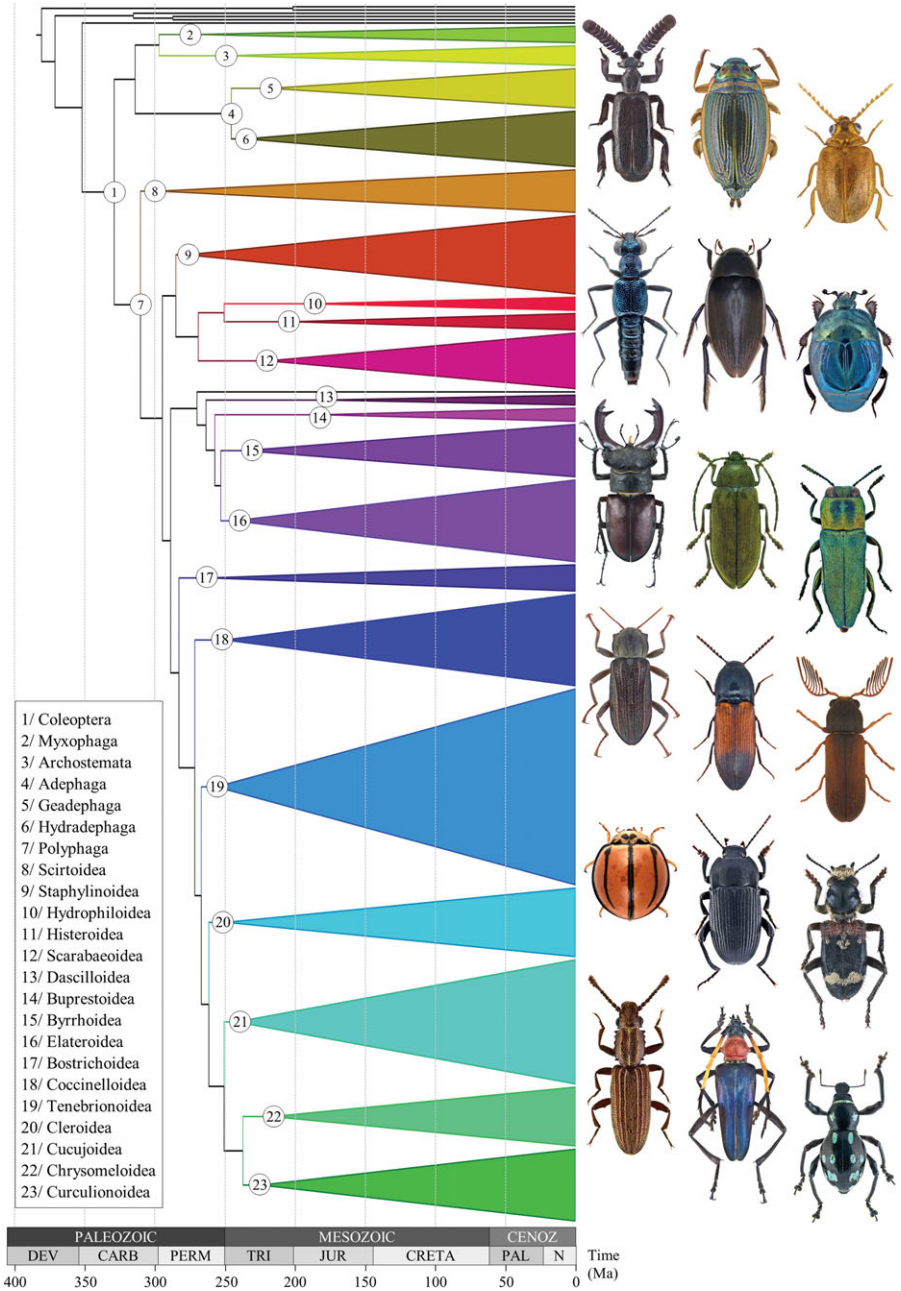

Fig. 1. Evolution of the main beetle clades through geological time. The chronogram shows the median ages derived from the BEAST dating analyses conducted on the dataset of McKenna *et al.* (2015) (MCK15) with new fossil calibrations (see text). Tips have been lumped into triangles representative of the sampling effort of the higher rank clades numbered in the tree. Triangles represent crown groups and not stem groups that would be older, as summarised in Fig. 2 and Table 2. A habitus picture of a species belonging to each of the 20 clades (except Myxophaga and Archostemata) is presented on the right of the topology in order of appearance. All pictures taken by Udo Schmidt. From top to bottom: *Arthropterus* sp. (Geadephaga), *Aulonogyrus concinnus* (Hydradephaga), *Prionocyphon serricornis* (Scirtoidea), *Dianous biformis* (Staphylinoidea), *Hydrophilus piceus* (Hydrophiloidea), *Saprinus splendens* (Histeroidea), *Lucanus cervus* (Scarabaeoidea), *Dascillus cervinus* (Dascilloidea), *Anthaxia diadema* (Buprestoidea), *Stenelmis canaliculata* (Byrrhoidea), *Ampedus balteatus* (Elateroidea), *Ptilinus pectinicornis* (Bostrichoidea), *Declivitata olivieri* (Coccinelloidea), *Colpotus godarti* (Tenebrionoidea), *Clerus mutillarius* (Cleroidea), *Oryzaephilus mercator* (Cucujoidea), *Pachyteria kurosawai* (Chrysomeloidea), *Metapocyrtus elegans* (Curculionoidea). [Colour figure can be viewed at wileyonlinelibrary.com].

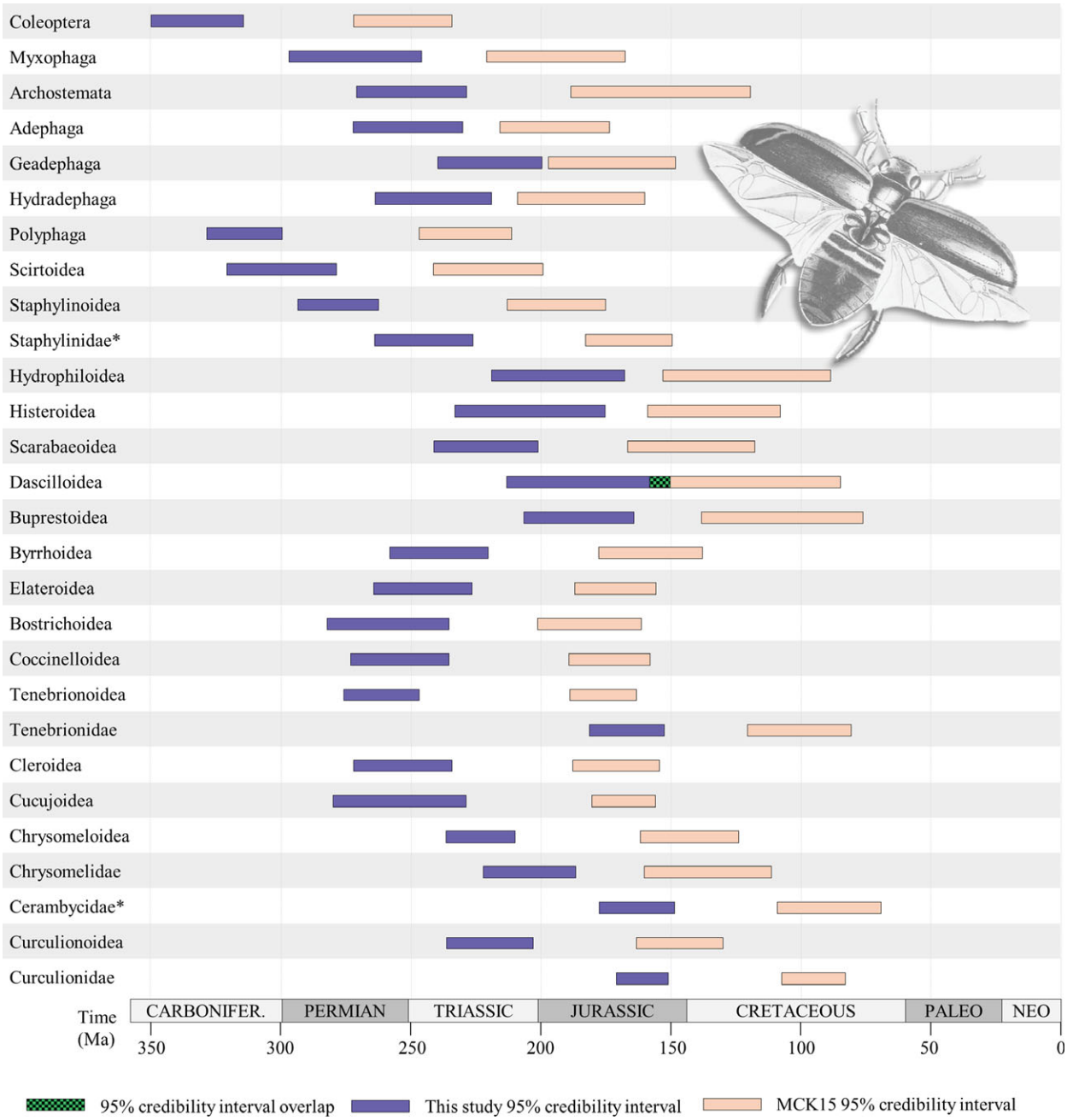

Fig. 2. Comparison of divergence time estimates for crowns of main beetle clades between McKenna *et al.* (2015) (MCK15) and the present study. Graph showing the 95% credibility intervals for the crown age of major beetle clades (see Table 2) in MCK15 and in the present study. The asterisk following the name of certain taxa indicates that these have been recovered as paraphyletic in MCK15 (see Table 2 and MCK15 for more information). On the top right corner is presented a drawing of *Dytiscus dimidiatus* taken from James Duncan's notorious book The Natural History of Beetles (1852). [Colour figure can be viewed at wileyonlinelibrary.com].

intervals are consistent with the latest dating for the crown of flowering plants in the Jurassic (e.g. Bell *et al.*, 2010; Clarke *et al.*, 2011; but see Beaulieu *et al.*, 2015). These estimates push back in time the old hypothesis of coevolution between phytophagan beetles and angiosperms (e.g. McKenna *et al.*, 2009). The ancestral plant association of phytophagan beetles therefore remains somewhat enigmatic as their origin largely pre-dates the diversification and dominance of angiosperms in the Cretaceous (Friis *et al.*, 2011).

The Mid Carboniferous origin of Coleoptera is older than all previous estimates that dated it back to the Late Carboniferous/Early Permian (Hunt *et al.*, 2007; McKenna &

Farrell, 2009; Misof *et al.*, 2014, MCK15). On one hand, a Mid–Late Carboniferous origin was suggested in recent studies for major holometabolan lineages including Hymenoptera – the clade strongly supported as sister to other Holometabola (Ronquist *et al.*, 2012; Misof *et al.*, 2014). On the other hand, the oldest definite beetle fossils with clearly developed elytra (i.e. bearing the principal apomorphy of the order) are known from the Early Permian deposits of Germany, Russia, Czech Republic and USA dated as 295 to 260 Ma (Kukalová, 1969; Ponomarenko, 1969; Lubkin & Engel, 2005; Beckemeyer & Engel, 2008; Kirejtshuk *et al.*, 2014). This indicates a *c.* 35–40 Ma-long gap between the supposed origin of Coleoptera and the oldest confirmed fossil of the clade (*Coleopsis archaica*, ~295 Ma; see Table 1 and File S3), which is comparable to the gaps between the estimated origin and oldest fossil of other holometabolan orders (e.g. Hymenoptera, see Ronquist *et al.*, 2012).

The Late Carboniferous to Early Permian origin of all four beetle suborders (Adephaga, Archostemata, Myxophaga and Polyphaga) and the Late Permian origin of several major clades (superfamilies) are the most surprising result of our analysis. If accurate, this suggests that the basic diversity of Coleoptera evolved during the Late Paleozoic, with 8–11 modern lineages surviving the End-Permian Mass Extinction (Fig. 1). Our analysis dates the divergences of most principal polyphagan clades in a rather narrow window in the Late Permian and Early Triassic, around the Palaeozoic–Mesozoic boundary. These results stand in contrast to the current understanding of the Permian–Triassic fossil record of Coleoptera, in which the oldest definite representatives of all four modern suborders date to Early Triassic or earliest Middle Triassic (Ponomarenko, 1969, 1977, 1992; Lawrence, 1999; Chatzimanolis *et al.*, 2012; Grebennikov & Newton, 2012; Tan *et al.*, 2012; Lawrence & Ślipiński, 2013; Prokin *et al.*, 2013a, 2013b).

The crown ages of the superfamilies as well as origins of families pre-date the first fossils known for these groups, and our estimates at this level differ from those of MCK15, in which origins of many clades were younger than known fossils of the respective clade. For example, the crown age of Hydrophiloidea s.s. in MCK15 was estimated as 124 Ma (CI: 88–155 Ma) and the divergence of modern hydrophiloid families was dated to *c.* 100 Ma (CI not provided). However, the oldest fossils of the modern hydrophiloid families Helophoridae, Spercheidae and Hydrophilidae are already known from the Late Jurassic (*c.* 145–155 Ma; Prokin, 2009; Fikáček *et al.*, 2012a, 2012b, 2014). Increased congruence between estimates of family-level divergence times in our analysis and the fossil record were expected, as we mainly used fossils reliably assigned to the deeper nodes of modern clades (subfamilies, tribes, genera) to calibrate the divergence dates at family/subfamily levels. Consequently, we also estimate a much older origin for the largest beetle families (e.g. Staphylinidae: Late Triassic; Tenebrionidae: Early Jurassic) including the phytophagous groups (Middle Triassic origin of stem chrysomeloids and curculionoids, and Late Triassic origin of Chrysomelidae and Mid–Late Jurassic origins of Curculionidae and Cerambycidae). These results are largely congruent with the time tree analyses of phytophagous clades by Wang *et al.* (2014) based on a recently discovered fossil prionine beetle, and of Tenebrionidae by Kergoat *et al.* (2014) based on combination of fossil and geological calibrations.

Reliability of divergence time estimates and analytical considerations

The exercise of this paper was to provide an alternative temporal framework of beetle evolution given the MCK15 topology by comparing the fossil set of MCK15 with a new and more comprehensive one. To do so, we replicated the analyses of MCK15 using two sets of fossils. However, we want to emphasise that we do not believe some of the parameter settings used in MCK15 (and therefore in this study) are the most appropriate considering the latest developments in molecular dating (some of which were not available at the time of MCK15). For instance, recent studies have shown that the effect of clock partitioning on estimates of evolutionary rates and timescales can be important in empirical datasets (e.g. Duchêne & Ho, 2014). Some methods have been introduced to take into account this issue, by identifying the best clock partitioning strategy in a Bayesian framework (Duchêne *et al.*, 2014). Likewise, the choice of fossil calibration prior densities should be examined in a comparative framework (Ho & Phillips, 2009). At a minimum, it is recommended to conduct comparative approaches using different prior densities to understand their impact on posterior age estimates, in particular when maximum ages are not easy to justify (Toussaint & Condamine, 2016). The fit of different parameter settings to empirical datasets can be tested by comparing the marginal likelihoods of different analyses using statistical tests (e.g. Bayes Factors; Kass & Raftery, 1995). The latest developments of dating programs such as BEAST (Drummond *et al.*, 2012) incorporate means to estimate these marginal likelihoods in a more sensitive and sound way than before (Baele *et al.*, 2012), thereby improving the robustness of the statistical framework in which comparative dating analyses are conducted.

Supporting Information

Additional Supporting Information may be found in the online version of this article under the DOI reference: 10.1111/syen.12198

File S1. BEAST chronogram derived from the replicated analysis of MCK15. Divergence time estimates recovered from the BEAST analysis conducted with the same set of fossil calibrations used in MCK15 and the same node constraints as described in MCK15 (the topology was unfixed). This analysis replicated that performed in MCK15 with 300 million generations, a sampling every 3000 cycles and a burn-in of 50%. The posterior median age in million years is given at each node of the topology.

File S2. BEAST chronogram derived from the analysis with the set of calibration of MCK15 but a fixed topology. Divergence time estimates recovered from the BEAST analysis conducted with the same set of fossil calibrations used in MCK15 but with the final BEAST topology of MCK15 as a fixed input (all parameters allowing topology changes were unchecked in BEAUti. This analysis was performed with 300 million generations, a sampling every 3000 cycles and a burn-in of 50%. The posterior median age in million years is given at each node of the topology.

File S3. Detailed information of fossil calibrations and justification after Parham *et al.* (2012) criteria.

File S4. BEAUti .xml file used for the new analysis based on the set of 34 beetle fossils.

File S5. Maximum Clade Credibility Tree of Toussaint *et al.* fully annotated.

Acknowledgements

We want to thank Shaun Winterton as well as three anonymous reviewers for helpful comments on an earlier version of this paper. We thank Duane McKenna for sending us the original dataset and chronogram published in *Systematic Entomology* (MCK15). We also want to thank Petr Švácha and Steve Davis for discussions on chrysomeloid and curculionoid fossils and latest opinions about the phylogenies of these clades, Rafał Ruta for discussions concerning the fossil record of the Scirtoidea, Alexey Solodovnikov for advice concerning the current views of the phylogeny of the Staphylinoidea, Zbyněk Kejval for comments on fossil Anthicidae, and Alexander Prokin for providing many relevant literature and discussions on fossils from the Russian deposits. This work was supported in part by NSF-DEB grant #1453452 to AEZS, the European Union's Horizon 2020 research and innovation programme under the Marie Skłodowska-Curie grant agreement No. 542241 to MS and EAV, the Ministry of Culture of the Czech Republic (DKRVO 2016/14, National Museum, 00023272) to MF, JH and LS, and the institutional support from resources of the Ministry of Education, Youth and Sports of the Czech Republic to DK. The work of MS and EAV at the Department of Zoology, Charles University in Prague was partly supported by grant SVV 260 313/2016.

References

Ahrens, D., Schwarzer, J. & Vogler, A.P. (2014) The evolution of scarab beetles tracks the sequential rise of angiosperms and mammals. *Proceedings of the Royal Society of London B: Biological Sciences*, **281**, 20141470.

Baele, G., Lemey, P., Bedford, T., Rambaut, A., Suchard, M.A. & Alekseyenko, A.V. (2012) Improving the accuracy of demographic and molecular clock model comparison while accommodating phylogenetic uncertainty. *Molecular Biology and Evolution*, **29**, 2157–2167.

Bai, M., Beutel, R.G., Liu, W.G. *et al.* (2014) Description of a new species of Glaresidae (Coleoptera: Scarabaeoidea) from the Jehol Biota of China with a geometric morphometric evaluation. *Arthropod Systematics & Phylogeny*, **72**, 223–236.

Batelka, J., Collomb, F.M. & Nel, A. (2006) *Macrosiagon deuvei* n. sp. (Coleoptera: Ripiphoridae) from the French Eocene amber. *Annales de la Société Entomologique de France*, **42**, 75–78.

Beaulieu, J.M., O'Meara, B.C., Crane, P. & Donoghue, M.J. (2015) Heterogeneous rates of molecular evolution and diversification could explain the Triassic age estimate for angiosperms. *Systematic Biology*, **64**, 869–878.

Beckemeyer, R.J. & Engel, M.S. (2008) A second specimen of *Permocoleus* (Coleoptera) from the lower Permian Wellington formation of noble County, Oklahoma. *Journal of the Kansas Entomological Society*, **81**, 4–7.

Bell, C.D., Soltis, D.E. & Soltis, P.S. (2010) The age and diversification of the angiosperms re-revisited. *American Journal of Botany*, **97**, 1296–1303.

Bloom, D.D., Fikáček, M. & Short, A.E. (2014) Clade age and diversification rate variation explain disparity in species richness among water scavenger beetle (Hydrophilidae) lineages. *PLoS One*, **9**, e98430.

Bocák, L., Kundrata, R., Fernández, C.A. & Vogler, A.P. (2016) The discovery of Iberobaeniidae (Coleoptera: Elateroidea): a new family of beetles from Spain, with immatures detected by environmental DNA sequencing. *Proceedings of the Royal Society of London Series B: Biological Sciences*, **283**, 20152350.

Boucher, S., Bai, M., Wang, B., Zhang, W. & Yang, X. (2016) †Passalopalpidae, a new family from the Cretaceous Burmese amber, as the possible sister group of Passalidae Leach (Coleoptera: Scarabaeoidea). *Cretaceous Research*, **64**, 67–78.

Cai, C.Y., Lawrence, J.F., Ślipiński, A. & Huang, D. (2014a) First fossil tooth-necked fungus beetle (Coleoptera: Derodontidae): *Juropeltastica sinica* gen. n. sp. n. from the Middle Jurassic of China. *European Journal of Entomology*, **111**, 299.

Cai, C.Y., Thayer, M.K., Engel, M.S. *et al.* (2014b) Early origin of parental care in Mesozoic carrion beetles. *Proceedings of the National Academy of Sciences*, **111**, 14 170–14 174.

Cai, C.Y., Ślipiński, A. & Huang, D. (2015a) First false jewel beetle (Coleoptera: Schizopodidae) from the Lower Cretaceous of China. *Cretaceous Research*, **52**, 490–494.

Cai, C.Y., Lawrence, J.F., Ślipiński, A. & Huang, D.Y. (2015b) Jurassic artematopodid beetles and their implications for the early evolution of Artematopodidae (Coleoptera). *Systematic Entomology*, **40**, 779–788.

Cai, C.Y., Ślipiński, A. & Huang, D.Y. (2015c) The oldest root-eating beetle from the Middle Jurassic of China (Coleoptera, Monotomidae). *Alcheringa: An Australasian Journal of Palaeontology*, **39**, 488–493.

Cassola, F. & Werner, K. (2004) A fossil tiger beetle specimen from the Brazilian Mesozoic: *Oxycheilopsis cretacicus* n. gen., n. sp. *Mitteilungen der Münchener Entomologischen Gesellschaft*, **94**, 75–81.

Chatzimanolis, S., Grimaldi, D.A., Engel, M.S. & Fraser, N.C. (2012) *Leehermania prorova*, the earliest staphyliniform beetle, from the Late Triassic of Virginia (Coleoptera: Staphylinidae). *American Museum Novitates*, **3761**, 1–28.

Clarke, J.T., Warnock, R. & Donoghue, P.C. (2011) Establishing a time-scale for plant evolution. *New Phytologist*, **192**, 266–301.

Crowson, R.A. (1962) Observations on the beetle family Cupedidae, with descriptions of two new fossil forms and a key to the recent genera. *Journal of Natural History*, **5**, 147–157.

Drummond, A.J., Suchard, M.A., Xie, D. & Rambaut, A. (2012) Bayesian phylogenetics with BEAUti and the BEAST 1.7. *Molecular Biology and Evolution*, **29**, 1969–1973.

Duchêne, S. & Ho, S.Y. (2014) Using multiple relaxed-clock models to estimate evolutionary timescales from DNA sequence data. *Molecular Phylogenetics and Evolution*, **77**, 65–70.

Duchêne, S., Molak, M. & Ho, S.Y. (2014) ClockstaR: choosing the number of relaxed-clock models in molecular phylogenetic analysis. *Bioinformatics*, **30**, 1017–1019.

Engel, M.S. & Grimaldi, D.A. (2008) A jugular-horned beetle in Cretaceous amber from Myanmar (Coleoptera: Prostomidae). *Alavesia*, **2**, 215–218.

Falin, Z.H. & Engel, M.S. (2010) Notes on Cretaceous Ripidiini and revised diagnoses of the Ripidiinae, Ripidiini, and Eorhipidiini (Coleoptera: Ripiphoridae). *Alavesia*, **3**, 35–42.

Fikáček, M., Prokin, A., Angus, R.B., Ponomarenko, A., Yue, Y., Ren, D. & Prokop, J. (2012a) Revision of Mesozoic fossils of the helophorid lineage of the superfamily Hydrophiloidea (Coleoptera: Polyphaga). *Acta Entomologica Musei Nationalis Pragae*, **52**, 89–127.

Fikáček, M., Prokin, A., Angus, R.B., Ponomarenko, A., Yue, Y., Ren, D. & Prokop, J. (2012b) Phylogeny and the fossil record of the Helophoridae reveal Jurassic origin of extant hydrophiloid lineages (Coleoptera: Polyphaga). *Systematic Entomology*, **37**, 420–447.

Fikáček, M., Prokin, A., Yan, E., Yue, Y., Wang, B., Ren, D. & Beattie, R. (2014) Modern hydrophilid clades present and widespread in the Late Jurassic and Early Cretaceous (Coleoptera: Hydrophiloidea: Hydrophilidae). *Zoological Journal of the Linnean Society*, **170**, 710–734.

Friis, E.M., Crane, P.R. & Pedersen, K.R. (2011) *Early Flowers and Angiosperm Evolution*. Cambridge University Press, Cambridge.

Ge, S.Q., Friedrich, F. & Beutel, R.G. (2010) On the systematic position and taxonomic rank of the extinct myxophagan †*Haplochelus* (Coleoptera). *Insect Systematics & Evolution*, **41**, 329–338.

Grebennikov, V.V. & Newton, A.F. (2012) Detecting the basal dichotomies in the monophylum of carrion and rove beetles (Insecta: Coleoptera: Silphidae and Staphylinidae) with emphasis on the Oxyteline group of subfamilies. *Arthropod Systematics & Phylogeny*, **70**, 133–165.

Grimaldi, D. & Engel, M.S. (2005) *Evolution of the Insects*. Cambridge University Press, Cambridge, New York, Melbourne, Madrid, Cape Town, Singapore, Sao Paulo.

Gunter, N.L., Weir, T.A., Ślipiński, A., Bocák, L. & Cameron, S.L. (2016) If dung beetles (Scarabaeidae: Scarabaeinae) arose in association with dinosaurs, did they also suffer a mass co-extinction at the K-Pg boundary? *PLoS One*, **11**, e0153570.

Ho, S.Y. & Phillips, M.J. (2009) Accounting for calibration uncertainty in phylogenetic estimation of evolutionary divergence times. *Systematic Biology*, **58**, 367–380.

Hunt, T., Bergsten, J., Levkanicova, Z. *et al.* (2007) A comprehensive phylogeny of beetles reveals the evolutionary origins of a superradiation. *Science*, **318**, 1913–1916.

Jin, Z., Ślipiński, A., Pang, H. & Ren, D. (2013) A new Mesozoic species of soft-bodied plant beetle (Coleoptera: Dascillidae) from the Early Cretaceous of Inner Mongolia, China with a review of fossil Dascillidae. *Annales Zoologici*, **63**, 501–509.

Kass, R.E. & Raftery, A.E. (1995) Bayes factors. *Journal of the American Statistical Association*, **90**, 773–795.

Kergoat, G.J., Bouchard, P., Clamens, A.L. *et al.* (2014) Cretaceous environmental changes led to high extinction rates in a hyperdiverse beetle family. *BMC Evolutionary Biology*, **14**, 220.

Kim, S.I. & Farrell, B.D. (2015) Phylogeny of world stag beetles (Coleoptera: Lucanidae) reveals a Gondwanan origin of Darwin's stag beetle. *Molecular Phylogenetics and Evolution*, **86**, 35–48.

Kirejtshuk, A.G. & Nel, A. (2012) The oldest representatives of the family Coccinellidae (Coleoptera: Polyphaga) from the lowermost Eocene Oise amber (France). *Zoosystematica Rossica*, **21**, 131–144.

Kirejtshuk, A.G. & Poinar, G. (2006) Haplochelidae, a new family of Cretaceous beetles (Coleoptera: Myxophaga) from Burmese amber. *Proceedings of the Entomological Society of Washington*, **108**, 155–164.

Kirejtshuk, A.G., Azar, D., Tafforeau, P., Boistel, R. & Fernandez, V. (2009a) New beetles of Polyphaga (Coleoptera, Polyphaga) from Lower Cretaceous Lebanese amber. *Denisia*, **26**, 119–130.

Kirejtshuk, A.G., Azar, D., Beaver, R.A., Mandelshtam, M.Y. & Nel, A. (2009b) The most ancient bark beetle known: a new tribe, genus and species from Lebanese amber (Coleoptera, Curculionidae, Scolytinae). *Systematic Entomology*, **34**, 101–112.

Kirejtshuk, A.G., Nabozhenko, M.V. & Nel, A. (2012) First mesozoic representative of the subfamily tenebrioninae (Coleoptera, Tenebrionidae) from the lower cretaceous of Yixian (China, Liaoning). *Entomological review*, **92**, 97–100.

Kirejtshuk, A.G., Poschmann, M., Prokop, J., Garrouste, R. & Nel, A. (2014) Evolution of the elytral venation and structural adaptations in the oldest Palaeozoic beetles (Insecta: Coleoptera: Tshekardocoleidae). *Journal of Systematic Palaeontology*, **12**, 575–600.

Kukalová, J. (1969) On the systematic position of the supposed Permian beetles, Tshecardocoleidae, with a description of a new collection from Moravia. *Sborník Geologických Věd, Řada P Paleontologie*, **11**, 139–162.

Lawrence, J.F. (1999) The Australian Ommatidae (Coleoptera: Archostemata): new species, larva and discussion of relationships. *Invertebrate Systematics*, **13**, 369–390.

Lawrence, J.F. & Ślipiński, S.A. (2013) *Australian Beetles*. CSIRO Publishing, Collingwood, Victoria.

Legalov, A.A. (2013) Review of the family Anthribidae (Coleoptera) from the Jurassic of Karatau: subfamily Protoscelinae. Genus *Protoscelis* Medvedev. *Paleontological Journal*, **47**, 292–302.

Liu, M., Lu, W. & Ren, D. (2007) A new fossil mordellid (Coleoptera: Tenebrionoidea: Mordellidae) from the Yixian Formation of western Liaoning province, China. *Zootaxa*, **1415**, 49–56.

Liu, Z., Ślipiński, A., Leschen, R.A., Ren, D. & Pang, H. (2015) The oldest Prionoceridae (Coleoptera: Cleroidea) from the Middle Jurassic of China. *Annales Zoologici*, **65**, 41–52.

Lubkin, S.H. & Engel, M.S. (2005) *Permocoleus*, new genus, the first Permian beetle (Coleoptera) from North America. *Annals of the Entomological Society of America*, **98**, 73–76.

McKenna, D.D. & Farrell, B.D. (2009) Beetles (Coleoptera). *The Timetree of Life* (ed. by S.B. Hedges and S. Kumar), pp. 278–289. Oxford University Press, Oxford.

McKenna, D.D., Sequeira, A.S., Marvaldi, A.E. & Farrell, B.D. (2009) Temporal lags and overlap in the diversification of weevils and flowering plants. *Proceedings of the National Academy of Sciences of the United States of America*, **106**, 7083–7088.

McKenna, D.D., Wild, A.L., Kanda, K. *et al.* (2015) The beetle tree of life reveals that Coleoptera survived end-Permian mass extinction to diversify during the Cretaceous terrestrial revolution. *Systematic Entomology*, **40**, 835–880.

Misof, B., Liu, S., Meusemann, K. *et al.* (2014) Phylogenomics resolves the timing and pattern of insect evolution. *Science*, **346**, 763–767.

Nikolajev, G.V. & Ren, D. (2010) The oldest fossil Ochodaeidae (Coleoptera: Scarabaeoidea) from the Middle Jurassic of China. *Zootaxa*, **2553**, 65–68.

Nikolajev, G.V. & Ren, D. (2011) The oldest species of the genus *Glaphyrus* Latr. (Coleoptera: Scarabaeoidea: Glaphyridae) from the Mesozoic of China. *Paleontological Journal*, **45**, 179–182.

Pan, X., Chang, H., Ren, D. & Shih, C. (2011) The first fossil buprestids from the Middle Jurassic Jiulongshan Formation of China (Coleoptera: Buprestidae). *Zootaxa*, **2745**, 53–62.

Parham, J.F., Donoghue, P.C., Bell, C.J. *et al.* (2012) Best practices for justifying fossil calibrations. *Systematic Biology*, **61**, 346–359.

Peris, D., Delclós, X., Soriano, C. & Perrichot, V. (2014) The earliest occurrence and remarkable stasis of the family Bostrichidae (Coleoptera: Polyphaga) in Cretaceous Charentes amber. *Palaeontologica Electronica*, **17**, 1–8. Available at: palaeo-electronica.org/content/2014/706-new-cretaceous-auger-beetle.

Peris, D., Maier, C.A., Sánchez-García, A. & Delclòs, X. (2015a) The oldest known riffle beetle (Coleoptera: Elmidae) from Early Cretaceous Spanish amber. *Comptes Rendus Palevol*, **14**, 181–186.

Peris, D., Philips, T.K. & Delclòs, X. (2015b) Ptinid beetles from the Cretaceous gymnosperm-dominated forests. *Cretaceous Research*, **52**, 440–452.

Perrichot, V., Nel, A. & Néraudeau, D. (2004) Two new wedge-shaped beetles in Albo-Cenomanian ambers of France (Coleoptera: Ripiphoridae: Ripiphorinae). *European Journal of Entomology*, **101**, 583–589.

Poinar, G. (2005) A Cretaceous palm bruchid, *Mesopachymerus antiqua*, n. gen., n. sp. (Coleoptera: Bruchidae: Pachymerini) and biogeographical implications. *Proceedings of the Entomological Society of Washington*, **107**, 392–397.

Ponomarenko, A.G. (1969) Historical development of the Coleoptera-Archostemata. *Trudy Paleontologichcskogo Instituto*, **125**, 1–240 (in Russian).

Ponomarenko, A.G. (1977) [suborder Adephaga]. *Mesozoic Coleoptera*, *Proceedings of the Paleontological Institute of Academy of Sciences of the USSR*, Vol. **161** (ed. by L.V. Arnoldi, V.V. Zherikhin, L.M. Nikritin and A.G. Ponomarenko), pp. 17–104. Nauka, Moscow (in Russian).

Ponomarenko, A.G. (1992) Upper Liassic beetles (Coleoptera) from Lower Saxony, Germany. *Senckenbergiana Lethaeal*, **72**, 179–188.

Prokin, A.A. (2009) New water scavenger beetles (Coleoptera: Hydrophilidae) from the Mesozoic of Mongolia. *Paleontological Journal*, **43**, 660–663.

Prokin, A.A. & Ren, D. (2011) New species of variegated mud-loving beetles (Coleoptera: Heteroceridae) from mesozoic deposits of China. *Paleontological Journal*, **45**, 284–286.

Prokin, A.A., Makarov, K.V., Ponomarenko, A.G. & Bashkuev, A.S. (2013a) New beetles larvae (Coleoptera: Coptoclavidae, Carabidae, Polyphaga) from the Upper Triassic of Germany. *Russian Entomological Journal*, **22**, 259–274.

Prokin, A.A., Petrov, P.N., Wang, B. & Ponomarenko, A.G. (2013b) New fossil taxa and notes on the Mesozoic evolution of Liadytidae and Dytiscidae (Coleoptera). *Zootaxa*, **3666**, 137–159.

Ronquist, F., Klopfstein, S., Vilhelmsen, L., Schulmeister, S., Murray, D.L. & Rasnitsyn, A.P. (2012) A total-evidence approach to dating with fossils, applied to the early radiation of the Hymenoptera. *Systematic Biology*, **61**, 973–999.

Shen, S.Z., Crowley, J.L., Wang, Y. *et al.* (2011) Calibrating the end-Permian mass extinction. *Science*, **334**, 1367–1372.

Tan, J., Ren, D. & Shih, C. (2006) First record of fossil *Priacma* (Coleoptera: Archostemata: Cupedidae) from the Jehol Biota of western Liaoning, China. *Zootaxa*, **1326**, 55–68.

Tan, J., Wang, Y., Ren, D. & Yang, X. (2012) New fossil species of ommatids (Coleoptera: Archostemata) from the Middle Mesozoic of China illuminating the phylogeny of Ommatidae. *BMC Evolutionary Biology*, **12**, 1.

Tong, K.J., Duchêne, S., Ho, S.Y. & Lo, N. (2015) Comment on "Phylogenomics resolves the timing and pattern of insect evolution". *Science*, **349**, 487–487.

Toussaint, E.F.A. & Condamine, F.L. (2016) To what extent do new fossil discoveries change our understanding of clade evolution? A cautionary tale from burying beetles (Coleoptera: *Nicrophorus*). *Biological Journal of the Linnean Society*, **117**, 686–704.

Wang, B., Zhang, H. & Jarzembowski, E.A. (2013) Early Cretaceous angiosperms and beetle evolution. *Frontiers in Plant Science*, **4**, 360.

Wang, B., Ma, J., McKenna, D.D., Yan, E.V., Zhang, H. & Jarzembowski, E.A. (2014) The earliest known longhorn beetle (Cerambycidae: Prioninae) and implications for the early evolution of Chrysomeloidea. *Journal of Systematic Palaeontology*, **12**, 565–574.

Yu, Y., Ślipiński, A., Leschen, R.A., Ren, D. & Pang, H. (2015) New genera and species of bark-gnawing beetles (Coleoptera: Trogossitidae) from the Yixian Formation (Lower Cretaceous) of Western Liaoning, China. *Cretaceous Research*, **53**, 89–97.

Zhang, X. & Zhou, H.-Z. (2013) How old are the rove beetles (Insecta: Coleoptera: Staphylinidae) and their lineages? Seeking an answer with DNA. *Zoological Science*, **30**, 490–501.

Accepted 21 June 2016
First published online 15 August 2016

Supplementary material

to the paper

Toussaint, E. A. F., Seidel, M., Arriaga-Varela, E., Hájek, J., Král, D., Sekerka, L., Short, A. E. Z. & Fikáček, M. (2017). The peril of dating beetles. *Systematic Entomology*, 42(1): 1-10.

File S1. BEAST chronogram derived from the replicated analysis of MCK15

Divergence time estimates recovered from the BEAST analysis conducted with the same set of fossil calibrations used in MCK15 and the same node constraints as described in MCK15 (the topology was unfixed). This analysis is an exact replica of the analysis performed in MCK15 with 300 million generations, a sampling every 3000 cycles and a burnin of 50%. The posterior median age in million years is given at each node of the topology.

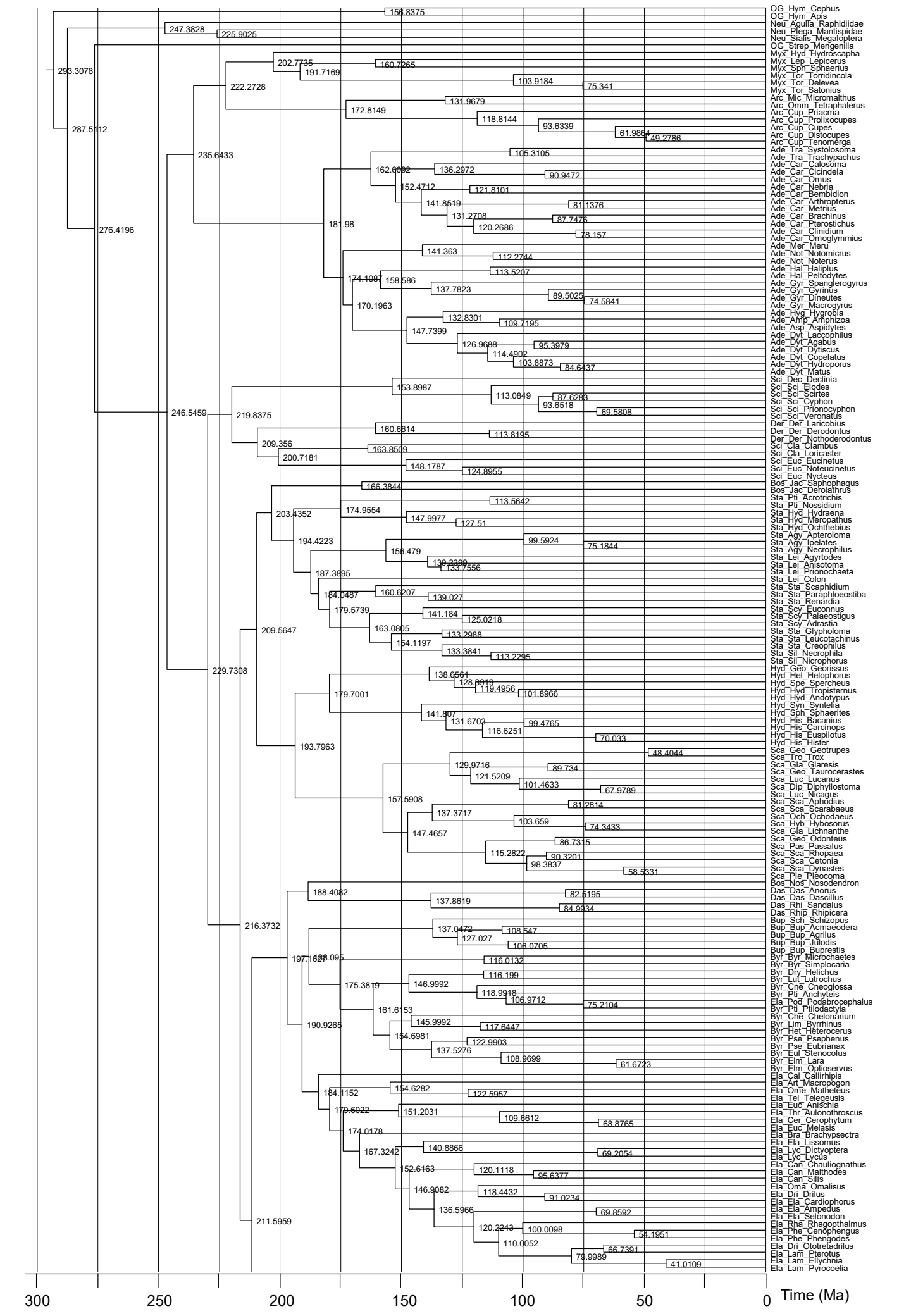
OG_Hym_Cephus
OG_Hym_Apis
Neu_Agulla_Raphidiidae
Neu_Plega_Mantispidae
Neu_Sialis_Megaloptera
OG_Strep_Mengenilla
Myx_Hyd_Hydroscapha
Myx_Lep_Lepicerus
Myx_Sph_Sphaerius
Myx_Tor_Torridincola
Myx_Tor_Delevea
Myx_Tor_Satonius
Arc_Mic_Micromalthus
Arc_Omm_Tetraphalerus
Arc_Cup_Priacma
Arc_Cup_Prolixocupes
Arc_Cup_Cupes
Arc_Cup_Distocupes
Arc_Cup_Tenomerga
Ade_Tra_Systolosoma
Ade_Tra_Trachypachus
Ade_Car_Calosoma
Ade_Car_Cicindela
Ade_Car_Omus
Ade_Car_Nebria
Ade_Car_Bembidion
Ade_Car_Arthropterus
Ade_Car_Metrius
Ade_Car_Brachinus
Ade_Car_Pterostichus
Ade_Car_Clinidium
Ade_Car_Omoglymmius
Ade_Mer_Meru
Ade_Not_Notomicrus
Ade_Not_Noterus
Ade_Hal_Haliplus
Ade_Hal_Peltodytes
Ade_Gyr_Spanglerogyrus
Ade_Gyr_Gyrinus
Ade_Gyr_Dineutes
Ade_Gyr_Macrogyrus
Ade_Hyg_Hygrobia
Ade_Amp_Amphizoa
Ade_Asp_Aspidytes
Ade_Dyt_Laccophilus
Ade_Dyt_Agabus
Ade_Dyt_Dytiscus
Ade_Dyt_Copelatus
Ade_Dyt_Hydroporus
Ade_Dyt_Matus
Sci_Dec_Declinia
Sci_Sci_Elodes
Sci_Sci_Scirtes
Sci_Sci_Cyphon
Sci_Sci_Prionocyphon
Sci_Sci_Veronatus
Der_Der_Laricobius
Der_Der_Derodontus
Der_Der_Nothoderodontus
Sci_Cla_Clambus
Sci_Cla_Loricaster
Sci_Euc_Eucinetus
Sci_Euc_Noteucinetus
Sci_Euc_Nycteus
Bos_Jac_Saphophagus
Bos_Jac_Derolathrus
Sta_Pti_Acrotrichis
Sta_Pti_Nossidium
Sta_Hyd_Hydraena
Sta_Hyd_Meropathus
Sta_Hyd_Ochthebius
Sta_Agy_Apteroloma
Sta_Agy_Ipelates
Sta_Agy_Necrophilus
Sta_Lei_Agyrtodes
Sta_Lei_Anisotoma
Sta_Lei_Prionochaeta
Sta_Lei_Colon
Sta_Sta_Scaphidium
Sta_Sta_Paraphloeostiba
Sta_Sta_Renardia
Sta_Scy_Euconnus
Sta_Scy_Palaeostigus
Sta_Scy_Adrastia
Sta_Sta_Glypholoma
Sta_Sta_Leucotachinus
Sta_Sta_Creophilus
Sta_Sil_Necrophila
Sta_Sil_Nicrophorus
Hyd_Geo_Georissus
Hyd_Hel_Helophorus
Hyd_Spe_Spercheus
Hyd_Hyd_Tropisternus
Hyd_Hyd_Andotypus
Hyd_Syn_Syntelia
Hyd_Sph_Sphaerites
Hyd_His_Bacanius
Hyd_His_Carcinops
Hyd_His_Euspilotus
Hyd_His_Hister
Sca_Geo_Geotrupes
Sca_Tro_Trox
Sca_Gla_Glaresis
Sca_Geo_Taurocerastes
Sca_Luc_Lucanus
Sca_Dip_Diphyllostoma
Sca_Luc_Nicagus
Sca_Sca_Aphodius
Sca_Sca_Scarabaeus
Sca_Och_Ochodaeus
Sca_Hyb_Hybosorus
Sca_Gla_Lichnanthe
Sca_Geo_Odonteus
Sca_Pas_Passalus
Sca_Sca_Rhopaea
Sca_Sca_Cetonia
Sca_Sca_Dynastes
Sca_Ple_Pleocoma
Bos_Nos_Nosodendron
Das_Das_Anorus
Das_Das_Dascillus
Das_Rhi_Sandalus
Das_Rhip_Rhipicera
Bup_Sch_Schizopus
Bup_Bup_Acmaeodera
Bup_Bup_Agrilus
Bup_Bup_Julodis
Bup_Bup_Buprestis
Byr_Byr_Microchaetes
Byr_Byr_Simplocaria
Byr_Dry_Helichus
Byr_Lut_Lutrochus
Byr_Cne_Cneoglossa
Byr_Pti_Anchyteis
Ela_Pod_Podabrocephalus
Byr_Pti_Ptilodactyla
Byr_Che_Chelonarium
Byr_Lim_Byrrhinus
Byr_Het_Heterocerus
Byr_Pse_Psephenus
Byr_Pse_Eubrianax
Byr_Eul_Stenocolus
Byr_Elm_Lara
Byr_Elm_Optioservus
Ela_Cal_Callirhipis
Ela_Art_Macropogon
Ela_Ome_Matheteus
Ela_Tel_Telegeusis
Ela_Euc_Anischia
Ela_Thr_Aulonothroscus
Ela_Cer_Cerophytum
Ela_Euc_Melasis
Ela_Bra_Brachypsectra
Ela_Ela_Lissomus
Ela_Lyc_Dictyoptera
Ela_Lyc_Lycus
Ela_Can_Chauliognathus
Ela_Can_Malthodes
Ela_Can_Silis
Ela_Oma_Omalisus
Ela_Dri_Drilus
Ela_Ela_Cardiophorus
Ela_Ela_Ampedus
Ela_Ela_Selonodon
Ela_Rha_Rhagopthalmus
Ela_Phe_Cenophengus
Ela_Phe_Phengodes
Ela_Dri_Ototretadrilus
Ela_Lam_Pterotus
Ela_Lam_Ellychnia
Ela_Lam_Pyrocoelia
156.8375
247.3828
225.9025
293.3078
202.7735
160.7265
191.7169
103.9184
75.341
222.2728
131.9679
172.8149
118.8144
93.6339
61.9864
49.2786
287.5112
105.3105
235.6433
162.6092
136.2972
90.9472
152.4712
121.8101
141.8519
81.1376
131.2708
87.7476
120.2686
78.157
181.98
276.4196
141.363
112.2744
113.5207
174.1087
158.586
137.7823
89.5025
74.5841
170.1963
132.8301
109.7195
147.7399
126.9688
95.3979
114.4902
103.8873
84.6437
153.8987
113.0849
87.6283
93.6518
69.5808
246.5459
219.8375
160.6614
113.8195
209.356
163.8509
200.7181
148.1787
124.8955
166.3844
113.5642
203.4352
174.9554
147.9977
127.51
99.5924
194.4223
75.1844
156.479
139.2399
133.7556
187.3895
184.0487
160.6207
139.027
179.5739
141.184
125.0218
209.5647
163.0805
133.2988
154.1197
133.3841
113.2295
229.7308
138.6561
128.8919
119.4956
101.8966
179.7001
141.807
131.6703
99.4765
116.6251
70.033
193.7963
48.4044
129.9716
89.734
121.5209
101.4633
67.9789
157.5908
81.2614
137.3717
103.659
74.3433
147.4657
86.7315
115.2822
90.3201
98.3837
58.5331
188.4082
82.5195
137.8619
84.9934
216.3732
137.0472
108.547
127.027
106.0705
197.1627
188.095
116.0132
116.199
175.3819
146.9992
118.9918
106.9712
75.2104
161.6153
190.9265
145.9992
117.6447
154.6981
122.9903
137.5276
108.9699
61.6723
154.6282
184.1152
122.5957
179.6022
151.2031
109.6612
68.8765
174.0178
167.3242
140.8866
69.2054
152.6163
120.1118
95.6377
146.9082
118.4432
91.0234
136.5966
69.8592
211.5959
120.2243
100.0098
54.1951
110.0052
66.7391
79.9989
41.0109
300
250
200
150
100
50
0
Time (Ma)

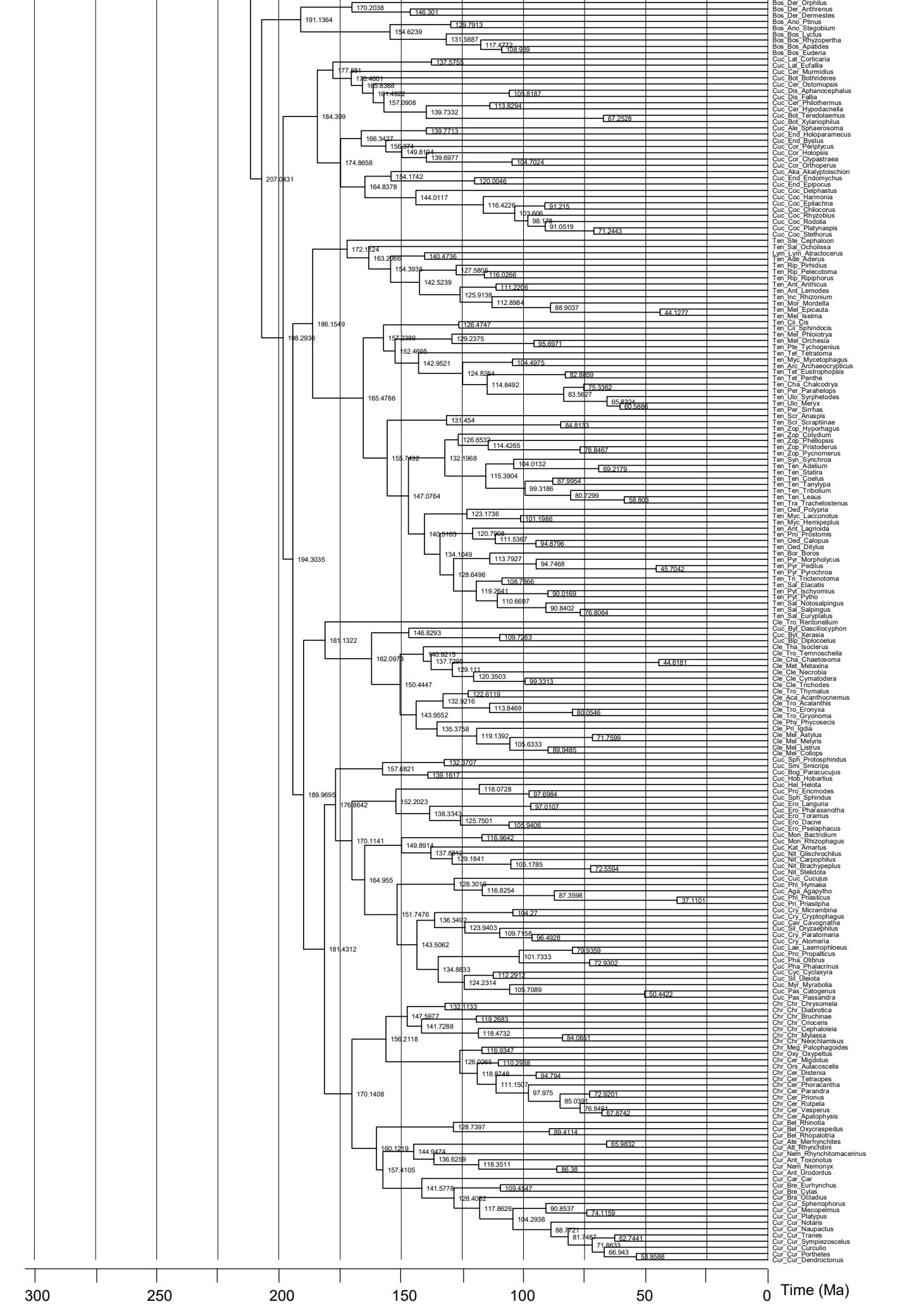
Bos_Der_Orphilus
Bos_Der_Anthrenus
Bos_Der_Dermestes
Bos_Ano_Ptinus
Bos_Ano_Stegobium
Bos_Bos_Lyctus
Bos_Bos_Rhyzopertha
Bos_Bos_Apatides
Bos_Bos_Euderia
Cuc_Lat_Corticaria
Cuc_Lat_Eufallia
Cuc_Cer_Murmidius
Cuc_Bot_Bothrideres
Cuc_Cer_Ostomopsis
Cuc_Dis_Aphanocephalus
Cuc_Dis_Fallia
Cuc_Cer_Philothermus
Cuc_Cer_Hypodacnella
Cuc_Bot_Teredolaemus
Cuc_Bot_Xylariophilus
Cuc_Ale_Sphaerosoma
Cuc_End_Holoparamecus
Cuc_End_Bystus
Cuc_Cor_Periptycus
Cuc_Cor_Holopsis
Cuc_Cor_Clypastraea
Cuc_Cor_Orthoperus
Cuc_Aka_Akalyptoischion
Cuc_End_Endomychus
Cuc_End_Epipocus
Cuc_Coc_Delphastus
Cuc_Coc_Harmonia
Cuc_Coc_Epilachna
Cuc_Coc_Chilocorus
Cuc_Coc_Rhyzobius
Cuc_Coc_Rodolia
Cuc_Coc_Platynaspis
Cuc_Coc_Stethorus
Ten_Ste_Cephaloon
Ten_Sal_Ocholissa
Lym_Lym_Atractocerus
Ten_Ade_Aderus
Ten_Rip_Pirhidius
Ten_Rip_Pelecotoma
Ten_Rip_Ripiphorus
Ten_Ant_Anthicus
Ten_Ant_Lemodes
Ten_Inc_Rhizonium
Ten_Mor_Mordella
Ten_Mel_Epicauta
Ten_Mel_Iselma
Ten_Cli_Cis
Ten_Cli_Sphindocis
Ten_Mel_Phlaiotrya
Ten_Mel_Orchesia
Ten_Pte_Tychogenius
Ten_Tet_Tetratoma
Ten_Myc_Mycetophagus
Ten_Arc_Archaeocrypticus
Ten_Tet_Eustrophopsis
Ten_Tet_Penthe
Ten_Cha_Chalcodrya
Ten_Per_Parahelops
Ten_Ulo_Syrphetodes
Ten_Ulo_Meryx
Ten_Per_Sirrhas
Ten_Scr_Anaspis
Ten_Scr_Scraptiinae
Ten_Zop_Hyporhagus
Ten_Zop_Colydium
Ten_Zop_Phellopsis
Ten_Zop_Pristoderus
Ten_Zop_Pycnomerus
Ten_Syn_Synchroa
Ten_Ten_Adelium
Ten_Ten_Statira
Ten_Ten_Coelus
Ten_Ten_Tanylypa
Ten_Ten_Tribolium
Ten_Ten_Leaus
Ten_Tra_Trachelostenus
Ten_Oed_Polypria
Ten_Myc_Lacconotus
Ten_Myc_Hemipeplus
Ten_Ant_Lagrioida
Ten_Pro_Prostomis
Ten_Oed_Calopus
Ten_Oed_Dityllus
Ten_Bor_Boros
Ten_Pyr_Morpholycus
Ten_Pyr_Pedilus
Ten_Pyr_Pyrochroa
Ten_Tri_Trictenotoma
Ten_Sal_Elacatis
Ten_Pyt_Ischyomius
Ten_Pyt_Pytho
Ten_Sal_Notosalpingus
Ten_Sal_Salpingus
Ten_Sal_Eurysplatus
Cle_Tro_Rentonellum
Cuc_Byt_Dascillocyphon
Cuc_Byt_Xerasia
Cuc_Bip_Diplocoelus
Cle_Tha_Isoclerus
Cle_Tro_Temnoscheila
Cle_Cha_Chaetosoma
Cle_Met_Metaxina
Cle_Cle_Necrobia
Cle_Cle_Cymatodera
Cle_Cle_Trichodes
Cle_Tro_Thymalus
Cle_Aca_Acanthocnemus
Cle_Tro_Acalanthis
Cle_Tro_Eronyxa
Cle_Tro_Gryonoma
Cle_Phy_Phycosecis
Cle_Pri_Igdia
Cle_Mel_Astylus
Cle_Mel_Melyris
Cle_Mel_Listrus
Cle_Mel_Collops
Cuc_Sph_Protosphindus
Cuc_Smi_Smicrips
Cuc_Bog_Paracucujus
Cuc_Hob_Hobartius
Cuc_Hel_Helota
Cuc_Pro_Ericmodes
Cuc_Sph_Sphindus
Cuc_Ero_Languria
Cuc_Ero_Pharaxanotha
Cuc_Ero_Toramus
Cuc_Ero_Dacne
Cuc_Ero_Pselaphacus
Cuc_Mon_Bactridium
Cuc_Mon_Rhizophagus
Cuc_Kat_Amartus
Cuc_Nit_Glischrochilus
Cuc_Nit_Carpophilus
Cuc_Nit_Brachypeplus
Cuc_Nit_Stelidota
Cuc_Cuc_Cucujus
Cuc_Phl_Hymaea
Cuc_Aga_Agapytho
Cuc_Phl_Priasticus
Cuc_Pri_Priasilpha
Cuc_Cry_Micrambina
Cuc_Cry_Cryptophagus
Cuc_Cav_Cavognatha
Cuc_Sil_Oryzaephilus
Cuc_Cry_Paratomaria
Cuc_Cry_Atomaria
Cuc_Lae_Laemophloeus
Cuc_Pro_Propalticus
Cuc_Pha_Olibrus
Cuc_Pha_Phalacrinus
Cuc_Cyc_Cyclaxyra
Cuc_Sil_Uleiota
Cuc_Myr_Myrabolia
Cuc_Pas_Catogenus
Cuc_Pas_Passandra
Chr_Chr_Chrysomela
Chr_Chr_Diabrotica
Chr_Chr_Bruchinae
Chr_Chr_Crioceris
Chr_Chr_Cephaloleia
Chr_Chr_Mylassa
Chr_Chr_Neochlamisus
Chr_Meg_Palophagoides
Chr_Oxy_Oxypeltus
Chr_Cer_Migdolus
Chr_Ors_Aulacoscelis
Chr_Cer_Distenia
Chr_Cer_Tetraopes
Chr_Cer_Phoracantha
Chr_Cer_Parandra
Chr_Cer_Prionus
Chr_Cer_Rutpela
Chr_Cer_Vesperus
Chr_Cer_Apatophysis
Cur_Bel_Rhinotia
Cur_Bel_Oxycraspedus
Cur_Bel_Rhopalotria
Cur_Ate_Merhynchites
Cur_Att_Rhynchitini
Cur_Nem_Rhynchitomacerinus
Cur_Ant_Toxonotus
Cur_Nem_Nemonyx
Cur_Ant_Urodontus
Cur_Car_Car
Cur_Bre_Eurhynchus
Cur_Bre_Cylas
Cur_Bra_Ocladius
Cur_Cur_Sphenophorus
Cur_Cur_Mecopelmus
Cur_Cur_Platypus
Cur_Cur_Notaris
Cur_Cur_Naupactus
Cur_Cur_Tranes
Cur_Cur_Sympiezoscelus
Cur_Cur_Curculio
Cur_Cur_Porthetes
Cur_Cur_Dendroctonus
300
250
200
150
100
50
0
Time (Ma)

File S2. BEAST chronogram derived from the analysis with the set of calibration of MCK15 but a fixed topology

Divergence time estimates recovered from the BEAST analysis conducted with the same set of fossil calibrations used in MCK15 but with the final BEAST topology of MCK15 as a fixed input (all parameters allowing topology changes were unchecked in BEAUti). This analysis was performed with 300 million generations, a sampling every 3000 cycles and a burnin of 50%. The posterior median age in million years is given at each node of the topology.

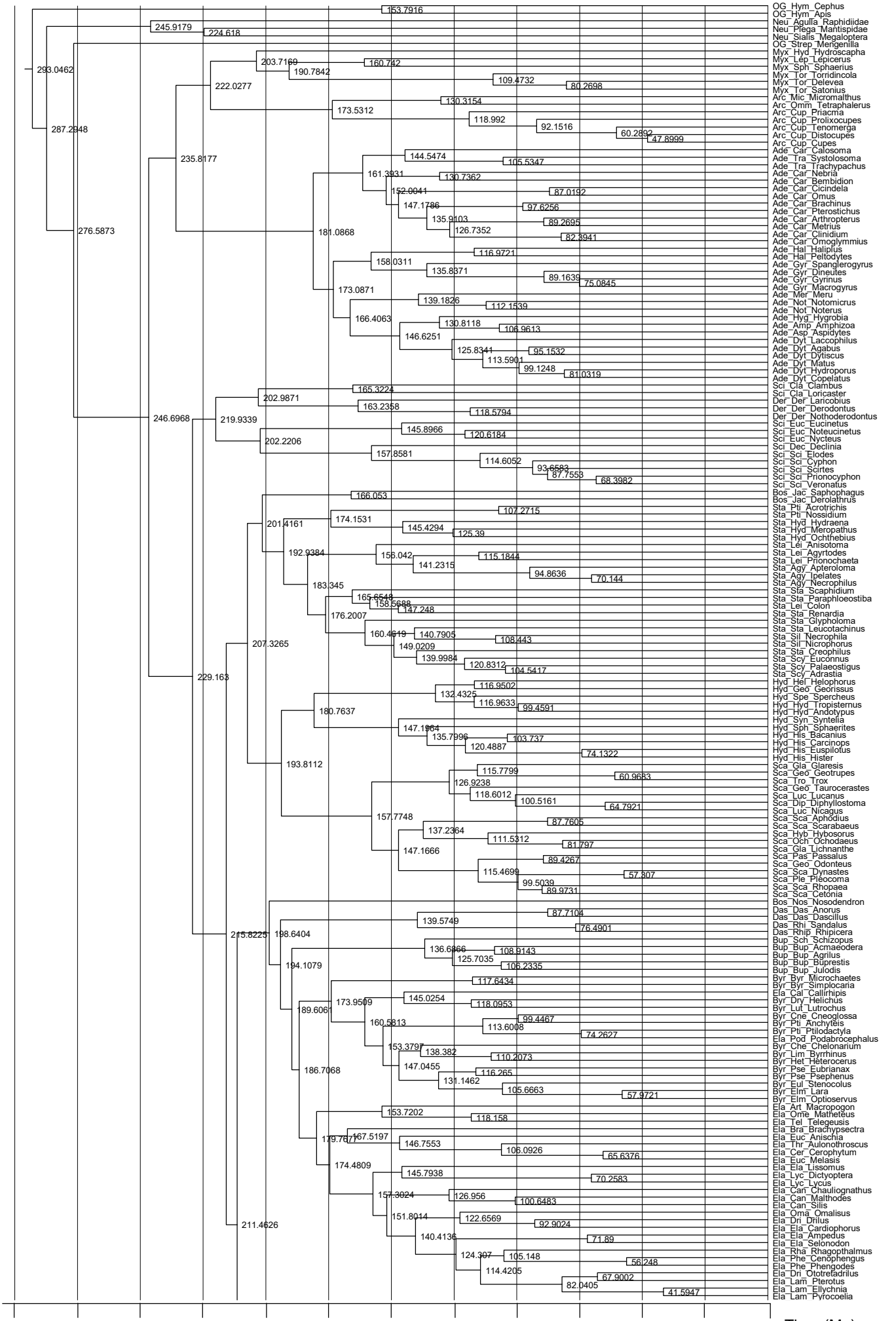
OG_Hym_Cephus
OG_Hym_Apis
Neu_Agulla_Raphidiidae
Neu_Plega_Mantispidae
Neu_Sialis_Megaloptera
OG_Strep_Mengenilla
Myx_Hyd_Hydroscapha
Myx_Lep_Lepicerus
Myx_Sph_Sphaerius
Myx_Tor_Torridincola
Myx_Tor_Delevea
Myx_Tor_Satonius
Arc_Mic_Micromalthus
Arc_Omm_Tetraphalerus
Arc_Cup_Priacma
Arc_Cup_Prolixocupes
Arc_Cup_Tenomerga
Arc_Cup_Distocupes
Arc_Cup_Cupes
Ade_Car_Calosoma
Ade_Tra_Systolosoma
Ade_Tra_Trachypachus
Ade_Car_Nebria
Ade_Car_Bembidion
Ade_Car_Cicindela
Ade_Car_Omus
Ade_Car_Brachinus
Ade_Car_Pterostichus
Ade_Car_Arthropterus
Ade_Car_Metrius
Ade_Car_Clinidium
Ade_Car_Omoglymmius
Ade_Hal_Haliplus
Ade_Hal_Peltodytes
Ade_Gyr_Spanglerogyrus
Ade_Gyr_Dineutes
Ade_Gyr_Gyrinus
Ade_Gyr_Macrogyrus
Ade_Mer_Meru
Ade_Not_Notomicrus
Ade_Not_Noterus
Ade_Hyg_Hygrobia
Ade_Amp_Amphizoa
Ade_Asp_Aspidytes
Ade_Dyt_Laccophilus
Ade_Dyt_Agabus
Ade_Dyt_Dytiscus
Ade_Dyt_Matus
Ade_Dyt_Hydroporus
Ade_Dyt_Copelatus
Sci_Cla_Clambus
Sci_Cla_Loricaster
Der_Der_Laricobius
Der_Der_Derodontus
Der_Der_Nothoderodontus
Sci_Euc_Eucinetus
Sci_Euc_Noteucinetus
Sci_Euc_Nycteus
Sci_Dec_Declinia
Sci_Sci_Elodes
Sci_Sci_Cyphon
Sci_Sci_Scirtes
Sci_Sci_Prionocyphon
Sci_Sci_Veronatus
Bos_Jac_Saphophagus
Bos_Jac_Derolathrus
Sta_Pti_Acrotrichis
Sta_Pti_Nossidium
Sta_Hyd_Hydraena
Sta_Hyd_Meropathus
Sta_Hyd_Ochthebius
Sta_Lei_Anisotoma
Sta_Lei_Agyrtodes
Sta_Lei_Prionochaeta
Sta_Agy_Apteroloma
Sta_Agy_Ipelates
Sta_Agy_Necrophilus
Sta_Sta_Scaphidium
Sta_Sta_Paraphloeostiba
Sta_Lei_Colon
Sta_Sta_Renardia
Sta_Sta_Glypholoma
Sta_Sta_Leucotachinus
Sta_Sil_Necrophila
Sta_Sil_Nicrophorus
Sta_Sta_Creophilus
Sta_Scy_Euconnus
Sta_Scy_Palaeostigus
Sta_Scy_Adrastia
Hyd_Hel_Helophorus
Hyd_Geo_Georissus
Hyd_Spe_Spercheus
Hyd_Hyd_Tropisternus
Hyd_Hyd_Andotypus
Hyd_Syn_Syntelia
Hyd_Sph_Sphaerites
Hyd_His_Bacanius
Hyd_His_Carcinops
Hyd_His_Euspilotus
Hyd_His_Hister
Sca_Gla_Glaresis
Sca_Geo_Geotrupes
Sca_Tro_Trox
Sca_Geo_Taurocerastes
Sca_Luc_Lucanus
Sca_Dip_Diphyllostoma
Sca_Luc_Nicagus
Sca_Sca_Aphodius
Sca_Sca_Scarabaeus
Sca_Hyb_Hybosorus
Sca_Och_Ochodaeus
Sca_Gla_Lichnanthe
Sca_Pas_Passalus
Sca_Geo_Odonteus
Sca_Sca_Dynastes
Sca_Ple_Pleocoma
Sca_Sca_Rhopaea
Sca_Sca_Cetonia
Bos_Nos_Nosodendron
Das_Das_Anorus
Das_Das_Dascillus
Das_Rhi_Sandalus
Das_Rhip_Rhipicera
Bup_Sch_Schizopus
Bup_Bup_Acmaeodera
Bup_Bup_Agrilus
Bup_Bup_Buprestis
Bup_Bup_Julodis
Byr_Byr_Microchaetes
Byr_Byr_Simplocaria
Ela_Cal_Callirhipis
Byr_Dry_Helichus
Byr_Lut_Lutrochus
Byr_Cne_Cneoglossa
Byr_Pti_Anchyteis
Byr_Pti_Ptilodactyla
Ela_Pod_Podabrocephalus
Byr_Che_Chelonarium
Byr_Lim_Byrrhinus
Byr_Het_Heterocerus
Byr_Pse_Eubrianax
Byr_Pse_Psephenus
Byr_Eul_Stenocolus
Byr_Elm_Lara
Byr_Elm_Optioservus
Ela_Art_Macropogon
Ela_Ome_Mathetes
Ela_Tel_Telegeusis
Ela_Bra_Brachypsectra
Ela_Euc_Anischia
Ela_Thr_Aulonothroscus
Ela_Cer_Cerophytum
Ela_Euc_Melasis
Ela_Ela_Lissomus
Ela_Lyc_Dictyoptera
Ela_Lyc_Lycus
Ela_Can_Chauliognathus
Ela_Can_Malthodes
Ela_Can_Silis
Ela_Oma_Omalisus
Ela_Dri_Drilus
Ela_Ela_Cardiophorus
Ela_Ela_Ampedus
Ela_Ela_Selonodon
Ela_Rha_Rhagopthalmus
Ela_Phe_Cenophengus
Ela_Phe_Phengodes
Ela_Dri_Ototretadrilus
Ela_Lam_Pterotus
Ela_Lam_Ellychnia
Ela_Lam_Pyrocoelia
293.0462
287.2948
276.5873
246.6968
229.163
215.8225
211.4626
235.8177
222.0277
181.0868
219.9339
207.3265
198.6404
194.1079
193.8112
189.6061
186.7068
183.345
179.767
176.2007
173.9509
173.5312
173.0871
161.3931
157.7748
157.3024
153.7916
153.3797
152.0041
147.1786
147.1666
146.6251
145.8966
144.5474
140.7905
139.1826
139.9984
139.7749
137.2364
136.6866
135.9103
135.8371
132.4325
131.1462
130.8118
130.7362
130.3154
126.956
126.9238
126.7352
125.8341
125.7035
125.39
124.307
122.6569
120.8312
120.6184
120.4887
118.9953
118.6012
118.5794
118.158
118.992
117.6434
116.9721
116.9633
116.9502
116.265
115.7799
115.4699
115.1844
114.6052
114.4205
113.6008
113.5901
112.1539
111.5312
110.2073
109.4732
108.9143
108.443
107.2715
106.9613
106.2335
106.0926
105.6663
105.5347
105.148
104.5417
103.737
102.4591
100.6483
100.5161
99.9731
99.5039
99.4591
99.4467
97.6256
95.1532
94.8636
93.6583
92.9024
92.1516
89.4267
89.2695
89.1639
87.7104
87.7007
87.7605
87.0192
82.3941
81.797
81.0319
80.2698
76.4901
75.0845
74.2627
74.1322
71.89
70.2583
70.144
68.3982
67.9002
65.6376
64.7921
60.9683
60.2892
57.9721
57.307
56.248
47.8999
41.5947
300
250
200
150
100
50
0
Time (Ma)

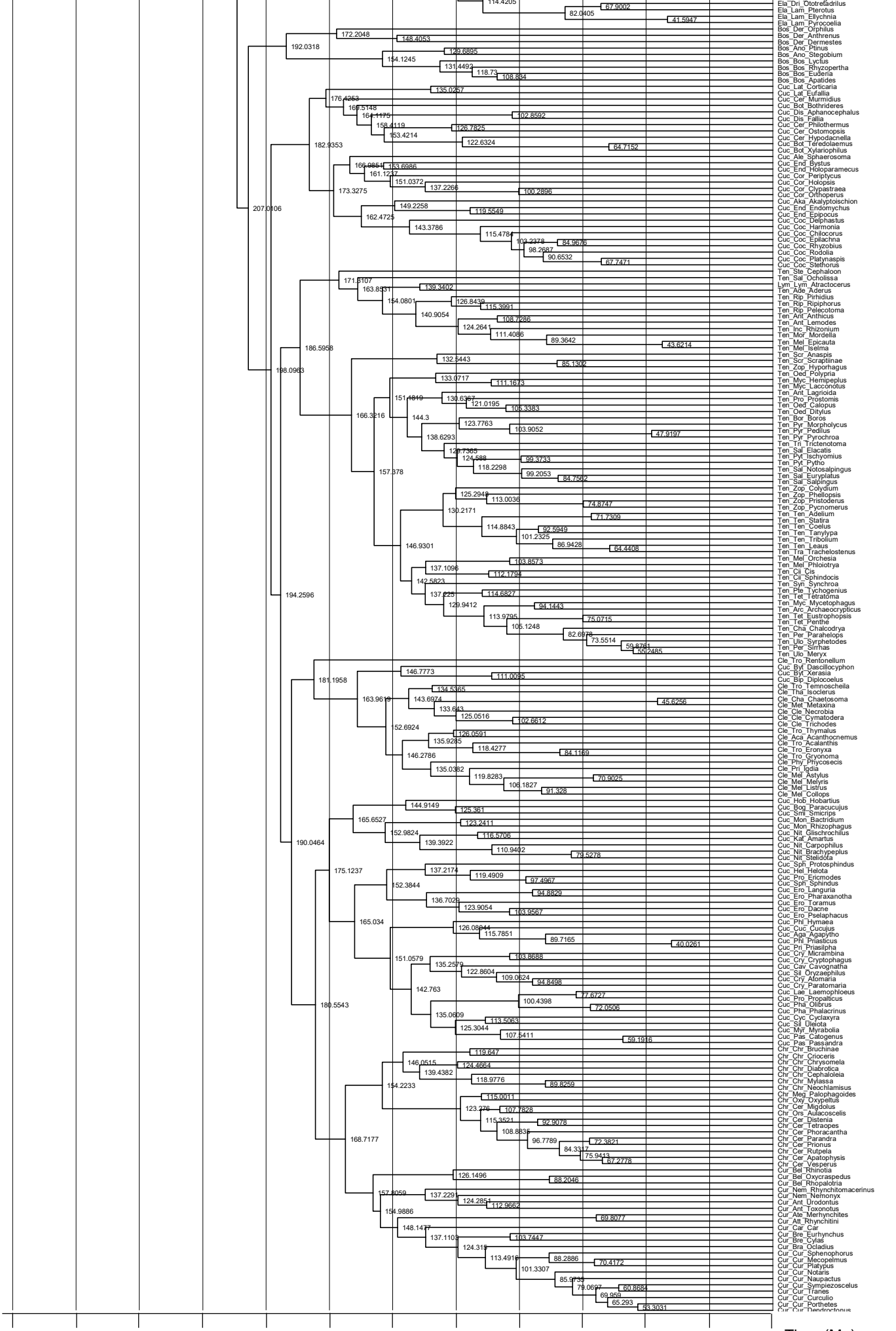
Ela_Dri_Ototretadrilus
Ela_Lam_Pterotus
Ela_Lam_Ellychnia
Ela_Lam_Pyrocoelia
Bos_Der_Orphilus
Bos_Der_Anthrenus
Bos_Der_Dermestes
Bos_Ano_Ptinus
Bos_Ano_Stegobium
Bos_Bos_Lyctus
Bos_Bos_Rhyzopertha
Bos_Bos_Euderia
Bos_Bos_Apatides
Cuc_Lat_Corticaria
Cuc_Lat_Eufallia
Cuc_Cer_Murmidius
Cuc_Bot_Bothrideres
Cuc_Dis_Aphanocephalus
Cuc_Dis_Fallia
Cuc_Cer_Philothermus
Cuc_Cer_Ostomopsis
Cuc_Cer_Hypodacnella
Cuc_Bot_Teredolaemus
Cuc_Bot_Xylariophilus
Cuc_Ale_Sphaerosoma
Cuc_End_Bystus
Cuc_End_Holoparamecus
Cuc_Cor_Periptycus
Cuc_Cor_Holopsis
Cuc_Cor_Clypastraea
Cuc_Cor_Orthoperus
Cuc_Aka_Akalyptoischion
Cuc_End_Endomychus
Cuc_End_Epipocus
Cuc_Coc_Delphastus
Cuc_Coc_Harmonia
Cuc_Coc_Chilocorus
Cuc_Coc_Epilachna
Cuc_Coc_Rhyzobius
Cuc_Coc_Rodolia
Cuc_Coc_Platynaspis
Cuc_Coc_Stethorus
Ten_Ste_Cephaloon
Ten_Sal_Ocholissa
Lym_Lym_Atractocerus
Ten_Ade_Aderus
Ten_Rip_Pirhidius
Ten_Rip_Ripiphorus
Ten_Rip_Pelecotoma
Ten_Ant_Anthicus
Ten_Ant_Lemodes
Ten_Inc_Rhizonium
Ten_Mor_Mordella
Ten_Mel_Epicauta
Ten_Mel_Iselma
Ten_Scr_Anaspis
Ten_Scr_Scraptiinae
Ten_Zop_Hyporhagus
Ten_Oed_Polyaria
Ten_Myc_Hemipeplus
Ten_Myc_Lacconotus
Ten_Ant_Lagrioida
Ten_Pro_Prostomis
Ten_Oed_Calopus
Ten_Oed_Ditylus
Ten_Bor_Boros
Ten_Pyr_Morpholycus
Ten_Pyr_Pedilus
Ten_Pyr_Pyrochroa
Ten_Tri_Trictenotoma
Ten_Sal_Elacatis
Ten_Pyt_Ischyomius
Ten_Pyt_Pytho
Ten_Sal_Notosalpingus
Ten_Sal_Eurysplatus
Ten_Sal_Salpingus
Ten_Zop_Colydium
Ten_Zop_Phellopsis
Ten_Zop_Pristoderus
Ten_Zop_Pycnomerus
Ten_Ten_Adelium
Ten_Ten_Statira
Ten_Ten_Coelus
Ten_Ten_Tanylypa
Ten_Ten_Tribolium
Ten_Ten_Leaus
Ten_Tra_Trachelostenus
Ten_Mel_Orchesia
Ten_Mel_Phloiotrya
Ten_Cii_Cis
Ten_Cii_Sphindocis
Ten_Syn_Synchroa
Ten_Pte_Tychogenius
Ten_Tet_Tetratoma
Ten_Myc_Mycetophagus
Ten_Arc_Archaeocrypticus
Ten_Tet_Eustrophopsis
Ten_Tet_Penthe
Ten_Cha_Chalcodrya
Ten_Per_Parahelops
Ten_Ulo_Syrphetodes
Ten_Per_Sirrhas
Ten_Ulo_Meryx
Cle_Tro_Rentonellum
Cuc_Byt_Dasicliocyphon
Cuc_Byt_Xerasia
Cuc_Bip_Diplocoelus
Cle_Tro_Temnoscheila
Cle_Tha_Isoclerus
Cle_Cha_Chaetosoma
Cle_Mel_Metaxina
Cle_Cle_Necrobia
Cle_Cle_Cymatodera
Cle_Cle_Trichodes
Cle_Tro_Thymalus
Cle_Aca_Acanthocnemus
Cle_Tro_Acalanthis
Cle_Tro_Eronyxa
Cle_Tro_Gryonoma
Cle_Phy_Phycosecis
Cle_Pri_Ipidia
Cle_Mel_Astylus
Cle_Mel_Melyris
Cle_Mel_Listrus
Cle_Mel_Collops
Cuc_Hob_Hobartius
Cuc_Bog_Paracucujus
Cuc_Smi_Smicrips
Cuc_Mon_Bactridium
Cuc_Mon_Rhizophagus
Cuc_Nit_Glischrochilus
Cuc_Kat_Amartus
Cuc_Nit_Carpophilus
Cuc_Nit_Brachypeplus
Cuc_Nit_Stelidota
Cuc_Sph_Protosphindus
Cuc_Hel_Helota
Cuc_Pro_Ericmodes
Cuc_Sph_Sphindus
Cuc_Ero_Languria
Cuc_Ero_Pharaxanotha
Cuc_Ero_Toramus
Cuc_Ero_Dacne
Cuc_Ero_Pselaphacus
Cuc_Phl_Hymaea
Cuc_Cuc_Cucujus
Cuc_Aga_Agapytho
Cuc_Phl_Priasticus
Cuc_Pri_Priasilpha
Cuc_Cry_Micrambina
Cuc_Cry_Cryptophagus
Cuc_Cav_Cavognatha
Cuc_Sil_Oryzaephilus
Cuc_Cry_Atomaria
Cuc_Cry_Paratomaria
Cuc_Lae_Laemophloeus
Cuc_Pro_Propalticus
Cuc_Pha_Olibrus
Cuc_Pha_Phalacrinus
Cuc_Cyc_Cyclaxyra
Cuc_Sil_Dieota
Cuc_Myr_Myrabolia
Cuc_Pas_Catogenus
Cuc_Pas_Passandra
Chr_Chr_Bruchinae
Chr_Chr_Crioceris
Chr_Chr_Chrysomela
Chr_Chr_Diabrotica
Chr_Chr_Cephaloleia
Chr_Chr_Mylassa
Chr_Chr_Neochlamisus
Chr_Meg_Palophagoides
Chr_Oxy_Oxypeltus
Chr_Cer_Migdolus
Chr_Ors_Aulacoscelis
Chr_Cer_Distenia
Chr_Cer_Tetraopes
Chr_Cer_Phoracantha
Chr_Cer_Parandra
Chr_Cer_Prionus
Chr_Cer_Rutpela
Chr_Cer_Apatophysis
Chr_Cer_Vesperus
Cur_Bel_Rhinotia
Cur_Bel_Oxycraspedus
Cur_Bel_Rhopalotria
Cur_Nem_Rhynchitomacerinus
Cur_Nem_Nemonyx
Cur_Ant_Urodontus
Cur_Ant_Toxonotus
Cur_Ate_Merhynchites
Cur_Att_Rhynchitini
Cur_Car_Car
Cur_Bre_Eurhynchus
Cur_Bre_Cylas
Cur_Bra_Ocladius
Cur_Cur_Sphenophorus
Cur_Cur_Mecopelmus
Cur_Cur_Platypus
Cur_Cur_Notaris
Cur_Cur_Naupactus
Cur_Cur_Sympiezoscelus
Cur_Cur_Tranes
Cur_Cur_Curculio
Cur_Cur_Porthetes
Cur_Cur_Pandeleteius
300
250
200
150
100
50
0
Time (Ma)

File S3. Detailed information of fossil calibrations and justification after Parham *et al.* (2012) criteria

Fossil Calibration 1:
Taxon: *Coleopsis archaica*
Calibrated stem: Coleoptera
Geological deposit: Grügelborn, Germany
Minimum age: 295.5 Ma
Reference: Kirejtshuk *et al*. (2014)
Justification of Parham *et al*. (2012) criteria:
CR1 (single/multiple OTUs with museum numbers): A single specimen. Full Museum data in the reference above.
CR2 (apomorphy-based or phylogenetic analysis): Presence of apomorphies.
CR3 (agreement of morphology and molecular data): Belongs to the monophyletic Coleoptera.
CR4 (detailed locality and stratigraphy data provided): Locality and stratigraphy data provided in the original paper, double-checked for accuracy with The Paleobiology Database (https://paleobiodb.org/).
CR5 (radioisotopic age or numeric age references given): Age derived from The Paleobiology Database (https://paleobiodb.org/).

Fossil Calibration 2:
Taxon: *Omma liassicum*
Calibrated stem: Ommatidae
Geological deposit: Hasfield, United Kingdon
Minimum age: 201.3 Ma
Reference: Crowson (1962)
Justification of Parham *et al*. (2012) criteria:
CR1 (single/multiple OTUs with museum numbers): Multiple specimens. Full Museum data in the reference above.
CR2 (apomorphy-based or phylogenetic analysis): Presence of apomorphies.
CR3 (agreement of morphology and molecular data): Belongs to an extant genus.
CR4 (detailed locality and stratigraphy data provided): Locality and stratigraphy data adopted from The Paleobiology Database (https://paleobiodb.org/).
CR5 (radioisotopic age or numeric age references given): Age derived from The Paleobiology Database (https://paleobiodb.org/).
Additional fossils of similar age: Fossils of two recent ommatid genera, *Omma avus* Ponomarenko, 1969 and *Tetraphalerus incertus* Ponomarenko, 1969, are known from the deposits of Issyk-Kul, Kazakhstan (Ponomarenko 1969), dated for 201.3–190.8 Ma. Both are fulfilling Parham *et al.* (2012) criteria CR1 to CR5, and are assigned to modern genera of Ommatidae based on apomorphies.

Fossil Calibration 3:
Taxon: *Priacma tuberculosa*
Calibrated stem: Priacminae
Geological deposit: Huangbanjigou, Yixian Formation, China

Minimum age: 125.5 Ma
Reference: Tan *et al.* (2006)
Justification of Parham *et al.* (2012) criteria:
CR1 (single/multiple OTUs with museum numbers): A single specimen. Full Museum data in the reference above.
CR2 (apomorphy-based or phylogenetic analysis): Presence of apomorphies.
CR3 (agreement of morphology and molecular data): Belongs to an extant genus.
CR4 (detailed locality and stratigraphy data provided): Locality and stratigraphy data provided in the original paper, double-checked for accuracy with The Paleobiology Database (https://paleobiodb.org/).
CR5 (radioisotopic age or numeric age references given): Age derived from The Paleobiology Database (https://paleobiodb.org/).
Additional fossils of similar age: Two additional fossils were described from the same locality as *P. tuberculosa* by Tan *et al.* (2006) and can be reliably assigned to *Priacma* based on presence of apomorphies: *P. clavata* Tan *et al.* 2006 and *P. renaria* Tan *et al.* 2006. Both of them fulfill Parham *et al.* (2012) criteria CR1 to CR5.

Fossil Calibration 4:
Taxon: *Haplochelus georissoides*
Calibrated stem: Lepiceridae
Geological deposit: Burmese amber, Myanmar
Minimum age: 93.5 Ma
References: Kirejtshuk & Poinar (2006), Ge *et al.* (2010).
Justification of Parham *et al.* (2012) criteria:
CR1 (single/multiple OTUs with museum numbers): A single specimen. Full Museum data in the reference above.
CR2 (apomorphy-based or phylogenetic analysis): Phylogenetic analysis.
CR3 (agreement of morphology and molecular data): Strongly supported as sister of *Lepicerus*.
CR4 (detailed locality and stratigraphy data provided): Locality and stratigraphy data provided in the original paper, double-checked for accuracy with The Paleobiology Database (https://paleobiodb.org/).
CR5 (radioisotopic age or numeric age references given): Age derived from The Paleobiology Database (https://paleobiodb.org/).
Additional fossils of similar age: An additional fossil assigned to Lepiceridae based on several unique apomorphies of that family, *Leptoceroides pretiosus* Kirejtshuk & Poinar, 2013, was described by Kirejtshuk & Poinar (2013) from the same deposit as *Haplochelus georissoides* (i.e. Burmese amber). It also fulfills Parham *et al.* (2012) criteria CR1 to CR5.

Fossil Calibration 5:
Taxon: *Protonectes germanicus*
Calibrated stem: Hydradephaga
Geological deposit: Schönbachsmühle, Hassberge Formation
Minimum age: 221.5 Ma
Reference: Prokin *et al.* (2013)
Justification of Parham *et al.* (2012) criteria:

CR1 (single/multiple OTUs with museum numbers): A single specimen. Full Museum data in the reference above.
CR2 (apomorphy-based or phylogenetic analysis): Based on careful examination of type photos, clearly belongs to Coptoclavidae which are well documented and share apomorphies with other Hydradephaga.
CR3 (agreement of morphology and molecular data): Assigned to a hydradephagan family which are highly supported as monophylum.
CR4 (detailed locality and stratigraphy data provided): Locality and stratigraphy data provided in the original paper, double-checked for accuracy with The Paleobiology Database (https://paleobiodb.org/).
CR5 (radioisotopic age or numeric age references given): Age derived from The Paleobiology Database (https://paleobiodb.org/).
Additional fossils of similar age: A fossil larva assigned to Hydradephaga, *Colymbotethis antecessor* Ponomarenko, 1993 was described by Ponomarenko (1993) based on apomorphies related to aquatic life style; it was found in the deposit of Kenderlyk, Tologoi Formation, Kazakhstan 228.0–208.5 Ma and assigned to a separate family †Colymbotethidae. The fossil fulfills Parham *et al.* (2012) criteria CR1 to CR5.

Fossil Calibration 6:
Taxon: *Oxycheilopsis cretacicus*
Calibrated stem: Cicindelinae
Geological deposit: Crato Formation, Brazil
Minimum age: 112 Ma
Reference: Cassola & Werner, (2004)
Justification of Parham *et al.* (2012) criteria:
CR1 (single/multiple OTUs with museum numbers): A single specimen. Full Museum data in the reference above.
CR2 (apomorphy-based or phylogenetic analysis): Presence of apomorphies.
CR3 (agreement of morphology and molecular data): Assigned deeply into the monophyletic Cicindelinae.
CR4 (detailed locality and stratigraphy data provided): Locality and stratigraphy data provided in the original paper, double-checked for accuracy with The Paleobiology Database (https://paleobiodb.org/).
CR5 (radioisotopic age or numeric age references given): Age derived from The Paleobiology Database (https://paleobiodb.org/).

Fossil Calibration 7:
Taxon: *Juropeltastica sinica*
Calibrated stem: Derodontidae
Geological deposit: Daohugou, Nei Mongol, China
Minimum age: 157.3 Ma
Reference: Cai *et al.* (2014a)
Justification of Parham *et al.* (2012) criteria:
CR1 (single/multiple OTUs with museum numbers): A single specimen. Full Museum data in the reference above.
CR2 (apomorphy-based or phylogenetic analysis): Presence of apomorphies.

CR3 (agreement of morphology and molecular data): Assigned to a modern subfamily of Derodontidae (Peltasticinae).
CR4 (detailed locality and stratigraphy data provided): Locality and stratigraphy data provided in the original paper, double-checked for accuracy with The Paleobiology Database (https://paleobiodb.org/).
CR5 (radioisotopic age or numeric age references given): Age derived from The Paleobiology Database (https://paleobiodb.org/).

Fossil Calibration 8:
Taxon: undescribed species
Calibrated stem: Silphidae
Geological deposit: Daohugou, Nei Mongol, China
Minimum age: 157.3 Ma
Reference: Cai *et al*. (2014b)
Justification of Parham *et al*. (2012) criteria:
CR1 (single/multiple OTUs with museum numbers): Multiple specimens. Full Museum data in the reference above.
CR2 (apomorphy-based or phylogenetic analysis): Presence of apomorphies.
CR3 (agreement of morphology and molecular data): Assigned by a unique synapomorphy to a strongly supported monophyletic clade.
CR4 (detailed locality and stratigraphy data provided): Locality and stratigraphy data provided in the original paper, double-checked for accuracy with The Paleobiology Database (https://paleobiodb.org/).
CR5 (radioisotopic age or numeric age references given): Age derived from The Paleobiology Database (https://paleobiodb.org/).

Fossil Calibration 9:
Taxon: undescribed species
Calibrated stem: Nicrophorinae
Geological deposit: Daohugou, Nei Mongol, China
Minimum age: 157.3 Ma
Reference: Cai *et al*. (2014b)
Justification of Parham *et al*. (2012) criteria:
CR1 (single/multiple OTUs with museum numbers): Multiple specimens. Full Museum data in the reference above.
CR2 (apomorphy-based or phylogenetic analysis): Presence of apomorphies.
CR3 (agreement of morphology and molecular data): Assigned by a unique synapomorphy to a strongly supported monophyletic clade.
CR4 (detailed locality and stratigraphy data provided): Locality and stratigraphy data provided in the original paper, double-checked for accuracy with The Paleobiology Database (https://paleobiodb.org/).
CR5 (radioisotopic age or numeric age references given): Age derived from The Paleobiology Database (https://paleobiodb.org/).

Fossil Calibration 10:
Taxon: *Protochares brevipalpis*

Calibrated stem: Hydrophilidae
Geological deposit: Talbragar Fossil Fish Beds, Australia
Minimum age: 152.1 Ma
Reference: Fikáček *et al*. (2014)
Justification of Parham *et al*. (2012) criteria:
CR1 (single/multiple OTUs with museum numbers): A single specimen. Full Museum data in the reference above.
CR2 (apomorphy-based or phylogenetic analysis): Combination of diagnostic characters.
CR3 (agreement of morphology and molecular data): Belongs to Hydrophilidae.
CR4 (detailed locality and stratigraphy data provided): Locality and stratigraphy data provided in the original paper, double-checked for accuracy with The Paleobiology Database (https://paleobiodb.org/).
CR5 (radioisotopic age or numeric age references given): Age derived from The Paleobiology Database (https://paleobiodb.org/).
Additional fossils of similar age: *Prospercheus cristatus* Prokin, 2009 assigned reliably to Spercheidae, i.e. sister group of Hydrophilidae, based on unique apomorphy of maxilla (M. Fikáček, unpubl. data) was described by Prokin (2009) from the deposit of Shar-Teg, Mongolia, 152.1–145.0 Ma. The fossil fulfills Parham *et al*. (2012) criteria CR1 to CR5 and dates the same node as the hydrophilid fossil listed above.

Fossil Calibration 11:
Taxon: *Mesochodaeus daohugouensis*
Calibrated stem: Ochodaeidae
Geological deposit: Daohugou, Nei Mongol, China
Minimum age: 157.3 Ma
Reference: Nikolajev & Ren (2010)
Justification of Parham *et al.* (2012) criteria:
CR1 (single/multiple OTUs with museum numbers): A single specimen. Full Museum data in the reference above.
CR2 (apomorphy-based or phylogenetic analysis): Based on careful examination of type photos, presence of apomorphies.
CR3 (agreement of morphology and molecular data): Assigned by apomorphy to Ochodaeidae.
CR4 (detailed locality and stratigraphy data provided): Locality and stratigraphy data provided in the original paper, double-checked for accuracy with The Paleobiology Database (https://paleobiodb.org/).
CR5 (radioisotopic age or numeric age references given): Age derived from The Paleobiology Database (https://paleobiodb.org/).

Fossil Calibration 12:
Taxon: *Sinaesalus longipes*
Calibrated stem: Lucanidae
Geological deposit: Yangshuwanzi, Yixian Formation, China
Minimum age: 122.5 Ma
Reference: Nikolajev & Ren (2011)
Justification of Parham *et al.* (2012) criteria:

CR1 (single/multiple OTUs with museum numbers): A single specimen. Full Museum data in the reference above.
CR2 (apomorphy-based or phylogenetic analysis): Based on careful examination of type photos, presence of apomorphies.
CR3 (agreement of morphology and molecular data): Assigned deeply into Lucanidae.
CR4 (detailed locality and stratigraphy data provided): Locality and stratigraphy data provided in the original paper, double-checked for accuracy with The Paleobiology Database (https://paleobiodb.org/).
CR5 (radioisotopic age or numeric age references given): Age derived from The Paleobiology Database (https://paleobiodb.org/).

Fossil Calibration 13:
Taxon: *Glaresis tridentata*
Calibrated stem: Glaresidae
Geological deposit: Chaomidian, Yixian Formation, China
Minimum age: 125.5 Ma
Reference: Bai *et al.* (2014)
Justification of Parham *et al.* (2012) criteria:
CR1 (single/multiple OTUs with museum numbers): A single specimen. Full Museum data in the reference above.
CR2 (apomorphy-based or phylogenetic analysis): Based on careful examination of type photos, presence of apomorphies.
CR3 (agreement of morphology and molecular data): Assigned deeply into Glaresidae.
CR4 (detailed locality and stratigraphy data provided): Locality and stratigraphy data provided in the original paper, double-checked for accuracy with The Paleobiology Database (https://paleobiodb.org/).
CR5 (radioisotopic age or numeric age references given): Age derived from The Paleobiology Database (https://paleobiodb.org/).
Additional fossil of similar age: *Glaresis orthochilus* Bai *et al.*, 2010 was described from the same deposit as *G. tridentata* by Bai *et al.* (2010). It may be reliably assigned to Glaresidae based on presence of apomorphies, and fulfills Parham *et al*. (2012) criteria CR1 to CR5.

Fossil Calibration 14:
Taxon: *Cretodascillus sinensis*
Calibrated stem: Dascillidae
Geological deposit: Liutiaogou, Yixian Formation, China
Minimum age: 122.5 Ma
Reference: Jin *et al*. (2013)
Justification of Parham *et al*. (2012) criteria:
CR1 (single/multiple OTUs with museum numbers): A single specimen. Full Museum data in the reference above.
CR2 (apomorphy-based or phylogenetic analysis): Presence of apomorphies.
CR3 (agreement of morphology and molecular data): Reliably assigned to Dascillidae.
CR4 (detailed locality and stratigraphy data provided): Locality and stratigraphy data provided in the original paper, double-checked for accuracy with The Paleobiology Database (https://paleobiodb.org/).

CR5 (radioisotopic age or numeric age references given): Age derived from The Paleobiology Database (https://paleobiodb.org/).

Fossil Calibration 15:
Taxon: *Sinoparathyrea bimaculata*
Calibrated stem: Schizopodidae
Geological deposit: Daohugou, Nei Mongol, China
Minimum age: 157.3 Ma
Reference: Pan *et al*. (2011), Cai *et al*. (2015a)
Justification of Parham *et al.* (2012) criteria:
CR1 (single/multiple OTUs with museum numbers): A single specimen. Full Museum data in the reference above.
CR2 (apomorphy-based or phylogenetic analysis): Combination of diagnostic characters.
CR3 (agreement of morphology and molecular data): Reliably assigned to Schizopodidae.
CR4 (detailed locality and stratigraphy data provided): Locality and stratigraphy data provided in the original paper, double-checked for accuracy with The Paleobiology Database (https://paleobiodb.org/).
CR5 (radioisotopic age or numeric age references given): Age derived from The Paleobiology Database (https://paleobiodb.org/).

Fossil Calibration 16:
Taxon: *Elmadulescens rugosus*
Calibrated stem: Elmidae
Geological deposit: El Soplao amber, Las Peñosas Formation, Spain
Minimum age: 109 Ma
Reference: Peris *et al.* (2015a)
Justification of Parham *et al.* (2012) criteria:
CR1 (single/multiple OTUs with museum numbers): A single specimen. Full Museum data in the reference above.
CR2 (apomorphy-based or phylogenetic analysis): Combination of diagnostic characters.
CR3 (agreement of morphology and molecular data): Reliably assigned to Elmidae.
CR4 (detailed locality and stratigraphy data provided): Locality and stratigraphy data provided in the original paper, double-checked for accuracy with The Paleobiology Database (https://paleobiodb.org/).
CR5 (radioisotopic age or numeric age references given): Age derived from The Paleobiology Database (https://paleobiodb.org/).
Additional fossils of similar age: An elmid beetle is currently under description from the Burmese amber (99 Ma; M. A. Jäch & C. Maier, pers. comm).

Fossil Calibration 17:
Taxon: *Heterocerites magnus*
Calibrated stem: Heteroceridae
Geological deposit: Chaomidian, Yixian Formation, China
Minimum age: 125.5 Ma
Reference: Prokin & Ren, (2011)
Justification of Parham *et al.* (2012) criteria:

CR1 (single/multiple OTUs with museum numbers): Multiple specimens. Full Museum data in the reference above.
CR2 (apomorphy-based or phylogenetic analysis): Based on careful examination of type photos, presence of apomorphies.
CR3 (agreement of morphology and molecular data): Reliably assigned to Heteroceridae.
CR4 (detailed locality and stratigraphy data provided): Locality and stratigraphy data provided in the original paper, double-checked for accuracy with The Paleobiology Database (https://paleobiodb.org/).
CR5 (radioisotopic age or numeric age references given): Age derived from The Paleobiology Database (https://paleobiodb.org/).

Fossil Calibration 18:
Taxon: *Sinobrevipogon jurassicus*
Calibrated stem: Artematopodidae
Geological deposit: Daohugou, Nei Mongol, China
Minimum age: 157.3 Ma
Reference: Cai *et al.* (2015b)
Justification of Parham *et al.* (2012) criteria:
CR1 (single/multiple OTUs with museum numbers): Multiple specimens. Full Museum data in the reference above.
CR2 (apomorphy-based or phylogenetic analysis): Phylogenetic analysis.
CR3 (agreement of morphology and molecular data): Reliably assigned to Artematopodidae.
CR4 (detailed locality and stratigraphy data provided): Locality and stratigraphy data provided in the original paper, double-checked for accuracy with The Paleobiology Database (https://paleobiodb.org/).
CR5 (radioisotopic age or numeric age references given): Age derived from The Paleobiology Database (https://paleobiodb.org/).

Fossil Calibration 19:
Taxon: *Stephanopachys vetus*
Calibrated stem: Dinoderinae
Geological deposit: Font-de-Benon Quarry, Charentese amber, France
Minimum age: 99.6 Ma
Reference: Peris *et al.* (2014)
Justification of Parham *et al.* (2012) criteria:
CR1 (single/multiple OTUs with museum numbers): A single specimen. Full Museum data in the reference above.
CR2 (apomorphy-based or phylogenetic analysis): Combination of diagnostic characters.
CR3 (agreement of morphology and molecular data): Belongs to an extant genus.
CR4 (detailed locality and stratigraphy data provided): Locality and stratigraphy data provided in the original paper, double-checked for accuracy with The Paleobiology Database (https://paleobiodb.org/).
CR5 (radioisotopic age or numeric age references given): Age derived from The Paleobiology Database (https://paleobiodb.org/).

Fossil Calibration 20:
Taxon: *Actenobius magneoculus*
Calibrated stem: Anobiinae
Geological deposit: San Just amber, Spain
Minimum age: 105.3 Ma
Reference: Peris *et al.* (2015b)
Justification of Parham *et al.* (2012) criteria:
CR1 (single/multiple OTUs with museum numbers): A single specimen. Full Museum data in the reference above.
CR2 (apomorphy-based or phylogenetic analysis): Combination of diagnostic characters.
CR3 (agreement of morphology and molecular data): Belongs to an extant genus.
CR4 (detailed locality and stratigraphy data provided): Locality and stratigraphy data provided in the original paper, double-checked for accuracy with The Paleobiology Database (https://paleobiodb.org/).
CR5 (radioisotopic age or numeric age references given): Age derived from The Paleobiology Database (https://paleobiodb.org/).

Fossil Calibration 21:
Taxon: *Rhyzobius antiquus*
Calibrated stem: Coccidulinae
Geological deposit: Oise amber, France
Minimum age: 47.8 Ma
Reference: Kirejtshuk & Nel (2012)
Justification of Parham *et al.* (2012) criteria:
CR1 (single/multiple OTUs with museum numbers): Multiple specimens (all morphological characters seen on the holotype). Full Museum data in the reference above.
CR2 (apomorphy-based or phylogenetic analysis): Combination of diagnostic characters.
CR3 (agreement of morphology and molecular data): Reliably assigned to Coccidulinae.
CR4 (detailed locality and stratigraphy data provided): Locality and stratigraphy data provided in the original paper, double-checked for accuracy with The Paleobiology Database (https://paleobiodb.org/).
CR5 (radioisotopic age or numeric age references given): Age derived from The Paleobiology Database (https://paleobiodb.org/).
Additional fossils of similar age: *Rhyzobius gratiosus* Kirejtshuk & Nel, 2012 was described from the same deposit as *R. antiquus* based on combination of diagnostic characters. It fulfills Parham et al. (2012) criteria CR1 to CR5

Fossil Calibration 22:
Taxon: *Archelatrius marinae*
Calibrated stem: Latridiinae
Geological deposit: Lebanese amber, Lebanon
Minimum age: 122.5 Ma
Reference: Kirejtshuk & Azar (2009)
Justification of Parham *et al.* (2012) criteria:
CR1 (single/multiple OTUs with museum numbers): A single specimen. Full Museum data in the reference above.

CR2 (apomorphy-based or phylogenetic analysis): Combination of diagnostic characters.
CR3 (agreement of morphology and molecular data): Assigned to Latridiinae based on diagnostic characters only.
CR4 (detailed locality and stratigraphy data provided): Locality and stratigraphy data provided in the original paper, double-checked for accuracy with The Paleobiology Database (https://paleobiodb.org/).
CR5 (radioisotopic age or numeric age references given): Age derived from The Paleobiology Database (https://paleobiodb.org/).

Fossil Calibration 23:
Taxon: *Paleoripiphorus deploegi*
Calibrated stem: Ripidiinae
Geological deposit: Archingeay/Les Nouillers amber
Minimum age: 99.6 Ma
Reference: Perrichot *et al.* (2004), Batelka *et al.* (2006), Falin & Engel (2010)
Justification of Parham *et al.* (2012) criteria:
CR1 (single/multiple OTUs with museum numbers): A single specimen. Full Museum data in the reference above.
CR2 (apomorphy-based or phylogenetic analysis): Combination of diagnostic characters.
CR3 (agreement of morphology and molecular data): Reliably assigned to Ripidiinae.
CR4 (detailed locality and stratigraphy data provided): Locality and stratigraphy data provided in the original paper, double-checked for accuracy with The Paleobiology Database (https://paleobiodb.org/).
CR5 (radioisotopic age or numeric age references given): Age derived from The Paleobiology Database (https://paleobiodb.org/).

Fossil Calibration 24:
Taxon: *Vetuprostomis consimilis*
Calibrated stem: Prostomidae
Geological deposit: Burmese amber, Myanmar
Minimum age: 93.5 Ma
Reference: Engel & Grimaldi (2008)
Justification of Parham *et al.* (2012) criteria:
CR1 (single/multiple OTUs with museum numbers): A single specimen. Full Museum data in the reference above.
CR2 (apomorphy-based or phylogenetic analysis): Combination of diagnostic characters.
CR3 (agreement of morphology and molecular data): Reliably assigned to Prostomatidae.
CR4 (detailed locality and stratigraphy data provided): Locality and stratigraphy data provided in the original paper, double-checked for accuracy with The Paleobiology Database (https://paleobiodb.org/).
CR5 (radioisotopic age or numeric age references given): Age derived from The Paleobiology Database (https://paleobiodb.org/).

Fossil Calibration 25:
Taxon: *Mirimordella gracilicruralis*
Calibrated stem: Mordellidae

Geological deposit: Huangbanjigou, Yixian Formation, China
Minimum age: 125.5 Ma
Reference: Liu *et al.* (2007)
Justification of Parham *et al.* (2012) criteria:
CR1 (single/multiple OTUs with museum numbers): A single specimen. Full Museum data in the reference above.
CR2 (apomorphy-based or phylogenetic analysis): Presence of apomorphies and combination of diagnostic characters.
CR3 (agreement of morphology and molecular data): Assigned to the extinct subfamily Praemordellinae in the extant family Mordellidae.
CR4 (detailed locality and stratigraphy data provided): Locality and stratigraphy data provided in the original paper, double-checked for accuracy with The Paleobiology Database (https://paleobiodb.org/).
CR5 (radioisotopic age or numeric age references given): Age derived from The Paleobiology Database (https://paleobiodb.org/).
Additional fossils of similar age: Three fossils reliably assigned to Mordellidae based on apomorphies and set of diagnostic characters, *Bellimordella capitulifera* Liu *et al*., 2008*, B. longispina* Liu *et al*., 2008 and *B. robusta* Liu *et al*., 2008 were described from the same locality by Liu *et al.* (2008). All three fossils fulfill the Parham *et al.* (2012) criteria CR1 to CR5.
Additional fossils of similar age: *Mediumiuga sinespinis* Peris & Ruzzier, 2013 from the Peñacerrada amber (112.6–109.0 Ma) is a definite mordellid showing unambiguous autapomorphies of the family.

Fossil Calibration 26:
Taxon: undescribed species
Calibrated stem: Aderidae
Geological deposit: Lebanese amber, Lebanon
Minimum age: 122.5 Ma
Reference: Grimaldi & Engel (2005)
Justification of Parham *et al.* (2012) criteria:
CR1 (single/multiple OTUs with museum numbers): A single specimen. Full Museum data in the reference above.
CR2 (apomorphy-based or phylogenetic analysis): Combination of diagnostic characters.
CR3 (agreement of morphology and molecular data): Reliably assigned to Aderidae.
CR4 (detailed locality and stratigraphy data provided): Locality and stratigraphy data provided in the original paper, double-checked for accuracy with The Paleobiology Database (https://paleobiodb.org/).
CR5 (radioisotopic age or numeric age references given): Age derived from The Paleobiology Database (https://paleobiodb.org/).
Additional fossils of similar age: *Cratoatractocerus grimaldi* Wolf-Schwenninger, 2011 assigned reliably to Lymexylidae, i.e. sister group of Aderidae, based on apomorphies and set of diagnostic characters was described by Wolf-Schwenninger (2011) from the deposit of Crato Formation, Brazil, 122.5-112.0 Ma. The fossil fulfills Parham *et al.* (2012) criteria CR1 to CR5 and dates the same node as the aderid fossil listed above.

Fossil Calibration 27:
Taxon: *Alphitopsis initialis*
Calibrated stem: Tenebrioninae
Geological deposit: Beipiao City, Yixian Formation, China
Minimum age: 125.5 Ma
Reference: Kirejtshuk *et al*. (2012)
Justification of Parham *et al*. (2012) criteria:
CR1 (single/multiple OTUs with museum numbers): A single specimen. Full Museum data in the reference above.
CR2 (apomorphy-based or phylogenetic analysis): Combination of diagnostic characters.
CR3 (agreement of morphology and molecular data): Reliably assigned to Tenebrioninae.
CR4 (detailed locality and stratigraphy data provided): Locality and stratigraphy data provided in the original paper, double-checked for accuracy with The Paleobiology Database (https://paleobiodb.org/).
CR5 (radioisotopic age or numeric age references given): Age derived from The Paleobiology Database (https://paleobiodb.org/).

Fossil Calibration 28:
Taxon: *Idgiaites jurassicus*
Calibrated stem: Prionoceridae
Geological deposit: Daohugou, Nei Mongol, China
Minimum age: 157.3 Ma
Reference: Liu *et al.* (2015)
Justification of Parham *et al.* (2012) criteria:
CR1 (single/multiple OTUs with museum numbers): A single specimen. Full Museum data in the reference above.
CR2 (apomorphy-based or phylogenetic analysis): Combination of diagnostic characters.
CR3 (agreement of morphology and molecular data): Reliably assigned to Prionoceridae.
CR4 (detailed locality and stratigraphy data provided): Locality and stratigraphy data provided in the original paper, double-checked for accuracy with The Paleobiology Database (https://paleobiodb.org/).
CR5 (radioisotopic age or numeric age references given): Age derived from The Paleobiology Database (https://paleobiodb.org/).

Fossil Calibration 29:
Taxon: *Paracretocateres bellus*
Calibrated stem: Lophocaterinae
Geological deposit: Huangbanjigou, Yixian Formation, China
Minimum age: 125.5 Ma
Reference: Yu *et al.* (2015)
Justification of Parham *et al*. (2012) criteria:
CR1 (single/multiple OTUs with museum numbers): Multiple specimens. Full Museum data in the reference above.
CR2 (apomorphy-based or phylogenetic analysis): Combination of diagnostic characters.
CR3 (agreement of morphology and molecular data): Reliably assigned to Lophocaterinae.

CR4 (detailed locality and stratigraphy data provided): Locality and stratigraphy data provided in the original paper, double-checked for accuracy with The Paleobiology Database (https://paleobiodb.org/).
CR5 (radioisotopic age or numeric age references given): Age derived from The Paleobiology Database (https://paleobiodb.org/).

Fossil Calibration 30:
Taxon: *Jurorhizophagus alienus*
Calibrated stem: Monotomidae
Geological deposit: Daohugou, Nei Mongol, China
Minimum age: 157.3 Ma
Reference: Cai *et al.* (2015)
Justification of Parham *et al.* (2012) criteria:
CR1 (single/multiple OTUs with museum numbers): A single specimen. Full Museum data in the reference above.
CR2 (apomorphy-based or phylogenetic analysis): Combination of diagnostic characters.
CR3 (agreement of morphology and molecular data): Reliably assigned to Monotomidae.
CR4 (detailed locality and stratigraphy data provided): Locality and stratigraphy data provided in the original paper, double-checked for accuracy with The Paleobiology Database (https://paleobiodb.org/).
CR5 (radioisotopic age or numeric age references given): Age derived from The Paleobiology Database (https://paleobiodb.org/).

Fossil Calibration 31:
Taxon: *Cretoprionus liutiaogouensis*
Calibrated stem: Prioninae+Parandrinae
Geological deposit: Liutiaogou, Yixian Formation, China
Minimum age: 122.5 Ma
Reference: Wang *et al*. (2013)
Justification of Parham *et al.* (2012) criteria:
CR1 (single/multiple OTUs with museum numbers): A single specimen. Full Museum data in the reference above.
CR2 (apomorphy-based or phylogenetic analysis): Presence of apomorphies (consultation with Petr Švácha).
CR3 (agreement of morphology and molecular data): Reliably assigned to Prioninae+Parandrinae.
CR4 (detailed locality and stratigraphy data provided): Locality and stratigraphy data provided in the original paper, double-checked for accuracy with The Paleobiology Database (https://paleobiodb.org/).
CR5 (radioisotopic age or numeric age references given): Age derived from The Paleobiology Database (https://paleobiodb.org/).

Fossil Calibration 32:
Taxon: *Mesopachymerus antiquus*
Calibrated stem: Bruchinae
Geological deposit: Canadian amber, Grassy Lake, Canada

Minimum age: 70.6 Ma
Reference: Poinar (2005)
Justification of Parham *et al.* (2012) criteria:
CR1 (single/multiple OTUs with museum numbers): A single specimen. Full Museum data in the reference above.
CR2 (apomorphy-based or phylogenetic analysis): Presence of apomorphies.
CR3 (agreement of morphology and molecular data): Reliably assigned to Bruchinae.
CR4 (detailed locality and stratigraphy data provided): Locality and stratigraphy data provided in the original paper, double-checked for accuracy with The Paleobiology Database (https://paleobiodb.org/).
CR5 (radioisotopic age or numeric age references given): Age derived from The Paleobiology Database (https://paleobiodb.org/).

Fossil Calibration 33:
Taxon: multiple fossils
Calibrated stem: Nemonychidae
Geological deposit: Karatau-Mikhailovka, Kazakhstan
Minimum age: 157.3 Ma
Reference: Legalov (2013)
Justification of Parham *et al.* (2012) criteria:
CR1 (single/multiple OTUs with museum numbers): Some species with a single specimen, others with multiple specimens. Full Museum data in the reference above.
CR2 (apomorphy-based or phylogenetic analysis): Presence of apomorphies (consultation with Steve Davis).
CR3 (agreement of morphology and molecular data): Reliably assigned to Nemonychidae.
CR4 (detailed locality and stratigraphy data provided): Locality and stratigraphy data provided in the original paper, double-checked for accuracy with The Paleobiology Database (https://paleobiodb.org/).
CR5 (radioisotopic age or numeric age references given): Age derived from The Paleobiology Database (https://paleobiodb.org/).
Additional fossils of similar age: *Talbragarus averyi* Oberprier & Oberprier (2012) was described from Talbragar Fossil Fish Beds, Australia (157.3–152.1 Ma), and reliably assigned to Nemonychidae based on combination of diagnostic characters. The fossil fulfills Parham *et al.* (2012) criteria CR1 to CR5.

Fossil Calibration 34:
Taxon: *Cylindrobrotus pectinatus*
Calibrated stem: Scolytinae
Geological deposit: Lebanese amber, Lebanon
Minimum age: 122.5 Ma
Reference: Kirejtshuk *et al*. (2009)
Justification of Parham *et al*. (2012) criteria:
CR1 (single/multiple OTUs with museum numbers): A single specimen. Full Museum data in the reference above.
CR2 (apomorphy-based or phylogenetic analysis): Presence of apomorphies.
CR3 (agreement of morphology and molecular data): Reliably assigned to Scolytinae.

CR4 (detailed locality and stratigraphy data provided): Locality and stratigraphy data provided in the original paper, double-checked for accuracy with The Paleobiology Database (https://paleobiodb.org/).
CR5 (radioisotopic age or numeric age references given): Age derived from The Paleobiology Database (https://paleobiodb.org/).
Additional fossils of similar age: *Microborus inertus* Cognato & Grimaldi (2009) was described from Burmese amber, Myanmar, 99.6-93.5 Ma and reliably assigned to Scolytinae based on apomorphies. The fossil fulfills Parham et al. (2012) criteria CR1 to CR5.

References to additional fossils not listed in the main paper:

Bai, M., Krell, F.T., Ren, D. & Yang, X. (2010) A new, well-preserved species of Glaresidae (Coleoptera: Scarabaeoidea) from the Jehol Biota of China. *Acta Geologica Sinica (English Edition)* **84**(4), 676–679.

Cognato, A.I. & Grimaldi, D. (2009) 100 million years of morphological conservation in bark beetles (Coleoptera: Curculionidae: Scolytinae). *Systematic Entomology* **34**, 93–100.

Kirejtshuk, A.G. & Poinar, G. Jr. (2013) On the systematic position of the genera *Lepiceroides* gen. n. and *Haplochelus*, with notes on the taxonomy and phylogeny of the Myxophaga (Coleoptera). Pp. 55–69. In: Azar, D., Engel, M.S., Jarzembowski, E., Krogmann, L., Nel, A. & Santiago-Blay, J. (eds) *Insect Evolution in an Amberiferous and Stone Alphabet. Proceedings of the 6th International Congress on Fossil Insects, Arthropods and Amber.* Brill, Leiden – Boston.

Liu, M., Zhao, Y.Y., Ren, D. (2008) Discovery of three new mordellids (Coleoptera, Tenebrionoidea) from the Yixian Formation of western Liaoning, China. *Cretaceous Research* **29**, 445-450.

Oberprier, R.G. & Oberprier, S.K. (2012) *Talbragarus averyi* gen. et sp. n., the first Jurassic weevil from the southern hemisphere (Coleoptera: Curculionoidea: Nemonychidae). *Zootaxa* **3478**, 256–266.

Peris, D. & Ruzzier, E. (2013) A new tribe, new genus, and new species of Mordellidae (Coleoptera: Tenebrionoidea) from the Early Cretaceous amber of Spain. *Cretaceous Research*, **45**, 1–6.

Ponomarenko, A.G. (1993) Two new species of Mesozoic dysticoid [sic!] beetles from Asia. *Paleontological Journal* **27**(1A), 182–191.

Wolf-Schwenninger, K. (2011) The oldest fossil record of Lymexylidae (Insecta: Coleoptera) from the Lower Cretaceous Crato Formation of Brazil. *Insect Systematics & Evolution* **42**, 205–212.

CHAPTER 2

Seidel, M., Sýkora, V., Leschen, R. A. B., & Fikáček, M. Systematics and biogeography of the Southern Hemisphere endemic Cylominae beetles (Coleoptera: Hydrophilidae) (manuscript draft).

MS, VS, MF and RL performed the field work; MS performed the principal laboratory work and molecular phylogenetic analyses; MS, VS and MF run the biogeography analyses; MS and MF drafted the manuscript, all authors contributed to the writing.

Systematics and biogeography of the Southern Hemisphere endemic Cylominae beetles (Coleoptera: Hydrophilidae)

Matthias Seidel[1,2*], Vít Sýkora[1], Richard Leschen[3] & Martin Fikáček[2,1*]

[1]Department of Zoology, Faculty of Science, Charles University, Prague, Czech Republic

[2]Department of Entomology, National Museum, Prague, Czech Republic

[3]Manaaki Whenua, New Zealand Arthropod Collection, Auckland, New Zealand

*corresponding authors

Abstract

Cylominae is an enigmatic subfamily of water scavenger beetles (Coleoptera: Hydrophilidae) with a conspicuous Southern Hemisphere distribution. Here we present the first comprehensive molecular phylogeny of this subfamily and explore the historical biogeography and processes that led to the current disjunct distribution of the group in Australia, New Zealand, austral South America, and South Africa. Our results reveal the subfamily to consist of two principal clades whose reciprocal monophyly is supported by larval morphology; these clades are re-instated as tribes Cylomini **stat. nov**. (14 genera) and Andotypini **stat. nov.** (containing 9 genera including *Thomosis* Broun, 1904, **stat. nov.**). Three genera from New Zealand remain undescribed. Our study demonstrates that Cylominae originated in the Early Cretaceous in temperate southern Gondwana and subsequently reached their current distribution by a combination of vicariance and long-distance dispersal events. Most interestingly, the presence of the subfamily in South Africa is revealed as a result of a long-distance dispersal postdating the separation of the African continent from Southern Gondwana by more than 50 million years. The New Zealand fauna originated by a mixture of vicariance and long distance dispersal, all genera arriving prior to the Oligocene bottleneck.

Introduction

The Southern Hemisphere distribution of notable plants and animals, such as southern beech (*Nothofagus*), *Hebe* (now *Veronica*) bushes, ratite birds, velvet worms and others, immediately reminds us of the ancient supercontinent Gondwana and its break-up into the continents as we know them today. For a long time vicariance was the dominant explanation for disjunct distribution patterns (e.g. Brundin 1966, Heads 2016) but in the last two decades many studies have shown a mix of dispersal and vicariance explanations for Gondwanan distributions (e.g. de Quieroz 2005, Sanmartín & Ronquist 2004, McCulloch et al. 2016, Renner et al. 2010). Still today molecular studies, dated based on fossil evidence, highlight Southern Hemisphere vicariant patterns i.e. in stoneflies (Krosch & Crantson 2013) or some Southern Hemisphere lucanids (Kim & Farrel 2015). Studies concerning Gondwanan biogeography often lack crucial taxa in their sampling, biogeographic analyses to determine the direction of dispersal and, more importantly, reliable fossils for dating. Therefore, those studies often only imply biogeographic scenarios rather than testing them. One such lineage with an "obvious Gondwana pattern" is the hydrophilid subfamily Cyclominae that has a disjunct Southern Hemisphere distribution pattern and an origin estimated in the Cretaceous (Bloom et al. 2014). Most genera and species are found in New Zealand and Australia, four genera in South America and one in South Africa. If this distribution is caused by vicariant events through break up of Gondwana the phylogenetic relationships must have followed this sequence of events (synthesis of events after Sanmartín & Ronquist 2004): (1) 135 million years ago (Mya) – separation of South America and Southern Africa through opening of the South Atlantic Ocean (e.g. Scotese et al. 1988, Gheerbrant & Rage 2006); (2) 90 Mya – separation of Australia and Antarctica, but connected via Tasmania (Sanmartin & Ronquist, 2004); (3) 80 Mya – separation of Zealandia and East Gondwana through opening of the Tasman Sea (McLoughlin 2001); (4) 55 Mya – drowning of Weddellian Isthmus land bridge between South America and Antarctic Peninsula (Reguero et al 2014) and start of biotic separation of Australia and Antarctica (Woodburne & Case 1996); (5) 34 Mya – separation of South America and Antarctica through opening of the Drake passage and full glaciation of Antarctica (e.g. Livermore et al. 2006; Pross et al. 2012; Houben et al. 2019).

Taxonomically, Cylominae were until recently treated as an assemblage of basal Sphaeridiinae lineages. The first considerable attempts to unite the group were those by Orchymont (1916, 1919, 1933) who joined mainly New Zealand hydrophilids with a few Australian and Chilean genera in the tribe Rygmodini Orchymont, 1916 (= Cylominae Zaitzev, 1908). Hansen (1990, 1991) added four more Australian genera and redistributed the genera in six different tribes based on the first morphology-based phylogenetic analysis: Sperchopsini (*Anticura* Spangler, 1979 and *Cylomissus* Broun, 1903), Coelostomatini (*Adolopus* Sharp, 1884 and *Cyloma* Sharp, 1872), Borborophorini (*Borborophorus* Hansen, 1990 and *Petasopsis* Hansen, 1990), Andotypini (*Andotypus* Spangler, 1979 and *Coelostomopsis* Hansen, 1990), Tormissini (*Tormissus* Broun, 1893, *Tormus* Sharp, 1884, *Afrotormus* Hansen, 1999, *Exydrus* Broun, 1886 and *Hydrostygnus* Sharp, 1884) and Rygmodini (*Cylorygmus* Orchymont, 1933, *Pseudorygmodus* Hansen, 1999, *Saphydrus* Sharp, 1884, *Eurygmus* Hansen, 1990, *Pseudohydrobius* Blackburn, 1898, *Rygmostralia* Orchymont, 1933 and *Rygmodus* White, 1846). In their landmark study, Short & Fikáček (2013) provided the first molecular dataset containing eight genera of the subfamily Cylominae: *Adolopus*, *Borborophorus*, *Coelostomopsis*, *Cyloma*, *Cylomissus*, *Hydrostygnus*, *Rygmodus* and *Saphydrus.* They revealed that all of them group in a monophyletic clade sister to the Sphaeridiinae and were hence transferred in a reinstated separate subfamily Rygmodinae (now Cylominae). The limited genus sampling did not provide enough evidence for keeping Hansen's (1991) tribes and were therefore synonymized under Rygmodinae (Short & Fikáček 2013). *Afrotormus* and *Tormus* (Short & Fikáček 2013, Fikáček et al. 2013), and *Pseudorygmodus* (Fikáček & Vondráček 2014) were removed from the subfamily based on the molecular data supported by adult and larval morphology. Recent studies added *Andotypus*, *Cylorygmus*, *Anticura*, *Exydrus*, *Tormissus*, *Pseudohydrobius* and *Rygmostralia* to the list of sequenced cylomine genera (McKenna et al. 2014, Minoshima et al. 2015, Gunter et al. 2016), but did not re-analyze the phylogeny of the subfamily in detail. Most recently, the South African *Relictorygmus* Seidel et al. 2018 and the New Zealand *Enigmahydrus* Seidel et al. (in prep.) were added to the subfamily Cylominae.

In this study, we address three questions: 1) Are Cylominae a Gondwanan group that tracks the subsequent break-up of the southern supercontinent? 2) Are New Zealand cylomines old paleoendemics or more recent colonizers? and 3) Is there a support for Hansen's (1991) tribal classification within the subfamily? To answer these questions,

we assembled the most comprehensive molecular dataset for the group containing 96% of all genera and 71% of all species of the subfamily.

Material and methods

Taxon sampling

The molecular study is based on specimens collected by the Fikáček lab between 2013 and 2017 in Chile, New Zealand and South Africa. We also included specimens from Australia supplied by CSIRO through Nicole Gunter (Cleveland Museum of Natural History, USA). Our sampling includes 23 of 24 genera of the Cylominae including three undescribed ones, and a total of 60 of 84 species preliminarily recognized in the subfamily (Seidel & Fikáček, unpubl.). Our sampling covers most species occurring in New Zealand (82%), austral South America (60%) and Africa (1 sp., 50%). Australian species are only represented by a single species per genus (6 spp. in total, 37.5%). South American, South African and Australian species were identified according to the published revisions (Hansen 1991, 1997; Fikáček et al. 2014; Seidel et al. 2018). The New Zealand fauna is a subject of ongoing revision (Seidel & Fikáček, unpubl.) with most species undescribed. We used the dataset of 263 sequenced specimens of New Zealand Cylominae covering all morphospecies available to us in DNA-grade to identify candidate species clades; the morphology of the representatives of these clades was subsequently examined and clades showing at least some morphological differences were considered as potential species. This delimitation will be reconfirmed in the prepared taxonomic studies (Seidel & Fikáček, unpubl.). For the final analysis, each species was represented by a single specimen. In few cases, we combined sequences of multiple conspecific specimens in order to reduce gaps in the concatenated dataset. Collecting data on all specimens used can be found in the Supplementary Table S1. All sequenced New Zealand specimens are currently stored in the National Museum Prague, Czech Republic and will be deposited in the New Zealand Arthropod Collection (Auckland, New Zealand).

DNA extraction and sequencing

Total genomic DNA was extracted using the Qiagen Blood and Tissue DNA extraction kit following the manufacturer's instructions. Eight gene fragments were amplified using

polymerase chain reaction (PCR): 12S rDNA (350 bp), 16S rDNA (569 bp), 18S rDNA (1856 bp), 28S rDNA (1075 bp), cox1-3' mtDNA (796 bp), cox1-5' mtDNA (640 bp), topoisomerase nDNA (632 bp), and H3 nDNA (326 bp). The 18S sequence was composed of three smaller fragments amplified and sequenced separately. See Supplementary Table S2 for the list of primers and the PCR amplification programs. Sanger sequencing was performed by Macrogen Europe (Amsterdam, The Netherlands). Sequences obtained in this study are listed in the Supplementary Table S4 and the sequences of outgroups adopted from Toussaint and Short (2018) are listed in Supplementary Table S5.

Sequence editing and phylogenetic analyses

Sequences were edited in Geneious 9.1.3 (Kearse et al. 2012). Edited sequences were aligned using first the Muscle and subsequently the ClustalW algorithms as implemented in Geneious, using the default settings.

The concatenated dataset has a length of 6250 bp with 26% of missing data in the Cylominae and 44.3% of missing data in outgroups. The dataset was divided into partitions by genes; protein-coding genes were subdivided by codon position; in total, 16 partitions were defined. Substitution models were tested in PartitionFinder2 (version 2.1.1) (Lanfear et al. 2016) on the CIPRES Science Gateway (Miller et al. 2010); the MrBayes block with the best-fitting models for each partition is listed in Supplementary Table S6. The phylogenetic reconstruction and divergence dating were conducted in MrBayes 3.2.6 (Ronquist et al. 2012) on the CIPRES Science Gateway (Miller et al. 2010). All analyses used two runs and four chains running for 30 million generations, with trees sampled every 1000 generations. Convergence of both runs was checked in TRACER 1.7 (Rambaut et al. 2018). Due to long initial phase until convergence, we used a conservative burn-in of 50% in all analyses. The consensus trees were further analyzed in FigTree v1.4.3 (Rambaut 2012).

Divergence dating

Our dating analysis used eight fossils to constrain the age of the selected nodes; their ages were incorporated using the uniform, exponential and lognormal distribution as specified

in Supplementary Table S3. The uniform distribution analysis, which we consider as the most conservative since it only requires fossil age as priors, followed the setting used by Bloom et al. (2014) with the following differences: (1) we used the highest value of the 95% credibility interval of the crown age of the Hydrophiloidea s. str. (214.68 Mya) adopted from Toussaint et al. (2016) as the maximum age for *Protochares brevipalpis*, *Helophorus paleosibiricus*, *Hydrochara* sp. and *Baissalarva hydrobioides*; (2) we replaced *Crenitulus paleodominicus* with the much older fossil of *Cretocrenis burmanicus* Fikáček et al. 2017, setting its minimum age at 99 Mya (Fikáček et al. 2017) and the maximum age at 214.68 Mya; (3) we constrained the age of the stem *Hydrobiomorpha* with *Hydrobiomorpha eopalpalis*, setting its minimum age at 47 Mya and maximum age at 214.68 Mya; (4) we used 146 Mya (the maximum age of the deposit with *Baissalarva*) as the maximum age for *Limnoxenus olenus*; (5) we omitted the *Cercyon* fossil. The tree was rooted with *Spercheus* in all analyses.

Biogeography analyses

For the reconstruction of the historical biogeography of Cyclominae, we used the time tree produced by the divergence dating analysis with uniform priors, from which all non-Cyclominae outgroups were removed. We reduced the Cyclominae tree to one species per genus except for *Cyloma* for which each principal clade was retained in the analysis. The distribution ranges divided the Southern Hemisphere into principal continents as follows: A – South America; B – South Africa; C – Australia; D – New Zealand; E – Antarctica. We used the time-stratified analysis with the time periods defined as follows: (1) 34–0 Mya: the period when temperate South America separates from Antarctica and Antarctica becomes fully covered by glaciers; (2) 55–34 Mya: drowning of Weddellian Isthmus land bridge between South America and Antarctic Peninsula and start of biotic separation of Australia and Antarctica complete biotic separation of Australia and Antarctica; (3) 80–55 Mya: New Zealand completely separates from the rest of Gondwana; (4) 90–80 Mya: Australia separates from Antarctica but stays connected with it by Tasmania; (5) 135–90 Mya: temperate Southern America and Southern Africa get separated. Dispersal probabilities were set arbitrarily to reflect the paleogeography as follows: 1.0 for adjacent continental areas; 0.2 for non-adjacent areas (e.g. Antarctica and Australia connected via island chain); 0.05 for areas separated by wide ocean (e.g. New Zealand and Australia

today); 0.000001 when dispersal is not possible (i.e. via completely glaciated Antarctica; we followed the BioGeoBEARS manual in setting extremely low instead of zero probabilities (Matzke 2015)). We constrained South Africa in areas allowed with 0 in the time period between 90 and 135 Mya to prevent unrealistic wide areas including Africa after its complete separation 135 Mya. For the complete setting of the analyses (matrices of Areas allowed and Dispersal multipliers), see Supplementary Table S7. The historical biogeography analyses were carried out with the R package BioGeoBEARS (Matzke 2014). The package implements three models: DEC, DIVALIKE and BAYAREALIKE; each of them may include an additional parameter *j* representing the founder event (i.e. speciation following the long-distance dispersal). Hence, six different models were used and tested.

Results

Phylogenetic analyses

The Bayesian analysis corroborated the tribal topology of Short & Fikáček (2013) and Toussaint & Short (2018), including the strongly supported (posterior probability, pp=1.0) monophyly of Cylominae and its sister position to the Sphaeridiinae. The non-dated and time-calibrated analyses resulted in nearly identical topologies, only with slight differences in the internal topology in the genus *Cyloma* (with *C. guttulatus* revealed as sister to other species in the non-dated analysis) and in the position of *Borborophorus* – it is placed as a weakly supported sister group to New Genus 1 in the non-dated analysis whereas as a weakly supported sister clade to New genus 1 + New Genus 2 in the time-calibrated one. In both cases, the topology revealed in the time-calibrated analysis corresponds better to the morphology and is followed here. All main clades of Cylominae were resolved with strong support (pp>0.99) and none of the revealed clades is geographically limited; all of them group genera from Chile, Australia and New Zealand. The basal-most divergence splits Cylominae into two major clades: (1) a species-poor assemblage (13 recent species) of genera originally classified as Tormissini, Andotypini and Southern Hemisphere Sperchopsini by Hansen (1991), and (2) a species-rich assemblage (ca. 60 species) containing the genera originally classified in Rygmodini, Borborophorini and Southern Hemisphere Coelostomatini by Hansen (1991). The monophyly of both groups is strongly supported by larval morphology (see Discussion)

and both clades are hence re-instated here as tribes Andotypini **stat. nov.** (the species-poor clade) and Cylomini **stat. nov.** (the species-rich clade). The Andotypini clade consists of two sub-clades: the *Cylomissus* group (pp=0.84) containing aquatic genera (Chilean *Anticura* sister to a clade of two New Zealand genera) and the *Andotypus* group (pp=1.0) with early-branching Chilean and Australian clades and a deeply nested New Zealand clade composed of *Tormissus*, *Hydrostygnus*, *Exydrus* and the subantarctic island endemic *Thomosis*. The Cylomini clade subdivides into five clades: the *Saphydrus* group (pp=1.0) contains the only South African representative, *Relictorygmus*, as the earliest-branching clade and the Australian and New Zealand genera *Eurygmus*, *Saphydrus* and *Enigmahydrus* as deeper assemblages. The monotypic *Cylorygmus* represents an isolated lineage well-supported (pp=0.99) as sister to the following Australian and New Zealand principal clades. *Rygmodus* group (pp=1.0) includes four genera including the flower-visiting *Rygmodus* and *Pseudohydrobius*; the New Zealand *Rygmodus* is revealed as sister to the three Australian genera. The *Coelostomopsis*, which was originally placed in Andotypini by Hansen (1991), is revealed as a member inside the *Rygmodus* group. The *Rygmodus* group is sister to the clade formed by the *Cyloma* group (pp=1.0) sister to the *Adolopus* group (pp=0.93). The *Cyloma* group only contains the New Zealand endemic and diverse *Cyloma* whose internal topology corresponds to two former genera *Psephoboragus* Broun, 1893 and *Cyloma* Sharp, 1872 (both were synonymized by Hansen 1997); the position of *Cyloma pictus* confirms the synonymy of *Namostygnus* Broun, 1909 with *Cyloma.* The *Adolopus* group is composed of *Adolopus,* two undescribed genera from New Zealand and the Australian genus *Borborophorus*.

Divergence dating

The relaxed clock model was selected as the best fitting model and used for the MrBayes time tree analysis. The analysis using lognormal priors gave the youngest age estimates, implementing exponential priors led to the oldest estimates, ages revealed by uniform priors were intermediate between lognormal and exponential ones (e.g. stem Cylominae median age being 13 Mya younger in lognormal analysis and 13 Mya older in exponential analysis compared to the uniform estimate) (Table 1). We consider the uniform priors as the most conservative ones: they use the age of the fossil as the minimum age of the clade but do not imply that the clade originated shortly before the fossil occurrence. The Cylominae were estimated to have originated during the Early Cretaceous (ca. 143.6 million years ago, Mya), with diversification of modern clades starting at ca. 114 Mya.

The modern groups of the Andotypini started to diverge in the Late Cretaceous (ca. 86.8 Mya), with the Chilean *Andotypus* and *Anticura* diverging from the New Zealand/Australian sister clades at similar times at the very end of the Late Cretaceous (71.2 Mya and 70.2 Mya, respectively). The modern clades of the Cylomini started to diverge in the middle Cretaceous (ca. 101.5 Mya) and all major subclades diverged until the end of the Cretaceous (between 92.7– 69.8 Mya). The African genus *Relictorygmus* diverged from its sister genera during the Late Cretaceous (ca. 82.1 Mya) and *Cylorygmus* represents the oldest split (92.7 Mya) leading to an extant genus. All generic lineages diverged by the end of the Eocene, and the modern species of the species-rich genera mostly originated during the Miocene to Pliocene (ca. 21–4 Mya).

Biogeography

Of the six models included in BioGeoBEARS, the models BAYAREALIKE and BAYAREALIKE+J performed the worst. The DEC and DIVALIKE models performed better, especially when allowed for the founder event or jump dispersal (DEC+J, DIVALIKE+J) (Table 2). Models not implementing the jump dispersal resulted in reconstructed joint areas that did not exist at the respective time-slice as ancestral for some basal nodes. The DEC+J and DIVALIKE+J models generated almost identical scenarios which only differ in the most probable area inferred for the most recent common ancestor (MRCA) of the Andotypini at 86.8 Mya: DIVALIKE+J inferred South America and DEC+J inferred South America+New Zealand. We follow the DEC+J scenario for our interpretations, since New Zealand remained connected to the other Gondwanan landmasses, including South America at 80 Mya. The area composed of South America, Australia and New Zealand was inferred as the ancestral range of the MRCA of Cylominae; Antarctica was not revealed in any ancestral state. All principal clades of Cylominae originated after the separation of Africa from Gondwana (at ca. 135 Mya) and before the final break-up of the supercontinent at ca. 80 Mya and later. Only the divergence of the *Rygmodus* group (Australia) from the common ancestor of the *Cyloma+Adolopus* groups (New Zealand) corresponds temporarily to the separation of Zealandia from Australia at ca. 80 Mya and may be a vicariant event. Few biogeographical events pre-dated the separation of the respective continents (e.g. the colonization of Australia from South America at the base of the *Andotypus* clade). Six biogeographic events largely post-dated the separation of the respective continents, indicating long-distance over-water dispersal in these lineages. Most notably, the

colonization of Africa by *Relictorygmus* at ca. 80 Mya post-dated the separation of Africa from Gondwana by 40 My. Of the six suggested long-distance dispersals, two lineages (*Enigmahydrus*+*Saphydrus* and *Anticura*) overlap marginally with their 95% credibility intervals from dating with the age New Zealand and East Gondwana split (80 Mya), and can therefore not completely be excluded from a vicariance scenario. The above reconstruction reveals the historical biogeography of Cylominae as very poorly fitting the vicariant model and explains the low values for dispersal (d=0.0) and high values for jump dispersal (j=0.758) revealed in all analyses.

Monophyly of Cylominae

Here we present the first phylogeny with a main focus on the subfamily Cylominae, the smallest subfamily of water scavenger beetles (Bloom et al. 2014) including eight previously not sequenced genera (*Austrotypus, Enigmahydrus, Eurygmus, Relictorygmus* and *Thomosis*, and three undescribed ones). Our Cylominae phylogeny confirms the subfamily as monophyletic with highest support (pp=1.0) and all genera listed in Short and Fikáček (2013) as members of the subfamily, except *Petasopsis* (not available for DNA studies) and *Pseudorygmodus* (transferred to Chaetarthriinae by Fikáček & Vondráček 2014). Furthermore, we discovered three undescribed New Zealand genera and up to 25 new species belonging to Cylominae.

Systematics

Tribe Cylomini stat. nov.

Cylomini Zaitzev, 1908 (type genus: *Cyloma* Sharp, 1872)

=Borborophorini Hansen, 1991 (type genus*:* *Borborophorus* Hansen, 1990; synonymized with Rygmodinae by Short & Fikáček 2013)

=Rygmodini Orchymont, 1916 (type genus: *Rygmodus* White, 1846; synonymized with Cylominae by Seidel et al. 2016)

Composition. 15 genera containing ca. 60 species: *Adolopus, Borborophorus, Coelostomopsis, Cyloma, Cylorygmus, Enigmahydrus, Eurygmus, Petasopsis, Pseudohydrobius, Relictorygmus, Rygmodus, Rygmostralia* and *Saphydrus* and two undescribed ones from New Zealand. The Australian *Petasopsis* was not available in DNA-grade and is provisionally assigned to this tribe based on the presence of the median pit on the mesoventrite, which it shares with *Cyloma* and *Adolopus*; *Petasopsis* is however morphologically very unusual and its position in the subfamily and in Cylomini needs to be ascertained by molecular data.

Synonymies of family-group names. Type genera of all three family-level names (i.e. *Cyloma, Borborophorus* and *Rygmodus*) are revealed as members of the same principal clade which confirms the synonymies proposed previously by Short & Fikáček (2013) and Seidel et al. (2016).

Morphological diagnosis. We could not find synapomorphies in adults, but the monophyly of the tribe is supported by the following larval characters: larval nasale with three to five teeth (five in *Borborophorus, Enigmahydrus, Cylorygmus, Rygmodus* and *Saphydrus*; three in *Cyloma*); mesal part of maxillary stipes with five setae.

Species groups. The ***Saphydrus* group** is the earliest diverging lineage of Cylomini; it contains four genera. The only African cylomine lineage, *Relictorygmus*, is the earliest diverging lineage, followed by the Australian *Eurygmus* and the New Zealand *Saphydrus* and *Enigmahydrus*; the latter two genera are revealed as sister taxa which is supported by the larval morphology (adults of *Enigmahydrus* are unknown; Seidel et al., in prep.): they share the number of teeth of the nasale, the symmetry of labrofrontoclypeus, mandibular morphology and the presence of fine cuticular projections on the dorsal body surface (Seidel et al., in prep.). The larvae of *Eurygmus* and *Relictorygmus* remain unknown.

The ***Cylorygmus* group.** The clade contains a single Chilean species of the genus *Cylorygmus*. It diverged from the Australian/New Zealand ancestors of the *Rygmodus*, *Adolopus* and *Cyloma* groups at ca. 92 Mya. Its morphology is very similar to that of *Relictorygmus* and may largely correspond to the ancestral morphology of the early diverging lineages of Cylomini (for characters see Seidel et al. 2018). Our analyses confirm with high support that *Cylorygmus* and *Relictorygmus* are separate non-sister lineages and reconfirm the establishment of *Relictorygmus* for the African species by Seidel et al. (2018).

The ***Rygmodus* group** is composed of the two flower-visiting genera, *Rygmodus* (New Zealand) and *Pseudohydrobius* (Australia), as well as the Australian *Rygmostralia* and *Coelostomopsis* for which the biology is unknown. *Rygmodus* is the only New Zealand genus of the clade, inferred as colonizing New Zealand ca. 60 Mya by over-water dispersal. Larvae have only been described for *Rygmodus* (Minoshima et al. 2018) and no attempts to compare adult morphology of the four genera were made so far.

The ***Adolopus* group** is a principally New Zealand clade containing four genera, with *Adolopus* being the earliest-diverging and the most species-rich genus in the group. Two new New Zealand genera and the Australian genus *Borborophorus* form a monophyletic clade, which is statistically not supported (pp=0.51). Both new New Zealand genera are morphologically similar to *Adolopus*, sharing the pit-like grove on the mesoventrite. The placement of the Australian *Borborophorus* within the *Adolopus* group is surprising since *Borborophorus* lacks the pit-like groove on the mesoventrite. However, *Borborophorus* bears a series of spine-like setae at the abdominal apex, a character only present in members of the *Adolopus* group in the Cylominae.

The ***Cyloma* group** contains a single New Zealand genus *Cyloma*; it can be easily distinguished from all other Cylominae by antennae with eight antennomeres. The position of *Cyloma* as close to *Adolopus* was already shown in previous studies (e.g. Short & Fikáček 2013) and is supported by the presence of the pit-like groove on the mesoventrite in *Cyloma* and the *Adolopus* group of genera (except *Borborophorus*).

Tribe Andotypini stat. nov.

Andotypini Hansen, 1991 (type genus*: Andotypus* Spangler, 1979)

=Tormissini Hansen, 1991 **syn. nov**. (type genus*: Tormissus* Broun, 1893; previously in synonymy with Cylominae by Short & Fikáček (2013))

Composition. Nine genera containing 14 species: *Andotypus*, *Anticura*, *Austrotypus*, *Cylomissus*, *Exydrus*, *Hydrostygnus, Thomosis*, *Tormissus* and one undescribed genus from New Zealand.

Synonymies of family-group names. The type genera of both family-group names (*Andotypus* and *Tormissus*) belong to the same principal clade, which allows us to synonymize Tormissini under Andotypini.

Morphological diagnosis. We were not able to find synapomorphies in adults, but the monophyly of the tribe is supported by the following larval characters: larval nasale with one or two teeth (one tooth: *Andotypus*, *Austrotypus*, *Cylomissus*, *Tormissus*; two teeth: *Anticura*, *Cylomissus*); mesal part of maxillary stipes with many more than five setae.

Species groups. The ***Cylomissus* group** contains three genera: the Chilean *Anticura* and the New Zealand *Cylomissus* and one undescribed genus. The close relationship of *Cylomissus* and *Anticura* was already suggested by Minoshima et al. (2015) based on morphological characters of larvae. In contrast to Minoshima et al. (2015) who revealed *Anticura* and *Cylomissus* as a paraphyletic assemblage at the base of the *Andotypus* group, our analysis based on a larger set of genes and with more complete taxon sampling reveals the group as a moderately supported monophylum (pp=0.84). All three genera are aquatic, inhabiting submerged moss along stream margins in New Zealand and Chile.

The ***Andotypus* group** contains six genera originally classified in tribes Andotypini and Tormissini by Hansen (1991). The similarity of the genera *Austrotypus* and *Andotypus* with the New Zealand *Tormissus* and related genera was mentioned already by Fikáček et al. (2014). Our data confirm this hypothesis and reveal that South American/Australian *Austrotypus* and *Andotypus* as early diverging lineages and show the New Zealand genera as a strongly supported monophylum sister to *Austrotypus*. The lack of the Peruvian *Austrotypus peruanus* Fikáček, Minoshima & Newton, 2014 for molecular analyses did not allow us to test the monophyly of the genus. We revealed *Tormissus* sensu Hansen (1991) polyphyletic, with *Tormissus guanicola* from New Zealand subantarctic islands being sister to the rest of the New Zealand taxa (genera *Exydrus*+*Hydrostygnus*+*Tormissus*). For this reason, we reinstate the monotypic genus *Thomosis* Broun, 1904 **stat. nov.** as a valid genus name and re-establish the original combination *Thomosis guanicola* Broun for its only species. The New Zealand subclade of the *Andotypus* group of genera is characterized by largely modified adult mouthparts, with a pentagonal mentum, large well sclerotized labrum that is not retracted under the clypeus and mandibles without basal mola (which is otherwise present in all Hydrophilidae), indicating specialized (possibly predatory) feeding habits. The armed

left and bare right epistomal lobe of larvae suggested as a synapomorphy for *Austrotypus* and *Andotypus* by Fikáček et al. (2014) is also present in the larva of *Thomosis* and *Tormissus* (Seidel & Fikáček, unpubl.) and strongly supports the monophyly of the *Andotypus* group.

Discussion

Biogeography of Cylominae

The Cylominae lineage diverged from Sphaeridiinae at 143.6 Mya (124.7–162.5), at a time when Gondwana was already splitting into the East and West Gondwana (sea-floor spreading in the Somali basin was at ca. 165 Mya; McLoughlin 2001, Rabinowitz et al. 1983). At that time, Southern Gondwana had a cool temperate climate (Scotese et al. 1999), i.e. climatic conditions that may have restricted the distribution of most cylomine species (e.g. Fikáček et al. 2014). The modern Cylominae originated at around 114 Mya (95.9–133.6) and were likely widespread in southern Gondwana, including Antarctica. The latter continent was not inferred as ancestral for any node in our analyses but it was interconnected to other continents, and at that time covered by evergreen forests (Brentnall et al. 2005, Cantrill & Poole, 2012); it was the only route between austral South America and Australia/New Zealand until ca. 35 Mya. We assume that Cylominae inhabited Antarctica until the Eocene-Oligocene transition when Antarctica became glaciated (Pross et al. 2012).

The most apparent long-distance dispersal of Cylominae is the presence of *Relictorygmus* in Africa. Southern Africa broke away from the rest of Gondwana by 135 Mya (Sanmartín & Ronquist 2004), ca. 53 million years before the *Relictorygmus* lineage appeared. The presence of the *Relictorygmus* lineage before 135 Mya is excluded irrespective of the dating strategy used. Furthermore, with the molecular evidence of *Relictorygmus* and *Cylorygmus* being separate lineages (as postulated in Seidel et al. 2018), the South America-South Africa disjunct distribution is confirmed impossible. We are not aware of a similar Australia to Africa dispersal of animals during that time, and in beetles that have a similar distribution to cylomines, phylogenetic information is wanting (e.g. camiarine Leiodidae (Newton 1998)).

Our analysis reveals five possible independent long-distance over-water dispersals from/to New Zealand between the Latest Cretaceous and Early Eocene, i.e. in the time when Zealandia was already widely isolated from other continents (Fig. 3). Two lineages dispersed from New Zealand (ancestors of the genera *Anticura* and *Borborophorus*) and three lineages reached New Zealand (ancestors of *Enigmahydrus*+*Saphydrus*, *Rygmodus* and of the New Zealand Andotypini). Divergences between Australian and New Zealand *Sticocladius* midges (Krosch & Cranston 2013) show similar ages to the split between *Borborophorus* and its New Zealand sisters, but the direction of dispersal (to or from New Zealand) has not been reconstructed. Other studies in further invertebrate groups such as stoneflies (McGulloch et al. 2016) show generally much younger ages of splits between New Zealand and Australian clades, compared to the Cylominae.

The dispersal event of *Anticura* to South America coincides with the arrival of *Andotypus* in South America, with the only difference that *Anticura* had a New Zealand ancestor. Since the 95% confidence interval of *Anticura* partly overlaps with the split of New Zealand from Gondwana, it is also possible that the taxonomic distribution is of vicariant origin. Therefore, the South American Andotypini might share a similar underlying pathway of reaching current-day Chile. Similarly, a vicariant scenario cannot be excluded as an explanation for the split from the ancestor of New Zealand *Enigmahydrus*+*Saphydrus,* at a time (ca. 70 Mya) when New Zealand and Australia were separating and were much closer to each other than nowadays.

The divergence of the *Rygmodus* group from the ancestor of the *Adolopus* and *Cyloma* groups coincides with the time when New Zealand separated from Australia (ca. 80 Mya; Lawver et al. 1992) and is the only solid example of a vicariance event revealed by our analyses. Both clades resulting from this vicariance were later able to cross the Tasman Sea by over-water dispersal: *Rygmodus* colonized New Zealand from Australia during the Paleocene and *Borborophorus* reached Australia in the early Eocene.

Ancestors of all New Zealand genera reached Zealandia before the Oligocene bottleneck (36–24 Mya; Cooper & Cooper 1995) that was caused by the significant reduction of continental land area (Landis et al. 2008). Most speciation events within the New Zealand genera seem to have happened before ca. 21 Mya and could be correlated with the availability of new habitats and niches after the Oligocene drowning. Similar speciation times have been observed in stoneflies (McCulloch et al. 2016), chironomid midges

(Krosch & Cranston 2013) and pettalid harvestmen (Giribet et al. 2011). The appearance of New Zealand cylomine lineages before the Oligocene drowning and the diversification thereafter indicates them to be paleoendemic and renders a scenario of a complete submergence of the islands very unlikely. A similar conclusion was drawn by Giribet & Boyer (2010) who estimated an early arrival in New Zealand and survival of the Oligocene drowning of soil-dwelling invertebrates such as Pettalidae (mite harvestmen), *Craterostigmus* (centipedes), *Paralamyctes* (stone centipedes) and Peripatopsidae (velvet worms).

Conclusions

Our study confirms the monophyly of Cylominae and reveals two strongly supported principal clades re-instated as tribes Cylomini and Andotypini; the monophyly of both clades is supported by larval morphological characters. Our phylogenetic analyses and studies of morphological characters reveal that Cylominae include in total 24 genera and 84 modern species (of these, three genera and 30 species are still undescribed). No fossil species are known for Cylominae so far, and may be difficult to recognize due to the absence of clear synapomorphies for the subfamily and the relatively simple (likely plesiomorphic) morphology of many of its genera. The only fossils that are currently known to us and could represent Cylominae are impression fossils from Foulden Maar (New Zealand) with an age of ca. 23 Mya (Kaulfuss et al. 2014). Those fossils might represent members of the *Adolopus* or *Cyloma* group, but will unlikely be of use for improving the dating analysis of the subfamily through their young age and bad preservation.

Our results confirm the separate status of *Relictorygmus* and *Cylorygmus* (Seidel et al. 2018) and disprove Hebauer's (2002) assumption about the disjunct distribution of *Cylorygmus* in Chile and South America. The presence of Cylominae in South Africa can only be explained by long-distance over-water dispersal from Australia or adjacent areas and does not follow the traditional Gondwanan vicariance pattern. In a similar way, long distance dispersals from/to New Zealand best explain the observed distribution of at least three younger lineages (New Zealand Andotypini, *Rygmodus* and *Borborophorus*). Older divergences mostly pre-dated the break-up of Eastern Gondwana, and a single divergence (*Rygmodus* group from the *Cyloma*+*Adolopus* groups) coincides with the tectonic events

(separation of New Zealand from Gondwana) and may be explained by vicariance. The pre-Oligocene appearance and post-Oligocene diversification/radiation of some New Zealand lineages refutes the idea of a complete drowning of Zealandia. The phylogenetic position of two taxa, *Petasopsis brevitarsis* and *Austrotypus peruanus*, needs to be tested in the future.

Acknowledgements

We are grateful to Nicole Gunter (Cleveland Museum of Natural History, Cleveland, USA) and Dominik Vondráček (National Museum, Prague) for providing part of the Cylominae sequences used in this study. We thank Jiří Hájek (National Museum, Prague, Czech Republic), Peter Hlaváč (Prague, Czech Republic), Crystal Maier (Museum of Comparative Zoology, Cambridge, MA, USA), David Sadílek (Charles University, Prague, Czech Republic), Jiawei Shen (Shanghai Normal University, Shanghai, China) and Matt Gimmel (Santa Barbara Museum of Natural History, Santa Barbara, CA, USA) for collecting New Zealand Hydrophilidae for our study. This work was supported by the European Union's Horizon 2020 research and innovation program under the Marie Skłodowska-Curie grant agreement No. 642241 to M. Seidel and by the Ministry of Culture of the Czech Republic (DKRVO 2019-2023/5.I.a, National Museum, 00023272) to Martin Fikáček. The work of M. Seidel and V. Sýkora at the Department of Zoology, Charles University, Prague was partly supported by grant SVV 260 434 /2019. R. Leschen was funded in part by core funding from the Crown Research Institute from the Ministry of Business, Innovation and Employment's Science and Innovation Group.

Author contribution

MS, VS, MF and RL performed the field work; MS performed the principal laboratory work and molecular phylogenetic analyses; MS, VS and MF run the biogeography analyses; MS and MF drafted the manuscript, all authors contributed to the writing.

References.

Bloom, D. D., Fikáček, M., & Short, A. E. Z. (2014). Clade age and diversification rate variation explain disparity in species richness among water scavenger beetle (Hydrophilidae) lineages. *PLoS One*, 9(6), e98430.

Brentnall, S. J., Beerling, D. J., Osborne, C. P., Harland, M., Francis, J. E., Valdes, P. J., & Wittig, V. E. (2005). Climatic and ecological determinants of leaf lifespan in polar forests of the high CO_2 Cretaceous 'greenhouse' world. *Global Change Biology*, 11(12), 2177-2195.

Brundin, L. 1966. Transantarctic relationships and their significance, as evidenced by chironomid midges, with a monograph of the subfamilies Podonominae and Aphroteniinae and the Austral Heptagyiae. *Kungliga Svenska Vetenskapsakademiens Handlingar*, 11: 1–472.

Cantrill, D. J., & Poole, I. (2012). *The vegetation of Antarctica through geological time*. Cambridge University Press.

Cooper, A., & Cooper, R. A. (1995). The Oligocene bottleneck and New Zealand biota: genetic record of a past environmental crisis. *Proceedings of the Royal Society of London. Series B: Biological Sciences*, 261(1362), 293-302.

Gunter, N. L., Weir, T. A., Slipinksi, A., Bocak, L., & Cameron, S. L. (2016). If dung beetles (Scarabaeidae: Scarabaeinae) arose in association with dinosaurs, did they also suffer a mass co-extinction at the K-Pg boundary?. *PloS one*, 11(5), 1-47.

Fikáček, M., Minoshima, Y. N., & Newton, A. F. (2014). A review of Andotypus and Austrotypus gen. nov., rygmodine genera with an austral disjunction (Hydrophilidae: Rygmodinae). *Annales Zoologici.* 64(4): 557-596.

Fikáček, M., Minoshima, Y. N., Komarek, A., Short, A. E., Huang, D., & Cai, C. (2017). Cretocrenis burmanicus, the first Mesozoic amber inclusion of a water scavenger beetle (Coleoptera: Hydrophilidae). *Cretaceous Research*, 77, 49-55.

Fikáček, M., Minoshima, Y., Vondráček, D., Gunter, N., & Leschen, R. A. (2013). Morphology of adults and larvae and integrative taxonomy of Southern Hemisphere genera Tormus and Afrotormus (Coleoptera: Hydrophilidae). *Acta Entomologica Musei Natioalis Pragae*, 53(1).

Fikáček, M., & Vondráček, D. (2014). A review of Pseudorygmodus (Coleoptera: Hydrophilidae), with notes on the classification of the Anacaenini and on distribution of genera endemic to southern South America. *Acta Entomologica Musei Nationalis Pragae*, 54(2), 479-514.

Gheerbrant, E., & Rage, J. C. (2006). Paleobiogeography of Africa: how distinct from Gondwana and Laurasia?. *Palaeogeography, Palaeoclimatology, Palaeoecology*, 241(2), 224-246.

Giribet, G., & Boyer, S. L. (2010). 'Moa's Ark' or 'Goodbye Gondwana': is the origin of New Zealand's terrestrial invertebrate fauna ancient, recent, or both?. *Invertebrate Systematics*, 24(1), 1-8.

Giribet, G., Sharma, P.P., Benavides, L.R., Boyer, S.L., Clouse, R.M., de Bivort, B.L., Dimitrov, D., Kawauchi, G.Y., Murienne, J. & Schwendinger, P.J. (2011). Evolutionary and biogeographical history of an ancient and global group of arachnids (Arachnida: Opiliones: Cyphophthalmi) with a new taxonomic arrangement. *Biological Journal of the Linnean Society*, 105, 92–130.

Hansen, M. (1990). Australian Sphaeridiinae (Coleoptera: Hydrophilidae): A taxonomic outline with descriptions of new genera and species. *Invertebrate Taxonomy*, 4, 317–395.

Hansen, M. (1991). The hydrophiloid beetles. Phylogeny, classification and a revision of the genera (Coleoptera, Hydrophiloidea). *Biologiske Skrifter,* 40, 1–367.

Hansen M (1997). Synopsis of the endemic New Zealand genera of the beetle subfamily Sphaeridiinae (Coleoptera: Hydrophilidae). New Zealand Journal of Zoology, 24, 351–370.

Heads, M. (2016). *Biogeography and evolution in New Zealand*. CRC Press.

Hebauer, F. (2002). New Hydrophilidae of the Old World (Coleoptera, Hydrophilidae). *Acta Coleopterologica*, 18(3), 3-24.

Houben, A. J., Bijl, P. K., Sluijs, A., Schouten, S., & Brinkhuis, H. (2019). Late Eocene Southern Ocean cooling and invigoration of circulation preconditioned Antarctica for full-scale glaciation. *Geochemistry, Geophysics, Geosystems,* 20(5), 2214-2234.

Kaulfuss, U., Lee, D. E., Barratt, B. I., Leschen, R. A., Larivière, M. C., Dlussky, G. M., Henderson, I. M. & Harris, A. C. (2015). A diverse fossil terrestrial arthropod fauna from New Zealand: evidence from the early Miocene Foulden Maar fossil lagerstätte. *Lethaia*, 48(3), 299-308.

Kearse, M., Moir, R., Wilson, A., Stones-Havas, S., Cheung, M., Sturrock, S., Buxton, S., Cooper, A., Markowitz, S., Duran, C., Thierer, T., Ashton, B., Meintjes, P. & Drummond, A. (2012). Geneious Basic: an integrated and extendable desktop software platform for the organization and analysis of sequence data. *Bioinformatics*, 28(12), 1647-1649.

Kim, S. I., & Farrell, B. D. (2015). Phylogeny of world stag beetles (Coleoptera: Lucanidae) reveals a Gondwanan origin of Darwin's stag beetle. *Molecular Phylogenetics and Evolution*, 86, 35-48.

Krosch, M., & Cranston, P. S. (2013). Not drowning,(hand) waving? Molecular phylogenetics, biogeography and evolutionary tempo of the 'Gondwanan'midge Stictocladius Edwards (Diptera: Chironomidae). *Molecular Phylogenetics and Evolution*, 68(3), 595-603.

Landis, C. A., Campbell, H. J., Begg, J. G., Mildenhall, D. C., Paterson, A. M., & Trewick, S. A. (2008). The Waipounamu Erosion Surface: questioning the antiquity of the New Zealand land surface and terrestrial fauna and flora. *Geological Magazine*, 145(2), 173-197.

Lanfear, R., Frandsen, P. B., Wright, A. M., Senfeld, T., & Calcott, B. (2016). PartitionFinder 2: new methods for selecting partitioned models of evolution for molecular and morphological phylogenetic analyses. *Molecular Biology and Evolution*, 34(3), 772-773.

Lawver, L. A., Gahagan, L. M., & Coffin, M. F. (1992). The development of paleoseaways around Antarctica. *The Antarctic Paleoenvironment: A Perspective on Global Change: Part One*, 7-30.

Livermore, R., Nankivell, A., Eagles, G., & Morris, P. (2005). Paleogene opening of Drake passage. *Earth and Planetary Science Letters*, 236(1-2), 459-470.

Matzke, N. J. (2014). Model selection in historical biogeography reveals that founder-event speciation is a crucial process in island clades. *Systematic Biology*, 63(6), 951-970.

Matzke, N.J. (2015). BioGeoBEARS [WWW Document] PhyloWiki. http://phylo.wikidot.com/biogeobears#dispersal_multipliers2

McCulloch, G. A., Wallis, G. P., & Waters, J. M. (2016). A time-calibrated phylogeny of Southern Hemisphere stoneflies: Testing for Gondwanan origins. *Molecular Phylogenetics and Evolution*, 96, 150-160.

McKenna, D. D., Farrell, B. D., Caterino, M. S., Farnum, C. W., Hawks, D. C., Maddison, D. R., Seago, A. E., Short, A. E. Z., Newton, A. F. & Thayer, M. K. (2014). Phylogeny and evolution of Staphyliniformia and Scarabaeiformia: forest litter as a stepping stone for diversification of nonphytophagous beetles. *Systematic Entomology*, 40(1), 35-60.

McLoughlin, S. (2001). The breakup history of Gondwana and its impact on pre-Cenozoic floristic provincialism. *Australian Journal of Botany*, 49(3), 271-300.

Miller, M. A., Pfeiffer, W., & Schwartz, T. (2010, November). Creating the CIPRES Science Gateway for inference of large phylogenetic trees. In *2010 gateway computing environments workshop (GCE)* (pp. 1-8). IEEE.

Minoshima, Y. N., Fikáček, M., Gunter, N., & Leschen, R. A. (2015). Larval Morphology and Biology of the New Zealand-Chilean Genera Cylomissus Broun and Anticura Spangler (Coleoptera: Hydrophilidae: Rygmodinae). *The Coleopterists Bulletin*, 69(4), 687-713.

Minoshima, Y. N., Seidel, M., Wood, J. R., Leschen, R. A., Gunter, N. L., & Fikáček, M. (2018). Morphology and biology of the flower-visiting water scavenger beetle genus Rygmodus (Coleoptera: Hydrophilidae). *Entomological science*, 21(4), 363-384.

Newton, A. F. (1998). Phylogenetic problems, current classification and generic catalog of World Leiodidae (including Cholevi- dae). *In*: Giachino, P.M. & Peck, S.B. (Eds.), *Phylogeny and evolution of subterranean and endogean Cholevidae (= Leio- didae Cholevinae). Proceedings of a Symposium (30 August, 1996, Florence, Italy), XX International Congress of Entomology.* Museo Regionale di Scienze Naturali di Torino, Turin, pp. 41–178

Orchymont, A. d'. (1916). De la place que doivent occuper dans la classification les sous-familles des Sphaeridiinae et des Hydrophilinae [Col. Hydrophilidae]. *Bulletin de la Societe entomologique de France*, 21(15), 235-240.

Orchymont, A. d'. (1919). Contribution a l'étude des sous-familles des Sphaeridiinae et des Hydrophilinae (Col. Hydrophilidae). *Annales de la Société entomologique de France,* 88, 105-168.

Orchymont, A. d'. (1933). Contribution a l'etude des Palpicornia. VIII. *Bulletin et Annales de la Societe entomologique de Belgique*, 73, 271-314.

Pross, J., Contreras, L., Bijl, P.K., Greenwood, D.R., Bohaty, S.M., Schouten, S., Bendle, J.A., Röhl, U., Tauxe, L., Raine, J.I., Huck, C.E., Flierdt, T. van de, Jamieson, S.S.R., Stickley, C.E., Schootbrugge, B. van de, Escutia, C., Brinkhuis, H., Scientists, I.O.D.P.E. 318, Brinkhuis, H., Dotti, C.E., Klaus, A., Fehr, A., Williams, T., Bendle, J.A.P., Bijl, P.K., Bohaty, S.M., Carr, S.A., Dunbar, R.B., Gonzàlez, J.J., Hayden, T.G., Iwai, M., Jimenez-Espejo, F.J., Katsuki, K., Kong, G.S., McKay, R.M., Nakai, M., Olney, M.P., Passchier, S., Pekar, S.F., Pross, J., Riesselman, C.R., Röhl, U., Sakai, T., Shrivastava, P.K., Stickley, C.E., Sugisaki, S., Tauxe, L., Tuo, S., Flierdt, T. van de, Welsh, K., Yamane, M., (2012). Persistent near-tropical warmth on the Antarctic continent during the early Eocene epoch. *Nature*, 488(7409), 73.

De Queiroz, A. (2005). The resurrection of oceanic dispersal in historical biogeography. *Trends in Ecology & Evolution*, 20(2), 68-73.

Rabinowitz, P. D., Coffin, M. F., & Falvey, D. (1983). The separation of Madagascar and Africa. *Science*, 220(4592), 67-69.

Rambaut A. (2012). Figtree v 1.4.0. http://tree.bio.ed.ac.uk/software/figtree/

Rambaut, A., Drummond, A. J., Xie, D., Baele, G., & Suchard, M. A. (2018). Posterior summarization in Bayesian phylogenetics using Tracer 1.7. *Systematic Biology*, 67(5), 901-904.

Reguero, M. A., Gelfo, J. N., López, G. M., Bond, M., Abello, A., Santillana, S. N., & Marenssi, S. A. (2014). Final Gondwana breakup: the Paleogene South American native ungulates and the demise of the South America–Antarctica land connection. *Global and Planetary change*, 123, 400-413.

Renner, S. S., Strijk, J. S., Strasberg, D., & Thébaud, C. (2010). Biogeography of the Monimiaceae (Laurales): a role for East Gondwana and long-distance dispersal, but not West Gondwana. *Journal of Biogeography*, 37(7), 1227-1238.

Ronquist, F., Teslenko, M., van der Mark, P., Ayres, D. L., Darling, A., Höhna, S., Larget, B., Liu, L., Suchard, M. A., & Huelsenbeck, J. P. (2012). MrBayes 3.2: efficient Bayesian phylogenetic inference and model choice across a large model space. *Systematic Biology*, 61, 539–542.

Sanmartín, I., & Ronquist, F. (2004). Southern Hemisphere biogeography inferred by event-based models: plant versus animal patterns. *Systematic Biology*, 53(2).

Scotese, C. R., Gahagan, L. M., & Larson, R. L. (1988). Plate tectonic reconstructions of the Cretaceous and Cenozoic ocean basins. *Tectonophysics*, 155(1-4), 27-48.

Scotese, C. R., Boucot, A. J., & McKerrow, W. S. (1999). Gondwanan palaeogeography and paleoclimatology. *Journal of African Earth Sciences*, 28(1), 99-114.

Seidel, M., Arriaga-Varela, E., & Fikáček, M. (2016). Establishment of Cylominae Zaitzev, 1908 as a valid name for the subfamily Rygmodinae Orchymont, 1916

with an updated list of genera (Coleoptera: Hydrophilidae). *Acta Entomologica Musei Nationalis Pragae, 56(*1), 159-165.

Seidel, M., Minoshima, Y. N., Arriaga-Varela, E., & Fikáček, M. (2018). Breaking a disjunct distribution: a review of the Southern Hemisphere genera Cylorygmus and Relictorygmus gen. nov. (Hydrophilidae: Cylominae). *Annales Zoologici,* 68(2): 375-403.

Seidel, M., Minoshima, Y. N., Leschen, R. A. B., & Fikáček, M. (in prep.). Phylogeny, systematics and rarity assessment of New Zealand endemic Saphydrus beetles and related enigmatic larvae (Coleoptera: Hydrophilidae: Cylominae)

Short, A. E. Z., & Fikáček, M. (2013). Molecular phylogeny, evolution and classification of the Hydrophilidae (Coleoptera). *Systematic Entomology*, 38(4), 723-752.

Toussaint, E. A. F., Seidel, M., Arriaga-Varela, E., Hájek, J., Král, D., Sekerka, L., Short, A. E. Z. & Fikáček, M. (2017). The peril of dating beetles. *Systematic Entomology* 42(1): 1-10.

Toussaint, E. F., & Short, A. E. (2018). Transoceanic Stepping–stones between Cretaceous waterfalls? The enigmatic biogeography of pantropical Oocyclus cascade beetles. *Molecular Phylogenetics and Evolution*, 127, 416-428.

Woodburne, M. O., & Case, J. A. (1996). Dispersal, vicariance, and the Late Cretaceous to early Tertiary land mammal biogeography from South America to Australia. *Journal of Mammalian Evolution*, 3(2), 121-161.

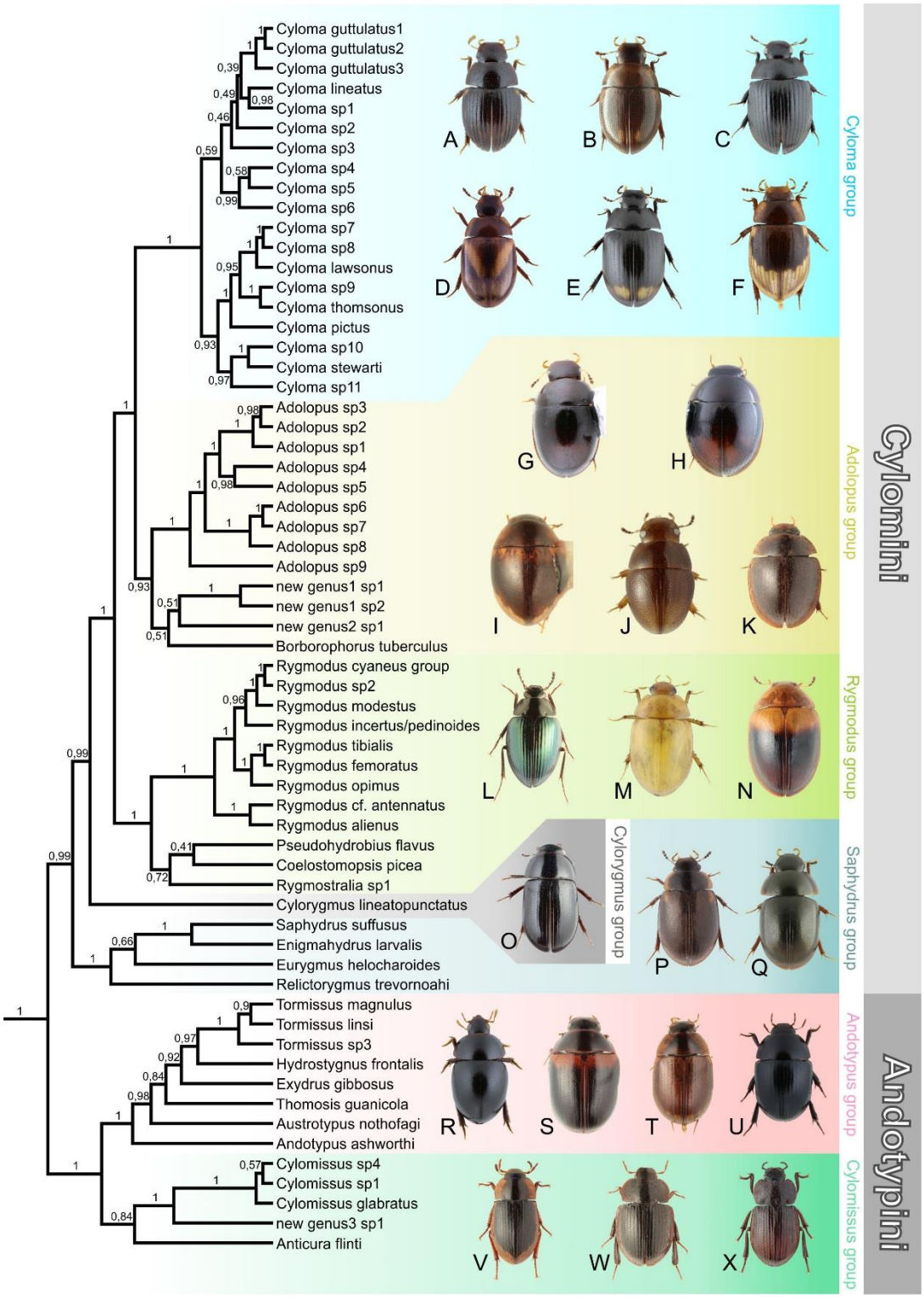

Figure 1. The species-level phylogeny of the Cylominae (fully resolved consensus tree from Bayesian analysis). Tribes and species groups recognized are indicated. Illustrated taxa: A–F – *Cyloma* Sharp, 1872; G–H – *Adolopus* Sharp, 1884; I – New Genus 2; J – New Genus 1; K – *Borborophorus* Hansen, 1990; L – *Rygmodus* White, 1846; M – *Pseudohydrobius* Blackburn, 1898; N – *Rygmostralia* Orchymont, 1933; O – *Cylorygmus* Orchymont, 1933; P – *Saphydrus* Sharp, 1884; Q – *Relictorygmus* Seidel et al. 2018; R – *Exydrus* Broun, 1886; S – *Austrotypus* Fikáček et al. 2014; T – *Andotypus* Spangler, 1979; U – *Hydrostygnus* Sharp, 1884; V – *Cylomissus* Broun, 1903; W – New Genus 3; X – *Anticura* Spangler, 1979.

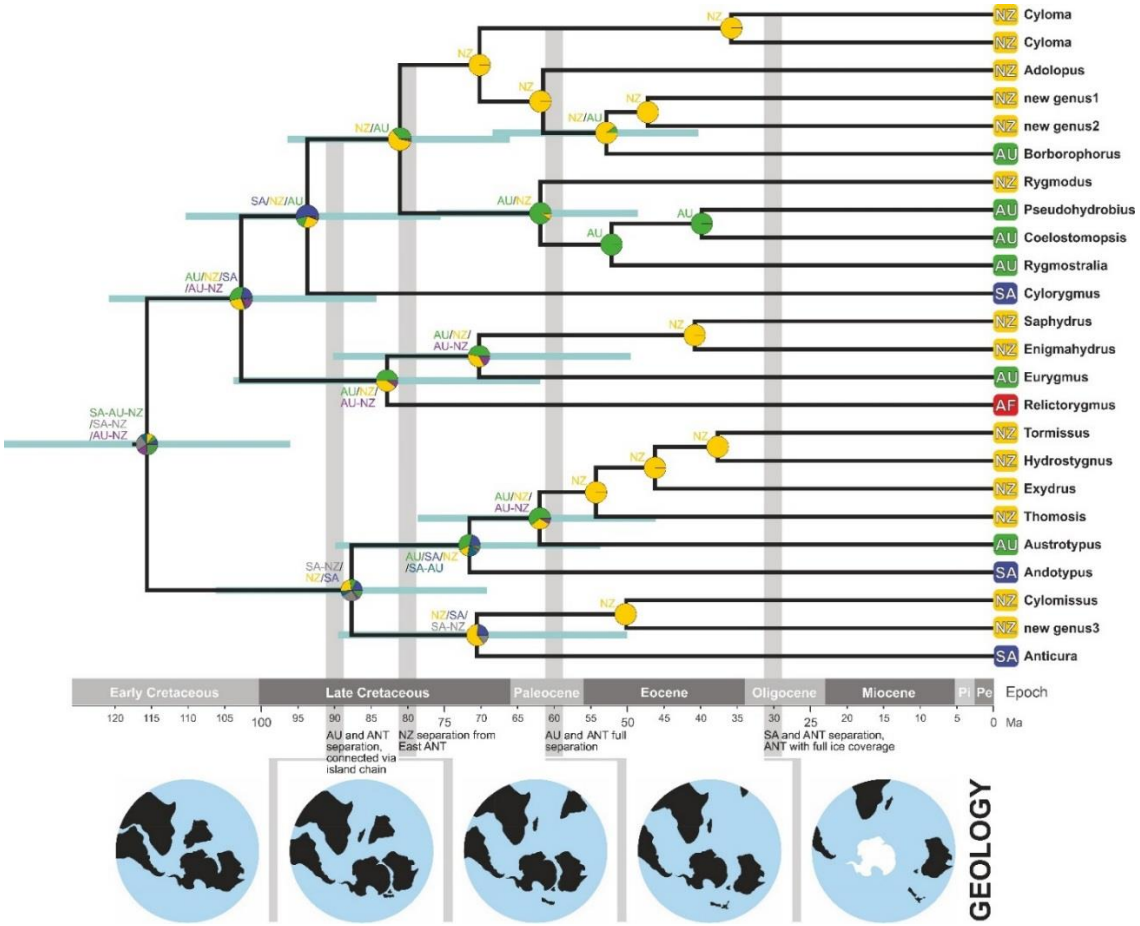

Figure 2. Results of the ancestral area estimation using the time-stratified DEC+J model of BioGeoBEARS. Pie charts show the probabilities of inferred ancestral areas for the particular node. Area codes: AF - Africa, ANT - Antarctica, AU - Australia, NZ - New Zealand, SA - South America.

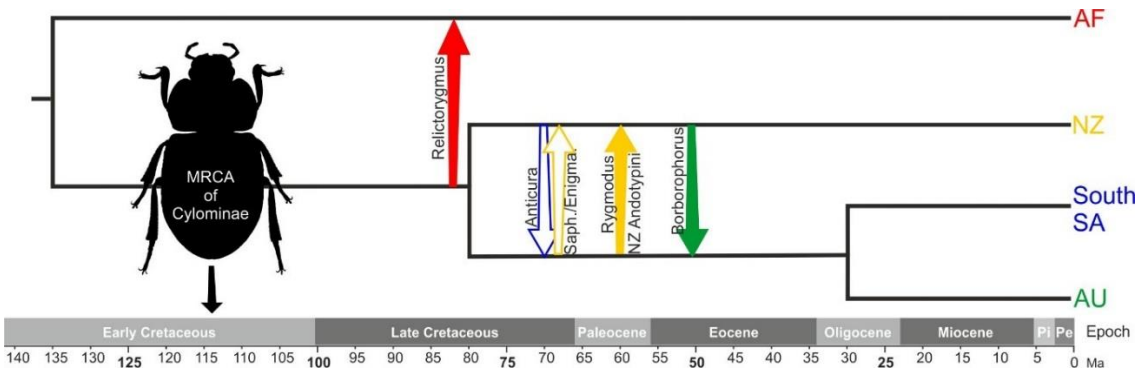

Figure 3. Cladogram of the break-up of parts of Gondwana indicating over-water long-distance dispersal events of Cylominae lineages revealed by our analyses. Color of arrows indicates the current distribution of the respective clade, full arrows indicate highly supported long distance dispersal, empty arrows indicate events in which median age post-dates the NZ/Gondwana split but the wide 95% CI does not exclude vicariance.

Table 1. Age estimates (median ages and 95% confidence intervals) of selected nodes of the Cylominae, as inferred from the divergence dating analyses using lognormal, uniform and exponential priors.

age	lognormal	uniform	exponential
stem Cylominae	129.00 [115.80 - 143.36]	143.56 [124.73 - 162.45]	156.72 [124.49 - 205.74]
crown Cylominae	101.60 [87.05 - 118.98]	114.05 [95.87 - 133.55]	123.30 [96.25 - 165.42]
crown Andotypini	76.39 [61.64 - 92.89]	86.83 [67.66 - 105.49]	95.27 [66.23 - 126.51]
crown Cylomini	89.69 [76.05 - 105.74]	101.53 [84.36 - 120.63]	109.10 [84.13 - 146.36]
stem *Cyloma*	62.74 [51.19 - 74.77]	69.82 [56.99 - 83.22]	74.37 [55.19 - 101.27]
stem *Rygmodus* gr.	71.68 [60.18 - 83.39]	80.42 [65.94 - 96.34]	85.10 [62.18 - 115.56]
stem *Relictorygmus*	72.99 [54.32 - 89.81]	82.12 [61.69 - 104.02]	90.18 [63.50 - 124.24]
stem *Cylorygmus*	89.69 [76.05 - 105.74]	92.73 [76.54 - 110.36]	98.38 [84.13 - 146.36]
stem *Andotypus*	63.29 [48.38 - 77.00]	71.16 [52.6 - 91.03]	78.73 [51.59 - 107.36]
stem *Anticura*	61.16 [44.79 -78.62]	70.19 [48.28 - 89.08]	76.24 [48.77 - 107.39]

Table 2. Comparison of parameters of the time-stratified analyses: AIC, Akaike information criterion; AICc, size-corrected AIC; LnL, log likelihood; n par, number of parameters in the analysis; d, e, j, parameres of the model (d, dispersal; e, extinction, j, founder event).

model	LnL	npar	d	e	j	AICc
DEC	-40.959	2	0.0129	0.0023	0	86.490
DEC+J	-31.631	3	<0.0001	<0.0001	0.758	70.462
DIVALIKE	-37.752	2	0.0139	0.0006	0	80.076
DIVALIKE+J	-31.639	3	0.0015	<0.0001	0.560	70.477
BAYAREALIKE	-46.167	2	0.0049	0.0112	0	96.905
BAYAREALIKE+J	-46.167	3	0.0049	0.0112	<0.0001	99.533

Supplementary material

to the paper

Seidel, M., Sýkora, V., Leschen, R. A. B., & Fikáček, M. Systematics and biogeography of the Southern Hemisphere endemic Cylominae beetles (Coleoptera: Hydrophilidae) (manuscript draft).

continued on
following page

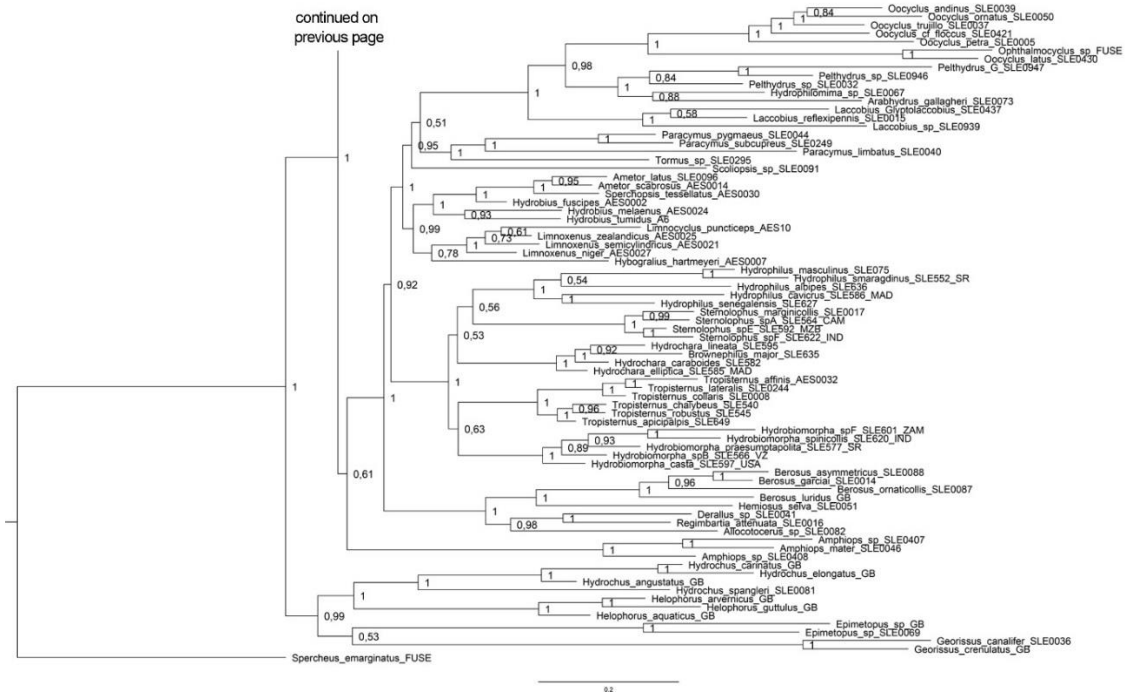

Supplementary Figure S1. Fully resolved consensus tree from the Bayesian analysis. Node values represent posterior probabilities.

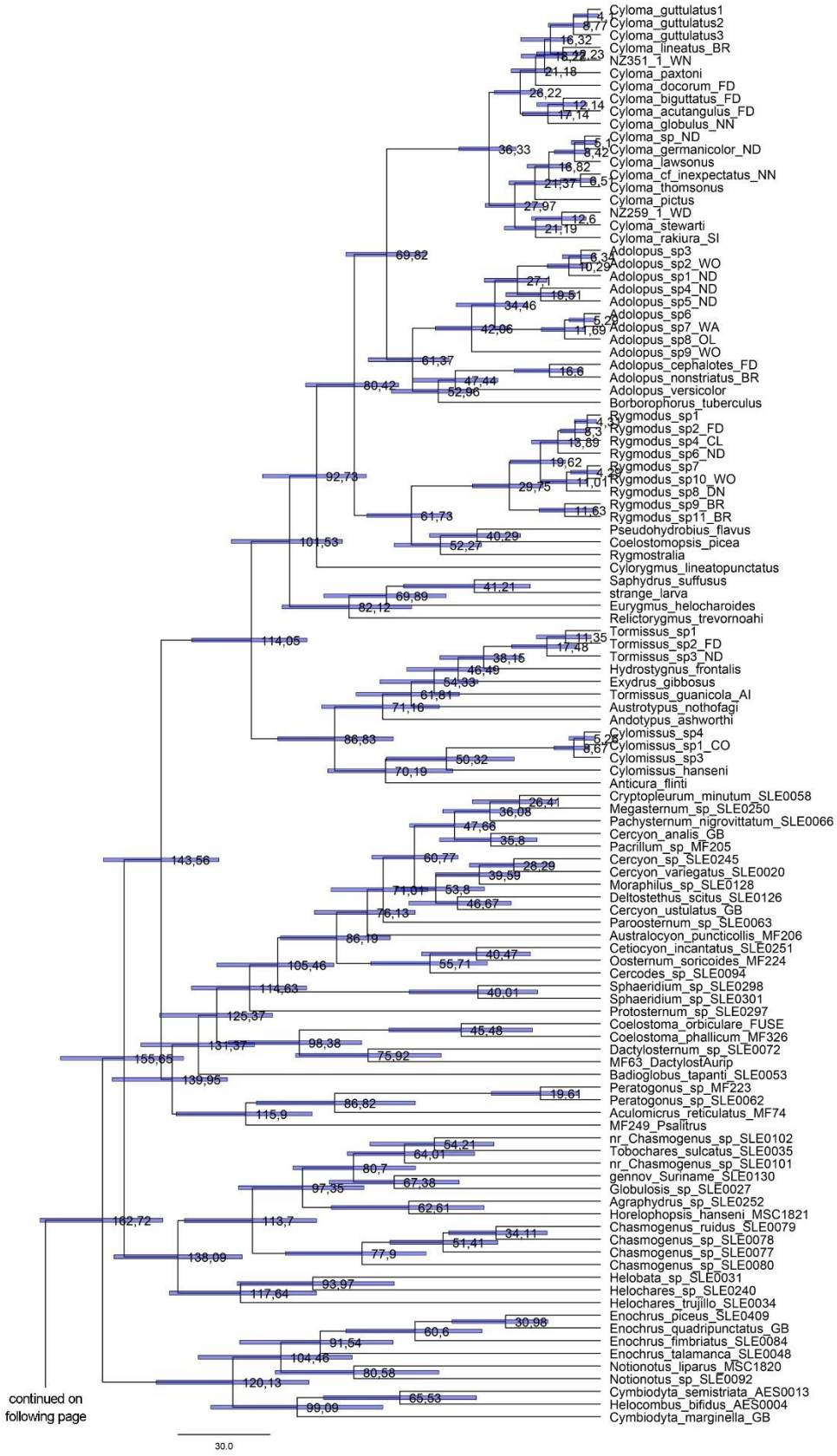
Cyloma_guttulatus1
Cyloma_guttulatus2
Cyloma_guttulatus3
Cyloma_lineatus_BR
NZ351_1_WN
Cyloma_paxtoni
Cyloma_docorum_FD
Cyloma_biguttatus_FD
Cyloma_acutangulus_FD
Cyloma_globulus_NN
Cyloma_sp_ND
Cyloma_germanicolor_ND
Cyloma_lawsonus
Cyloma_cf_inexpectatus_NN
Cyloma_thomsonus
Cyloma_pictus
NZ259_1_WD
Cyloma_stewarti
Cyloma_rakiura_SI
Adolopus_sp3
Adolopus_sp2_WO
Adolopus_sp1_ND
Adolopus_sp4_ND
Adolopus_sp5_ND
Adolopus_sp6
Adolopus_sp7_WA
Adolopus_sp8_OL
Adolopus_sp9_WO
Adolopus_cephalotes_FD
Adolopus_nonstriatus_BR
Adolopus_versicolor
Borborophorus_tuberculus
Rygmodus_sp1
Rygmodus_sp2_FD
Rygmodus_sp4_CL
Rygmodus_sp6_ND
Rygmodus_sp7
Rygmodus_sp10_WO
Rygmodus_sp8_DN
Rygmodus_sp9_BR
Rygmodus_sp11_BR
Pseudohydrobius_flavus
Coelostomopsis_picea
Rygmostralia
Cylorygmus_lineatopunctatus
Saphydrus_suffusus
strange_larva
Eurygmus_helocharoides
Relictorygmus_trevornoahi
Tormissus_sp1
Tormissus_sp2_FD
Tormissus_sp3_ND
Hydrostygnus_frontalis
Exydrus_gibbosus
Tormissus_guanicola_AI
Austrotypus_nothofagi
Andotypus_ashworthi
Cylomissus_sp4
Cylomissus_sp1_CO
Cylomissus_sp3
Cylomissus_hanseni
Anticura_flinti
Cryptopleurum_minutum_SLE0058
Megasternum_sp_SLE0250
Pachysternum_nigrovittatum_SLE0066
Cercyon_analis_GB
Pacrillum_sp_MF205
Cercyon_sp_SLE0245
Cercyon_variegatus_SLE0020
Moraphilus_sp_SLE0128
Deltostethus_scitus_SLE0126
Cercyon_ustulatus_GB
Paroosternum_sp_SLE0063
Australocyon_puncticollis_MF206
Cetiocyon_incantatus_SLE0251
Oosternum_soricoides_MF224
Cercodes_sp_SLE0094
Sphaeridium_sp_SLE0298
Sphaeridium_sp_SLE0301
Protosternum_sp_SLE0297
Coelostoma_orbiculare_FUSE
Coelostoma_phallicum_MF326
Dactylosternum_sp_SLE0072
MF63_DactylostAurip
Badioglobus_tapanti_SLE0053
Peratogonus_sp_MF223
Peratogonus_sp_SLE0062
Aculomicrus_reticulatus_MF74
MF249_Psalitrus
nr_Chasmogenus_sp_SLE0102
Tobochares_sulcatus_SLE0035
nr_Chasmogenus_sp_SLE0101
gennov_Suriname_SLE0130
Globulosis_sp_SLE0027
Agraphydrus_sp_SLE0252
Horelophopsis_hanseni_MSC1821
Chasmogenus_ruidus_SLE0079
Chasmogenus_sp_SLE0078
Chasmogenus_sp_SLE0077
Chasmogenus_sp_SLE0080
Helobata_sp_SLE0031
Helochares_sp_SLE0240
Helochares_trujillo_SLE0034
Enochrus_piceus_SLE0409
Enochrus_quadripunctatus_GB
Enochrus_fimbriatus_SLE0084
Enochrus_talamanca_SLE0048
Notionotus_liparus_MSC1820
Notionotus_sp_SLE0092
Cymbiodyta_semistriata_AES0013
Helocombus_bifidus_AES0004
Cymbiodyta_marginella_GB
continued on following page
30.0

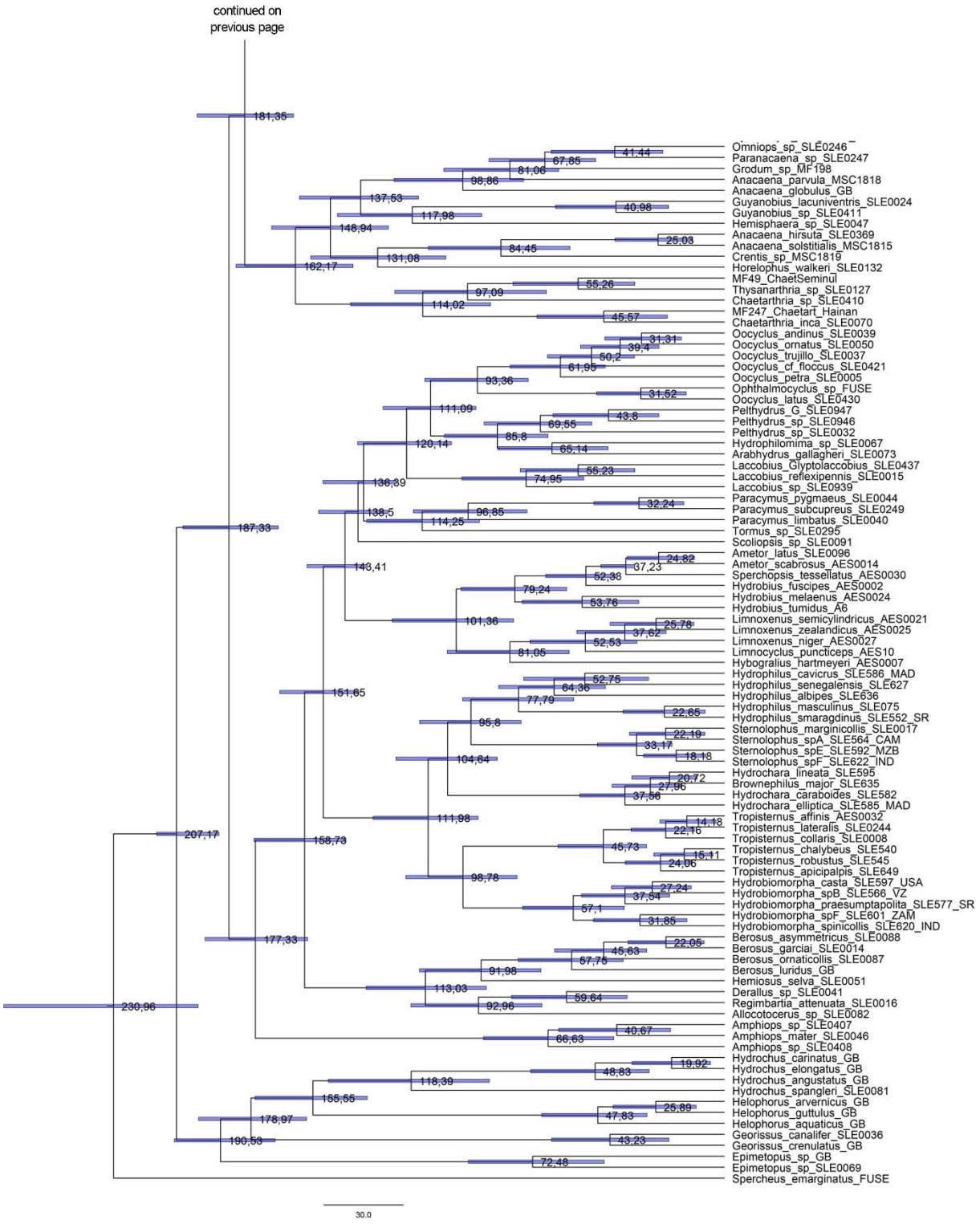

Supplementary Figure S2. Fully resolved divergence-time dated consensus tree from Bayesian analysis using uniform parameters. Node values represent median ages, node bars show 95% credibility intervals.

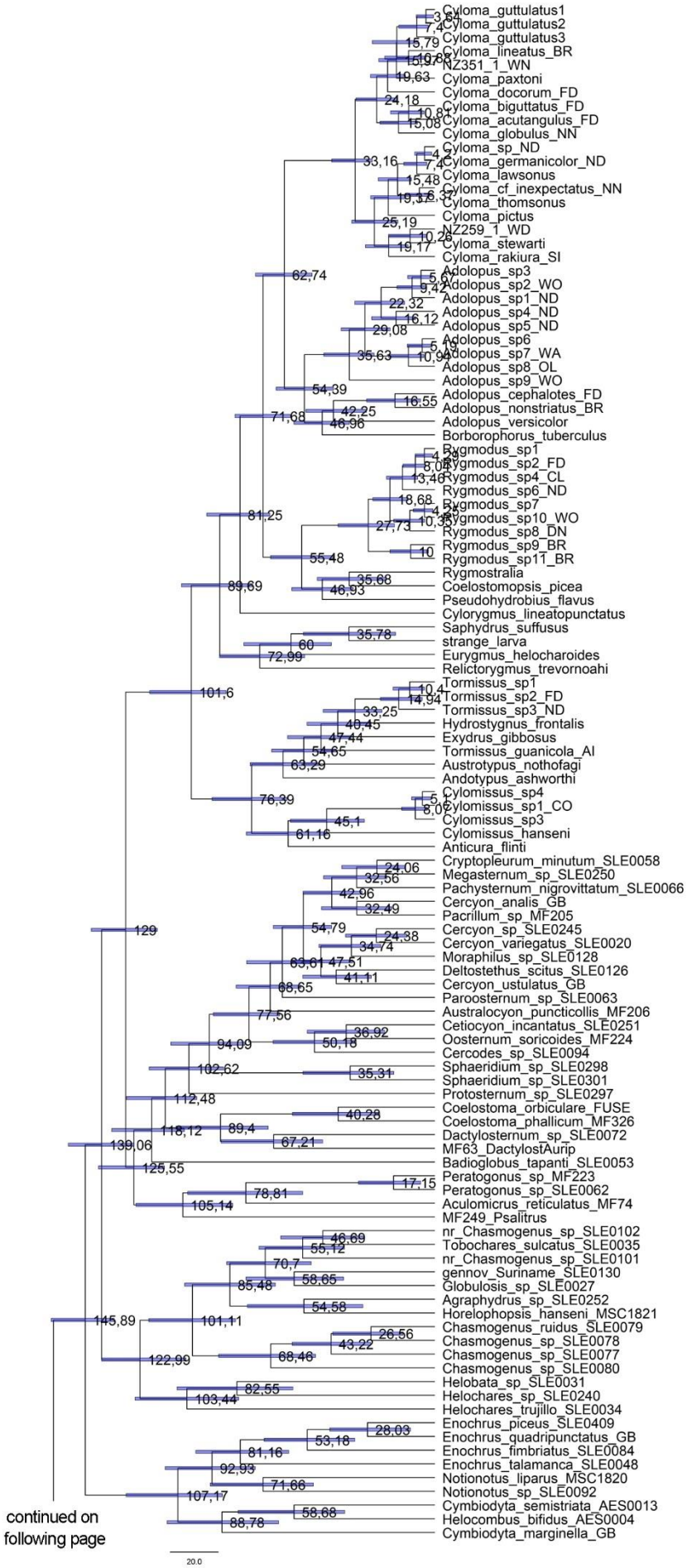
Cyloma_guttulatus1
Cyloma_guttulatus2
Cyloma_guttulatus3
Cyloma_lineatus_BR
NZ351_1_WN
Cyloma_paxtoni
Cyloma_docorum_FD
Cyloma_biguttatus_FD
Cyloma_acutangulus_FD
Cyloma_globulus_NN
Cyloma_sp_ND
Cyloma_germanicolor_ND
Cyloma_lawsonus
Cyloma_cf_inexpectatus_NN
Cyloma_thomsonus
Cyloma_pictus
NZ259_1_WD
Cyloma_stewarti
Cyloma_rakiura_SI
Adolopus_sp3
Adolopus_sp2_WO
Adolopus_sp1_ND
Adolopus_sp4_ND
Adolopus_sp5_ND
Adolopus_sp6
Adolopus_sp7_WA
Adolopus_sp8_OL
Adolopus_sp9_WO
Adolopus_cephalotes_FD
Adolopus_nonstriatus_BR
Adolopus_versicolor
Borboropharus_tuberculus
Rygmodus_sp1
Rygmodus_sp2_FD
Rygmodus_sp4_CL
Rygmodus_sp6_ND
Rygmodus_sp7
Rygmodus_sp10_WO
Rygmodus_sp8_DN
Rygmodus_sp9_BR
Rygmodus_sp11_BR
Rygmostralia
Coelostomopsis_picea
Pseudohydrobius_flavus
Cylorygmus_lineatopunctatus
Saphydrus_suffusus
strange_larva
Eurygmus_helocharoides
Relictorygmus_trevornoahi
Tormissus_sp1
Tormissus_sp2_FD
Tormissus_sp3_ND
Hydrostygnus_frontalis
Exydrus_gibbosus
Tormissus_guanicola_AI
Austrotypus_nothofagi
Andotypus_ashworthi
Cylomissus_sp4
Cylomissus_sp1_CO
Cylomissus_sp3
Cylomissus_hanseni
Anticura_flinti
Cryptopleurum_minutum_SLE0058
Megasternum_sp_SLE0250
Pachysternum_nigrovittatum_SLE0066
Cercyon_analis_GB
Pacrillum_sp_MF205
Cercyon_sp_SLE0245
Cercyon_variegatus_SLE0020
Moraphilus_sp_SLE0128
Deltostethus_scitus_SLE0126
Cercyon_ustulatus_GB
Paroosternum_sp_SLE0063
Australocyon_puncticollis_MF206
Cetiocyon_incantatus_SLE0251
Oosternum_soricoides_MF224
Cercodes_sp_SLE0094
Sphaeridium_sp_SLE0298
Sphaeridium_sp_SLE0301
Protosternum_sp_SLE0297
Coelostoma_orbiculare_FUSE
Coelostoma_phallicum_MF326
Dactylosternum_sp_SLE0072
MF63_DactylostAurip
Badioglobus_tapanti_SLE0053
Peratogonus_sp_MF223
Peratogonus_sp_SLE0062
Aculomicrus_reticulatus_MF74
MF249_Psalitrus
nr_Chasmogenus_sp_SLE0102
Tobochares_sulcatus_SLE0035
nr_Chasmogenus_sp_SLE0101
gennov_Suriname_SLE0130
Globulosis_sp_SLE0027
Agraphydrus_sp_SLE0252
Horelophopsis_hanseni_MSC1821
Chasmogenus_ruidus_SLE0079
Chasmogenus_sp_SLE0078
Chasmogenus_sp_SLE0077
Chasmogenus_sp_SLE0080
Helobata_sp_SLE0031
Helochares_sp_SLE0240
Helochares_trujillo_SLE0034
Enochrus_piceus_SLE0409
Enochrus_quadripunctatus_GB
Enochrus_fimbriatus_SLE0084
Enochrus_talamanca_SLE0048
Notionotus_liparus_MSC1820
Notionotus_sp_SLE0092
Cymbiodyta_semistriata_AES0013
Helocombus_bifidus_AES0004
Cymbiodyta_marginella_GB
62,74
81,25
71,68
89,69
101,6
76,39
129
94,09
102,62
112,48
118,12
139,06
125,55
145,89
101,11
122,99
82,55
103,44
107,17
92,93
81,16
53,18
28,03
58,68
88,78
71,66
105,14
78,81
17,15
89,4
67,21
40,28
50,18
36,92
35,31
68,65
77,56
63,61
47,51
41,11
54,79
24,88
34,74
42,96
32,49
24,06
32,56
33,25
48,45
47,44
54,65
63,29
45,1
61,16
72,99
60
35,78
55,48
35,68
46,93
27,73
10,35
18,68
13,46
8,01
10
16,55
42,25
46,96
54,39
35,63
10,94
29,08
22,32
16,12
25,19
19,17
10,28
15,48
33,16
7,4
15,79
15,08
10,81
24,18
19,63
15,97
7,4
3,84
55,12
46,69
70,7
58,65
85,48
54,58
26,56
43,22
68,46
20.0
continued on
following page

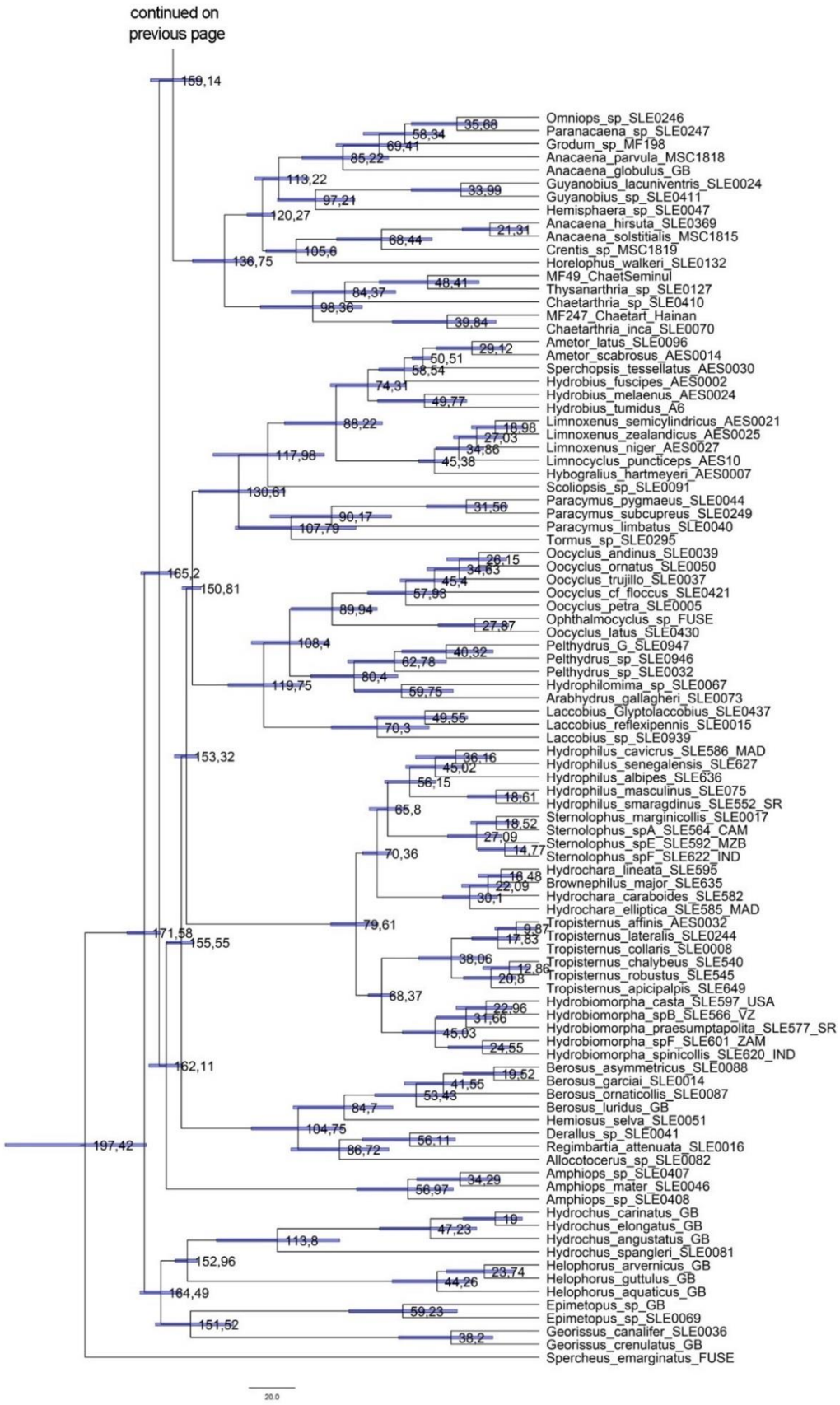

Supplementary Figure S3. Fully resolved divergence-time dated consensus tree from Bayesian analysis using lognormal parameters. Node values represent median ages and node bars show 95% credibility intervals.

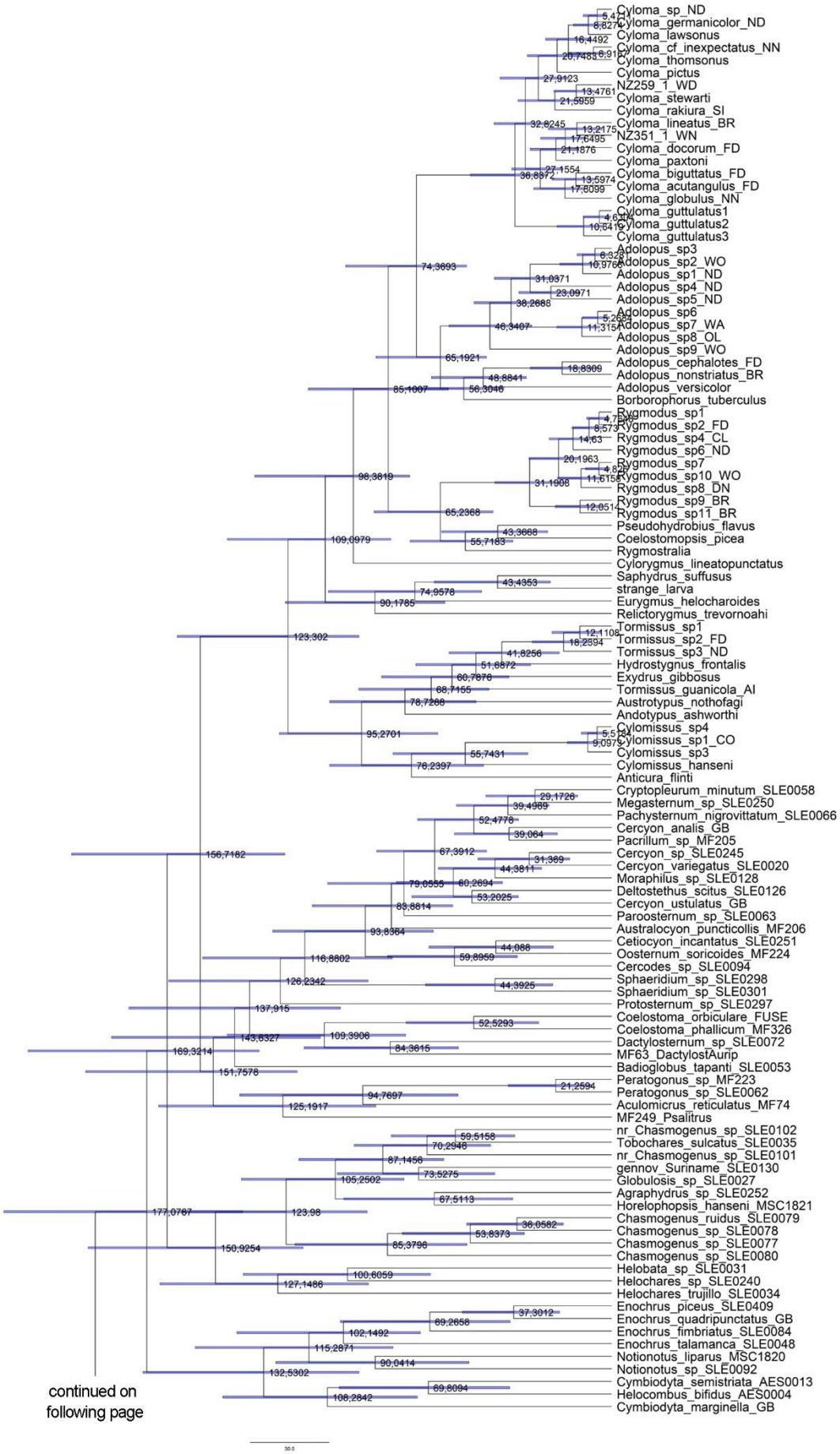
Cyloma_sp_ND
Cyloma_germanicolor_ND
Cyloma_lawsonus
Cyloma_cf_inexpectatus_NN
Cyloma_thomsonus
Cyloma_pictus
NZ259_1_WD
Cyloma_stewarti
Cyloma_rakiura_SI
Cyloma_lineatus_BR
NZ351_1_WN
Cyloma_docorum_FD
Cyloma_paxtoni
Cyloma_biguttatus_FD
Cyloma_acutangulus_FD
Cyloma_globulus_NN
Cyloma_guttulatus1
Cyloma_guttulatus2
Cyloma_guttulatus3
Adolopus_sp3
Adolopus_sp2_WO
Adolopus_sp1_ND
Adolopus_sp4_ND
Adolopus_sp5_ND
Adolopus_sp6
Adolopus_sp7_WA
Adolopus_sp8_OL
Adolopus_sp9_WO
Adolopus_cephalotes_FD
Adolopus_nonstriatus_BR
Adolopus_versicolor
Borborophorus_tuberculus
Rygmodus_sp1
Rygmodus_sp2_FD
Rygmodus_sp4_CL
Rygmodus_sp6_ND
Rygmodus_sp7
Rygmodus_sp10_WO
Rygmodus_sp8_DN
Rygmodus_sp9_BR
Rygmodus_sp11_BR
Pseudohydrobius_flavus
Coelostomopsis_picea
Rygmostralia
Cylorygmus_lineatopunctatus
Saphydrus_suffusus
strange_larva
Eurygmus_helocharoides
Relictorygmus_trevornoahi
Tormissus_sp1
Tormissus_sp2_FD
Tormissus_sp3_ND
Hydrostygnus_frontalis
Exydrus_gibbosus
Tormissus_guanicola_AI
Austrotypus_nothofagi
Andotypus_ashworthi
Cylomissus_sp4
Cylomissus_sp1_CO
Cylomissus_sp3
Cylomissus_hanseni
Anticura_flinti
Cryptopleurum_minutum_SLE0058
Megasternum_sp_SLE0250
Pachysternum_nigrovittatum_SLE0066
Cercyon_analis_GB
Pacrillum_sp_MF205
Cercyon_sp_SLE0245
Cercyon_variegatus_SLE0020
Moraphilus_sp_SLE0128
Deltostethus_scitus_SLE0126
Cercyon_ustulatus_GB
Paroosternum_sp_SLE0063
Australocyon_puncticollis_MF206
Cetiocyon_incantatus_SLE0251
Oosternum_soricoides_MF224
Cercodes_sp_SLE0094
Sphaeridium_sp_SLE0298
Sphaeridium_sp_SLE0301
Protosternum_sp_SLE0297
Coelostoma_orbiculare_FUSE
Coelostoma_phallicum_MF326
Dactylosternum_sp_SLE0072
MF63_DactylostAurip
Badioglobus_tapanti_SLE0053
Peratogonus_sp_MF223
Peratogonus_sp_SLE0062
Aculomicrus_reticulatus_MF74
MF249_Psalitrus
nr_Chasmogenus_sp_SLE0102
Tobochares_sulcatus_SLE0035
nr_Chasmogenus_sp_SLE0101
gennov_Suriname_SLE0130
Globulosis_sp_SLE0027
Agraphydrus_sp_SLE0252
Horelophopsis_hanseni_MSC1821
Chasmogenus_ruidus_SLE0079
Chasmogenus_sp_SLE0078
Chasmogenus_sp_SLE0077
Chasmogenus_sp_SLE0080
Helobata_sp_SLE0031
Helochares_sp_SLE0240
Helochares_trujillo_SLE0034
Enochrus_piceus_SLE0409
Enochrus_quadripunctatus_GB
Enochrus_fimbriatus_SLE0084
Enochrus_talamanca_SLE0048
Notionotus_liparus_MSC1820
Notionotus_sp_SLE0092
Cymbiodyta_semistriata_AES0013
Helocombus_bifidus_AES0004
Cymbiodyta_marginella_GB
74,3693
85,1007
65,1921
98,3819
109,0979
95,2701
123,302
156,7182
169,3214
177,0767
150,9254
continued on
following page

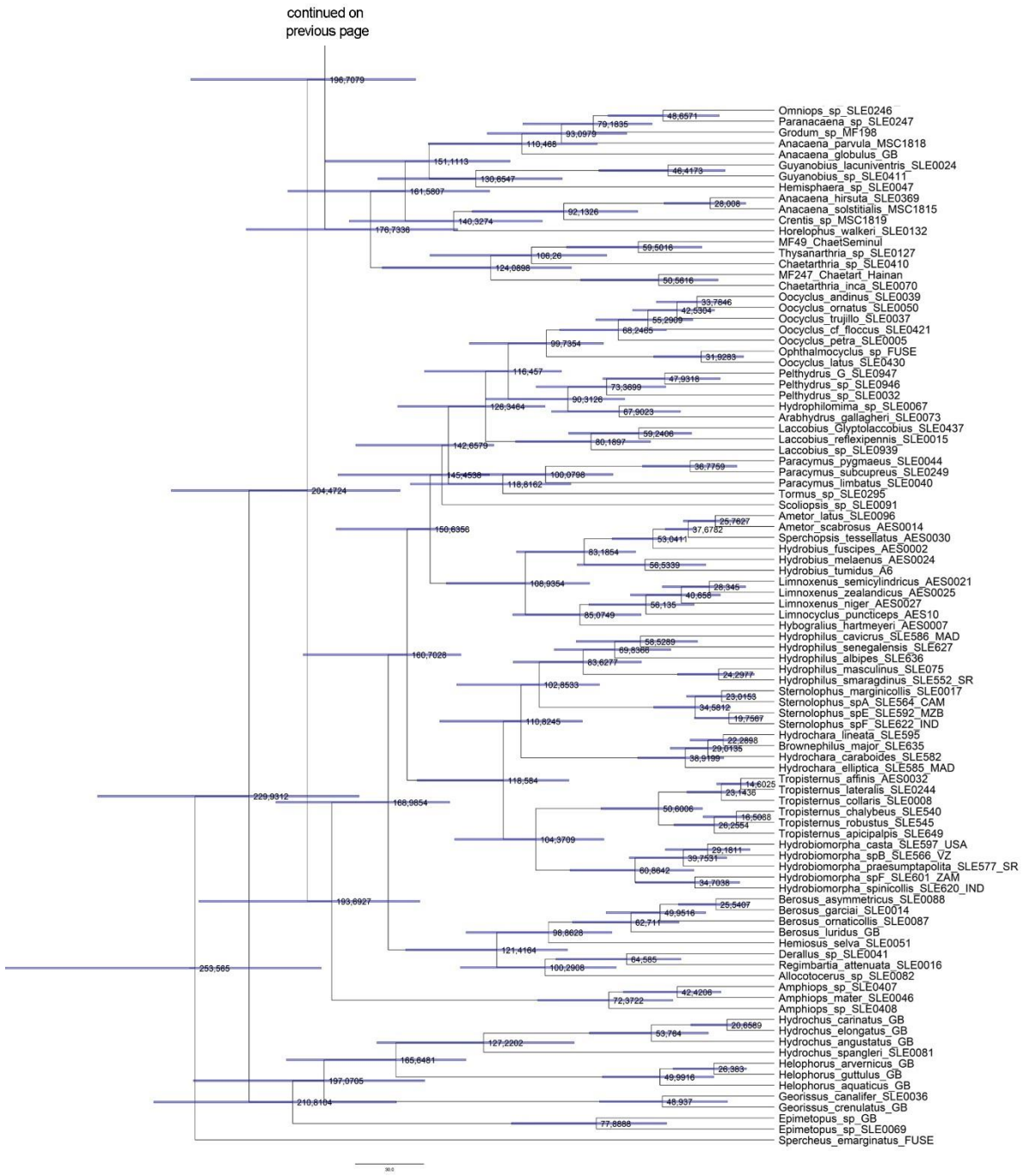

Supplementary Figure S4. Fully resolved divergence-time dated consensus tree from the Bayesian analysis using exponential parameters. Node values represent median ages and node bars show 95% credibility intervals.

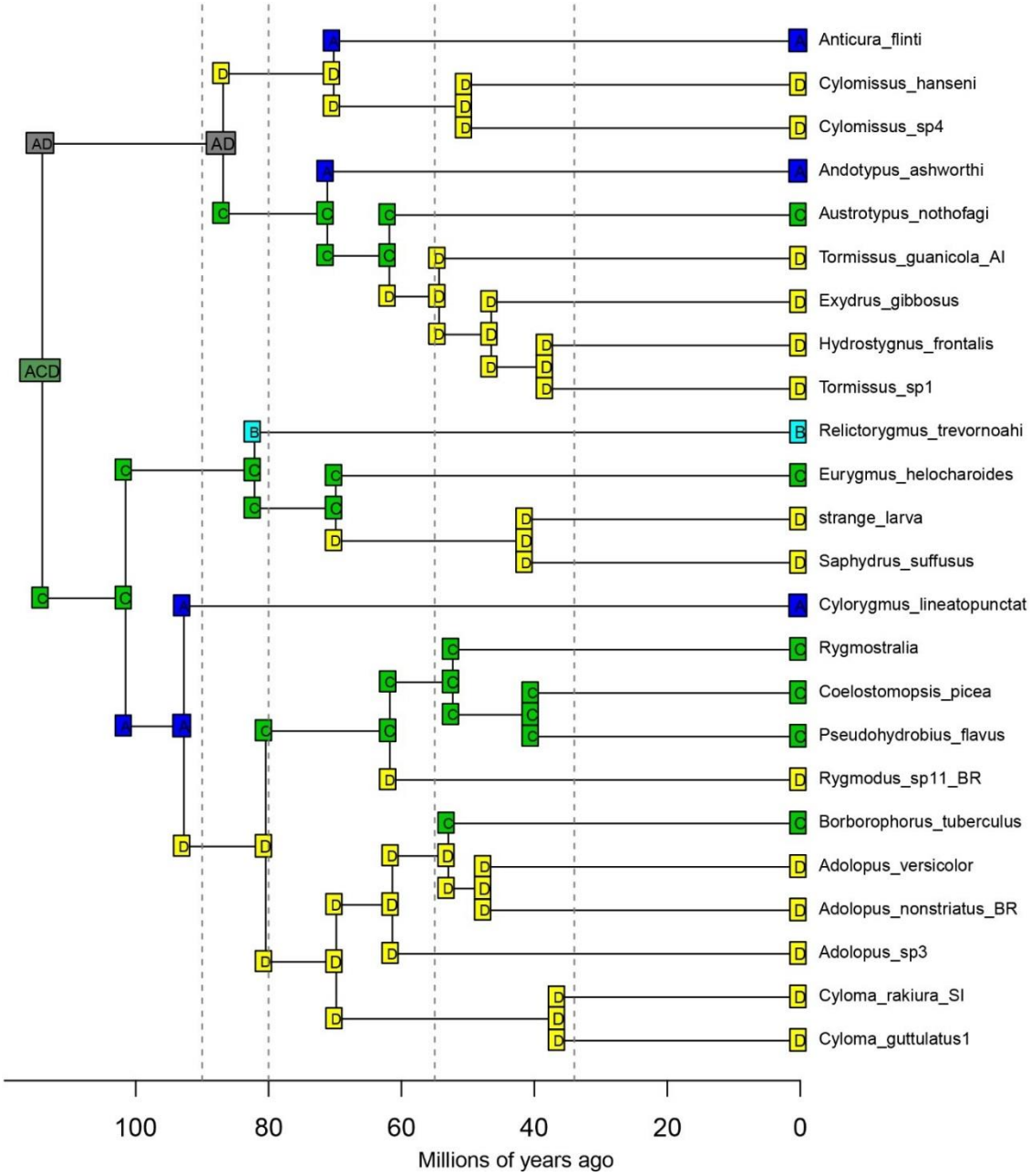

Supplementary Figure S5. Ancestral area estimation using the time-stratified DEC+J model of BioGeoBEARS (parameters: global optim, 4 areas max. d=0; e=0; j=0.758; LnL=−31.63)

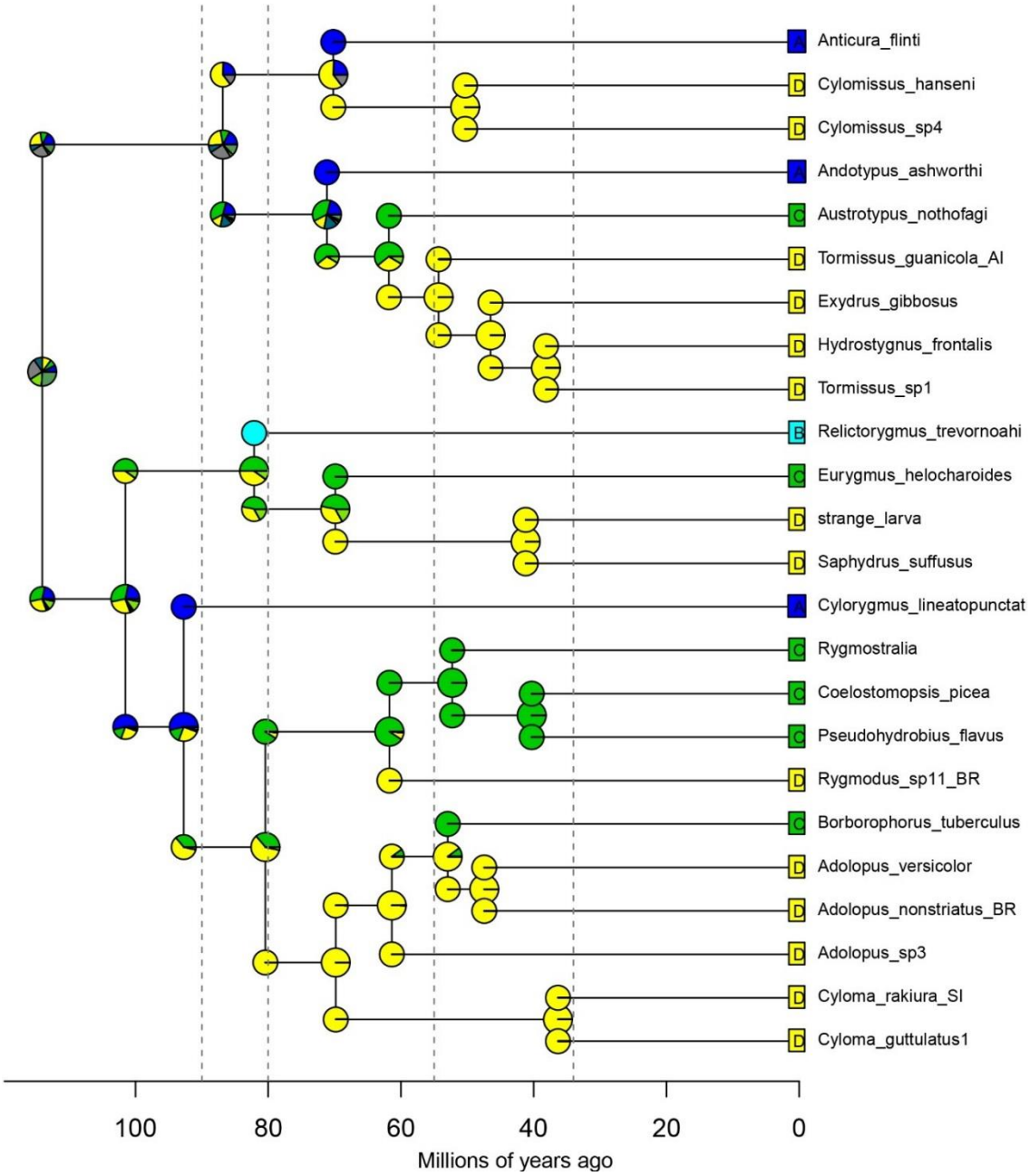

Supplementary Figure S6. Ancestral area estimation using the time-stratified DEC+J model of BioGeoBEARS (parameters: global optim, 4 areas max. d=0; e=0; j=0.758; LnL=−31.63)

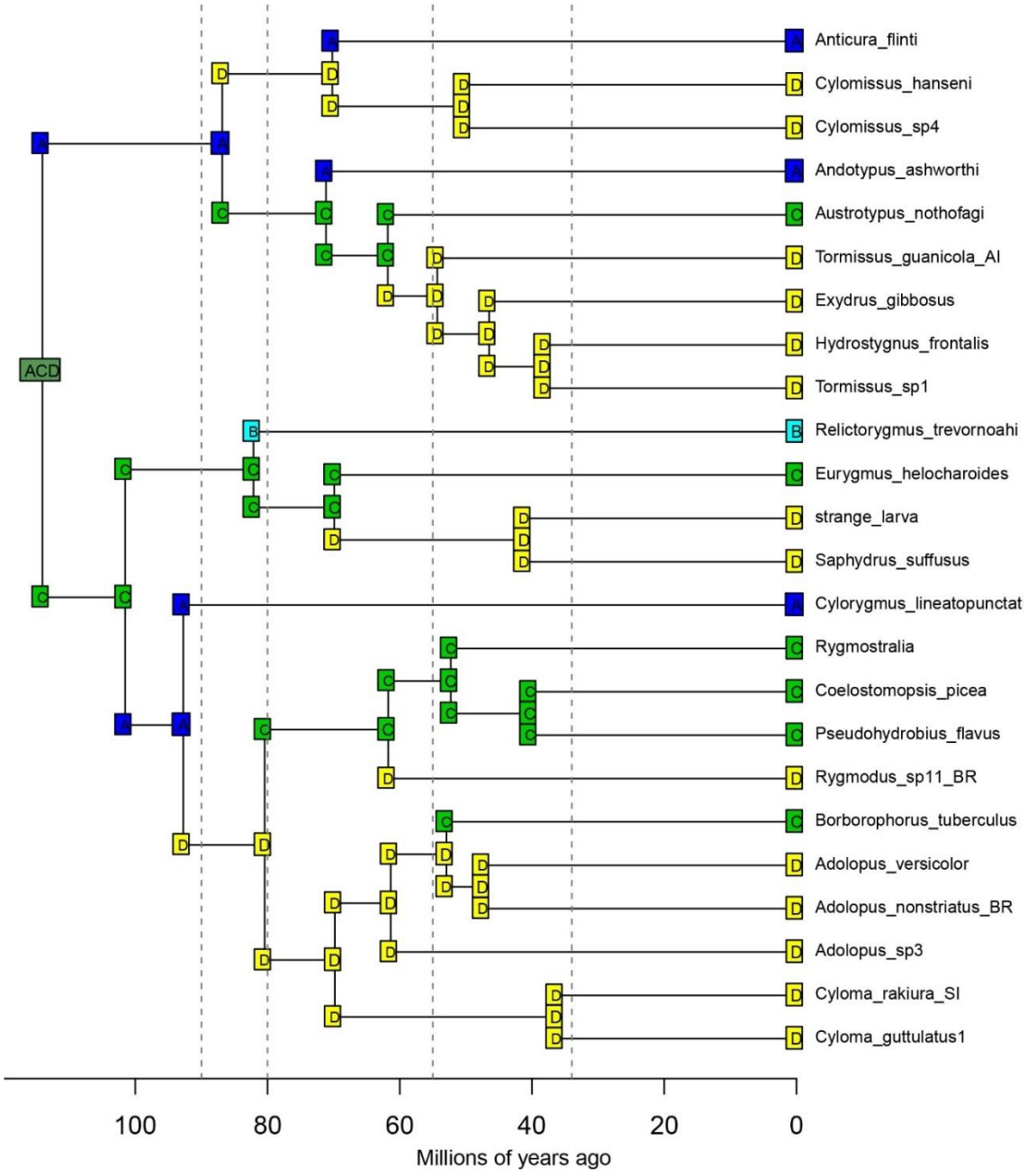

Supplementary Figure S7. Ancestral area estimation using the time-stratified DIVALIKE+J model of BioGeoBEARS (parameters: global optim, 4 areas max. d=0.0015; e=0; j=0.5599; LnL=−31.64)

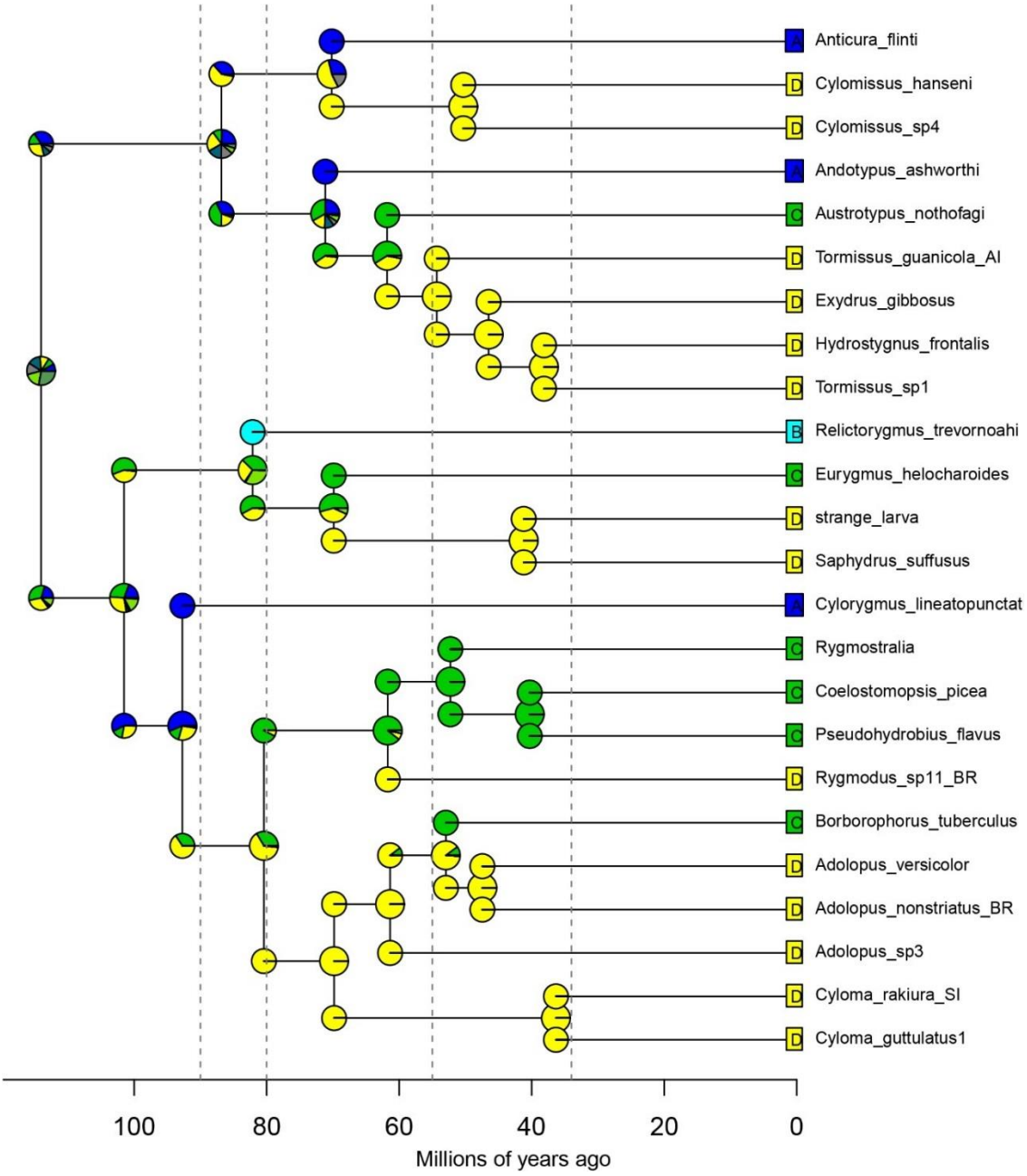

Supplementary Figure S8. Ancestral area estimation using the time-stratified DIVALIKE+J model of BioGeoBEARS (parameters: global optim, 4 areas max. d=0.0015; e=0; j=0.5599; LnL=−31.64)

Supplementary Table S1. Collectiong data of Cylominae specimens included in the phylogenetic study.

Species	Code	Collecting events	Collecting information
Cyloma sp9	NZ464	New Zealand, NN, Nelson Lakes NP, N end of Lake Rotoroa at Braeburn Track, 41.7987°S 172.58421°E, 522m, 5-9.xii.2016, Fikáček & Seidel lgt. MM57	lowland wet *Nothofagus* forest with huge amount of sooty moulds and with continuous layer of *Blechnum* fern understory, baited pitfall traps (rotten squid)
*Cyloma guttulatus*1	NZ111.1	New Zealand, SC, Peel Forest Reserve, Emily Falls track, 43°53.9′S 171°13.8′E, 400m, 9.ii.2016, J. Hájek & P. Hlaváč lgt.	
*Cyloma guttulatus*1	NZ243.1	New Zealand, FD, Borland Walk at Borland Lodge, 45°46.35-48'S 167°32.18-25'E, 180m, 23-28.i.2016, Seidel & Fikáček lgt., 2016-NZ020	baited pitfall traps (rotten squid) in mossy *Nothofagus* forest, in places with numerous ferns in understory
*Cyloma guttulatus*2	NZ262	New Zealand, WD, Pleasant Flat at Haast Pass Highway, 44°00.75'S 169°22.86'E 100m, 18-21.ii.2016, Seidel, Sýkora, Leschen & Maier lgt., 2016-NZ-MS29	baited pitfall traps (rotten squid) in native forest
*Cyloma guttulatus*2	NZ213.1	New Zealand, WD, Kelly Creek at Otira Hwy., 42°48.06'S 171°34.26'E, 380m, 24-26.ii.2016, Seidel, Sýkora, Leschen, Maier & Lambert lgt., 2016-NZ-MS73	sifting of leaf litter in native forest
*Cyloma guttulatus*3	NZ468.1	New Zealand, TO, Pureora Forest Park, Waituhi Lookout, 38.860°S 175.5465°E, 975m, 19-22.xi.2016, Fikáček & Seidel lgt., MM08	low broadleaf forest with very abundant mosses on ground and trunks, and large accumulations of leaf litter, baited pitfall traps (rotten squid)
*Cyloma guttulatus*3	NZ729.1	New Zealand, HB, Kaweka Range, Whittle Rd., 39°16'36"S 176°26'48"E, 995m, 28.xi.2018, J. Shen lgt., JWS086	sifted leaf litter
Cyloma lineatus	NZ83	New Zealand, BR, Klondyke Trk, Victoria Ra, 12.i.2011, T.R. Buckley & R. Leschen lgt., TB452, 42°18.842'S 172°07.065'E, 699m	sifting wet dead wood
Cyloma stewarti	COL1778	New Zealand, WN, W.A. Miller Scenic Reserve, Makakahi River, 29.i.2008, K. Marske, R. Leschen & T. Buckley lgt., 40°42.329'S 175°39.316'E, 267m, KM278	sifted flood debris-wood and leaf litter
Cyloma stewarti	NZ31	New Zealand, WO, Whareorino Forest, Mangatoa Tk, 4.iii.2012, M. Gimmel & R. Leschen lgt., 38°24.985'S 174°43,312'E, RL1673	sifting litter and rotten wood
Cyloma stewarti	NZ728.1	New Zealand, GB, Lake Waikaremoana, Rahuinui Stream, 38°44'41"S 177°06'58"E, 600m, 26.xi.2018, J. Shen lgt., JWS082	sifted leaf litter & moss
Cyloma lawsonus	NZ434	New Zealand, WO, Pirongia Forest Park, Ruapane Link Track (lower part), 37.966°S 175.144°E, 235m,18-21.xi.2016 M.Fikáček & M.Seidel lgt., MM02	lowland broadleaf forest with podocarps, nikau palms and *Ripogonum* lianas, sparse understory, baited pitfall traps (rotten squid)
Cyloma lawsonus	NZ117.1	New Zealand, Auckland, Waitakere Ranges, 2.i.2016, Karekare - Whatipu reserve, 37°00.0-6′S 174°28.6-29.0′E, 12m, J.Hájek & P. Hlaváč lgt.	
Cyloma sp2	NZ178	New Zealand, WD, Ship Creek at Swamp Forest Walk and Beach, 43°45.64'S 169°08.97'E, 0m, 19-21.ii.2016, Seidel, Sýkora, Leschen & Maier lgt., 2016-NZ-MS30	baited pitfall traps (rotten squid) in native forest
Cyloma sp4	NZ69.1	New Zealand, FD, Chalky Inlet, Middle Passage Island, 46.02394°S 166.53805°E, 5-30m, 20.i.2011, S.A. Forgie lgt., SAF045	sifting litter/bark/lichen/moss/log scrapings
Cyloma pictus	NZ676	New Zealand, AU, Hanfield Inlet, 26.iii.2006, R. Leschen & E. Edwards lgt., 50°44.310'S 166°06.376'E, AU036	rotten wood and lichen
Cyloma pictus	NZ566.1	New Zealand, AU, Adams Is., Fairchilds Garden, 22.iii.2006, R. Leschen & E. Edwards lgt., 50°50.248'S 165°55.342'E, AU007	*Dracophyllum*, *Metrosideros*, *Poa*, and Megaherb leaf litter
Cyloma sp11	NZ187.1	New Zealand, Stewart Island, end of Fern Gully Tk. W of Oban, 17.-21.i.2016, 46°53.34'S 168°5.51'E, 65m, Seidel, Sýkora & Fikáček lgt., 2016-NZ005	flight intercept trap in dense young forest with numerous ferns in understory
Cyloma sp3	NZ157	New Zealand, FD, Borland Road 24km NWW of Monowai, 45°41.13'S 167°20.29'E, 320m, 24-27.i.2016, Seidel, Sýkora & Fikáček lgt., 2016-NZ024	on dead possum carcass
Cyloma sp3	NZ156.1	New Zealand, FD, Monowai Lookout Tk at Monowai campsite, 45°48.67'S 167°31.21'E, 210m, 26-28.i.2016 Seidel, Sýkora & Fikáček, 2016-NZ030	baited pitfall traps (rotten squid) in mossy *Nothofagus* forest
Cyloma thomsonus	NZ158	New Zealand, SL, Kaka Point Scenic Reserve, 46°23.04'S 169°46.45'E, 20m, 2-6.ii.2016, Seidel, Sýkora & Fikáček lgt., 2016-NZ050	baited pitfall traps (rotten squid) in native coastal forest with podocarps and ferns

Cyloma thomsonus	NZ248.1	New Zealand, SL, Catlins, McLean Falls Tk. at Tautuku River, 46°34.26'S169°20.98'E, 50m, 3-10.ii.2016, Seidel, Sýkora & Fikáček lgt., 2016-NZ051	baited pitfall traps (rotten squid) in wet to moderately wet area in native coastal forest with numerous tree ferns and falled/rotten trunks
Cyloma sp7	NZ577.1	New Zealand, ND, Warawara St Forest, 7.xii.2008, R. Leschen, T. Buckley & D. Seldon lgt., RL1375	sifting rotten wood and leaf litter
Cyloma sp7	NZ577.2	New Zealand, ND, Warawara St Forest, 7.xii.2008, R. Leschen, T. Buckley & D. Seldon lgt., RL1375	sifting rotten wood and leaf litter
Cyloma sp8	NZ61	New Zealand, ND, Waiatua Strm, Herekino Heads, 8-23.xii.2010, D. Seldon & F. Brook lgt., TB534, 25253281E, 6659141N	pit trap
Cyloma sp5	NZ237.1	New Zealand, FD, Borland Road along Percy Stream, 45°36.43'S 167°20.78'E, 430m, 25-27.i.2016, Seidel & Fikáček lgt., 2016-NZ028	baited pitfall traps (rotten squid) in mossy *Nothofagus* forest with large stony blocks
Cyloma sp6	NZ32.1	New Zealand, NN, Oparara Basin, Oparara Arches Track, mixed *Nothofagus* and podocarp forest, 30.i.2012, R. Leschen lgt., 41.149821°S 172.189917°E, RL1642	sifted rotten wood
Cyloma sp1	NZ351.1	New Zealand, WN, Tararua Forest Park, southern crossing btwn. Kime Hut & Dennan Peak, 1200-1300m, 40°56'S 175°16'E, 25.xi.2005, FMHD#2005-038, A. Solodovnikov & D. Clarke lgt., ANMT site 1154	alpine zone w/scrub *Olearia*
Cyloma sp10	NZ259.1	New Zealand, WD, Cockayne Nature Walk at Otira Hwy., 42°48.06'S 171°34.26'E, 380m, 24-26.ii.2016, Seidel, Sýkora, Leschen, Maier & Lambert lgt., 2016-NZ-MS66	baited pitfall traps (rotten squid) in stony forest
Enigmahydrus larvalis	MF665	New Zealand, Taranaki, unnamed stream 0.2km S of Pukeiti Garden, 9km E of Okato, 370m, 30.xi.2012, 39°12.1'S 173°58.9'E, Becker, Fikáček & Hájek lgt.	in mosses on stones in/along the stream in lowland *Nothofagus* forest
Saphydrus suffusus	NZ462	New Zealand, NN, Nelson Lakes NP, N end of Lake Rotoroa at Braeburn Track 41.7987°S 172.58421°E, 522m, 5-9.xii.2016, Fikáček & Seidel lgt., MM57	lowland wet *Nothofagus* forest with huge amount of sooty moulds and with continuous layer of *Blechnum* fern understory, baited pitfall traps (rotten squid)
Saphydrus suffusus	COL1786	New Zealand, BR, Rough Crk, Maruia Springs, 12.i.2011, R. Leschen & T.R. Buckley lgt., TB455, 42°22.825'S 172°16.798'E, 550m	
Cylorygmus lineatopunctatus	MF790	Chile, Valparaiso, PN La Campana, Sector Ocoa, 4.75km SE of park entrance, "La Cascada", 870m, 20.xi.2013, 32°57.7'S 71°3.2'W, Fikáček, Kment & Vondráček lgt., CH03	
Relictorygmus trevornoahi	MF1727.2	South Africa, Western Cape, 13.3km SEE Stanford (wetland), 100m, 4-5.xii.2015, 34°27.84S 19°35.75E, Arriaga, Fikáček, Seidel & Vondráček, RSA50	
Rygmostralia sp1	COL800	Australia, QLD, Mt. Bartle Frere, NW peak, 1426m, 19.xi.2009, 17.385°S 145.802°E, Monteith & Turco lgt.	sieved litter
Borborophorus tuberculus	COL666	Australia, QLD, Baldy Mt. Rd., RF, 1100m, 11.x.2008, 17°17'20"S 145°25'34"E, G. Monteith lgt.	pyrethrum trees
Exydrus gibbosus	NZ114.1	New Zealand, Auckland, Auckland - Lynfield, 31.i.2016, Wattle Bay reserve, 36°56.1′S 174°43.6′E, 2-30m, J.Hájek & P. Hlaváč lgt.	sifting in secondary coastal forest
Exydrus gibbosus	COL1791	New Zealand, BP, Ohope, 8.ix.2009, R. Leschen & E. Hilario lgt., RL1493, 37.97338°S 177.07198°E	
Exydrus gibbosus	NZ747	New Zealand, ND, Tangihua Forest, Te Haua Ura Tk., 35°53'01"S 174°07'38"E, 80m, 18.xi.2018, J. Shen lgt., JWS073	sifted leaf litter, moss & rotten woods
Thomosis guanicola	NZ640	New Zealand, Antipodes Islands, 24.vii.2016	
Hydrostygnus frontalis	COL1777	New Zealand, ND, Waipoua NP, Yakas Tk, 14.ii.2008, R. Leschen, B. Michaux lgt., 35.61717°S173.52986°E, RL1340	under rotten logs
Hydrostygnus frontalis	NZ70.1	New Zealand, ND, Puketi Forest, Nature Walk, 16.iii.2011, R. Leschen & N. Lord lgt., 35°12.714'S 173°47.461'E, 358m, RL1555	beating and under bark (night)
new genus2 sp1	COL1775	New Zealand, WD, Wharekai Te Kau Walk, Jackson Bay, 5.xi.2007, 43 58.286S, 168 36.738E, R. Leschen & C. Carlton lgt., RL1293	leaf litter and rotten log berlesate
new genus2 sp1	NZ185.1	New Zealand, WD, Lake Wombat Track 2.5km S of Franz Josef, 43°24.80'S 170°10.43'E, 200m, 21-23.ii.2016, Seidel, Sýkora, Leschen & Maier lgt., 2016-NZ-MS50	sifting of leaf litter in native forest

new genus1 sp1	NZ161	New Zealand, FD, Borland Road at right-bank tributary of Percy Stream, 45°36.46'S 167°20.64'E, 400m 25-27.i.2016, Seidel, Sýkora & Fikáček lgt., 2016-NZ027	sifting of mosses and leaf litter (in rain) in mossy *Nothofagus* forest
new genus1 sp2	NZ358.1	New Zealand, BR, Mt Faraday, 17.ii.2015, R. Leschen, T. Buckley lgt., RL1817A, 128m, 42°01.972'S 171°34.638'E	sifting alpine leaf litter
Coelostomopsis picea	COL119	Australia, QLD, Mt Finnigan summit, 1100m, 20.x.2008, 15°49'16S 145°16'35E, G. Monteith lgt.	berlesate moss
Eurygmus helocharoides	COL2028	Australia, QLD, Polly Ck., Garradunga, malaise 6, 58m, 13.i.-14.ii.2010, 17.458°S 146.021°E, J. Hasenpusch lgt.	
Andotypus ashworthi	MF792	Chile, Los Lagos, PN Puyehue, Aguas Calientes, lower part of Sendero Pionero, 520m, 5-9.xii.2013, 40°44.3'S 72°18.6'W, Fikáček, Kment & Vondráček lgt., CH27	baited pitfall traps (rotten fish) in Valvidian (evergreen laurel-leaf) rainforest
Anticura flinti	MF793	Chile, Los Lagos, PN Puyehue, Anticura, Río Anticura between Salto Pudú and confluence with Río Golgol, 350-460m, 6-9.xii.2013, 40°40.0-40.5'S 72°9.9-10.6'W, Fikáček, Kment & Vondráček lgt., CH29	floating, mosses from the stone in the river (submerged + just above water) and the flood debris accumulated in logjam
Austrotypus nothofagi	MF540	Australia, Queensland, Lamington NP, 800m, 13-15.iii.2013, 28°11.9'S, 153°11.2'E, G. Monteith lgt.	
new genus3 sp1	MF515	New Zealand, Taranaki, unnamed stream 0.2km S of Pukeiti Garden, 9km E of Okato, 370m, 30.xi.2012, 39°12.1'S 173°58.9'E, Becker, Fikáček & Hájek lgt., NZ27	in mosses on stones in/along the stream in lowland *Nothofagus* forest
Cylomissus sp1	NZ146.1	New Zealand, Central Otago, Remarkables Mts, 16.ii.2016, Wye Creek track, 45°08.3′S 168°46.1′E, 590m, M. Fikáček, J. Hájek & P. Hlaváč lgt.	stream collecting in submerged moss in small forest stream (Wye Creek)
Cylomissus sp1	NZ186	New Zealand, CO, Stream at Symes Road (Old Man Range), 45°20.63'S 169°13.91'E, 1340m, 15.ii.2016, Seidel, Sýkora, Leschen & Maier lgt., 2016-NZ-MS07	stream collecting in very small subalpine stream (tributary to Butchers Creek), collecting in submerged moss and gravel
Cylomissus sp4	NZ512.1	New Zealand, WO, Pirongia Forest Park, Mangakara Nature Walk + lower part of Ruapane Link Track, 37.966°S 175.144-149°E, 177-235m, 18.xi.2016, Fikáček & Seidel lgt., MM01	lowland broadleaf forest with podocarps, nikau palms and *Ripogonum* lianas, sparse understory, floating emerged mosses in small stream
Cylomissus sp4	NZ273	New Zealand, AK, Nihotupu Stream at waterfall, 36°56.50'S 174°33.47'E, 260m, 6.iii.2016, Seidel & Leschen lgt., 2016-NZ-MS87	stream collecting in small forest stream (Nihotupu Stream), collecting in submerged moss
Cylomissus glabratus	NZ138.1	New Zealand, FD, Tutoko Valley Tk. ca. 0.5 km from Milford Sound Hwy, 44°40.35'S 167°57.99'E, 90m, 1.ii.2016, Seidel, Sýkora & Fikáček lgt., 2016-NZ046	small stream in *Nothofagus* forest with many ferns/tree ferns, largely dried-up, with some submerged moss
Cylomissus glabratus	NZ540.1	New Zealand, BR, Ten Mile Creek at Matakitaki Rd. 13.4km S of Murchinson 41.92019°S 172.31994°E, 275m 9.xii.2016, Fikáček & Seidel lgt.	large stony stream in the *Nothofagus* forest, submerged moss
Adolopus sp1	NZ75	New Zealand, ND, Puketi Forest, Nature Walk, 16.iii.2011, R. Leschen & N. Lord lgt., 35°12.714'S 173°47.461'E, 358m, RL1549	sifting leaf litter
Adolopus sp2	NZ46.1	New Zealand, WO, Marokopa Falls, 3.iii.2012, M. Gimmel & R. Leschen lgt., 38°15.560'S 174°50.926'E, RL1654	ex beating
Adolopus sp3	NZ665.1	New Zealand, WN, Mount Holdsworth, Tararua Forest Park, 29.i.2008, K. Marske, R. Leschen & T. Buckley lgt., 40°54.408'S 175°28.432'E, 282m	sifted wood and leaf litter
Adolopus sp4	NZ560	New Zealand, ND, Mangamuka, 8.xii.2008, 35°11.463'S 173°27.323'E, R. Leschen, T. Buckley & D. Seldon lgt., RL1389	ex rotten wood
Adolopus sp5	NZ735	New Zealand, ND, Warawara Forest, Warawara Tk., 35°22'12"S 173°16'59"E, 370 m, 22.xi.2018, J. Shen lgt., JWS077	sifted leaf litter, moss & rotten wood
Adolopus sp5	NZ606.1	New Zealand, ND, Warawara St Forest, 7.xii.2008, R. Leschen, T. Buckley & D. Seldon lgt., RL1376	ex rotten logs
Adolopus sp6	NZ565.1	New Zealand, MK, Temple Valley, 10.i.2006, R. Leschen, T. Buckley & R. Hoare lgt., RL1043, 44.10676°N 169.81697°E	leaf litter
Adolopus sp6	NZ168.1	New Zealand, FD, Borland Walk at Borland Lodge, 45°46.35-48'S 167°32.18-25'E, 180 m, 23-28.i.2016, Seidel & Fikáček lgt., 2016-NZ020	on/under moist rotten logs and polypore fungi
Adolopus sp7	NZ672	New Zealand, WA Waikuku Lodge, Aorangi Range, 24.i.2008. K. Marske, R. Leschen & T. Buckley lgt., 41°24.616'S E175°21.880'E, 458m	ex leaf litter/rotten wood

Adolopus sp7	NZ649.1	New Zealand, WA, Sutherland Vehicle Track, Aorangi Range, 24.i.2008, K. Marske, R. Leschen & T. Buckley lgt., 41°25.239'S E175°21.551'E, 398m	sifted wood and leaf litter in secondary forest on former grazing land
Adolopus sp8	NZ666.1	New Zealand, OL, Thunder Ck, 13.i.2006, R. Leschen, T. Buckley & R. Hoare lgt., RL1065, 44.03749°S 169.36664°E	rotten logs
Adolopus sp8	NZ643.1	New Zealand, OL, Pleasant Flat, 13.i.2006, R. Leschen, T. Buckley & R. Hoare lgt., RL1066, 44.01224°S 169.38128°E	at night
Adolopus sp8	NZ643.2	New Zealand, OL, Pleasant Flat, 13.i.2006, R. Leschen, T. Buckley & R. Hoare lgt., RL1066, 44.01224°S 169.38128°E	at night
Adolopus sp9	NZ52	New Zealand, WO, Marokopa Falls, 3.iii.2012, M. Gimmel, R. Leschen lgt., 38°15.560'S 174°50.926'E, RL1653	ex rotten wood
Rygmodus sp1	COL1794	New Zealand, Northern Cartenbury, Arthur's Pass Village, 750m, 17.i.2011, 42°56.321'S 171°33.706'E, R. Leschen lgt., TB497	ex *Hoheria*
Rygmodus sp1	COL1832	New Zealand, Westland, Kellys Creek, Otira, 332m, 17.i.2011, 42 48.123 S 171 34.298 E, R. Leschen & T.R. Buckley lgt., TB490	beating *Hoheria*
Rygmodus opimus	NZ162	New Zealand, DN, Taieri Mouth, Picknick Gully, 46°3.25'S 170°11.27'E, 25m, 12.ii.2016, Seidel, Sýkora & Fikáček lgt., 2016-NZ073	sifting of small accumulations of leaf litter + hand collecting in small remnant of native coastal forest (very dry)
Rygmodus sp2	NZ155.1	New Zealand, FD, Borland Rd., at stream just below Borland Saddle, 45°44.79'S 167°23.17'E, 940m, 24.i.2016, Seidel, Sýkora & Fikáček lgt., 2016-NZ022	sweeping/beating flowering *Hebe* bushes along the mountain stream at the border of forest and subalipine tussock area
Rygmodus cf. *antennatus*	MF875	New Zealand, Buller, Sewell Peak, 146m, 13.i.2014, 42°25.382'S 171°17.753'E, T. Buckley, M. Gimmel & R. Leschen lgt., RL1709	beating *Leptospermum*
Rygmodus cf. *antennatus*	MF549	New Zealand, Buller, Whareata Mine, Denniston, 650m, 27.i.2012, 41°46.031'S 171°47.255'E, R. Leschen, L. Dunning & C. Williams lgt., RL1638	ex flowers of manuka (*Leptospermum scoparium*),
Rygmodus alienus	MF550	New Zealand, Buller, Whareata Mine, Denniston, 650m, 27.i.2012, 41°46.031'S 171°47.255'E, R. Leschen, L. Dunning & C. Williams lgt., RL1638	ex flowers of manuka (*Leptospermum scoparium*)
Rygmodus alienus	COL1826	New Zealand, Buller, Klondyke spur, Victoria Ra, 1293m, 11.i.2011, 42°18.032'S 172°07.511'E, R. Leschen & T.R. Buckley lgt., TB441	ex *Celmisia*
Rygmodus sp4	COL1841	New Zealand, Coromandel, Tapu, Coroglen Track, 16.xi.2009, 36°59'S 175°35'E, D. Seldon lgt., RL1580	ex *Cordyline austalis* flowers
Rygmodus sp4	MF560	New Zealand, Coromandel, Tapu, Coroglen Track, 16.xi.2009, 36°59'S 175°35'E, D. Seldon lgt., RL1580	ex *Cordyline austalis* flowers
Rygmodus tibialis	COL1845	New Zealand, Westland, Cattle Walk Tr, Waita River, 7.xi.2007, 43°47.508'S 169°7.233'E, R. Leschen & C. Carlton lgt., RL1302	under stones along river
Rygmodus cf. *incertus*	COL1818	New Zealand, Northland, Warawara St Forest, 13.xii.2009, 35°22.011' S 173°16.695' E, R. Leschen, T. Buckley & D. Seldon lgt., RL1446	ex *Cordyline banksii* flowers
Rygmodus femoratus	COL1824	New Zealand, WO, Mt. Te Aroha, 8.xii.2007, D. Seldon lgt., 37°32'S 175°44'E, RL1581	ex *Cordyline indivisa* flowers
Tormissus magnulus	NZ461.1	New Zealand, NN, Nelson Lakes NP, N end of Lake Rotoroa at Braeburn Track 41.7987°S 172.58421°E, 522m 5-9.xii.2016, Fikáček & Seidel lgt., MM57	lowland wet *Nothofagus* forest with huge amount of sooty moulds and with continuous layer of *Blechnum* fern understory, baited pitfall traps (rotten squid)
Tormissus magnulus	COL1806	New Zealand, WN, Kapiti Island, Wilkinson Track, 21.i.2008, K. Marske, R. Leschen & T. Buckley lgt., 40°51.145'S 174°55.722'E, 260m, KM227	under/in dead wood
Tormissus linsi	NZ160.1	New Zealand, FD, Borland Road 24km NWW of Monowai, 45°41.13'S 167°20.29'E, 320m, 24-27.i.2016, Seidel, Sýkora & Fikáček lgt., 2016-NZ024	baited pitfall traps (rotten squid) in degraded remnants of *Nothofagus* forest with numerous rotten logs
Tormissus sp3	NZ754.1	New Zealand, ND, Lower Waipapa River Track, Omahuta Forest, 35.2749361°S 173.688°E, 12m, 17.xi.2018, J. Shen & V. Sýkora lgt., 2018-NZ27	baited pitfall traps in a native kauri/podocarp forest
Pseudohydrobius flavus	COL803	Australia, QLD, Mt. Lewis Rd., hut 12km NW Julatten, 1187m, 21.xi.2009, 16.511°S 145.269°E, Monteith & Turco lgt.	

Supplementary Table S2. Primer sequences and programs used for PCRs for the gene fragments used in our study.

Cox1-5'							
LCO1490	GGTCAACAAATCATAAAGATATTGG (Folmer et al. 1994)						
HCO2198	TAAACTTCAGGGTGACCAAAAAATCA (Folmer et al. 1994)						
PROGRAM							
Step	1	2	3	4	5	6	7
Temp.	94°C	94°C	48°C	72°C	repeat 2-4	72°C	12°C
Time	3:00	0:30	0:45	1:00	34x	8:00	forever
Cox1-3'							
SJerryF	CAACATYTATTYTGATTYTTTGG (Timmermans et al. 2010)						
SPatR	GCACTAWTCTGCCATATTAGA (Timmermans et al. 2010)						
PROGRAM							
Step	1	2	3	4	5	6	7
Temp.	95°C	95°C	50°C	72°C	repeat 2-4	72°C	12°C
Time	5:00	0:30	0:40	2:00	40x	8:00	forever
H3							
H3aR	ATGGCTCGTACCAAGCAGACGGC (Colgan et al. 1998)						
H3aF	ATATCCTTGGGCATGATGGTGAC (Colgan et al. 1998)						
PROGRAM							
Step	1	2	3	4	5	6	7
Temp.	95°C	95°C	50°C	72°C	repeat 2-4	72°C	12°C
Time	3:00	0:30	0:30	1:00	34x	10:00	forever
12S							
12s ai	AAACTACGATTAGATACCCTATTAT (Simon et al. 1994)						
12s bi	AAGAGCGACGGGCGATGTGT (Simon et al. 1994)						
PROGRAM							
Step	1	2	3	4	5	6	7
Temp.	94°C	94°C	50°C	72°C	repeat 2-4	72°C	12°C
Time	3:00	0:30	0:45	1:00	34x	8:00	forever
16S							
16S-1472-JJ	GGTCCTTTCGTACTAA (Astrin & Stüben 2008)						
16S-ar-JJ	CRCCTGTTTATTAAAAACAT (Astrin & Stüben 2008)						
PROGRAM							
Step	1	2	3	4	5	6	7
Temp.	94°C	94°C	50°C	72°C	repeat 2-4	72°C	12°C
Time	3:00	0:30	0:45	1:00	34x	8:00	forever
28S							
28S NLF 184-21	ACCCGCTGAAYTTAAGCATAT (Van der Auwera et al. 1994)						
28S LS1041R	TACGGACRTCCATCAGGGTTTCCCCTGACTTC (Maddison 2008)						
PROGRAM							
Step	1	2	3	4	5	6	7
Temp.	94°C	94°C	52°C	72°C	repeat 2-4	72°C	12°C
Time	3:00	0:30	0:45	1:00	34x	10:00	forever
Topoisomerase							
external primers (1 µl of DNA extract/10 µl PCR reaction)**:**							
TP643F	GACGATTGGAARTCNAARGARATG (Wild & Maddison 2008)						
TP932R	GGWCCDGCATCDATDGCCCA (Wild & Maddison 2008)						
internal primers (0.7 µl of external primer PCR product/10 µl PCR reaction)**:**							
TP675F	GAGGACCAAGCNGAYACNGTDGGTTGTTG (Wild & Maddison 2008)						
TP919R	GTCTCTTTGCGTYTTRTTRTADATYTTYTC (Wild & Maddison 2008)						
PROGRAM							
Step	1	2	3	4	5	6	7
Temp.	95°C	95°C	56°C	72°C	repeat 2-4	72°C	12°C
Time	3:00	0:30	0:45	1:30	37x	8:00	forever
18S5							
18S5'	GACAACCTGGTTGATCCTGCCAGT (Shull et al. 2001)						
18Sb5.0	TAACCGCAACAACTTTAAT (Shull et al. 2001)						
PROGRAM							
Step	1	2	3	4	5	6	7
Temp.	95°C	95°C	50°C	72°C	repeat 2-4	72°C	4°C
Time	5:00	0:30	0:40	2:00	40x	8:00	forever

18Sce							
18Sai	CTTGAGAAACGGCTACCACATC (Whiting et al 1997)						
18Sb0.5	GTTTCAGCTTTGCAACCAT (Whiting et al 1997)						
PROGRAM							
Step	1	2	3	4	5	6	7
Temp.	95°C	95°C	50°C	72°C	repeat 2-4	72°C	4°C
Time	5:00	0:30	0:40	2:00	40x	8:00	forever
18S3							
18Sa1.0	GGTGAAATTCTTGGACCGTC (Shull et al. 2001)						
18S3´I	CACCTACGGAAACCTTGTTACGAC (Shull et al. 2001)						
PROGRAM							
Step	1	2	3	4	5	6	7
Temp.	95°C	95°C	50°C	72°C	repeat 2-4	72°C	4°C
Time	5:00	0:30	0:40	2:00	40x	8:00	forever

Supplementary Table S3. Node calibration parameters used for the divergence dating analyses in MrBayes.

		lognormal			uniform		exponential	
fossil	group dated	min age	mean age	stdev	min age	max age	min age	mean age
Protochares brevipalpis	Hydrophiloidea s. str.	145.0	164.0	3	145.0	214.68	145.0	214.68
Helophorus paleosibiricus	stem Helophoridae	135.0	155.1	3	135.0	214.68	135.0	214.68
Hydrobiomorpha eopalpalis	stem Hydrobiomorpha	47.0	67.09	3	47.0	214.68	47.0	214.68
Hydrochara sp.	stem *Hydrochara*	47.0	67.09	3	47.0	214.68	47.0	214.68
Baissalarva hydrobioides	stem Laccobiini	135.0	155.1	3	135.0	214.68	135.0	214.68
Limnoxenus olenus	stem *Limnoxenus*	22.5	42.59	3	22.5	146.0	22.5	146.0
Hydrobius titan	stem *Sperchopsis*	33.9	53.99	3	33.9	146.0	33.9	146.0
Cretocrenis burmanicus	crown Anacaenini	99.0	119.1	3	99.0	214.68	99.0	214.68

Supplementary Table S4. Taxon names, codes and GenBank accession numbers of Cylominae [when available: sequences to be submitted to GenBank after the submission of the paper for publication are provided with specimen codes only].

	GenBank accession numbers							
Taxon (alternative name in parenthesis)	**Cox1-5'**	**Cox1-3'**	**H3**	**12S**	**16S**	**18S**	**28S**	**Topo-isomerase**
Adolopus sp1	NZ75	NZ75	NZ75	NZ75	NZ75	NZ75	NZ71.1	NZ75
Adolopus sp2	NZ46.1	NZ46.1	NZ46.1	NZ46.1	NZ46.1	NZ46.1	NZ46.1	NZ46.1
Adolopus sp3	NZ665.1	NZ665.1	NZ665.1	NZ665.1	NZ665.1	NZ665.1	NZ655.1	NZ665.1
Adolopus sp4	NZ560	NZ560	NZ560	-	NZ560	NZ560	-	-
Adolopus sp5	NZ735	NZ735	NZ735	NZ735	NZ606.1	NZ606.1	-	NZ735
Adolopus sp6	NZ565.1	NZ565.1	NZ565.1	NZ565.1	NZ565.1	NZ565.1	NZ168.1	NZ565.1
Adolopus sp7	NZ672	NZ672	NZ672	NZ672	NZ672	NZ672	NZ649.1	NZ672
Adolopus sp8	NZ666.1	NZ666.1	NZ666.1	NZ643.1	NZ666.1	NZ643.2	NZ666.1	-
Adolopus sp9	NZ52	NZ52	NZ52	-	NZ52	NZ52	NZ52	NZ52
Andotypus ashworthi	MF792	MF792	MF792	-	-	MF792	MF792	-
Anticura flinti	MF793	KM262054.1	MF793	MF793	MF793	KT447582.1	MF793	-
Austrotypus nothofagi	MF540	MF540	MF540	MF540	MF540	MF540	MF540	MF540
Borborophorus tuberculus	-	KC935232.1	-	COL666	-	KC935009.1	KJ845053.1	-
Coelostomopsis picea	-	KC935245.1	COL119	COL119	-	KC935022.1	KC992551.1	-
Cyloma guttulatus1	NZ243.1	NZ243.1	NZ243.1	NZ243.1	NZ243.1	NZ111.1	NZ243.1	NZ243.1
Cyloma guttulatus2	NZ213.1	NZ213.1	NZ213.1	NZ213.1	NZ213.1	NZ262	NZ213.1	NZ213.1
Cyloma guttulatus3	NZ729.1	NZ729.1	NZ729.1	NZ729.1	NZ729.1	NZ468.1	-	NZ729.1
Cyloma lawsonus	NZ434	NZ434	NZ117.1	NZ434	NZ434	NZ434	NZ117.1	NZ434
Cyloma lineatus	NZ83	NZ83	NZ83	NZ83	NZ83	NZ83	NZ83	NZ83
Cyloma pictus	NZ676	NZ676	NZ676	NZ676	NZ676	NZ676	-	NZ566.1
Cyloma sp1 (NZ351.1)	NZ351.1	NZ351.1	NZ351.1	NZ351.1	-	NZ351.1	-	NZ351.1
Cyloma sp10 (NZ259.1)	NZ259.1	NZ259.1	NZ259.1	NZ259.1	NZ259.1	-	-	-
Cyloma sp2 (Cyloma paxtoni)	NZ178	NZ178	NZ178	NZ178	NZ178	NZ178	COL1789	-
Cyloma sp3 (Cyloma docorum)	NZ157	NZ157	NZ157	NZ157	NZ157	NZ157	NZ156.1	NZ157
Cyloma sp4 (Cyloma biguttatus)	NZ69.1	NZ69.1	NZ69.1	NZ69.1	NZ69.1	NZ69.1	NZ69.1	NZ69.1
Cyloma sp5 (Cyloma acutangulus)	NZ237.1	NZ237.1	NZ237.1	NZ237.1	NZ237.1	NZ237.1	NZ237.1	NZ237.1
Cyloma sp6 (Cyloma globulus)	NZ32.1	-	NZ32.1	-	NZ32.1	-	-	-
Cyloma sp7 (Cyloma sp ND)	NZ577.2	NZ577.2	NZ577.2	NZ577.1	NZ577.2	NZ577.2	-	NZ577.1
Cyloma sp8 (Cyloma germanicolor)	NZ61	NZ61	NZ61	NZ61	NZ61	NZ61	NZ61	NZ61
Cyloma sp9 (Cyloma cf inexpectatus)	NZ464	NZ464	NZ464	NZ464	NZ464	NZ464	-	NZ464
Cyloma stewarti	NZ31	NZ31	NZ31	NZ728.1	NZ31	NZ31	COL1778	NZ31
Cyloma thomsonus	NZ158	NZ158	NZ158	NZ158	NZ158	NZ158	NZ248.1	NZ158

Cylomasp11 (Cyloma rakiura)	NZ187.1	NZ187.1	NZ187.1	NZ187.1	NZ187.1	NZ187.1	NZ187.1	NZ187.1
Cylomissus glabratus (Cylomissus sp3)	NZ540.1	NZ540.1	NZ540.1	NZ540.1	NZ540.1	NZ540.1	NZ138.1	NZ540.1
Cylomissus sp1	NZ186	NZ186	NZ186	NZ186	NZ186	NZ146.1	NZ186	NZ186
Cylomissus sp4	NZ512.1	NZ512.1	NZ512.1	NZ273	NZ512.1	NZ512.1	-	NZ512.1
Cylorygmus lineatopunctatus	MF790	MF790	MF790	MF790	-	MF790	-	MF790
Enigmahydrus larvalis (strange larva)	-	MF665	-	-	MF665	MF665	MF665	-
Eurygmus helocharoides	COL2028	COL2028	COL2028	COL2028	COL2028	COL2028	COL2028	-
Exydrus gibbosus	NZ114.1	COL1791	COL1791	NZ747	NZ114.1	COL1791	COL1791	COL1791
Hydrostygnus frontalis	NZ70.1	KC935285.1	COL1777	COL1777	NZ70.1	COL1777	COL1777	COL1777
new genus1 sp1 (Adolopus cephalotes)	NZ161	NZ161	NZ161	NZ161	NZ161	NZ161	NZ161	NZ161
new genus1 sp2 (Adolopus nonstriatus)	NZ358.1	NZ358.1	NZ358.1	NZ358.1	NZ358.1	NZ358.1	NZ358.1	NZ358.1
new genus2 sp1 (Adolopus versicolor)	NZ185.1	NZ185.1	-	NZ185.1	NZ185.1	COL1775	NZ185.1	-
new genus3 sp1 (Cylomissus hanseni)	MF515	MF515	MF515	MF515	MF515	MF515	MF515	MF515
Pseudohydrobius flavus	COL803	KF801992.1	COL803	COL803	COL803	COL803	KF802155.1	COL803
Relictorygmus trevornoahi	MF1727.2	MF1727.2	-	-	MF1727.2	MF1727.2	MF1727.2	MF1727.2
Rygmodus alienus (Rygmodus sp11)	MF550	MF550	MF550	MF550	-	MF550	-	COL1826
Rygmodus cf antennatus (Rygmodus sp9)	MF875	MF875	MF875	MF875	MF875	MF549	-	MF875
Rygmodus cf. incertus (Rygmodus sp6)	-	COL1818	COL1818	-	-	COL1818	-	-
Rygmodus femoratus (Rygmodus sp10)	COL1824	COL1824	COL1824	-	-	COL1824	-	-
Rygmodus opimus (Rygmodus sp8)	NZ162	NZ162	NZ162	-	NZ162	NZ162	NZ162	NZ162
Rygmodus sp1	COL1794	COL1794	COL1794	COL1794	COL1794	COL1794	COL1794	COL1832
Rygmodus sp2	NZ155.1	NZ155.1	NZ155.1	NZ155.1	NZ155.1	NZ155.1	NZ155.1	NZ155.1
Rygmodus sp4	COL1841	COL1841	COL1841	MF560	COL1841	COL1841	COL1841	COL1841
Rygmodus tibialis (Rygmodus sp7)	COL1845	COL1845	COL1845	MF556	-	COL1845	COL1845	COL1845
Rygmostralia sp1	COL800	KF801989.1	COL800	COL800	KF801824.1	COL800	KF802152.1	COL800
Saphydrus suffusus	NZ462	NZ462	NZ462	NZ462	NZ462	COL1786	COL1786	NZ462
Thomosis guanicola	NZ640	NZ640	NZ640	NZ640	-	NZ640	-	-
Tormissus linsi (Tormissus sp2)	-	NZ160.1	-	NZ160.1	NZ160.1	-	-	NZ160.1
Tormissus magnulus (Tormissus sp1)	NZ461.1	COL1806	COL1806	COL1806	NZ461.1	COL1806	COL1806	COL1806
Tormissus sp3	NZ754.1	NZ754.1	NZ754.1	NZ754.1	NZ754.1	NZ754.1	-	NZ754.1

Supplementary Table S5. Taxon names, codes and GenBank accession numbers of outgroups adopted from Toussaint & Short (2018). GenBank accession numbers indicated with 'T&S 2018' (=Toussaint & Short 2018) will be added upon availability.

	GenBank accession numbers				
Taxon (alternative name in parenthesis)	**Cox1-3'**	**16S**	**18S**	**28S**	**H3**
Aculomicrus reticulatus MF94	-	-	KC934982	KC992514	-
Agraphydrus sp. SLE0252	KC935211	KC992640	KC934985	-	-
Allocotocerus yalumbaboothbyi SLE0082	-	KC992641	KC934986	KC992517	-
Ametor latus SLE0096	KC935212	-	KC934987	-	-
Ametor scabrosus AES0014	KC935213	-	KC934988	KC992518	-
Amphiops mater SLE0046	KC935214	-	KC934989	KC992519	-
Amphiops sp. SLE0407	KC935215	KC992642	KC934990	KC992520	-
Amphiops sp. SLE0408	KC935216	KC992643	KC934991	KC992521	-
Anacaena globulus	AM287086	AM287064	AM287125	-	-
Anacaena parvula MSC1818	KC935222	-	KC934997	KC992527	-
Anacaena lucida SLE0247 (Paranacaena_sp)	KC935221	KC992646	KC934992	-	-
Anacaena sp. MF198 (Grodum_sp)	KC935224	-	KC934999	KC992529	-
Anacena lineata SLE0246 (Omniops_sp)	KC935296	KC992645	KC934996	KC992526	-
Arabhydrus gallagheri SLE0073	KC935227	KC992650	KC935003	KC992532	T&S 2018
Australocyon puncticollis MF206	KC935228	-	KC935004	KC992533	-
Badioglobus tapanti SLE0053	KC935229	-	KC935005	KC992534	-
Berosus asymmetricus SLE0088	KC935230	KC992651	KC935006	KC992535	T&S 2018
Berosus garciai SLE0014	KC935231	KC992652	KC935007	KC992536	-
Berosus luridus	AM287087	AM287065	AJ810721	AJ810756	-
Berosus ornaticollis SLE0087	-	KC992653	KC935008	KC992537	-
Brownephilus major SLE0635	T&S 2018	T&S 2018	T&S 2018	T&S 2018	T&S 2018
Cercyodes laevigatus SLE0094	KC935233	-	KC935010	KC992538	-
Cercyon analis Chimera	DQ156007	-	EF213786	-	-
Cercyon ustulatus Chimera	DQ155947	AM287071	AM287129	AM287137	-
Cercyon variegatus SLE0020	KC935234	KC992654	KC935011	KC992539	-
Cercyon versicolor SLE0245	KC935235	-	KC935012	-	-
Cetiocyon incantatus SLE0251	KC935236	-	KC935013	KC992540	-
Chaetarthria incisa SLE0070	-	KC992655	KC935014	KC992541	-
Chaetarthria seminulum MF49	KC935238	-	KC935015	KC992542	-
Chaetarthria sp. SLE0410	KC935239	KC992656	KC935016	KC992544	-
Chaetarthria sp. MF247	KC935237	-	-	KC992543	-
Chasmogenus ruidus SLE0079	KC935240	KC992657	KC935017	KC992545	-
Chasmogenus sp. SLE0077	KC935241	KC992658	-	KC992546	-
Chasmogenus sp. SLE0078	KC935242	KC992659	KC935018	KC992547	-
Chasmogenus sp. SLE0080	KC935243	-	KC935019	KC992548	-
Coelostoma orbiculare Chimera	AM287094	AM287072	EF213785	KC992549	-
Coelostoma phallicum MF326	KC935244	-	KC935021	KC992550	-
Crenitulus hirsuta SLE0369 (Anacaena_hirsuta)	KC935217	KC992644	KC934993	KC992522	-
Crenitulus solstitialis MSC1815 (Anacaena_solstitialis)	KC935223	KC992647	KC934998	KC992528	-
Crentis sp. MSC1819	KC935246	KC992660	KC935023	KC992552	-
Cryptopleurum minutum SLE0058	KC935248	-	KC935024	KC992553	-
Cryptopleurum subtile SLE0250 (Megasternum_sp)	KC935247	KC935025	-	-	-
Cymbiodyta marginella	AM287088	-	AM287126	AM287134	-
Cymbiodyta semistriata AES0013	KC935252	-	KC935029	KC992557	-
Dactylosternum auripes MF63	KC935253	-	KC935030	KC992558	-
Dactylosternum sp. SLE0072	KC935254	KC992664	KC935031	KC992559	-
Deltostethus scitus SLE0126	KC935255	KC992665	KC935032	KC992560	-
Derallus sp. SLE0041	KC935256	KC992666	KC935033	KC992561	-

Enochrus fimbriatus SLE0084	KC935258	KC992668	KC935034	KC992563	-
Enochrus piceus SLE0409	KC935261	KC992670	KC935037	KC992565	-
Enochrus quadripunctatus	AM287090	AM287068	AM287127	AM287135	-
Enochrus talamanca SLE0048	KC935263	KC992672	KC935039	KC992567	-
Epimetopus sp.	AM287082	AM287060	AJ810724	AJ810759	-
Epimetopus sp. SLE0069	KC935264	KC992673	KC935040	KC992568	-
Gen. nov. sp. SLE0130	KC935282	-	KC935062	KC992588	-
Gen. nov. sp. SLE0101 (nr_Chasmogenus)	-	KC992684	KC935061	KC992600	-
Gen. nov. sp. SLE0102 (nr_Chasmogenus)	KC935283	KC992685	KC935060	KC992601	-
Georissus canalifer SLE0036	KC935265	KC992674	KC935041	KC992569	-
Georissus crenulatus BMNH679200	DQ221983	DQ202580	AY745584	-	-
Globulosis sp. SLE0027	KC935266	KC992675	KC935042	KC992570	-
Guyanobius lacuniventris SLE0024	KC935267	KC992676	KC935043	KC992571	-
Guyanobius sp. SLE0411	KC935268	KC992677	KC935044	KC992572	-
Helobata sp. SLE0031	KC935269	KC992678	KC935045	KC992573	-
Helochares sp. SLE0240	KC935271	KC992679	KC935047	KC992575	-
Helochares trujillo SLE0034	KC935270	-	KC935046	KC992574	-
Helocombus bifidus AES0004	KC935272	-	KC935048	KC992576	-
Helophorus aquaticus	AM287078	AM287056	AJ810741	AJ810749	-
Helophorus arvernicus	AM287079	AM287057	AM287122	AM287130	-
Helophorus guttulus	AM278080	AM287058	AM287123	AM287131	-
Hemiosus selva SLE0051	-	KC992680	KC935049	KC992577	-
Hemisphaera seriatopunctata SLE0047	KC935273	-	KC935050	KC992578	-
Horelophopsis hanseni MSC1821	KC935274	-	KC935051	KC992579	-
Horelophus walkeri SLE0032	KC935275	-	KC935052	KC992580	-
Hybogralius hartmeyeri AES0007	KC935277	-	KC935054	KC992582	-
Hydrobiomorpha casta SLE0597	T&S 2018	T&S 2018	T&S 2018	T&S 2018	T&S 2018
Hydrobiomorpha praesumptapolita SLE0577	T&S 2018	T&S 2018	T&S 2018	T&S 2018	T&S 2018
Hydrobiomorpha sp. SLE0566	T&S 2018	T&S 2018	T&S 2018	T&S 2018	T&S 2018
Hydrobiomorpha sp. SLE0601	T&S 2018	T&S 2018	T&S 2018	T&S 2018	T&S 2018
Hydrobiomorpha spinicollis SLE0620	T&S 2018	T&S 2018	T&S 2018	T&S 2018	T&S 2018
Hydrobius fuscipes AES0002	KC935279	-	KC935056	KC992584	-
Hydrobius melaenus AES0024	KC935280	-	KC935057	KC992585	-
Hydrobius tumidus A6	T&S 2018	T&S 2018	T&S 2018	T&S 2018	T&S 2018
Hydrochara caraboides SLE0582	T&S 2018	T&S 2018	T&S 2018	T&S 2018	T&S 2018
Hydrochara elliptica SLE0585	T&S 2018	T&S 2018	T&S 2018	T&S 2018	T&S 2018
Hydrochara lineata SLE0595	T&S 2018	T&S 2018	T&S 2018	T&S 2018	T&S 2018
Hydrochus angustatus Chimera	HM569417	-	-	AF427601	-
Hydrochus carinatus	AM287084	AM287062	AM287124	AM287132	-
Hydrochus elongatus Chimera	HM569423	-	AJ810717	AJ810752	-
Hydrochus spangleri SLE0081	-	KC992683	KC935059	KC992587	-
Hydrophilomima sp. SLE0067	-	KC992686	KC935063	KC992589	T&S 2018
Hydrophilus albipes SLE0636	-	-	KC935064	KC992590	-
Hydrophilus cavicrus SLE0586	T&S 2018	T&S 2018	T&S 2018	T&S 2018	T&S 2018
Hydrophilus masculinus SLE0075	T&S 2018	T&S 2018	T&S 2018	T&S 2018	T&S 2018
Hydrophilus senegalensis SLE0627	T&S 2018	T&S 2018	T&S 2018	T&S 2018	T&S 2018
Hydrophilus smaragdinus SLE0552	T&S 2018	T&S 2018	T&S 2018	T&S 2018	T&S 2018
Laccobius sp. SLE0437	T&S 2018	T&S 2018	T&S 2018	T&S 2018	T&S 2018
Laccobius reflexipennis SLE0015	KC935287	KC992689	KC935067	KC992592	-
Laccobius sp. SLE0939	T&S 2018	T&S 2018	T&S 2018	T&S 2018	T&S 2018
Laccobius serratus SLE0057	KC935288	KC992690	KC935068	KC992593	-
Laccobius sp. SLE0433	T&S 2018	T&S 2018	T&S 2018	T&S 2018	T&S 2018
Limnocyclus puncticeps AES0010	T&S 2018	T&S 2018	T&S 2018	T&S 2018	T&S 2018
Limnoxenus niger AES0027	KC935289	-	KC935069	KC992594	-
Limnoxenus semicylindricus AES0021	KC935290	KC992691	KC935070	KC992595	-
Limnoxenus zealandicus AES0025	KC935291	-	KC935071	KC992596	-
Moraphilus sp. SLE0128	KC935292	-	KC935072	KC992597	-
Notionotus liparus MSC1820	KC935293	-	KC935073	KC992598	-

Notionotus sp. SLE0092	KC935294	KC992692	KC935074	KC992599	-
Oocyclus andinus SLE0039	T&S 2018	T&S 2018	T&S 2018	T&S 2018	T&S 2018
Oocyclus sp. SLE0421 (Oocyclus_cf_floccus)	T&S 2018	T&S 2018	T&S 2018	T&S 2018	T&S 2018
Oocyclus latus SLE0430	T&S 2018	T&S 2018	T&S 2018	T&S 2018	T&S 2018
Oocyclus ornatus SLE0050	KC935299	KC992694	-	KC992605	-
Oocyclus petra SLE0005	KC935300	KC992695	KC935078	KC992606	-
Oocyclus trujillo SLE0037	KC935305	KC992699	-	KC992611	-
Oosternum soricoides MF224	KC935306	-	KC935079	KC992612	-
Opthalmocyclus sp. Chimera	KC935307	KC992700	KC935080	KC992613	-
Pachysternum nigrovittatum SLE0066	KC935308	-	KC935081	KC992614	-
Pacrillum sp. MF205	KC935309	-	KC935082	KC992615	-
Paracymus limbatus SLE0040	KC935310	KC992701	KC935083	KC992616	-
Paracymus pygmaeus SLE0044	KC935311	KC992702	KC935084	KC992617	-
Paracymus subcupreus SLE0249	KC935312	-	KC935085	KC992618	-
Paroosternum saundersi SLE0063	-	-	KC935086	KC992619	-
Pelthydrus sp. SLE0947	T&S 2018	T&S 2018	T&S 2018	T&S 2018	T&S 2018
Pelthydrus sp. SLE0032	KC935313	-	KC935087	KC992620	-
Pelthydrus sp. SLE0946	T&S 2018	T&S 2018	T&S 2018	T&S 2018	T&S 2018
Peratogonus sp. MF223	KC935314	-	KC935088	KC992621	-
Peratogonus sp. SLE0062	-	-	KC935089	KC992622	-
Protosternum sp. SLE0297	-	KC992703	KC935091	KC992624	-
Psalitrus sp. MF249	KC935316	-	KC935092	KC992625	-
Regimbartia attenuata SLE0016	KC935317	KC992704	KC935093	KC992626	-
Scoliopsis sp. SLE0091	KC935321	KC992708	KC935097	KC992630	-
Spercheus emarginatus Chimera	AM287085	KC992709	AJ810718	AJ810753	-
Sperchopsis tessellata AES0030	KC935322	-	KC935098	KC992631	-
Sphaeridium bipustulatum SLE0298	KC935323	-	KC935099	-	-
Sphaeridium lunatum SLE0301	KC935324	-	KC935100	-	-
Sternolophus marginicollis SLE0017	KC935325	KC992711	KC935101	KC992632	-
Sternolophus sp. SLE0564	T&S 2018	T&S 2018	T&S 2018	T&S 2018	T&S 2018
Sternolophus sp. SLE0592	T&S 2018	T&S 2018	T&S 2018	T&S 2018	T&S 2018
Sternolophus sp. SLE0622	T&S 2018	T&S 2018	T&S 2018	T&S 2018	T&S 2018
Thysanarthria sp. SLE0127	KC935326	KC992712	KC935102	KC992633	-
Tobochares sulcatus SLE0035	KC935327	KC992713	KC935103	KC992634	-
Tormus sp. SLE0295	KC935328	-	KC935104	KC992635	-
Tropisternus affinis AES0032	KC935329	-	KC935105	KC992636	-
Tropisternus apicipalpis SLE0649	T&S 2018	T&S 2018	T&S 2018	T&S 2018	T&S 2018
Tropisternus chalybeus SLE0540	T&S 2018	T&S 2018	T&S 2018	T&S 2018	T&S 2018
Tropisternus collaris SLE0008	KC935330	KC992714	KC935106	KC992637	-
Tropisternus lateralis SLE0244	KC935331	KC992715	KC935107	KC992638	-
Tropisternus robustus SLE0545	T&S 2018	T&S 2018	T&S 2018	T&S 2018	T&S 2018

Supplementary Table S6. PartionFinder2 output of MrBayes block for partition definitions. (Subset 1-3= Cox1-5', Subset 4-6= Cox1-3', Subset 7-9= H3, Subset 10-12= Topoisomerase, Subset 13= 12S, Subset 14= 16S, Subset 15= 18S, Subset 16= 28S).

```
begin mrbayes;

        charset Subset1 = 1-640\3;
        charset Subset2 = 2-640\3;
        charset Subset3 = 3-640\3;
        charset Subset4 = 641-1437\3;
        charset Subset5 = 642-1437\3;
        charset Subset6 = 643-1437\3;
        charset Subset7 = 1438-1764\3;
        charset Subset8 = 1439-1764\3;
        charset Subset9 = 1440-1764\3;
        charset Subset10 = 1765-2397\3;
        charset Subset11 = 1766-2397\3;
        charset Subset12 = 1767-2397\3;
        charset Subset13 = 2398-2748;
        charset Subset14 = 2749-3318;
        charset Subset15 = 3319-5174;
        charset Subset16 = 5175-6250;

        partition PartitionFinder = 16:Subset1, Subset2, Subset3, Subset4, Subset5,
Subset6, Subset7, Subset8, Subset9, Subset10, Subset11, Subset12, Subset13,
Subset14, Subset15, Subset16;
        set partition=PartitionFinder;

        lset applyto=(1) nst=6 rates=invgamma;
        prset applyto=(1) statefreqpr=fixed(equal);
        lset applyto=(2) nst=6 rates=invgamma;
        lset applyto=(3) nst=6 rates=invgamma;
        lset applyto=(4) nst=6 rates=invgamma;
        lset applyto=(5) nst=6 rates=invgamma;
        lset applyto=(6) nst=6 rates=gamma;
        lset applyto=(7) nst=6 rates=gamma;
        lset applyto=(8) nst=1 rates=propinv;
        prset applyto=(8) statefreqpr=fixed(equal);
        lset applyto=(9) nst=6 rates=invgamma;
        lset applyto=(10) nst=6 rates=invgamma;
        prset applyto=(10) statefreqpr=fixed(equal);
        lset applyto=(11) nst=2 rates=invgamma;
        lset applyto=(12) nst=6 rates=invgamma;
        lset applyto=(13) nst=6 rates=invgamma;
        lset applyto=(14) nst=6 rates=invgamma;
        lset applyto=(15) nst=6 rates=invgamma;
        lset applyto=(16) nst=6 rates=invgamma;

        prset applyto=(all) ratepr=variable;
        unlink statefreq=(all) revmat=(all) shape=(all) pinvar=(all) tratio=(all);
```

Supplementary Table S7. Areas allowed and dispersal multipliers used in BioGeoBEARS (area codes: A – South America; B – South Africa; C – Australia; D – New Zealand; E – Antarctica).

Areas allowed				
34 - 0 Mya				
A	B	C	D	E
1	0	0	0	0
0	1	0	0	0
0	0	1	0	0
0	0	0	1	0
0	0	0	0	1
55 - 34 Mya				
A	B	C	D	E
1	0	0	0	1
0	1	0	0	0
0	0	1	0	0
0	0	0	1	0
1	0	0	0	1
80 - 55 Mya				
A	B	C	D	E
1	0	1	0	1
0	1	0	0	0
1	0	1	0	1
0	0	0	1	0
1	0	1	0	1
90 - 135 Mya				
A	B	C	D	E
1	0	1	1	1
1	1	1	1	1
1	0	1	1	1
1	0	1	1	1
1	0	1	1	1
135 Mya				
A	B	C	D	E
1	0	1	1	1
0	0	0	0	0
1	0	1	1	1
1	0	1	1	1
1	0	1	1	1

Dispersal multipliers				
34 - 0 Mya				
A	B	C	D	E
1	0.05	0.05	0.05	0.000001
0.05	1	0.05	0.05	0.000001
0.05	0.05	1	0.05	0.000001
0.05	0.05	0.05	1	0.000001
0.000001	0.000001	0.000001	0.000001	0.000001
55 - 34 Mya				
A	B	C	D	E
1	0.05	0.05	0.05	0.2
0.05	1	0.05	0.05	0.05
0.05	0.05	1	0.05	0.05
0.05	0.05	0.05	1	0.05
0.2	0.05	0.05	0.05	1
80 - 55 Mya				
A	B	C	D	E
1	0.05	0.05	0.05	1
0.05	1	0.05	0.05	0.05
0.05	0.05	1	0.05	0.2
0.05	0.05	0.05	1	0.05
1	0.05	0.2	0.05	1
90 - 135 Mya				
A	B	C	D	E
1	0.05	1	1	1
0.05	1	0.05	0.05	0.05
1	0.05	1	1	0.2
1	0.05	1	1	1
1	0.05	0.2	1	1
135 Mya				
A	B	C	D	E
1	0.2	1	1	1
0.2	1	0.05	0.05	0.05
1	0.05	1	1	1
1	0.05	1	1	1
1	0.05	1	1	1

Supplementary References

Astrin, J. J., & Stüben, P. E. (2008). Phylogeny in cryptic weevils: molecules, morphology and new genera of western Palaearctic Cryptorhynchinae (Coleoptera: Curculionidae). *Invertebrate Systematics*, 22(5), 503-522.

Colgan, D. J., McLauchlan, A., Wilson, G. D. F., Livingston, S. P., Edgecombe, G. D., Macaranas, J., Cassis, G. & Gray, M. R. (1998). Histone H3 and U2 snRNA DNA sequences and arthropod molecular evolution. *Australian Journal of Zoology*, 46(5), 419-437.

Folmer O, Black M, Hoeh W, Lutz R, Vrijenhoek R (1994) DNA primers for amplification of mitochondrial cytochrome c oxidase subunit I from diverse metazoan invertebrates. *Molecular Marine Biology and Biotechnology*, 3, 294–299.

Maddison, D. R. (2008). Systematics of the North American beetle subgenus Pseudoperyphus (Coleoptera: Carabidae: Bembidion) based upon morphological, chromosomal, and molecular data. *Annals of Carnegie Museum*, 77(1), 147-193.

Shull, V. L., Vogler, A. P., Baker, M. D., Maddison, D. R., & Hammond, P. M. (2001). Sequence alignment of 18S ribosomal RNA and the basal relationships of adephagan beetles: evidence for monophyly of aquatic families and the placement of Trachypachidae. *Systematic Biology*, 50(6), 945-969.

Simon, C., Frati, F., Beckenbach, A., Crespi, B., Liu, H., & Flook, P. (1994). Evolution, weighting, and phylogenetic utility of mitochondrial gene sequences and a compilation of conserved polymerase chain reaction primers. *Annals of the Entomological Society of America*, 87(6), 651-701.

Timmermans, M. J., Dodsworth, S., Culverwell, C. L., Bocak, L., Ahrens, D., Littlewood, D. T. J., Pons, J. & Vogler, A. P. (2010). Why barcode? High-throughput multiplex sequencing of mitochondrial genomes for molecular systematics. *Nucleic Acids Research*, 38(21), e197-e197.

Van der Auwera, G., Chapelle, S., & De Wächter, R. (1994). Structure of the large ribosomal subunit RNA of Phytophthora megasperma, and phylogeny of the oomycetes. *FEBS Letters*, 338(2), 133-136.

Whiting, M. F., Carpenter, J. C., Wheeler, Q. D., & Wheeler, W. C. (1997). The Strepsiptera problem: phylogeny of the holometabolous insect orders inferred from 18S and 28S ribosomal DNA sequences and morphology. *Systematic Biology*, 46(1), 1-68.

Wild, A. L., & Maddison, D. R. (2008). Evaluating nuclear protein-coding genes for phylogenetic utility in beetles. *Molecular phylogenetics and evolution*, 48(3), 877-891.

CHAPTER 3

Seidel, M., Arriaga-Varela, E. & Fikáček, M. (2016). Establishment of Cylominae Zaitzev, 1908 as a valid name for the subfamily Rygmodinae Orchymont, 1916 with an updated list of genera (Coleoptera: Hydrophilidae). *Acta Entomologica Musei Nationalis Pragae,* 56(1): 159-165.

Author contributions: MS, drafted the manuscript, all authors contributed to the writing.

ACTA ENTOMOLOGICA MUSEI NATIONALIS PRAGAE
Published 15.vii.2016 Volume 56(1), pp. 159–165 ISSN 0374-1036
http://zoobank.org/urn:lsid:zoobank.org:pub:221A7F58-99D6-4C58-B357-CDA7DAE0BF49

Establishment of Cylominae Zaitzev, 1908 as a valid name for the subfamily Rygmodinae Orchymont, 1916 with an updated list of genera (Coleoptera: Hydrophilidae)

Matthias SEIDEL[1,2], Emmanuel ARRIAGA-VARELA[1,2] & Martin FIKÁČEK[2,1]

[1)] Department of Zoology, Faculty of Science, Charles University, Viničná 7, CZ-123 83 Praha 2, Czech Republic; e-mails: seidelma@natur.cuni.cz, arriagavarelae@natur.cuni.cz

[2)] Department of Entomology, National Museum, Cirkusová 1740, CZ-19300 Praha 9 – Horní Počernice, Czech Republic; e-mail: mfikacek@gmail.com

Abstract. Cylominae Zaitzev, 1908 is established as a valid subfamily name for Rygmodinae Orchymont, 1916, syn. nov., due to the recent transfer of *Cyloma* Sharp, 1872 to the subfamily. The history of nomenclature of the subfamily is reviewed and an updated overview of family-group and genus-group names currently assigned to the subfamily is provided.

Key words. Coleoptera, Hydrophilidae, Cylominae, Rygmodinae, genus, new synonym, new status, nomenclature

Introduction

Recent advances in the phylogenetic studies stabilized the subfamiliar classification of the family Hydrophilidae. Six major clades of Hydrophilidae were recognized in the multigene analysis performed by Short & Fikáček (2013) and established as subfamilies: mainly aquatic Hydrophilinae, Chaetarthriinae, Enochrinae and Acidocerinae, and mostly terrestrial Sphaeridiinae and Rygmodinae. The subfamily assignment of most genera was also revised in the course of the study. Subsequent studies either corroborated the proposed classification (Bloom et al. 2014, Fikáček et al. 2015, Toussaint et al. 2016) or corrected the subfamily assignment of genera previously not available for studies (Fikáček & Vondráček 2014). However, nomenclatural issues concerning some family-group names resulting from these changes were not addressed properly. For this reason, the nomenclature of the family-group and genus-group names of the subfamily Rygmodinae is revised here, in order to make it stable before the ongoing revision of this clade will be published.

History of the subfamily

The tribe Cylomina was the first established family-group taxon (Zaitzev 1908) encompassing the New Zealand genera *Cyloma* Sharp, 1872, *Psephoboragus* Broun, 1893 (currently a junior subjective synonym of *Cyloma*) and *Cylomissus* Broun, 1903. Several years later, Orchymont (1916) proposed the tribe Rygmodini, providing just a very inaccurate diagnosis. His concept of Rygmodini became clear after a more detailed definition was provided by Orchymont (1919) – the group encompassed 14 genera endemic to New Zealand, i.e. *Adolopus* Sharp, 1884, *Cyloma*, *Gitocyloma* Broun, 1915 (junior subjective synonym of *Cyloma*), *Namostygnus* Broun, 1909 (junior subjective synonym of *Cyloma*), *Psephoboragus*, *Cylomissus*, *Exydrus* Broun, 1886, *Hydrostygnus* Sharp, 1884, *Rygmodus* White, 1846, *Saphydrus* Sharp, 1884, *Tormissus* Broun, 1893, *Thomosis* Broun, 1904 (junior subjective synonym of *Tormissus*), *Tormus* Sharp, 1884, *Stygnohydrus* Broun, 1893 (junior subjective synonym of *Tormus*), and the Australian endemic *Pseudohydrobius* Blackburn, 1898. Orchymont (1919) explained the establishment of the Rygmodini by the fact that *Rygmodus* (the type genus) is the oldest described taxon in the group. Although he commented on the name Cylomina Zaitzev, 1908, he ignored its priority over Rygmodini. The status proposed by Orchymont (1919), i.e. Rygmodini as a valid name, with Cylomina as its synonym, was corroborated by Knisch (1924).

Hansen (1991) performed the first phylogenetic analysis of the Hydrophilidae and proposed a new classification of the family (the so-called Hansen's Classification). In the course of this work, he redefined Rygmodini as containing six genera only: *Pseudohydrobius*, *Rygmostralia* Orchymont, 1933, *Saphydrus*, *Rygmodus*, *Eurygmus* Hansen, 1990, and *Cylorygmus* Orchymont, 1933. The genera *Tormus*, *Tormissus*, *Hydrostygnus* and *Exydrus* were transferred to a newly established tribe Tormissini, and the genera *Cyloma* and *Adolopus* to the tribe Coelostomatini; several genus-level synonymies were also proposed. The transfer of *Cyloma* from Rygmodini to Coelostomatini resulted in placing Cylomina Zaitzev, 1908 in synonymy with Coelostomatini Heyden, 1891.

Short & Fikáček (2013) reassessed the phylogeny and classification of Hydrophilidae based on a multigene dataset. They found a strong support for most of the genera assigned to 'basal sphaeridiine clades' in Hansen's Classification (i.e. Rygmodini, Tormissini, Andotypini and Borborophorini) to form a monophyletic group. Based on these results, the subfamily Rygmodinae was established for the clade, and the remaining family-group names were synonymized with it. The genera *Adolopus* and *Cyloma* were transferred back to Rygmodinae from Coelostomatini, and the genera *Tormus* and *Afrotormus* Hansen, 1999 (previously classified in Tormissini) were moved to Hydrophilinae. Furthermore, *Anticura* Spangler, 1979 was moved from Hydrophilinae to Rygmodinae. Due to the ongoing revision of the group, no formal family-group taxa (tribes, subtribes) were established inside of the subfamily. In this revised concept, Rygmodinae contained 18 genera. Subsequently, one new genus was described by Fikáček et al. (2014) and *Pseudorygmodus* Hansen, 1999 was transferred from Rygmodinae to Chaetarthriinae by Fikáček & Vondráček (2014).

When reassigning *Cyloma* back from Coelostomatini to Rygmodinae, Short & Fikáček (2013) did not resurrect the family-group name Cylomina from synonymy with Coelostomatini and therefore overlooked its nomenclatural priority over Rygmodinae. Here we fix

this issue, and establish Cylominae Zaitzev, 1908, stat. nov., as a valid subfamily name, with Rygmodinae Orchymont, 1916 standing as its synonym. The names standing previously in synonymy with Rygmodinae Orchymont, 1916 are transferred under Cylominae Zaitzev, 1908. An updated overview of family-group and genus-group names currently assigned to the subfamily is provided below.

Spelling corrections

When Zaitzev (1908) introduced Cylomina in his catalogue, the name was listed as 'Cyl(l)omina', corresponding to his spelling of the type genus – '*Cyl*(*l*)*oma*'. This is the reason why Cylomina was listed as Cyllomina by some subsequent authors (e.g. Hansen 1991, Bouchard et al. 2011), but all of them considered this spelling as an unjustified emendation, since Sharp's (1872) original spelling of the genus was *Cyloma.* In agreement with that, we are using Cylomina as the correct original spelling of Zaitzev's (1908) name.

Bouchard et al. (2011: 7–9, 157) considered *Cyloma* as a neuter noun of Greek origin, based on the ending *-loma* (Greek word for margin), and in agreement with that corrected the genitive stem for formation of family-group names from '*Cylom-*' used by all previous authors to '*Cylomat-*'. However, as discussed by Newton & Thayer (1992: 15), *Cyloma* was explicitly stated as 'a word without any classical derivation' in the original description by Sharp (1872: 152). As such, the stem formation for the family-group name follows Article 29.3.3 of the International Code of Zoological Nomenclature (ICZN 1999). This Article states that 'if a generic name is or ends in a word not Greek or Latin, *or is an arbitrary combination of letters*, the stem for the purposes of the Code is that adopted by the author who establishes the new family-group taxon'. Zaitzev's (1908) establishment of Cylomina (stem: *Cylom-*) hence determined the stem formation for family-group names derived from *Cyloma*. Consequently, we consider the stem formation done by Bouchard et al. (2011) as incorrect, and establish the subfamily name as Cylominae.

Updated overview of family- and genus-group names within Cylominae

Subfamily Cylominae Zaitzev, 1908

Cylominae Zaitzev, 1908: 400. Type genus: *Cyloma* Sharp, 1872.

= Cyllomina: Zaitzev (1908): 400 (incorrect original spelling based on incorrect subsequent spelling of the name of type genus).

= Rygmodini Orchymont, 1916: 238, **syn. nov.** Type genus: *Rygmodus* White, 1846.

= Andotypini Hansen, 1991: 186. Type genus: *Andotypus* Spangler, 1979. Synonymized with Rygmodinae by Short & Fikáček (2013).

= Borborophorini Hansen, 1991: 190. Type genus: *Borborophorus* Hansen, 1990. Synonymized with Rygmodinae by Short & Fikáček (2013).

= Tormissini Hansen, 1991: 181. Type genus: *Tormissus* Broun, 1893. Synonymized with Rygmodinae by Short & Fikáček (2013).

Adolopus Sharp, 1884

Adolopus Sharp, 1884: 478. Type species: *Adolopus helmsi* Sharp, 1884 (designated by Knisch 1924: 108).

Distribution. New Zealand (Hansen 1999).

Andotypus Spangler, 1979

Andotypus Spangler, 1979a: 303. Type species: *Andotypus ashworthi* Spangler, 1979 (by original designation).

Distribution. Chile (Fikáček et al. 2014).

Anticura Spangler, 1979

Anticura Spangler, 1979b: 698. Type species: *Anticura flinti* Spangler, 1979 (by original designation).

Distribution. Argentina, Chile (Hansen 1999, Fikáček & Vondráček 2014).

Austrotypus Fikáček, Minoshima & Newton, 2014

Austrotypus Fikáček, Minoshima & Newton, 2014: 559. Type species: *Austrotypus nothofagi* Fikáček, Minoshima & Newton, 2014 (by original designation).

Distribution. Australia (New South Wales, Queensland), Peru (Fikáček et al. 2014).

Borborophorus Hansen 1990

Borborophorus Hansen, 1990: 326. Type species: *Borborophorus pubescens* Hansen, 1990 (by original designation).

Distribution. Australia (New South Wales, Queensland) (Hansen 1999).

Coelostomopsis Hansen, 1990

Coelostomopsis Hansen, 1990: 333. Type species: *Coelostomopsis picea* Hansen, 1990 (by original designation).

Distribution. Australia (Queensland) (Hansen 1999).

Cyloma Sharp, 1872

Cyloma Sharp, 1872: 152. Type species: *Cyloma lawsonus* Sharp, 1872 (by monotopy).
= *Cylloma*: Zaitzev (1908): 400 (incorrect subsequent spelling).
= *Psephoboragus* Broun, 1893b: 1402. Type species: *Psephoboragus signatus* Broun, 1983 (designated by Knisch 1924: 109). Synonymized by Hansen (1991).
= *Namostygnus* Broun, 1909: 98. Type species: *Namostygnus rufipes* Broun, 1909 (by monotypy). Synonymized by Hansen (1991).
= *Gitocyloma* Broun, 1915: 277. Type species: *Gitocyloma nigratus* Broun, 1915 (by monotypy). Synonymized by Hansen (1991).

Distribution. New Zealand (Hansen 1999).

Cylomissus Broun, 1903

Cylomissus Broun, 1903: 613. Type species: *Cylomissus glabratus* Broun, 1903 (by monotypy).
= *Cyclomissus* Zaitzev, 1908: 400 (incorrect subsequent spelling).

Distribution. New Zealand (Hansen 1999).

Cylorygmus Orchymont, 1933

Cylorygmus Orchymont, 1933: 293. Type species: *Cylorygmus lineatopunctatus* Orchymont, 1933 (by original designation).

Distribution. Chile (Hansen 1999, Fikáček & Vondráček 2014), South Africa (Western Cape) (Hebauer 2002).

Eurygmus Hansen, 1990

Eurygmus Hansen, 1990: 322. Type species: *Eurygmus helocharoides* Hansen, 1990 (by original designation).

Distribution. Australia (Queensland) (Hansen 1999).

Exydrus Broun, 1886

Exydrus Broun, 1886: 940. Type species: *Cyclonotum flavicorne* Broun, 1886 (designated by Knisch 1924: 106).

Distribution. New Zealand (Hansen 1999).

Hydrostygnus Sharp, 1884

Hydrostygnus Sharp, 1884: 475. Type species: *Hydrostygnus brouni* Sharp, 1884 (designated by Hansen 1999: 238)

Distribution. New Zealand (Hansen 1999).

Petasopsis Hansen, 1990

Petasopsis Hansen, 1990: 331. Type species: *Petasopsis brevitarsis* Hansen, 1990 (by original designation).

Distribution. Australia (Queensland) (Hansen 1999).

Pseudohydrobius Blackburn, 1898

Pseudohydrobius Blackburn, 1898: 231. Type species: *Pseudohydrobius floricola* Blackburn, 1898 (by monotypy).

Distribution. Australia (New South Wales, Victoria, Queensland) (Hansen 1999, Fikáček & Watts 2015).

Rygmodus White, 1846

Rygmodus White, 1846: 11. Type species: *Rygmodus modestus* White, 1846 (designated by Knisch 1924: 107).

Distribution. New Zealand (Hansen 1999).

Rygmostralia Orchymont, 1933

Rygmostralia Orchymont, 1933: 293. Type species: *Rygmostralia brunnea* Orchymont, 1933 (by original designation).

Distribution. Australia (New South Wales) (Hansen 1999).

Saphydrus Sharp, 1884

Saphydrus Sharp, 1884: 467. Type species: *Saphydrus suffusus* Sharp, 1884 (designated by Knisch 1924: 108).

Distribution. New Zealand (Hansen 1999).

Tormissus Broun, 1893

Tormissus Broun, 1893a: 1021. Type species: *Tormissus magnulus* Broun, 1893 (designated by Knisch 1924: 107).
= *Thomosis* Broun, 1904: 273. Type species: *Thomosis guanicola* Broun, 1904 (by monotypy). Synonymized by Hansen (1991).

Distribution. New Zealand (Hansen 1999).

Acknowledgements

We thank Petr Kment, Jiří Hájek and Lukáš Sekerka (National Museum, Prague) for help and discussions on nomenclatural problems treated in this paper, and to Alfred F. Newton (Field Museum, Chicago) for comments on the stem formation of family-group names derived from *Cyloma* and further corrections of the manuscript. This work was supported by the European Union's Horizon 2020 research and innovation program under the Marie Skłodowska-Curie grant agreement No. 542241 to M. Seidel and E. Arriaga-Varela, and the Ministry of Culture of the Czech Republic (DKRVO 2016/14, National Museum, 00023272) to Martin Fikáček. The work of the first two authors at the Department of Zoology, Charles University in Prague was partly supported by grant SVV 260 313/2016.

References

BLACKBURN T. 1898: Further notes on Australian Coleoptera, with descriptions of new genera and species. XXIV. *Transactions of the Royal Society of South Australia* **22**: 221–233.

BLOOM D. D., FIKÁČEK M. & SHORT A. E. Z. 2014: Clade age and diversification rate variation explain disparity in species richness among water scavenger beetle (Hydrophilidae) lineages. *PLoS ONE* **9(6)(e98430)**: 1–9. doi:10.1371/journal.pone.0098430

BOUCHARD P., BOUSQUET Y., DAVIES A. E., ALONSO-ZARAZAGA M. A., LAWRENCE J. F., LYAL C. H. C., NEWTON A. F., REID C. A. M., SCHMITT M., ŚLIPIŃSKI S. A. & SMITH A. B. T. 2011: Family-group names in Coleoptera (Insecta). *ZooKeys* **88**: 1–972.

BROUN T. 1886: *Manual of the New Zealand Coleoptera. Part IV.* Colonial Museum and Geological Survey Department, Wellington, pp. 817–973.

BROUN T. 1893a: *Manual of the New Zealand Coleoptera. Part V.* Colonial Museum and Geological Survey Department, Wellington, pp. 975–1320.

BROUN T. 1893b: *Manual of the New Zealand Coleoptera. Part VII.* Colonial Museum and Geological Survey Department, Wellington, pp. 1395–1504.

BROUN T. 1903: Descriptions of new genera and species of New Zealand Coleoptera. *Annals and Magazine of Natural History, Series 7* **11**: 602–618.

BROUN T. 1904: Description of a new Coleopterous Insect from Bounty Island. *Annals and Magazine of Natural History*, *Series 7* **14**: 273–274.

BROUN T. 1909: Descriptions of Coleoptera from the Subantarctic Islands of New Zealand; with remarks on the affinities of the genera, etc. *Subantarctic Islands of New Zealand* **1**: 78–123.

BROUN T. 1915: Descriptions of new genera and species of Coleoptera. Part IV. *Bulletin of the New Zealand Institute* **1**: 267–346.

FIKÁČEK M., MARUYAMA M., KOMATSU T., VON BEEREN C., VONDRÁČEK D. & SHORT A. E. 2015: Protosternini (Coleoptera: Hydrophilidae) corroborated as monophyletic and its larva described for the first time: a review of the myrmecophilous genus Sphaerocetum. *Invertebrate Systematics* **29**: 23–36.

FIKÁČEK M., MINOSHIMA Y. N. & NEWTON A. F. 2014: A review of Andotypus and Austrotypus gen. nov., rygmodine genera with an austral disjunction (Hydrophilidae: Rygmodinae). *Annales Zoologici* (Warszawa) **64**: 557–596.

FIKÁČEK M. & VONDRÁČEK D. 2014: A review of Pseudorygmodus (Coleoptera: Hydrophilidae), with notes on the classification of the Anacaenini and on distribution of genera endemic to southern South America. *Acta Entomologica Musei Nationalis Pragae* **54**: 479–514.

FIKÁČEK M. & WATTS C. H. S. 2015: Notes on the Australian Anacaenini (Coleoptera: Hydrophilidae): description of male of Phelea breviceps Hansen and unravelling the identity of Crenitis neogallica Gentili. *Zootaxa* **3980**: 427–434.

HANSEN M. 1990: Australian Sphaeridiinae (Coleoptera: Hydrophilidae): A taxonomic outline with descriptions of new genera and species. *Invertebrate Taxonomy* **4**: 317–395.

HANSEN M. 1991: The hydrophiloid beetles. Phylogeny, classification and a revision of the genera (Coleoptera, Hydrophiloidea). *Biologiske Skrifter* **40**: 1–367.

HANSEN M. 1999: *World Catalogue of Insects, Vol. 2: Hydrophiloidea (Coleoptera).* Apollo Books, Stenstrup, 416 pp.

HEBAUER F. 2002: New Hydrophilidae of the Old World (Coleoptera, Hydrophilidae). *Acta Coleopterologica* **18(3)**: 3–24.

INTERNATIONAL COMISSION ON ZOOLOGICAL NOMENCLATURE (ICZN) 1999: *International Code of Zoological Nomenclature, Fourth Edition.* International Trust for Zoological Nomenclature, London, 306 pp.

KNISCH A. 1924: Hydrophilidae. In: SCHENKLING S. (ed.): *Coleopterorum Catalogus, Pars 79.* W. Junk, Berlin, 306 pp.

NEWTON A. F. Jr. & THAYER M. K. 1992: Current classification and family-group names in Staphyliniformia (Coleoptera). *Fieldiana: Zoology (New Series)* **67**: 1–92.

ORCHYMONT A. d' 1916: De la place qui doivent occuper dans la classification les sous-familles des Sphaeridiinae et des Hydrophilinae. *Bulletin de la Société Entomologique de France* **1916**: 235–240.

ORCHYMONT A. d' 1919: Contribution a l'étude des sous-familles des Sphaeridiinae et des Hydrophilinae (Col. Hydrophilidae). *Annales de la Société Entomologique de France* **88**: 105–168.

ORCHYMONT A. d' 1933: Contribution à l'étude des Palpicornia VIII. *Bulletin et Annales de la Société Entomologique de Belgique* **73**: 271–314.

SHARP D. 1872: Description of a new genus and species of Hydrophilidæ from New Zealand, and of a new species of Philhydrus from Great Britain. *Entomologist's Monthly Magazine* **9**: 152–153.

SHARP D. 1884: Revision of the Hydrophilidæ of New Zealand. *Transactions of the Entomological Society of London* **1884**: 465–480.

SHORT A. E. Z. & FIKÁČEK M. 2013: Molecular phylogeny, evolution and classification of the Hydrophilidae (Coleoptera). *Systematic Entomology* **38**: 723–752.

SPANGLER P. J. 1979a: A new genus of water scavenger beetle from Chile (Coleoptera: Hydrophilidae: Sphaeridiini). *Coleopterists Bulletin* **33**: 303–308.

SPANGLER P. J. 1979b: A new genus of water beetle from austral South America (Coleoptera: Hydrophilidae). *Proceedings of the Biological Society of Washington* **92**: 697–718.

TOUSSAINT E. F., FIKÁČEK M. & SHORT A. E. 2016: India-Madagascar vicariance explains cascade beetle biogeography. *Biological Journal of the Linnean Society*, in press, doi: 10.1111/bij.12791.

WHITE A. 1846: Insects. Pp. 1–24. In: RICHARDSON J. & GRAY J. E. (eds): *The Zoology of the Voyage of H. M. S. Erebus & Terror. Vol. 2.* E. W. Janson, London.

ZAITZEV F. A. 1908: Catalogue des Coléoptères aquatiques des familles Dryopidae, Georyssidae, Cyathoceridae, Heteroceridae et Hydrophilidae. *Horae Societatis Entomologicae Rossicae* **38**: 283–420.

CHAPTER 4

Seidel, M., Minoshima, Y. N., Arriaga-Varela, E., & Fikáček, M. (2018). Breaking a disjunct distribution: a review of the Southern Hemisphere genera *Cylorygmus* and *Relictorygmus* gen. nov. (Hydrophilidae: Cyclominae). *Annales zoologici,* 68(2): 375-403.

Author contributions: MS, EAV and MF performed the field work and accumulated additional museum material; MS performed the majority of morphological studies on adult beetles; YNM performed the morphological studies on larvae; MS, drafted the manuscript, all authors contributed to the writing.

ANNALES ZOOLOGICI (Warszawa), 2018, 68(2): 375-402

BREAKING A DISJUNCT DISTRIBUTION: A REVIEW OF THE SOUTHERN HEMISPHERE GENERA *CYLORYGMUS* AND *RELICTORYGMUS* GEN. NOV. (HYDROPHILIDAE: CYLOMINAE)

MATTHIAS SEIDEL[1,2,*], YÛSUKE N. MINOSHIMA[3], EMMANUEL ARRIAGA-VARELA[1,2] and MARTIN FIKÁČEK[2,1,*]

[1]*Department of Zoology, Faculty of Science, Charles University, Viničná 7, CZ-123 83 Praha 2, Czech Republic; e-mail: seidelma@natur.cuni.cz*
[2]*Department of Entomology, National Museum, Cirkusová 1740, CZ-19300 Praha 9 - Horní Počernice, Czech Republic*
[3]*Natural History Division, Kitakyushu Museum of Natural History and Human History, Higashida 2-4-1, Yahatahigashi-ku, Kitakyushu-shi, Fukuoka, 805-0071; Japan; e-mail: minoshima@kmnh.jp*
[*]*Corresponding author*

Abstract.— The southern hemisphere water scavenger beetle genus *Cylorygmus* Orchymont, 1933 (Coleoptera: Hydrophilidae: Cyclominae) is revised. Three species are recognized, one in Chile and two in South Africa. The morphological differences indicate that the African species are not congeneric with the Chilean one. *Relictorygmus* **gen. nov.** is established for the African *R. trevornoahi* **sp. nov.** (type species) and *R. repentinus* (Hebauer, 2002), both known from few localities in the Western Cape province of the Republic of South Africa. The genus *Cylorygmus* with the only species *C. lineatopunctatus* Orchymont, 1933 is endemic to a small region in central Chile. Its larva is described in detail based on specimens collected in association with adults. Both genera and all species are diagnosed, described and illustrated, and an identification key for adults is provided. Our study demonstrates that the trans-Atlantic disjunct distribution of *Cylorygmus* was based on inaccurate taxonomic treatment and did not reflect the real evolutionary history of these beetles.

Key words.— disjunct distribution, South Africa, Chile, new genus, new species, larval morphology.

INTRODUCTION

Organisms with widely disjunct distribution are frequent model groups for biogeographers since they help us to reconstruct the history of landmasses and their past interconnections, and to understand the processes which led to modern distributional patterns (e.g., Brundin 1966, de Quieroz 2014). The beetle family Hydrophilidae, a diverse group containing about 3000 known species, includes some examples of putatively disjunct generic distributions: *Austrotypus* Fikáček *et al.*, 2014 occurring in Peru and Australia (Fikáček *et al.* 2014) and *Cetiocyon* Hansen, 1990 found in Papua New Guinea and Suriname (Fikáček and Short 2010) are the most recently published examples. Five more genera with African–American disjunct distribution are known in the primarily terrestrial subfamilies Cyclominae and Sphaeridiinae. Four of them, the cylomine genus *Cylorygmus* Orchymont, 1933, coelostomatine genera *Phaenonotum* Sharp, 1882 and *Cyclotypus*

PL ISSN 0003-4541 © Museum and Institute of Zoology PAS
doi: 10.3161/00034541ANZ2018.68.2.011

Sharp, 1882, and the omicrine genus *Omicrus* Sharp, 1879 are mainly distributed in the Neotropics, but few African species were also assigned to them by Bameul (1992), Régimbart (1907) and Hebauer (2002): *Cylorygmus repentinus* Hebauer, 2002 from South Africa, *Phaenonotum africanum* Régimbart, 1907 from Cameroon, *Omicrus hebaueri* Bameul, 1992 from the Ivory Coast, and two species of *Cyclotypus* from Madagascar. The African species of these genera were not reviewed taxonomically, and their generic placement requires confirmation (Seidel and Fikáček personal observation). The North American megasternine species *Tectosternum naviculare* (Zimmerman, 1869) is the only case which has been reviewed in detail. Smetana (1978, 1984) confirmed its assignment to the genus *Tectosternum* Balfour-Browne, 1958, previously considered being an African endemic.

The aforementioned genus *Cylorygmus* is the only African genus belonging to the subfamily Cyclominae, a small assemblage of 'relict' genera distributed in the southern hemisphere (Seidel *et al.* 2016) and having the highest genus and species diversity in New Zealand and Australia, with several endemic genera in austral South America (Fikáček *et al.* 2014, Fikáček and Vondráček 2014, Minoshima *et al.* 2015). *Cylorygmus* was originally described from Chile with the single species *C. lineatopunctatus* Orchymont, 1933. Hebauer (2002) added *C. repentinus*, based on two specimens collected in the Western Cape Province of South Africa. This discovery was not only the first record of the subfamily Cyclominae in Africa, but it also implied a trans-Atlantic disjunct distribution for the genus *Cylorygmus*. The assignment of the African species to *Cylorygmus* was only based on overall morphological similarity, lacking a thorough comparison to *C. lineatopunctatus*, and was hence considered as requiring confirmation (e.g., Fikáček *et al.* 2014). To facilitate the revision of its generic placement, we organized an expedition to Western Cape in 2015. Surprisingly, the specimens we collected revealed to be related to *C. repentinus*, but representing another, as yet undescribed, species. These fresh specimens also allowed us to test the generic placement of the African species of *Cylorygmus*, of which the morphological and taxonomical implications are discussed in this paper. We are also summarizing all know data about the Chilean *Cylorygmus*, including the description of its larva, based on specimens collected in association with adults.

Material and methods

Adult morphological examination. For generic character examination, specimens were dissected after short treatment in 10% KOH (in case of *C. lineatopunctatus*) or after extracting the dissolved internal tissues in the solution of 180 μl of Qiagen ATL and 20 μl of proteinase K, bleached in 15% hydrogen peroxide solution and mounted on permanent slides in Euparal. For habitus illustration, partially focused photographs were taken using Canon EOS 550D digital camera with attached Canon MP-E65 mm f/2.8 1–5× macro lens, followed by a combination in Helicon Focus software. Photographs of slide-mounted parts were taken using Canon EOS 1100D digital camera attached to an Olympus BX41 compound microscope and subsequently combined in Helicon Focus software. SEM micrographs were taken using a Hitachi S-3700N environmental electron microscope at the Department of Paleontology, National Museum (Prague, Czech Republic). All pictures were subsequently adapted in Adobe Photoshop CS6 (e.g., cleaning background, cropping). Original unedited photos, including those only used for comparative purposes and not included into this paper were submitted as a .zip file to Zenodo archive under the doi: 10.5281/zenodo.1065382.

Larval morphological examination. The methodology for larval examination followed Minoshima and Hayashi (2011). The specimens were cleared using 10% KOH solution, dissected and mounted on H-S Slides (Shirayama *et al.* 1993) with Euparal resin or preserved in ethanol. Observations and dissections were carried out using an Olympus SZX12 stereoscopic microscope and Nikon Eclipse E600 compound light microscope. Illustrations were made with the aid of a drawing tube attached to the E600. Line drawings were prepared using the software Paint tool SAI (Systemax Inc., Japan) and Photoshop CC (Adobe Systems Inc., USA). Habitus photographs were taken using the same methodology and equipment as adult ones. The morphological terminology of larva generally follows Archangelsky (1997) and Minoshima and Hayashi (2011), for terminology of antennal segments we followed Beutel (1999). For the chaetotaxy of the larval head we referred to Fikáček *et al.* (2008) and Bytteebier and Torres (2009). Following abbreviations are used:

AN – antenna,
FR – frontale,
gAN – group of antennal sensilla,
gAPP – group of sensilla on inner appendage of maxilla,
gFR – group of sensilla on frontale,
gLA – group of sensilla on labium,
gMX – group of sensilla on maxilla,
L1, L2, L3 – – first, second and third instar,
LA – labium,
MN – mandible,
MX – maxilla,
PA – parietale,
SE – sensorium.

Specimen depositories. Examined material is housed in the following collections:

BMNH – Natural History Museum, London, United Kingdom (M. Barclay);
CDTB – collection of D. T. Bilton, Plymouth, United Kingdom;
FMNH – Field Museum of Natural History, Chicago, Illinois, USA (A. Newton, C. Maier);
HNHM – Hungarian Natural History Museum, Budapest, Hungary (O. Merkl);
ISAM – Iziko South African Museum, Cape Town, South Africa;
JBCC – Juan E. Barriga collection, Curico, Chile;
KMNH – Kitakyushu Museum of Natural History and Human History, Kitakyushu, Japan (Y. Minoshima);
MNNC – Museo Nacional de Historia Natural, Santiago de Chile, Chile (M. Elgueta);
NHMW – Naturhistorisches Museum Wien, Wien, Austria (M. Jäch);
NMPC – Department of Entomology, National Museum, Prague, Czech Republic (J. Hájek, M. Fikáček);
SEMC – Snow Entomological Museum, University of Kansas, Lawrence, USA (A. Short);
ZMHB – Museum für Naturkunde, Berlin (J. Frisch, B. Jäger).

TAXONOMY

Key to species of *Cylorygmus* and *Relictorygmus* gen. nov.

1. Body dorso-ventrally compressed (Figs 1A–B). Labrum dorsally with a median group of stout setae (Fig. 3A). Gula narrowing anteriad to a half of its width at base (Fig. 3B); femora pubescent with intermixed stout setae (Figs 3D–E, G–I); pubescence of ventrite 1 intermixed with stout setae (Fig. 2K); abdominal apex with stout setae (Fig. 2L); male genitalia with median lobe ca. twice as wide as parameres, gonopore apical (Fig. 9A). Chile . . . . . ***Cylorygmus lineatopunctatus*** Orchymont

–. Body moderately convex (Figs 10B, E). Labrum without median group of setae dorsally (Fig. 12D). Gula narrowing anteriad to a fourth of its width at base (Figs 12F, K); femora pubescent, lacking intermixed stout setae (Figs 12A–C, I); pubescence of ventrite 1 without intermixed stout setae (Fig. 11K); abdominal apex without stout setae (Fig. 11L); male genitalia with median lobe at midlength ca. half as wide as parameres, gonopore subapical (Figs 9C, E); South Africa . . . . . **2** (***Relictorygmus*** gen. nov.)

2. Ventral surface of profemora densely pubescent at base (Fig. 12I); elevated anterior part of mesoventrite sub-triangular with weakly sinuate posterior margin (Fig. 10M), transverse ridge of mesoventrite straight (Figs 12L–M); anterior metaventral process narrowly triangular (Fig. 12L); male genitalia with parameres curved inwards in apical half, median lobe of aedeagus rather narrow at base, slightly narrowing apicad (Fig. 9C) . . . . . ***Relictorygmus repentinus*** (Hebauer)

–. Ventral surface of profemora sparsely pubescent at base (Fig. 12A); elevated anterior part of mesoventrite heart-shaped (Fig. 12H), transverse ridge of mesoventrite angulate (Fig. 12H); anterior metaventral process widely triangular (Fig. 12G); male genitalia with parameres relatively straight, median lobe of aedeagus basally ca. 2.0× as wide as apical part narrowing anteriad to half of its width (Fig. 9E) . . . . . ***Relictorygmus trevornoahi*** sp. nov.

Cylorygmus Orchymont, 1933

Type species. *Cylorygmus lineatopunctatus* Orchymont, 1933 (by original designation).

Differential diagnosis from co-occurring genera. In southern South America, *Cylorygmus* can be confused with *Enochrus* Thomson, 1859 both as adult and larva. Adult *Cylorygmus* differs from *Enochrus* in maxillary palps (Fig. 1C) bent inwards (in contrast to zigzag shaped palpomeres in *Enochrus*) and flattened mesoventrite (Fig. 3D) (in contrast to posteromedially raised mesoventrite forming a high keel or large cone-shaped tooth in *Enochrus*). Larvae can be distinguished from *Enochrus* by (1) the absence of prolegs on abdominal segments III–VII (Fig. 1E) (with spinose prolegs on these segments in *Enochrus*), and (2) the nasale with five very large and distinct teeth, epistomal lobes large and symmetrical (Figs 4C, 6A, 7C) (nasale with five to more irregular and much smaller teeth, epistomal lobes narrow, asymmetrical, right one projecting further than left one in *Enochrus* (see Archangelsky 2002 and Byttebier and Torres 2009). Larva of *Cylorygmus* also resembles the larva of Argentinian endemic genus *Hydramara* Knisch, 1925 which inhabits streams, but differs from it by mandibles with two retinacular teeth (with two large teeth and one small basal tooth in *Hydramara*) and by antennal sensorium well developed (minute and difficult to see in *Hydramara*).

Differential diagnosis from cylomine genera. **Adult.** Labrum (Figs 1C, 3A) exposed (in contrast to *Adolopus* Sharp, 1884, *Andotypus* Spangler, 1979, *Anticura* Spangler, 1979, *Austrotypus*, *Coelostomopsis* Hansen, 1990, *Cyloma* Sharp, 1872, *Eurygmus* Hansen, 1990, *Petasopsis* Hansen, 1990 and *Rygmodus* White, 1846 which have completely or largely concealed labrum); mesoventrite (Fig. 3D) not

Figure 1. *Cylorygmus lineatopunctatus* Orchymont, 1933. (A–C) adult habitus: (A) dorsal; (B) lateral; (C) frontal view of the head. (D–H) habitus of third instar larva: (D) dorsal; (E) ventral; (F) detail of thorax and head in dorsal view; (G) detail of thorax and head in ventral view; (H) tergite on abdominal segment VIII.

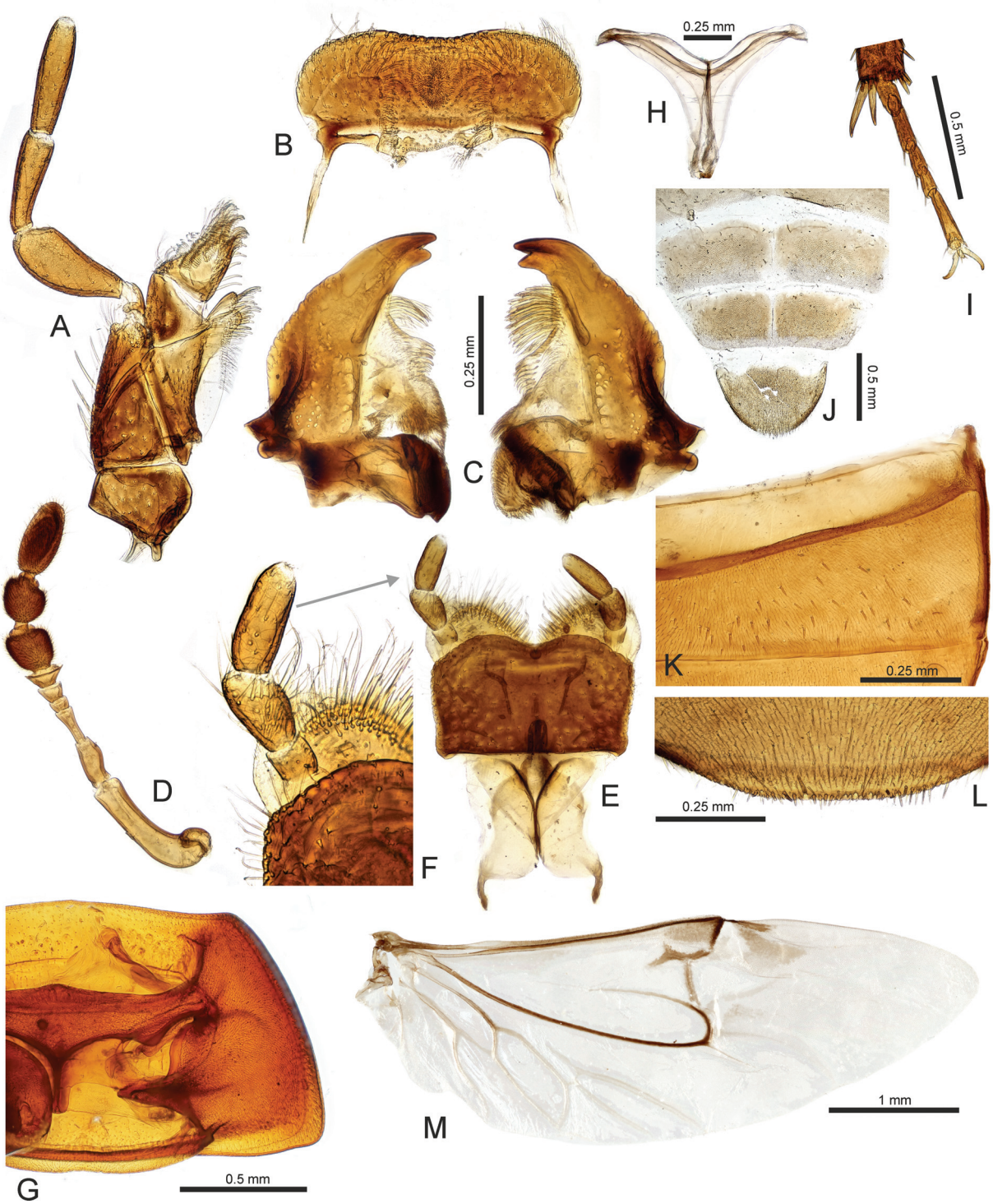

Figure 2. Detailed adult morphology of *Cylorygmus lineatopunctatus* Orchymont, 1933. (A) maxilla; (B) labrum; (C) mandibles; (D) antennae; (E) mentum and prementum; (F) detail of the labial palp; (G) prothorax in ventral view; (H) metafurca; (I) metatarsus; (J) abdominal tergites VI–VII; (K) detail of abdominal ventrite I with intermixed stout setae; (L) apex of ventrite V with stout setae; (M) hindwing.

distinctly elevated posteromesally (in contrast to *Adolopus*, *Andotypus*, *Borborophorus* Hansen, 1990, *Coelostomopsis*, *Cyloma*, *Exydrus* Broun, 1886, *Hydrostygnus* Sharp, 1884 and *Tormissus* Broun, 1893 which have a posteromesal elevation), but with transverse ridge (in contrast to *Anticura*, *Cylomissus* Broun, 1903, *Eurygmus*, *Pseudohydrobius* Blackburn, 1898, *Rygmodus*, *Rygmostralia* Orchymont, 1933 and *Saphydrus* Sharp, 1884 which also have non-elevated mesoventrite, but lack the transverse ridge); first metatarsomere (Fig. 2I) shorter than second (in contrast to *Andotypus*, *Austrotypus* and *Coelostomopsis* with very long first metatarsomere); elytra not explanate (Figs 1A–B) and epipleura very narrow at apex (in contrast to *Borborophorus* and *Petasopsis* with explanate elytra and epipleura very wide throughout).

Cylorygmus differs from *Relictorygmus* gen. nov. in the following combination of characters: labrum dorsally with median group of stout setae (Fig. 3A); gula (Fig. 3B) moderately wide anteriorly (ca. half of its width at base); anterior margin of mentum (Fig. 3B) very weakly indented below the palpal insertions; femora (Figs 3G–I) pubescent with intermixed stout setae; mesoventrite (Fig. 3D) with weakly developed transverse groove posteromesally, setose centrally; anterior metaventral process narrow, about 2.3× longer than wide at base (Fig. 3D); abdominal ventrite I (Fig. 2K) with intermixed stout setae; posterior margin of abdominal ventrite V (Fig. 2L) with series of stout setae mesally; abdominal tergites VI–VII (Fig. 2J) subdivided mesally; male genitalia (Fig. 7A) with median lobe ca. twice as wide as parameres, gonopore apical.

Larva. The symmetrical wide mandibles, each with two retinacular teeth (Figs 5C, 8C), nasale with five large teeth and symmetrical epistomal lobes (Figs 4C, 6A, 7C), antennal sensorium shorter than antennomere 3 (Figs 5A–B, 8A–B), inner face of maxillary stipes with 5 setae only (Figs 5E, 8E), prementum only slightly narrower than mentum and with distinctly developed ligula (Figs 5G–H, 8G–H), abdomen without projections or tracheal gills (Figs 1D–E) and legs well developed (Figs 1G, 6B) diagnoses the larva of *Cylorygmus* easily from members of Amphiopini (mandibles slender, mentum very wide, ligula absent), Berosini (abdomen usually with projections or gills, mandibles asymmetrical or slender and symmetrical, epistomal lobes strongly asymmetrical or nearly absent), Laccobiini (mandibles and epistomal lobes either asymmetrical, or nasale with less than 5 large teeth), Hydrobiusini (mandibles with a small tooth below the basal retinacular tooth), Hydrophilini (head appendages long and slender, mentum much wider than prementum, abdomen with at least short projections), Chaetarthriinae (antennal sensorium as long as antennomere 3, ligula projecting further than labial palps, coronal sulcus usually absent) and Sphaeridiinae (nasale with less than 5 teeth, inner face of stipes mostly with many stout setae, legs often shortened to completely reduced). The larva may be hence confused only with those of the subfamilies Acidocerinae, Enochrinae and Cylominae, to some of which it is also very similar by external habitus. Larvae of all known Enochrinae differ from *Cylorygmus* by nasale with multiple irregularly shaped small toothlets (rather than five large well-defined teeth in *Cylorygmus*) and by the dorsal surface of mentum completely covered by cuticular spines (with two submedian bare areas in *Cylorygmus*). All known larvae of Acidocerinae differ from *Cylorygmus* by nasale with at least 6 teeth.

Within Cylominae, *Cylorygmus* can be easily distinguished from *Anticura*, *Cylomissus*, *Andotypus* and *Austrotypus* and *Tormissus* by nasale with 5 teeth and inner face of stipes with 5 setae only (with 1–2 teeth on nasale and multiple setae on inner face of stipes in the latter genera), and from *Cyloma* by nasale with 5 teeth (nasale with 3 teeth in *Cyloma*). All mentioned genera except *Borborophorus* differ in the configuration of the teeth of the nasale: *Saphydrus* with the median and lateral teeth large and the intermediate small, *Rygmodus* in both right and left tooth more widely isolated from the median three teeth (plus mandibles, maxillae and prementum very elongate), and *Adolopus* with all teeth grouped together (i.e. without any tooth more widely isolated or distinctly smaller than others). The supposed larva of *Borborophorus* is very similar to that of *Cylorygmus* in the form of nasale and epistomal lobes, as well as in most other characters examined (but slides were not done and chaetotaxy not examined), and seems to differ only by the shape of head capsule (slightly widened posteriorly, compared to parallel-sided in *Cylorygmus*), smaller stemmata and antennal sensorium as long as antennomere 3 (slightly shorter in first instar larva and much shorter in third instar larva in *Cylorygmus*).

Redescription of adult. Body elongate oval (Fig. 1A), compressed in lateral view (Fig. 1B). General coloration brown to black.

Head. Clypeus and frons (Fig. 1C) distinctly punctate; frontoclypeal suture very weakly marked, by lack of punctures; clypeus not excised above antennal insertions, anterior margin concave, marginal bead absent, surface with only few isolated trichobothria. Frons with trichobothria next to inner margin of each eye. Eyes (Figs 1B–C) small, slightly protruding from head outline; facets ca. 16–17 μm in diameter. Labrum (Figs 1C, 2B, 3A) well sclerotized, exposed in front of clypeus, visible in dorsal view, ca. 3.0× wider than long, bisinuate anteriorly, rounded laterally; anterolateral margin with long setae, anteromedian part with group of stout setae; epistome with two groups of long spine-like setae anteriorly and with two parallel series of

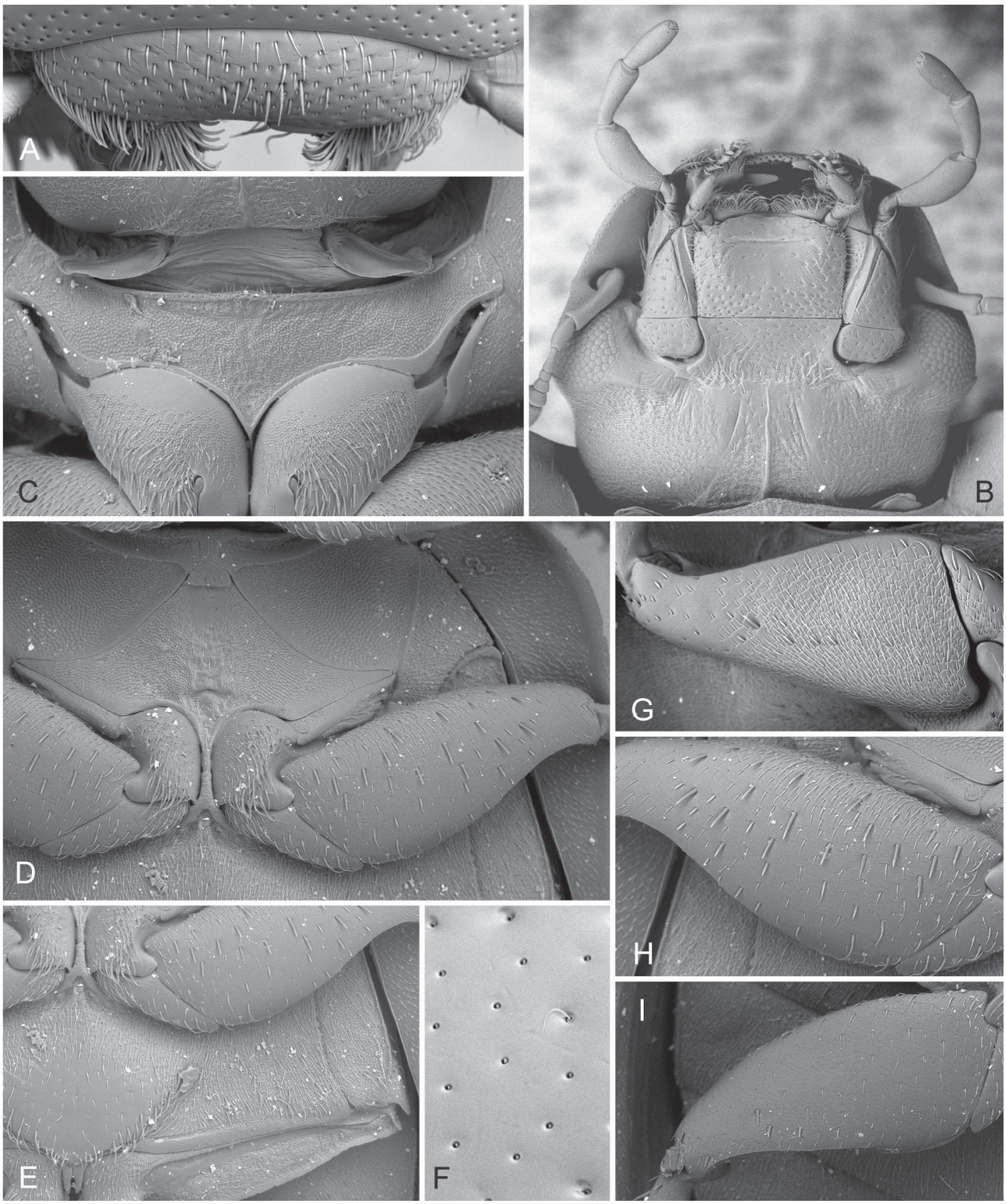

Figure 3. *Cylorygmus lineatopunctatus* Orchymont, 1933, details of adult morphology, SEM micrographs. (A) labrum, dorsal view; (B) head, ventral view; (C) prosternum; (D) mesothorax, ventral view; (E) metaventrite; (F) elytral interval with trichobothrium; (G–I) femora in ventral view: (G) profemur; (H) mesofemur; (I) metafemur.

long hair-like projections posteriorly. Mandibles (Fig. 2C) slightly asymmetrical, without developed mandibular angle, apex bidentate; prostheca with series of long projections, slender and elongate in anterior part, stout and shorter at base; outer margin sparsely pubescent; mola large, with small cuticular projections. Maxilla (Fig. 2A) with large sub-pentagonal cardo, lacking trichobothria; basistipes widely triangular, moderately pubescent, bearing one or two trichobothria; mediostipes vaguely defined from lacinia; lacinia membranous, with distally situated finger-like projection, pubescent, setae more thickened and rounded towards anterior part of lacinia and on the projection, galea long, apical membranous portion blunt at apex, densely pubescent, the pubescence regularly ordered in rows, setae thickened, bent and apically rounded; maxillary palpus four-segmented, palpomere 1 minute, palpomere 2 slightly swollen distally, about as long as palpomere 3 and 4 each; palpomere 4 without digitiform sensilla. Labium with submentum (Fig. 2E) about as long as mentum, pubescent; mentum (Fig. 3B) transverse, ca. 1.5× wider than long, widening anteriad, anterior margin almost continuously rounded, very weakly indented below palpal insertions, surface flat, with a weak transverse groove parallel to anterior margin; lateral margins with dense series of setae; prementum (Fig. 2F) subdivided into two large lateral lobes bearing long, apically acute and slender setae, as well as short, apically rounded and thickend setae; palpifer weakly sclerotized; labial palpus with 3 palpomeres (Fig. 2F), basal palpomere minute, second palpomere widened, bearing numerous setae, palpomere 3 thin, only with few setae. Antenna with 9 antennomeres (Fig. 2D); scapus long and thin, widest at midlength; pedicel widest at midlength; antennomere 3 about 0.7× as long as pedicel and as long as antennomeres 4–6 combined; antennomere 6 (cupule) small, slightly narrower than antennal club; antennomeres 7–9 forming a loosely segmented pubescent antennal club, antennomere 9 elongate ca. 1.7× as long as each of antennomeres 7–8. Gula wide (Fig. 3B), narrowing anteriad to a half of its width at base, with median ridge, tentorial pits reduced. Temporae (Fig. 3B) rugose and sparsely pubescent, with weakly defined ridge arising from inner margin of each eye.

Prothorax. Pronotum (Fig. 1A) widest at base (ca. 0.45× as long as wide, ca. 1.5× wider at base than in front angles), continuously arcuately narrowing anteriad; anterior angles acute (Figs 1B, 2G); dorsal punctation similar to that on frons; trichobothria present in anterolateral corner; anterior, posterior and lateral margins with narrow marginal bead. Hypomeron (Fig. 2G) with very narrow lateral glabrous part and densely pubescent mesal part divided by a very fine ridge; antennal grooves absent; hypomeral process simply pointed, not reaching prosternal process. Prosternum (Figs 2G, 3C) slightly shorter than procoxal cavity anteriorly to procoxae, flat, with weak transverse impression, angulate and beaded on anterior margin, with evenly distributed short setae; exposed part of prosternal process pointing between procoxae, posterior part concealed by procoxae slightly widened posteriorly, truncate at apex. Coxal cavities (Fig. 2G) closed internally, open posteriorly, coxal fissure long, widely open. Profurca short and weakly sclerotized, profurcal arms widely separated basally, in form of asymmetrical apically slightly widened stalks.

Mesothorax. Scutum with finely microsculptured median portion, bearing sparsely arranged setae laterally; scutellar shield (Fig. 1A) exposed, triangular, pointed posteriorly, as long as wide, bearing punctation similar to frons and a series of stout setae below the anterior margin. Elytron (Figs 1A–B) elongate, ca. 2.3× as long as wide, evenly convex; with 10 series of punctures, serial punctures distinctly larger than punctures in intervals; trichobothria present on alternate intervals (Fig. 3F); sutural stria present, adjacent to punctural series 1; scutellar stria absent; lateral margin of elytra beaded, very narrowly explanate, lateral margin bare, without stout setae; epipleuron wide at base, gradually narrowing towards level of metacoxae, then narrow but distinct, reaching elytral apex; lateral narrow bare part not delimited from mesal pubescent one by a ridge; ventral face of elytron without elevated ridges. Mesoventrite (Fig. 3D) divided from mesanepisterna by anapleural sutures; subtriangular in shape in anterior two thirds, narrowing anteriorly, widely extending in posterior third, lateral extensions with distinct coxal lobes; anapleural sutures arcuate; median part of mesoventrite flat, with rugose surface, without elevated projection, with weakly developed transverse groove posteromesally; anterior portion without anteromedian pit-like groove; mesoventral process narrow, abutting to metaventral process, not elevated above it. Mesanepisterna (Fig. 3D) not meeting mesally, very narrowly divided by anterior portion of mesoventrite; anterior collar well-defined, rather wide, sparsely pubescent along anterior bead. Mesepimeron with large ventral portion, not reaching anterior collar of mesanepisternum; forming lateral margin of mesocoxal cavity; whole surface with densely arranged setae. Mesocoxal cavities obliquely transverse, very narrowly separated from each other by meso- and metaventral processes; internal postcoxal wall developed mesally and posteriorly, narrow. Mesofurca well developed, rather short, furcal arm not developed; basal portion fused and rather wide, bifurcating only very dorsally into two arms, each with narrow asymmetrical plate-like apical extension.

Metathorax. Metanotum weakly sclerotized, ca. 2× wider than long, alacristae slightly diverging posteriad. Metaventrite (Fig. 3E) ca. 2.9× wider than long, slightly

longer than mesoventrite, evenly convex, with median area bare and slightly raised posteriorly, margin of elevated area with thick long setae, discrimen reaching mid of metaventrite, surrounded by sparsely pubescent area, lateral part of metaventrite with dense short pubescence, interspersed with longer thick setae; anteromesal area with shallow impression; katepisternal suture weakly developed, vanishing towards lateral margin of mesoventrite, katepisternum narrow and bare; posterior metaventral process bifid. Metanepisternum ca. 4.5× longer than wide, with oblique ridge subanteriorly, anterior margin straight; surface pubescent. Metafurca (Fig. 2H) Y-shaped; stalk long, grooved, without basal extensions; arms long and wide, with apical plate-like extensions. Hind wing (Fig. 2M) well developed, widest at mid-length, ca. 1.6× longer than elytron, venation well-developed in basal portion, absent in distal part; anal lobe moderately large, defined by well-developed anal notch; RA tightly attached to ScA except subbasally, both reaching triangular radial cell, RA_{3+4} as long as radial cell, r4 arising from its midlength; distal portion of RP and MP_{1+2} forming a strong loop, distally with long median spur; vein complex of MP_3+MP_4+Cu+AA well developed, not connected to MP_{1+2} by cross-veins, with well-developed and completely closed basal and wedge cells; distal portion of MP_4+CuA complex H-shaped, arising from anterior portion of wedge cell; AA_4 long, reaching posterior margin; AP_{3+4} long, reaching over the midlength of anal lobe.

Legs. Mesotrochantin ca. 0.6× as long as mesocoxal cavity, narrow, exposed ventrally anterior of mesocoxae. Coxae: procoxae subglobular, pubescent ventrally; mesocoxae transverse, narrowly separated, pubescent ventrally; metacoxae transverse, finely pubescent except anterior part, all coxae with interspersed thick setae. Trochanters with proximal parts concealed by coxae, distal portion subtriangular, pubescent ventrally; meso- and metatrochanters bisinuate on posterior margin, posterior margin not continuous with that of femora. Femora attached to trochanters by their posertobasal (in meso- and metafemora) or anterobasal (in profemora) parts only; anterobasal (in meso and metafemora) or posterobasal (in profemora) part free, angulate; pubescence of ventral surface in profemora (Fig. 3G) dense and in meso and metafemora (Figs 3H–I) sparse; all femora with tibial grooves well defined by sharp ventral edges. Tibiae slightly longer than femora, slightly widening distally; each tibia with longitudinal series of setae on dorsal, ventral and lateral faces; apex with group of short to very long spines, protibia with two long, meso- and metatibia with one moderately long and one very long spurs mesally, the longer one ca. 1.5–2.0× as long as the first tarsomere. Tarsi (Fig. 2I) with 5 tarsomeres; protarsus with tarsomeres 1–4 short, subequal in length, tarsomere 5 longer, ca. as long as tarsomeres 1–3 combined; meso- and metatarsi with basal tarsomere shorter than tarsomere 2, tarsomeres 3 and 4 ca. subequal in length to tarsomere 1, tarsomere 5 ca. 2× longer than tarsomere 3; ventral surface of all tarsomeres with sparse long pubescence; claws small, simply arcuate.

Abdomen with five exposed ventrites; ventrites evenly convex, without median carina, densely pubescent; ventrite I (Fig. 2K) with intermixed stout setae; posterior margin of ventrite V (Fig. 2L) entire, with stout setae. Laterotergite III without stridulatory file; tergites VI–VII (Fig. 2J) subdivided mesally.

Genitalia. Aedeagus (Fig. 9A) of simple trilobed type; phallobase subequal in length to parameres, with wide, indistinctly defined, posteriorly rounded manubrium; parameres distinctly longer than median lobe; median lobe wider than parameres, weakly narrowing apicad, apex cut off and pubescent, gonopore distinct, apical. Sternite 9 (Fig. 9B) with wide median part constricted subbasally, widened and notched posteriorly, lateral struts shorter than median part. Female genitalia of the general morphology similar to other Hydrophilidae (see e.g. Fikáček 2010), with very long coxostyli and gonostyli, otherwise not examined in detail.

Cylorygmus lineatopunctatus Orchymont, 1933 (Figs 1–8, 9A–B, 13)

Philhydrus lineato-punctatus Germain, 1911: 58 (nomen nudum).
Cylorygmus lineatopunctatus Orchymont, 1933: 293.

Type material examined. **Neotype** (designated by Moroni 1985): 1 male (MNNC): "Quillota [printed] / XI-96 [in red handwriting] // 810 // Colección / P. Germain [printed] // ♂ // Museo Nacional / Santiago-Chile // NEOTIPO [blue label, handwritten] // CHILE M.N.H.N. / Tipo No 3779 // *Cylorygmus* / *lineatopunctatus* D'Orch. 33 / Det. J. Moroni 1970".

Comments on type material. There was long-lasting confusion about the identity of *Cylorygmus lineatopunctatus*. Orchymont (1933) described the genus and species according to a single female collected by P. Germain in Quillota in November 1896 deposited in the Hamburg Museum, which was however destroyed during the Second World War. Spangler (1974) associated the specimens collected in Magallanes (southern Chile) with Orchymont's (1933) description, designated a neotype and later described the larva of this taxon (Spangler 1979). He noted the large distance between the original type locality and that of his neotype, and cast doubt whether the original type locality is in the Valparaíso region near Santiago de Chile, or in Aysén Region in the south. Moroni (1985) examined the material collected by P. Germain deposited in MNNC

including specimens which were likely collected together with the lost holotype, and realized that the specimens redescribed by Spangler (1974) in fact belonged to a different species [later it was found that Spangler's (1974) specimens in fact represent the genus *Pseudorygmodus* Hansen, 1999 and are not related to *Cylorygmus*; Hansen 1999, Fikáček and Vondráček 2014]. Moroni (1985) recognized the invalidity of the neotype designation by Spangler (1974) since Spangler was not in compliance with Art. 75.3.6 (ICZN) which requires "evidence that the neotype came as nearly as practicable from the original type locality [Art. 76.1]". Moroni selected the above specimen collected by P. Germain likely together with the original holotype as a neotype. We examined the specimen of *C. lineatopunctatus* from Orchymont collection in IRSNB mentioned by Hansen (1999): this specimen corresponds by the label data with the lost holotype as well as Moroni's neotype and bears Orchymont's identification label. It is moreover conspecific with Moroni's neotype and with additional specimens examined by us. Very likely all examined specimens including the lost holotype and the neotype by Moroni belonged to the same series of specimens from the Germain collection. This confirms that the identity of *C. lineatopunctatus* fixed by Moroni (1985) corresponds to the original meaning of the name by Orchymont (1933).

Additional adult material examined. **CHILE: Región Metropolitana de Santiago**: 4 spec. (MNNC): Hospital Lo Águila [33°54'S 70°46'W], without date and collector; 1 ♂, 4 spec. (MNNC): Lo Águila, Chile central // Lo Águila, 33°54'S 70°46'W, J. Moroni det., P. Germain coll.; 1 ♀, 7 spec. (MNNC): Santiago, Lo Águila, lgt. P. Germain; 1 ♂, 11 spec. (MNNC): Chile, P. Germain coll. [considered as collected in Lo Águila by Moroni]; 1 spec. (MNNC): Santiago, Rungua [33°0'24.12"S 70°53'20.4"W], 7.xi.[18]69 [remaining text illegible]; 2 spec. (MNNC): Maipo, Rangue [33°51'19"S 70°53'11"W], 4.vi.2004, lgt. M. Elgueta & M. Guerrero; 3 spec. (JBCC): Mina La Disputada [33°10'14"S 70°18'16"W], x.1989, J. E. Barriga lgt.; 1 ♀, 5 spec. (NHMW, NMPC): Quebrada La Plata [33°29'38"S 70°53'23"W] / Prov. Santiago de Chile /lg. H. Franz / Sa 6-7; 1 spec. (FMNH): Peñalolén 14 km SE of Santiago [33°33'21"S 70°31'41.3"W], 7.x.1945, lgt. L. Peña Guzmán; 1 ♂, 20 spec. (HNHM, NMPC): Farellones, 6.x.1965, Hungarian Soil-Zool. Exp. Nr. P-B.36, Andrássy, Balogh & Mahunka lgt. [further collecting details provided by Andrássy *et al*. (1967): Farellones, 2100 m, singled in surroundings, but always along streamlets, mostly beneath stones]. **Valparaíso Región:** 1 ♀ (IRSNB): Chile, Quillota / XI. 1896 // A. d'Orchymont det. / *Cylorygmus* / *lineatopunctatus* // Para- / type // Coll. R. I. Sc. N. B.; 1 spec. (MNNC): Valparaíso / Quillota [32°52'S 71°15'0"W] // *Philydrus* / *lineatopunctatus* P. G. [= Ph. Germain] / Paulo / Quillota // *lineatopunctatus* P. G. ined. 1911; 2 spec. (MNNC): Quillota [32°52'S 71°15'0"W] / XI-96 // Chile / Valparaíso / Quillota 11.1896 // castaneno P. G. ined. 1627; 1 ♂, 1 spec. (MNNC): Quillota, ii.[1897], lgt. P. Germain; 1 ♀ (MNNC): Quillota, xi.[18]96, lgt. P. Germain [labelled as topotype by Moroni]; 1 ♀ (MNNC): 810 // Quillota xi.96 // TOPOTIPO; 15 spec. (MNNC): Quillota [32°52'S 71°15'0"W], without date and collector; 8 spec. (FMNH): La Vega vicinity, 33°2.71'S 71°1.63'W (ANMT1014), 940 m a.s.l., sclerophyll forest with Eucalyptus, berlesate damp litter in dry stream bed, 15.xii.1996, lgt. A. Newton & M. Thayer (FMHD #96-207); 3 spec. (FMNH): Parque Nacional La Campana (Sector Granizo), Cajón La Opositora, 32°58.78'S 71°6.93'W (ANMT1045), 685 m a.s.l., sclerophyll forest with *Nothofagus obliqua*, berlesate wet debris at stream, 29.xii.2002, lgt. M. Thayer & A. Newton (FMHD#2002-101); 1 spec. (FMNH): Parque Nacional La Campana (Sector Ocoa), vicinity of Quebrada Buitrera, 32°55.89'S 71°5.1'W (ANMT 1047), 415 m a.s.l., sclerophyll woodland with *Jubaea chilensis* palms and *Trichocereus* cacti, in cow dung near stream edge, 28.xii.2002, lgt. M. Chani; 3 spec. (FMNH): same locality, but in debris at pool in dry creek bed, 28.xii.2002, lgt. D. Clarke (FMHD#2002-100); 3 spec. (FMNH): same locality, but in moss at base of tree at stream edge, 28.xii.2002, lgt. M. Chani; 2 spec. (FMNH): same locality, but wet debris at stream edge, 28.xii.2002, lgt. A. Solodovnikov; 10 spec. (FMNH, NMPC, KMNH): same locality, but berlesate from flood debris at small stream, 30.xi.2002, lgt. M. Thayer, A. Newton, A. Solodovnikov & D. Clarke (FMHD#2002-026); 1 ♂ (FMNH): 4 km E of Quebrada Alvarado, 33°3'S 71°3'W (ANMT668.2), 500 m a.s.l., gallery forest along stream, wet leaves, stream edge, 5.i.1983, lgt. A. Newton & M. Thayer; 1 ♂, 2 spec. (NMPC): Parque Nacional La Campana (Sector Ocoa), 4.75 km SE of park entrance, "La Cascada", 32°57.7'S 71°3.2'W, 870 m a.s.l., sifting of wet/humid flood debris and leaf litter at sides of the pool below the waterfall, 20.xi.2013, lgt. M. Fikáček, D. Vondráček & P. Kment (CH03); 1 ♂ (HNHM): Between Concon and Quintero, 14.xii.1965, Hungarian Soil-Zool. Exp. Nr. P-B.300, Mahunka lgt. [more details from Andrássy *et al*. 1967: "netted from trees and bushes"].

Larval material examined. **CHILE: Valparaíso Región:** 2 first instar larvae, 2 likely second instar larvae, 4 third instar larvae (FMNH, NMPC, KMNH: 1 L1 and 2 L3 dissected and examined in detail): Parque Nacional La Campana (Sector Ocoa), vicinity of Quebrada Buitrera, 32°55.89'S 71°5.1'W, berlesate from flood debris at small stream, 30.xi.2002, lgt. M. Thayer, A. Newton, A. Solodovnikov & D. Clarke (FMHD#2002-026). The larvae were collected together with adults of *Cylorygmus* and two early-instar larvae of *Enochrus* (*Hugoscottia*) sp., no other hydrophilids co-occurred

in the sample. Adults of *Enochrus* (*H.*) *fulvipes* (Solier, 1849) were found by us in similar habitats on several localities in La Campana National Park in 2013, which also indicates that adults and larvae of *Cylorygmus* and *Enochrus* (*Hugoscottia*) co-occur in the same microhabitat in the region. Larvae of all other hydrophiloid genera occurring in Chile (see Jerez and Moroni 2006) except of that of *Cylorygmus* are known (e.g., Archangelsky 1997), and may be easily diagnosed from the examined larvae. Hence, despite not being able to confirm the identification of the larvae by means of DNA barcoding, we consider the identification of the larvae by association with adults and by exclusion of other Chilean genera as reliable.

***Further published records*. CHILE: Región Metropolitana de Santiago:** Peñalolén [33°33'21"S 70°31'41.3"W], 7.x.1945, lgt. L. Peña (Moroni 1985); Maipú, 15.xi.1982, lgt. R. Honour (Moroni 1985)

***Redescription of adult*.** 4.4–5.1 mm long, 2.2–2.5 mm wide (ca. 1.9× as long as wide), elongate oval, compressed in lateral view. **Coloration** (Figs 1A–C). Dorsal coloration dark brown to black; margins of pronotum yellow to light brown; ventral coloration dark brown, only hypomeron, epipleuron and legs light brown. **Head.** Eyes (Figs 1B–C) moderately small, interocular distance ca. 5.5× the transverse diameter of eye. Mentum (Fig. 3B) with anterior margin evenly rounded mesally, slightly concave laterally, surface becoming rugose and moderately setose towards lateral margins. **Prothorax.** Prosternum (Fig. 3C) mesally with moderately long setae, setae evenly distributed, surface of anterior marginal bead rugose, anterior portion with a weak transverse impression. **Mesothorax.** Mesoventrite (Fig. 3D) with weakly developed transverse groove posteromesally, not reaching coxal cavities, surface posterior of transverse groove sparsely setose; elevated anterior part of mesoventrite sub-triangular with straight posterior margin. **Metathorax** (Fig. 3E). Raised median area of metaventrite sparsely setose; anterior metaventral process narrow, elongated, ca. 2.3× as long as maximum width. **Legs.** Ventral surface of profemora (Fig. 3G) densely pubescent at base, bare at apex; mesofemora (Fig. 3H) sparsely pubescent with intermixed stout setae; metafemora (Fig. 3I) sparsely pubescent with only few intermixed stout setae. **Male genitalia.** Parameres (Fig. 9A) weakly arcuate on outer face, rounded at apices; median lobe ca. 2× as wide as parameres in ventral view, apex cut off and pubescent, slightly constricted subapically, gonopore apical.

***Description of larvae*. Third instar. General morphology** (Figs 1D–E). Body slender, widest between abdominal segments 2–3. Colour. Head capsule (Figs 1D–G) reddish brown with yellowish anterolateral part; appendage yellowish, only mandibles reddish brown. Sclerites (Figs 1D–H) on thorax and abdomen reddish brown, legs (Fig. 1G) yellowish brown; membranous parts slightly infuscate yellowish white, median part of abdominal segments 1–7 with one pair of oblong reddish brown patches dorsally (Fig. 1D).

Head. Head capsule subquadrate (Fig. 6A), widest medially. Cervical sclerites subquadrate. Frontal lines lilyform, coronal line very short. Surface of head capsule smooth. Six stemmata on each anterolateral portion of head capsule. Posterior tentorial pits present on median part close to junction of gular and submental sulci. Clypeolabrum (Fig. 7C) slightly asymmetrical. Nasale asymmetrical, with five distinct teeth; right four teeth aggregated, right upward; left one not projecting further than fight four teeth. Lateral lobes of epistome present, almost symmetrical but right lobe slightly projecting further than left lobe. Antenna (Figs. 8A–B) 3-segmented, slender; surface of antenna bare. Antennomere 1 widest, somewhat longer than antennomere 2, antennomere 3 the shortest and narrowest. Antennal sensorium present. Mandibles (Figs. 8C–D) moderately stout, symmetrical. Two inner teeth present on median part of inner face each; apical inner tooth slightly larger than proximal one. Maxilla (Figs. 8E–F) slender, 6-segmented, longer than antenna. Cardo moderate in size, irregularly shaped. Stipes the longest, ca. 1.7 times as long as palpomeres 1–4 combined; tooth-like cuticular projections present basally on inner face. Maxillary palpus short, 4-segmented. Palpomere 1 widest, incompletely cylindrically sclerotised, partly membranous dorsally. Inner process sclerotised. Palpomere 2 short, wider than palpomeres 3 and 4; palpomere 3 longest, wider than palpomere 4; palpomere 4 rather short and narrowest. Labium (Figs. 8G–H) well-developed. Submentum fused to head capsule, transverse; submental sulcus indistinct. Mentum trapezoidal, widest at base. Dorsal and lateral surface densely covered with small cuticular teeth, dorsal surface partly bare. Prementum subquadrate, without cuticular teeth. Ligula slender, mostly sclerotised, strongly curved towards dorsally, ca. as long as labial palpomere 2. Labial palpus slender, long, palpomere 1 wider and much shorter than palpomere 2; palpomere 2 long; intersegmental membrane between palpomere 1 and 2 bearing several cuticular projections dorsally.

Thorax (Figs 1F–G). Membranous parts very densely covered with short, hair-like, cuticular projections. Prothorax wider than head capsule. Proscutum formed by one large plate subdivided by fine sagittal line, anterior and posterior margins weakly sclerotised; proscutal plate covered with setae of variable length and densely distributed fine cuticular structures. Prosternal sclerite incompletely subdivided by fine sagittal line at posterior half; bearing numerous short setae on anterior part. Mesonotum with three pairs of dorsal sclerites; two pairs on anterior margin, median pair transverse, each attached mesally, lateral pair small; one large pair behind anterior pairs,

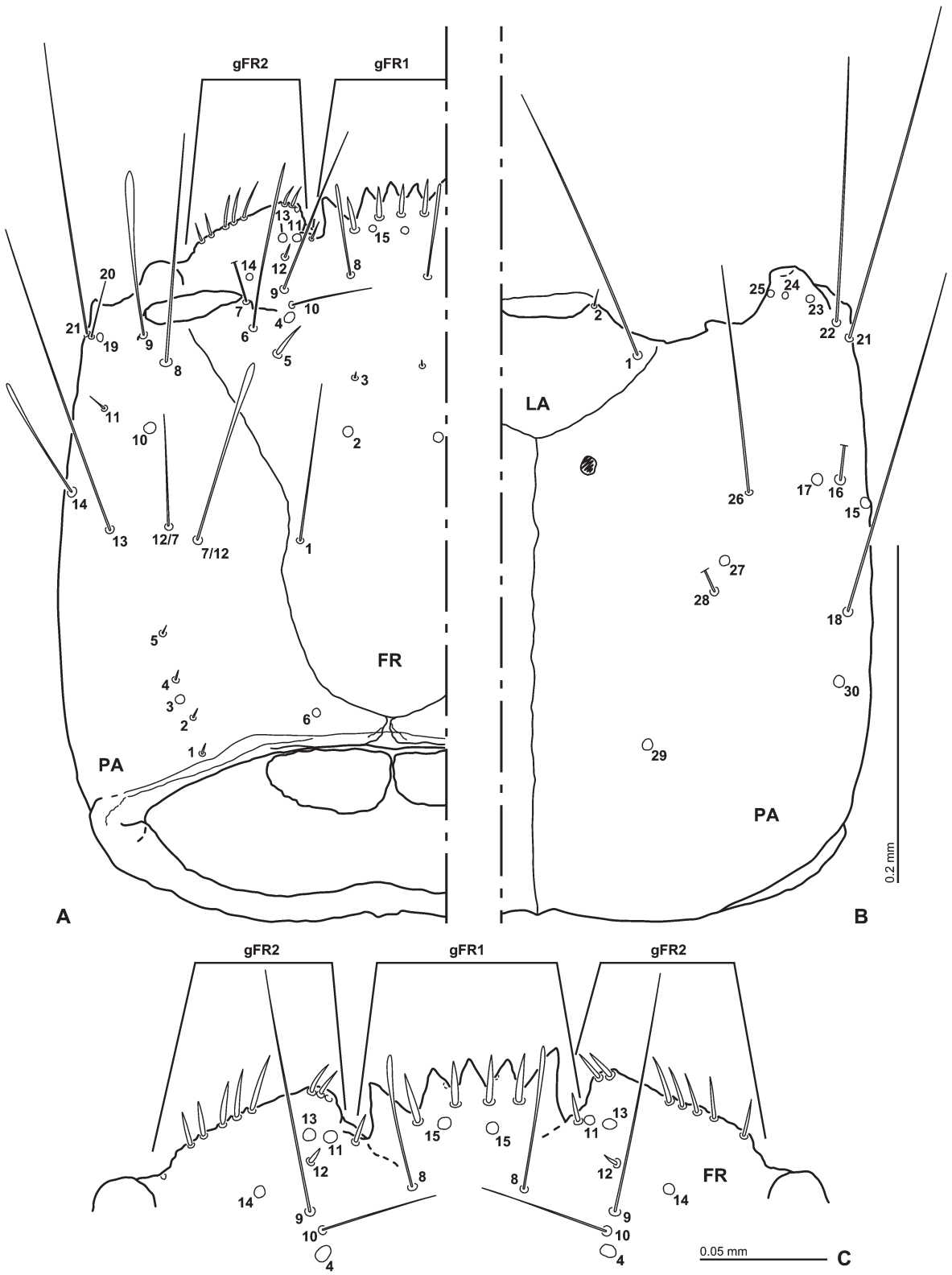

Figure 4. Head capsule of the first instar larva of *Cylorygmus lineatopunctatus* Orchymont, 1933. (A) head capsule in dorsal view; (B) head capsule in ventral view; (C) clypeolabrum.

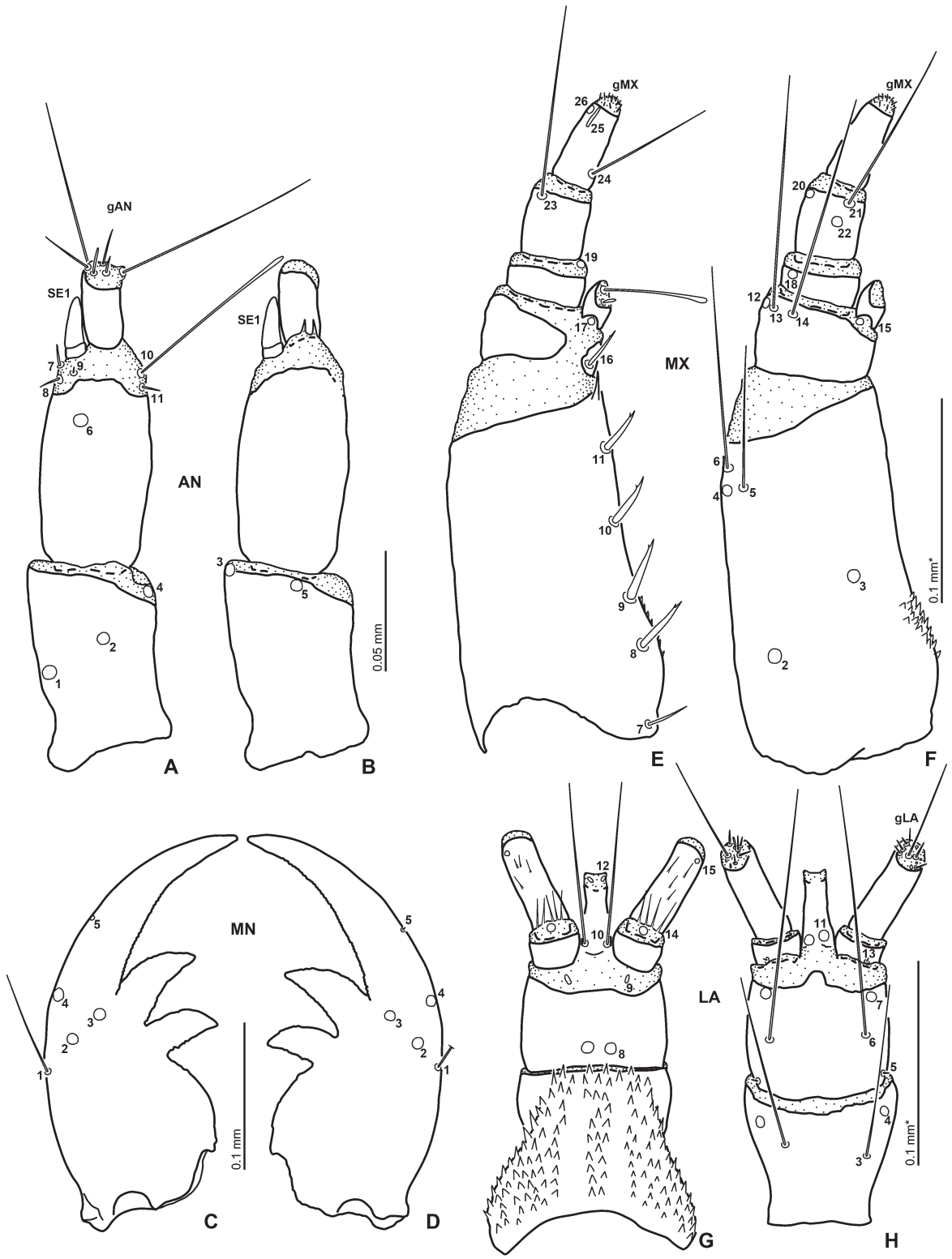

Figure 5. Head appendages of the first instar larva of *Cylorygmus lineatopunctatus* Orchymont, 1933. (A–B) antenna: (A) dorsal view; (B) ventral view; (C–D) mandibles in dorsal view: (C) left one; (D) right one; (E–F) maxilla: (E) dorsal view; (F) ventral view, cardo omitted; (G–H) mentum and prementum: (G) dorsal view; (H) ventral view.

subpentagonal, subdivided by transverse ridge and shallow transverse groove; each attached mesally. A pair of spiracles on anterolateral face, projecting laterally. Metanotum with three pair of dorsal sclerites; one pair on anterior margin, transverse, attached mesally, lateral pair very small, almost reduced. One large pair behind anterior pair, transverse, subquadrate, anterior halves shallowly concave; last pair behind large sclerite, transverse. Legs (e.g., Fig. 6B) rather short and slender, 5-segmented; all three pairs similar in shape.

Abdomen (Figs 1D–E, H). Abdomen 10 segmented, widest at segments 2 and 3, then slightly tapering posteriad; membranous parts covered with densely arranged short cuticular projections. Segment 1 with two pairs of small dorsal sclerites medially; posterior pair bearing seta. One pair of spiracles on lateral part of dorsal surface, tuberculate. Segments 2–7 similar to segment 1, but with one pair of small dorsal sclerites. Spiracular atrium (Fig. 6C): Segment 8 with large, oval dorsal plate (Figs 1H, 6C). Procercus short, partly sclerotised. Segment 9 trilobed. Lateral lobe of spiracular atrium large, widest basally, narrowing apically; inner part partly sclerotised; acrocercus absent, or stout and short present on ventral face of lateral lobe. Median lobe of spiracular atrium large, partly sclerotised, almost parallel-sided; a pair of slightly projecting lateral projection on basal part of median lobe.

First instar (Figs 4–5, 6B). Similar to third instar larvae, but sclerites weakly pigmented than third instar. Thorax. Prothorax as wide as or slightly wider than head capsule. Dorsal sclerites on meso- and metanotum weakly visible, lateral pair on mesonotum may be absent.

Chaetotaxy of head. First instar. Frontale (Figs 4A, C). Central part with three pairs of sensilla (FR1–3) slightly divergent posteriad; FR1 long seta; FR2 pore-like, situated more anteriorly and more mesally to FR1; FR3 very short seta, anteriorly to FR2. Pore-like sensillum FR4 and setae FR5–6 located posteromesally to antennal socket; FR5 stout, short seta, posteromesally to FR6, FR6 long seta, laterally to FR4–5; FR4 anteriorly to FR5. FR7 rather long seta, situated on inner

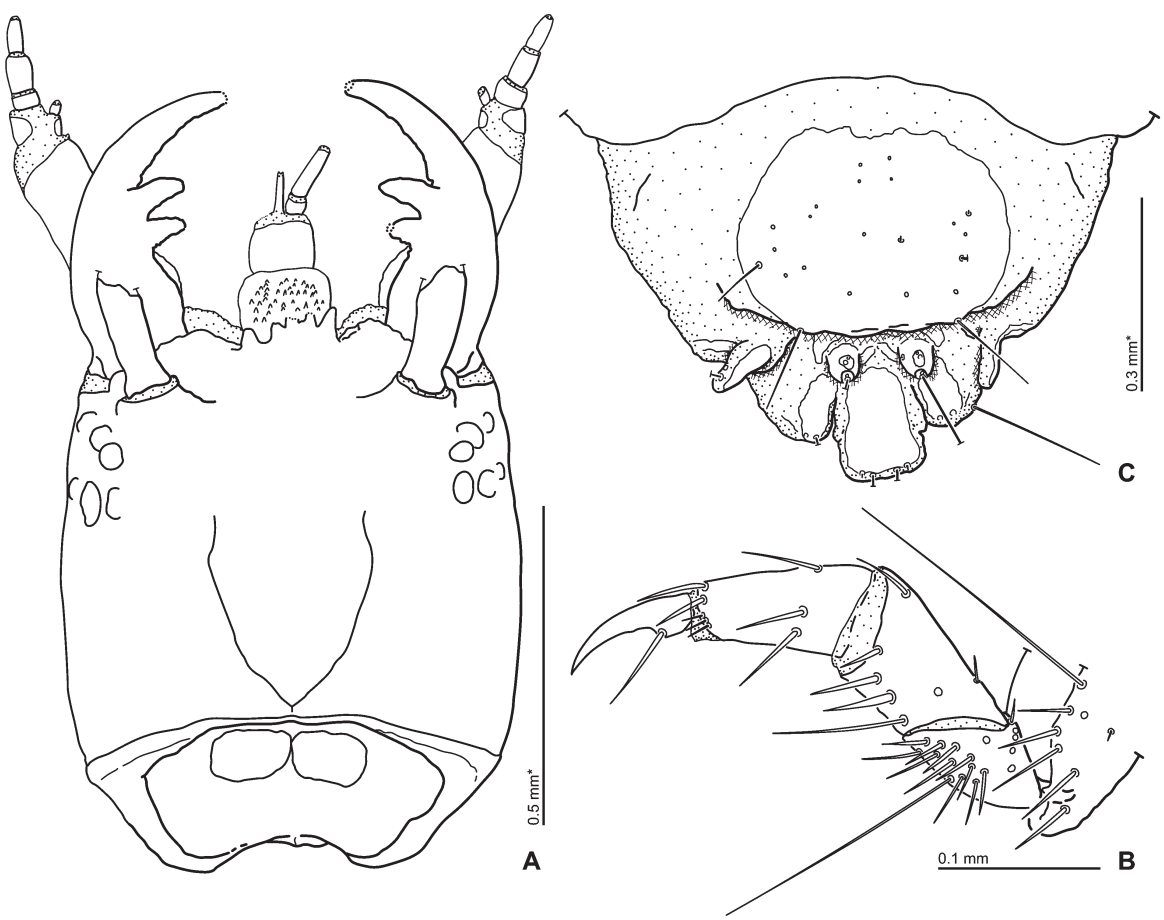

Figure 6. Larva of *Cylorygmus lineatopunctatus* Orchymont, 1933. (A) head in dorsal view; (B) mesothoracic leg in anterior view; (C) abdominal segments VIII–X in dorsal view. (A, C) – 3rd instar larva, (B) 1st instar larva.

face of antennal socket. Setae FR9–10 mesally to antennal socket; FR9 long, FR10 rather long. Pore-like sensillum FR15 and rather long, paddle shaped seta FR8 situated mesally on clypeolabrum, behind nasale; from FR15 anteriorly to FR8. Sensilla FR11-14 situated on epistome, anteromesally to antennal socket; FR11, 13–14 pore-like, FR12 short seta; FR11–13 closely aggregated, situated on inner part of epistome, FR12

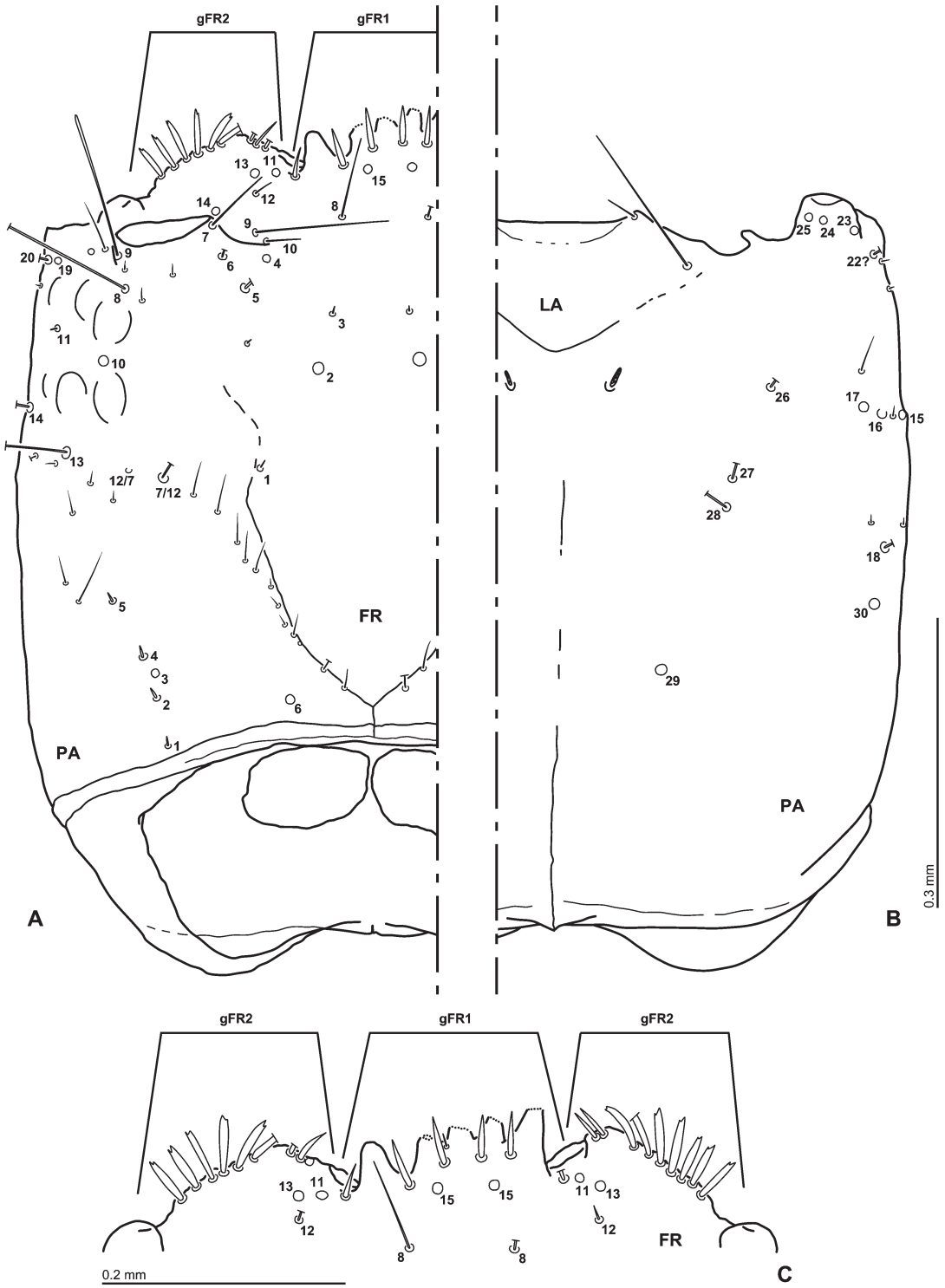

Figure 7. Head capsule of the third instar larva of *Cylorygmus lineatopunctatus* Orchymont, 1933. (A) head capsule in dorsal view; (B) head capsule in ventral view; (C) clypeolabrum.

posteriorly to FR11 and FR13, FR11 mesally to FR1213. FR14 located close to inner margin of antennal socket. Nasale with a group of six stout and short setae (gFR1); two minute ventral sensilla on laterally to median tooth of nasale. Epistomal lobe with stout short setae on anterior margin, composed by two groups; nine (six lateral, three mesal; lateral-most seta missing in the figured specimen) on left lobe, seven (five lateral, two mesal) on lateral lobe. **Parietale** (Figs 4A–B) Dorsal surface with a group of five sensilla (PA1–5) forming longitudinal row in posterior part; PA1–2 and 4–5 very short setae, PA3 pore-like. PA6 pore-like, located posteromesally close to coronal line. Sensilla PA7, 12–17 situated medially on dorsal to

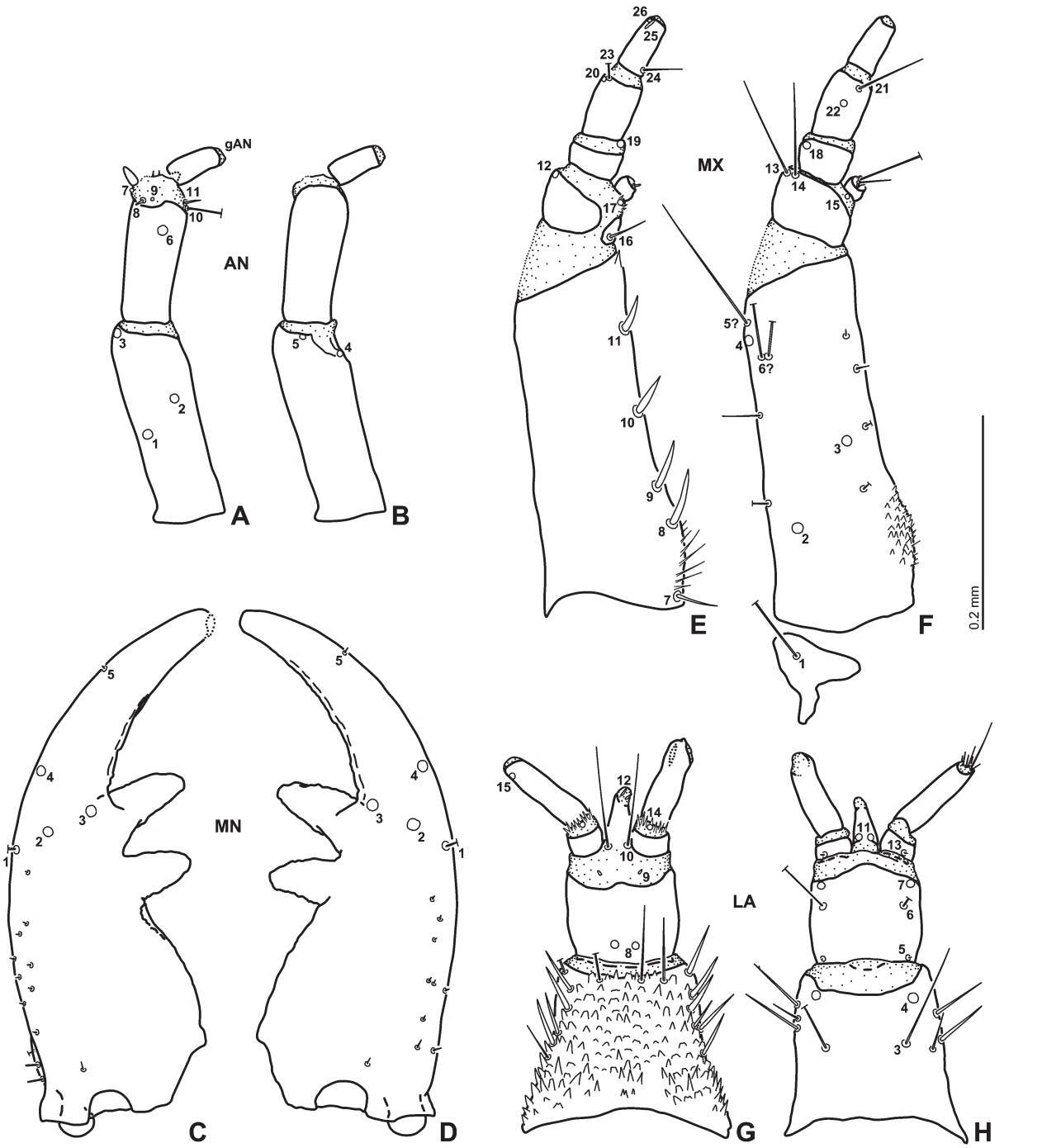

Figure 8. Head appendages of the third instar larva of *Cylorygmus lineatopunctatus* Orchymont, 1933. (A–B) antenna: (A) dorsal view; (B) ventral view; (C–D) mandibles in dorsal view: (C) left one; (D) right one; (E–F) maxilla: (E) dorsal view; (F) ventral view; (G–H) mentum and prementum: (G) dorsal view; (H) ventral view.

lateroventral surface, forming irregularly transverse row; from dorsal to ventral, PA7, PA12, 13, 14, 15, 16, 17. PA7 very long, paddle shaped; PA12 rather long seta; PA13 very long, on laterodorsal face; PA14 long seta, paddle shaped; PA15 and PA17 pore-like, PA16 long seta. Pore-like sensillum PA10 and short seta PA11 located between anterior and posterior rows of stemmata; PA10 mesally to PA11. PA8 very long seta, situated behind outer part of antennal socket. PA9 long seta, paddle shaped, on outer margin of antennal socket. PA19–22 located laterally on anterior corner of head capsule, closely aggregated; PA19 pore-like, PA20 rather short seta, PA21 and PA22 very long setae; from dorsal to ventral, PA19, 20, 21, 22. Pore-like sensilla PA23–25 on ventral mandibular articulation; PA23 on outer part; PA25 on inner part, PA24 between PA23 and PA25. Very long seta PA18 situated posteriorly to PA15–17, pore-like sensilla PA30 posteriorly to PA18. PA26–28 located median part of ventral surface of parietale; PA26 very long seta, anteriorly to PA27–28; PA27 pore-like, between PA26 and PA27; PA28 seta. PA29 pore-like, situated posteromesal part of ventral face of parietale. **Antenna** (Figs 5A–B). Antennomere 1 with five pore-like sensilla (AN1–5). AN1 situated laterally on median part of inner surface; AN2 dorsally on mesal part of anterior third; AN3–5 subapically, AN3 on lateral face, AN4 on inner face, AN5 ventrally on mesal part. Antennomere 2 with one pore-like sensillum (AN6) situated dorsally on subapical part of sclerite and five seta (AN7–11) dorsally on intersegmental membrane between antennomeres 2 and 3, and sensorium (SE1). Setae AN7–9 on outer face, posteriorly and close to SE1, AN7 and AN8 short, AN9 very short; AN7 anteriorly to AN8, AN9 mesally to AN7–8. AN10–11 on inner face, AN10 very long, paddle shaped; AN11 short. Sensorium SE1 on outer face, stout, slightly shorter than antennomere 3. Antennomere 3 with group of apical sensilla (gAN) in apical membranous area. **Mandibles** (Figs 5C–D). Three pore-like sensilla (MN2–4) on median part; MN4 situated on dorsolateral face, anterolaterally to MN2–3, anteriorly to MN1; MN2 posterolaterally to MN3. Rather long seta MN1 placed on lateral face, behind MN4; MN5 on apical third of lateral face. MN6 undetectable. Positions of sensilla identical in both mandibles. **Maxilla** (Figs 5E–F). Cardo with one ventral seta (MX1). Inner face of stipes with a row of five stout setae (MX7–11); simple seta MX7 at base, MX8–11 with small apical tooth, at equal intervals. Pore-like sensilla MX2–3 situated ventrally, MX2 laterally on posterior third, MX3 mesally on midlength. Pore-like sensilla MX4 and setae MX5–6 lateroventrally on subapical part of sclerite; MX5 long, MX6 very long. Dorsal surface of palpomere 1 with one rather short, stout seta (MX16) situated basally on inner face. Three sensilla (MX12–14) located laterally on distal part of ventral surface of sclerite; MX12 pore-like, MX13–14 very long seta; MX12 dorsally to MX13–14, MX13 between MX14 and MX12. Pore-like sensilla MX15 and MX17 situated on membrane behind inner appendage, MX17 dorsally, MX15 ventrally. Inner appendage with one long, paddle shaped seta and a few short setae apically (gAPP). Palpomere 2 with two pore-like sensilla (MX18–19); MX18 ventrally on lateral part; MX19 dorsomesally on intersegmental membrane between palpomeres 2 and 3; MX27 undetectable. Palpomere 3 with two pore-like sensilla (MX20 and MX22), and very long setae (MX21 and MX23). MX22 located ventrally on median part of sclerite; MX20-21 and MX23 distally on borderline between sclerite and intersegmental membrane; MX21 ventrally on inner face, MX23 dorsally on outer face, MX20 laterodorsally. Palpomere 4 with one rather long seta (MX24) situated subbasally on inner face, and with digitiform (MX25) and pore-like (MX26) sensilla apically on outer face of sclerite; MX25 dorsally to MX26. Apical membranous area of palpomere 4 with several minute setae (gMX). **Labium** (Figs 5E–H). Submentum with two pairs of setae (LA1–2); LA1 very long on lateral corner, LA2 short on anterolateral corner. Ventral surface of mentum with one pair of very long setae (LA3) and pore-like sensilla (LA4) on anterolateral part; LA3 behind LA4, LA4 subapically. Prementum and its anterior membranous area with five pairs of sensilla (LA5–9). LA5-7 situated lateroventral surface of prementum, minute seta LA5 at base, extremely long seta LA6 on midlength, pore-like sensillum LA7 apically on sclerite, close to borderline between sclerite and membrane. Pore-like sensilla LA8–9 situate median part of dorsal surface; LA8 on subbasally, LA9 situated on anterior membranous area. Ligula with one pair of very long setae (LA10) and two pairs of pore-like sensilla (LA11-12); LA10 dorsally at base; LA12 dorsally at apex, LA11 ventrally on subbasal part. Palpomere 1 with two sensilla (LA13–14); LA13 minute seta, situated basally on lateral part of ventral surface of sclerite; LA14 pore-like, dorsally on median part of intersegmental membrane between palpomeres 1 and 2. Palpomere 2 with one pore-like sensillum LA15 situated apically on outer face; several setae of variable shape (gLA) on apical membranous area.

Third instar. Frontale (Figs 7A, C). One small secondary seta situated posteriorly to FR5, laterally to FR2–3; one very short secondary seta behind antennal socket. **Parietale** (Figs 7A–B). Slightly oblique longitudinal row of short secondary setae present along frontal line. Two rather short secondary setae close to PA5. Longitudinal row of short, irregularly arranged secondary setae situated between PA7 and PA17; two minute secondary setae anterior to PA18; one short secondary seta anterior to PA17. Two secondary sensilla between PA9 and PA19, mesal one seta, lateral one pore-like. Few minute secondary setae on anterior

corner of head capsule. **Antenna** (Figs 8A–B) without secondary sensilla. Mandibles with minute secondary setae on posterior half of lateral face; a few basal secondary sensilla longer than others. **Maxilla** (Figs 8E–F) with secondary sensilla on stipes. Lateral face with two moderately short secondary setae on anterior third and posterior third respectively. One long secondary seta close to MX 5–6, undetectable from the primary setae. Ventral face with four short secondary setae on inner part, almost equidistant; anterior seta close to MX11, posterior seta close to MX9, but positions of the sensilla variable. Labium with secondary setae on mentum: 8 to 9 stout secondary setae of variable length present laterally, three moderately long setae on anterior margin.

Distribution. The species has very restricted distribution. Actual records are known between latitudes of ca. 33°S and 34°S in the Metropolitan and Valparaiso Region in Chile central Chile (Fig. 13A). It occurs both in the coastal range and in the foothills of the Andes. up to ca. 2100 m of altitude. The reconstruction of the potential distribution based on climatic data was performed by Fikáček and Vondráček (2014) and indicated that the species may be potentially distributed from northern parts of Valparaíso Region to northern O'Higgins only, i.e. in the region which

Figure 9. Aedeagus (A, C, E) and male sternite 9 (B, D, F) of *Cylorygmus* and *Relictorygmus* species. (A–B) *Cylorygmus lineatopunctatus* Orchymont, 1933; (C–D) *Relictorygmus repentinus* (Hebauer, 2002), holotype; (E–F) *Relictorygmus trevornoahi* sp. nov., paratype.

is strongly influenced by agriculture. Since it represents a very isolate and ancient clade of the Hydrophilidae (see Discussion), having a very restricted distribution, *C. lineatopunctatus* surely deserves protection.

Natural history. All known specimens were collected from September to February, i.e. during the summer season in Chile. Most adults and all larval specimens were collected from humid to wet debris, leaf litter and moss, in or along stream beds in sclerophyll or *Nothofagus* forests (Figs 13C–E). Incidentally, the specimens are probably hiding in other wet places near streams; for example, there were also found in cow dung near the edge of a stream.

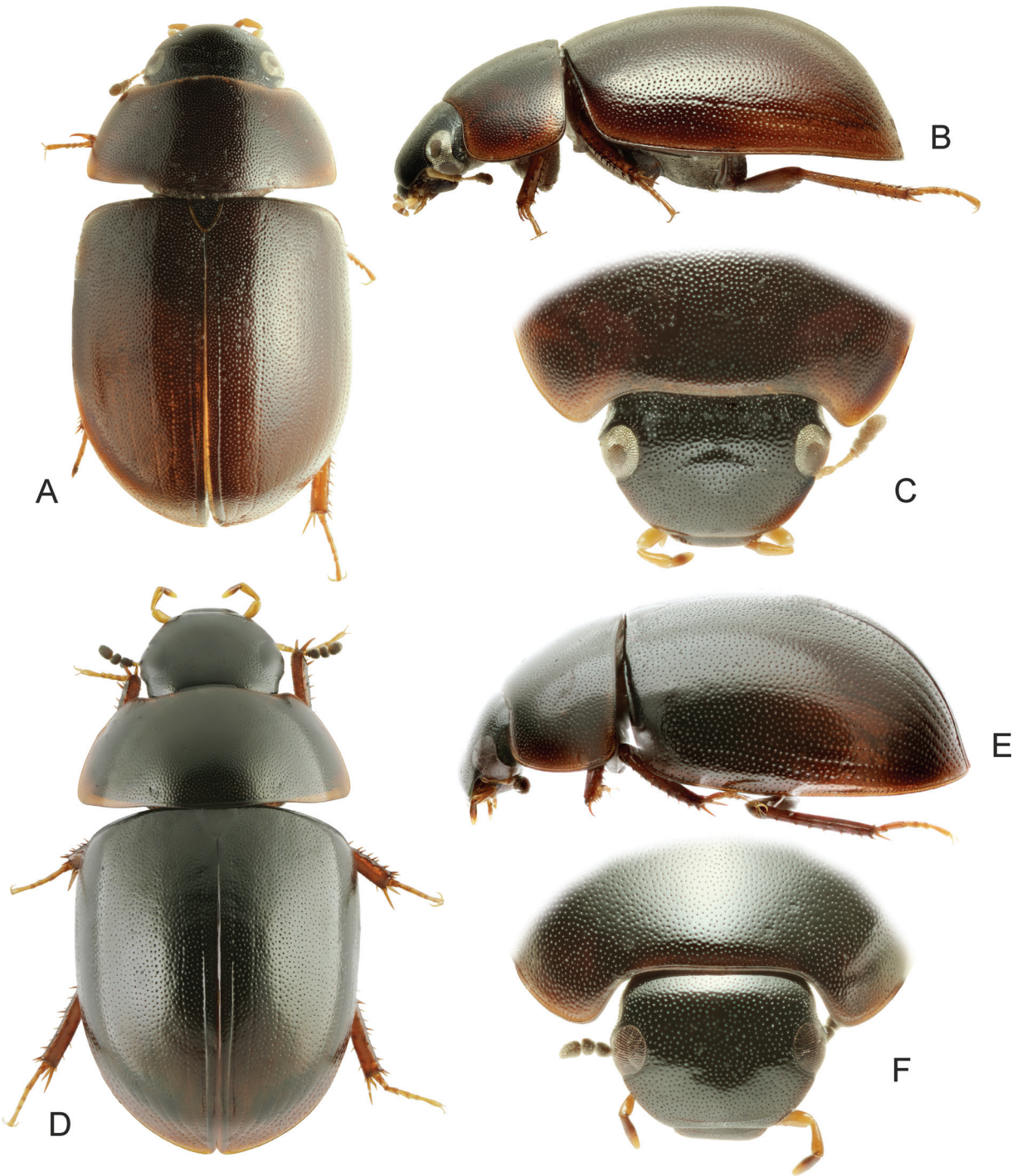

Figure 10. Habitus of *Relictorygmus* species. (A–C) *R. repentinus* (Hebauer, 2002), paratype: (A) dorsal habitus; (B) lateral habitus; (C) frontal view of the head. (D–F) *R. trevornoahi* sp. nov., paratype: (A) dorsal habitus; (B) lateral habitus; (C) frontal view of the head.

Relictorygmus gen. nov.

Type species. *Relictorygmus trevornoahi* gen. et sp. nov. (by present designation).

Etymology. The genus name is formed from the Latin adjective *relictus* (abandoned) and the core *-rygmus* which refers to *Cylorygmus* to which species of the new genus were assigned until now. The name refers to the genus being a remnant and supposed last member of the cylomine fauna in Africa. The gender is masculine.

Differential diagnosis from co-inhabiting genera. In South Africa, *Cylorygmus* may be confused with *Enochrus* and *Coelostoma* Brullé, 1835. *Relictorygmus* differs from *Enochrus* in maxillary palps (Figs 10C, F) bend inwards (in contrast to zigzag shaped palpomeres in *Enochrus*) and flattened mesoventrite (Figs 12H, M) (in contrast to posteromedially raised mesoventrite forming a high keel or large cone-shaped tooth in *Enochrus*). It differs from *Coelostoma* by the flat mesoventrite (Figs 12H, M) (in contrast to mesoventrite with high arrow-head shaped elevation and anterior pit-like groove in *Coelostoma*), and metatarsomere 1 shorter than metatarsomere 2 (Fig. 11I) (much longer than metatarsomere 2 in *Coelostoma*).

Differential diagnosis from cylomine genera. *Relictorygmus* gen. nov. corresponds to *Cylorygmus* in most external characters, but differs from it in the following combination of characters: labrum dorsally without median group of stouter setae (Fig. 12D); gula narrow anteriorly (Figs 12D, K) (ca. one fourth of its width at base); mentum with anterior margin markedly indented below palpal insertions (Figs 12F, K); femora pubescent but lacking intermixed stout setae (Figs 12A–C, I); mesoventrite (Figs 12H, M) with well-developed transverse groove posteromesally, pubescent centrally; anterior metaventral process wide and triangular (Figs 12G, L); abdominal ventrite I (Fig. 11K) without intermixed stout setae; posterior margin of abdominal ventrite V (Fig. 11L) without stout setae mesally; abdominal tergites VI–VII (Fig. 11J) not subdivided mesally; male genitalia (Figs 9C, E) with narrow median lobe, gonopore subapical.

Description of adult (characters marked by an asterisk were not examined for *R. repentinus*). Body (Fig 10) widely elongate, moderately convex. General coloration dark brown.

Head. Clypeus and frons (Figs 10C, F) distinctly punctate; frontoclypeal suture very weakly marked, by lack of punctures; clypeus not excised above antennal insertions, anterior margin concave, marginal bead absent, surface with only few isolated trichobothria. Frons with trichobothria next to inner margin of each eye. Eyes (Figs 10B–C, E–F) moderately large, slightly protruding from head outline; facets ca. 16–17 μm in diameter. Labrum (Figs 10C, F; 11C, 12D) well sclerotized, exposed in front of clypeus, visible in dorsal view, ca. 3.3× wider than long*, bisinuate anteriorly, rounded laterally; anterolateral margin with long setae, dorsal surface with transverse series of slightly stouter setae; epistome with two groups of long spine-like setae anteriorly and with two parallel series of long hair-like projections posteriorly. Mandibles* (Fig. 11C) slightly asymmetrical, without developed mandibular angle, apex bidentate; prostheca with series of long projections, slender and elongate in anterior part, stout and shorter at base; outer margin sparsely pubescent; mola large, with small cuticular projections. Maxilla (Fig. 11A) with large sub-pentagonal cardo, lacking trichobothria; basistipes widely triangular, moderately pubescent, bearing one or two trichobothria; mediostipes vaguely defined from lacinia; lacinia* membranous, with distally situated finger-like projection, pubescent, setae more thickened and rounded towards anterior part of lacinia and on the projection, galea* long, apical membranous portion blunt at apex, densely pubescent, pubescence regularly ordered in rows, setae thickened, bent and apically rounded; maxillary palpus four-segmented, palpomere 1 minute, palpomere 2 slightly swollen distally, about as long as palpomere 3 and 4 each; palpomere 4 without digitiform sensilla. Labium with submentum (Figs 12E, K) about as long as mentum, pubescent; mentum transverse, ca. 1.3–1.4× wider than long, slightly widening anteriad, anterior margin rounded mesally (Figs 12F, K), surface moderately concave, with weak transverse groove parallel to anterior margin; lateral margins with sparse series of setae; prementum (Fig. 11E–F) subdivided into two large lateral lobes bearing long, apically acute and slender setae, as well as short, apically rounded and thickend setae; palpifer weakly sclerotized; labial palpus with 3 palpomeres (Fig. 11F), basal palpomere minute, second palpomere widened, bearing numerous setae, palpomere 3 thin, only with few setae. Antenna with 9 antennomeres (Fig. 11A); scapus long and thin, widest at midlength; pedicel widest at midlength; antennomere 3 about as long as pedicel and as long as antennomeres 4–6 combined; antennomere 6 (cupule) small, slightly narrower than antennal club; antennomeres 7–9 forming a loosely segmented pubescent antennal club, antennomere 9 elongate ca. twice as long as each of antennomeres 7–8. Gula (Figs 12F, H) wide, narrowing anteriad to a fourth its length at base, with median ridge, tentorial pits reduced. Temporae (Figs 12H, F) rugose and sparsely pubescent, with weakly defined ridge arising from inner margin of each eye.

Prothorax. Pronotum (Figs 10A, D) widest at base (ca. 0.45× as long as wide, ca. 1.5–1.6× wider at base than in front angles), continuously arcuately narrowing anteriad; anterior angles acute; dorsal punctation similar to that on frons; trichobothria present in

anterolateral corner; anterior, posterior and lateral margins with narrow marginal bead. Hypomeron (Fig. 11G) with very narrow lateral glabrous part and densely pubescent mesal part divided by a very fine ridge; antennal grooves absent; hypomeral process simply pointed, not reaching prosternal process. Prosternum (Figs 11G, 12E, 12J) slightly shorter than procoxal cavity anteriorly to procoxae, flat, with or without weak transverse impression, arcuate and beaded on anterior margin, mesally with sparsely arranged moderately

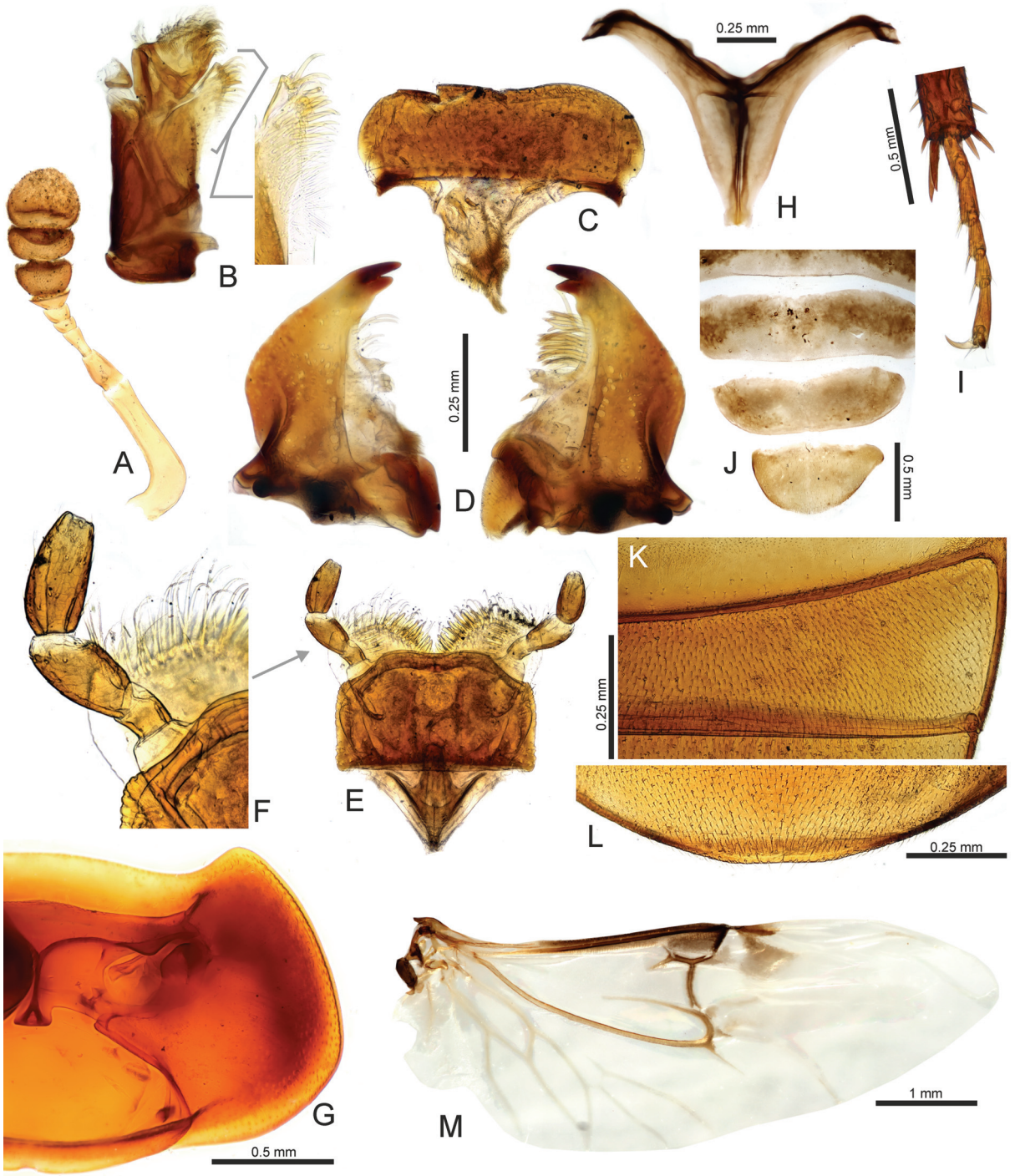

Figure 11. Detailed adult morphology of *Relictorygmus trevornoahi* sp. nov. (A) antenna (distal part of antennal club not in horizontal position); (B) maxilla (maxillary palpus missing) and detail of galea; (C) labrum; (D) mandibles; (E) mentum with prementum; (F) detail of labial palp; (G) prothorax in ventral view; (H) metafurca; (I) metatarsus; (J) abdominal tergites VI–VIII; (K) detail of abdominal ventrite I without setae; (L) apex of abdominal ventrite V without stout setae; (M) hindwing.

long setae; exposed part of prosternal process pointing between procoxae, posterior part concealed by procoxae slightly widened posteriorly, truncate at apex*. Coxal cavities* (Fig. 11G) closed internally, open posteriorly, coxal fissure long, widely open. Profurca* short and weakly sclerotized, profurcal arms widely separated basally, in form of asymmetrical apically slightly widened stalks.

Mesothorax. Scutum* with finely microsculptured median portion, bearing sparsely arranged setae laterally; scutellar shield (Figs 10A, D) exposed, triangular, pointed posteriorly, as long as wide, bearing punctation similar to frons and a series of stout setae below the anterior margin. Elytron elongate (Figs 10A–B, D–E), 2.3–2.4× as long as wide, evenly convex; with 10 series of punctures, serial punctures distinctly larger than punctures in intervals; trichobothria absent in all intervals; sutural stria present, adjacent to punctural series 1; scutellar stria absent; lateral margin of elytra beaded, very narrowly explanate, lateral margin bare, without stout setae; epipleuron wide at base, gradually narrowing towards level of metacoxae, then narrow but distinct, reaching elytral apex; lateral narrow bare part not delimited from mesal pubescent one by a ridge; ventral face without elevated ridges. Mesoventrite (Figs 12G–H, L–M) divided from mesanepisterna by anapleural sutures, slowly narrowing anteriorly (suture well defined), subtriangular in shape in anterior two thirds, widely extending in posterior third, lateral extensions with distinct coxal lobes; anapleural sutures arcuate, converging but not meeting anteriad; median part of mesoventrite flat, without projection, with moderately developed transverse groove posteromesally; anterior portion without anteromedian pit-like groove; mesoventral process narrow, abutting to metaventral process, not elevated above it. Mesanepisterna (Figs 12G–H, L–M) not meeting mesally, very narrowly divided by anterior portion of mesoventrite; anterior collar well-defined, rather wide, sparsely pubescent along anterior bead. Mesepimeron with large ventral portion, not reaching anterior collar of mesanepisternum; forming lateral margin of mesocoxal cavity; whole surface with densely arranged setae. Mesocoxal cavities obliquely transverse, very narrowly separated from each other by meso- and metaventral processes; internal postcoxal wall developed mesally and posteriorly, narrow. Mesofurca* well developed, rather short, furcal arm not developed; basal portion fused and rather wide, bifurcating only very dorsally into two arms, each with narrow asymmetrical plate-like apical extension.

Metathorax. Metanotum* weakly sclerotized, ca. 2× wider than long, alacristae slightly diverging posteriad. Metaventrite (Figs 12G, L) ca. 2.9× wider than long, slightly longer than mesoventrite, evenly convex, with raised median area, median area more distinct posteriorly, margin of elevated area bearing same setae as metaventral surface, discrimen reaching mid of metaventrite, surrounded by sparsely pubescent area, lateral part of metaventrite with dense short pubescence, without interspersed thick setae; anteromesal area with small to wider shallow impression; katepisternal suture weakly developed, vanishing towards lateral margin of mesoventrite, katepisternum narrow and asetose; posterior metaventral process bifid. Metanepisternum ca. 3.7× longer than wide, with oblique ridge subanteriorly, anterior margin straight; surface pubescent. Metafurca* (Fig. 11H) Y-shaped; stalk long, grooved, without basal extensions; arms long and wide, with apical plate-like extensions. Hind wing (Fig. 11M) well developed, widest sub-basally, ca. 1.6× longer than elytron*, venation well-developed in basal portion, absent in distal part; anal lobe large, defined by well-developed anal notch; RA tightly attached to ScA except subbasally, both reaching triangular radial cell, RA_{3+4} as long as radial cell, r4 arising from its midlength; distal portion of RP and MP_{1+2} forming a strong loop, distally with long median spur; vein complex of MP_3+MP_4+Cu+AA well developed, not connected to MP_{1+2} by cross-veins, with well-developed and completely closed basal and wedge cells; distal portion of MP_4+CuA complex H-shaped, arising from anterior portion of wedge cell; AA_4 long, reaching posterior margin; AP_{3+4} long, reaching over the midlength of anal lobe.

Legs. Coxal surface without interspersed thick setae; femora (Figs 12A–C, I) ventrally with sparse to dense pubescence lacking intermixed stout setae. In other characters corresponding to those of *Cylorygmus*.

Abdomen with five exposed ventrites; ventrites evenly convex, without median carina, densely pubescent; ventrite I (Fig. 11K) without intermixed stout setae; posterior margin of ventrite V (Fig. 11L) entirely without stout setae; laterotergite III without stridulatory file; tergites VI–VII (Fig. 11J) not subdivided mesally.

Genitalia. Aedeagus (Figs 9C, E) of simple trilobed type; phallobase subequal in length to parameres, with wide, weakly to distinctly defined posteriorly rounded manubrium; parameres slightly longer than median lobe; median lobe narrower than parameres, gonopore distinct, subapical. Male sternite 9 (Figs 7D, F) and female genitalia as in *Cylorygmus*.

Relictorygmus repentinus (Hebauer, 2002) comb. nov.

Cylorygmus repentinus Hebauer, 2002: 11.

Type material examined. **Holotype:** male (ZMHB): "R. S. Africa 17.xi.1993 / 34°27'S/20°24'E, leg. Uhlig / Cape Province: / De Hoop Nat. Res. / lake shore, reed sievings // ♂// *Cylorygmus* sp. / M. Hansen det. // HOLOTYPUS / *Cylorygmus* / *repentinus* sp.n. / des.

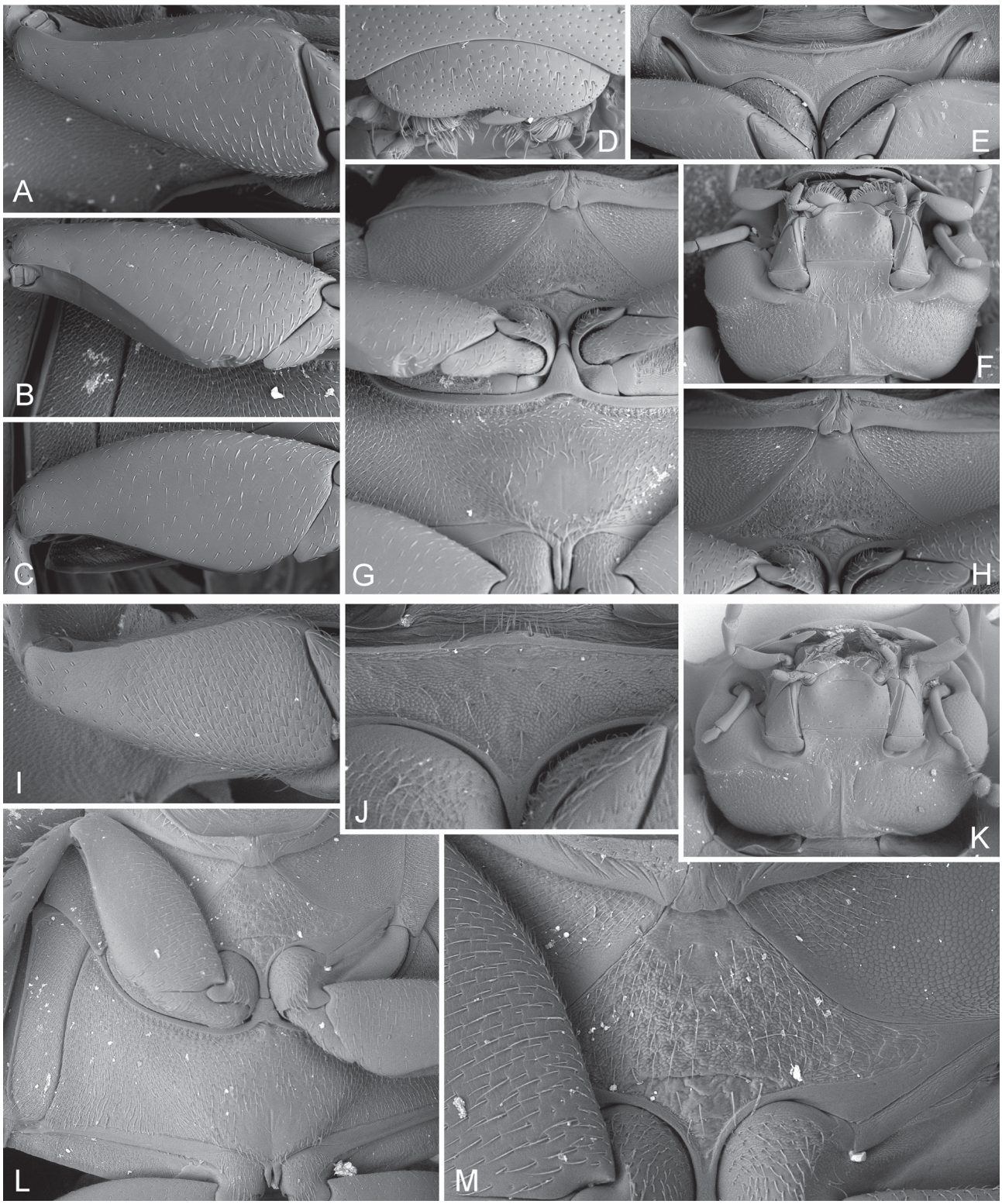

Figure 12. Details of adult morphology of *Relictorygmus* gen. nov., SEM micrographs. (A–H) *Relictorygmus trevornoahi* sp. nov., paratype: (A–C) femora in ventral view: (A) profemur; (B) mesofemur; (C) metafemur. (D) labrum in dorsal view; (E) prosternum; (F) head in ventral view; (G) meso- and metathorax in ventral view; (H) detail of mesoventrite. (I–M) *R. repentinus* (Hebauer, 2002), holotype: (I) profemur in ventral view; (J) median portion of prosternum; (K) head in ventral view; (L) meso- and metathorax in ventral view; (M) detail of mesoventrite.

F.Hebauer // *Relictorygmus repentinus* / (Hebauer, 2002) / det. M. Seidel 2017". **Paratype:** female (SEMC): "R. S. Africa 17.xi.1993 / 34°27'S/20°24'E, leg. Uhlig / Cape Province: / De Hoop Nat. Res. / lake shore, reed sievings // ♀// HOLOTYPUS / *Cylorygmus* / *repentinus* sp.n. / des. F.Hebauer // ex. F. Hebauer / Exchange 2008 // *Relictorygmus repentinus* / (Hebauer, 2002) / det. M. Seidel 2017".

Additional material examined. 1♀ (NMPC): South Africa, Western Cape, Bot River near R43 bridge, 34°18.7'S 19°8.8'E, 17.-18.x.2013 (P. Bulirsch leg.).

Redescription of adult. 5.0–5.1 mm long, 2.8–2.9 mm wide (ca. 1.8× as long as wide), elongate oval, moderately convex (Figs 10A–B). **Coloration.** Dorsal coloration dark brown; margins of pronotum yellowish to light brown; ventral coloration dark brown, only hypomeron, epipleuron and legs light brown. **Head.** Eyes (Figs 10B–C) moderately large, interocular distance ca. 3.1× transverse diameter of eye. Mentum (Fig. 12K) with anterior margin arcuate mesally, moderately concave laterally, surface smooth and becoming sparsely setose towards lateral margins; gula (Fig. 12K) with median ridge strongly developed; gular sutures strongly concave. **Prothorax.** Prosternum (Fig. 12J) mesally with long setae, sparsely setose, surface of anterior marginal bead rather smooth; transverse ridge absent. **Mesothorax.** Mesoventrite (Figs 12L–M) with well-developed transverse groove posteromesally, reaching coxal cavities laterally, straight, surface posterior to the groove sparsely setose; elevated anterior part of mesoventrite subtriangular with weakly sinuate posterior margin. **Metathorax** (Fig. 12L). Raised median area of metaventrite with asetose anteriomedial area; anterior metaventral process wide, triangular, ca. 1.2× as long as maximum width. **Legs.** Ventral surface of profemora (Fig. 12I) densely pubescent at base, sparsely pubescent at apex; mesofemora with moderately dense pubescence anterobasally, becoming sparser towards posterior margin and apex; metafemora sparsely pubescent. **Male genitalia.** Parameres (Fig. 9C) curved inwards, rounded at apices; median lobe ca. 0.5× as wide as parameres, rounded at apex, gonopore subapical.

Distribution. Only known from two localities in the southern extremes of Western Cape Province, South Africa (Fig. 12B).

Natural history. Specimens were collected in the middle of October and November, which correspond to the spring season in South Africa. The type specimens were obtained by sifting litter in reed stands at the shore of a nearly dried-up freshwater lake (Figs 13H–I). The additional specimen from the Bot River was collected by stepping its reed-covered muddy banks. Immature stages unknown.

Relictorygmus trevornoahi sp. nov.

Type material. **Holotype**: male (SAIM): "R. SOUTH AFRICA: W. Cape / 13.3 km SEE Stanford (wetland) / 34°27.85'S 19°35.75'E; 100 m / 4-5.xii.2015; Arriaga, Fikáček, Seidel & Vondráček lgt. RSA50 // isolated shallow/partly dried-up / pools in a small grassy wetland with / patches of *Juncus* and *Phragmites*: / in water and stepping/flooding the / mud/dried pools at sides". **Paratypes**: 8 spec. (NMPC, BMNH, CDTB, ISAM, SEMC), 1 spec. (BMNH): same data as the holotype.

Description. 4.7–4.9 mm long, 2.7–2.9 mm wide (ca. 1.7× as long as wide), elongate oval, (holotype measurements: length = 4.8 mm, width = 2.9 mm, height = 1.8 mm); moderately convex (Figs 10D–E). **Coloration.** Dorsal coloration dark brown to black; margins of pronotum only slightly paler; ventral coloration including hypomeron, epipleuron and legs dark brown to black. **Head.** Eyes (Figs 10E–F) moderately large, interocular distance ca. 3.3× transverse diameter of eye. Mentum (Fig. 12F) with anterior margin blunt mesally, moderately concave laterally, surface becoming rugose and sparsely setose towards lateral margins; gula (Fig. 12F) with strongly developed median ridge; gular sutures strongly concave. **Prothorax.** Prosternum (Figs 11G, 12E) mesally with sparse moderately long setae on anterior half, posterior part bare; surface of anterior marginal bead rather smooth; anterior portion with weakly developed transverse ridge. **Mesothorax.** Mesoventrite (Figs 12G–H) with strongly developed transverse groove posteromesally, reaching coxal cavities laterally, angulate in shape, surface posterior to the groove bare; elevated anterior part of mesoventrite heart-shaped with deeply sinuate posterior margin. **Metathorax.** Raised median area of metaventrite with a setose anteriomedial area; anterior metaventral process wide, triangular, ca. 1.2× as long as maximum width. **Legs.** Ventral surface of profemora (Fig. 12A) sparsely pubescent at base and apex; with moderately dense pubescence anterobasally, becoming sparser towards posterior margin and apex; meso- and metafemora (Figs 12B–C) sparsely pubescent. **Male genitalia.** Parameres (Fig. 9E) with outer faces subparallel at basal half, then slightly converging apicad; inner face very weakly arcuate in apical third; apices widely rounded. Median lobe narrow, width at base ca. 2.0× the width at apical half, apex rounded, gonopore subapical.

Etymology. The species is dedicated to the South African comedian Trevor Noah whose performances were a welcomed entertainment to the first author.

Distribution. Only known from the type locality close to Stanford, Western Cape Province, South Africa (Fig. 13B).

Natural history. Specimens were collected at the beginning of December which corresponds to the end of

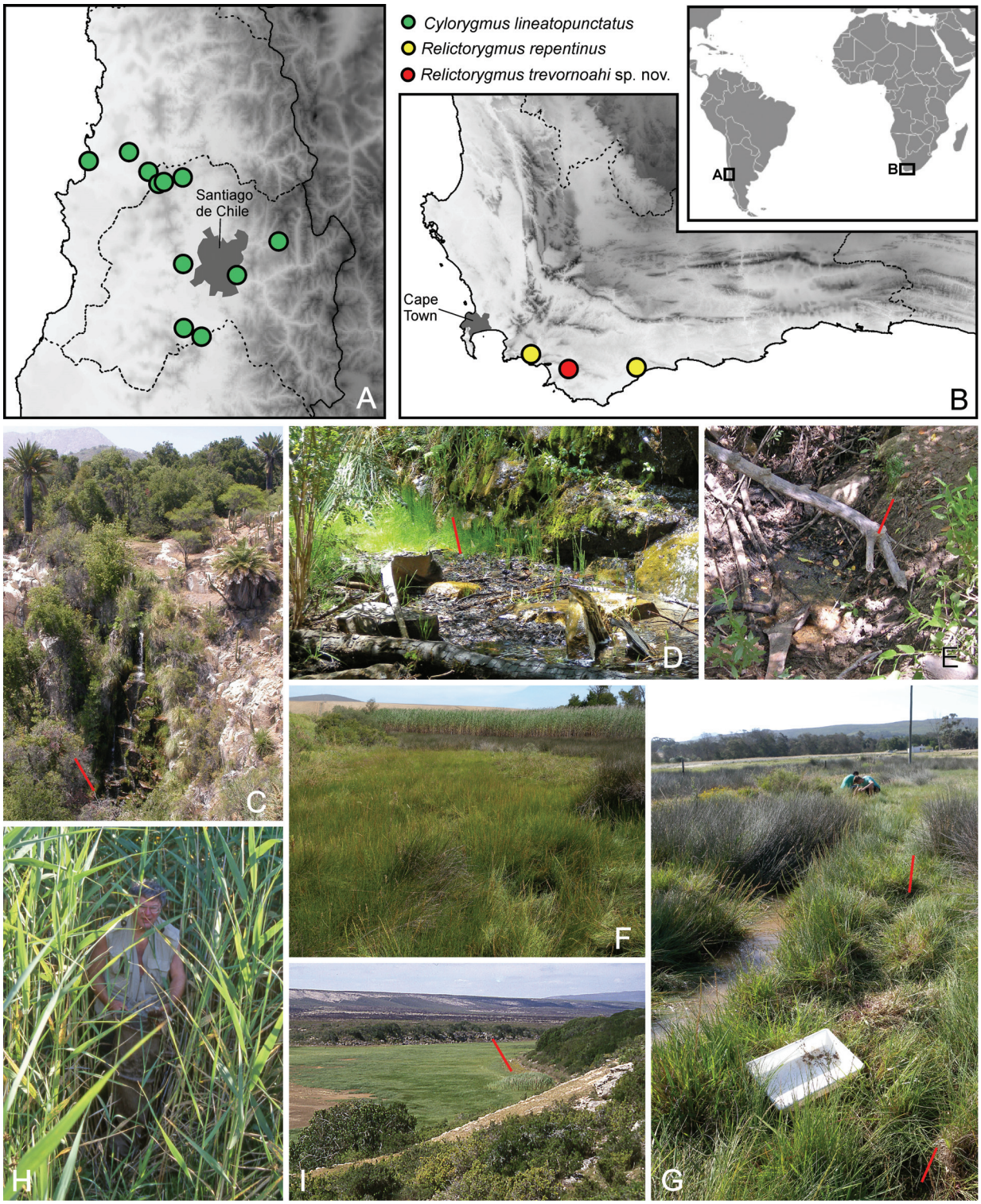

Figure 13. Distribution and habitats of *Cylorygmus* and *Relictorygmus* species. (A) known distribution in Chile; (B) known distribution in Western Cape, RSA (inset map shows position of maps A and B). (C–E) habitats of *Cylorygmus lineatopunctatus* Orchymont, 1933 in Sector Ocoa, PN La Campana, Chile: (C) small waterfall "La Cascada"; (D) water-soaked plant debris at base of the waterfall from which specimens were collected in 2013; (E) small pools in dried-up streambed in Quebrada Buitrera with debris from which specimens were collected in 2003. (F–G) type locality of *Relictorygmus trevornoahi* sp. nov.: (F) general view of the marshy meadow; (G) detail of dried-up pools with exposed bottom at side of main pools from which specimens were flooded. (H–I) type locality of *Relictorygmus repentinus* (Hebauer, 2002) at De Hoop village in De Hoop NR, Western Cape, RSA: (H) – M. Uhlig sifting litter in reed stands at the type locality; (I) general view of dried-up De Hoop vlei [= lake] north of De Hoop village, with the sampled reed stand). Photo credits: (C) – P. Kment; (D, F, G) – M. Fikáček; (E) – M. Thayer; (H, I) – M. Uhlig.

the spring season in South Africa. The habitat (Figs 13F–G) was a marshy meadow with few small shallow water pools that were drying out. The nearly dried-up pools (without free water, but with the muddy bottom still wet) were flooded which resulted in specimens floating on the water surface. The following hydrophilid species were collected at the same locality as *R. trevornoahi* (but mostly in the pools still having some water): *Allocotocerus simplex* (Régimbart, 1906), *Laccobius praecipuus* Kuwert, 1890, *Paracymus amplus* Wooldridge, 1977, *Limnoxenus sjostedti* Knisch, 1924, *Anacaena capensis* Hebauer, 1999, *Enochrus hartmanni* Hebauer, 1998, *Enochrus* cf. *circumductus* (Régimbart, 1905), *Helochares dilutus* (Erichson, 1843), *Coelostoma austrine* Mouchamps, 1958, *Cercyon dieganus* Régimbart, 1903 and *Cercyon martialis* Hebauer, 1997. An unidentified species of tiny *Aulacochthebius* Kuwert, 1887 (Coleoptera: Hydraenidae) was collected in the same microhabitat with the same method as *R. trevornoahi*, i.e. by floating the nearly dried-up pools.

Discussion

Both genera treated in this paper, *Cylorygmus* and *Relictorygmus* gen. nov., are very similar to each other, and as such it is not surprising that they were not distinguished from each other until now. When examining their adult morphology, we discovered a number of differences (e.g. width of gula, presence/absence of the stout setae on metafemora and abdominal ventrite I, presence/absence of stout setae on abdominal apex, sclerotization of abdominal tergites, general morphology of male genitalia, and different body shape) which indicated that the Chilean and South African species might not be closely related. On the other hand, characters so far considered as genus-specific in the Cylominae (morphology of mouthparts, the form of the mesoventrite) are very similar in both genera. A preliminary analysis of molecular data (Fikáček *et al*. in prep.) suggest that *Cylorygmus* and *Relictorygmus* are not closely related. This indicates that *Cylorygmus* and *Relictorygmus* may possess shared similarities that are plesiomorphies (characters inherited from ancestors) rather than apomorphies which would indicate their close relationships. The adult and larval synapomorphies of Cylominae are still unknown, but the assignment of both genera to the Cylominae was confirmed by our preliminary analysis, and that of *Cylorygmus* also by the analysis by McKenna *et al*. (2015).

The morphology of both adults and larvae seems to be congruent with the suggested plesiomorphic status of both genera, as both adults and larvae lack apparent derived structures and in most characters are in fact similar to genera of the subfamilies Hydrophilinae, Chaetarthriinae, Enochrinae and Acidocerinae. For example, larval nasale with five teeth and symmetrical mandibles with two large retinacular teeth as in *Cylorygmus* can be found in many genera of Hydrobiusini, in *Sternolophus* Solier, 1834 (Hydrophilini) and many Anacaenini (Archangelsky 1997, Archangelsky and Fikáček 2004, Minoshima and Hayashi 2011a,b). In many of those (Hydrobiusini, *Sternolophus*, but also the laccobiine genus *Tritonus* Mulsant, 1844: Fikáček *et al*. 2017), the left lateralmost tooth of nasale is more distant from the other teeth, and the dorsal structure of mentum has a specific structure (i.e. it is covered by spinose cuticular projections except for two submedian bare areas: present in Hydrobiusini, *Tritonus* and *Cylorygmus*). All these characters shared with early branching representatives of different subfamilies indicate that the larval and adult morphology of *Cylorygmus* and *Relictorygmus* is plesiomorphic, and may stand close to the morphology of the supposed most recent common ancestor of the Hydrophilidae. Also, the habitat preferences of both genera (i.e. very humid but not submerged places at sides of water bodies) are shared with many groups of aquatic hydrophilids and may represent the ancestral state for the Hydrophilidae.

The separate generic status of *Cylorygmus* and *Relictorygmus* is more congruent with the distribution of both taxa. Besides South Africa and austral South America, Cylominae are only known from Australia, New Zealand, i.e. only from continents forming Gondwana during the Mesozoic. The break-up of Gondwana is hence supposed to play an important role in their current distribution. In contrast to Australia, New Zealand and South America, which kept some interconnections (or at least close proximity) until rather recently (ca. 50–30 millions of years ago (mya)), the African continent split from the others very early: it started to rift apart from southern South America ca. 135 mya and only northern South America stayed connected to Africa until ca. 110–95 mya (Sanmartín and Ronquist 2004). Bloom *et al*. (2014) estimated that the most recent common ancestor of Cylominae to have slived ca. 121.6 mya (HDP: 145–95 mya), i.e. at the time when Africa was already largely separated from South America, except in its northern part. If both *Cylorygmus* and *Relictorygmus* really represent ancient early branching clades of Cylominae as the preliminary molecular analyses suggest, available data would not allow to reject the hypothesis that ancestors of *Cylorygmus* and *Relictorygmus* originated by vicariant events corresponding to the break-up of Gondwana. On the other hand, the fact that the African *Relictorygmus* seems to stand closer to Australian and New Zealand genera, and Chilean *Cylorygmus* seems to form a lineage separated from all other cylomines does

not fully correspond to the sequence of Gondwana break-up (this would predict South African clades as the most isolated ones). Further studies are necessary to understand this incongruence.

Conclusions

The limited set of characters applied by Hebauer (2002) in his description of the first African member of Cylominae resulted in the assumption of the trans-Atlantic disjunct distribution of the genus *Cylorygmus*. A detailed examination of the morphology of the Chilean and African species and the discovery of the third new species revealed that the Chilean and South African species are not closely related. This justifies the placement of the African species into a new genus, *Relictorygmus* gen. nov., breaking up an incorrectly assumed disjunct distribution of *Cylorygmus*. Understanding the presence of cylomine beetles in Africa will be crucial to understand the evolutionary and biogeographical history of these Gondwanan relicts. Molecular phylogenetics is necessary to be applied in future studies.

Author contribution

MS, EAV and MF performed the field work and accumulated additional museum material; MS performed the majority of morphological studies on adult beetles; YNM performed the morphological studies on larvae; MS prepared the first draft and photo documentation; all authors commented drafts of the paper at different stages and helped with completing the manuscript for submission.

Acknowledgements

We are grateful to Dominik Vondráček and Jiří Šmíd (National Museum, Prague) for their collaboration during the expedition to Western Cape province in 2015, to Manfred Uhlig (Museum für Naturkunde, Berlin) for sharing pictures of the type locality of *R. repentinus* with us, to Petr Bulirsch (Prague) for the donation of the only *R. repentinus* specimen known besides the type series, to Renzo Perissinotto (Nelson Mandela Metropolitan University) for his help with the logistics of our field trip and to the authorities of CapeNature for providing access to protected areas under their control. We are grateful to Vít Sýkora (Charles University, Prague) for providing his preliminary results on the Cylominae phylogeny. Alberto Ballerio (Brescia) is thanked for the discussion of the neotype issues. Furthermore, we thank all the curators listed in material and methods for loaning specimens to us. This work was supported by the European Union's Horizon 2020 research and innovation program under the Marie Skłodowska-Curie grant agreement No. 642241 to M. Seidel and E. Arriaga-Varela, by JSPS KAKENHI Grant Number JP17K15187 to Y. Minoshima, and by the Ministry of Culture of the Czech Republic (DKRVO 2018/13, National Museum, 00023272) to Martin Fikáček. The work of M. Seidel and E. Arriaga-Varela at the Department of Zoology, Charles University, Prague was partly supported by grant SVV 260 434 /2018. The Synthesys project. http://www.synthesys.info/ funded the stay of EA-V at the HNHM under the grant No. HU-TAF-6176.

References

Andrássy, I., Balogh, J., Loksa, I., Mahunka, S. and A. Zicsi. 1965. The scientific results of the Hungarian Soil Zoological Expedition to Chile, Argentina and Brasil 1. Report on the collectings. Folia Entomologica Hungarica, 20: 247–296.

Archangelsky, M. 1997. Studies on the biology, ecology, and systematics of the immature stages of New World Hydrophiloidea (Coleoptera: Staphyliniformia). Bulletin of the Ohio Biological Survey, New Series, 12: 1–207.

Archangelsky, M. 2002. Immature stages of Neotropical *Enochrus* (Coleoptera: Hydrophilidae): *E.* (*Methydrus*) *lampros* Knisch, 1924 and *E.* (*Hugoscottia*) *tremolerasi* Knisch, 1922. Aquatic Insects, 24(1): 41–52.

Archangelsky, M. and M. Fikáček. 2004. Descriptions of the egg case and larva of *Anacaena* and a review of the knowledge and relationships between larvae of Anacaenini (Coleoptera: Hydrophilidae: Hydrophilinae). European Journal of Entomology, 101: 629–636.

Bameul, F. 1992. Première découverte d'un *Omicrus* Sharp dans la région éthiopienne: *O. hebaueri* n. sp. (Coleoptera, Hydrophilidae). Bulletin de la Société entomologique de France, 97(4): 373–379.

Beutel, R. G. 1999. Morphology and evolution of the larval head of Hydrophiloidea and Histeroidea (Coleoptera: Staphyliniformia). Tijdschrift voor Entomologie, 142: 9–30.

Bloom, D. D., Fikáček, M. and A. E. Z. Short. 2014. Clade age and diversification rate variation expain disparity in species richness among water scavenger beetle (Hydrophilidae) lineages. PLoS One, 9(6): e98430.

Brundin, L. 1966. Transantarctic relationships and their significance, as evidenced by chironomid midges, with a monograph of the subfamilies Podonominae and Aphroteniinae and the Austral Heptagyiae. Kungliga Svenska Vetenskapsakademiens Handlingar, 11: 1–472.

Byttebier, B. and P. L. M. Torres. 2009. Description of the preimaginal stages of *Enochrus* (*Hugoscottia*) *variegatus* (Steinheil, 1869) and *E.* (*Methydrus*) *vulgaris* (Steinheil, 1869) (Coleoptera: Hydrophilidae), with emphasis on larval morphometry and chaetotaxy. Zootaxa, 2139: 1–22.

De Queiroz, A. 2014. The monkey's voyage: how improbable journeys shaped the history of life. Basic Books, New York, 360 pp.

Fikáček, M., Archangelsky, M. and P. L. M. Torres. 2008. Primary chaetotaxy of the larval head capsule and head appendages of the Hydrophilidae (Coleoptera) based on larva of *Hydrobius fuscipes* (Linnaeus, 1758). Zootaxa, 1874: 16–34.

Fikáček, M., Minoshima, Y. N. and A. F. Newton. 2014. A review of *Andotypus* and *Austrotypus* gen. nov., rygmodine genera with Austral disjuction (Hydrophilidae: Rygmodinae). Annales Zoologici (Warszawa), 64(4): 557–596.

Fikáček, M. and D. Vondráček. 2014. A review of *Pseudorygmodus* (Coleoptera: Hydrophilidae), with notes on the classification of the Anacaenini and on distribution of genera endemic to southern South America. Acta Entomologica Musei Nationalis Pragae, 54(2): 479–514.

Fikáček, M. and C. H. S. Watts. 2015. Notes on the Australian Anacaenini (Coleoptera: Hydrophilidae): description of male of *Phelea breviceps* Hansen and unravelling the indentity of *Crenitis neogallica* Gentili. Zootaxa, 3980(3): 427–434.

Fikáček, M. and A. E. Z. Short. 2010. Taxonomic revision and phylogeny of the genus *Cetiocyon* and its discovery in the Neotropical Region (Insecta: Coleoptera: Hydrophilidae). Arthropod Systematics & Phylogeny, 68(3): 309–329.

Fikáček, M., Gustafson, G. T. and A. E. Z. Short. 2017. On wet rocks with snorkels: immature stages of *Tritonus* cascade beetles with unusual modification of spiracles (Coleoptera: Hydrophilidae: Laccobiini). Annales Zoologici (Warszawa), 67(1): 97–107.

Germain, P. 1911. Catálogo de los coleopteros chilenos del Museo Nacional. Boletín del Museo nacional de Chile 3: 47–73.

Hansen, M. 1999. Fifteen new genera of Hydrophilidae (Coleoptera), with remarks on the generic classification of the family. Insect Systematics & Evolution, 30(2): 121–172.

Hebauer, F. 2002. New Hydrophilidae of the Old World (Coleoptera, Hydrophilidae). Acta Coleopterologica, 18(3): 3–24.

Jerez, V. and J. Moroni. 2006. Diversidad de coleópteros acuáticos en Chile. Gayana, 70(1): 72–81.

Jia, F.-L., Tang, Y. and Y. N. Minoshima. 2016. Description of three new species of *Crenitis* Bedel from China, with additional faunistic records for the genus (Coleoptera: Hydrophilidae: Chaetarthriinae). Zootaxa, 4208(6): 561–576.

McKenna, D. D., Farrell, B. D., Caterino, M. S., Farnum, C. W., Hawks, D. C., Maddison, D. R., Seago, A. E., Short, A. E. Z., Newton, A. F. and M. K. Thayer. 2015. Phylogeny and evolution of Staphyliniformia and Scarabaeiformia: forest litter as a stepping stone for diversification of nonphytophagous beetles. Systematic Entomology, 40(1): 35–60.

Minoshima, Y. and M. Hayashi. 2011a. Larval morphology of the Japanese species of the tribes Acidocerini, Hydrobiusini and Hydrophilini (Coleoptera: Hydrophilidae). Acta Entomologica Musei Nationalis Pragae, 51 (supplementum): 1–118.

Minoshima, Y. and M. Hayashi. 2011b. Larval morphology of the genus *Hydrocassis* Fairmaire (Coleoptera: Hydrophilidae). Journal of Natural History, 45(45–46): 2757–2784.

Minoshima, Y. N., Fikáček, M., Gunter, N. and R. A. B. Leschen. 2015a. Larval morphology and biology of the New Zealand-Chilean genera *Cylomissus* Broun and *Anticura* Spangler (Coleoptera: Hydrophilidae: Rygmodinae). Coleopterists Bulletin, 69(4): 687–712.

Minoshima, Y. N., Komarek, A. and M. Ôhara. 2015b. A revision of *Megagraphydrus* Hansen (Coleoptera: Hydrophilidae): synonymization with *Agraphydrus* Régimbart and description of seven new species. Zootaxa, 3930(1): 1–63.

Moroni, B. J. C. 1985. Redescripcion de *Cylorygmus lineatopunctatus* d'Orchymont, 1933 (Coleoptera: Hydrophilidae: Sphaeridiinae: Rygmodini). Revista Chilena de Entomología, 12: 145–151.

d'Orchymont, A. 1933. Contribution a l'etude des Palpicomia VIII. Bulletin et Annales de la Société Entomologique de Beige, 73: 271–313.

Régimbart, M. 1907. Hydrophilides provenant du Voyage de ML Fea dans l'Afrique Occidentale. Ann. Mus. Civ. Stor. Nat. Genova (3. Sér.), 3: 46–62.

Sanmartín, I. and F. Ronquist. 2004. Southern hemisphere biogeography inferred by event-based models: plant versus animal patterns. Systematic Biology, 53(2): 216–243.

Seidel, M., Arriaga-Varela, E. and M. Fikáček. 2016. Establishment of Cylominae Zaitzev, 1908 as a valid name for the subfamily Rygmodinae Orchymont, 1916 with an updated list of genera (Coleoptera: Hydrophilidae). Acta Entomologica Musei Nationalis Pragae, 56(1): 159–165.

Short A. E. Z. and M. M. García. 2007. *Tobochares sulcatus*, a new genus and species of water scavenger beetle from Amazonas State, Venezuela (Coleoptera: Hydrophilidae: Hydrophilini). Aquatic Insects, 29(1): 1–7.

Smetana, A. 1978. Revision of the subfamily Sphaeridiinae of America north of Mexico (Coleoptera: Hydrophilidae). Memoirs of the Entomological Society of Canada, 105: 1–292.

Smetana, A. 1984. Revision of the subfamily Sphaeridiinae of America north of Mexico (Coleoptera: Hydrophilidae). Supplementum 2. Canadian Entomologist, 116: 555–566.

Spangler, P. J. 1974. The rediscovery of *Cylorygmus lineatopunctatus* (Coleoptera: Hydrophilidae: Sphaeridiinae: Rygmodini). Journal of the Kansas Entomological Society, pp. 244–248.

Spangler, P. J. 1979. Description of the larva and pupa of *Cylorygmus lineatopunctatus* (Coleoptera: Hydrophilidae: Rygmodini) [in Chile]. Proceedings of the Biological Society of Washington.

Shirayama, Y., Kaku, T. and R. P. Higgins. 1993. Double-sided microscopic observation of meiofauna using an HS-slide. Benthos Research, 44: 41–44. [In Japanese with English title and abstract].

Short, A. E. Z. and M. Fikáček. 2013. Molecular phylogeny, evolution and classification of the Hydrophilidae (Coleoptera). Systematic Entomology, 38: 723–752.

Received: August 23, 2017
Accepted: December 12, 2017

CHAPTER 5

Seidel, M., Minoshima, Y. N., Leschen, R. A. B., & Fikáček, M. Phylogeny, systematics and rarity assessment of New Zealand endemic *Saphydrus* beetles and related enigmatic larvae (Coleoptera: Hydrophilidae: Cylominae) (manuscript draft).

Author contributions: MS, MF and RL performed the field work; MS run the molecular and phylogenetic analyses; MF prepared the rarity and conservation status assessment; MS and MF studied the adult morphology and taxonomy; YM and MF studied the studies of immature stages; MF, MS and YM drafted the manuscript, all authors contributed to the writing.

Phylogeny, systematics and rarity assessment of New Zealand endemic *Saphydrus* beetles and related enigmatic larvae (Coleoptera: Hydrophilidae: Cylominae)

Matthias SEIDEL[1,2)], Yûsuke N. MINOSHIMA[3)], Richard A. B. LESCHEN[4)] & Martin FIKÁČEK[1,2*)],

[1)] Department of Zoology, Faculty of Science, Charles University, Viničná 7, CZ-12843 Praha 2, Czech Republic; e-mails: matth.seidel@gmail.com, mfikacek@gmail.com

[2)] Department of Entomology, National Museum in Prague, Cirkusová 1740, CZ-19300 Praha 9 – Horní Počernice, Czech Republic

[3)] Natural History Division, Kitakyushu Museum of Natural History and Human History, 2-4-1 Higashida, Yahatahigashi-ku, Kitakyushu-shi, Fukuoka, 805-0071 Japan; e-mail: minoshima@kmnh.jp

[4)] Manaaki Whenua – Landcare Research, New Zealand Arthropod Collection, Auckland, New Zealand; e-mail: leschenr@landcareresearch.co.nz

*corresponding author

Abstract. The New Zealand endemic beetle genus *Saphydrus* Sharp, 1884 (Coleoptera: Hydrophilidae. Cylominae) is studied in order to understand its phylogenetic position, species-level systematics, biology and distribution, and to reveal reasons for its rarity. The first complete genus-level phylogeny of Cylominae based on two mitochondrial (*cox1*, 16S) and two nuclear genes (18S, 28S) covering 18 of 19 genera of the subfamily reveals *Saphydrus* as an isolated lineage situated in a clade with *Cylorygmus* (South America), *Relictorygmus* (South Africa) and *Eurygmus* (Australia). We use DNA to associate two larval morphotypes with *Saphydrus*: one of them represents the larvae of *S. suffusus* Sharp, 1884; the other, characterized by unique characters of the head and prothorax morphology, is revealed as sister but not closely related to *Saphydrus*. It is described here as *Enigmahydrus* gen. nov. with a single species, *E. larvalis* sp. nov., whose adult stage remains unknown. *Saphydrus* includes five species, two of which (*S. moeldnerae* sp. nov. and *S. tanemahuta* sp. nov.) are described as new. Larvae of *Enigmahydrus larvalis* and *Saphydrus suffusus* are described and illustrated in detail based on DNA-identified specimens, candidate larvae for *Saphydrus obesus* Sharp, 1884

and *S. tanemahuta* are illustrated and diagnosed. Specimen data are used to evaluate the range, altitudinal distribution, seasonality and population dynamics over time for all species. Strongly seasonal occurrence of adults combined with other factors (winter occurrence in *S. obesus*, occurrence at high altitudes in *S. tanemahuta*) is hypothesized as the primary reason of the rarity for *Saphydrus* species. In contrast, *Enigmahydrus larvalis* underwent a massive decline in population number and size since the 1970s and is currently known from a single, locally limited population; we propose the 'nationally threatened' status for this species.

Introduction

A series of recent reports indicate a large decline of insect diversity worldwide and in all studied groups (e.g., Thomas 2005, Hallmann *et al.* 2017, Lister and García 2018). Habitat loss, the conversion of wild areas to agriculture land, climate change and the introduction of alien species are among the principal drivers of this decline in abundance and number of species (Sánchez-Bayo & Wyckhuys 2019). Consequently, local surveys around the globe report the once-common species becoming rare, hard-to-collect, vulnerable to extinction or even locally extinct (e.g., Muggleton and Benham, 1975, Thogmartin *et al.* 2017). Island taxa with relatively small populations inhabiting geographically limited areas may be most susceptible to population decline and eventual extinction (Gray *et al.* 2018, Gillespie and Will, 2018). The case of the Lord Howe Island stick insect (*Dryococelus australis*), which became extinct on the main island around 1920 after the introduction of rats and was re-discovered in 2001 as a small population counting only 24 individuals on a nearby tiny islet (Priddel *et al.* 2003), is one famous example. Yet in most, less extreme cases of rare insect species, we are lacking even the basic data to assess the reasons of rarity and to evaluate their conservation status. This lack of data may result both in an underestimation of conservation risks in threatened taxa (McKinney 1999) or in considering common species as threatened when its specialized but unknown biology makes it hard to find.

New Zealand consists of three main islands and hundreds of smaller islets situated in subtropical to subantarctic waters of the Pacific Ocean, east of Australia (Wallis and Trewick 2009). Until the Early Mesozoic, it was a part of the Gondwana, from which a small continent of Zealandia split and became sub-fragmented 85 to 65 million years ago (Goldberg *et al.* 2008, Mortimer *et al.* 2017). Being situated at the boundary of Pacific

and Australian tectonic plates, Zealandia underwent drastic geological changes including massive drowning, rifting and volcanism, which resulted in what are today New Zealand, New Caledonia, and smaller islands which make up 7% of the original landmass that remains emergent (Mortimer and Campbell 2014). The main New Zealand islands were more recently affected by the uplift of the Southern Alps (Tippett and Kamp 1995), volcanism (McGlone *et al.* 2001) and massive glaciation (Barrell 2011). All these events underlined the effect of long-term isolation from other continents, and made New Zealand's fauna almost entirely endemic (Daugherty *et al.* 1993), consisting of old relicts which survived since Gondwana times (e.g., tuatara: Herrera-Flores *et al.* 2017) or later colonizers which evolved into morphologically and ecologically unique taxa (e.g., kakapo and kea parrots: Prum *et al.* 2015). These paleo- and neo-endemic taxa of New Zealand may be threatened by habitat degradation and loss or by the introduction of invasive species acting as predators or competitors (e.g., Rawlence *et al.* 2019). However, taxonomic and distribution data are fragmentary or missing for invertebrate taxa (McKinney 1999, Fattorini *et al.* 2012), which makes the evaluation of the threat and potential decline of New Zealand endemic insects a difficult task (Leschen *et al.* 2012, Ward *et al.* 2014, Hoare *et al.* 2015, Grainger *et al.* 2018).

Water scavenger beetles (Coleoptera: Hydrophilidae) is a moderately large beetle family with ca. 3000 known species (Short and Fikáček 2013). Although known mostly for its aquatic forms, two large clades of this family colonized terrestrial habitats (Bloom *et al.* 2014). One of them, the subfamily Cylominae, is the principal component of New Zealand fauna: 61 of 85 New Zealand species belong to this group (Seidel and Fikáček, unpubl. data). All New Zealand cylomine genera are endemic ancient relicts dating back to the Late Cretaceous to Eocene (Seidel *et al*., unpubl. data) similarly as more iconic tuataras, kiwis or kakapos. Similarly as in the latter vertebrate groups, they also evolved into unusual ecological forms, such as pollen-feeding flower visitors (Minoshima et al. 2018), and some re-colonized aquatic habitats (Minoshima et al. 2015). Yet, the New Zealand fauna of Cylominae is poorly known, with all published data based on historical museum specimens (e.g., Broun 1880, 1893a,b, Sharp 1884) or their recent re-examination (Hansen 1997). To fill this gap, we performed field work in New Zealand from 2010 to 2018 and examined material collected within the last decades available in museum collections. This study is the first in the series summarizing and evaluating this data to understand the phylogenetic position, morphology, distribution and biology of the particular genera and to evaluate the conservation status of their species.

Based on museum collections and our survey work, members of *Saphydrus* Sharp constitute the rarest species among New Zealand Cylominae. The genus was described in 1884 based on few specimens collected in South Island by Richard Helms and originally included four species (Sharp 1884). Three more species were added later by Broun (1893b, 1921), but later revision by Hansen (1997) synonymized some of them, and moved another genus, at the end revealing *Saphydrus* to contain three species only. During our field work, we succeeded to collect fresh specimens of the genus including immature stages which we were able to associate with adults by means of DNA. DNA data also allowed us to assess the phylogenetic position of *Saphydrus* within Cylominae. Here we summarize field-based data as well as those of all specimens available in collections, in order to revise the systematics of the group, evaluate its distribution and biology, and to assess reasons for the rarity of *Saphydrus* species. One new genus and three new species are described.

Material and methods

DNA sequencing. Genomic DNA was extracted from whole specimens using Qiagen Blood and Tissue Kit following the manufacturer's instructions. Four gene fragments were amplified using polymerase chain reaction (PCR): 3' part of *cox1* mtDNA (796 bp),16S rDNA (573 bp), 18S rDNA (1825 bp) and 28S rDNA (1042 bp). The 18S fragment was amplified and sequenced as three separate smaller fragments. See Supplementary Table S1 for the list of primers and amplification programs. Sanger sequencing was performed by Macrogen Europe (Amsterdam, the Netherlands). Sequences of few Cylominae and all outgroup taxa were adopted from previous studies: Short & Fikáček (2013): *Borborophorus*, *Coelostomopsis*, *Cylomissus, Hydrostygnus, Rygmodus*, one specimen of *Saphydrus* and all outgroup taxa; Gunter et al. (2016): *Pseudohydrobius*, *Rygmostralia*; McKenna et al. (2015): *Andotypus* (part of sequences); Minoshima et al. (2015): *Anticura*. All sequences used for the analysis are listed in the Supplementary Table S2; locality data for the newly sequences specimens are listed in Supplementary Table S3.

Phylogenetic analysis. Sequences were edited in Geneious 9.1.3 (Kearse et al. 2012). Edited sequences were aligned using first the Muscle and subsequently the ClustalW algorithm as implemented in Geneious, using the default settings. The concatenated dataset has a length of 4226 bp with 18.1% of missing data. The dataset was divided into

partitions by genes, protein-coding genes were subdivided by codon position; in total, six partitions were defined. Substitution models were tested in PartitionFinder2 (Lanfear et al. 2017) on the CIPRES Science Gateway (Miller et al. 2010). The MrBayes block with the best-fitting models for each partition is listed in Supplementary Table S4. The phylogenetic reconstruction was conducted using MrBayes 3.2.6 (Ronquist et al. 2012) on the CIPRES Science Gateway. The analysis used two runs, each with two chains, for 25 million generations with tree sampling every 1000 generations. The convergence of both runs was checked in Tracer 1.7 (Rambaut et al. 2018). Due to the long initial phase needed to reach convergence, we used a conservative burn-in of 50%. The consensus tree was edited in FigTree v1.4.3 (Rambaut 2012).

Specimen depositories. We examined all available specimens in the institutions which hold important collections of New Zealand beetles. Both dry collections (pinned specimens) and alcohol collections (mainly larva specimens) were examined. The newly collected material accumulated during our field work in 2010–2018 was also included. Specimens are deposited in the following collections:

BMNH Natural History Museum, London, United Kingdom (Max Barclay, Michael Geiser);

KMNH Kitakyushu Museum of Natural History & Human History, Kitakyushu, Japan (Yûsuke Minoshima);

LUNZ Lincoln University, Lincoln, New Zealand (John Marris);

MONZ Museum of New Zealand Te Papa Tongarewa, Wellington, New Zealand (Julia Kasper);

NHMW Naturhistorisches Museum Wien, Vienna, Austria (Manfred A. Jäch);

NMPC Department of Entomology, National Museum, Prague, Czech Republic (Lukáš Sekerka, Jiří Hájek);

NZAC New Zealand Arthropod Collection, Landcare Research, Auckland, New Zealand (Richard Leschen).

Adult morphology. A part of the specimens was dissected, with genitalia embedded in a drop of alcohol-soluble Euparal resin. External morphology of uncoated specimens of *Saphydrus suffusus* and *S. monticola* was examined using a Hitachi S-3700N environmental electron microscope at the Department of Paleontology, National Museum in Prague. Two specimens of *S. suffusus* were treated in 10% KOH and mounted in

permanent slides with Euparal resin; morphological details of these specimens were photographed using Canon EOS1100D camera attached to an Olympus BX41 compound microscope; multilayer photographs were stacked using Helicon Focus software. Habitus photographs were taken using Canon D-550 digital camera with attached Canon MP-E65mm f/2.8 1–5× macrolens, and subsequently adapted in Adobe Photoshop CS2. Drawings were traced from photographs taken using the above equipment.

Larval morphology. Protocols of larval examination generally followed those of Minoshima & Hayashi (2011) and Minoshima (2018). Observations were carried out using a Leica MZ16 and an Olympus BX50 microscopes. Illustrations were made with the aid of a drawing tube attached to the BX50. Some larvae were cleared using 10% KOH solution (ca. 50 min at 50 °C) or Proteinase K (Qiagen DNeasy Blood & Tissue Kit; 20 µl proteinase K solution and 180 µl Buffer ATL, approximately 24 h at 55 °C, mixed several times), and were dissected when needed. The parts were examined on H-S Slide (Shirayama et al., 1993) with Euparal or lactic acid. Habitus of the larvae were photographed using the same equipment as for adults.

Morphological terminology and classification. Higher-level classification follows Short & Fikáček (2013) and Seidel et al. (2016). Adult morphological terminology follows Lawrence et al. (2011). Larval morphological terminology follows Archangelsky (1997) and Minoshima and Hayashi (2011) for general morphology, Fikáček et al. (2008) and Byttebier and Torres (2009) for chaetotaxy. The following abbreviations are used: AN: antenna; FR: frontale; gAN: group of the apical antennal sensilla; gAPP: group of sensilla on inner appendage of maxilla; gFR: group of sensilla on frontale; gLA: group of the apical sensilla on labial palpus; gMX: group of the apical sensilla on maxilla; LA: labium; MN: mandible; MX: maxilla; PA: parietale; SE: sensorium; ■ (black square): additional sensillum.

Distribution data analysis. Distribution map was prepared in QGIS software (https://www.qgis.org/en/site/) using the freely available GLOBE altitude data (https://www.ngdc.noaa.gov/mgg/topo/globe.html) and the shape file 'NZ Area Codes for recording specimen localities' available at LRIS portal (https://lris.scinfo.org.nz/layer/48165-nz-area-codes-for-recording-specimen-localities/). GPS and altitude data were either adopted from locality labels or assigned based on locality data available using the topomap webpage (https://www.topomap.co.nz/); specimens in which locality data likely cover larger area were assigned an approximate GPS but were not included in the altitude distribution

analysis. For seasonality analysis, collecting events based on traps exposed for several weeks were assigned to the month in which the majority of exposure days belongs. The conservation status criteria discussed follow Townsend et al. (2008).

Species distribution data and original photos. Complete data of all adult and larval specimens examined were databased in a DarwinCore (DwC) format; this spreadsheet was also used for the creation of the distribution maps and analyzing the seasonality, altitudinal distribution and the records through time. The DwC spreadsheet and all original unedited photographs and SEM micrographs of adults and larvae were uploaded as a .zip file to the Zenodo depository (https://zenodo.org/) under [DOI will be added once manuscript is accepted]. See Arriaga-Varela et al. (2017) for details on databasing and archiving strategy.

Results

Phylogeny of Cylominae and the position of *Saphydrus* and larval forms

The phylogenetic analysis of the genera of Cylominae resulted in nearly completely resolved tree (Fig. 1, see also Supplementary Fig. S1). Cylominae were found as a strongly supported monophylum (posterior probability, pp=1.0). Three strongly supported principal clades were revealed: (1) the clade comprising the genera *Exydrus*, *Austrotypus*, *Andotypus*, *Hydrostygnus*, *Tormissus*, *Anticura* and *Cylomissus* (pp=1.0); (2) the clade consisting of *Saphydrus* and both larval morphotypes sequenced here, *Cylorygmus*, *Relictorygmus* and *Eurygmus* (pp=0.9), and (3) the clade comprising *Rygmodus*, *Pseudohydrobius*, *Rygmostralia*, *Coelostomopsis*, *Borborophorus*, *Cyloma* and *Adolopus* (pp=1.0). *Saphydrus* and the sequenced larvae are members of the clade grouping New Zealand, South American (*Cylorygmus*), Australian (*Eurygmus*) and South African clades (*Relictorygmus*), but relationships among these genera remain unresolved. Of the sequenced larvae, the one without lateral lobes on the abdomen (MF529) is revealed as genetically almost identical with the sequenced adults of *Saphydrus suffusus* (NZ462 and SLE0099); its genetic distance from adults varies between 0.9-1.5% for *cox1*. The larva with large projection on the abdomen (MF665) is strongly supported as sister clade to *Saphydrus suffusus* (pp=1.0) but is gentically rather distant from it (genetic distance to the sequenced specimens of *S. suffusus* varies between

14.3–15.3%). Attempts to sequence species not available in fresh specimens using ancient DNA sequencing protocols failed.

Adult systematics

Saphydrus Sharp, 1884

(Figs 2–4)

Type species. *Saphydrus suffusus* Sharp, 1884 (designated by Knisch 1924: 108).

Literature. Sharp (1884): original description; Broun (1893a): diagnosis, key to species; Broun (1893b): notes in taxonomic status; Orchymont (1916): discussion on taxonomic position; Orchymont (1919): assigned to Rygmodini; Knisch (1924): catalogue; Hansen (1991): redescription; Hansen (1997): diagnosis, key to species, new synonymies; Hansen (1999): catalogue; Leschen *et al.* (2003): list of New Zealand beetle genera; Short and Fikáček (2013): transferred to Rygmodinae; Seidel *et al.* (2016): transferred to Cylominae.

Diagnosis. Body length 4.2–7.1 mm; body elongate oval, moderately convex; general body coloration brown (Figs 2A–E); labrum partly to totally exposed; eyes small to large, slightly to distinctly protruding laterally (Figs 2F, H, J, L, N); antenna with 9 antennomeres; antennal club loosely segmented (Figs 4N–R); mentum with subparallel lateral sides (Figs 3A, D); prosternum flat, without median carina (Figs 3B, E); anapleural sutures well developed (Figs 3C,E, 4D,H); mesoventrite triangular in shape, narrow anteriorly, reaching anterior margin of mesothorax, flat, without protuberances (Figs 3C, 4D, H); mesocoxal cavities narrowly separated from each other (Fig. 4H); elytra with with 10 elytral series (lateral ones frequently indistinct among interval punctation); apical half of series 1 sharply impressed (sutural stria present); scutellar stria absent; elytral interval punctures each with a decumbent seta (Fig. 3H; often abrased dorsally, see lateral parts of elytra); metaventrite flat, nearly completely pubescent except posteromesally (Fig 4H); abdomen with 5 ventrites; first abdominal ventrite not carinate mesally; fifth abdominal ventrite entire and without stout setae posteromesally (Fig 4H); legs moderately long, tips of femora not overlapping body outline; meso- and metatrochanter not continuous with femora at posterior margin; all femora with dense ventral pubescent

except on extreme apex (Fig 4H); claws simple, without basal tooth (Fig 4M); meso- and metatarsus with 5 tarsomeres, basal one short (Fig. 4M).

Differential diagnosis from New Zealand Hydrophilidae. By the combination of medium body size, brownish coloration (Figs 2A–E), striate elytra and flat mesoventrite without any median elevation (Figs 3C,F), *Saphydrus* may be only confused with some species of *Rygmodus* in New Zealand. It differs them by simple claws without basal tooth (Fig. 4M; always with a tooth in *Rygmodus*). By the general habitus and medium size, *Saphydrus* may also resemble some species of the genus *Cyloma*, *Enochrus* and the only species of *Limnoxenus*, which are all easily distinguishable by strongly elevated median portion of the mesoventrite (except of that, *Enochrus* has the second maxillary palpomere excised basally, *Enochrus* and *Limnoxenus* bear small small emargination at abdominal apex, and *Cyloma* has antennae with 8 antennomeres only).

Distribution. Endemic to North and South Islands of New Zealand.

Key to species of *Saphydrus* (adults)

All species of *Saphydrus* are similar and are best diagnosed by the morphology of the male genitalia. Proportion of antennomere 9 mentioned in the key needs to be examined from dorsal or ventral view (often antennal club is slightly rotated and antennomere 9 looks longer and narrower than it really is).

1. Small species (4.5–4.7 mm). Pronotum quadratic, with lateral sides subparallel (Figs 2L,N, 4I). Elytral series distinctly impressed (Figs 2D, E). Anterior margin of the clypeus with distinct marginal bead (Figs 2L,N). Eyes strongly protruding laterally (Figs 2L,N). Dorsal punctation coarse. … 2
– Small to large species (4.2–7.1 mm). Pronotum distinctly narrowing anteriorly, lateral sides not subparallel (Figs 2F,H,J). Elytral series not impressed. Anterior margin of clypeus without marginal bead. Eyes less protruding laterally. Dorsal punctation finer. … 3
2. Pronotum ca. 2.1× as wide as long, much wider than head (Fig. 2L). Eyes large, interocular distance ca. 4.2× the width of one eye in dorsal view. Anterior margin of the clypeus angular, weakly concave mesally. Mesal elytral intervals with ca. 3 punctures across (Fig. 2M). Elytra highly convex in lateral view (Fig. 2D). … ***Saphydrus monticola***
– Pronotum ca. 1.8× as wide as long, slightly wider than head (Fig. 2N). Eyes smaller,

interocular distance ca. 5.9× the width of one eye in dorsal view. Anterior clypeal margin rounded, straight mesally. Mesal elytral intervals with 1–2 punctures across (Fig. 2O). Elytra moderately convex in lateral view (Fig. 2E). … ***Saphydrus moeldnerae*** **sp. nov.**

3. Small species (4.2-4.8 mm). Body widest at posterior third of elytral length (Fig. 2C). Eyes small, separated by 6× of width of one eye in dorsal view (Fig. 2J). Antennomere 9 distinctly longer than wide (Fig. 4P). Elytral intervals with rather coarse punctation, mesal intervals with 2–3 puctures across (Fig. 2K). Median lobe wider than paramere, gonopore subapical (Fig. 4K). … ***Saphydrus tanemahuta*** **sp. nov.**

– Small to large species (4.2-7.1 mm). Body widest at mid-length (Figs 2A,B). Eyes larger, separated by 4–5× of width of one eye in dorsal view (Figs 2F,H). Antennomere 9 only slightly longer than wide (Figs 4N,O). Elytral intervals with rather fine punctation, mesal intervals with 3–7 punctures across (Figs 2G,I). Median lobe narrower than paramere, gonopore basal (Figs 4I,J). … 4

4. Smaller (4.2–5.7 mm). Aedeagus (Fig. 4I) with phallobase much shorter than parameres, apical portion of median lobe narrowly acute, parameres sinuate laterally and obtusely pointed apically. Pale coloration along lateral margins of pronotum usually rather wide (Fig. 2F), elytra with or without paler humeral spot. Elytral intervals 2 and 3 each with 3–4 punctures across (Fig. 2G). … ***Saphydrus suffusus***

– Larger (5.7–7.1 mm). Aedeagus (Fig. 4J) with phallobase nearly as long as parameres, apical portion of median lobe slightly widened and rounded, parameres continuously arcuate laterally and widely rounded at apex. Pale coloration along lateral margins of pronotum usually narrower (Fig. 2H), elytra at most with very indistinct pale humeral spot. Elytral intervals 2 and 3 each with 5–7 punctures across (Fig. 2I). … ***Saphydrus obesus***

Saphydrus moeldnerae **sp. nov.**

(Figs 3E,N–O, 3R)

Type locality. New Zealand, North Island, Wellington Region, Tararua Forest Park.

Type material. ***Holotype:*** dissected female (NZAC): **NEW ZEALAND: Wellington:** ‘NEW ZEALAND: Wellington / Tararua For. Park, above / Akatarawa Saddle, 455m, / 40°56.936’S 175°6.529’E / 26.xi.-21.xii.2005, Newton & / Thayer lgt. FMHD#2005-112

// flight intercept trap, broadleaf- / podocarp forest on slope / ANMT site 1151 / FIELD MUSEUM NAT. HIST.'.

Diagnosis. Body length 4.5 mm. Body narrowly elongate, widest at mid-length, constricted between pronotum and elytra; elytra moderately convex in lateral view. Whole dorsal surface pale brown; anterior margin of clypeus, wide lateral portions of pronotum, humeral, lateral and apical portions of elytra slightly paler. ***Head.*** Anterior margin of clypeus nearly rounded, with distinct marginal bead, anterior margin straight. Punctation of clypeus and frons very coarse and rather dense, interstices without microsculpture. Eyes small, isolated by 5.9× the width of one eye in dorsal view, strongly protruding laterally. Antennal club with antennomere 9 slightly longer than wide. ***Thorax.*** Pronotum subquadrate, with lateral margins subparallel, anterior and posterior corners rounded, 1.8× wider than long; punctation coarse and dense, slightly shallower than that on head. Elytra combined widest at mid-length; elytral series distinctly impressed, serial punctures slightly larger than interval ones; interval punctation coarse and rather dense, intervals 2 and 3 each usually with 1–2 punctures across. ***Male genitalia.*** Unknown.

Differential diagnosis. *Saphydrus moeldnerae* is very distinct from all other species of the genus except *S. monticola* by small body size, subquadrate pronotum and anterior margin of clypeus with marginal bead. See under *S. monticola* for differential characters from that species.

Biology. Unknown; the only known specimen was collected to the flight intercept trap in broadleaf-podocarp forest.

Etymology. The species is named after Karina Möldner a former natural sciences teacher, in appreciation for her early encouragement to the first author to pursue biological studies.

***Saphydrus monticola* Broun, 1893**

(Figs 2D,L–M, 3D–I, 4L,Q)

Saphydrus monticola Broun, 1893b: 1401.

Type locality. New Zealand, North Island, Waikato district, Mt. Pirongia.

Type material. ***Holotype:*** female (BMNH, Broun collection): **NEW ZEALAND: Waikato:** 'Pirongia // New Zealand / Broun Coll. / Brit. Mus. / 1922-482 // 2443 // Saphydrus / monticola // Type'. The original description includes more information: Collected amongst leaf-mould, A. T. Urquhart lgt.

Additional material examined. NEW ZEALAND: Northland: 1 male, 3 females, 1 spec. (NZAC): Waipoua Forest, Yakas Tk entrance, 06-11.ii.1995, J. Klimaszewski, pit trap baited with carrion; 1 female (NZAC): Waipoua Forest, nr. Info Centre, 06-11.ii.1995, J. Klimaszewski, pit trap with carrion & apple, mixed bush at edge of grass. **Auckland:** 1 female (ZMUC): Waitakere Ranges Reg. Park, Kauri Grove Tk., 36°57'52.68"S 174°30'44.65"E, 300m, 02.ii.2011, A. Schomann & J. Pedersen leg., deciduous forest with Kauri, sifted litter & handpick, [DNA isolation: NZ374].

Diagnosis. Body length 4.7 mm. Body elongate oval, widest at mid-length, constricted between pronotum and elytra. Whole dorsal surface pale brown; anterior margin of clypeus, wide lateral portions of pronotum, humeral, lateral and apical portions of elytra slightly paler. ***Head.*** Anterior margin of clypeus angulate, with distinct marginal bead, anteromesal part slightly concave, angulate. Punctation of clypeus and frons very coarse and dense, interstices without microsculpture. Eyes large, isolated by 4.2× the width of one eye in dorsal view, strongly protruding laterally. Antennal club with antennomere 9 distinctly longer than wide. Mentum finely rugose on surface, with few coarse, sparsely arranged punctures posterolaterally. ***Thorax.*** Pronotum subquadrate, with lateral margins subparallel, anterior and posterior corners rounded; 2.1× wider than long; punctation coarse and dense, slightly finer than that on head. Elytra combined widest at mid-length; elytral series distinctly impressed, serial punctures slightly larger than interval ones; interval punctation coarse and rather dense, intervals 2 and 3 each usually with 2–3 punctures across. ***Male genitalia*** (Fig. 4L). Aedeagus 0.9 mm long. Phallobase ca. as long as parameres, with weakly delimited manubrium. Parameres narrowing from base to apex, sinuate on outer margin, nearly straight on inner margin, pointed apically. Median lobe subtriangular, blunt apically, gonopore large, subapical.

Differential diagnosis. *Saphydrus monticola* is very distinct from all other species of the genus except *S. moeldnerae* by small body size, subquadrate pronotum and anterior margin of clypeus with marginal bead. Compared to *S. moeldnerae*, it is bigger and more robust with elytra much more convex in lateral view (compare Figs 2D and 2E); its clypeus is angulate with slightly concave anteromesal part exposing the labrum (Fig. 2L);

the pronotum is much wider than head and proportionally wider and shorted (Fig. 2L); punctation of elytral intervals is more dense (compare Figs 2M and 2O) and terminal antennomere is relatively smaller (compare Figs 4Q and 4R).

Biology. Unknown. Based on Broun (1893b), the holotype was collected 'amongst leaf mould', recently found specimens were attracted to baited pitfall traps or found in sifted kauri leaf litter.

Distribution. Known from eight specimens only collected in Waikato, Auckland and Northland regions of North Island. It seems to co-occur with *S. suffusus*.

***Saphydrus obesus* Sharp, 1884**

(Figs 2B,H–I, 4J,O)

Saphydrus obesus Sharp, 1884: 469.

Type locality. New Zealand, South Island, Buller district: Greymouth.

Type material examined. ***Lectotype*** (designated by Hansen 1997): unsexed specimen (BMNH, Sharp collection): 'Saphydrus obe- / sus. / Type D. S. / Greymouth Helms // Type / H. T. / Greymouth / New Zealand / Helms. // Sharp Coll. / 1905-313. // LECTOTYPE / Saphydrus obesus Sharp / M. Hansen des. 1996'. ***Paralectotypes:*** 1 male, 2 unsexed spec. (BMNH, Sharp collection): 'Saphydrus / obesus D. S. / Greymouth. // Greymouth. / New Zealand / Helms // Sharp. Coll. / 1905-313.'; 1 unsexed spec. (BMNH, Sharp collection): 'Saphydrus / obesus D. S. / Greymouth N. Z^{d}. // Greymouth. / New Zealand / Helms // Sharp. Coll. / 1905-313.'; 1 unsexed spec. (BMNH, Sharp collection): 'Saphydrus o- / besus / Greymouth // Greymouth. / New Zealand / Helms // Sharp. Coll. / 1905-313.'; 2 unsexed spec. on the same label (BMNH, Sharp collection): 'Saphydrus obesus D. S. / Greymouth. Helms. 1881 // Greymouth. / New Zealand / Helms // Sharp. Coll. / 1905-313.'. [Note: Sharp collection in BMNH includes only historical specimens, all of which may have been part of the original type series. We consider those bearing the species name as paralectotypes (see above) and attached the syntype label to them.]

Additional material examined. NEW ZEALAND: Northland: 1 female (NZAC): New Zealand; Northland; Mangamuka Walk, 28.vii.-01.viii.1998, 36°11'S 173°28'E, R. Leschen, R. Hoare, FIT 223 [DNA isolate: ANC01]. **Waikato:** 1 male, 3 spec. (AMNZ): New Zealand, Waikato, Mt. Maungatautari, Tari Rd., 13.viii.-01-ix.2003, P. A. Maddinson et al. leg., pitfall trap T10. **Nelson:** 1 spec. (NZAC): Big R, Kahurangi.

03.viii.1970, F. Black & N.W. Nelson leg. **Buller:** 1 female (NZAC): New Zealand, Westland, SH13 2.5km E of Turiwhate, 91 m, Fitzgerald Ck., 9.vi.1983, H.P. McColl, litter; 1 spec. (NZAC): Cape Foulwind, Westport, 2.ix.1971, O.L. Townsend leg.; 1 spec. (LUNZ): Arthurs Pass National Park, Kellys Creek, 460m, 11.xi.1985, R. M. Emberson & P. Syrett leg., under logs, Kamahi/Rata forest. **Unknown locality:** 1 spec. (NHMW): 'Sharp 1890 / Neuseeland // Saphydrus / obesus / D.S. N. Zealand // TYPE' [the specimen does not agree with the data provided in the original description and we do not consider it as type].

Diagnosis. Body length 5.7–7.1 mm. Body broadly oval, widest at mid-length. Clypeus brown, anterior and anterolateral margins of clypeus narrowly yellowish, frons dark brown; pronotum dark brown to black on disc, lateral margins widely yellowish; elytral disc brown, lateral margins and apices narrowly yellowish. ***Head.*** Anterior margin of clypeus arcuate, not elevated and without marginal bead. Punctation of clypeus and frons fine and dense, interstices without microsculpture. Eyes moderately large, isolated by 4.0× the width of one eye in dorsal view, moderately protruding laterally. Antennal club with antennomere 9 only slightly longer than wide. Mentum impunctate mesally, with coarse sparse punctation posterolaterally. ***Thorax.*** Pronotum distinctly narrowing anteriad, punctation very fine and dense, similar to that on head. Elytra combined widest at mid-length; elytral series not impressed, serial punctures subequal in size to slightly larger than interval ones; interval punctation fine and dense, intervals 2 and 3 each with 5–7 punctures across. ***Male genitalia*** (Fig. 4J). Aedeagus 1.15 mm long. Phallobase ca. as long as parameres, with large and distictly defined manubrium. Parameres wide basally, gradually narrowing apicad, continually arcuate on outer margin, slightly sinuate on inner margin, widely rounded at apex. Median lobe narrow in apical 0.7, slightly widening basally, much narrower than parameres at midlength; apex slightly widened, rounded; gonopore situated on the base of median lobe.

Differential diagnosis. Largest species of *Saphydrus*, it may be only confused by body size and shape with *S. suffusus* with which it may co-occur. Differential characters are mentioned in the key, identification by external characters may be difficult without comparative material, but it is easy when male genitalia are examined (compare Figs 4J and 4I).

Biology. Some of the specimens were collected by pitfall and flight intercept traps or from leaf litter. Adults seem to occur in winter (June to November), see Discussion for

details.

Distribution. Known from North Island (Northland, Waikato) and northwestern part of South Island (Buller, Nelson). The species is probably largely sympatric with the more common *S. suffusus*.

***Saphydrus suffusus* Sharp, 1884**

(Figs 2A,G,H; 3A–C; 4H–I,M–N)

Saphydrus suffusus Sharp, 1884: 468.

= *Saphydrus consonus* Broun, 1921: 478 (synonymized by Hansen 1997:354).

= *Saphydrus collaris* Broun, 1921: 478 (synonymized by Hansen 1997: 354).

Type locality. New Zealand, South Island, Buller district: Greymouth.

Type material. *S. suffusus*: ***Lectotype*** (designated by Hansen 1997): unsexed specimen (BMNH, Sharp collection): 'Saphydrus / suffusus / Type / D.S. / Greymouth. Helms // Type / H. T. // Greymouth / New Zealand. / Helms. // Sharp Coll. / 1905-313 // LECTOTYPE / Saphydrus suffusus Sharp / M. Hansen des. 1996'. ***Paralectotypes:*** 1 spec. (BMNH, Sharp collection): 'Saphydrus / suffusus D. S. / Greymouth // Greymouth / New Zealand / Helms. // Sharp Coll. / 1905-313.'; 1 unsexed spec. (BMNH, Sharp collection): 'Saphydrus / suffusus D. S. / Greymouth N. Z^{d}. // // Greymouth / New Zealand / Helms. // Sharp Coll. / 1905-313.'; 1 unsexed spec. (BMNH, Sharp collection), 3 spec. (NZAC): 'Saphydrus / suffusus / Greymouth. Helms // // Greymouth / New Zealand / Helms. // Sharp Coll. / 1905-313.'; 1 male (BMNH, Sharp collection): 'Saphydrus / suffusus D. S. / Mauri Creek / Greymnouth // // Greymouth / New Zealand / Helms. // Sharp Coll. / 1905-313.'; 1 unsexed spec. (BMNH, Sharp collection): 'Saphydrus / suffusus D. S. / Mauri Creek / Greymouth N. Z^{d}. // // Greymouth / New Zealand / Helms. // Sharp Coll. / 1905-313.'; 3 unsexed spec. on the same label (BMNH, Sharp collection): 'Saphydrus suffusus / Mauri Creek Greymouth // // Greymouth / New Zealand / Helms. // Sharp Coll. / 1905-313.' 4 spec. (NHMW): 'Saphydrus suffusus / mihi D. S. / Greymouth, N. Zealand // Sharp 1890 / Neuseeland // TYPUS // suffusus / N. Seeld Sharp' [Note: Sharp collection in BMNH only include historical specimens from Greymouth and Mauri Creek (= Maori Creek). We consider those bearing the species name and the locality on the same label as the paralectotypes. The specimens from NZAC and NHMW are undoubtedly originally from Sharp's collection and correspond to the

data mentioned in the original description, and are hence all considered as paralectotypes.]

S. consonus: ***Holotype:*** unsexed specimen (BMNH, Broun collection): '3980. // New Zealand / Broun Coll. / Brit. Mus. / 1922-482. // HOLO- / TYPE // Buller. / 17. 1. 1915 // Saphydrus / collaris'.

S. collaris: ***Holotype:*** unsexed specimen (BMNH, Broun collection): '3981. // New Zealand / Broun Coll. / Brit. Mus. / 1922-482. // Te Aroha / March 1894 // Saphydrus / collaris.'.

Additional material examined. NEW ZEALAND: Waikato: 136 spec. (FMNH): Pirongia Forest Park, Tahuanui Track, 840m, 37°58.953'S 175°5.523'E, 18.xi.–27.xii.2005, Solodovnikov & Clarke leg., FMHD#2005-012, flight intercept trap, mixed forest near subalpine zone, ANMT site 1143; 99 spec. (NMPC): same data as previous specimens; 3 spec. (BMNH): same data as previous specimens. **Coromandel:** 2 spec. (NMPC): Mahakirau Forest Estate, Lot 19, 36°51.975'S,175°32.861'E, 14.i.2017, at light, beating vegetation, R. Leschen & C. Maier, RL1898 [DNA grade specimens: NZ610 and NZ616]. **Taranaki:** 1 male (NZAC): Dawson Falls Tk., 914 m, 23.i.1972, G.W.Ramsay, litter; 1 spec. (LUNZ): Mount Egmont National Park, Potaema Picnic area, 650 m, R. M. Emberson & P. Syrett leg., 26.xii.1985, in tent. **Gisborne:** 1 spec. (FMNH): Te Urewera NP, Waikaremoana Rd., S end Matanunui Ridge, 38°44.404'S 177°5.806'E, 22.xi.-23.xii.2005, 720 m, Newton, Thayer & Solodovnikov leg., FMHD#2005-028, flight intercept trap, mixed broadleaf (incl. *Nothofagus fusca*)-podocarp forest, AMNT site 1149; 1 spec. (NMPC): same data as previous specimen; 1 spec. (FMNH): Te Urewera NP, Waikaremoana Rd., S end Matanunui Ridge, 38°44.404'S 177°5.806'E, 720 m, 22.xi.-23.xii.2005, Solodovnikov & Clarke leg., FMHD#2005-026, carrion trap (octopus), mixed broadleaf (incl. *Nothofagus fusca*)-podocarp forest, AMNT site 1149. **Wellington:** 1 spec. (FMNH): Tararua Forest Park, Waitewaewae Tk., 40°51.98'S 175°15.319'E, 220 m, 26.xi.-21.xii.2005, Newton & Thayer leg., FMHD#2005-035, carrion trap (octopus), broadleaf (much *Knightia excelsa*)-podocarps forest, ANMT site 1152; 1 male, 1 female, 1 spec. (NZAC): Wellington, Orongorono's pig droppings, 16.i.1961, D. N. Edwards leg.; 1 spec. (NZAC): Waiotauru Road, Tararua Forest Park, 28.ii.1993, J. T. Nunn collection. **Nelson:** 83 spec. (FMNH): Kahurangi NP, Cobb Dam Rd., Asbestos Tk., 450 m, 41°6.333'S 172°43.174'E, 29.xi.–18.xii.2005, A. Solodovnikov & D. Clarke leg., FMNH#2005-057, carrion trap (octopus), mixed broadleaf (incl. *Nothofagus fusca*)-podocarp forest, AMNT site 1160 [DNA specimens:

NZ401, NZ402]; 9 spec. (FMNH): Kahurangi NP, Cobb Dam Rd., Asbestos Tk., 450 m, 41°6.333'S 172°43.174'E, 29.xi.-18.xii.2005, A. Solodovnikov & D. Clarke leg., FMNH#2005-056, flight intercept trap, mixed broadleaf (incl. *Nothofagus fusca*)-podocarp forest; 2 spec. (NMPC): Nelson Lakes NP, N end of Lake Rotoroa at Braeburn Track 41.7987°S, 172.58421°E, 522 m 5-9.xii.2016, Fikáček & Seidel lgt. MM57, lowland wet *Nothofagus* forest with huge amount of sooty moulds and with continuous layer of *Blechnum* fern understory: baited pitfall traps (rotten squid) [DNA isolation: NZ418, NZ462]; 1 spec. (LUNZ): Punakaiki Scenic Reserve, Porarari River, 29.xii.1983-3.i.1984, J. W. Early & L. Masner leg., yellow pan trap, *Nothofagus* forest. **Buller:** 14 spec. (NZAC): Rough Creek, Maruia Springs, 550 m, 42°22.825'S 172°16.798'E, 12.i.2011, R. Leschen & T. Buckley, TB455; 1 male, 5 spec. (NMPC): same data as previous specimens, [DNA isolations: COL1786, COL1825, COL1843]; 19 spec. (FMNH): Nelson Lakes NP, Rotoiti, St. Arnaud Tk., 645m, 14.xii.1984–6.i.1985, A. Newton & M. Thayer leg., #705, *Nothofagus* forest, flight intercept trap; 1 male, 8 spec. (NMPC): same data as previous specimens [2 specimens slide mounted]; 1 male, 1 spec. (NMPC): Waterfall Creek Tk., Maruia Springs, 42°21.717'S 172°15.332'E, 499 m, 10.i.2011, R. Leschen & T. Buckley leg, TB435, ex. dead wood [DNA isolation: NZ82, COL1787); 1 spec. (NZAC): same label data; 1 spec. (LUNZ): Lake Rotoroa, near camp ground, 9.i.1993, J. W. M. Marris, at night, logs/trees; 1 spec. (NZAC): Pororari River mouth, Punakaiki, 29.xii.2010, J. T. Nunn collection, in flood debris; 3 spec. (NZAC): Maruia Springs, 550 m, 2.ii.2014, J. T. Nunn collection, *Nothofagus* forest. **Westland:** 1 spec. (NMPC): Cockayne Nature Walk at Otira Hwy., 42°48.06'S 171°34.26'E, 380 m, 24.–26.ii.2016, Seidel, Sýkora, Leschen, Maier & Lambert lgt., 2016-NZ-MS66, baited pitfall traps (rotten squid) in stony forest, [DNA isolation: NZ263]. **Unknown locality:** 2 females (NMPC): Helms, 1886; 1 spec. (MONZ): Lewis coll.

Diagnosis. Body length 4.2–5.7 mm. Body elongate oval, widest at midlength. Clypeus and frons dark brown, anterior and anterolateral margins of clypeus narrowly yellowish; pronotum dark brown on disc, lateral margins narrowly yellowish; elytral disc brown, lateral margins narrowly yellowish. ***Head.*** Anterior margin of clypeus arcuate, not elevated and without marginal bead. Punctation of clypeus and frons fine and dense, interstices without microsculpture. Eyes large, isolated by 5× the width of one eye in dorsal view, strongly protruding laterad. Antennal club with ultimate antennomere only slightly longer than wide. Mentum with shallow sparsely arranged punctires posteriorly.

Thorax. Pronotum distinctly narrowing anteriad, punctation very fine and dense, similar to that on head. Elytra combined widest at mid-length; elytral series not impressed, serial punctures subequal in size to slightly larger than interval ones; interval punctation fine and dense, intervals 2 and 3 each usually with 3–4 punctures across. ***Male genitalia*** (Fig. 4I). Aedeagus 1.25 mm long. Phallobase ca. half as long as parameres, with small and very indistict manubrium. Parameres wide throughout, narrowing in apical 0.15, slightly bisinuate on outer margin, slightly convex on inner margin, obtusely pointed at apex. Median lobe very narrow in apical 0.7, widening basally, much narrower than parameres at midlength; apex narrowly acute in ventral view; gonopore distinct, situated basally.

Differential diagnosis. By the body size and shape, *S. suffusus* may be only confused with *S. obesus* with which it may co-occur. Differential characters are mentioned in the key. Identification by external characters may be difficult without comparative material, but it is easy when male genitalia are examined (compare Figs. 4I and 4J).

Notes on synonymies. When describing *S. consonus* and *S. collaris*, Broun (1921) knew *S. suffusus* solely from its original description. He based his diagnosis of both taxa from *S. suffusus* on the absence of the pale humeral spot on elytra, and distinguished *S. consonus* from *S. collaris* on the basis of the difference of pronotal shape and elytral convexity. The inspection of both Broun's types revealed that both are identical in pronotal and elytral shape (the seeming difference was possibly caused by different posture of beetles on the labels) as well as in all other diagnostic characters. These two taxa only differ from the type of *S. suffusus* in the coloration of elytra, which are however variable even within a population: compare Fig. 2A (specimen with dark elytra) and Fig. 2F (specimen with pale elytral spot). For all these reasons, we consider all three taxa as synonyms, in agreement with the synonymy established by Hansen (1997).

Biology. Adults are occasionally collected using flight intercept traps, baited pitfall traps or by beating vegetation. Sometimes they may be collected in masses using flight intercept or pitfall traps, and in one instance, there were hundreds of specimens crawling slowly on the surfaces of vegetation and rotting wood along the track at Rough Creek, near Maruia (Leschen, pers. obs.). See Discussion for further details.

Distribution. North Island (Waikato, Coromandel, Taranaki, Gisborne, Wellington) and northwestern part of South Island (Buller, Nelson, northern Westland) up to ca. 900 m a.s.l. Probably rather common and widespread, but overlooked.

***Saphydrus tanemahuta* sp. nov.**
(Figs 2C,J–K; 4K,P)

Type locality. New Zealand, South Island, Fiordland: Wilmot Pass, Mt. Barber.
Type material. ***Holotype:*** dissected male (NZAC): 'Mt. Barber / 2700-4200′ // Willmot Pass / Fiordland // 8Jan70 / J. S. Dugdale // sweeping / in alpine / zone'. ***Paratype:*** 1 female (NZAC): 'Mt. Dewar / 1060m // Dec. 69 / J. S. Dugdale // ♀'.

Diagnosis. Body length 4.2–4.8 mm. Body elongate oval, widest at posterior third of elytral length. Clypeus and frons dark brown, anterior and anterolateral margins of clypeus yellowish; pronotum dark brown on disc, lateral margins narrowly yellowish; elytral disc brown, lateral margins and apical third yellowish. ***Head.*** Anterior margin of clypeus subangulate, very slightly elevated, but without marginal bead. Punctation of clypeus and frons rather coarse and sparse, interstices without microsculpture. Eyes small, isolated by 6× the width of one eye in dorsal view, slightly protruding laterad. Antennal club with ultimate antennomere distictly longer than wide. Mentum with coarse sparse punctation posteriorly and laterally, interstices without microsculpture. ***Thorax.*** Pronotum distinctly narrowing anteriad, punctation moderately coarse and sparse, similar to that on head. Elytra combined widest at posterior third; elytral series not impressed, serial punctures subequal in size to interval ones; interval punctation rather coarse and sparse, intervals 2 and 3 each usually with 2–3 punctures across. ***Male genitalia*** (Fig. 4K)**.** Aedeagus 0.9 mm long. Phallobase slightly longer than parameres, with large and distictly defined manubrium. Parameres narrow, slightly narrowing apicad, weakly sinuate on outer margin, nearly straight on inner margin, rounded at apex. Median lobe wide throughout, wider than parameres at midlength, narrowing in apical 0.2 to an obtusely pointed apex; gonopore distinct, situated apically.
Differential diagnosis. By its small body size, *S. tanemahuta* may be only confused with *S. moeldnerae* or *S. monticola*, from which it may be easily distinguished by the shape of the pronotum (narrowing anteriad in *S. tanemahuta*, with subparallel lateral margins in *S. moeldnerae* and *S. monticola*) and the form of elytra (widest at posterior third and without impressed series in *S. tanemahuta*, widest at midlength and with impressed series in *S. monticola*).
Etymology. The species is named after Tāne-mahuta, the Maori god of forests and birds. Noun in apposition.

Biology. Unknown. The holotype was swept from vegetation in the alpine zone.
Distribution. Endemic to South Island (Buller, Fiordland), known only from two distant localities (ca. 520 km apart), in both cases at rather high altitudes. The species is possibly more widespread over Southern Alps and may be confined to the alpine zone.

Morphology of immature stages

Four larval morphotypes were found in the examined samples. Two of them were associated with *Saphydrus* by means of DNA (Fig. 1) and are described in detail below (Figs 5A–D,P–S; 6–13). Two additional morphotypes were associated with *Saphydrus* based on morphological characters and body size, and are here only briefly illustrated (Figs 5E–O) and diagnosed. Based on the morphological characters, three of these morphotypes clearly represent the genus *Saphydrus*. The fourth morphotype is genetically distant, and differs substantially in morphology; we are assigning it to a new genus *Enigmahydrus*. Larvae of both genera are characterized by symmetrical nasale with 5 teeth, and may be distinguished using the following key:

1. Head subquadrate (Fig. 5C–D,G–H,N–O, 8A–B); nasale in all instars with alternating larger and smaller teeth (Figs 6C, 8A). Mentum and prementum divided from each other, ligula short and membranous (Figs 7D, 9D). Proscutum without subquadrate projections (Figs 5C,G,N). Prosternum in form of one plate subdivided by a fine saguittal line (Figs 5D,H,O; 8C). Abdominal segments without or with small lateral finger-like projections (Figs 5A,E,I). … ***Saphydrus***
- Head pentagonal (Figs 5R–S, 12A–B); nasale with all teeth of the same size in second and third instar (Fig. 5R, 12A), and only slightly varying in size in the first instar (Fig. 10E). Mentum and prementum fused, projecting in large, strongly sclerotized ligula-like projection anteriorly (11E, 13E). Proscutum with two subquadrate projections on each side (Fig 5R). Prosternum in form of a pair of sclerited divided by a narrow gap (Figs 5S, 12C). Abdominal segment with large finger-like projections (Fig. 5P). … ***Enigmahydrus*** **gen. nov.**

Genus *Saphydrus* Sharp, 1884

Diagnosis of larva. Dorsal surface of head and all head appendages with numerous fine cuticular projections; head quadratic; eyes distinct, but not on projecting bulges; nasale with 5 teeth, three large alternating with two small; epistomal lobes low, symmetrical; antennal sensorium slender, as long as or slightly longer than antennomere 3; mandible with two inner teeth; maxillary stipes with 5 inner setae; maxillary palpomere 1 short; mentum separated from prementum; prementum with a short ligula; legs short, not visible in dorsal view; proscutum without large lateral projections; prosternum largely sclerotized, in form of one sclerite subdivided by sagittal line; meso- and metathorax with large transverse tergites; abdomen slightly wider than thorax; abdominal segments with short to medium-sized lateral projections; abdominal tergite 8 large, quadrate; abdominal prolegs absent; spiracular atrium developed.

Differential diagnosis. The nasale with five teeth alternating in size distinguishes *Saphydrus* from larvae of all other New Zealand genera except of the first instar of *Enigmahydrus*. For the diagnostic characters from *Enigmahydrus* see the key above.

***Saphydrus suffusus* Sharp, 1884**

Larval material examined in detail. 1 L1, 2 L3, 8 larvae (KMNH, NMPC): **NEW ZEALAND: Taranaki:** Mt. Egmont NP., Curtis Falls Tk. 0.9 km NW of Mountain House, sifting of leaf litter in montane *Nothophagus* forest with many tree ferns and moss, 39°18.1′S 174°6.8′E, 950 m, 28.xi.2012, Becker, Fikáček & Hájek lgt. (NZ20); 1 sequenced larva [MF529] (NMPC): Mt. Egmont NP, Potaema Walk, 6.8 km W of Pembroke, sifting of leaf litter accumulated in depression of lower montane forest, 650 m, 174.15°S 39.31°E,28.xi.2012, lgt. Becker, Fikáček, Hájek (NZ16);

Additional larval material examined. 1 larva (NMPC): **NEW ZEALAND: Taranaki:** Mt. Egmont NP, Potaema Walk, 6.8 km W of Pembroke, sifting of leaf litter accumulated in depression of lower montane forest, 650 m, 174.15°S 39.31°E,28.xi.2012, lgt. Becker, Fikáček, Hájek (NZ16); 1 larva (NMPC): Mt. Egmont NP, Mangaoraka Tk. at Egmont Road, sifting of mosses on ground, bases of trunks and decaying logs in mossy lower montane forest, 600 m, 174.11°S 39.24°E, 1.xii.2012, lgt. Fikáček (NZ29); 7 larvae (NMPC): Mt. Egmont NP, Murphys Lake 1.8 km SE of Dawson Falls area, sifting of leaf litter, tree roots and moss in montane forest at banks of the pond,710 m, 174.11°S

39.33°E, 29.xi.2012, lgt. Becker, Fikáček & Hájek (NZ22); 1 larva (NMPC): Te Urewera NP, Waipai swamp at Waipai-Ruapani Tk, 1.6 km NWW of Aniwaniwa, sifting of leaf litter under tree ferns, 780 m, 171.57°S 38.74°E, 23.xi.2012, lgt. Becker, Fikáček & Hájek (NZ05). **Gisborne:** 1 larva (NMPC): Te Urewera NP, at small lakes of Mokau Tk., 5.7 km NW of Aniwaniwa, sifting of leaf litter and mosses in *Nothofagus* forest around peatbog lakes, 880 m, 177.11°S, 38.71°E, 24.xi.2012, lgt. Becker, Fikáček, Hájek (NZ09); 1 larva (NMPC): Te Urewera NP, Te Kumi stream at Waipai-Ruapani Tk., sifting *Nothofagus* leaf litter near stream, 690 m, 177.15°S, 38.74°E, 23.xi.2012, lgt. Becker, Fikáček & Hájek (NZ06); 1 larva (NZAC): Lake Waikaremoana, 7.i.1972, lgt. G. W. Ramsay (72/19). **Marlborough:** 1 larva (FMNH): Pelorus Bridge Scenic Reserve, sifting in mixed broadleaf (incl. Nothofagus spp.)-podocarp forest, 35 m,173.56°S 41.30°E, 27.xi.2005 lgt. M. Thayer (FMHD#2005-041). **Westland:** 2 larvae (NMPC): Kellys Creek at Otira Hwy., 3 km N of Otira, sifting of moss + leaf litter in the mossy forest on flood plain of small mountain river, 350 m, 171.57°S 42.80°E, 3.xii.2012, lgt. Fikáček, Hájek, Leschen (NZ30).

Description of larva. First instar. ***General morphology.*** *Head.* Anterior part bearing very fine cuticular projections dorsally and laterally; posterior part with wrinkles dorsally and laterally. Antenna proportionally shorter and stouter than that of third instar. Antennomere 1 slightly wider and much shorter than antennomere 2; antennomere 2 about 1.4 times as long as antennomere 1. Antennomere 3 relatively wider than in third instar. Antenna and maxilla with dense cuticular projections on mesal face, mentum and prementum dorsally. Mandible without fine surface structures. Maxilla proportionally stouter than third instar. Prosternal sclerite subdivided by sagittal line, bearing few sensilla.

Primary chaetotaxy of head capsule. *Frontale* (Figs 6A,C). Central part with three pairs of sensilla (FR1–3) forming slightly oblique longitudinal row; FR1 and FR3 short seta; FR3 slightly stouter than FR1; FR2 pore-like. Rather long seta FR5 and rather short seta FR6 located posteriorly to inner margin of antennal socket; FR5 posterior to FR6. Pore-like sensillum FR4 posteromesally to inner margin of antennal socket. FR7 short seta, on inner face of antennal socket. Setae FR9 and FR10 mesally to antennal socket, rather short seta FR10 behind rather long seta FR9. FR8 and FR15 situated mesally on anterior part of head capsule; rather long seta FR8 behind pore-like FR15. Sensilla FR11–14 on epistome; FR11, FR13, and FR14 pore-like, FR12 short seta. FR11–13 behind

gFR2; FR11 mesally to FR12–13, FR13 between FR11 and FR12. FR14 anteriorly to inner margin of antennal socket. Nasale with a group of six rather short, slightly stout setae and two ventral setae (gFR1); four setae on dorsal surface, two on ventral. Epistomal lobe bearing four rather short setae (gFR2) on anterior margin; mesal one stouter than lateral three.

Parietale (Figs 6A–B). Dorsal surface with group of five setae (PA1–5) forming slightly irregular longitudinal row posteriorly; PA3 pore-like, remaining four short setae. Pore-like sensillum PA6 close to posterior end of frontal line. Very long seta PA7 on mesal part of dorsal surface of parietale, on midlength of parietale. Very long seta PA8 behind lateral part of antennal socket. Long seta PA9 laterally to antennal socket. Pore-like sensillum PA10 behind PA8; rather short seta PA11 behind PA9. Homology of PA12–14 unclear. Short seta ?PA12 mesal to PA10; Very long seta ?PA14 posterior to PA10; ?PA13 midlength between ?PA14 and PA5. PA15–17 on anterior third of lateral face; PA15 pore-like, dorsally to PA16 and PA17; very long seta PA16 between PA15 and PA17; PA17 pore-like, mesally to PA16. PA19–22 on anterior corner of head capsule, forming transverse row; PA19 pore-like, PA20 rather short seta, PA21 extremely long seta, PA22 rather long seta. Pore-like sensilla PA23–25 on ventral mandibular articulation; PA23 on outer margin; PA25 on inner part; PA24 between PA23 and PA25, close to PA25. Very long seta PA18 and pore-like sensillum PA30 located posterior to PA16 and PA17; PA30 mesally to PA18. Three sensilla (PA26–28) situated mesal part of ventral surface of parietale; PA26 long seta, PA27 pore-like, PA28 seta; PA26 anterior to PA27 and PA28, PA27 between PA26 and PA28. Pore-like sensillum PA29 posteromesally to PA28.

Antenna (Fig. 7A). Antennomere 1 bearing five pore-like sensilla; possible AN1 medially on anterior third of dorsal surface; possible AN2 on anterior third of lateral face; AN3 laterally on anterior margin; AN4 anterior margin of inner face; AN5 medially on anterior margin of ventral surface. Antennomere 2 with one pore-like sensillum (AN6) situated dorsally on subapical part of sclerite and five sensilla on intersegmental membrane between antennomeres 2 and 3. Sensorium SE1 slender, as long as or slightly longer than antennomere 3. Short seta AN7 and minute seta AN8 on lateral face, behind SE1. Very long seta AN10 and short stout seta AN11 on inner face; AN11 behind AN10. Antennomere 3 with group of six apical sensilla of variable length (gAN).

Mandibles (Fig. 7B). Three pore-like sensilla (MN2–4) forming triangle posterolaterally to inner tooth; rather long seta MN1 posterolaterally to MN2. Minute seta MN5 on median part of outer face. MN6 minute, possibly present but undetectable.

Maxilla (Fig. 7C). Cardo with one rather long ventral seta (MX1). Inner face of stipes with longitudinal row of five stout, rather short setae (MX7–11). MX7 shortest and narrowest, on basal part. MX8–9 equidistant on inner face. Pore-like sensilla MX2 and MX3 located ventrally on posterior third of stipes; MX2 on outer face, MX3 on inner face. Pore-like sensillum MX4 and very long setae MX5 and MX6 subapically on lateral face; MX4 behind MX6; MX5 mesally to MX4. Dorsal face of palpomere 1 bearing one rather short, stout seta (MX16) situated medially on inner face. MX12–14 situated ventrally on apical part of outer face of palpomere 1; MX12 pore-like; MX13 very long seta, between MX14 and MX12; MX14 long seta mesally to MX13. Pore-like sensilla MX15 and MX17 on membrane behind inner appendage, MX17 dorsally, MX15 ventrally. Inner appendage bearing setae of variable length apically (gAPP). Palpomere 2 with two pore-like sensilla (MX18 and MX19) and one minute seta (MX27). MX18 situated ventrally on anterior margin of sclerite; MX19 on inner face of intersegmental membrane between palpomeres 2 and 3; MX27 subbasally on lateral face. Palpomere 3 with four sensilla (MX20–23). MX20 and MX23 apically on outer face; MX20 pore, ventrally to MX23, MX23 seta. MX21 and MX22 on ventral surface; very long seta MX21 on apical part; MX22 pore-like, behind MX21. Palpomere 3 with three sensilla (MX24–26), and several minute setae (gMX) on apical membranous area. MX24 rather long seta situated basally on inner face; MX25 and MX26 subapically; MX25 digitiform, dorsally; MX26 pore-like, ventrally.

Labium (Fig. 7D). Submentum with two pairs of setae (LA1–2). LA1 extremely long on lateral margin, LA2 minute on anterolateral corner. Mentum with two ventral sensilla (LA3 and LA4); short seta LA3 situated mesally to pore-like sensillum LA4. Prementum and its anterior membranous area with five pairs of sensilla (LA5–9). LA8 and LA9 pore-like, on median part of dorsal surface; LA8 behind LA9. LA5–7 laterally on ventral surface; minute seta LA5 on subbasal part; very long seta LA6 and pore-like sensillum LA7 on apical margin of sclerite; LA7 laterally to LA6. Ligula bearing three pairs of sensilla (LA10–12). Rather long seta LA10 basally on dorsal face; pore-like sensillum LA11 basally on ventral face; LA12 pore-like on apical part. Palpomere 1 with two sensilla (LA13–14); LA13 minute seta on basal part of ventral surface; LA14 pore-like, dorsally on intersegmental membrane between palpomeres 1 and 2. Palpomere 2 with

one pore-like sensillum LA15 situated subapically on outer face; several setae of variable shape and length (gLA) on apical membranous area.

Description of third instar larva. ***Body*** (Figs 5A–B) slender, widest between abdominal segments 4–5. Colour. Head capsule reddish brown. Thorax and abdomen light brownish with reddish brown sclerites. Dorsal surface covered by small particles (dirt) in most larvae examined.

Head. *Head capsule* subquadrate, cervical sclerites small, subquadrate. Frontal lines visible only basally, coronal line absent. Surface of head capsule covered dorsally with minute cuticular projections except on anterior and posterior margins; ventral surface of head capsule smooth. Cuticular projections variable in shape, circular, scale-like, scale-like with row of minute cuticular spines, short fringe-like transverse row of minute cuticular spines. Six stemmata on each anterolateral portion of head capsule. Posterior tentorial pits present close to junction of submentum sulcus and gular sulcus. Clypeolabrum almost symmetrical. Nasale slightly projecting further than epistomal lobes, with five teeth: three teeth (lateralmost and median ones) large, two intermediate teeth between large ones small; all teeth bearing small cuticular projections. Lateral lobe of epistome present, almost symmetrical, rounded apically at mesal part. Epistomal lobe bearing fringe of cuticular projections on anterior margin.

Antenna 3-segmented, slender. Surface of antennomeres bearing very densely arranged hair-like cuticular projections except on part of ventral surface of antennomeres 1 and 3 and ventral surface of antennomere 2. Antennomere 1 the widest, slightly shorter than antennomeres 2 and 3 combined. Antennomere 3 very short and narrow, much smaller than other segments, as long as sensorium SE1. Mandibles slender, strongly curved, distinctly widened posteriad, symmetrical, with two inner teeth of almost equal in size on median part of inner face. Basal part of inner face bearing fine cuticular projections.

Maxilla 6-segmented, slender, longer than antenna, bearing fine to long hair-like cuticular projections. Cardo subtriangular, large. Stipes the longest, inner face and outer face bearing densely arranged hair-like cuticular projections; the projections on outer face much longer than those on inner face. Maxillary palpus short, covered with fine cuticular projections. Palpomere 1 the longest and widest. Inner process sclerotized. Palpomeres 2–4 almost same in length, palpomere 2 the widest, palpomere 4 the narrowest.

Labium well developed. Submentum fused to head capsule, transverse. Mentum subquadrate, widest at base, slightly wider than prementum. Dorsal surface densely

covered with fine hair-like cuticular projections except with a pair of median patches. Prementum subquadrate, widened anteriad, dorsal surface covered with fine hair-like cuticular projections. Ligula short, partly sclerotized. Labial palpus rather short, densely covered with fine hair-like cuticular projections; palpomere 1 wider than palpomere 2, palpomere 2 much longer than palpomere 1.

Thorax. Membranous parts very densely covered with fine hair-like cuticular projections. Prothorax wider than head capsule. Proscutum formed by one large plate subdivided by fine sagittal line; anterior and posterior margins weakly sclerotized; proscutal plate covered with fine cuticular projections and setae of variable length. Prosternal sclerites subdivided mesally by a sagittal line, bearing numerous setae on anterior margin. Mesonotum with three pairs of dorsal sclerites. Anterior pair narrow, transverse; posterior pair large, transverse; lateral pair small. One small and one moderately large lateral tubercles present. Mesothoracic spiracles on lateral face, anterior to lateral tubercles, forming a small finger-like projection. Metanotum with two pairs of dorsal sclerites; anterior pair large, oval, transverse; posterior pair small, transverse. Legs short but well developed, 5-segmented.

Abdomen. Abdomen 10-segmented, membranous parts covered with densely arranged cuticular projections. Spiracles laterodorsally on anterior part of segments 1–7, slightly projecting as tubercle. Segment 1 with one pair of small dorsal sclerites on median part. Segments 2–7 similar to segment 1, but dorsal sclerites absent; lateral projection on segment 7 finger-like, longer than those on segments 1–6. Spiracular atrium: Segment 8 bearing one pair of finger-like lateral projections; dorsal plate large, subquadrate, sinuate posteriorly. Procercus short. Segment 9 trilobed, partly sclerotized. Lateral lobe of spiracular atrium large, dorsal face largely sclerotized; acrocercus present, stout, truncate apically. Median lobe of spiracular atrium subquadrate, largely sclerotized dorsally; one pair of moderately long, membranous projections present between median and lateral lobes.

Chaetotaxy of head. Head capsule bearing numerous rather short secondary sensilla on dorsal and lateral faces; median part of ventral face without secondary setae. Secondary sensilla on dorsal head capsule rather short, those on lateral face rather long.

Antenna (Fig. 9A). Antennomere 1 bearing 12 secondary sensilla dorsally and laterally. Antennomere 2 with six secondary setae on dorsal face. Sensorium SE1 as long as antennomere 3.

Mandible (Fig. 9B). Mandible bearing minute setae on posterior half of lateral face (ca. 10 setae) and group of rather long setae on basal part of lateral face (ca. 10 setae). Minute sensilla-like structures on subapical part.

Maxilla (Fig. 9C). Ventral face of stipes bearing numerous secondary setae of variable length; ca. 8 on inner face, 10 on ventral, 16 on lateral.

Labium (Fig. 9D). Anterior part of mentum bearing numerous rather short to moderately long secondary setae; two pairs on anterodorsal margin, four pairs of stout setae on lateral corners, 3 to 5 setae on lateral corner of ventral face.

***Saphydrus* cf. *obesus* Sharp, 1884**

Material examined. NEW ZEALAND: Nelson: 1 L3 (NZAC): Dun Mountain, very wet moss, 440 m [c. 173.37°S 41.31°E], 29.iii.1966, lgt. J. I. Townsend.

Diagnosis of third instar. *Body* with thorax and abdomen nearly of the same width, hence body narrowly parallel-sided (compared to widened posteriorly of thorax in *S. suffusus*). Body length ca. 11.4 mm (compared to ca. 7.8 mm in L3 of *S. suffusus*), width of head capsule 1.4 mm (compared to 1.1 mm in *S. suffusus*). The morphology of the head capsule very similar to that of *S. suffusus*, including nasale with alternating larger and smaller teeth and mentum rather small, with distinctly separated mentum and prementum and without modified ligular region. Proscutum without lateral projections. Thorax and abdomen with small tubercle-like projections only.

Identification of the larva. The larva was collected without association with adults. Taking into account the head morphology which is nearly identical to that of *S. suffusus*, and its larger body size, we suppose it may belong to *S. obesus* (i.e. the species likely closely related to *S. suffusus* but slightly larger in size).

***Saphydrus* cf. *tanemahuta* Seidel et. al., 2019**

Material examined. NEW ZEALAND: Westland: 2 larvae (NZAC): Paparoa Range, Mt. Dewar, moss, 1131 m [c. 171.54°S 42.08°E], 12.xii.1969, lgt. J. S. Dugdale; 2 larvae (NZAC): Paparoa Range, Mt. Dewar, moss, 1208 m [c. 171.54°S 42.08°E], 10.xii.1969, J.S.Dugdale lgt.

Diagnosis of third instar. *Body* widely elongate, widened ca. at midlength of abdomen. Body length 7.2 mm, width of head capsule 0.9 mm. Head subquadrate, dorsal surface with finely tuberculate microstructure. Nasale with 5 teeth, larger ones alternating with smaller ones. Epistomal lobes slightly lower than nasale, nearly symmetrical. Antenna with antennomere 1 slightly longer than antennomere 2, antennomere 3 minute; sensorium narrow, slightly longer than antennomere 3. Mandibles symmetrical, with two inner teeth. Maxilla with stipes ca. 2× longer than maxillary palpus. Labium of moderate size; mentum separated from prementum; ligula normally developed, semi-membranous. Prothorax wider than head capsule. Proscutum weakly lobate laterally. Prosternal sclerite subdivided mesally by a sagittal line. Mesothorax and metathorax each with two pairs of finger-like lobes laterally. Legs short, 5-segmented. Abdominal segments 1–7 each with two lobes, anterior lobe projecting laterally, posterior lobe with two pairs of lateral projections. Abdominal segment 8 with two pairs of lateral projections. Tergite 8 elongate subquadrate, with sinuate posterior margin.

Identification of the larva. The larva shares the head morphology with that of *S. suffusus*, i.e. the nasale consists of alternating larger and smaller teeth, head is subquadrate, maxillary stipes is much longer than maxillary palpus, mentum is divided from submentum, ligula is present, small and largely membranous, and proscutum lacks large lateral projections. Based on these characters, the larva seems to belong to the genus *Saphydrus*, despite its lobate abdomen may resemble the conditions found in *Enigmahydrus larvalis*. Based on the label data, the examined larvae were collected during the same expedition and in the same area as the paratype of *S. tanemahuta* sp. nov., although not syntopically with the adult specimen. We hence suppose that this larval morphotype belongs to *S. tanemahuta*. The size of the larva does not contradict this association.

***Enigmahydrus* gen. nov.**

Type species. *Enigmahydrus larvalis* sp. nov., by monotypy.

Phylogenetic position and generic status. Molecular data unambiguously reveals the larva described below as a sister clade to *Saphydrus suffusus* (Fig. 1). This corresponds to the larval morphology which is similar in both clades in basic characters (number of teeth of the nasale, symmetry of labrofrontoclypeus, mandibular morphology, dorsal

surface sclerotized body parts with numerous fine cuticular projections). Molecular data indicated that the larva is not genetically close to *Saphydrus suffusus* which made its generic status uncertain. The large differences in morphology between larval *Saphydrus* and the larva described below underlines this finding, as they in many aspects exceed the differences between other hydrophilid genera. The combination of large genetic distance to *Saphydrus* and large morphological differences from larvae of *Saphydrus* allows us to define a new genus for this larval taxon.

Diagnosis. The genus is only known in larval stage. It can be diagnosed from larvae of all other New Zealand Hydrophilidae as well as from all other hydrophilid genera with known larvae by the following combination of characters: ***Head***. widely subpentagonal; frontal lines converging posteriorly; coronal line absent; nasale with 5 teeth which are of slightly unequal size (alternating larger and smaller) in L1 and of equal size in L3; epistomal lobes symmetrical both in shape and chaetotaxy, low; cervical sclerites present; antenna with antennomere 1 shorter than antennomere 2; sensorium long and narrow, longer than antennomere 3; mandibles symmetrical, each with 2 inner teeth; maxila with stipes shorter (in L1) or as long as (in L3) maxillary palpus; inner appendage of palpomere 1 large, sclerotized; submentum divided from parietale by a sulcus; mentum fused with prementum; prementum projecting anteriorly into ligula-like projection as long as (in L1) or longer (in L3) than labial palps; head surface and appendages with numerous cuticular projections. ***Thorax*.** All three segments with dorsal sclerites; proscutum projecting laterally into large subquadrate lobes; prosternum subdivided into a pair of sclerites divided by a narrow gap; legs short, 5-segmented with well-developed claw. Meso- and metathorax each with two pairs of pubescent finger-like lateral projections. ***Abdomen*.** Abdominal segments 1–7 each with two pairs of pubescent finger-like lateral projections; segment 8 with an elongate dorsal sclerite, its posterior margin sinuate; stigmatic atrium well-developed.

Association with adults. We sequenced all genera of the subfamily Cylominae world-wide except of the Australian genus *Petasopsis*, and may positively eliminate the possibility that the larva described below belongs to any of them. *Petasopsis* is known by a single small species (body length = 1.9–2.0 mm) occurring in northern Australia. The body size of this species does not correspond to *Enigmahydrus*, and also the distribution of *Petasopsis* makes it very unlikely that it can be congeneric with *Enigmahydrus*. *Enigmahydrus* is clearly revealed as sister to the New Zealand-endemic genus *Saphydrus*, but differs from all known larval forms assigned to this genus above. Considering the

usual ratio of the body size of L3 larva and corresponding adults (Figs 5a–i), the adult of *Enigmahydrus* has to be a beetle of about the size of *S. obesus*. The latter species can be excluded due to its supposed close relationship to *S. suffusus* (assuming that its larva should be morphologically similar to *S. suffusus*), which is further supported by the fact that the candidate larva for *S. obesus* diagnosed above clearly differs from that of *Enigmahydrus*. The remaining two species of *Saphydrus* for which no candidate larvae are available (*S. monticola* and *S. moeldnerae* sp. nov.) are too small to be adults of *Enigmahydrus* species described below.

Etymology. The name is formed from the simplified version of the Latin *aenigma* (mystery) and *-hydrus*, a common ending in generic names in the Hydrophilidae; the names refers to the fact that the adult stage of this genus was not yet collected and remains a mystery. Gender masculine.

***Enigmahydrus larvalis* sp. nov.**

Type material. ***Holotype:*** 1 L3 (sequenced: MF665) (NZAC): **NEW ZEALAND: Taranaki:** unnamed stream 0.2 km S of Pukeiti Garden, 9 km E of Okato, lowland *Nothofagus* forest, sifting of leaf litter, 370 m, 173.98°S 39.20°E, 30.xi.2012, lgt. Becker, Fikáček, Hájek (NZ27). ***Paratypes used for morphology description:*** **NEW ZEALAND: Waikato:** 3 L1, 11 L2, 8 L3 (KMNH, NMPC): NEW ZEALAND: AK: Kohukohunui, Hunua Ra., 600 m, 30. Mar. 74, G. Kuschel litter 74/20. ***Additional paratypes:*** **NEW ZEALAND: Northland:** 1 L1, 3 L2, 3 L3 (NZAC): Omahuta Reserve [c. 173.62°S 35.24°E], 21.i.1972, G. W. Ramsay (72/58); 1 L1, 2 L2, 4 L3 (NZAC): Waipoua Kauri Forest, litter [c. 173.55°S 35.65°E], 19.i.1972, lgt. G. W. Ramsay (41/72); 1 L3 (NZAC): Waipoua State Forest, Te Matua Ngahere, leaf litter [c. 173.52°S 35.60°E], 4.ii.1975, lgt. J. C. Watt (75/94); 3 L3 (NZAC): Ngaiotonga Scenic Reserve, litter [c. 174.26°S 35.31°E], 20.i.1972, lgt. G. W. Ramsay (72/52); 1 L1, 3 L2, 1 L1 (NZAC): Mangamuka Range, litter [c. 173.47°S 35.18°E], 21.i.1972, lgt. G. W. Ramsay (72/61); 25 larvae (NZAC): Puketi State Forest, litter [c. 173.73°S 35.22°E], 21.i.1972, lgt. G. W. Ramsay (72/56); 7 L3, 1 L1 (NZAC): Waipoua Kauri Forest, litter [173.55°S 35.65°E], 19.i.1972, lgt. G. W. Ramsay (40/72); 8 L3, 1 L2 (NZAC): same label data, but 72/42; 2 L3, 2 L1 (NZAC): same label data but 39/72; 27 larvae (NZAC): Mangamuka Range, summit, litter [c. 173.47°S 35.18°E], 21.i.1972, lgt. G. W. Ramsay (72/50); 2 L3, 2 L2,

1 L1 (NZAC): Trounson Kauri Park, Kaihu [c. 173.64°S 35.72°E], 19.i.1972, lgt. G. W. Ramsay (38/72); 1 L2 (NZAC): Omahuta State Forest, moss on fallen tree [c. 173.62°S 35.24°E], 30.vi.1965, lgt. M. S. Luxton; 10 L1, 4 L2, 1 L3 (NZAC): Trounson Kauri Park, Kaihu [c. 173.64°S 35.72°E], 19.i.1972, lgt. G. W. Ramsay (72/37); 2 L3 (NZAC): Kauri Sanctuary, Anahutu Forest, Kaitaia, litter under *Agathis australis* [c. 173.26°S 35.17°E], 8.v.1974, lgt. G. Kuschel (74/34); 1 L1, 2 L2, 3 L3 (NZAC): Waipoua [c. 173.55°S 35.65°E], 19.x.1962, lgt. R. A. Cumber; 1 L1, 2 L2, 6 L3 (NZAC): Omahuta Kauri Reserve [c. 173.62°S 35.24°E], 21.i.1972, lgt. G. W. Ramsay (72/59). **Auckland:** 1 L1, 6 L2, 2 L3 (NZAC): Hunua Range, Kohukohunui [c. 175.21°S 37.03°E], 30.iii.1974. lgt. G. Kuschel (74/19); 5 larvae (NZAC): Hunua Range, Kohukohunui, 600 m [c. 175.21°S 37.03°E], 30.iii.1974, lgt, G. Kuschel (74/20). **Waikato:** 2 L1, 2 L3 (NZAC): Mamaku Range, Rotorua, litter [c. 176.04°S 38.07°E], 18.i.1972, lgt. G. W. Ramsay (72/26); 22 larvae (NZAC): Mt. Pirongia, 350 m [c. 175.13°S 37.97°E], 2.x.1970, lgt. A. W. Don. **Coromandel:** 6 L1, 1 L2, 4 L3 (NZAC): Coromandel Range, near summit Auckland, litter, lgt. G. W. Ramsay. **Bay of Plenty:** 2 L2, 3 L3 (NZAC): Horohoro State Forest, Mamaku Plateau, litter, 550 m [c. 176.12°S 38.27°E], 27.vii.1976, lgt. J. S. Dudgale (76/45); 5 L2, 5 L2 (NZAC): Mamaku Range, Rotorua, litter [c. 176.12°S 38.27°E], 20.xi.1974. lgt. A. K. Walker (74/88). **Nelson:** 3 L2, 3 L3 (NZAC): Whangamoa Saddle, 312 m [c. 173.43°S 41.22°E], without date and collector data.

Description of larva. First instar. ***General morphology.*** First instar larva superficially similar to third instar. Frontal lines complete, lyriform; coronal line absent. Antenna proportionally stouter and shorter than third instar. Antennomeres 1 and 2 subequal in width; antennomere 3 relatively larger than third instar. Mandibles bearing fine cuticular projections situated basally on inner face and lateral face; finer and sparser than third instar. Two inner mandibular teeth subequal in size. Maxilla proportionally stouter than third instar. Labium: ligula-like projection (see general morphology of third instar and discussion) proportionally stouter than third instar; basal half of ligula-like projection sclerotized dorsally.

Primary chaetotaxy of head capsule. *Frontale* (Figs 10A,E). Central part with two sensilla (FR1, FR2); Pore-like sensillum FR2 situated anterolaterally to short, stout seta FR1. Rather long seta FR5 and pore-like sensilla FR4 posteromesal to antennal socket; FR4 close and mesal to FR5. Short setae FR6 and FR7 close to posteromesal margin of antennal socket; FR6 close to frontal line; FR7 on mesal face. Sensilla FR9–14 on

epistome; FR9 long seta, FR10 short seta, FR12 short, stout seta, FR11, FR13, FR14 pore-like. FR9 and FR14 on lateral part, close to antennal socket, FR9 behind FR14. FR10–13 on mesal part; FR11 and FR13 close to antennal margin; FR13 lateral to FR11. FR12 behind FR13; FR10 behind FR12. Three sensilla (FR3, FR8, FR15) behind teeth of nasale. Short stout seta FR3 situated mesally to short seta FR8; pore-like sensillum FR15 close to mesal setae of gFR1. Nasale with a group of six rather short, stout setae and two ventral setae (gFR1). Two rather short setae (gFR2) on epistomal lobe, close to lateral-most seta of gFR1.

Parietale (Figs 10A–D). Dorsal surface with a group of five setae (PA1–5) forming irregular row in posterior part; PA3 pore-like, remaining four short setae. Pore-like sensillum PA6 close to posterior end of frontal line. Very long seta PA7 on mesal part of dorsal surface of parietale, on midlength of parietale. One very long additional seta behind PA7 (presence of this seta variable even in the same individual; this is present on right side but absent on left in figured specimen; compare Fig. 10A and B). Long seta PA8 mesal to anterior row of stemmata. Long seta PA9 situated posterolaterally to antennal socket. Pore-like sensillum PA10 between mesal-most stemmata of anterior and posterior rows; short seta PA11 between median ones. Supposed PA12–14 short to rather short, stout setae on median part of dorsal face of parietale; their position variable (compare Fig. 10A and B; in the figured specimen, anterior one rather short on right side but posterior one rather short on left). PA19–22 on anterior corner of head capsule; PA19 pore-like on dorsolateral part; PA20 rather short seta, dorsal to PA21; PA21 extremely long seta; PA22 long seta, between PA23 and PA21. PA22 undetectable on one side of examined specimen (compare Fig. 10C and D). Pore-like sensilla PA23–25 behind ventral mandibular articulation; PA23 situated laterally; PA24 and PA25 on inner part; PA24 between PA23 and PA25, close to PA25. Rather short seta PA16 on lateral face, behind stemmata; PA16–18 and PA26 forming transverse row; Very long seta PA18 and pore-like sensilla PA17 on lateroventral face; PA17 situated ventrally to PA18; PA26 on lateral part of ventral surface. Pore-like sensillum PA15 situated on tubercle, on midlength of lateral face of parietale. Pore-like sensillum PA30 situated posteromesally to PA15. Three sensilla (PA27–29) situated on medioposterior part of ventral surface of parietale; PA27 pore-like, PA28 extremely long seta, PA29 pore-like. PA27 close and anterior to PA28; PA29 posteromesal to PA28.

Chaetotaxy of head appendages. *Antenna* (Fig. 11A). Antennomere 1 likely bearing five pore-like sensilla; AN1 laterally on anterior third; AN2 subapical of dorsal surface

of sclerite; AN3 may be situated laterally on anterior margin undetectable in examined L1 specimen; AN4 situated dorsally on inner part of borderline between sclerite and intersegmental membrane; AN5 medially on anterior margin of ventral surface. Antennomere 2 with one pore-like sensillum (AN6) situated dorsolaterally on subapical part of sclerite and five sensilla (AN7, 8, 10, 11, SE1) on intersegmental membrane between antennomeres 2 and 3. Sensorium SE1 slender, as long as or slightly longer than antennomere 3. very short setae AN7 and AN8 on lateral face, behind SE1. Long seta AN10 and short, rather stout seta AN11 on inner face. Antennomere 3 with group of six apical sensilla of variable length (gAN).

Mandibles (Fig. 11D). Three pore-like sensilla (MN2–4) forming triangle laterally to inner tooth. MN3 close to base of inner tooth; MN4 on lateral part; MN2 behind MN4. Long seta MN1 situated close and laterally to MN2. Minute seta MN5 on anterior part of outer face. MN6 minute, present subapically on incisors area.

Maxilla (Fig. 11B–C). Cardo with one ventral seta (MX1). Inner face of stipes with longitudinal row of five setae (MX7–11). MX7 narrowest, rather stout, rather long, situated subbasally. MX8–9 stout, rather short, nearly equidistant on inner face. Pore-like sensilla MX2 and MX3 located ventrally on posterior third of stipes; MX2 on outer face, MX3 on inner face. Pore-like sensillum MX4 and very long setae MX5 and MX6 subapically on lateral face; MX4 between MX5 and MX6; MX5 posteromesally to MX4. Dorsal face of palpomere 1 bearing one rather long, very stout seta (MX16) situated medially on inner face. MX12–14 situated lateroventrally on subapical part of sclerite; MX12 pore-like, MX13 very long seta, MX14 long seta; MX12 very close to MX13, behind MX13; MX14 mesal to MX12 and MX13. MX15 and MX17 pore-like, on membrane behind inner appendage, MX17 dorsal, MX15 ventral. Inner appendage bearing setae of variable length apically (gAPP). Palpomere 2 with two pore-like sensilla (MX18 and MX19) and one minute seta (MX27). MX18 situated ventrally on subapical part of lateral face; MX19 on inner face of intersegmental membrane between palpomeres 2 and 3; MX27 subbasally on lateral face. Palpomere 3 with four sensilla (MX20–23). MX20 and MX23 subapically on outer face; MX20 pore, ventrally to MX23, MX23 very long seta. MX21 and MX22 on inner part of ventral surface; rather long seta MX21 on apical part; MX22 pore-like, behind MX21. Palpomere 3 with four sensilla (MX24–26), and several minute setae (gMX) on apical membranous area. MX24 long seta situated subbasally on inner face; MX24 and MX25 subapically on outer face, MX25 digitiform on dorsal face; MX26 pore-like on ventral.

Labium (Fig. 11E). Submentum with two pairs of setae (LA1–2). LA1 very long on lateral margin, LA2 minute on anterolateral corner. Mentum with two ventral sensilla (LA3, LA4) situated laterally on subapical part; short, stout seta LA3 posteromesal to pore-like sensillum LA4. Prementum with four pairs of sensilla (LA5–8) on sclerite. LA8 pore-like, on dorsal face, behind ligula. LA5–7 situated laterally on ventral surface, minute seta LA5 at base, pore-like sensillum LA7 subapically, long seta LA6 between LA5 and LA7. Ligula-like projection with four pair of sensilla; LA9, LA10, LA12 on dorsal face, LA11 ventral. LA9 on membrane, about midlength of projection close to borderline between sclerite and membrane. LA10–12 on apical area; minute seta LA10 on lateral part; minute sensilla LA12 on median part; LA11 pore-like. Palpomere 1 with two sensilla (LA13–14); LA13 minute seta situated basally on ventral surface; LA14 pore-like, dorsally on intersegmental membrane between palpomeres 1 and 2. Palpomere 2 with one pore-like sensillum LA15 situated on anterior part of outer face; several setae of variable shape and length (gLA) on apical membranous area.

Third instar larva. ***General morphology. Body*** wide, elongated oval, rather flat, with long finger-like lateral projections. Body length ca. 9.3 mm. Colour. Head reddish brown. Thorax and abdomen yellowish with reddish brown sclerites; median part of abdomen darker than lateral part. Dorsal plate of spiracular atrium lighter in colour than other sclerites. Whole dorsal surface often covered by dirt and destritus in examined specimens.

Head. Head capsule subhexagonal, head width 1.3 mm; cervical sclerites moderately small, subquadrate. Frontal lines visible only basally. Surface of head capsule covered with small, scale-like microstructure bearing minute projections anteriorly on dorsal, lateral, lateroventral surfaces. Six stemmata on each anterolateral portion of head capsule. Posterior tentorial pits present close to junction of submentum sulcus and gular sulcus. Clypeolabrum almost symmetrical. Nasale projecting further than epistomal lobe, with five distinct teeth of the same length, each bearing small toothlets subapically. Epistomal lobe present, almost symmetrical, rounded apically. Epistomal lobe bearing fringe of hair-like cuticular projections on anterior margin; inner part of epistomal lobe and the part behind nasal teeth bearing numerous short, small fringes of hair-like cuticular projections.

Antenna (Fig. 13A) 3-segmented, slender. Surface of antennomeres bearing very densely arranged minute hair-like cuticular projections except on ventral surface of

posterior part of antennomere 1. Antennomere 1 widest, shorter than antennomere 2, antennomere 3 small, as long as sensorium SE1.

Mandibles (Fig. 13B) rather slender, symmetrical, strongly curved, with two inner teeth on median part. Anterior inner teeth slightly larger than posterior one. Inner part bearing densely arranged fine cuticular projections basally.

Maxilla (Fig. 13C–D) 6-segmented, slender, longer than antenna, bearing fine to long hair-like cuticular projections. Cardo subtriangular, large. Stipes the longest, inner face and outer face bearing very densely arranged hair-like cuticular projections of variable length. Maxillary palpus slender. Dorsal and inner part of ventral face of palpomeres 1–3, including intersegmental membrane, bearing densely arranged short hair-like cuticular projections; palpomere 4 bearing fine cuticular projections close to MX24. Palpomere 1 cylindrically sclerotized, longest and widest. Inner process sclerotized, bearing fine, hair-like cuticular projections. Palpomere 2 shorter than palpomere 3; length of palpomere 3 subequal to that of palpomere 4.

Labium (Fig. 13E) well developed. Submentum fused to head capsule, transverse. Mentum and prementum completely sclerotized, fused, borderline between mentum and prementum visible ventrally as fine sulcus. Prementum extending anteriorly at mesal area into ligula-like projection; ligula fused with anterior membranous area of prementum, situated on the top of the ligula-like projection (see Discussion). Dorsal surface of basal to lateral part of mentum covered with scale-like structures each bearing ca. 1 to 5 hair-like projections on its apex; lateral face of mentum and prementum (except ligula-like projection) bearing densely arranged hair-like cuticular projections. Anterior membranous area of prementum and membranous ligula bearing fine cuticular projections. Labial palpus rather short, densely covered with fine hair-like cuticular projections dorsally and laterally. Palpomere 1 wider and slightly shorter than palpomere 2.

Thorax. Membranous parts very densely covered with fine hair-like cuticular projections. Prothorax wider than head capsule. Proscutum formed by one large, transverse plate subdivided by fine sagittal line; anterior and posterior margins weakly sclerotized. Proscutal plate covered with cuticular microstructures and setae of variable length; surface of apical part of stout setae granulate; lateral part extending as two subquadrate projections. Prosternal sclerites divided into two plates separated from each other mesally, each bearing numerous setae on anterior part. Mesonotum with three pairs of dorsal sclerites. Anterior pair narrow, transverse; posterior pair large, transverse;

lateral pair narrow. Lateral face of mesonotum with one long finger-like projection projected laterally and one small projection bearing numerous short setae. Mesothoracic spiracles on lateral face, anterior to lateral finger-like projection, forming a small finger-like projection. Metanotum with one pair of large, oval, transverse dorsal sclerites. Lateral face with two projections similar to those on mesonotum. Legs short but well developed, 5-segmented.

Abdomen 10-segmented, membranous parts covered with densely arranged cuticular projections. Spiracles laterodorsally on anterior part of segments 1–7, slightly projecting as tubercle. Segment 1 with one pair of rather small, oval, transverse dorsal sclerites anteromedially; lateral face with two long finger-like projections laterally, posterior one slightly shorter than anterior one. The projections bearing densely arranged short, hair-like cuticular projections and numerous rather long, stout setae. Three transverse rows of tubercles present dorsally. Segments 2–7 similar to segment 1, but dorsal sclerites absent. Spiracular atrium: Segment 8 with one pair of finger-like projections projected posteriorly. Procercus short. Segment 9 trilobed, small, partly sclerotized. Lateral lobe of spiracular atrium subequal to median lobe of spiracular atrium in length, bearing one very long seta; median lobe of spiracular atrium sclerotized dorsally, subquadrate, wider than lateral lobe. Urogomphus short, not visible from dorsal and ventral views.

Chaetotaxy of head capsule. Arrangements of primary sensilla similar to first instar, but third instar larva bearing many secondary sensilla. *Frontale*. Posterior to central parts bearing sparsely arranged short stout secondary setae; numerous rather short, scale-like secondary setae present on anterior part behind nasale teeth and mesal part of epistomal lobe. *Parietale*. Irregular row of short, stout secondary setae along reduced frontal line;

dorsal, lateral and lateroventral surface bearing numerous secondary setae but some parts bare; setae on dorsal surface short, stout; those on ventral surface long. Distribution of secondary setae almost same as that of small, scale-like cuticular microstructures on the surface. *Antenna* (Fig. 13A). Sensorium SE1 proportionally slenderer than in first instar. *Mandibles* (Fig. 13B). Mandibles bearing numerous short, stout secondary setae; setae sparsely arranged on apical half, densely arranged on lateral part of basal half. MN1 between MN2 and MN4. *Maxilla* (Fig. 13C–D). Stipes bearing secondary setae on ventral face; four rather short, stout setae along inner face; six short setae on median and outer part. *Labium* (Fig. 13E). Labium with numerous secondary setae; short to very long setae on outer face of mentum and prementum; long setae forming lateral fringe. One pair of longitudinal rows of short stout setae present on

median part of prementum to ligula behind LA9. LA9 situated apical part of ligula-like projection.

Etymology. The species name *larvalis* refers to the fact that the species is so far known only by its larval stage.

Biology. Terrestrial species. Larvae were collected from by sifting moist leaf litter in lowland rainforests. Adults remain unknown.

Distribution. Larvae were common and widespread in 1970s (Fig. 14A). At the moment the only population is known in lowland part of Mt. Egmont National Park, based on a single larva collected in 2012. The locality was revisited and sampled in 2016, but no additional specimens were found.

Discussion

Why are *Saphydrus* and *Enigmahydrus* rarely collected?

Our study accumulated all available material of *Saphydrus* and *Enigmahydrus* and confirmed that all six species are very infrequently collected. Rarity could be the result of species existing at low population densities and/or in restricted geographical ranges. Or the species could be common, just overlooked and not often collected due to their unusual biology. We analyzed the specimen data for all species to disentangle these two possibilities.

Distribution (Fig. 14A). Based on known records, most species are widespread, distributed across the North Island and northern part of South Island (*Saphydrus suffusus*, *S. obesus* and *Enigmahydrus larvalis*), over the northern part of North Island (*S. monticola*) or across the Southern Alps in the South Island (*S. tanemahuta*). Only *S. moeldnerae* is known from a single locality and may be more local.

Rarity of adults. Larvae are collected rather frequently compared to adults of *Saphydrus*; in *Enigmahydrus larvalis* only larvae are known and adults were never collected. This is unusual for the life history of beetles: the adult is the freely living or active stage which is more apparent, often capable of flight, and easier to collect while larvae are more sedentary, actively feeding in their specific microhabitats (and, therefore, remain unknown for most beetle taxa). This suggests that adults of *Saphydrus* and *Enigmahydrus* are very seasonal and/or short-lived. In hydrophilid beetles. the larval stage lasts for 20–60 days (Fikáček 2019a). Hence, larvae may be more likely found using appropriate sampling methods than adults living for few days each year. The observations of mass

occurrence of *S. suffusus* may also indicate short-lived adults and swarming behavior: two samples examined (collected by FIT and pitfall traps) contain 80–160 specimens each. RL also observed a mass swarming of this species at Maruia Springs in 2011, i.e. once in 25 years of his regular field work across New Zealand. In contrast to adults, larvae of *S. suffusus* may be locally common in forest leaf litter: in December 2012 we found them in four of six samples of leaf litter collected at middle elevations of Mt. Egmont - an area frequently visited by entomologists where only two adult specimens were collected within the last 45 years. The absence of adult specimens of *E. larvalis* despite the frequent capture of larvae in the early 1970s also corresponds to this pattern.

Seasonality over the year (Fig. 14B). The most common *S. suffusus* shows the seasonal peak for adults in summer (December-January) which overlaps with the period of highest collecting activity (dotted line in Fig. 14B). The limited data for the other *Saphydrus* species do not contradict this pattern (summer occurrence); *Saphydrus obesus* is the only exception: all adult records are from winter and spring (June to November). This may be, in combination with the expected short lifespan of adults, the reason why this species is so infrequently collected. Larval data are more complete for *Enigmahydrus* only, likely due to the very apparent morphology of the larvae making it hard-to-overlook in the samples. They indicate the larval occurrence all over the year, a pattern not seen in the other species, and unusual for temperate and subtropical Hydrophilidae (Fikáček 2019a). The January peak in Fig. 14B seems to be an artifact caused by high collecting effort in this month (most examined samples from 1970 were collected in January).

Altitudinal distribution (Fig. 14C). At least three species (*S. obesus*, *S. monticola* and *E. larvalis*) mainly occur at low altitudes (up to 400 m a.s.l.), i.e. areas which are most affected by agriculture and timber plantations eliminating native forests which are habitats of these species (Ewers *et al.* 2006). The most common *S. suffusus* occurs mainly between 400–600 m a.s.l. which corresponds to the altitude of most forested protected areas and national parks. *Saphydrus tanemahuta* is the only species confined to alpine environment which might explain its rarity since alpine areas are not frequently visited by collectors. The recent intensive sampling in alpine tussock areas in South Island by one of us (RL) did not succeed in re-capturing this species.

Records through time (Fig. 14D). The population dynamics data are usually not available for insects; indirect information was gained by evaluating the number of records over years. This analysis shows a recent increase in the number of records for *S. suffusus*, partly corresponding to the increased collecting effort from 2000 onwards (but not to the

high collecting effort in the 1970s; dotted line in Fig. 14D). The use of flight intercept and baited pitfall traps, collecting methods which were infrequently used before, is a plausible reason for this pattern. In *S. obesus* and *S. monticola*, the records are infrequent but more or less randomly distributed through the history, which indicates small but stable, randomly sampled populations. The data for *E. larvalis* suggest that the species may have been common and widespread in the early 1970s. This contrasts strongly with the only post-1970s record based on a single larva, despite the intensive sampling of leaf litter across New Zealand within the last 20 years, including sampling in Northland which represents most 1970s records. We suppose that the records for *Enigmahydrus larvalis* indicate a strong decline in the number of populations.

Are the species threatened? We conclude that for most species rarity may be linked to an unusual biology (short-lived adults, in *S. obesus* with winter occurrence) possibly combined with low population densities or with locally restricted populations. Additional surveys are necessary to evaluate the status of *S. obesus*, *S. tanemahuta*, *S. monticola* and *S. moeldnerae*. In *S. suffusus*, the data indicate that the species is widespread, common, and was overlooked due to short bursts of adult activity. *Enigmahydrus larvalis* is the only taxon in which a strong decline in the number of populations and specimens is observed. At the moment, only a single population is known in restricted areas of lowland forest on the north-east foothills of Mt. Egmont (Taranaki); the repeated visits of that locality in 2016 failed to record the species. We hence suppose that the population is quite small and local, fulfilling the criteria by Townsend et al. (2008) to classify the species as nationally endangered. We moreover show that *Enigmahydrus* is a phylogenetically isolated ancient lineage and may be highly specialized in larval prey preference (see below), which further underlines the need for its conservation (e.g., Rolland *et al.* 2012).

Phylogenetic position of *Saphydrus* and *Enigmahydrus*

Our phylogenetic analysis shows that *Saphydrus* and *Enigmahydrus* form an isolated lineage of New Zealand Cylominae and are phylogenetically distant from other New Zealand endemic genera. The principal clade into which *Saphydrus* and *Enigmahydrus* belong has today an extremely disjunct distribution and is very poor in species: *Enigmahydrus*+*Saphydrus* lineage is the most speciose (New Zealand, 6 species), followed by *Relictorygmus* (South Africa, 2 species; Seidel *et al.* 2018), *Cylorygmus* (austral South America, 1 species; Seidel *et al.* 2018) and *Eurygmus* (Australia, 1 species; Hansen 1990, Fikáček 2019a). Divergence dating and historical biogeography analysis

are crucial to understand the reasons for this pattern. An ancient origin of the clade and a high background extinction may be a possible explanation, congruent with timing of the break-up of Gondwana (Africa separated from Gondwana ca. 135 million years ago (Mya), New Zealand from Australia ca. 85–65 Mya; Sanmartín and Ronquist 2004, Mortimer *et al.* 2017). Hence, *Saphydrus* and *Enigmahydrus* are likely old paleoendemic taxa (Giribet and Boyer 2010, Sharma and Wheeler 2013).

The sister-relationship of *Enigmahydrus* and *Saphydrus* corresponds well with the larval morphology of both genera, which share some unique characters like the nasale with five teeth of alternating size in the first instar, and the specific microsculpture of the dorsal head surface and head appendages. The surface structures may be an adaptation to camouflage: many examined larvae were covered by a layer of encrustation, which had to be carefully removed prior to the examination. The adult morphology cannot be compared since adults of *Enigmahydrus* are not known. However, the adult morphology of the genera in the whole clade is quite uniform, likely corresponding to the ancestral morphology of the Cylominae, and lacks apparent large-scale modifications (Seidel *et al.* 2018, Fikáček 2019a, this paper). Hence, adults of *Enigmahydrus* and *Saphydrus* may be quite similar to each other. In fact, we cannot completely exclude that *S. monticola* and *S. moeldnerae*, both with unknown larvae, may be congeneric with *E. larvalis*, since they differ from the other three *Saphydrus* species with known larvae by a few characters (quadrate pronotum, beaded clypeal margin). This possibility can only be rejected when the DNA-grade specimens of these two species will be available, or when adults of *E. larvalis* will be discovered and associated with the larva by DNA barcoding.

The larva of *Enigmahydrus* is at the moment the most unusual larva of the Hydrophilidae, both with respect to the details of its morphology and its general habitus. The most striking modification is that of the mouthparts which corresponds to the pattern in other hydrophilid larvae, genera often differ in details of mouthpart morphology, likely corresponding to different prey preferences. The differences mostly apply to the teeth of nasale (including their total loss in many Sphaeridiinae; e.g., Fikáček *et al.* 2015, Archangelsky 2018, Minoshima 2018) or the shape of mandibles (including their extreme asymmetry due to functional adaptations; Sato *et al.* 2017, Fikáček *et al.* 2018a,b). Less extreme modifications are found in the labium which is generally used to manipulate the food during the extraoral digestion (Fikáček 2019a): it bears a membranous ligula of varying size in many groups (Archangelsky 1997), a setose hypopharyngeal lobe likely facilitating the absorption of predigested food in few terrestrial groups (Archangelsky

1999, Fikáček *et al.* 2014), and it is reduced in size and likely not used for food manipulation in *Berosus*-like larvae (Fikáček *et al.* 2018a). In contrast, the labium of *Enigmahydrus* is enlarged, strongly sclerotized and bears two unique modifications: (1) mentum and prementum are fused, which is unknown for any other hydrophiloid larvae except for Spercheidae with filter-feeding habits (Fikáček 2019b), and (2) the anterior part of prementum is projecting in a long strongly sclerotized median process (this process resembles ligula, but the position of the sensilla LA9–12 on the tip of the projection indicates that only its apical membranous part is actually homologous with ligula of *Saphydrus*; compare Figs. 7D and 11E, 9D and 13E). Other unique characters are: (3) large protruding stemmata (Fig. 10A); (4) lateral parietal sensilla situated on tubercles (Fig. 10A); (5) antenna, maxillary stipes and base of premento-mentum with dense hair-like cuticular projections (e.g., Fig. 13); (6) proscutum with large subquadrate lobes (Fig. 5R; similar lobes, although much smaller, are only known in larvae of *Crenitis* and *Crenitulus* in Chaetarthriinae: Archangelsky and Fikáček 2004); (7) mesally separated prosternal sclerites (Figs 5S, 12C; only known in *Tormus* in Hydrophilinae: Fikáček *et al.* 2013); and (8) long pubescent lateral projections on abdominal segments 1–7 (slightly similar setose projections are present in aquatic larvae of *Regimbartia*, *Hydrochara* and *Crenitis* and are sometimes interpreted as tracheal gills; Archangelsky 1997; Minoshima and Hayashi 2011, 2015). As in other groups with unusual mouthparts, the strongly modified head morphology of *Enigmahydrus* indicates a specialized prey preference, unknown at the moment.

Acknowledgements

We are grateful to Nicole Gunter (Cleveland Museum of Natural History, Cleveland, USA) and Dominik Vondráček (National Museum, Prague) for providing part of the Cylominae sequences used in this study. We thank all the curators listed for making material from their instituions available to us for study. Tatiana Aghová (National Museum, Prague) is thanked for her help with the ancient DNA sequencing. This work was supported by the European Union's Horizon 2020 research and innovation program under the Marie Skłodowska-Curie grant agreement No. 642241 to M. Seidel and by the Ministry of Culture of the Czech Republic (DKRVO 2019-2023/5.I.a, National Museum, 00023272) to M. Fikáček and M. Seidel. The work of M. Seidel at the Department of Zoology, Charles University, Prague was partly supported by grant SVV 260 434 /2019.

R. Leschen was funded in part by core funding from the Crown Research Institute from the Ministry of Business, Innovation and Employment's Science and Innovation Group.

Author contribution

MS, MF and RL performed the field work; MS run the molecular and phylogenetic analyses; MF prepared the rarity and conservation status assessment; MS and MF studied the adult morphology and taxonomy; YM and MF studied the studies of immature stages; MF, MS and YM drafted the manuscript, all authors contributed to the writing.

References

Archangelsky, M. (1997). Studies on the biology, ecology, and systematics of the immature stages of New World Hydrophiloidea (Coleoptera: Staphyliniformia). *Bulletin of the Ohio Biological Survey, New Series* **12**, 1–207.

Archangelsky, M. (1999). Adaptations of immature stages of Sphaeridiinae (Staphyliniformia, Hydrophiloidea: Hydrophilidae) and state of knowledge of preimaginal Hydrophilidae. *Coleopterist Bulletin* **53**, 1, 64–79.

Archangelsky, M. (2018) Larval chaetotaxy and morphometry of Oosternum costatum (Coleoptera: Hydrophilidae) including a discussion of larval characters with phylogenetic relevance. *Acta Entomologica Musei Nationalis Pragae* **58**, 2, 499–511.

Archangelsky, M., and Fikáček, M. (2004). Descriptions of the egg case and larva of *Anacaena* and a review of the knowledge and relationships between larvae of Anacaenini (Coleoptera: Hydrophilidae: Hydrophilinae). *European Journal of Entomology* **101**, 629–636.

Arriaga-Varela, E., Seidel, M., Deler-Hernández, A., Senderov, V., and Fikáček, M. (2017). A review of the *Cercyon* Leach (Coleoptera, Hydrophilidae, Sphaeridiinae) of the Greater Antilles. *ZooKeys* **681**, 39-93. doi: 10.3897/zookeys.681.12522

Barrell, D. J. A. (2011). Quaternary glaciers of New Zealands. In: Ehlers, J., Gibbard, P. L., and Hughes, P. D. (eds). Quaternary Glaciations – extent and chronology. A closer look. *Developments in Quaternary Sciences* **15**, 1047–1064. doi: 10.1016/B978-0-444-53447-7.00075-1

Bloom, D. D., Fikáček, M., and Short, A. E. Z. (2014). Clade age and diversification rate variation explain disparity in species richness among water scavenger beetle

(Hydrophilidae) lineages. *PLoS ONE* **9**, e98430, 1–9. doi: 10.1371/journal.pone.0098430

Broun, T. (1880). Manual of the New Zealand Coleoptera. Colonial Museum & Geological Survey Department, Wellington, 651 pp.

Broun, T. (1893a). Manual of the New Zealand Coleoptera. Part V. Colonial Museum and Geological Survey Department, Wellington, pp. 975–1320.

Broun, T. (1893b). Manual of the New Zealand Coleoptera. Part VII. Colonial Museum and Geological Survey Department, Wellington, pp. 1395–1504.

Broun, T. (1921). Descriptions of new genera and species of Coleoptera. Part VI. *Bulletin of the New Zealand Institute* **1,** 6, 475–590.

Byttebier, B., and Torres, P. L. M. (2009). Description of the preimaginal stages of *Enochrus* (*Hugoscottia*) *variegatus* (Steinheil, 1869) and *E.* (*Methydrus*) *vulgaris* (Steinheil, 1869) (Coleoptera: Hydrophilidae), with emphasis on larval morphometry and chaetotaxy. *Zootaxa* **2139,** 1–22.

Daugherty, C. H., Gibbs, G. W., and Hitchmough, R. A. (1993). Mega-island or micro-continent? New Zealand and its fauna. *Trends in Ecology and Evolution* **8**, 12, 437–442. doi: 10.1016/0169-5347(93)90006-B

Ewers, R. M., Kliskey, A. D., Walker, S., Rutledge, D., Harding, J. S., and Didham, R. K. (2006). Past and future trajectories of forest loss in New Zealand. *Biological Conservation* **133**, 3, 312–325. doi: 10.1016/j.biocon.2006.06.018

Fattorini, S., Cardoso, P., Rigal, F., and Borges, P. V. A. (2012). Use of arthropod rarity for area prioritisation: insights from the Azorean Islands. *PLoS ONE* **7**, e33995. doi:10.1371/journal.pone.0033995

Fikáček, M. (2019a). 20. Hydrophilidae Leach, 1815. pp. 271–337. In: Slipinski, A., and Lawrence, J. (eds). Australian Beetles. Volume 2. Archostemata, Myxophaga, Adephaga, Polyphaga (part). CSIRO Publishing, Clayton South, 765 pp.

Fikáček, M. (2019b). 19. Spercheidae Erichson, 1837. pp. 265–270. In: Slipinski, A., and Lawrence, J. (eds). Australian Beetles. Volume 2. Archostemata, Myxophaga, Adephaga, Polyphaga (part). CSIRO Publishing, Clayton South, 765 pp.

Fikáček, M., Archangelsky, M., and Torres, P. L. M. (2008). Primary chaetotaxy of the larval head capsule and head appendages of the Hydrophilidae (Coleoptera) based on larva of *Hydrobius fuscipes* (Linnaeus, 1758). *Zootaxa* **1874**: 16–34.

Fikáček, M., Minoshima, Y., Vondráček, D., Gunter, N., and Leschen, R. A. B. (2013). Morphology of adults and larvae and integrative taxonomy of southern hemisphere

genera *Tormus* and *Afrotormus* (Coleoptera: Hydrophilidae). *Acta Entomologica Musei Nationalis Pragae* **53**, 1, 75–126.

Fikáček, M., Minoshima, Y. N., and Newton, A. F. (2014). A review of *Andotypus* and *Austrotypus* gen. nov., rygmodine genera with austral disjunction (Hydrophilidae: Rygmodinae). *Annales Zoologici* (Warszawa) **64**, 4, 557–596.

Fikáček, M., Maruyama, M., Komatsu, T., von Beeren, C., Vondráček, D., and Short, A. E. Z. (2015). Protosternini (Coleoptera: Hydrophilidae) corroborated as monophyletic and its larva described for the first time: a review of the myrmecophilous genus *Sphaerocetum*. *Invertebrate Systematics* **29**, 23–36.

Fikáček, M., Minoshima, Y. N., and Jäch, M. A. (2018a). Larval morphology of *Yateberosus*, a New Caledonian endemic subgenus of *Laccobius* (Coleoptera: Hydrophilidae), with notes on '*Berosus*-like' larvae in Hydrophiloidea, *Acta Entomologica Musei Nationalis Pragae* **58**, 1, 195–206.

Fikáček, M., Liang, W.-R., Hsiao, Y., Jia, F., and Vondráček, D. (2018b). Biology and morphology of immature stages of banana-associated *Protosternum* beetles, with comments on the status of Taiwanese endemic *P. abnormale* (Coleoptera: Hydrophilidae). *Zoologischer Anzeiger* **277**, 85–100.

Gillespie, R. G., and Will, K. (2018). Biodiversity of Arthropods on islands. Pp. 81–104. In: Foottit, R. G., and Adler, P. H. (eds). Insect Biodiversity: Science and Society II. Second Edition. Wiley-Blackwell, 1024 pp.

Giribet, G., and Boyer, S. L. (2010). 'Moa's Ark' or 'Goodbye Gondwana': Is the origin of New Zealand's terrestrial invertebrate fauna ancient, recent or both? *Invertebrate Systematics* **24**, 1, 1–8. doi: 10.1071/IS10009

Goldberg, J., Trewick, S. A., and Paterson, A. M. (2008). Evolution of New Zealand´s terrestrial fauna: a review of molecular evidence. *Philosophical Transactions of the Royal Society in London, B Biological Sciences* **363**, 1508, 3319–3334. doi: 10.1098/rstb.2008.0114

Grainger, N., Harding, J., Drinan, T., Collier, K., Smith, B., Death, R., Makan, T., and Rolfe, J. (2018). Conservation status of New Zealand freshwater invertebrates, 2018. *New Zealand Threat Classification Series* **28**, 1–25.

Gray, A., Wilkins, V., Pryce, D., Fowler, L., Key, R. S., Mendel, H., Jervois, M., Hochkirch, A., Cairns-Wicks, R., Dutton, A.-J., and Malan, L. (2018) The status of the invertebrate fauna on the South Atlantic islands of St. Helena: problems,

analysis and recommendations. *Biodiversity and Conservation* doi: 10.1007/s10531-018-1653-4

Gunter, N. L., Weir, T. A., Slipinski, A., Bocák, L., and Cameron, S. L. (2016). If dung beetles (Scarabaeidae: Scarabaeinae) arose in association with dinosaurs, did they also suffer a mass co-extinction at the K-Pg boundary? *PLoS ONE* 11, e0153570, 1–47. doi: 10.1371/journal.pone.0153570

Hallmann, C. A., Sorg, M., Jongejans, E., Siepel, H., Hofland, N., Schwan, H., Stenmans, W., Müller, A., Sumser, H., Hörren, T., Goulson, D., and de Kroon, H. (2017). More than 75 percent decline over 27 years in total flying insect biomass in protected areas. *PLoS One* **12**, e0185809, 1-21. doi: 10.1371/journal.pone.0185809

Hansen, M. (1990). Australian Sphaeridiinae (Coleoptera: Hydrophilidae): A taxonomic outline with descriptions of new genera and species. *Invertebrate Taxonomy* **4**, 317–395.

Hansen, M. (1991). The Hydrophiloid Beetles. Phylogeny, Classification and a Revision of the Genera (Coleoptera, Hydrophiloidea). *Biologiske Skrifter, Det Kongelige Danske Videnskabernes Selskab* **40,** 1–368.

Hansen, M. (1997). Synopsis of the endemic New Zealand genera of the beetle subfamily Sphaeridiinae (Coleoptera, Hydrophilidae). *New Zealand Journal of Zoology* **24**, 351–370.

Hansen, M. (1999). World Catalogue of Insects. Volume 2: Hydrophiloidea (s.str.) (Coleoptera). Apollo Books, Stestrup, 416 pp.

Herrera-Flores, J. A., Stubbs, T. L., and Benton, M. J. (2017). Macroevolutionary patterns in Rhynchocephalis: is the tuatara (*Sphenodon punctatus*) a living fossil? *Palaeontology* **60**, 3, 319–328. doi: 10.1111/pala.12284

Hoare, R. J. B., Dugdale, J. S., Edwards, E. D., Gibbs, G. W., Patrick, B. H., Hitchmough, R. A., and Rolfe, J. R. (2015) Conservation status of New Zealand butterflies and moths (Lepidoptera), 2015. *New Zealand Threat Classification Series* **20**, 1–13.

Kearse, M., Moir, R., Wilson, A., Stones-Havas, S., Cheung, M., Sturrock, S., Buxton, S., Cooper, A., Markowitz, S., Duran, C., Thierer, T., Ashton, B., Meintjes, P., and Drummond, A. (2012). Geneious Basics: an integrated and extendable desktop software for the organization and analysis of sequence data. *Bioinformatics* **25**, 12, 1647–1649. doi: 10.1093/bioinformatics/bts199

Knisch, A. (1924). Hydrophilidae. In Junk, W., and Schenkling, S. (eds). Coleopterorum Catalogus. Vol. 14, part 79. W. Junk, Berlin, 306 pp.

Lanfear, R., Frandsen, P. B., Wright, A. M., Senfeld, T., and Calcott, B. (2017). PartitionFinder2: New methods for selecting partitioned models of evolution for molecular and morphological phylogenetic analyses. *Molecular Biology and Evolution* **34**, 3, 772–773. doi: 10.1093/molbev/msw260

Lawrence, J. F., Slipinski, A., Seago, A. E., Thayer, M. K., Newton, A. F., and Marvaldi, A. E. (2011). Phylogeny of the Coleoptera based on morphological characters of adults and larvae. *Annales Zoologici* (Warszawa) **61**, 1, 1–217.

Leschen, R. A. B., Lawrence, J. F., Kuschel, G., Thorpe, S., and Wang, Q. (2003). Coleoptera genera of New Zealand. *New Zealand Entomologist* **26**, 15–28.

Leschen, R. A. B., Marris, J. W. M., Emberson, R. M., Nunn, J., Hitchmough, R. A., and Stringer, I. A. N. (2012)). The conservation status of New Zealand Coleoptera. *New Zealand Entomologist* **35,** 2, 91–98.

Lister, B. C., and García, A. (2018). Climate-driven declines in arthropod abundance restructure a rainforest food web. *Proceedings of the National Academy of Sciences on the United States of America* **115**, 44, E10397–E10406. doi: 10.1073/pnas.1722477115

McGlone, M. S., Duncan, R. P., and Heenan, P. B. (2001). Endemism, species selection and the origin and distribution of the vascular plant flora of New Zealand. *Journal of Biogeography* **28,** 2, 199–216.

McKenna, D. D., Wild, A. L., Kanda, K., Bellamy, C. L., Beutel, R. G., Caterino, M. S., Farnum, C. W., Hawks, D. C., Ivie M. A., Jameson, M. L., Leschen, R. A. B., Marvaldi, A. E., McHugh, J. V., Newton, A. F., Robertson, J. A., Thayer, M. K., Whiting, M. F., Lawrence, J. F., Slipinski, A., Maddison, D. R., and Farrell B. D. (2015). The beetle tree of life reveals that Coleoptera survived end-Permian mass extinction to diversify during the Cretaceous terrestrial revolution. *Systematic Entomology* **40**, 4, 835–880. doi: 10.1111/syen.12132

McKinney, M. L. (1999). High rates of extinction and threat in poorly studied taxa. *Conservation Biology* **13**, 6, 1273–1281. doi: 10.1046/j.1523-1739.1999.97393.x

Miller, M. A., Pfeiffer, W., and Schwartz, T. (2010). Creating the CIPRES Science Gateway for inference of large phylogenetic trees. *Gateway Computing Environments Workshop (GCE)* **2010**, 1–7. doi: 10.1109/GCE.2010.5676129

Minoshima, Y. N. (2018). Larval morphology of *Armostus ohyamatensis* Hoshina and Satô (Coleoptera: Hydrophilidae: Megasternini). *Coleopterists Bulletin*, **72,** 4, 767–778.

Minoshima, Y. N., Fikáček, M., Gunter, N., and Leschen, R. A. B. (2015). Larval morphology and biology of the New Zealand-Chilean genera *Cylomissus* Broun and *Anticura* Spangler (Coleoptera: Hydrophilidae: Rygmodinae). *Coleopterist Bulletin* **69**, 687–712.

Minoshima, Y., and Hayashi, M. (2011). Larval morphology of the Japanese species of the tribes Acidocerini, Hydrobiusini and Hydrophilini (Coleoptera: Hydrophilidae). *Acta Entomologica Musei Nationalis Pragae* **51,** supplementum, 1–118.

Minoshima, Y. N., and Hayashi, M. (2015). Description of the larval stages of the berosine genera *Berosus* and *Regimbartia* based on the Japanese species *B. japonicus* and *R. attenuata* (Coleoptera: Hydrophilidae). *Acta Entomologica Musei Nationalis Pragae* **55**, 47–83.

Minoshima, Y. N., Seidel, M., Wood, J. R., Leschen, R. A. B., Gunter, N. L., and Fikáček, M. (2018). Morphology and biology of the flower-visiting water scavenger beetle genus *Rygmodus* (Coleoptera: Hydrophilidae). *Entomological Science* **21**, 363–384.

Mortimer, N., and Campbell, H. (2014) Zealandia. Our continent revealed. Penguin Books, London, 271 pp.

Mortimer, N., Campbell, H. J., Tulloch, A. J., King, P. R., Stagpoole, V. M., Wood, R. A., Rattenbury, M. S., Sutherland, R., Adams, C. J., Collot, J., and Seton, M. (2017). Zealandia: Earth's Hidden Continent. GSA Today 27, 3, 27-35. doi: 10.1130/GSATG321A.1

Muggleton, J., and Benham, B. R. (1975). Isolation and the decline of the large blue butterfly (*Maculinea arion*) in Great Britain. *Biological Conservation* **7**, 2, 119–128. doi: 10.1016/0006-3207(75)90051-8

Orchymont, A. d'. (1916). De la place qui doivent occuper dans la classification les sous-familles des Sphaeridiinae et des Hydrophilinae. *Bulletin de la Société Entomologique de France* **(1916),** 235–240.

Orchymont, A. d' (1919). Notes complémentaires pour la classification et la phylogénie des "Palpicornia". *Revue Zoologique Africaine* **6,** 163–168.

Priddel, D., Carlile, N., Humphrey, M., Fellenberg, S., and Hiscox, D. (2003). Rediscovery of the 'extinct' Lord Howe Island stick-insect (*Dryococelus australis* (Montrouzier)) (Phasmatodea) and recommendations for its conservation. *Biodiversity & Conservation* **12**, 7, 1391–1403. doi: 10.1023/A:1023625710011

Prum, R. O., Berv, J. S., Dornburg, A., Field, D. J., Townsend, J. P., Lemmon, E. M., and Lemmon, A. R. (2015). A comprehensive phylogeny of birds (Aves) using targeted next-generation DNA sequencing. *Nature* **526**, 7574, 569–573. doi: 10.1038/nature15697

Rambaut, A. (2012). FigTree (version 1.4.0). Available at http://tree.bio.ed.ac.uk/software/figtree/

Rambaut, A., Drummond, A. J., Xie, D., Baele, G., and Suchard, M. A. (2018). Posterior summarization in Bayesian phylogenetics using Tracer 1.7. *Systematic Biology* **67**, 5, 901–904. doi: 10.1093/sysbio/syy032.

Rawlence, N., Scofield, R. P., McGlone, M. S., and Knapp, M. (2019). History repeats: large scale synchronous biological turnover in avifauna from the Plio-Pleistocene and Late Holocene of New Zealand. *Frontiers in Ecology and Evolution* **7**, 158, 1–8.

Rolland, J., Cadotte, M. W., Davies, J., Devictor, V., Lavergne, S., Mouquet, N., Pavoine, S., Rodrigues, A., Thuiller, W., Turcati, L., Winter, M., Zupan, L., Jabot, F., and Morlon, H. (2012). Using phylogenies in conservation: new perspectives. *Biology Letters* **8**, 5, 692–694. doi: 10.1098/rsbl.2011.1024

Ronquist, F., Teslenko, M., van der Mark, P., Ayres, D. L., Darling, A., Höhna, S., Larget, B., Liu, L., Suchard, M. A., and Huelsenbeck, J. P. (2012). *Systematic Biology* **61**, 3, 539–542. doi: 10.1093/sysbio/sys029

Sánchez-Bayo, F., and Wyckhuys K. A. G (2019). Worldwide decline of the entomofauna: A review of its drivers. *Biological Conservation* **232**, 8–27. doi: 10.1016/j.biocon.2019.01.020

Sanmartín, I., and Ronquist, F. (2004). Southern hemisphere biogeography inferred by event-based models: plant versus animal patterns. *Systematic Biology* **53**, 216–243.

Sato, S., Inoda, T., Niitsu, S., Kubota, S., Goto, Y., and Kobayashi, Y. (2017). Asymmetric larval head and mandibles of *Hydrophilus acuminatus* (Insecta: Coleoptera, Hydrophilidae): fine structure and embryonic development. *Arthropod Structure and Development* **46**, 6, 824e842.

Seidel, M., Arriaga-Varela, E., and Fikáček, M. (2016). Establishment of Cyclominae Zaitzev, 1908 as a valid name for the subfamily Rygmodinae Orchymont, 1916 with an updated list of genera (Coleoptera: Hydrophilidae). *Acta Entomologica Musei Nationalis Pragae* **56**, 1, 159–165.

Seidel, M., Minoshima, Y. N., Arriaga-Varela, E., and Fikáček, M. (2018). Breaking a disjunct distribution: a review of the southern hemisphere genera *Cylorygmus* and *Relictorygmus* gen. nov. (Hydrophilidae: Cylominae). *Annales Zoologici* (Warszawa) **68**, 2, 375–402. doi: 10.3161/00034541ANZ2018.68.2.011

Sharma, P. P., and Wheeler, W. C. (2013). Revenant clades in historical biogeography: the geology of New Zealand predisposes endemic clades to root age shifts. *Journal of Biogeography* **40**, 1609–1618.

Sharp, D. (1884). Revision of the Hydrophilidæ of New Zealand. *Transactions of the Entomological Society of London* **(1884),** 465–480.

Shirayama, Y., Kaku, T., and Higgins, R. P. (1993). Double-sided microscopic observation of meiofauna using an HS-slide. *Benthos Research* **44**, 41–44. (In Japanese with English title and abstract)

Short, A. E. Z., and Fikáček, M. (2013). Molecular phylogeny, evolution and classification of the Hydrophilidae (Coleoptera). *Systematic Entomology* **38**, 723–752. doi: 10.1111/syen.12024

Thogmartin, W. E., Wiederholt, R., Oberhauser, K., Drum, R. G., Diffendorfer, J. E., Altizer, S., Taylor, O. R., Pleasants, J., Semmens, D., Semmens, B., Erickson, R., Libby, K. and Lopez-Hoffman, L. (2017) Monarch butterfly population decline in North America: identifying the threatening processes. *Royal Society Open Science* **4**, 170760, 1–16. doi: 10.1098/rsos.170760

Thomas, J. A. (2005). Monitoring change in the abundance and distribution of insects using butterflies and other indicator groups. *Philosophical Transactions of the Royal Society in London, B Biological Sciences* **360**, 1454, 339–357. doi: 10.1098/rstb.2004.1585

Tippett, J. M., and Kamp, P. J. J. (1995). Geomorphic evolution of the Southern Alps, New Zealand. *Earth Surface Processes and Landforms* **20**, 177–192. doi: 10.1002/esp.3290200207

Townsend, A. J., de Lange, P. J., diffy, C. A. J., Miskelly, C. M., Molloy, J., and Norton, D. A. (2008). New Zealand threat classification system manual. Science & Technical Publishing, Department of Conservation, Wellington, 35 pp.

Wallis, G. P., and Trewick, S. A. (2009). New Zealand phylogeography: evolution on a small continent. *Molecular Ecology* **18**, 3548-3580. doi: 10.1111/j.1365-294X.2009.04294.x

Ward, D., Early, J., Schnitzler, F. R., Hitchmough, R., Rolfe, J., and Stringer, I. (2014). Conservation statusn of New Zealand Hymenoptera, 2014. *New Zealand Threat Classification Series* **20**, 1–14.

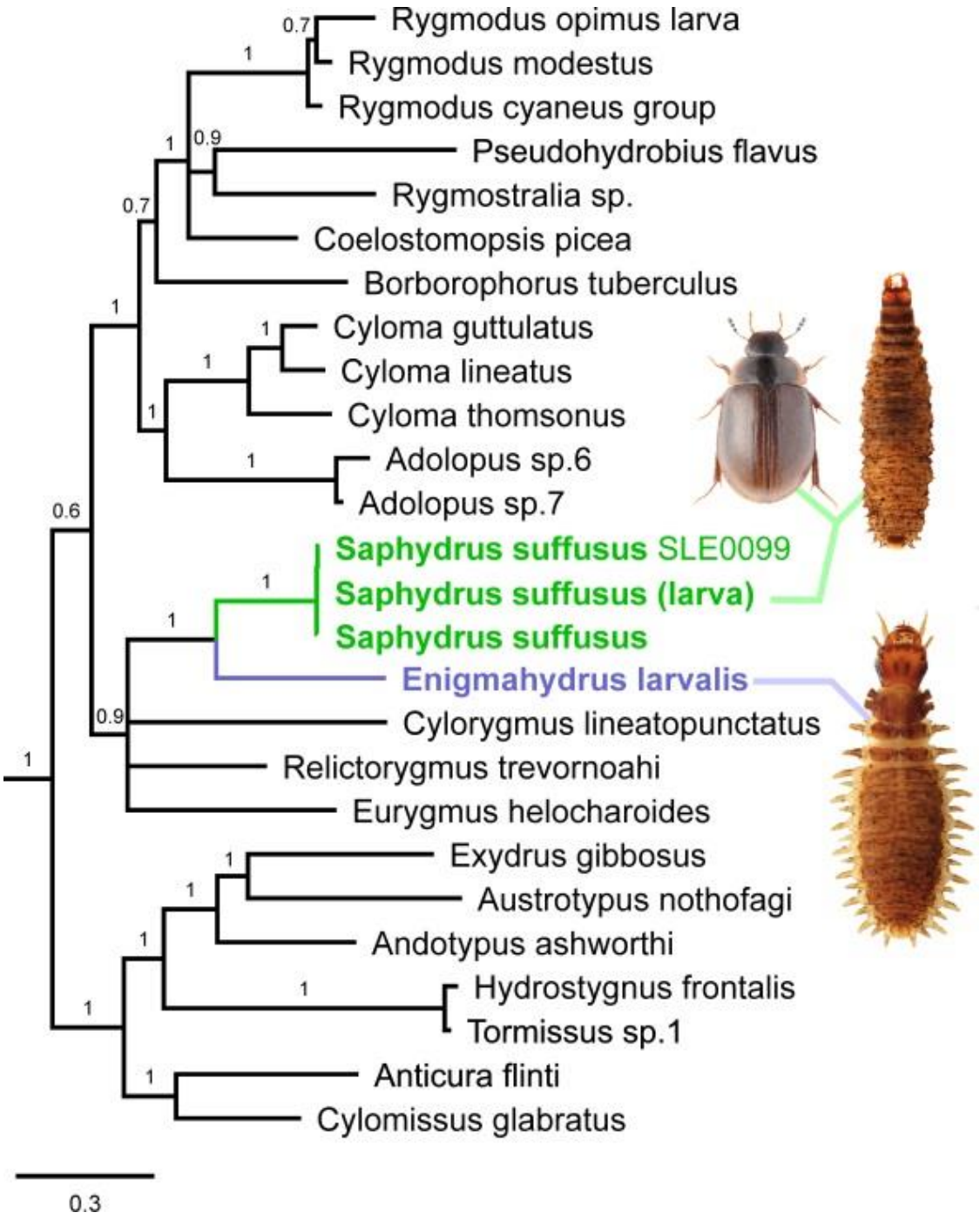

Figure 1. Phylogenetic relationships of the genera of Cylominae based on *cox1*, 16S, 18S and 28S sequences showing the position of *Saphydrus* and *Enigmahydrus*.

Figure 2. Adults of *Saphydrus*. A, F–G – *S. suffusus*, specimens from Buller, Rough Creek (TB455); B, H–I – *S. obesus*, paralectotype; C, J–K – *S. tanemahuta* sp. nov.; D, L–M – *S. monticola*, holotype; E, N–O – *S. moeldnerae* sp. nov., holotype. A–E – dorsal and lateral habitus. F, H, J, L, N – detail of head and pronotum; G, I, K, M, N – detail of punctation of elytral intervals. Figs F–O not to scale.

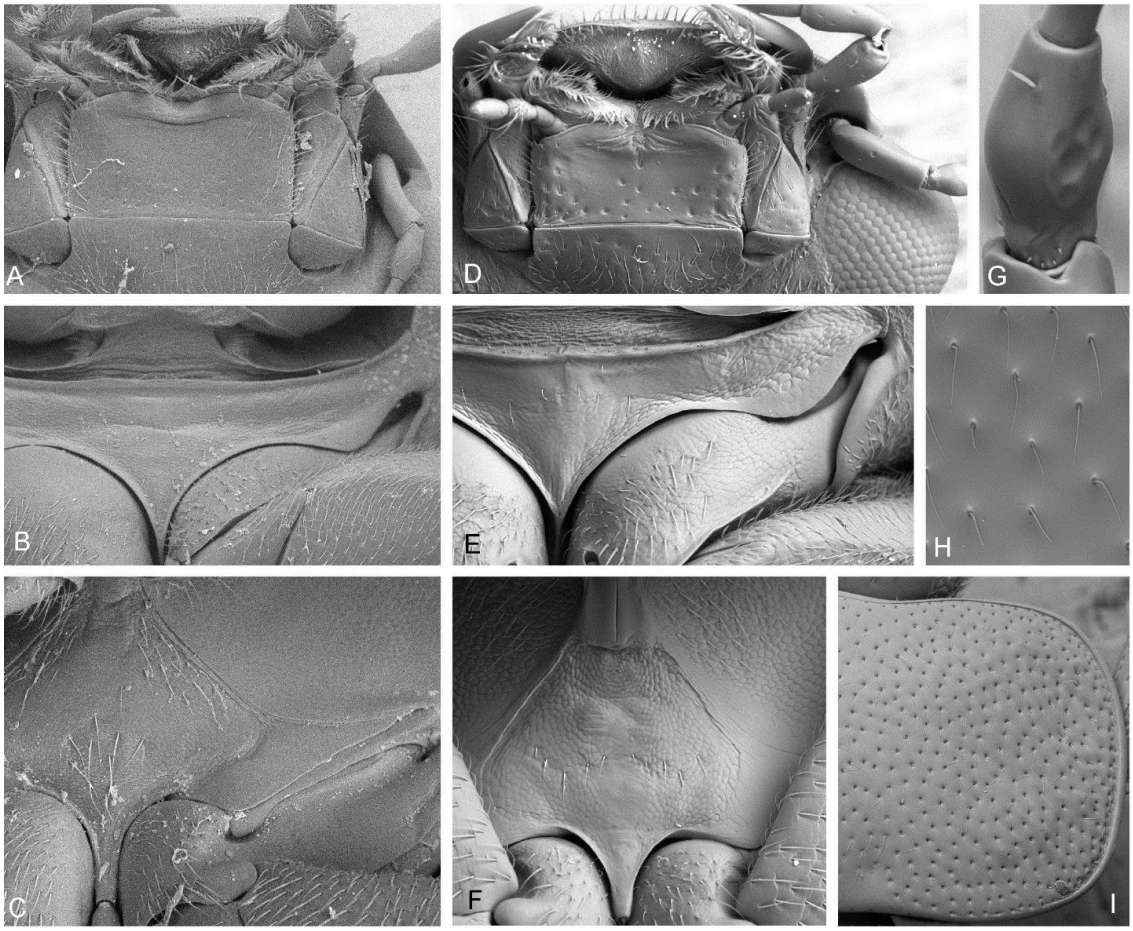

Figure 3. Adult morphology of *Saphydrus*. A–C – *S. suffuses*: A – mentum; B – prosternum; C – mesoventrite. D–I – *S. monticola*: D – mentum; E – prosternum; F – mesoventrite; G – antennal pedicel, dorsal view; H – setiferous punctation of elytra; I – pronotal shape and punctation.

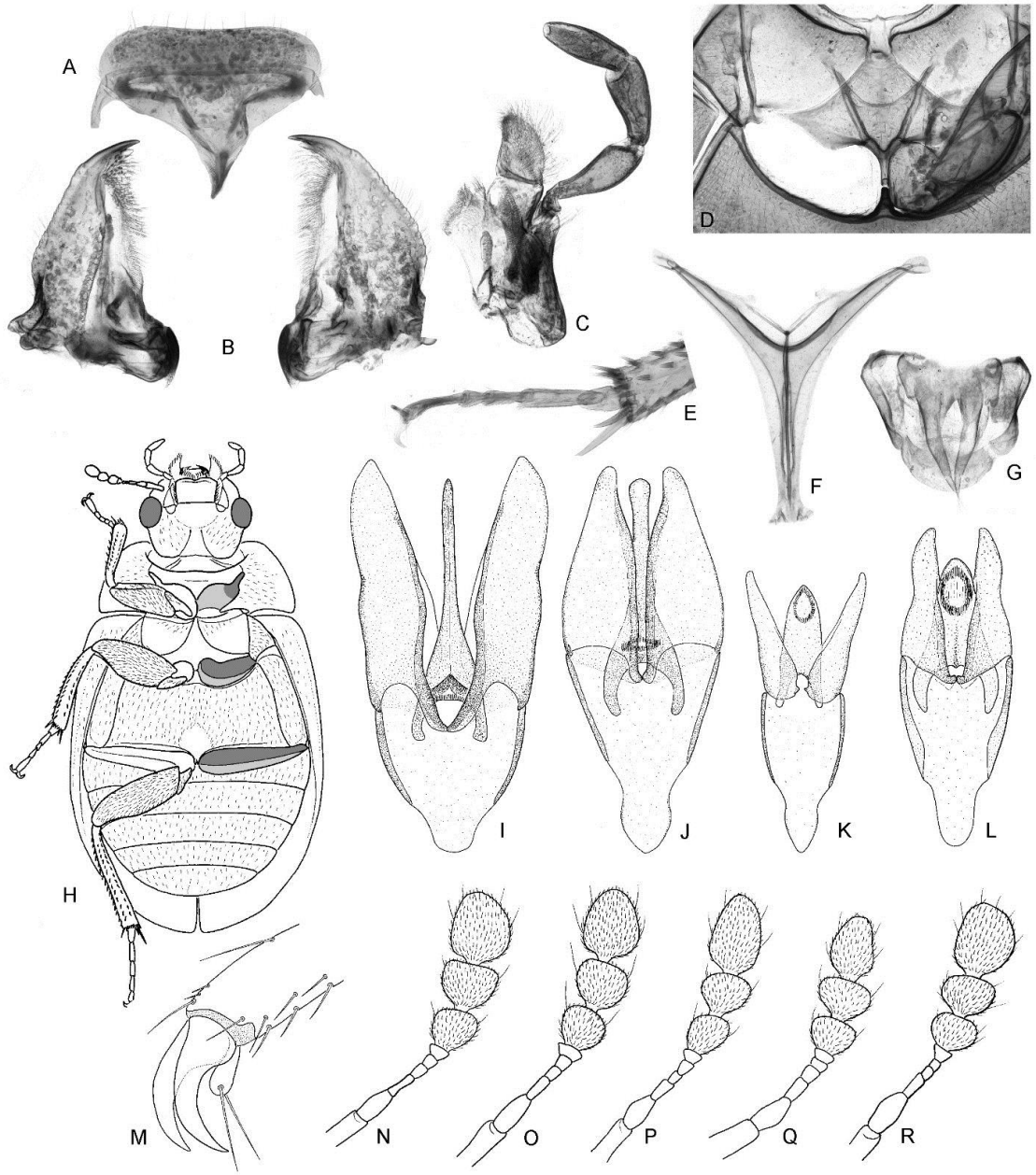

Figure 4. Adult morphology of *Saphydrus*. A–H – *S. suffusus*: A – labrum; B – mandibles; C – maxilla; D – mesoventrite and mesofurca; E – metatarsus; F – metafurca; G – ovopositor; H – ventral morphology. I–L – male genitalia of *Saphydrus*: I – *S. suffusus*; J – *S. obesus*; K – *S. tanemahuta* sp. nov.; L – *S. monticola*. M – tarsal claws of *S. suffusus*. N–R – antenna: N – *S. suffusus*; O – *S. obesus*; P – *S. tanemahuta* sp. nov.; Q – *S. monticola*; R – *S. moeldnerae* sp. nov.

Figure 5. Examined larval forms of *Saphydrus* and *Enigmahydrus*. A–D – *Saphydrus suffusus* (A, B – habitus dorsally and laterally; C, D – head and prothorax dorsally and ventrally). E–H – *Saphydrus* cf. *obesus* (E, F – habitus dorsally and laterally; G, H – head and prothorax dorsally and ventrally). I–O – *Saphydrus* cf. *tanemahuta* (I, J – habitus dorsally and laterally; K – detail of labroclypeus; L – detail of labium; M – abdominal apex; N, O – head and prothorax dorsally and ventrally). P–S – *Enigmahydrus larvalis* (P, Q – habitus dorsally and laterally; R, S – head and prothorax dorsally and ventrally). a–i – relative size of all third instar larvae and adults: a – *Enigmahydrus larvalis*; b – *Saphydrus suffusus*; c – larva of *S. suffusus*; d – *S. obesus*; e – supposed larva of *S. obesus*; f – *S. tanemahuta*; g – supposed larva of *S. tanamehuta*; h – *S. monticola*; i – *S. moeldnerae*.

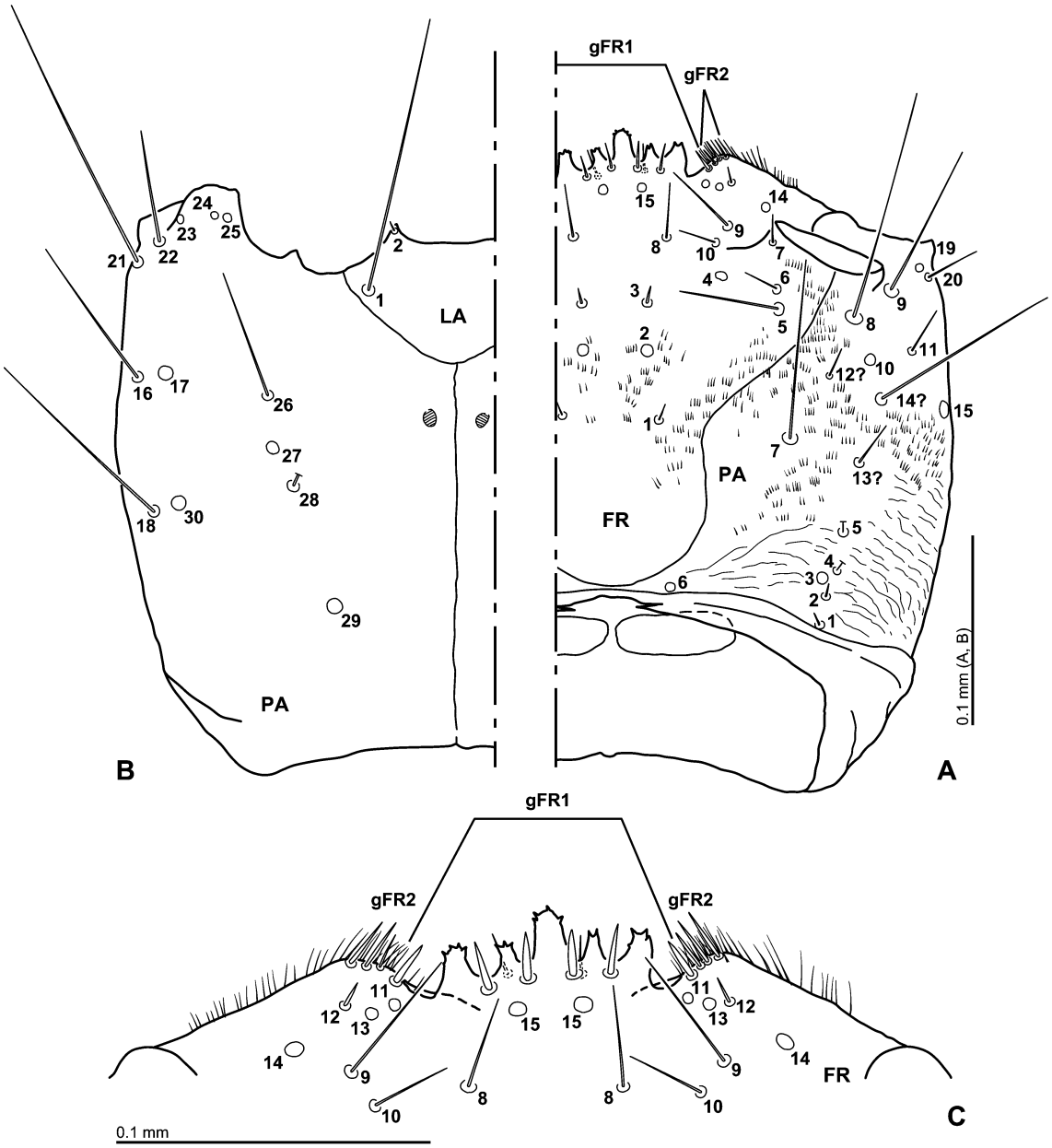

Figure 6. Larva of *Saphydrus suffusus*, head capsule of the first instar. A – dorsal view; B – ventral view; C – detail of labroclypeus in dorsal view.

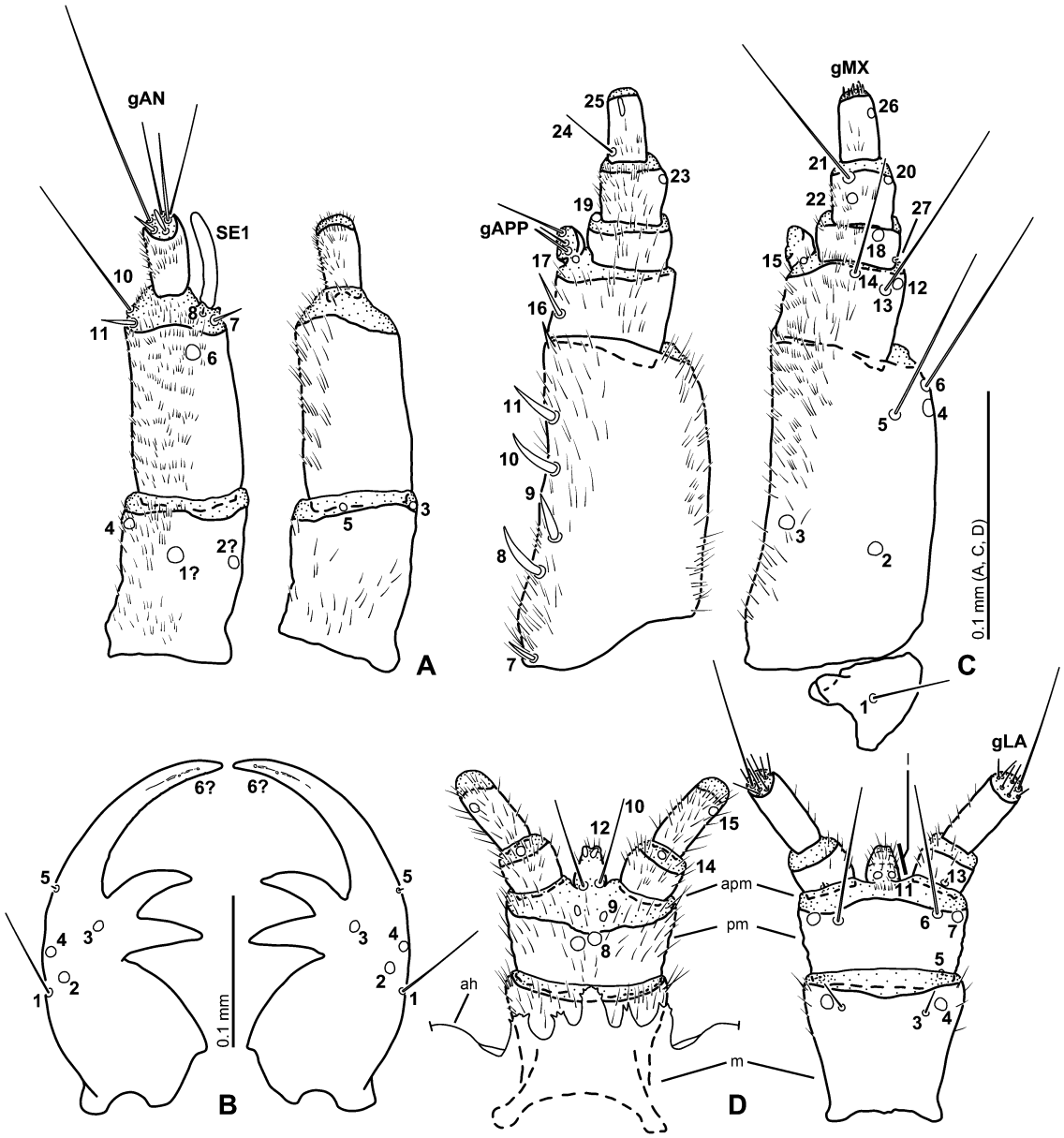

Figure 7. Larva of *Saphydrus suffusus*, head appendages of the first instar. A – antenna, dorsal (left) and ventral (right) surface; B – mandibles in dorsal view; C – maxilla, dorsal (left) and ventral (right) surface; D – mentum and prementum, dorsal with anterior margin of head capsule (left) and ventral (right) view. Abbreviations: ah: anterior margin of head capsule; apm: anterior membranous area of prementum; pm: prementum; l: ligula; m: mentum.

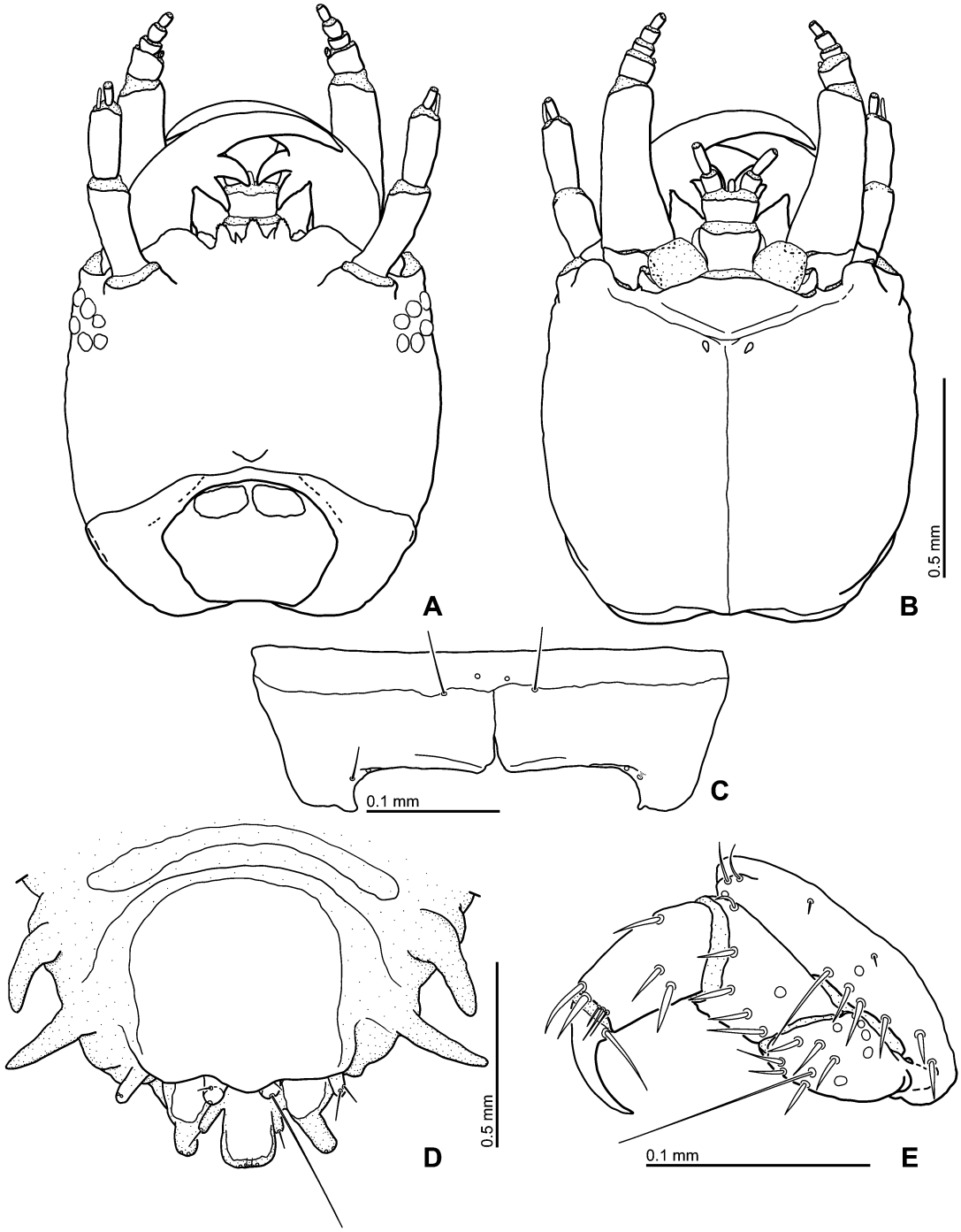

Figure 8. Larva of *Saphydrus suffusus*, third instar. A – head capsule, dorsal view; B – head capsule, ventral view; C – prosternum; D – abdominal apex, dorsal view; E – mesothoracic leg.

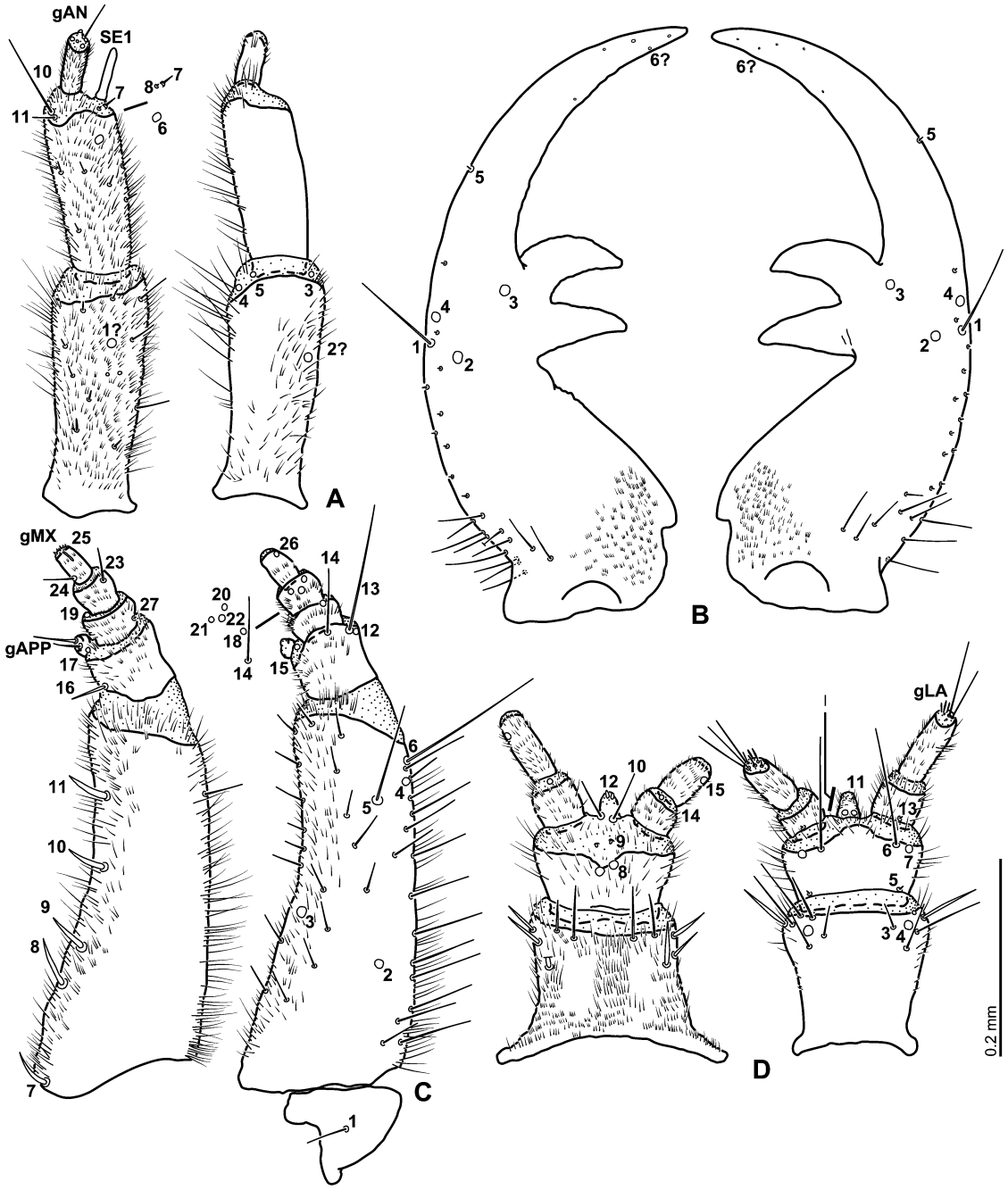

Figure 9. Larva of *Saphydrus suffusus*, head appendages of the third instar. A – antenna, dorsal (left) and ventral (right) surface; B – mandibles in dorsal view; C – maxilla, dorsal (left) and ventral (right) surface; D – mentum and prementum in dorsal and ventral view. Abbreviation: l: ligula.

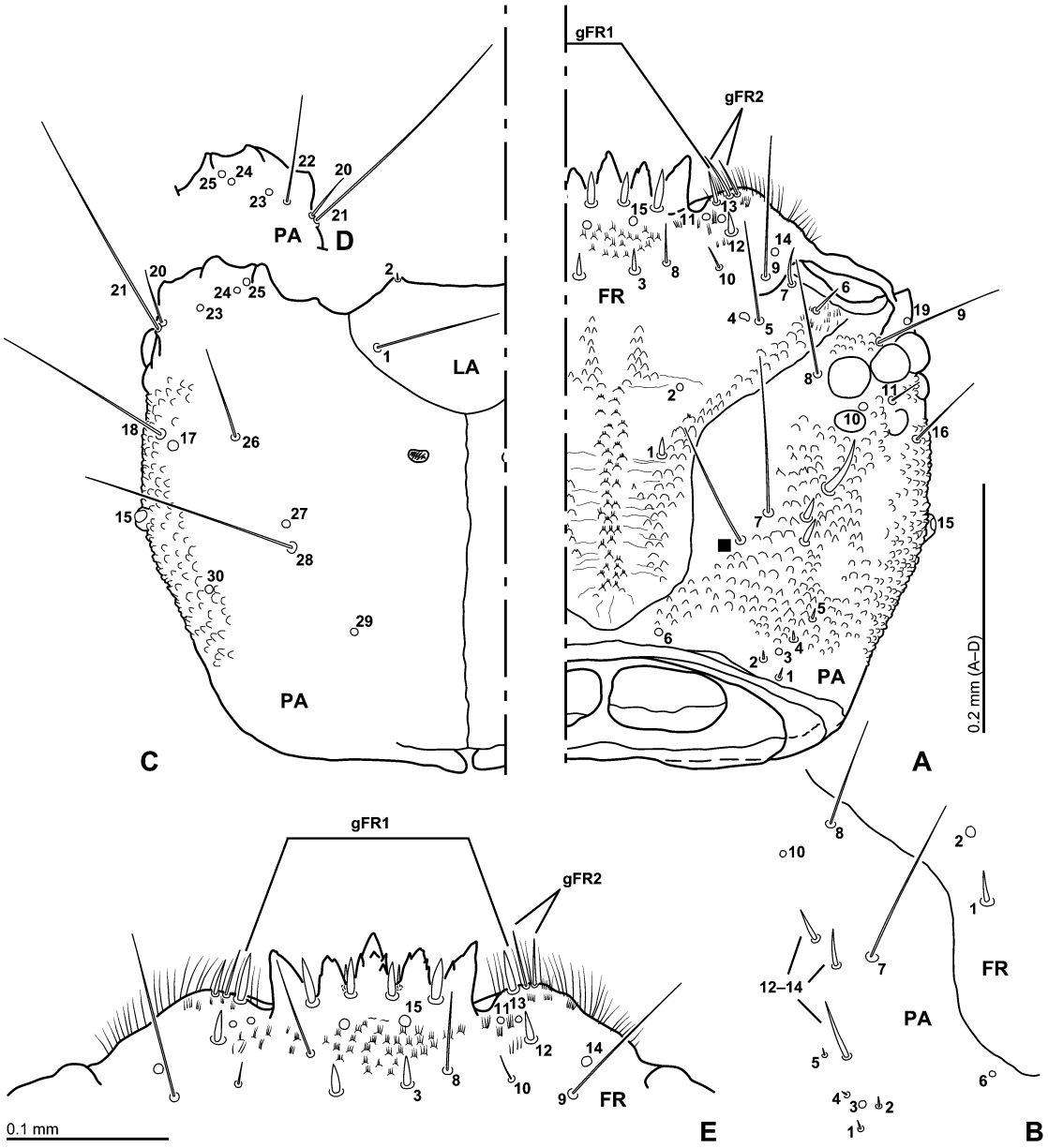

Figure 10. Larva of *Enigmahydrus larvalis*, head capsule of the first instar. A – dorsal view; B – variation on chaetotaxy of frontale and parietale; C – ventral view; D – variation of ventral chaetotaxy around mandibular articulation; E – detail of labroclypeus in dorsal view.

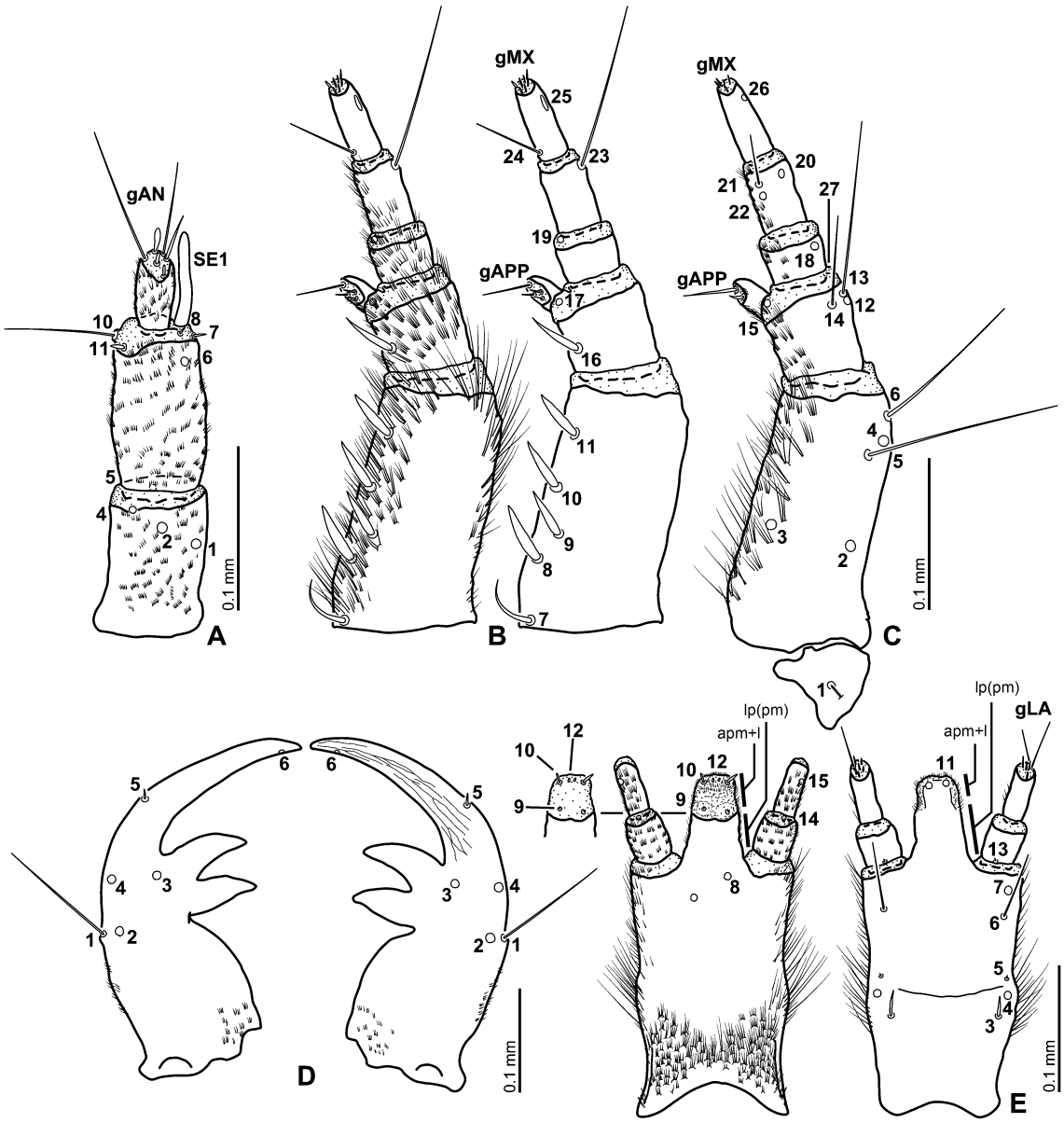

Figure 11. Larva of *Enigmahydrus larvalis*, head appendages of the first instar. A – antenna in dorsal view; B –maxilla in dorsal view, with pubescence illustrated (left) and omitted (right); C – maxilla, ventral surface; D – mandibles in dorsal view; E – mentum and prementum in dorsal and ventral view. Abbreviations: apm: anterior membranous area of prementum; lp: ligula-like projection; l: ligula; pm: prementum.

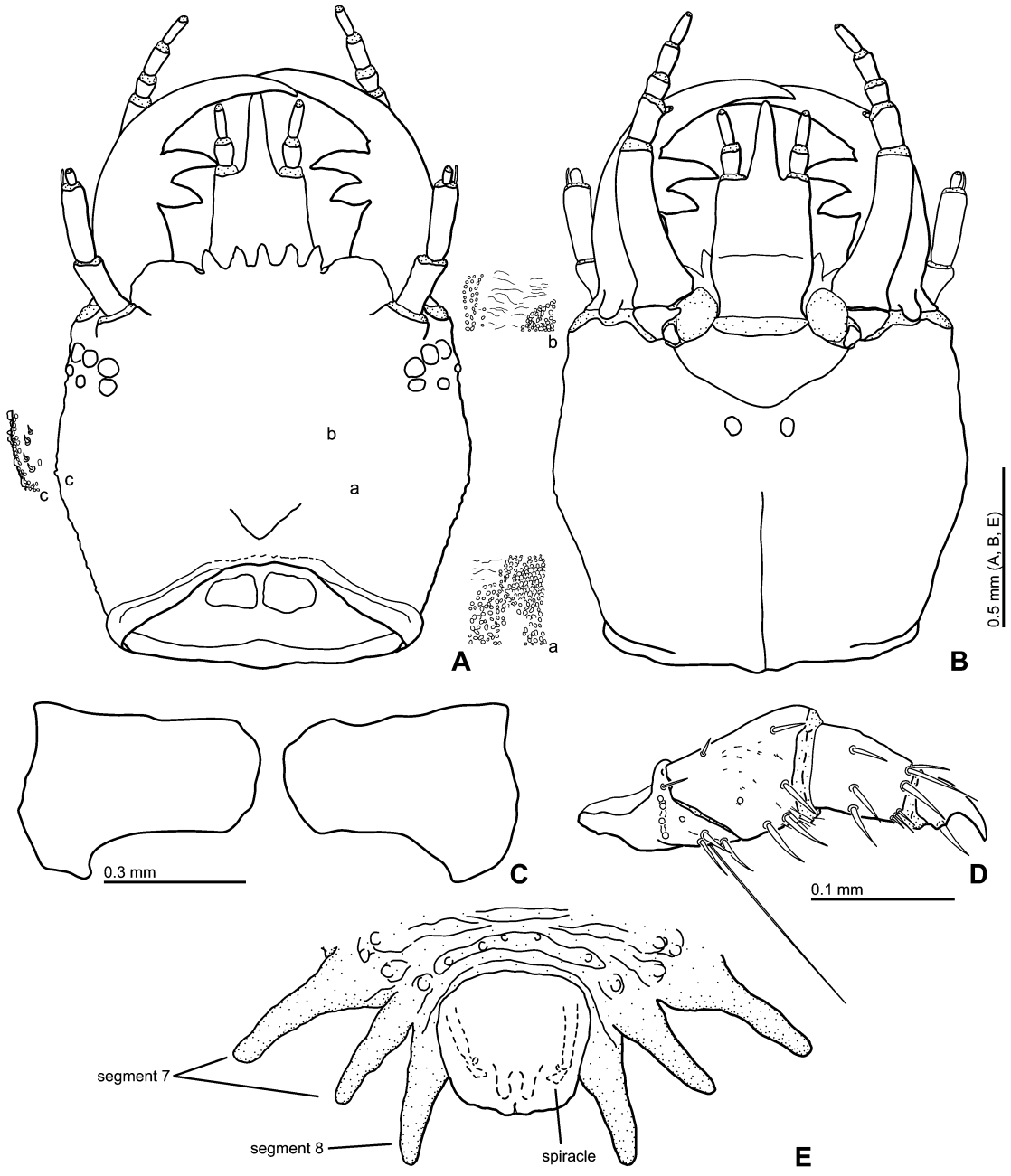

.

Figure 12. Larva of *Enigmahydrus larvalis*, third instar. A – head capsule, dorsal view; B – head capsule, ventral view; C – prosternum; D – mesothoracic leg; E – abdominal apex in dorsal view.

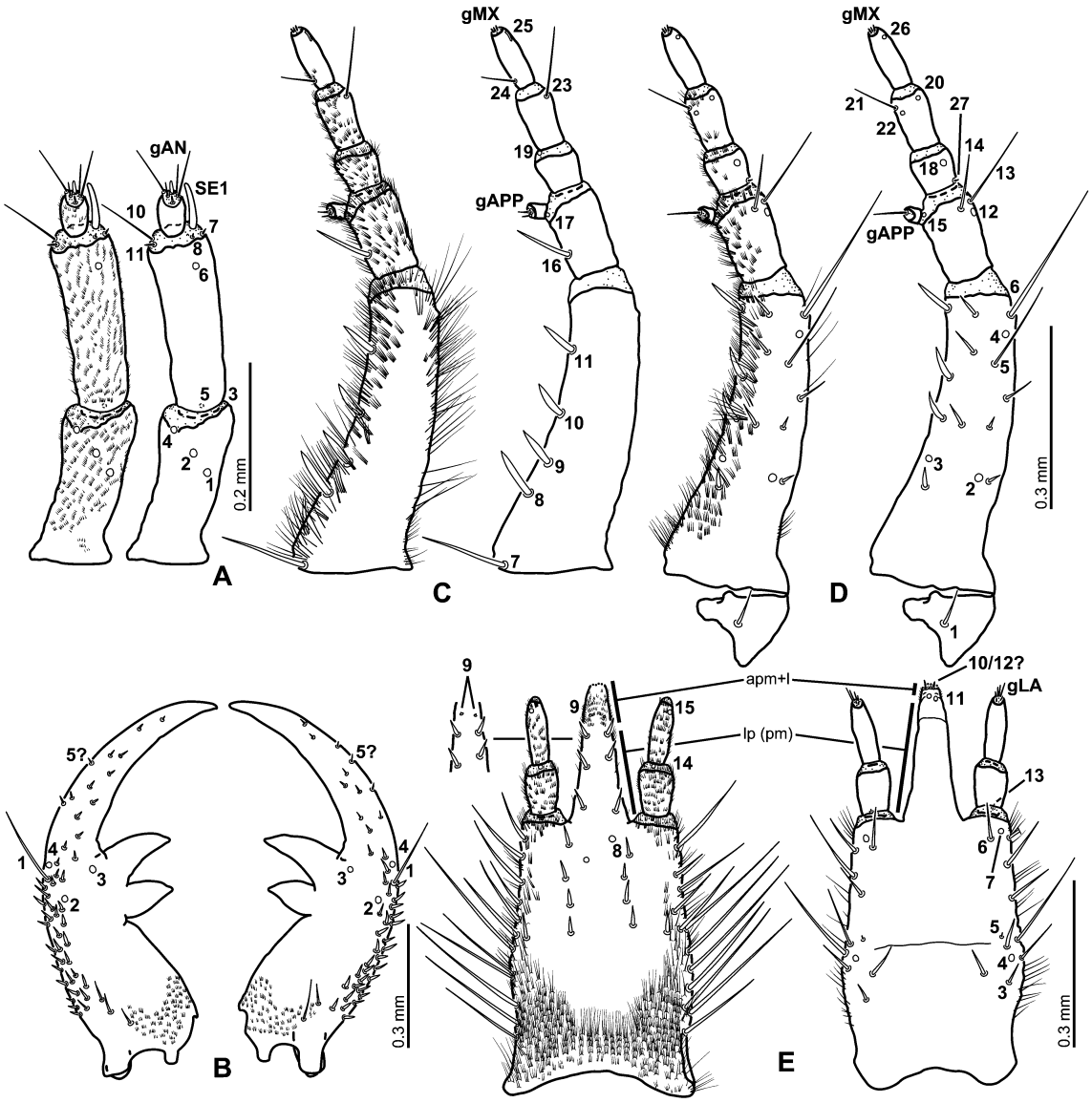

Figure 13. Larva of *Enigmahydrus larvalis*, head appendages of the third instar. A – antenna in dorsal view, with pubescence illustrated (left) and omitted (right); B – mandibles in dorsal view; C – maxilla in dorsal view; D – maxilla in ventral view with pubescence illustrated and omitted; E – mentum and prementum in dorsal and ventral view. Abbreviations: apm: anterior membranous area of prementum; lp: ligula-like projection; l: ligula; pm: prementum.

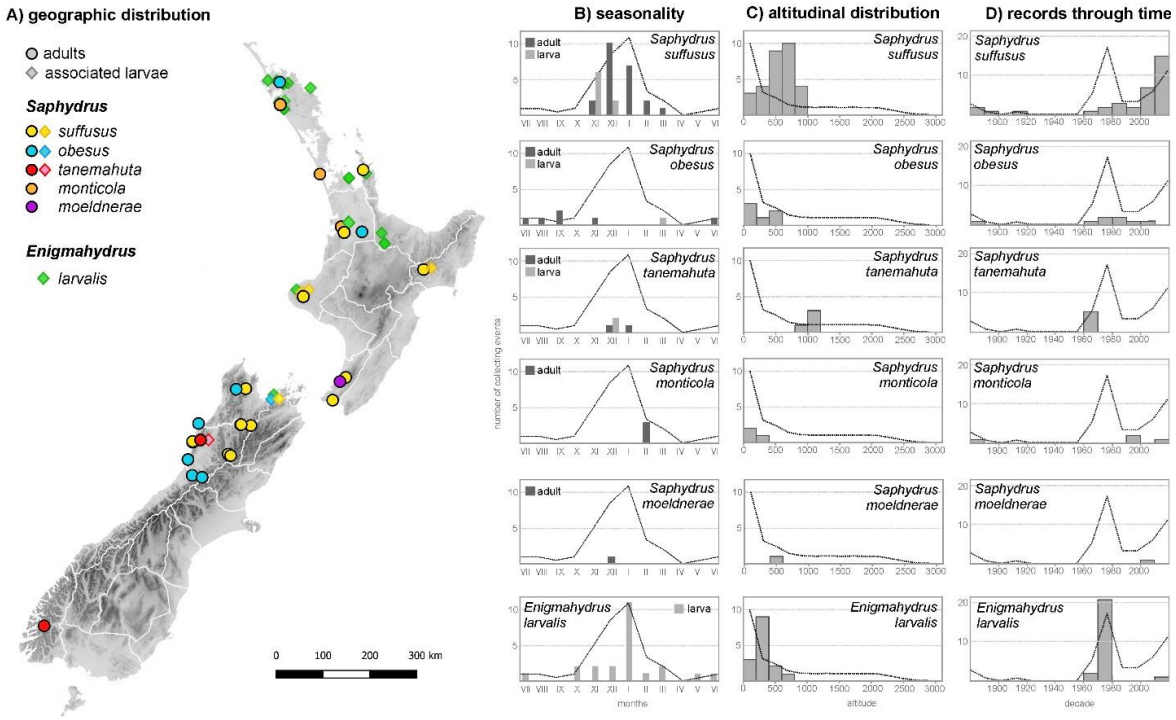

Figure 14. Known geographic distribution (A), altitudinal distribution (B), seasonal occurrence (C) and records through time (D) of *Saphydrus* and *Enigmahydrus* including the larval forms. Dotted line in graphs: seasonality – relative distribution of collecting effort through year; altitudinal distribution – relative area with the respektive altitude (hyprographic curve); record through time – relative collecting effort through time.

Supplementary material
to the paper

Seidel, M., Minoshima, Y. N., Leschen, R. A. B., & Fikáček, M. Phylogeny, systematics and rarity assessment of New Zealand endemic *Saphydrus* beetles and related enigmatic larvae (Coleoptera: Hydrophilidae: Cylominae) (manuscript draft).

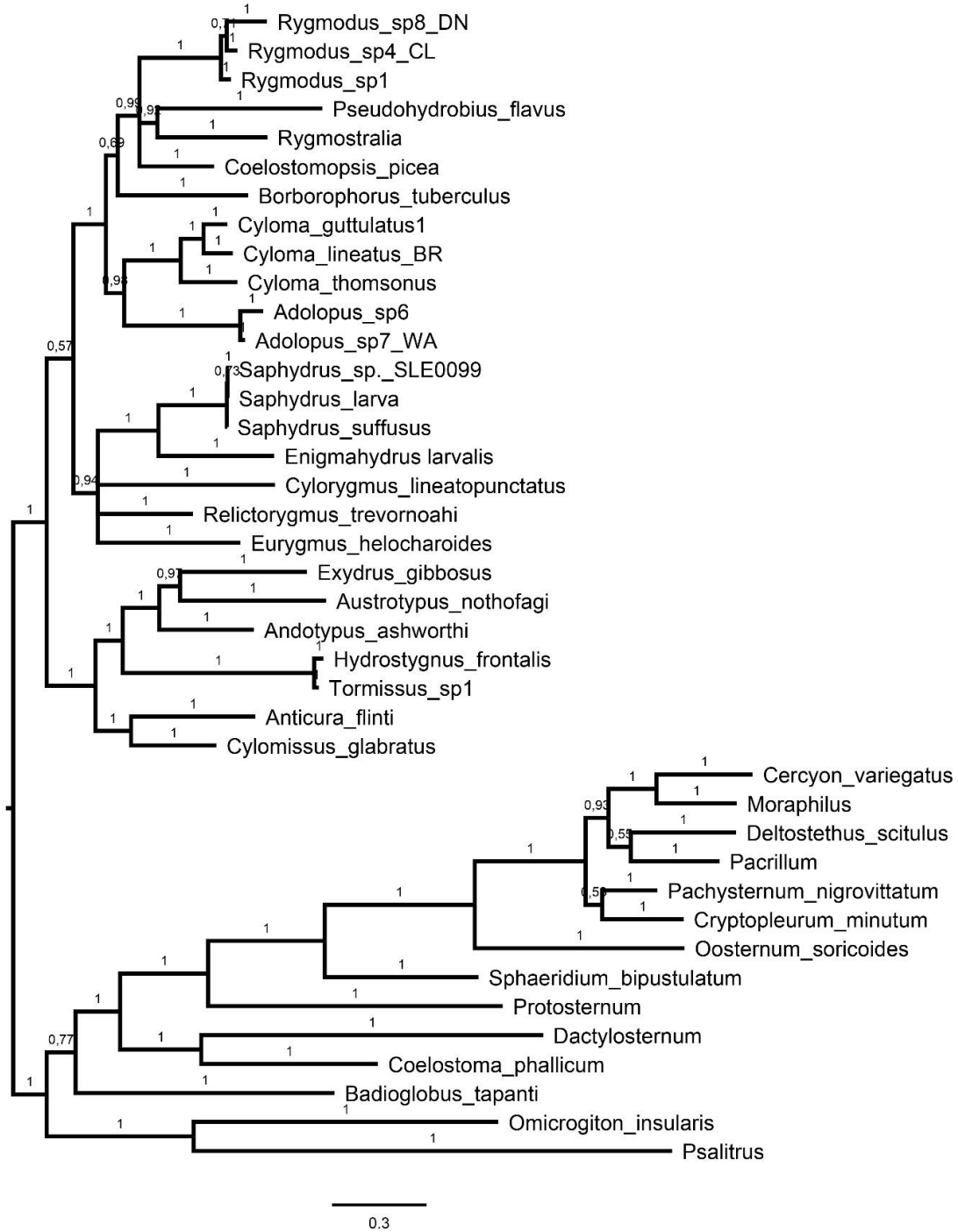

Supplementary Figure S1. The fifty percent majority rule tree from the Bayesian analysis.

Supplementary table S1. Primer sequences and programs used for PCRs for gene fragments used in our study.

cox1-3'							
SJerryF	CAACATYTATTYTGATTYTTTGG (Timmermans et al. 2010)						
SPatR	GCACTAWTCTGCCATATTAGA (Timmermans et al. 2010)						
PROGRAM							
Step	1	2	3	4	5	6	7
Temp.	95°C	95°C	50°C	72°C	repeat 2-4	72°C	12°C
Time	5:00	0:30	0:40	2:00	40x	8:00	forever
16S							
16S-1472-JJ	GGTCCTTTCGTACTAA (Astrin and Stüben 2008)						
16S-ar-JJ	CRCCTGTTTATTAAAAACAT (Astrin and Stüben 2008)						
PROGRAM							
Step	1	2	3	4	5	6	7
Temp.	94°C	94°C	50°C	72°C	repeat 2-4	72°C	12°C
Time	3:00	0:30	0:45	1:00	34x	8:00	forever
18S5							
18S5'	GACAACCTGGTTGATCCTGCCAGT (Shull et al. 2001)						
18Sb5.0	TAACCGCAACAACTTTAAT (Shull et al. 2001)						
PROGRAM							
Step	1	2	3	4	5	6	7
Temp.	95°C	95°C	50°C	72°C	repeat 2-4	72°C	4°C
Time	5:00	0:30	0:40	2:00	40x	8:00	forever
18Sce							
18Sai	CTTGAGAAACGGCTACCACATC (Whiting et al 1997)						
18Sb0.5	GTTTCAGCTTTGCAACCAT (Whiting et al 1997)						
PROGRAM							
Step	1	2	3	4	5	6	7
Temp.	95°C	95°C	50°C	72°C	repeat 2-4	72°C	4°C
Time	5:00	0:30	0:40	2:00	40x	8:00	forever
18S3							
18Sa1.0	GGTGAAATTCTTGGACCGTC (Shull et al. 2001)						
18S3´I	CACCTACGGAAACCTTGTTACGAC (Shull et al. 2001)						
PROGRAM							
Step	1	2	3	4	5	6	7
Temp.	95°C	95°C	50°C	72°C	repeat 2-4	72°C	4°C
Time	5:00	0:30	0:40	2:00	40x	8:00	forever
28S							
28S NLF 184-21	ACCCGCTGAAYTTAAGCATAT (Van der Auwera et al. 1994)						
28S LS1041R	TACGGACRTCCATCAGGGTTTCCCCTGACTTC (Maddison 2008)						
PROGRAM							
Step	1	2	3	4	5	6	7
Temp.	94°C	94°C	52°C	72°C	repeat 2-4	72°C	12°C
Time	3:00	0:30	0:45	1:00	34x	10:00	forever

Supplementary Table S2. Taxon names, codes and GenBank accession numbers of sequences [when available].

Taxon name	**Cox1-3'**	**28S**	**18S**	**16S**	**classification**
Adolopus sp2	xxx	xxx	xxx	xxx	Cylominae
Adolopus sp6	xxx	xxx	xxx	xxx	Cylominae
Adolopus sp7	xxx	xxx	xxx	xxx	Cylominae
Andotypus ashworthi	xxx	KP419352.1	KP419000.1	-	Cylominae
Anticura flinti	KM262054.1	xxx	KT447582.1	xxx	Cylominae
Austrotypus nothofagi	xxx	xxx	xxx	xxx	Cylominae
Borborophorus tuberculus	KC935232.1	KJ845053.1	KC935009.1	-	Cylominae
Coelostomopsis picea	KC935245.1	KC992551.1	KC935022.1	-	Cylominae

Cyloma guttulatus	xxx	xxx	xxx	xxx	Cylominae
Cyloma lineatus	xxx	xxx	xxx	xxx	Cylominae
Cyloma thomsonus	xxx	xxx	xxx	xxx	Cylominae
Cylomissus glabratus SLE0098	KC935251.1	KC992556.1	KC935028.1	KC992663.1	Cylominae
Cylorygmus lineatopunctatus	xxx	KJ845012.1	xxx	-	Cylominae
Enigmahydrus larvalis	xxx	xxx	xxx	xxx	Cylominae
Eurygmus helocharoides	xxx	xxx	xxx	xxx	Cylominae
Exydrus gibbosus	xxx	xxx	xxx	xxx	Cylominae
Hydrostygnus frontalis SLE0097	KC935285.1	KC992591.1	KC935066.1	KC992687.1	Cylominae
Pseudohydrobius flavus	KF801992.1	KF802155.1	xxx	KF801827.1	Cylominae
Relictorygmus trevornoahi	xxx	xxx	xxx	xxx	Cylominae
Rygmodus modestus	xxx	xxx	xxx	xxx	Cylominae
Rygmodus opimus	xxx	xxx	xxx	xxx	Cylominae
Rygmodus sp1 sp. SLE0129	KC935318.1	KC992627.1	KC935094.1	KC992705.1	Cylominae
Rygmostralia sp1	KF801989.1	KF802152.1	xxx	KF801824.1	Cylominae
Saphydrus suffusus	xxx	xxx	xxx	xxx	Cylominae
Saphydrus suffusus	KC935319.1	KC992628.1	KC935095.1	KC992706.1	Cylominae
Saphydrus suffusus larva	xxx	-	-	-	Cylominae
Tormissus magnulus	xxx	xxx	xxx	xxx	Cylominae
Sphaeridium bipustulatum	KC935323.1	-	KC935099.1	KC992710.1	Sphaeridinae
Psalitrus MF249	KC935316.1	KC992625.1	KC935092.1	-	Sphaeridinae
Protosternum sp. SLE0297	-	KC992624.1	KC935091.1	KC992703.1	Sphaeridinae
Pacrillum sp. MF205	KC935309.1	KC992615.1	KC935082.1	-	Sphaeridinae
Pachysternum nigrovittatum SLE0066	KC935308.1	KC992614.1	KC935081.1	-	Sphaeridinae
Oosternum soricoides MF224	KC935306.1	KC992612.1	KC935079.1	-	Sphaeridinae
Omicrogiton insularis MF284	KC935295.1	KC992602.1	KC935075.1	-	Sphaeridinae
Moraphilus sp. SLE0128	KC935292.1	KC992597.1	KC935072.1	-	Sphaeridinae
Deltostethus scitulus SLE0126	KC935255.1	KC992560.1	KC935032.1	KC992665.1	Sphaeridinae
Dactylosternum sp. SLE0072	KC935254.1	KC992559.1	KC935031.1	KC992664.1	Sphaeridinae
Cryptopleurum minutum SLE0058	KC935248.1	KC992553.1	KC935024.1	-	Sphaeridinae
Coelostoma phallicum MF326	KC935244.1	KC992550.1	KC935021.1	-	Sphaeridinae
Cercyon variegatus SLE0020	KC935234.1	KC992539.1	KC935011.1	KC992654.1	Sphaeridinae
Badioglobus tapanti SLE0053	KC935229.1	KC992534.1	KC935005.1	-	Sphaeridinae

Supplementary Table S3. Collectiong data of newly sequenced Cylominae specimens included in the phylogenetic study.

Species	code	Collecting events	collecting information
*Cyloma guttulatus*1	NZ111.1	New Zealand, SC, Peel Forest Reserve, Emily Falls track, 43°53.9′S 171°13.8′E, 400m, 9.ii.2016, J. Hájek & P. Hlaváč lgt.	
*Cyloma guttulatus*1	NZ243.1	New Zealand, FD, Borland Walk at Borland Lodge, 45°46.35-48'S 167°32.18-25'E, 180m, 23-28.i.2016, Seidel & Fikáček lgt., 2016-NZ020	baited pitfall traps (rotten squid) in mossy *Nothofagus* forest, in places with numerous ferns in understory
Cyloma lineatus	NZ83	New Zealand, BR, Klondyke Trk, Victoria Ra, 12.i.2011, T.R. Buckley & R. Leschen lgt., TB452, 42°18.842'S 172°07.065'E, 699m	sifting wet dead wood
Cyloma thomsonus	NZ158	New Zealand, SL, Kaka Point Scenic Reserve, 46°23.04'S 169°46.45'E, 20m, 2-6.ii.2016, Seidel, Sýkora & Fikáček lgt., 2016-NZ050	baited pitfall traps (rotten squid) in native coastal forest with podocarps and ferns
Cyloma thomsonus	NZ248.1	New Zealand, SL, Catlins, McLean Falls Tk. at Tautuku River, 46°34.26'S169°20.98'E, 50m, 3-10.ii.2016, Seidel, Sýkora & Fikáček lgt., 2016-NZ051	baited pitfall traps (rotten squid) in wet to moderately wet area in native coastal forest with numerous tree ferns and falled/rotten trunks
Enigmahydrus larvalis	MF665	New Zealand, Taranaki, unnamed stream 0.2km S of Pukeiti Garden, 9km E of Okato, 370m, 30.xi.2012, 39°12.1'S 173°58.9'E, Becker, Fikáček & Hájek lgt.	in mosses on stones in/along the stream in lowland *Nothofagus* forest
Saphydrus suffusus	NZ462	New Zealand, NN, Nelson Lakes NP, N end of Lake Rotoroa at Braeburn Track 41.7987°S 172.58421°E, 522m, 5-9.xii.2016, Fikáček & Seidel lgt., MM57	lowland wet *Nothofagus* forest with huge amount of sooty moulds and with continuous layer of *Blechnum* fern understory, baited pitfall traps (rotten squid)
Saphydrus suffusus	COL1786	New Zealand, BR, Rough Crk, Maruia Springs, 12.i.2011, R. Leschen & T.R. Buckley lgt., TB455, 42°22.825'S 172°16.798'E, 550m	
Saphydrus suffusus larva	MF529	New Zealand: Taranaki, Mt. Egmont NP, Potaema Walk, 6.8 km W of Pembroke, 650 m, 28.xi.2012, 39°18.9'S 174°9.1'E, Becker, Fikáček & Hájek lgt.	
Cylorygmus lineatopunctatus	MF790	Chile, Valparaiso, PN La Campana, Sector Ocoa, 4.75km SE of park entrance, "La Cascada", 870m, 20.xi.2013, 32°57.7'S 71°3.2'W, Fikáček, Kment & Vondráček lgt., CH03	
Relictorygmus trevornoahi	MF1727.2	South Africa, Western Cape, 13.3km SEE Stanford (wetland), 100m, 4-5.xii.2015, 34°27.84S 19°35.75E, Arriaga, Fikáček, Seidel & Vondráček, RSA50	
Rygmostralia sp1	COL800	Australia, QLD, Mt. Bartle Frere, NW peak, 1426m, 19.xi.2009, 17.385°S 145.802°E, Monteith & Turco lgt.	sieved litter
Borborophorus tuberculus	COL666	Australia, QLD, Baldy Mt. Rd., RF, 1100m, 11.x.2008, 17°17'20"S 145°25'34"E, G. Monteith lgt.	pyrethrum trees

Exydrus gibbosus	NZ114.1	New Zealand, Auckland, Auckland - Lynfield, 31.i.2016, Wattle Bay reserve, 36°56.1′S 174°43.6′E, 2-30m, J.Hájek & P. Hlaváč lgt.	sifting in secondary coastal forest
Exydrus gibbosus	COL1791	New Zealand, BP, Ohope, 8.ix.2009, R. Leschen & E. Hilario lgt., RL1493, 37.97338°S 177.07198°E	
Coelostomopsis picea	COL119	Australia, QLD, Mt Finnigan summit, 1100m, 20.x.2008, 15°49'16S 145°16'35E, G. Monteith lgt.	berlesate moss
Eurygmus helocharoides	COL2028	Australia, QLD, Polly Ck., Garradunga, malaise 6, 58m, 13.i.-14.ii.2010, 17.458°S 146.021°E, J. Hasenpusch lgt.	
Andotypus ashworthi	MF792	Chile, Los Lagos, PN Puyehue, Aguas Calientes, lower part of Sendero Pionero, 520m, 5-9.xii.2013, 40°44.3'S 72°18.6'W, Fikáček, Kment & Vondráček lgt., CH27	baited pitfall traps (rotten fish) in Valvidian (evergreen laurel-leaf) rainforest
Anticura flinti	MF793	Chile, Los Lagos, PN Puyehue, Anticura, Río Anticura between Salto Pudú and confluence with Río Golgol, 350-460m, 6-9.xii.2013, 40°40.0-40.5'S 72°9.9-10.6'W, Fikáček, Kment & Vondráček lgt., CH29	floating, mosses from the stone in the river (submerged + just above water) and the flood debris accumulated in logjam
Austrotypus nothofagi	MF540	Australia, Queensland, Lamington NP, 800m, 13-15.iii.2013, 28°11.9'S, 153°11.2'E, G. Monteith lgt.	
Adolopus sp2	NZ46.1	New Zealand, WO, Marokopa Falls, 3.iii.2012, M. Gimmel & R. Leschen lgt., 38°15.560'S 174°50.926'E, RL1654	ex beating
Adolopus sp6	NZ565.1	New Zealand, MK, Temple Valley, 10.i.2006, R. Leschen, T. Buckley & R. Hoare lgt., RL1043, 44.10676°N 169.81697°E	leaf litter
Adolopus sp7	NZ672	New Zealand, WA Waikuku Lodge, Aorangi Range, 24.i.2008. K. Marske, R. Leschen & T. Buckley lgt., 41°24.616'S E175°21.880'E, 458m	ex leaf litter/rotten wood
Adolopus sp7	NZ649.1	New Zealand, WA, Sutherland Vehicle Track, Aorangi Range, 24.i.2008, K. Marske, R. Leschen & T. Buckley lgt., 41°25.239'S E175°21.551'E, 398m	sifted wood and leaf litter in secondary forest on former grazing land
Rygmodus opimus	NZ162	New Zealand, DN, Taieri Mouth, Picknick Gully, 46°3.25'S 170°11.27'E, 25m, 12.ii.2016, Seidel, Sýkora & Fikáček lgt., 2016-NZ073	sifting of small accumulations of leaf litter + hand collecting in small remnant of native coastal forest (very dry)
Tormissus magnulus	NZ461.1	New Zealand, NN, Nelson Lakes NP, N end of Lake Rotoroa at Braeburn Track 41.7987°S 172.58421°E, 522m 5-9.xii.2016, Fikáček & Seidel lgt., MM57	lowland wet *Nothofagus* forest with huge amount of sooty moulds and with continuous layer of *Blechnum* fern understory, baited pitfall traps (rotten squid)
Tormissus magnulus	COL1806	New Zealand, WN, Kapiti Island, Wilkinson Track, 21.i.2008, K. Marske, R. Leschen & T. Buckley lgt., 40°51.145'S 174°55.722'E, 260m, KM227	under/in dead wood
Pseudohydrobius flavus	COL803	Australia, QLD, Mt. Lewis Rd., hut 12km NW Julatten, 1187m, 21.xi.2009, 16.511°S 145.269°E, Monteith & Turco lgt.	

Supplementary Table S4. PartionFinder2 output of MrBayes block for partition definitions (Subset 1-3= Cox1-3', Subset 4= 16S, Subset 5= 18S, Subset 6= 28S).

```
begin mrbayes;

        charset Subset1 = 1-786\3;
        charset Subset2 = 2-786\3;
        charset Subset3 = 3-786\3;
        charset Subset4 = 787-1359;
        charset Subset5 = 1360-3184;
        charset Subset6 = 3185-4226;

        partition PartitionFinder = 6:Subset1, Subset2, Subset3, Subset4, Subset5,
Subset6;
        set partition=PartitionFinder;

        lset applyto=(1) nst=6 rates=invgamma;
        lset applyto=(2) nst=6 rates=invgamma;
        lset applyto=(3) nst=6 rates=invgamma;
        lset applyto=(4) nst=6 rates=invgamma;
        lset applyto=(5) nst=6 rates=invgamma;
        lset applyto=(6) nst=6 rates=invgamma;

        prset applyto=(all) ratepr=variable;
        unlink statefreq=(all) revmat=(all) shape=(all) pinvar=(all) tratio=(all);
```

Supplementary References

Astrin, J. J., & Stüben, P. E. (2008). Phylogeny in cryptic weevils: molecules, morphology and new genera of western Palaearctic Cryptorhynchinae (Coleoptera: Curculionidae). *Invertebrate Systematics*, *22*(5), 503-522.

Maddison, D. R. (2008). Systematics of the North American beetle subgenus Pseudoperyphus (Coleoptera: Carabidae: Bembidion) based upon morphological, chromosomal, and molecular data. *Annals of Carnegie Museum*, *77*(1), 147-193.

Shull, V. L., Vogler, A. P., Baker, M. D., Maddison, D. R., & Hammond, P. M. (2001). Sequence alignment of 18S ribosomal RNA and the basal relationships of adephagan beetles: evidence for monophyly of aquatic families and the placement of Trachypachidae. *Systematic Biology*, *50*(6), 945-969.

Timmermans, M. J., Dodsworth, S., Culverwell, C. L., Bocak, L., Ahrens, D., Littlewood, D. T. J., Pons, J. & Vogler, A. P. (2010). Why barcode? High-throughput multiplex sequencing of mitochondrial genomes for molecular systematics. *Nucleic Acids Research*, *38*(21), e197-e197.

Van der Auwera, G., Chapelle, S., & De Wächter, R. (1994). Structure of the large ribosomal subunit RNA of Phytophthora megasperma, and phylogeny of the oomycetes. *FEBS Letters*, *338*(2), 133-136.

Whiting, M. F., Carpenter, J. C., Wheeler, Q. D., & Wheeler, W. C. (1997). The Strepsiptera problem: phylogeny of the holometabolous insect orders inferred from 18S and 28S ribosomal DNA sequences and morphology. *Systematic Biology*, *46*(1), 1-68.

CHAPTER 6

Minoshima, Y. N., **Seidel, M.**, Wood, J. R., Leschen, R. A., Gunter, N. L., & Fikáček, M. (2018). Morphology and biology of the flower-visiting water scavenger beetle genus *Rygmodus* (Coleoptera: Hydrophilidae). *Entomological Science*, 21(4): 363-384.

Author contributions: YM and MF prepared the larval descriptions; MS, MF and RL performed the field work; MS and MF run the molecular and phylogenetic analyses; MF and JW prepared the pollen analyses; MF, YM and MS drafted the manuscript, all authors contributed to the writing.

Entomological Science (2018) doi: 10.1111/ens.12316

ORIGINAL ARTICLE

Morphology and biology of the flower-visiting water scavenger beetle genus *Rygmodus* (Coleoptera: Hydrophilidae)

Yûsuke N. MINOSHIMA[1], Matthias SEIDEL[2,3], Jamie R. WOOD[4], Richard A. B. LESCHEN[5], Nicole L. GUNTER[6] and Martin FIKÁČEK[2,3]

[1]*Natural History Division, Kitakyushu Museum of Natural History and Human History, Kitakyushu-shi, Japan,* [2]*Department of Zoology, Faculty of Science, Charles University in Prague, Praha, Czech Republic,* [3]*Department of Entomology, National Museum, Praha, Czech Republic,* [4]*Long-term Ecology Laboratory, Manaaki Whenua, Lincoln, New Zealand,* [5]*Manaaki Whenua, New Zealand Arthropod Collection, Auckland, New Zealand and* [6]*Department of Invertebrate Zoology, Cleveland Museum of Natural History, Cleveland, Ohio, USA*

Abstract

Hydrophilidae (water scavenger beetles) is well known as an aquatic beetle family; however, it contains ca. 1,000 secondarily terrestrial species derived from aquatic ancestors. The New Zealand endemic genus *Rygmodus* White is a member of the hydrophilid subfamily Cylominae, which is the early-diverging taxon of the largest terrestrial lineage (Cylominae + Sphaeridiinae) within the Hydrophilidae. In this paper we report that *Rygmodus* beetles are pollen-feeding flower visitors as adults, but aquatic predators as larvae. Based on analyses of gut contents and a summary of collecting records reported on museum specimen labels, adult *Rygmodus* beetles are generalists feeding on pollen of at least 13 plant families. *Rygmodus* adult mouthparts differ from those of other (saprophagous) hydrophilid beetles in having the simple scoop-like apex and mola with roughly denticulate surface, resembling the morphology found in pollen-feeding staphylinid beetles. Larvae were found along the sides of streams, under stones and in algal mats and water-soaked moss; one collected larval specimen was identified using DNA barcoding of two molecular markers, mitochondrial cytochrome oxidase 1 (*cox1*) and nuclear histone 3 (H3). Larvae of two species, *Rygmodus modestus* and *Rygmodus* sp., are described in detail and illustrated; they closely resemble ambush-type predatory larvae of the hydrophilid tribe Hydrophilini in the head morphology. *Rygmodus* is the only known hydrophilid beetle with adults and larvae inhabiting different environments.

Key words: Cylominae, ecological divergence, gut content, immature stage, larval morphology, mouthpart, pollen-feeding.

INTRODUCTION

Larval stages of holometabolous insects frequently exhibit very different life styles from that of the conspecific adults, both in habitat and in food preferences. This ability to occupy multiple niches during the life of a single specimen, or "ecological divergence", is often considered as one of the reasons for increased diversification rates of Holometabola and for its immense species diversity (Yang 2001; Mayhew 2007; Rainford *et al*. 2014; but see Condamine *et al*. 2016). Numerous exceptions to the above pattern may be found, and in reality, the degree of "ecological divergence" varies within particular groups of hemimetabolous and holometabolous insects. For example, in many groups of hemimetabolous stoneflies (Plecoptera), larvae are aquatic and predatory or detritivorous, whereas terrestrial adults feed on lichens, fungal spores, pollen or arthropod corpses (e.g. Fenoglio & Tierno de Figueroa 2003; Rúa & Tierno de Figueroa 2013). In contrast, larvae and adults of aquatic beetles often co-occur in

Correspondence: Yûsuke N. Minoshima, Natural History Division, Kitakyushu Museum of Natural History and Human History, 2-4-1 Higashida, Yahatahigashi-ku, Kitakyushu-shi 805-0071, Japan.
Email: minoshima@kmnh.jp
Martin Fikáček, Department of Entomology, National Museum, Cirkusová 1740, CZ-193 00 Praha 9 - Horní Počernice, Czech Republic.
Email: mfikacek@gmail.com

Received 30 October 2017; accepted 4 April 2018.

the same habitat and feed on the same or very similar food source. For example, Dytiscidae with predatory adults and larvae, Elmidae with adults and larvae often living alongside each other on the same substrate, feeding on algae and detritus scraped from the surface, or on microorganisms from decaying wood (Brown 1987; Balke 2005; Kodada & Jäch 2005).

Hydrophilidae (water scavenger beetles) is well known as an aquatic beetle family; however, one-third of its members are secondarily terrestrial species derived from aquatic ancestors (Bernhard *et al.* 2006; Short & Fikáček 2013). Although habitat transitions have occurred independently in multiple lineages across Hydrophilidae, the majority of the terrestrial species are assigned to a single clade comprised of the subfamilies Cylominae and Sphaeridiinae (>1,000 species), which includes ca. 100 aquatic species (Short & Fikáček 2011, 2013; Fikáček *et al.* 2013; Minoshima *et al.* 2015; Girón & Short 2017). Hunt *et al.* (2007) reported that habitat shift from terrestrial to aquatic environments would have occurred at least ten times in the evolutionary history of Coleoptera, whereas only a few aquatic to terrestrial transitions are known outside of the Hydrophiloidea (e.g. Toussaint *et al.* 2016; Ruta *et al.* 2017). Adults and larvae of the Hydrophilidae always co-occur in the same (micro)habitat both in the aquatic groups and those inhabiting terrestrial environments like leaf litter, mammal excrements or ant nests (e.g. Fikáček *et al.* 2013, 2014, 2015; Minoshima *et al.* 2013, 2015; Clarkson *et al.* 2014; Arriaga-Varela *et al.* 2017). This allows relatively easy identification of conspecific adults and larvae by DNA barcoding on a limited number of candidate species (e.g. Fikáček *et al.* 2013, 2015; Minoshima *et al.* 2013, 2015). From an evolutionary point of view, transitions between different habitat types affect both adults and immature stages of the respective clade (Archangelsky 1999; Bloom *et al.* 2014). In contrast to the aforementioned Dytiscidae and Elmidae, food preferences differ between adults and larvae in Hydrophilidae: larvae are always predatory, feeding on various invertebrates, but adults are generally detritivorous, feeding on decaying organic matter, although precise food preferences are known in neither adult nor larval stage for most taxa (e.g. Archangelsky 1997).

Rygmodus White, 1846 is a New Zealand endemic genus of the hydrophilid subfamily Cylominae. This small subfamily is restricted to Australia, New Zealand, southern South America and South Africa, and is sister to the species-rich, largely terrestrial subfamily Sphaeridiinae (Short & Fikáček 2013; Minoshima *et al.* 2015; Seidel *et al.* 2016). Adults of *Rygmodus* have been reported to visit flowers (Thomson 1881; Broun 1886; Heine 1937; Primack 1983), which is an unusual life style in the family Hydrophilidae. No further information about the biology and life cycles of the genus is available, and adult food preferences and the habitat of their larvae remain unknown. Despite extensive collecting in New Zealand, including expeditions that targeted terrestrial water scavenger beetles, no hydrophilid larva of any kind has been found in flowers (with or without *Rygmodus* adults present). This suggests the larval habitat likely differs from that of adults in the genus.

In this study, we sequenced one larval specimen collected at the side of a stream in northern South Island of New Zealand and compared its DNA barcodes with those of adult Hydrophilidae. Consequently, the larva was surprisingly identified as *Rygmodus*, indicating the larvae of this flower-visiting hydrophilid beetle live in a totally different (aquatic) environment. We document some morphological and biological aspects of both adults and larvae: we investigate gut contents, mandibular morphology and host plants of *Rygmodus* adults, and describe the larval morphology based on detailed examination.

MATERIALS AND METHODS

Adult and larval specimens examined

The majority of adults included in this study represent *Rygmodus modestus* White, 1846 collected in Te Urewera National Park (North Island, New Zealand) in November 2012 by M. Fikáček, J. Hájek and A. Becker (see Table 1 for detailed collecting data). These specimens were used for dissection of mouthparts as well as for analyzing gut contents. In addition, we used freshly collected specimens of *R. modestus* and other *Rygmodus* species for DNA analyses. Currently, all these specimens are held in the entomological collection of the National Museum, Prague (NMPC); however vouchers will be deposited in the New Zealand Arthropod Collection, Auckland (NZAC) following a species-level taxonomic revision of the genus (M. Fikáček *et al.*, in prep.). The host plant data listed in Table 2 were compiled from collecting records of these specimens plus all available historical specimens deposited in NZAC and the Museum of Natural History, London (BMNH; Broun and Sharp collections); host plant data were available for 27 collecting events in total.

Larval specimens described here were collected directly from aquatic habitats in 2010 (see detailed label data in respective parts of descriptions) and preserved in ethanol. In addition, a few additional larval specimens corresponding morphologically with the

larvae of *Rygmodus* described herein were collected in 2012–2016; however, we have failed to sequence DNA of these specimens for barcoding, and therefore they are only briefly mentioned and not described here in detail. The larval specimens used in this study are deposited in Kitakyushu Museum of Natural History and Human History, Kitakyushu (KMNH) and NMPC.

Identification of adults and larvae

The taxonomy of *Rygmodus* was reviewed by Hansen (1997), who constructed an identification key of adult *Rygmodus* based on the examination of type specimens deposited in BMNH. This key does not deal with sexual dimorphism in some body parts (shape of claws and antennal club) in some species and completely omits the male genitalia. We re-examined the type specimens deposited in BMNH, alongside the newly collected specimens, and recognized that identification is straightforward for several species, that is, *R. modestus*, *R. tibialis* Broun, 1893, *R. femoratus* Sharp, 1884, and *R. alienus* Broun, 1893 but that detailed revision is required for other species or species complexes such as the *R. cyaneus* Broun, 1881 species complex, *R. incertus* Broun, 1880, and *R. pedinoides* White, 1846. Therefore, the species identification for the latter group is provisional in this study and will be investigated in detail in a future study.

We identified a single larval specimen (voucher #: COL1804) by DNA barcoding based on two molecular markers: a 268 bp fragment of nuclear histone 3 (H3) and a 776 bp fragment of mitochondrial cytochrome oxidase 1 (*cox1*) (Tables S1, S2). The H3 and *cox1* sequences of the larva were compared with those from identified adult specimens of *Rygmodus* and most New Zealand hydrophilid genera including all aquatic ones (Table S1). Most of the sequences were newly acquired; only one *cox1* sequence of *Rygmodus* (SLE0129) was taken from Short and Fikáček (2013). The sequence data were edited and aligned in Geneious 6.1 (Biomatters Ltd., Auckland, New Zealand) using the MUSCLE algorithm. The aligned data were analyzed using maximum likelihood with HKY + G (based on the best fitting model selected by jModelTest 2.1.1; Guindon & Gascuel 2003; Darriba *et al.* 2012) in the MEGA 7.0 software (Kumar *et al.* 2016); bootstrap values were calculated using 1,000 replicates in the same software.

Morphological studies of larvae and adults

For larval morphology, we largely followed the methods used by Minoshima and Hayashi (2011a). Given the limited larval specimens available for the study, our description is based on a few *R. modestus* larvae that were dissected and examined under a compound light microscope. The specimens were, unfortunately, partially damaged and some characters could not be observed; we described and illustrated them where possible. To assess intra- and inter-generic variation, these larvae were briefly compared with the additional larvae of other species. The specimens were cleared using ca. 10% KOH solution, dissected and examined on H-S Slides (Shirayama *et al.* 1993) with lactic acid or glycerol. The examined larvae are preserved in 80% ethanol and stored within screw-cap vials. Observations and dissections were carried out using Olympus SZX12 (Olympus, Tokyo, Japan) and Leica MZ16 (Leica Microsystems, Wetzlar, Germany) binocular microscopes and Nikon E600 (Nikon Instech, Tokyo, Japan) and Olympus BX50 compound light microscopes. Illustrations were made with the aid of a drawing tube attached to the E600. Photographs were taken with an Olympus PEN Lite E-PL5 digital camera attached to the SZX12. Composite images were created using the Image Stacking Software Helicon Focus (Helicon Soft, Kharkov, Ukraine). The images were modified using Adobe Photoshop CC and Lightroom CC (Adobe Systems, San Jose, CA, USA) as needed.

Adult mouthparts of *R. modestus* were examined in detail. They were dissected after treating the specimen with 10% KOH solution and embedded in Euparal resin (Waldeck GmbH & Co. KG, Münster, Germany) on a permanent microscopic slide following the protocol by Hanley and Ashe (2007). The mouthparts were photographed using a Canon EOS1100D (Canon, Tokyo, Japan) camera attached to an Olympus BX41 compound microscope; multilayer photographs were stacked using Helicon Focus software. Comparison with other cylomine genera was based on specimens dissected in the same way and deposited in NMPC. Detailed morphology of the mandible, especially the mandibular mola, was examined using an Hitachi S-3700 N environmental scanning electron microscope (Hitachi High-Technologies, Tokyo, Japan) after dissecting the mandible from the KOH-treated head and cleaning away organic dirt by 10% hydrogen peroxide solution. We examined the molar structure of four hydrophilid taxa for comparative purposes: *Rygmodus modestus* and *Saphydrus suffusus* Sharp, 1884 (both Cylominae, the former flower-visiting, the latter not; see Table 3), *Dactylosternum hydrophiloides* MacLeay, 1825 (Sphaeridiinae: Coelostomatini, terrestrial species feeding on decaying plant material) and *Helochares* (*Hydrobaticus*) sp. (Acidocerinae, saprophagous aquatic species).

The terminology of larval morphology follows Archangelsky (1997) and Minoshima *et al.* (2013).

For the primary chaetotaxy of the larval head we refer to Fikáček *et al.* (2008) and Byttebier and Torres (2009). The following abbreviations are used for description: AN, antenna; FR, frontale; gAN, group of antennal sensilla; gAPP, group of sensilla on inner appendage of maxilla; gFR, group of sensilla on frontale; gLA, group of sensilla on labium; gMX, group of sensilla on maxilla; LA, labium; MN, mandible; MX, maxilla; PA, parietale; SE, sensorium. The terminology of adult mouthparts follows Lawrence and Ślipiński (2013) as adopted for Hydrophilidae by Fikáček *et al.* (2014). Classification follows Short and Fikáček (2013) for Hydrophilidae, and Seidel *et al.* (2016) for Cylominae. Plant classification follows Stevens (2001 onwards) (see also Glenny *et al.* 2012; Angiosperm Phylogeny Group 2016).

Analysis of gut contents

In order to test whether *Rygmodus* adults feed on tissues or pollen of flowers they are visiting, we examined mid-gut contents of 15 specimens of at least four *Rygmodus* species collected from nine host plants. All the examined specimens were collected from flowers directly and stored in 96% ethanol until dissection. Each specimen was dissected as follows: the abdomen was removed, and then the middle to posterior part of the mid-gut and the hind-gut were dissected; the anterior part of the mid-gut, which reaches into the thorax, was not dissected in order to keep the remaining body parts of voucher specimens intact. We used one specimen to test whether any pollen grains could be observed in gut contents. The mid-gut contents were spread on a slide, stained and mounted with 0.25% safranine solution in glycerine (Jones 2012) and then examined at 100–200× magnification using an Olympus BX41 compound microscope. As pollen was observed in this test, the remaining specimens were sent to Landcare Research (Lincoln, New Zealand), where the contents of the intestines were extracted and processed. For each sample, the intestinal contents were washed in hot KOH for 10 min, followed by a wash in HCl and acetolysis. Pollen grains were then concentrated from the acetylized material using flotation with lithium polytungstate (specific gravity 2.2), and stained with fuchsin red and mounted with glycerol jelly on a slide. All pollen grains, or up to 200 in cases where more numbers of grains were present, were identified for each slide. In the latter cases, the samples were also checked for rare pollen grains; if present, they were indicated as "<1" in Table 1. The pollen grains were identified to the family, genus or species level, based on a reference collection of pollen grains held at Landcare Research and using pollen and spore identification keys (Large & Braggins 1991; Moar 1993).

RESULTS

DNA barcoding

The molecular phylogenetic tree resulting from the H3 sequences (Fig. 1A) revealed that all the examined *Rygmodus* adult specimens form a strongly supported (bootstrap, 99%) clade, and that the focal larval specimen (COL1804) belongs to this clade. Furthermore, the *cox1* tree (Fig. 1B) revealed that *R. modestus* is sister to the *R. cyaneus* complex (bootstrap, 100%), and that the larval specimen is nested inside of the *R. modestus* clade with strong support (bootstrap, 98%). Hence, the larva was reliably identified as *R. modestus*.

The topology outside of the *R. modestus* + *R. cyaneus* clade was incongruent between the H3 and *cox1* trees. The topology of the *cox1* tree seems congruent to the differentiation in the genital morphology among *Rygmodus* species: *R. alienus*, which is a member of the *R. alienus*–*R. antennatus* (Sharp, 1884) species complex characterized by the wide and short median lobe of aedeagus, was placed as the early-diverging taxon sister to the other sampled species, which are all characterized by the rather uniform genital morphology with the narrow and elongate median lobe of aedeagus. The H3 tree supported the close relationships of *R. femoratus* and *R. tibialis*, which are extremely similar in morphology.

Biology of *Rygmodus*

Adults

Rygmodus modestus adults (Fig. 2D) examined in detail for this study were collected in the middle of November 2012 on flowering bushes of *Olearia* in full sun at a picnic area along Aniwaniwa Road in the *Nothofagus* forest at the banks of the Aniwaniwa Stream, Te Urewera National Park. Several hundred specimens were found crawling on the blossoms on a single *Olearia* bush (Fig. 2A–C) and smaller numbers were collected by beating flowering bushes of *Brachyglottis repanda* in the same area (e.g. Fig. 3F). In addition to *Olearia* and *Brachyglottis* tree daisies (Asteraceae), adults of various species of *Rygmodus* were collected from flowers of a wide spectrum of white-flowering native bushes across New Zealand, in particular, those which have flowers accumulated in apparent inflorescences. Two additional host plants not recorded in our examined material were reported for *R. modestus* by Heine (1937): *Rubus australis* (Rosaceae) and *Euphrasia cuneata* (Orobanchaceae).

Table 1 Results of the analysis of mid-gut contents of *Rygmodus* adults

Species: collecting event (all New Zealand)	Collected from	Pollen type	Count[†]
R. modestus: GB: Te Urewera NP, Black Beech Tk, xi.2012[‡]	*Brachyglottis repanda*	*Aristotelia*	184
		Undetermined	1
R. modestus: GB: Te Urewera NP, Black Beech Tk, xi.2012[‡]	*Brachyglottis repanda*	Asteraceae	205
		Coprosma	39
		Pratia	27
		Prumnopitys taxifolia	6
R. modestus: GB: Te Urewera NP, Black Beech Tk, xi.2012[‡]	*Brachyglottis repanda*	*Aristotelia*	200
		Coprosma	<1
		Haloragaceae	<1
		Asteraceae	<1
		Hebe	<1
		Ericaceae	<1
R. cyaneus group: NC: Arthurs Pass, Temple basin Tk., i.2014	*Hebe*	*Hebe*	231
R. cyaneus group: NC: Arthurs Pass Village, i.2011	*Hoheria glabrata*	*Hoheria*	169
R. modestus: CL: Tapu, Coroglen Tk., xi.2009	*Cordyline australis*	*Cordyline*	200
		Cunoniaceae cf. *Weinmannia*	1
R. cyaneus group: WD: Otira, Kelly's Creek, i.2011	*Hoheria glabrata*	*Hoheria*	115
R. femoratus: BR: Lewis Pass, xii.2012	*Aciphylla*	*Aciphylla*	200
		Haloragaceae	1
		Poaceae	<1
R. cyaneus group: KA: Mt. Fyffe Hut, i.2012	*Celmisia*	*Pratia* cf. *angulata*	177
		Leptospermum	1
R. alienus: BR: Whareata Mine, Denniston, i.2012	*Leptospermum scoparium*	*Leptospermum*	200
		Asteraceae	<1
		Dacrydium cupressinum	<1
R. cyaneus group: Arthurs Pass, Temple Basin Tk., i. 2011	*Hebe* + *Ranunculus*	*Hebe*	87
		Poaceae	1
R. modestus: GB: Te Urewera NP, Aniwaniwa Rd., xi.2012	*Olearia*	Asteraceae	19
R. modestus: GB: Te Urewera NP, Aniwaniwa Rd., xi.2012	*Olearia*	Asteraceae	200
		Coprosma	<1

[†]Pollen grain count: "<1" refers to rare pollen types found after inspecting the whole slide but not in the subsample used for counting dominant pollen types.
[‡]Collected on the same inflorescence.

A summary of all known host plants is provided in Table 2.

Two of the 15 specimens analyzed had the mid-gut empty. The gut contents of the remaining 13 specimens consisted almost exclusively of pollen grains (e.g. Fig. 2E–J), with a very small amount of fine unidentified particles; larger non-pollen particles were very rare (unidentified parts of plant tissue and fungal sporangia; Fig. 2K,L). In all the specimens, one pollen type formed the majority of the mid-gut contents (in four specimens only one pollen type was found), and one to five additional pollen types were found in much smaller amounts. In ten specimens, the main pollen type corresponded to the flower from which the specimen was collected. Three specimens of *R. modestus* collected together from flowering *Brachyglottis repanda* showed very different contents of mid-gut (Table 1, rows 1–3); in two of them, the main pollen type did not correspond to the host plant from which they were collected. In total, the mid-guts of examined specimens contained pollen grains representing 14 plant families (Podocarpaceae, Apiaceae, Asteraceae, Asparagaceae, Campanulaceae, Cunoniaceae, Elaeocarpaceae, Ericaceae, Haloragaceae, Malvaceae, Myrtaceae, Plantaginaceae, Poaceae and Rubiaceae). Ten pollen types were identified to the genus level (*Dacrydium, Prumnopitys, Aciphylla, Aristotelia*, *Cordyline, Coprosma*, *Hebe, Hoheria*, *Leptospermum* and *Pratia*).

Pollen grains found in mid-guts of the dissected specimens largely agree with known plants on which museum specimens were collected (compare Tables 1 and 2: pollen grains of all known host plants except *Ranunculus* and *Pittosporum* were found). However, additional pollen types were recorded from the mid-guts: some of them (*Aristotelia*, *Coprosma* and *Pratia*) were subdominant or even dominant in mid-guts of a

Table 2 List of plant taxa, based on collection records of *Rygmodus* adults from their flowers/inflorescences in the present study and for museum specimens examined

Family	Genus/species
Asparagaceae	*Cordyline* spp. (*C. australis*, *C. banksii*, *C. indivisa*)
Apiaceae	*Aciphylla* sp.
Asteraceae	*Olearia* spp.
	Brachyglottis repanda
	Celmisia sp.
Ericaceae	*Gaultheria* sp.
Malvaceae	*Hoheria* sp.
Myrtaceae	*Leptospermum scoparium*
Orobanchaceae	*Euphrasia cuneata*[†]
Pittosporaceae	*Pittosporum eugenioides*
Ranunculaceae	*Ranunculus* sp. (white large-flower subalpine species)
Rosaceae	*Rubus australis*[†]
Plantaginaceae	Subalpine *Veronica* (*Hebe*) sp. (*Veronica subalpina* morphotype)

[†]After Heine (1937).

few dissected specimens and likely resulted from previous feeding of the respective specimens. Other pollen types were rare and may be remnants from previous feeding (especially for species with apparent inflorescences, such as *Prumnopitys* and *Weinmannia*) or contaminants brought to host plant flowers by other insects or by wind (e.g. Haloragaceae, grasses and podocarps).

Larvae

Larvae of *Rygmodus* were first found in 2010 at two localities in the Marlborough region, northern South Island: from moss growing on wet rocks beside the small waterfall in the Pelorus Bridge Scenic Reserve (Fig. 3E) and algal mats at sites of the Dead Horse Creek at Wakamarina Road south of Canvastown (Fig. 3G,H). The larvae collected in Dead Horse Creek were of a single morphotype. One (COL1804) of them was used for the species identification by DNA barcoding and identified as *R. modestus* (see above). These larvae were found in algal mats growing on exposed rocks with a thin film of water flowing over them, where they co-occurred with larvae of *Cylomissus glabratus* Broun, 1903 (see Minoshima *et al.* 2015 for details). At Pelorus Bridge, larvae of two morphotypes were found syntopically in the moss soaked by a thin film of water flowing through it. One type was morphologically identified as *R. modestus*, and the other as an unidentified *Rygmodus* species. The moss was inspected manually during the day and at night. At night, a single *Rygmodus* adult was found sitting on the moss in the waterfall; based on the larval identification presented in this paper, we suppose that it might have been an *R. modestus* female laying eggs there. During the later field work (undertaken 2012–2016 by M. Fikáček, M. Seidel, R. Leschen and M. Gimmel), a few larval specimens were found at several occasions: in wet moss at sides and below small waterfalls (Fig. 3F) of the Aniwaniwa Stream just below Aniwaniwa Falls, Te Urewera National Park, where numerous adults of *R. modestus* were collected as mentioned above, syntopically with adults and larvae of *Cylomissus glabratus*, in wet moss at the side of a tiny streamlet at Three Mile Pack Track south of Okarito (West Coast, South Island) (no adults found in this area), and in water under stones at the side of a small stream in the alpine tussock area at Arthur's Pass (West Coast/Canterbury, South Island) (Fig. 3I,J; adults of the *R. cyaneus* species group collected in the same area). In February 2016, three larval specimens of *Rygmodus* were sifted from leaf litter collected from two localities, Picnic Gully at the mouth of Taieri river south of Dunedin and along Matai Falls track in the Catlins area, in the very south of South Island. This area was very dry, without standing or flowing water at the time of collection, and large amounts of leaf litter accumulated in depressions and along drains, but we cannot exclude the possibility that the sifted leaf litter was originally accumulated at sides of streamlets flowing earlier in the season or flood debris. No adults were collected in February 2016 from this area, but we suppose that the larvae may be of *R. opimus* Broun, 1880 which is the only *Rygmodus* species recorded so far from this area (M. Fikáček, unpubl. data 2018).

Nothing is known about the length of larval development or the duration of adult stage. Our observations and label data from museum specimens suggest that adults appear mostly in spring and early summer (November–December) when the above-mentioned plant species bloom. In 2016, two adults were collected as late as at the end of January on *Hebe* bushes ending its bloom in the subalpine area below Borland Saddle, Fiordland, South Island.

Adult mouthparts of *Rygmodus*

Morphology of mouthparts of *R. modestus* (Figs 4A–G, S1) corresponds well with the general morphology of mouthparts of Hydrophilidae (Archangelsky *et al.* 2005; Fikáček & Vondráček 2014) and Cylominae (see Fikáček *et al.* 2014 for mouthparts of *Andotypus* Spangler, 1979 and *Austrotypus* Fikáček *et al.*, 2014). The following differences from other cylomine genera were found:

Labrum (Fig. S1B) moderately sclerotized, concealed under clypeus; transverse, ca. 2.6× wider than long, deeply concave on the anterior margin. Anterior margin with series of short setae mesally and very long setae on anterolateral corners; anterior third of dorsal portion bearing sparsely arranged very long setae.

Mandibles (Figs 4A–G, S1A) slightly asymmetrical, narrowly falcate in apical four fifths; mandibular angle very obsolete; apex simple, spoon-like. Inner face with fine long pubescence starting at apical fifth and reaching mola, mesal portion distally of mola membranous, finely pubescent. Mola large, hammer-shaped, strongly sclerotized on inner surface, asymmetrical; inner surface of both mandibles with strong denticles which are more massive on the left mandible, and finer (partly maybe abraded) in the right mandible.

Maxilla (Fig. S1D). Lacinia with sparse irregularly arranged long setae, sickle-shaped on distal parts; inner finger-like projection absent. Galea with a narrow basal sclerite extending over the inner surface; distal and outer surface membranous, bearing long irregularly arranged setae.

Labium (Fig. S1C). Mentum subquadrate, ca. 1.7× wider than long, lateral margins subparallel, with sparse setation, anterior margin bisinuate. Palpiger moderately sclerotized, rather narrow, partly concealed by mentum. Palpus with 3 palpomeres; basal palpomere minute, palpomeres II and III subequal in length, palpomere II with numerous fine sparsely arranged setae in distal portion. Prementum in form of two strongly sclerotized lobes reaching basal part of palpomere II, bearing very long setae along inner face. Hypostome projecting into a crescent-like lobe on each side below the premental lobe reaching distal part of palpomere II, each lobe bearing dense series on inner face.

DESCRIPTION OF LARVAL MORPHOLOGY

Rygmodus modestus White, 1846

Material examined

1 L2 (KMNH), Dead Horse Cr, south of Canvastown, Marlborough, South Island, New Zealand, 41°19.599′S, 173°39.579′E, wet stones with algae and moss along a stream (scraped slime on rock), 30. xi.2010, M. Fikáček & R. Leschen leg, RL1513.

Description of second-instar larva

Body (Fig. 3A–C). Slender, widest between abdominal segments III–V.

Color (Fig. 3A–C). Head capsule reddish brown with yellowish anterolateral and posteromedian parts; appendages reddish brown to yellowish. Thorax yellowish brown, sclerites darker. Abdomen yellowish brown; dorsal surface bicolored, with a regular pattern of dark areas on segments I–VII; ventral surface uncolored; sclerite of spiracular atrium brown.

Head. Head capsule (Fig. 7A) subtrapezoidal, slightly widened anteriorly. Cervical sclerite large, subquadrate. Frontal lines lyriform, coronal line short (Figs 5A, 7A). Surface of head capsule with minute microstructures distributed in posterior part of dorsal to lateroventral surface of parietale. Six stemmata on each anterolateral portion of head capsule. Posterior tentorial pits present on median part close to submental sulcus. Clypeolabrum almost symmetrical (Fig. 5C). Nasale with five large teeth; three median teeth smaller and more aggregated, both lateral teeth larger than median ones and more separated from them; all teeth subtriangular in shape. Nasale projecting slightly further than epistomal lobes. Lateral lobes of epistome present, almost symmetrical. Left lobe projecting anteriorly, rounded with widely obliquely truncate apex; right lobe similar to left lobe.

Chaetotaxy of head capsule. Frontale (Fig. 5A,C). Central part with three pairs of sensilla (FR1–3) slightly divergent posteriad; FR1 rather short seta; FR2 pore-like, situated more anteriorly and more mesally to FR1; FR3 short seta, close and anterior to FR2. Irregularly arranged longitudinal row of short setae present along frontal line. Pore-like sensillum FR4 and setae FR5–6 posteromesal to antennal socket; FR5 stout, rather short seta, posteromesal to FR6, FR6 rather long seta, lateral to FR4; FR4 mesal to FR5–6. FR7 rather short seta, on inner face of antennal socket. Setae FR9–10 closely aggregated, mesal to antennal socket; FR9 rather long, FR10 rather short. Pore-like sensillum FR15 and seta FR8 situated mesally on clypeolabrum, behind nasale; FR15 anterior to FR8, distance between left and right FR15 subequal to distance between left and right FR8. Sensilla FR11–14 on epistome, anteromesal to antennal socket; FR11, 13–14 pore-like, FR12 short seta; FR11–13 forming triangular group on inner part of epistome, FR12 posterior to FR11 and FR13, FR11 mesal to FR12–13. FR14 close to antennal socket, posterolateral to FR11–13. Nasale with a group of six stout and short setae (gFR1) and 2 minute ventral setae lateral to median tooth of nasale. Epistomal lobe with nine setae on anterior margin; seven lateral ones moderately long, bearing subapical tooth; inner two short.

Parietale (Fig. 5A,B). Dorsal surface with a group of five sensilla (PA1–5) forming slightly irregular longitudinal row in posterior part; PA1–2 and 4–5 short setae, PA3 pore-like. PA6 pore-like, located posteromesally close to coronal line. Densely arranged short setae

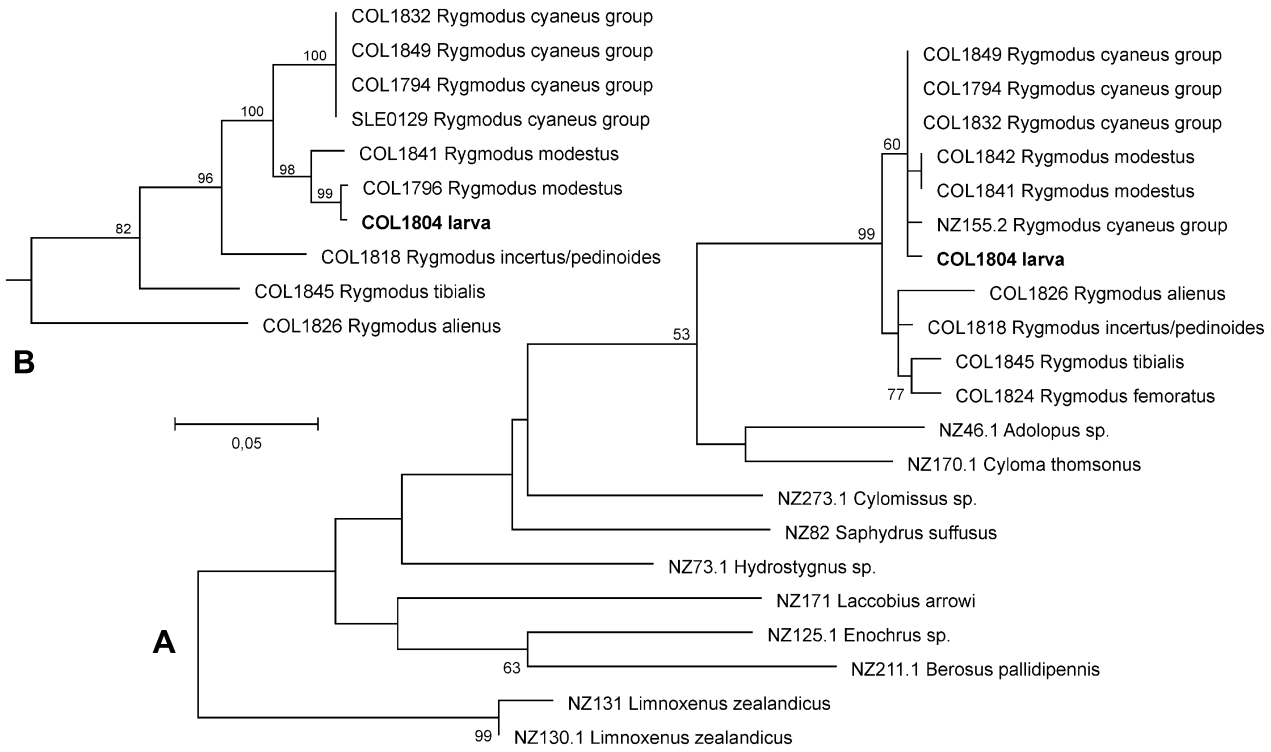

Figure 1 DNA barcoding of a larva (COL1804) in comparison with adult specimens of Hydrophilidae. (A) Maximum likelihood tree of nuclear H3 (histone 3) sequences of New Zealand hydrophilids, showing the monophyly of *Rygmodus*. (B) Maximum likelihood tree of mitochondrial cytochrome oxidase 1 (*cox1*) sequences of *Rygmodus*, showing that *R. cyaneus* and *R. modestus* form a clade and that the larva is identified as *R. modestus*. Bootstrap support values >50 are indicated above the branches.

present along frontal lines and anterior half of dorsal and lateral faces of parietale. Long setae PA7 and PA13 and short seta PA12 situated dorsally on median part of parietale, PA7 and PA12 closer than PA12 and PA13; PA7 mesal to PA12–13, PA12 between PA7 and PA13. PA14–17 in anterior third of lateral face of parietale, forming transverse row; PA14 and 16 long setae, PA15 and PA17 pore-like, arranged in following order (from dorsal to ventral ones): PA14, 15, 16, 17. Pore-like sensillum PA10 and short seta PA11 between anterior and posterior rows of stemmata; PA10 mesal to PA11. PA8–9 and PA19–22 on anterior corner of head capsule; PA8–9 and PA21 very long setae, PA20 and PA22 long setae, PA19 pore-like; PA8 posterior to lateral margin of antennal socket; PA9 lateral to antennal socket; PA19 between PA9 and PA20; PA20 and PA21 closely aggregated, PA20 dorsal to PA21; PA22 close and lateral to outer margin of ventral mandibular articulation. Pore-like sensilla PA23–25 on ventral mandibular articulation; PA23 on outer margin; PA24–25 on inner part, closely aggregated. Sensillum PA18 posterior to PA16–17, pore-like (but see Remarks). Pore-like sensillum PA30 posteromesal to PA18. PA26–28 aggregated, located ventrally on median part of anterior third of parietale, mesal to PA17 and PA18; PA26 possibly seta (seta missing, but socket of the same shape as PA28), anterior to PA27–28; PA27 pore-like, between PA26 and PA27; PA28 long seta. PA29 pore-like, posteromesal to PA28 and lateral to PA30, close to gular sulcus.

Antenna (Fig. 6A). Three-segmented, slender; surface of antenna smooth but a few very minute cuticular projections present on basal margin of dorsal surface of antennomere II. Antennomere I slightly longer than antennomeres II and III combined, antennomere I widest, antennomere III the shortest and narrowest. Approximate ratios of length of antennomeres I:II:III as follows: 1:0.6:0.2 (n = 1). Antennal sensorium present.

Chaetotaxy of antenna (Fig. 6A). Antennomere I with five pore-like sensilla (AN1–5) and 12 short setae sparsely distributed on dorsal surface. AN1 situated dorsolaterally on median part of inner surface, AN2 dorsally on distal fourth; AN3–5 subapical, AN3 on lateral face, AN4 on inner face, AN5 on inner part of ventral face. Antennomere II with one pore-like sensillum (AN6) situated dorsally on subapical part of sclerite. Setae AN7–8 and AN10–11 and sensorium (SE1) on intersegmental membrane between antennomeres II

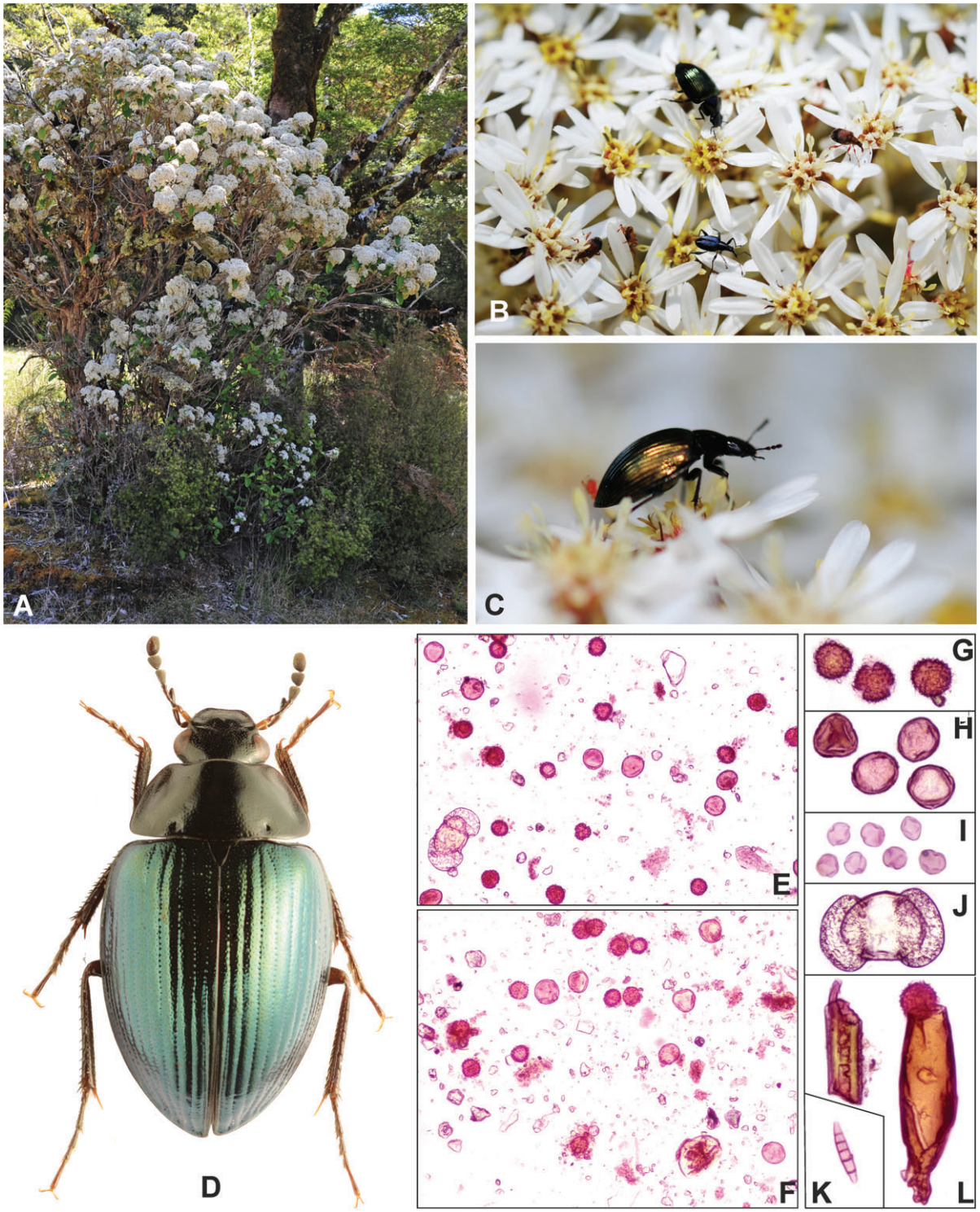

Figure 2 Adults of *Rygmodus modestus* White, 1846. (A–C) Mass occurrence of *R. modestus* adults at Aniwaniwa Road, Te Urewera National Park (New Zealand) in November 2012. (A) *Olearia* bushes from which adults were collected. (B,C) Alive *R. modestus* adults at *Olearia* flowers, together with *Rhopalomerus picipennis* (Pascoe) and *R. monachus* (Broun) (Curculionidae: Eugnominae) in (B). (D) Adult in dorsal view. (E–L) Safranine-dyed mid-gut contents of a specimen collected from *Brachyglottis repanda* at Black Beech Tk., Te Urewera National Park. (E,F) General view of the slide with dissected mid-gut contents. (G–J) Details of pollen grains found: (G) Asteraceae gen. sp.; (H) *Coprosma* sp.; (I) *Pratia* sp.; and (J) *Prumnopitys taxifolia*. (K,L) Other rarely occurring particles: (K) fungal sporangium and (L) fragment of plant tissue. Photographs (B,C) by J. Hájek.

Figure 3 Larvae and larval habitats of *Rygmodus* in New Zealand. (A–C) Second-instar larva of *R. modestus* (dorsal, lateral and ventral view, respectively). (D) Third-instar larva of *Rygmodus* sp. from Pelorus Bridge, dorsal view. (E–J) Habitats of larvae: (E) mossy waterfall at Pelorus Bridge (habitat of larvae of *Rygmodus* sp.); (F) small waterfall flowing over moss rock (habitat of larvae of *R. modestus*) with flowering *Brachyglottis repanda* at side (from which adults of the same species were collected) in Te Urewera National Park; (G,H) Dead Horse Creek, with detail of algal mats from which larvae of *R. modestus* were collected; (I,J) small stream in alpine tussock area at Arthur's Pass, with detail of stones under which larvae of *Rygmodus* were collected. Photographs (E,F) by M. Fikáček, (G,H) by R. Leschen, and (I,J) by M. Gimmel.

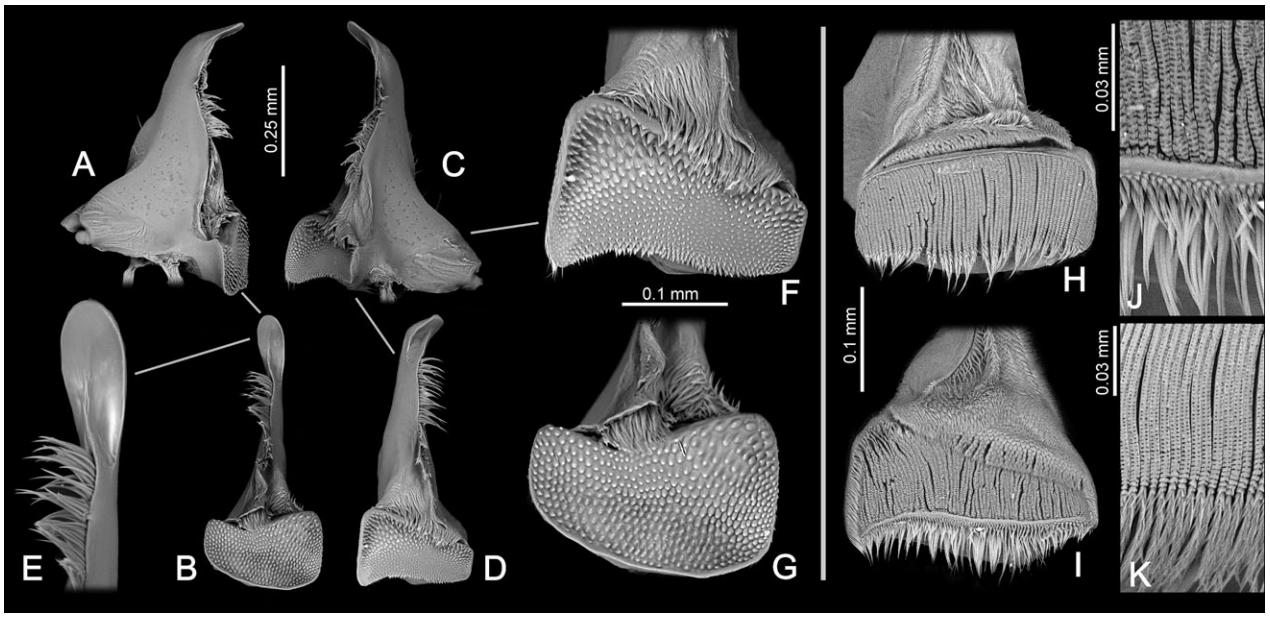

Figure 4 Mandibles of adult hydrophilid beetles. (A–G) *Rygmodus modestus*. (H–J) *Saphydrus suffusus* Sharp, 1884 (Cyclominae). (K) *Dactylosternum hydrophiloides* (MacLeay, 1825) (Sphaeridiinae). (A,C) Whole mandible, ventral view. (B,D) Whole mandible, mesal view. (E) Detail of mandibular apex in mesal view. (F–I) Detail of mola in mesal view. (J,K) Detail of fine structure of mola.

and III, AN9 absent; AN7–8 posterior and close to SE1, AN7 short, AN8 minute; AN10–11 on lateral face, AN10 very long, AN11 minute. Sensorium SE1 slender, as long as antennomere III, on outer face. Antennomere III with group of apical sensilla (gAN) in apical membranous area.

Mandibles (Fig. 6B). Slender, almost symmetrical, right mandible slightly longer than left one. Each mandible with two inner teeth present on median part of inner face; apical inner tooth larger than proximal one. Incisor area of left mandible roughly serrated, that of right one serrated in basal part only.

Chaetotaxy of mandibles (Fig. 6B). Three pore-like sensilla (MN2–4) on median part; MN4 on dorsolateral face, anterolateral to MN2–3, anterior to MN1; MN2 laterally to MN3; MN3 at base of apical inner tooth. Moderately long seta MN1 on lateral face, behind MN4; MN5 hard to distinguish, probably a minute seta on lateral face of subapical part. Outer face of mandibles bearing numerous short setae, except for apical part. MN6 undetectable.

Maxilla (Fig. 6C,D). Slender, 6-segmented, longer than antenna. Cardo moderate in size, irregularly shaped. Stipes the longest, ca. 1.75 times as long as palpomeres I–IV combined; inner face smooth except of few hair-like cuticular projections basally, between MX7 and MX8. Maxillary palpus short, 4-segmented. Palpomere I widest, incompletely cylindrically sclerotized dorsally. Inner process sclerotized. Palpomere II short, wider than palpomeres III and IV; palpomere III longest, wider than palpomere IV; palpomere IV rather short and narrowest. Approximate ratios of length of palpomeres I to IV as follows: 1.0:0.6:1.7:1.0 (n = 1).

Chaetotaxy of maxilla (Fig. 6C,D). Cardo with one ventral seta (MX1). Inner face of stipes with a row of five stout setae (MX7–11) and seven short setae; MX7 at base, MX8–9 subbasal, MX8 behind MX9, MX10 ca. at midlength, MX11 anterior to MX10. Pore-like sensilla MX2–3 situated ventrally on posterior two fifths; MX2 on lateral part, posterolateral to MX3. Pore-like sensilla MX4 and setae MX5–6 situated subapically on lateral face. Lateral half of ventral surface to lateral surface bearing numerous setae; lateral face with several long setae, remaining ones short to rather short. Dorsal surface of palpomere I with one rather short, stout seta (MX16) situated basally on inner face. Three sensilla (MX12–14) located laterally on distal part of sclerite (Fig. 3D); MX12 dorsal to MX13–14, MX13 between MX14 and MX12. Pore-like sensilla MX15 and MX17 on membrane behind inner appendage, MX17 dorsal, MX15 ventral. Inner appendage with one very long and a few short setae apically (gAPP). Palpomere II with two pore-like sensilla (MX18–19) and one minute seta (MX27); MX18 situated laterally on anterior margin of sclerite, MX27

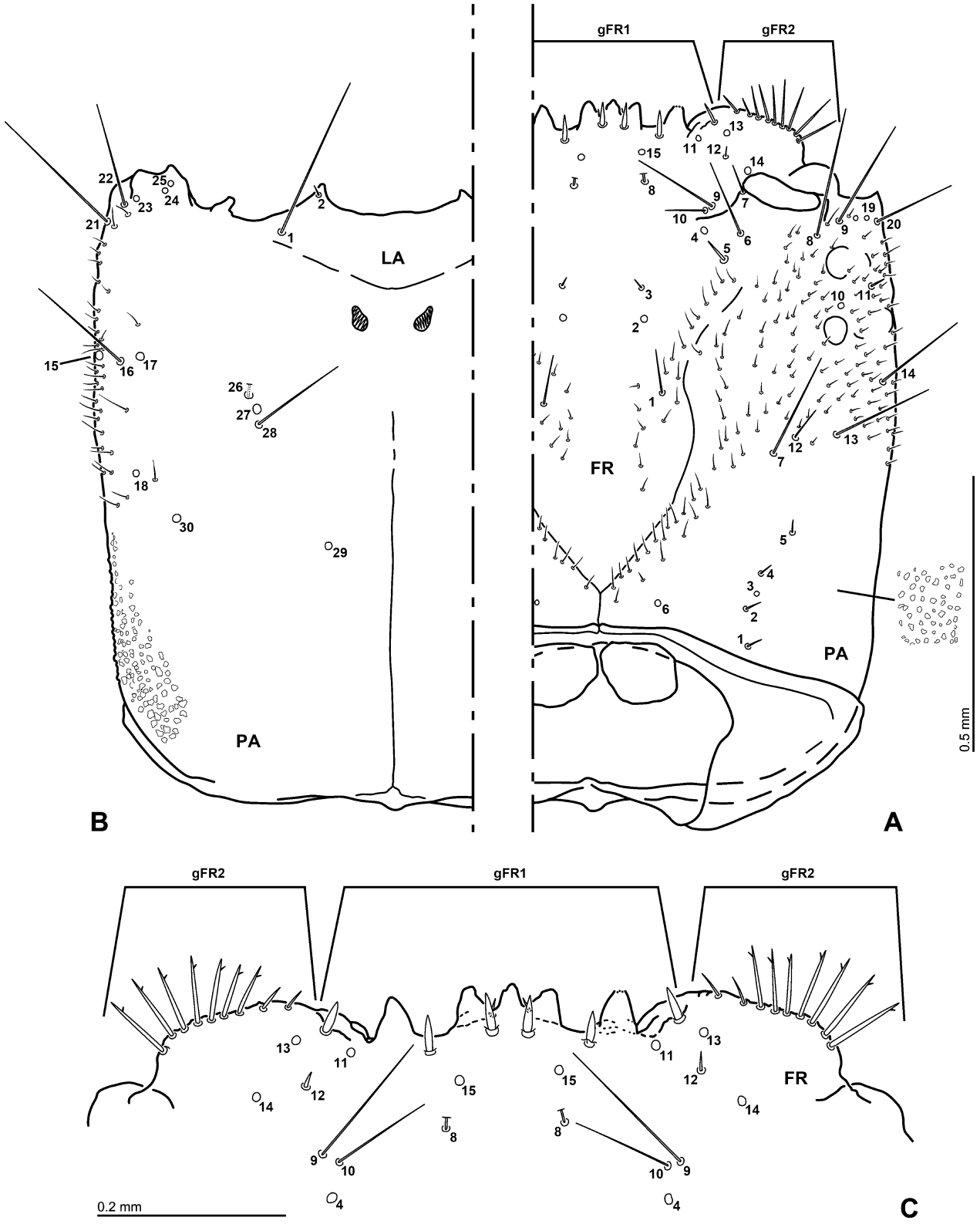

Figure 5 Head capsule of the second-instar larva of *Rygmodus modestus* and its chaetotaxy. (A) Dorsal view. (B) Ventral view. (C) Detail of clypeolabrum.

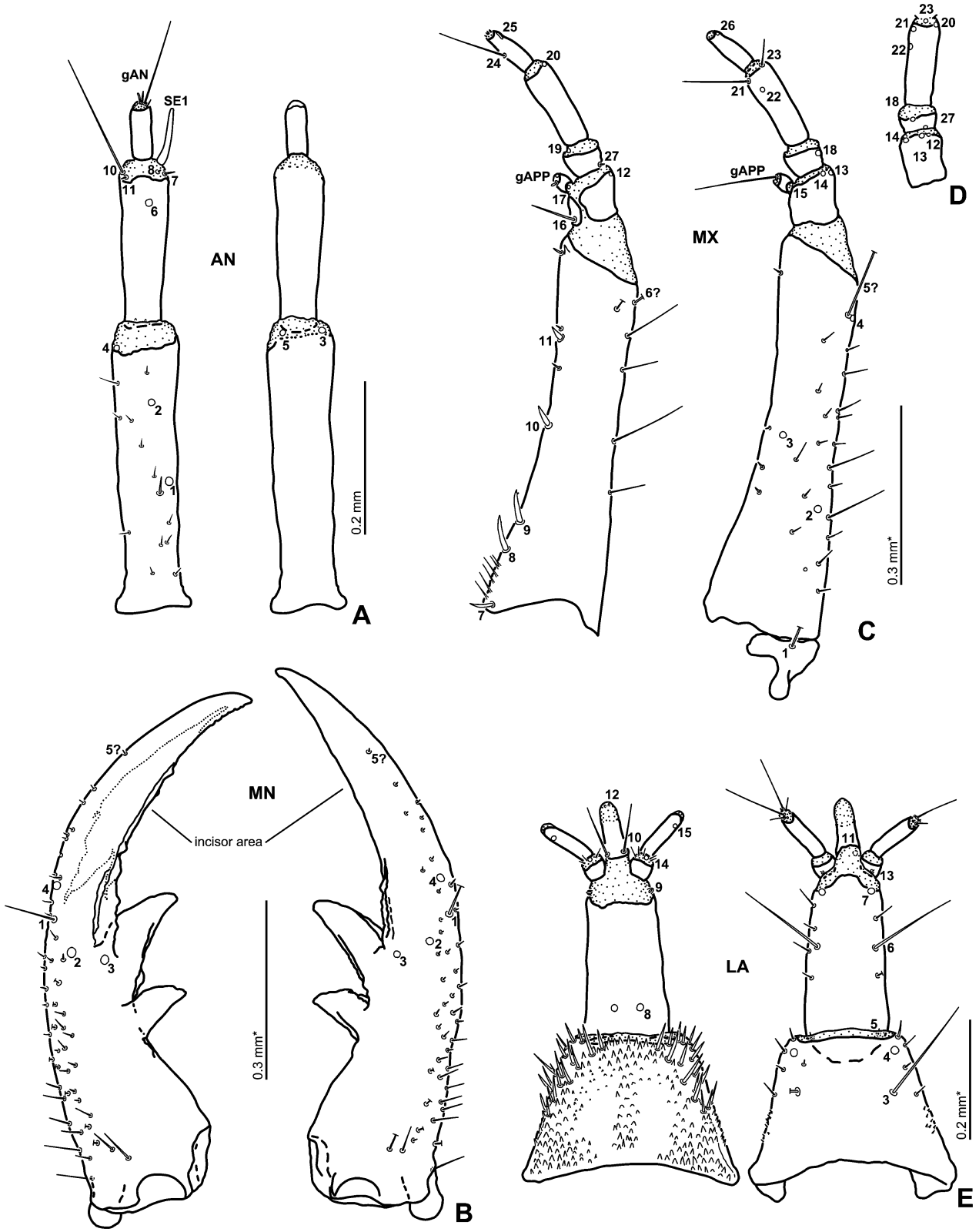

Figure 6 Head appendages of the second-instar larva of *Rygmodus modestus*. (A) Antenna, dorsal (left) and ventral (right) views. (B) Mandibles, dorsal view. (C) Maxilla, dorsal (left) and ventral (right) views. (D) Maxillary palpomeres 1–3, lateral view. (E) Labium in dorsal (left) and ventral (right) views.

on basal margin of lateral face; MX19 on inner face of intersegmental membrane between palpomeres II and III. Palpomere III with two pore-like sensilla (MX20 and MX22), and long (MX21) and short (MX23) setae. MX22 located ventrally on subapical part of sclerite; MX20–21 and MX23 distal, on borderline between sclerite and intersegmental membrane; MX21 on inner face, MX23 lateroventral, MX20 laterodorsal. Palpomere IV with one rather long seta (MX24) at midlength of inner face, and with digitiform (MX25) and pore-like (MX26) sensilla situated apically on outer face; MX25 dorsal, MX26 ventral. Apical membranous area of palpomere IV with several minute setae (gMX).

Labium (Fig. 6E). Developed. Submentum fused to head capsule, transverse; submental sulcus indistinct. Mentum trapezoid, widest at base. Dorsal and lateral surface densely covered with small cuticular teeth, dorsal surface with a pair of bare areas submedially. Prementum subquadrate, elongate, basal part slightly wider than apical part, without cuticular teeth; ca. 2.2 times longer than wide. Ligula slender, partly sclerotized medially, ca. as long as labial palpus. Labial palpus moderately long, palpomere I slightly wider than palpomere II; palpomere II long, parallel-sided, distinctly longer than palpomere I; intersegmental membrane between palpomeres I and II bearing a few short hair-like cuticular projections dorsally.

Chaetotaxy of labium (Fig. 6E). Submentum with two pairs of setae (LA1–2); LA1 very long on lateral margin, LA2 short on anterior corner. Mentum with a group of numerous rather short spiniform setae on dorsal to lateral surface of anterior corners; ventral face of anterior corners bearing a few short setae. Ventral surface of mentum with one pair of long setae (LA3) and pore-like sensilla (LA4) on anterior part; LA3 behind LA4, LA4 situated subapically on anterolateral corner. Prementum and its anterior membranous area with five pairs of sensilla (LA5–9), and a few short setae on lateral face of prementum. LA5–7 on lateroventral surface of prementum, minute seta LA5 at base, long seta LA6 at midlength; pore-like sensillum LA7 lateral, on borderline between sclerite and membrane; LA8 subbasal, on mesal part of dorsal surface. Sensillum LA9 situated laterally on anterior membranous area. Ligula with one pair of rather long setae (LA10) and two pairs of pore-like sensilla (LA11–12); LA10 situated dorsally on basal margin of sclerite, LA11 ventrally on subbasal part, LA12 at apex. Palpomere I with two sensilla (LA13–14); LA13 minute seta, situated ventrally at base; LA14 pore-like, situated dorsally on intersegmental membrane between palpomeres. Palpomere II with one pore-like sensillum LA15 situated apically on outer face of sclerite; several minute setae of variable shape (gLA) on apical membranous area.

Thorax. Membranous parts very densely covered with hair-like cuticular projections. Prothorax wider than head capsule (Fig. 3A). Proscutum formed by one large plate subdivided by fine sagittal line, anterior and posterior margins weakly sclerotized; proscutal plate covered with several very long setae, and densely distributed rather short setae and fine cuticular projections. Prosternal sclerite (Fig. 7D) incompletely subdivided by fine sagittal line at base; bearing numerous short setae on lateral part of anterior margins and along sagittal line. Mesonotum with three pairs of dorsal sclerites (Fig. 7B); two pairs on anterior margin, median pair transverse, attached mesally, lateral pair small; one large pair behind anterior pairs, subpentagonal, attached mesally, subdivided by transverse ridge anteriorly, with transverse shallow groove medially, covered with short setae and densely arranged fine cuticular projections in posterior half. One pair of tubercles situated anteriorly on lateral face. Mesothoracic spiracles projecting laterally, forming a small finger-like projection. Metanotum with four pairs of dorsal sclerites (Fig. 7C); two pairs on anterior margin, median pair transverse, attached mesally, lateral pair narrow, hardly visible; one large pair behind anterior two pairs, transverse, subquadrate, attached mesally, subdivided by transverse ridge, with transverse shallow groove, covered with short setae and densely arranged fine cuticular projections in posterior part; last pair behind large sclerite, transverse, mostly covered with short setae and densely arranged fine cuticular projections. Legs (Fig. 7E,F) rather short and slender, 5-segmented; all three pairs similar in shape.

Abdomen. Abdomen (Fig. 3A–C) 10-segmented, widest at segments III and IV, then tapering posteriad; membranous parts covered with densely arranged hair-like cuticular projections. Segment I with two pairs of dorsal sclerites; anterior pair smaller than posterior pair, these two pairs closely aggregated, and may thus appear as one large semicircular sclerite subdivided by fine sagittal and transverse lines. One pair of spiracles on lateral part of dorsal surface, weakly tuberculate. Segments II–VII similar to segment I, but dorsal sclerites absent. Spiracular atrium (Fig. 7G): Segment VIII bearing short to moderately long hair-like cuticular projections; dorsal plate present but margins of the plate weakly defined and hardly visible; dorsal plate may be oblong oval, bearing minute but stout spine-like cuticular projections. Procercus short, inner part sclerotized. Segment IX trilobed, partly sclerotized. Lateral lobe of spiracular atrium large, partly sclerotized,

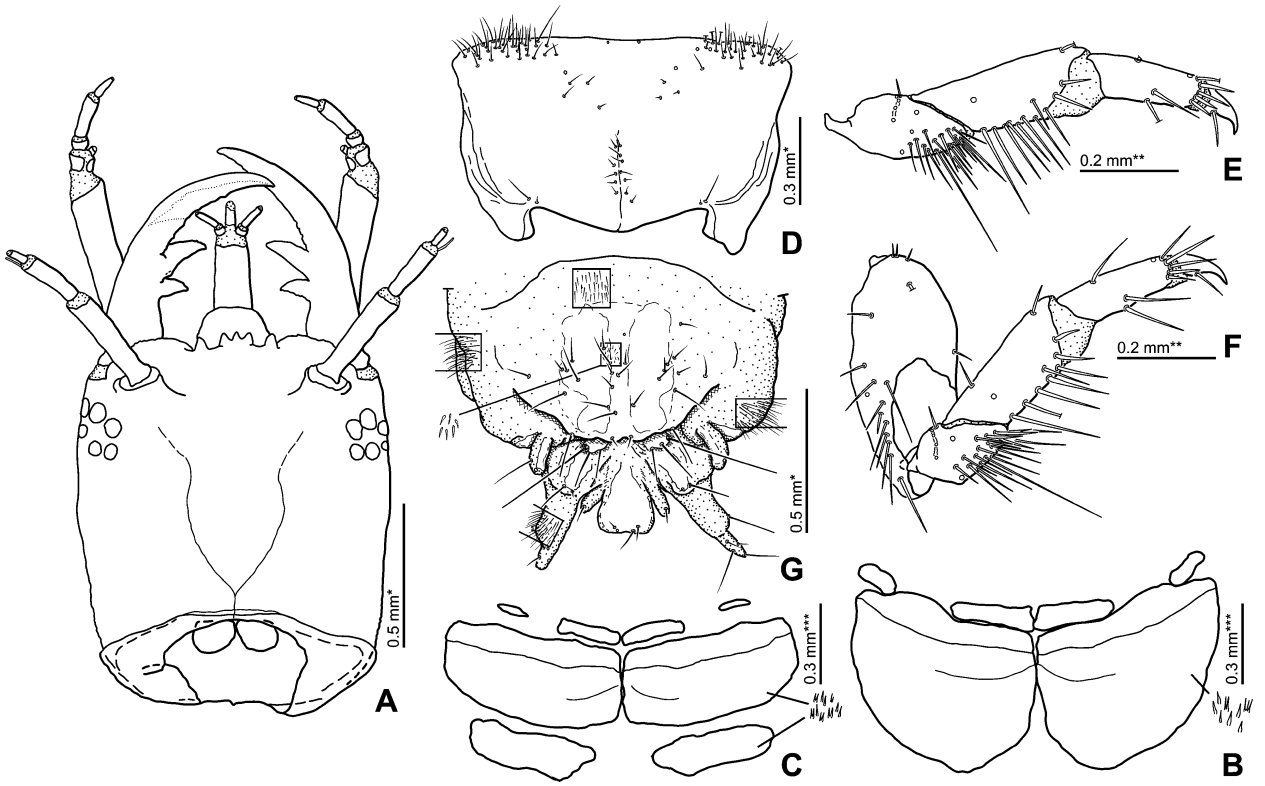

Figure 7 Details of larval morphology of the second-instar larva of *Rygmodus modestus*. (A) Head, dorsal view. (B) Mesonotum sclerites, dorsal view. (C) Metanotal sclerites, dorsal view. (D) Prosternal plate, ventral view. (E) Foreleg, anterior view. (F) Mesoleg, anterior view. (G) Abdominal apex with spiracular atrium.

narrowing apically, bearing rather long hair-like cuticular projections; acrocercus present but borderline between lateral lobe and acrocercus indistinguishable. Median lobe of spiracular atrium large, sclerotized dorsally, widest apically; a pair of moderately long projections present between median and lateral lobes.

Remarks

We examined only one second-instar larva in detail. Although many additional/secondary sensilla were present, especially on the frontale, almost all primary sensilla were detectable. A few sensilla which are problematic in terms of the homology or morphology (pore-like *vs*. seta) are commented below.

PA18: After comparison with other cylomine larvae examined by us (*Andotypus* and *Austrotypus*: Fikáček *et al*. 2014; *Cylomissus* Broun, 1903 and *Anticura* Spangler, 1979: Minoshima *et al*. 2015), the pore marked PA18 in Figure 5B is very likely the true PA18. Sensillum PA18 is a seta in all known hydrophilid larvae including Cylominae (e.g. Fikáček *et al*. 2008, 2014; Minoshima & Hayashi 2011b, 2012; Clarkson *et al*. 2014; Minoshima *et al*. 2015), hence it is possible that the seta has been broken before or during preparation.

PA26: We marked a pore closely aggregated with PA27–28 as PA26 (Fig. 5B), and assumed that this sensillum was originally a seta. This is based on the shape of the socket of PA26, which is very similar to that of PA28, and the fact that PA26 is a seta in *Rygmodus* sp. (Fig. S2B). PA26 and PA28 are usually setae in hydrophilid larvae (e.g. Fikáček *et al*. 2008, 2015; Minoshima & Hayashi 2011a; but see also Fikáček *et al*. 2008 and Minoshima *et al*. 2017 for arrangement of PA26–28 in Laccobiini).

MN5: Mandibular sensillum MN5 is undetectable from additional/secondary sensilla (Fig. 6B). To determine the precise position of the sensillum, examination of the first-instar larva is necessary. We treated an apical seta as MN5 for the moment.

MN6: MN6 seems to be absent (Fig. 6B), but usually this pore is hardly visible even when present (as in other cylomine larvae; Fikáček *et al*. 2014; Minoshima *et al*. 2015). The presence or absence of MN6 cannot be decided at the moment.

MX5–6: Maxillary sensilla MX5–6 are very often undetectable from closely situated secondary sensilla in second- and third-instar larvae (Minoshima & Hayashi 2011a); thus we labelled these with a question mark (Fig. 6C).

Rygmodus sp.

We examined the following material: 1 L3 (KMNH), Pelorus Bridge, Marlborough, South Island, New Zealand, 41°30.490′S, 173°56.747′E, 29.x.2010, night collecting around waterfall splash zone, RL1509, M. Fikáček & R. Leschen leg. Description and figures are presented in File S1 and Figures S1, S2.

DISCUSSION

Insect pollination in New Zealand

The flora of New Zealand is composed of a high diversity of plants that tend to have white flowers and are thought to be pollinated by wind or little specialized insect groups such as flies, beetles, basal groups of Lepidoptera and short-tongued bees (e.g. Heine 1937; Webb & Kelly 1993; Swenson & Bremer 1997; Newstrom & Robertson 2005; Newstrom-Lloyd 2013), in agreement with the observation that New Zealand insect fauna have a paucity of specialized day-active pollinators. The low diversity of bees and butterflies in New Zealand led Primack (1978) to describe the pollinator fauna as "unspecialized", which might be partly a consequence of the biogeographic history of New Zealand as a continental island (e.g. Buckley *et al.* 2015). However, Primack (1978) was especially interested in the montane fauna, and his conclusion should not be applied to the entire New Zealand fauna: although not all flower-feeding beetle lineages are present in New Zealand, there is a relatively rich fauna of galerucine beetles (Chrysomelidae), dasytine beetles (Melyridae) and weevils (Curculionidae: Curculioninae: Eugnomini) (e.g. Heine 1937; Kuschel 1990). There are also "unusual" day-time flower visitors that are unique to New Zealand or occur only in the Australian region: species of *Rygmodus* (Hydrophilidae) treated in this paper, cryptophagid beetles (Leschen & Gimmel 2012), the erotylid beetle *Loberonotha olivascens* (Broun, 1893) (Leschen 2003), some oxypodine Aleocharinae (Leschen & Newton 2015), and the extraordinarily high diversity of flower-visiting Scirtidae (Klimaszewski & Watt 1997). All these groups may be also pollen specialists and pollinators.

Pollen-feeding and pollination in *Rygmodus*

The early records of *Rygmodus* species from *Brachyglottis, Cordyline* and *Aciphylla* flowers were reported by Thomson (1881) and Broun (1886). Since then, a few faunistic studies (Heine 1937; Primack 1983) have listed *Rygmodus* species as "pollinators", but without demonstrating that the beetles can deliver viable pollen and facilitate fertilization. Our study is the first to demonstrate the specialized morphology of *Rygmodus* mandibles and confirm the presence of pollen in the guts of these beetles.

When *Rygmodus* mandibles are compared to those of other hydrophilid beetles, including members of the subfamily Cylominae to which *Rygmodus* belongs, two differences are apparent: the simple (rather than bidentate) scoop-like apex of the mandible (Fig. 4B,E), and the denticulate microstructure of molae (Fig. 4B,D,F, G). Inner surfaces of molae consist of high vertical lamellae with fine comb-like edges (together composing a fine sieve-like structure) in all hydrophilids examined, that is, aquatic *Helochares* Mulsant, 1844, a cylomine not visiting flowers (*Saphydrus* Sharp, 1884; Fig. 4H–J, Table 3) and terrestrial hydrophilids feeding on rotten plant material (*Dactylosternum* Wollaston, 1854; Fig. 4K) and excrements (*Sphaeridium* Fabricius, 1775; Holter 2004). All these hydrophilid groups likely feed on fine particles (16–19 μm in *Sphaeridium*; Holter 2004) extracted from water-soaked detritus, and the sieve may serve for drainage of superfluous fluid (Holter 2004) and/or size-selection of detritus particles. This "compression-sieve" involving complex molae is also present in other groups of beetles (e.g. scarabaeoids: Nel & Scholtz 1990; M. Seidel, pers. obs. 2017). The molar structure of *Rygmodus* clearly differs from this pattern: it lacks the vertical lamellae and bears irregularly arranged denticles, resembling the molar structure of pollen-feeding omaliine staphylinid beetles (Betz *et al.* 2003). Compared to other spore-feeding or microphagous beetles, *Rygmodus* differs in having an internally scooped-shaped incisor lobe for gathering pollen and broad, transverse molae with denticulate surfaces and raised borders (compared to striate and somewhat flattened molae in many other spore-feeding groups) and utilized as a pollen press.

The spectrum of pollen grains found in the mid-gut (Table 1) and the list of flowers from which the beetles were collected (Table 2) indicate that *Rygmodus* are generalist pollen-feeders exploiting a wide range of available flowers. Feeding specialization seems habitat-based: for example, species of the *R. cyaneus* complex mostly occur in subalpine habitats across North and South Islands of New Zealand, and are hence very frequently recorded from subalpine *Hebe* species. The pollen grains extracted from the mid-gut of *Rygmodus* are not punctured, abraded, or cracked as in other pollen-feeding beetles examined, for example, the New Zealand cryptophagid *Paratomaria crowsoni* Leschen, 1996 collected from *Brachyglottis repanda* (R. A. B. Leschen, pers. obs. 2016). *Paratomaria* Leschen, 1996 differs from *Rygmodus* in the smaller

body length (<2 mm) and mandibles more typical for spore-feeding beetles, with the bidentate incisor lobe (not scoop-like), the relatively smaller prostheca compared to the body of the entire mandible and the striate mola. In contrast to the cryptophagid, it is possible that more pollen grains are gathered into the oral space of *Rygmodus* and their subtle compression by molae is enough to make them ready to extract nutrients. Moreover, the ancestors of *P. crowsoni* were likely mycophagous (Leschen 1996) rather than saprophagous; different ways of food processing in *Paratomaria* and *Rygmodus* may hence also reflect difference in evolutionary history between these taxa.

A large part of the ventral surface of *Rygmodus* is covered with pubescence, which is sparser than in other hydrophilid beetles (in which it primarily holds an air bubble when the beetle is submerged: e.g. Fikáček *et al.* 2012). Denser pubescence is only present on ventral surface of tarsi, on antennal club and on mouthparts (labrum, galea, prementum and hypopharynx). No pollen grains were found from these densely pubescent body parts on inspection with safranine staining or electron microscopy; however, as the examined specimens were preserved in alcohol, we cannot rule out the possibility that pollen grains were washed out in the fixative fluid. We are hence unable to confirm that *Rygmodus* might serve as a pollinator at the moment, and additional observations of live specimens are necessary.

Habitat shifts in *Rygmodus*

The life style of *Rygmodus*, with flower-visiting, pollen-feeding adults and aquatic larvae, is unique within the Hydrophilidae; the larval habitat is different from the adult habitat, and adults' association with flowers is also unusual within the family. Only a few flower visitors have been reported within the Hydrophilidae: adults of *Pseudohydrobius* Blackburn, 1898 (Cyclominae) come to flowers of *Leptospermum* (Lea 1919), adults of *Cycreon* Orchymont, 1919 and *Nitidulodes* Sharp, 1882 (Sphaeridiinae: Megasternini) are known to be associated with inflorescences of Araceae (Bloom *et al.* 2014; Low *et al.* 2016; Arriaga-Varela *et al.* 2018), and *Pelosoma* Mulsant, 1844 (Megasternini) with inflorescences of *Heliconia* (Archangelsky 1997).

Within the subfamily Cyclominae, *Rygmodus* is unusual in only larvae being aquatic. Cyclominae contains 19 described genera (Short & Fikáček 2013; Seidel *et al.* 2016) that usually inhabit forest leaf litter, rotten organic matter or aquatic environments as both adults and larvae (Table 3). The most recent common ancestor of the subfamily was estimated as having a

Table 3 Summary of larval and adult habitats in the representatives of Cyclominae

Genus	Larval habitat	Adult habitat	References
Adolopus Sharp, 1884	Terrestrial (leaf litter, rotten wood)	Terrestrial (leaf litter, rotten wood)	M. Seidel & M. Fikáček, pers. obs. 2015, 2016
Andotypus Spangler, 1979	Terrestrial (leaf litter, baited traps)	Terrestrial (leaf litter, baited traps)	Fikáček *et al.* (2014)
Anticura Spangler, 1979	Aquatic	Aquatic (submerged moss)	Minoshima *et al.* (2015)
Austrotypus Fikáček *et al.* 2014	Terrestrial (rotten organic material)	Terrestrial (rotten organic material)	Fikáček *et al.* (2014)
Borborophorus Hansen 1990	? Terrestrial (log and bark litter)	Terrestrial (leaf litter, rotten wood)	Fikáček (2018)
Coelostomopsis Hansen 1990	Unknown	Terrestrial (leaf litter, FIT traps)	Fikáček (2018)
Cyloma Sharp, 1872	Terrestrial (leaf litter)	Terrestrial (leaf litter, baited traps)	M. Seidel & M. Fikáček, pers. obs. 2015, 2016
Cylomissus Broun, 1903	Aquatic	Aquatic (submerged moss)	Minoshima *et al.* (2015)
Cylorygmus Orchymont, 1933	Semiaquatic	Semiaquatic	Seidel *et al.* (2018)
Eurygmus Hansen 1990	Unknown	Terrestrial (FIT traps)	Fikáček (2018)
Exydrus Broun 1886	Unknown	Terrestrial (leaf litter, baited traps)	M. Seidel & M. Fikáček, pers. obs. 2015, 2016
Hydrostygnus Sharp, 1884	Unknown	Terrestrial (leaf litter, baited traps)	M. Seidel & M. Fikáček, pers. obs. 2015, 2016
Petasopsis Hansen 1990	Unknown	Terrestrial (leaf litter)	Hansen (1990)
Pseudohydrobius Blackburn, 1898	Unknown	Terrestrial (flower-visiting)	Fikáček (2018)
Relictorygmus Seidel *et al.*, 2018	Unknown	Semiaquatic	Seidel *et al.* (2018)
Rygmodus White, 1846	Aquatic/semiaquatic	Terrestrial (flower-visiting)	This paper
Rygmostralia Orchymont, 1933	Unknown	Terrestrial	Fikáček (2018)
Saphydrus Sharp, 1884	Terrestrial (leaf litter)	Terrestrial (sweeping, baited traps)	M. Seidel & M. Fikáček, pers. obs. 2015, 2016
Tormissus Broun, 1893	Terrestrial (rotten organic material)	Terrestrial (rotten organic material)	M. Seidel & M. Fikáček, pers. obs. 2015, 2016

Table 4 Comparison of larval morphology among genera of the subfamily Cylominae

Character	*Andotypus*	*Anticura*	*Austrotypus*	*Cylomissus*	*Cylorygmus*	*Rygmodus*	? *Borborophorus*
Nasale	One small tooth	Two teeth	One tooth	Single or two teeth	Five teeth	Five teeth	Five teeth
Epistomal lobe	Left lobe projecting further than right lobe	Almost symmetrical	Left lobe projecting further than right lobe	Almost symmetrical	Almost symmetrical	Almost symmetrical	Almost symmetrical
Number of setae of gFR2, left/right	8/2	8–9/5–8	11/0	6/4	7–8/7–9	9/9	4/4
Coronal line	Absent	Present	Absent	Present	Present	Present	Present
Mandible	Asymmetrical/stout	Symmetrical/stout	Asymmetrical/stout	Symmetrical/stout	Symmetrical/stout	Symmetrical/narrow	Symmetrical/stout
Prementum	Wider than long	Wider than long	Wider than long	Wider than long	As long as wide or slightly wider than long	Much longer than wide	Wider than long
Ligula	Reduced	Developed	Reduced	Developed	Developed	Developed	Developed
Hypopharyngeal lobe	Absent	Absent	Present	Absent	Absent	Absent	Absent
Antennal sensorium, SE1	Slightly shorter than antennomere III, thick	Very short, thick	Very short, thick	Half the length of antennomere III, stout	Shorter than antennomere III, thick	As long as antennomere III, thin	As long as antennomere III, thick
gMX2	Present	Present	Present	Present	Absent	Absent	Absent
Lateral projections abdominal segment VIII	Present	Absent	Present	Absent	Absent	Absent	Absent
Dorsal plate on segment VIII	Subdivided	Simple	Subdivided	Simple	Simple	Simple	Simple

gFR, group of sensilla on frontale; gMX, group of sensilla on maxilla; SE, sensorium.

terrestrial life style by Bloom *et al.* (2014), and subsequent unpublished analyses have reconstructed the cylomine ancestor as inhabiting decaying plant material in both larval and adult stages (V. Sýkora, unpubl. data 2015). Hence, it can be hypothesized that habitat shifts from decaying plant material to the association with flowers in adults and to aquatic habitats in larvae occurred in the ancestor of *Rygmodus*. The association with flowers is also known in the Australian genus *Pseudohydrobius* (Lea 1919). *Pseudohydrobius* has been placed in the principal clade of Cylominae, along with *Rygmodus*, by preliminary phylogenetic analyses (V. Sýkora *et al.*, unpubl. data 2015), but no detailed information about its biology or life cycle is available. Based on examination of slide-mounted specimens, *Pseudohydrobius* resembles *Rygmodus* in the simple mandibular apex, but the shape of its mandible is different (wider and shorter) and the mola seems to have the usual lamellate structure as shown in Figure 4H–K for other hydrophilids. It also lacks the basal tooth on tarsal claws, which is an autapomorphy for adult *Rygmodus* (Hansen 1997) and may facilitate crawling on plants/flowers. Additional research is therefore necessary to reveal whether *Rygmodus* and *Pseudohydrobius* have independently evolved the habit of association with flowers, or whether they are sister genera.

The association of *Rygmodus* larvae with aquatic habitats (stream edges and mossy spray zones) is secondary, and parallel to the terrestrial to aquatic transitions in the cylomine genera *Cylomissus* and *Anticura* (Short & Fikáček 2013; Bloom *et al.* 2014; Minoshima *et al.* 2015). Larval mouthparts of *Rygmodus* resemble those of the tribe Hydrophilini in having the long narrow falcate mandibles, long antenna-like maxillae and labium with far-projecting long prementum, differing from all other known cylomine larvae. Hydrophilinae larvae are ambush-type predators feeding on a wide spectrum of aquatic invertebrates (e.g. Hosseinie 1976; Matta 1982; Formanowicz & Brodie 1988). From the morphological similarity of mouthparts, we may expect that *Rygmodus* larvae are also predatory. When compared to other known Cylominae larvae (Table 4), *Rygmodus* shares the nasale with five teeth, low almost symmetrical epistomal lobes, presence of coronal line, long antennal sensorium and presence of only five stout setae on inner face of the maxillary stipes with larvae supposedly belonging to the Australian genus *Borborophorus* Hansen, 1990 (Fikáček 2018) and Chilean *Cylorygmus* Orchymont, 1933 (Seidel *et al.* 2018); it however differs in all these characters from the genera *Cylomissus*, *Anticura*, *Andotypus* and *Austrotypus* (Fikáček *et al.* 2014; Minoshima *et al.* 2015). These differences correspond to the preliminary results of phylogenetic analyses (M. Fikáček & V. Sýkora, unpubl. data 2015), in which *Rygmodus*, *Borborophorus* and *Cylorygmus* are members of the same principal clade but all the other aforementioned genera do not seem closely related to them, forming another big clade.

ACKNOWLEDGMENTS

We are indebted to the authorities of the Department of Conservation of New Zealand and responsible local DoC and iwi representatives for making our field work possible. We are grateful to Nicola Bolstridge (Manaaki Whenua, Lincoln) for the help with the pollen preparations, and to Matthew Gimmel (Santa Barbara Museum of Natural History, USA) and Axel Becker (Friedrich Schiller Universität, Jena, Germany) for the assistance during our field work. Maxwell Barclay and Christine Taylor (both Natural History Museum, London, UK) allowed the access to the historical Broun and Sharp collections without which we would not be able to provide species identification for the specimens examined in this paper; both collections were studied in 2013 by M.F. with the financial support of the SYNTHESYS project GB-TAF-2710. This work was partly supported by: JSPS KAKENHI Grant Number JP17K15187 to Y.M., the Ministry of Culture of the Czech Republic (DRKVO 2018/13, National Museum, 00023272) and Charles University Research Centre program No. 204069 to M.F. This project has received funding from the European Union's Horizon 2020 research and innovation programme under the Marie Skłodowska-Curie grant agreement No 642241. J.W. and R.L. were funded in part by core funding from the Crown Research Institute from the Ministry of Business, Innovation and Employment's Science and Innovation Group. The work of M.S. at the Department of Zoology, Charles University, was supported by grant SVV 260434/2017. N.G. was supported by the Commonwealth Environmental Research Facilities "Taxonomic Research Information Network" emerging priorities program and an OCE postdoctoral fellowship from CSIRO, Australia.

REFERENCES

Angiosperm Phylogeny Group (2016) An update of the Angiosperm Phylogeny Group classification for the orders and families of flowering plants: APG IV. *Botanical Journal of the Linnean Society* **181**, 1–20.

Archangelsky M (1997) Studies on the biology, ecology, and systematics of the immature stages of New World Hydrophiloidea (Coleoptera: Staphyliniformia). *Bulletin of the Ohio Biological Survey, New Series* **12**, 1–207.

Archangelsky M (1999) Adaptations of immature stages of Sphaeridiinae (Staphyliniformia, Hydrophiloidea: Hydrophilidae) and state of knowledge of preimaginal hydrophilidae. *Coleopterists Bulletin* **53**, 64–79.

Archangelsky M, Beutel RG, Komarek A (2005) Hydrophiloidea. 10.1. Hydrophilidae. In: Beutel RG, Leschen RAB (eds) *Handbook of Zoology. Volume IV: Arthropoda: Insecta. Part 38. Coleoptera, Beetles*, *Volume 1: Morphology and Systematics (Archostemata, Adephaga, Myxophaga, Polyphaga partim)*, pp 157–183. Walter De Gruyter, Berlin.

Arriaga-Varela E, Seidel M, Deler-Hernández A, Senderov V, Fikácek M (2017) A review of the *Cercyon* Leach (Coleoptera, Hydrophilidae, Sphaeridiinae) of the Greater Antilles. *ZooKeys* **681**, 39–93.

Arriaga-Varela E, Wong SY, Kirejtshuk A, Fikáček M (2018) Review of the flower-inhabiting water scavenger beetle genus *Cycreon* (Coleoptera: Hydrophilidae), with descriptions of new species and comments on its biology. *Deutsche Entomologische Zeitschrift* (in press).

Balke M (2005) 7.6. Dytiscidae Leach, 1915. In: Beutel RG, Leschen RAB (eds) *Handbook of Zoology. Volume IV: Arthropoda: Insecta. Part 38. Coleoptera, Beetles 1. Morphology and Systematice (Archostemata, Adephaga, Myxophaga, Polyphaga Partim)*, pp 90–116. Walter de Gruyter, Berlin.

Bernhard D, Schmidt C, Korte A, Fritzsch G, Beutel RG (2006) From terrestrial to aquatic habitats and back again – molecular insights into the evolution and phylogeny of Hydrophiloidea (Coleoptera) using multigene analyses. *Zoologica Scripta* **35**, 597–606.

Betz O, Thayer MK, Newton AF (2003) Comparative morphology and evolutionary pathways of the mouthparts in spore-feeding Staphylinoidea (Coleoptera). *Acta Zoologica* **84**, 179–238.

Bloom DD, Fikáček M, Short AEZ (2014) Clade age and diversification rate variation explain disparity in species richness among water scavenger beetle (Hydrophilidae) lineages. *PLoS ONE* **9**, Article ID, e98430. https://doi.org/10.1371/journal.pone.0098430

Broun T (1886) *Manual of the New Zealand Coleoptera. Part III*. Colonial Museum and Geological Survey Department, Wellington.

Brown HP (1987) Biology of riffle beetles. *Annual Review of Entomology* **32**, 253–273.

Buckley TR, Krosch M, Leschen RAB (2015) Evolution of New Zealand insects: summary and prospectus for future research. *Austral Entomology* **54**, 1–27.

Byttebier B, Torres PLM (2009) Description of the preimaginal stages of *Enochrus* (*Hugoscottia*) *variegatus* (Steinheil, 1869) and *E.* (*Methydrus*) *vulgaris* (Steinheil, 1869) (Coleoptera: Hydrophilidae), with emphasis on larval morphometry and chaetotaxy. *Zootaxa* **2139**, 1–22.

Clarkson B, Albertoni FF, Fikáček M (2014) Taxonomy and biology of the bromeliad-inhabiting genus *Lachnodacnum* (Coleoptera: Hydrophilidae: Sphaeridiinae). *Acta Entomologica Musei Nationalis Pragae* **54**, 157–194.

Condamine FL, Clapham ME, Kergoat GJ (2016) Global patterns of insect diversification: towards a reconciliation of fossil and molecular evidence? *Scientific Reports* **6** Article ID, 19208. https://doi.org/10.1038/srep19208

Darriba D, Taboada GL, Doallo R, Posada D (2012) jModelTest 2: more models, new heuristics and parallel computing. *Nature Methods* **9**, 772.

Fenoglio S, Tierno de Figueroa JM (2003) Observations on the feeding of adults of some *Neoperla* and *Anacroneuria* species (Plecoptera: Perlidae). *African Entomology* **11**, 138–139.

Fikáček M (2018) 10D. Hydrophilidae Latreille, 1802. In: Lawrence JF, Ślipiński A (eds) *Australian Beetles*, Vol. **2**. CSIRO Publishing, Melbourne. (in press).

Fikáček M, Vondráček D (2014) A review of *Pseudorygmodus* (Coleoptera: Hydrophilidae), with notes on the classification of the Anacaenini and on distribution of genera endemic to southern South America. *Acta Entomologica Musei Nationalis Pragae* **54**, 479–514.

Fikáček M, Archangelsky M, Torres PLM (2008) Primary chaetotaxy of the larval head capsule and head appendages of the Hydrophilidae (Coleoptera) based on larva of *Hydrobius fuscipes* (Linnaeus, 1758). *Zootaxa* **1874**, 16–34.

Fikáček M, Prokin A, Angus RB *et al.* (2012) Phylogeny and the fossil record of the Helophoridae reveal Jurassic origin of extant hydrophiloid lineages (Coleoptera: Polyphaga). *Systematic Entomology* **37**, 420–447.

Fikáček M, Minoshima Y, Vondráček D, Gunter N, Leschen RAB (2013) Morphology of adults and larvae and integrative taxonomy of Southern Hemisphere genera *Tormus* and *Afrotormus* (Coleoptera: Hydrophilidae). *Acta Entomologica Musei Nationalis Pragae* **53**, 75–126.

Fikáček M, Minoshima YN, Newton AF (2014) A review of *Andotypus* and *Austrotypus* gen. nov., rygmodine genera with an austral disjunction (Hydrophilidae: Rygmodinae). *Annales Zoologici* **64**, 557–596.

Fikáček M, Maruyama M, Komatsu T, Beeren C, von Vondráček D, AEZ S (2015) Protosternini (Coleoptera: Hydrophilidae) corroborated as monophyletic and its larva described for the first time: a review of the myrmecophilous genus *Sphaerocetum*. *Invertebrate Systematics* **29**, 23–36.

Formanowicz DR, Brodie ED (1988) Prey density and ambush site changes in *Tropisternus lateralis* larvae (Coleoptera, Hydrophilidae). *Journal of the Kansas Entomological Society* **61**, 420–427.

Girón JC, Short AEZ (2017) Revision of the Neotropical water scavenger beetle genus *Quadriops* Hansen, 1999 (Coleoptera, Hydrophilidae, Acidocerinae). *Zookeys* **705**, 115–141.

Glenny D, James T, Cruickshank J *et al.* (2012) *Key to Flowering Plant Genera of New Zealand*. [cited 19 Jun 2017.] Available from URL: http://www.landcareresearch.co.nz/resources/identification/plants/flowering-plants-key

Guindon S, Gascuel O (2003) A simple, fast, and accurate algorithm to estimate large phylogenies by maximum likelihood. *Systematic Biology* **52**, 696–704.

Hanley RS, Ashe JS (2007) Techniques for dissecting adult aleocharine beetles (Coleoptera: Staphylinidae). *Bulletin of Entomological Research* **93**, 11–18.

Hansen M (1990) Australian Sphaeridiinae (Coleoptera: Hydrophilidae): a taxonomic outline with descriptions of new genera and species. *Invertebrate Taxonomy* **4**, 317–395.

Hansen M (1997) Synopsis of the endemic New Zealand genera of the beetle subfamily Sphaeridiinae (Coleoptera: Hydrophilidae). *New Zealand Journal of Zoology* **24**, 351–370.

Heine EM (1937) Observations on the pollination of New Zealand flowering plants. *Transactions and Proceedings of the Royal Society of New Zealand* **67**, 133–148.

Holter P (2004) Dung feeding in hydrophilid, geotrupid and scarabaeid beetles: examples of parallel evolution. *European Journal of Entomology* **101**, 365–372.

Hosseinie SO (1976) Comparative life histories of three species of *Tropisternus* in the laboratory (Coleoptera: Hydrophilidae). *Internationale Revue der Gesamten Hydrobiologie und Hydrographie* **61**, 261–268.

Hunt T, Bergsten J, Levkanicova Z *et al.* (2007) A comprehensive phylogeny of beetles reveals the evolutionary origins of a superradiation. *Science* **318**, 1913–1916.

Jones GD (2012) Pollen analyses for pollination research, unacetolyzed pollen. *Journal of Pollination Ecology* **9**, 96–107.

Klimaszewski J, Watt JC (1997) Coleoptera: family-group review and keys to identification. *Fauna of New Zealand* **37**, 1–194.

Kodada J, Jäch MA (2005) 18.2. Elmidae Curtis, 1830. In: Beutel RG, Leschen RAB (eds) *Handbook of Zoology. Volume IV: Arthropoda: Insecta. Part 38. Coleoptera, Beetles 1. Morphology and Systematics (Archostemata, Adephaga, Myxophaga, Polyphaga partim)*, pp 471–496. Walter de Gruyter, Berlin.

Kumar S, Stecher G, Tamura K (2016) MEGA7: molecular evolutionary genetics analysis version 7.0 for bigger datasets. *Molecular Biology and Evolution* **33**, 1870–1874.

Kuschel G (1990) Beetles in a suburban environment: a New Zealand case study. *DSIR Plant Projection Report* **3**, 1–118.

Large MF, Braggins JE (1991) *Spore Atlas of New Zealand Ferns and Fern Allies*. SIR Publishing, Wellington.

Lawrence JF, Ślipiński A (2013) *Australian Beetles. Volume 1. Morphology, Classification and Keys*. CSIRO Publishing, Melbourne.

Lea AM (1919) Notes on some miscellaneous Coleoptera, with descriptions of new species. Part V. *Transactions of the Royal Society of South Australia* **43**, 166–261 pls xxv–xxvii.

Leschen RAB (1996) Phylogeny and revision of the genera of Cryptophagidae (Coleoptera: Cucujoidea). *The University of Kansas Science Bulletin* **55**, 549–634.

Leschen RAB (2003) Erotylidae (Insecta: Coleoptera: Cucujoidea): phylogeny and review. *Fauna of New Zealand* **47**, 1–108.

Leschen RAB, Gimmel ML (2012) Catalogue of the tribe Picrotini (Coleoptera: Cryptophagidae: Cryptophaginae). *New Zealand Entomologist* **35**, 14–28.

Leschen RAB, Newton AF (2015) Checklist and type designations of New Zealand Aleocharinae (Coleoptera: Staphylinidae). *Zootaxa* **4028**, 301–353.

Low SL, Wong SY, Ooi IH *et al.* (2016) Floral diversity and pollination strategies of three rheophytic Schismatoglottideae (Araceae). *Plant Biology* **18**, 84–97.

Matta JF (1982) The bionomics of two species of *Hydrochara* (Coleoptera: Hydrophilidae) with descriptions of their larvae. *Proceedings of the Entomological Society of Washington* **84**, 461–467.

Mayhew PJ (2007) Why are there so many insect species? Perspectives from fossils and phylogenies. *Biological Reviews* **82**, 425–454.

Minoshima Y, Hayashi M (2011a) Larval morphology of the Japanese species of the tribes Acidocerini, Hydrobiusini and Hydrophilini (Coleoptera: Hydrophilidae). *Acta Entomologica Musei Nationalis Pragae* **51** (Suppl), 1–118.

Minoshima Y, Hayashi M (2011b) Larval morphology of the genus *Hydrocassis* Fairmaire (Coleoptera: Hydrophilidae). *Journal of Natural History* **45**, 2757–2784.

Minoshima Y, Hayashi M (2012) Larval morphology of *Amphiops mater mater* Sharp (Coleoptera: Hydrophilidae: Chaetarthriini). *Zootaxa* **3351**, 47–59.

Minoshima Y, Hayashi M, Kobayashi N, Yoshitomi H (2013) Larval morphology and phylogenetic position of *Horelophopsis hanseni* Satô et Yoshitomi (Coleoptera, Hydrophilidae, Horelophopsinae). *Systematic Entomology* **38**, 708–722.

Minoshima YN, Fikáček M, Gunter N, Leschen RAB (2015) Larval morphology and biology of New Zealand–Chilean genera *Cylomissus* Broun and *Anticura* Spangler (Coleoptera: Hydrophilidae: Rygmodinae). *Coleopterists Bulletin* **69**, 687–712.

Minoshima YN, Iwata Y, Fikáček M, Hayashi M (2017) Description of immature stages of *Laccobius* (*Laccobius*) *kunashiricus*, with a key to genera of the Laccobiini based on larval characters (Coleoptera, Hydrophilidae). *Acta Entomologica Musei Nationalis Pragae* **57**, 97–119.

Moar NT (1993) *Pollen Grains of New Zealand Dicotyledonous Plants*. Manaaki Whenua Press, Lincoln.

Nel A, Scholtz CH (1990) Comparative morphology of the mouthparts of adult Scarabaeoidea (Coleoptera). *Entomology Memoirs, Department of Agricultural Development, Republic of South Africa* **80**, 1–84.

Newstrom L, Robertson A (2005) Progress in understanding pollination systems in New Zealand. *New Zealand Journal of Botany* **43**, 1–59.

Newstrom-Lloyd LE (2013) Pollination in New Zealand. In: Dymond JR (ed.) *Ecosystem Services in New Zealand: Conditions and Trends*, pp 408–431. Manaaki Whenua Press, Lincoln.

Primack RB (1978) Variability in New Zealand montane and alpine pollinator assemblages. *New Zealand Journal of Ecology* **1**, 66–73.

Primack RB (1983) Insect pollination in the New Zealand mountain flora. *New Zealand Journal of Botany* **21**, 317–333.

Rainford JL, Hofreiter M, Nicholson DB, Mayhew PJ (2014) Phylogenetic distribution of extant richness suggests metamorphosis is a key innovation driving diversification in insects. *PLoS ONE* **9**, Article ID, e109085. https://doi.org/10.1371/journal.pone.0109085

Rúa J, Tierno de Figueroa JM (2013) Adult feeding habits of three Perloidea species (Plecoptera: Perlidae and Chloroperlidae). *Aquatic Insects* **35**, 99–104.

Ruta R, Klausnitzer B, Prokin A (2017) South American terrestrial larva of Scirtidae (Coleoptera: Scirtoidea): the adaptation of Scirtidae larvae to saproxylic habitat is more common than expected. *Austral Entomology* **57**, 50–61.

Seidel M, Arriaga-Varela E, Fikáček M (2016) Establishment of Cylominae Zaitzev, 1908 as a valid name for the subfamily Rygmodinae Orchymont, 1916 with an updated list of genera (Coleoptera: Hydrophilidae). *Acta Entomologica Musei Nationalis Pragae* **56**, 159–165.

Seidel M, Minoshima YN, Arriaga-Varela E, Fikáček M (2018) Breaking a disjunct distribution: a review of the Southern Hemisphere genera *Cylorygmus* and *Relictorygmus* gen. nov. (Hydrophilidae: Cylominae). *Annales Zoologici* **68**, 375–402.

Shirayama Y, Kaku T, Higgins RP (1993) Double-sided microscopic observation of meiofauna using an HS-slide. *Benthos Research* **44**, 41–44. (In Japanese with English abstract.)

Short AEZ, Fikáček M (2011) World catalogue of the Hydrophiloidea (Coleoptera): additions and corrections II (2006–2010). *Acta Entomologica Musei Nationalis Pragae* **51**, 83–122.

Short AEZ, Fikáček M (2013) Molecular phylogeny, evolution and classification of the Hydrophilidae (Coleoptera). *Systematic Entomology* **38**, 723–752.

Stevens PF (2001 onwards) *Angiosperm Phylogeny Website, Version 13*. [Cited 19 Jun 2017.] Available from URL: http://www.mobot.org/MOBOT/research/APweb/

Swenson U, Bremer K (1997) Patterns of floral evolution of four Asteraceae genera (Senecioneae, Blennospermatinae) and the origin of white flowers in New Zealand. *Systematic Biology* **46**, 407–425.

Thomson GM (1881) The flowering plants of New Zealand, and their relation to the insect fauna. *Transactions of the Botanical Society of Edinburgh* **14**, 91–105.

Toussaint EFA, Hendrich L, Escalona HE, Porch N, Balke M (2016) Evolutionary history of a secondary terrestrial Australian diving beetle (Coleoptera, Dytiscidae) reveals a lineage of high morphological and ecological plasticity. *Systematic Entomology* **41**, 650–657.

Webb CJ, Kelly D (1993) The reproductive biology of the New Zealand flora. *Trends in Ecology & Evolution* **8**, 442–447.

Yang AS (2001) Modularity, evolvability, and adaptive radiations: a comparison of the hemi- and holometabolous insects. *Evolution & Development* **3**, 59–72.

SUPPORTING INFORMATION

Additional supporting information may be found online in the Supporting Information section at the end of the article.

File S1 Description of the second instar larva of *Rygmodus* sp.
Figure S1 Mouthparts of *Rygmodus modestus*.
Figure S2 Head capsule of the third instar larva of *Rygmodus* sp. from Pelorus Bridge and its chaetotaxy.
Figure S3 Head appendages of the third instar larva of *Rygmodus* sp. from Pelorus Bridge.
Table S1 List of specimens used for molecular analyses, along with GenBank accession numbers of their sequences.
Table S2 Primers used for amplification of molecular data.

Supplementary material

to the paper

Minoshima, Y. N., Seidel, M., Wood, J. R., Leschen, R. A., Gunter, N. L., & Fikáček, M. (2018). Morphology and biology of the flower-visiting water scavenger beetle genus *Rygmodus* (Coleoptera: Hydrophilidae). *Entomological Science*, 21(4): 363-384.

File S1. Description of the third instar larva of *Rygmodus* sp.

***Rygmodus* sp.**
(Figs. 3D, S2, S3)

Description of third instar larva.
Dorsal and ventral habitus similar to *R. modestus*, but head morphology and head chaetotaxy differ from that species in many aspects. Morphology of head hence described below.

Head. Head capsule subtrapezoidal, widest anteriorly (Fig. S2A, B). Cervical sclerite large, subquadrate. Frontal lines lyriform, coronal line short. Surface of head with minute microstructures distributed in posterior part of dorsal to ventral surface of parietale. Six stemmata on each anterolateral portion of head capsule. Posterior tentorial pits present on median part close to submental sulcus. Clypeolabrum almost symmetrical. Nasale with five large teeth; three median teeth smaller and more aggregated, both lateral teeth larger than median ones and more separated from them; all teeth subtriangular in shape, submedian teeth sometimes slightly bifid at apex. Nasale projecting slightly further than epistomal lobes. Lateral lobes of epistome present, almost symmetrical. Left lobe projecting anteriorly, rounded with widely obliquely truncate apex; right lobe similar to left lobe.

Chaetotaxy of head capsule. Frontale (Fig. S2A, C). Central part with three pairs of sensilla (FR1–3) slightly divergent posteriad; FR1 rather short seta; FR2 pore-like, anterior and mesal to FR1; FR3 short seta, close and anterior to FR2. A few short setae close to FR1. Pore-like sensillum FR4 and setae FR5–6 posteromesal to antennal socket; FR5 stout, rather short seta, posteromesal to FR6, FR6 rather long seta, lateral to FR4; FR4 mesal to FR5–6. FR7 rather short seta on inner face of antennal socket. Sensilla FR9–10 closely aggregated, mesal to antennal socket; FR9 possibly seta (based on morphology of socket), broken in examined specimen, FR10 rather short. Pore-like sensillum FR15 and seta FR8 situated mesally on clypeolabrum, behind nasale; FR15 anteromesal to FR8. Sensilla FR11-14 on epistome, anteromesal to antennal socket; FR11, 13–14 pore-like, FR12 short seta; FR11–13 forming triangular group on inner part of epistome, FR12 posterior to FR11 and FR13, FR11 mesal to FR12–13. FR14 close to antennal socket, posterolateral to FR11–13. Nasale with a group of six stout and short setae (gFR1) and two minute ventral setae lateral to median tooth of nasale. Epistomal lobe with eight setae and one pore-like sensillum on anterior margin; setae bearing subapical tooth.

Parietale (Fig. S2A–B). Dorsal surface with a group of five sensilla (PA1–5) forming slightly irregularly longitudinal row in posterior part; PA1–2 and 4–5 short setae, PA3 pore-like. PA6 pore-like, located posteromesally close to coronal lines. Densely arranged short setae present along frontal lines, numerous short setae on anterior half of dorsal and lateral face of parietale. PA7 and PA12–13 on median part of dorsal surface, PA12 at midlength between PA7 and PA13. PA14 on anterior third of lateral part of parietale. PA8 posterior to lateral margin of antennal socket. PA9 close and lateral to PA8. PA19–22 on anterior corner of head capsule; PA19–21 closely aggregated on dorsal part, PA22 close to ventral mandibular articulation. PA10–11 behind PA8–19. PA15–17 on anterior fourth of lateral face, closely aggregated. PA18 and PA30 at midlength of lateral part of ventral face, PA30 posteromesal to PA18. Pore-like sensilla PA23–25 on ventral mandibular articulation; PA23 on outer margin; PA24–25 on inner part, aggregated. Setae PA26 and PA28 and pore PA27 on median part of anterior third of ventral surface. PA29 situated ventrally on midlength of parietale, close to gular sulcus.

Antenna (Fig. S3A) (antennomere 1 of the specimen examined in detail was broken during fixation or preparation). Antenna 3-segmented, slender; surface of antenna smooth but minute cuticular projections present on ventral surface of antennomere 1. Antennomere 1 distinctly longer than antennomeres 2 and 3 combined, antennomere 1 widest, antennomere 3 the shortest and narrowest. Approximate ratios of length of antennomeres 1 to 3 as follows: 1:0.6:0.3 (n=1). Antennal sensorium present.

Chaetotaxy of antenna (Fig. S3A). Antennomere 1 with five pore-like sensilla (AN1–5); AN1 situated dorsally on basal two-fifths; AN2 dorsally on anterior fourth of mesal part; AN3–5 subapical, AN3 on lateral face, AN4 on inner face, AN5 on inner part of ventral surface. Antennomere 2 with one pore-like sensillum (AN6) situated dorsally on anterior fourth of sclerite. Setae AN7–8 and AN10–11 and sensorium (SE1) on intersegmental membrane between antennomeres 2 and 3, AN9 absent; AN7–8 posterior and close to SE1, AN7 short, AN8 minute; AN10–11 on lateral face, AN11 minute. Sensorium SE1 slender, as long as antennomere 3, on outer face. Antennomere 3 with group of apical sensilla (gAN) in apical membranous area.

Mandibles (Fig. S3B) (apical part of right mandible of the specimen broken) slender, may almost symmetrical. Two inner teeth present on median part of inner face each; apical inner tooth larger than proximal one.

Chaetotaxy of mandibles (Fig. S3B). Three pore-like sensilla (MN2–4) on median part; MN4 on dorsolateral face, anterolateral to MN2–3, anterior to MN1; MN2 between MN1 and MN3; MN3 at base of apical inner tooth. Moderately long seta MN1 on lateral face, behind MN4; MN5 situated subapically on lateral face. Outer face of mandibles bearing numerous minute setae excluding apical part, basal part bearing ca 10 short setae. MN6 not detected.

Maxilla (Fig. S3C) slender, 6-segmented, longer than antenna. Cardo moderate in size, irregularly shaped. Stipes the longest, ca. twice as long as palpomeres 1–4 combined; a few hair-like cuticular projections present basally on inner face, between MX7 and MX8. Maxillary palpus short, 4-segmented. Palpomere 1 widest, incompletely cylindrically sclerotised dorsally. Inner process sclerotised. Palpomere 2 short, slightly wider than palpomeres 3 and 4; palpomere 3 longest; palpomere 4 rather short and narrowest. Approximate ratios of length of palpomeres 1 to 4 as follows: 1.0:0.7:1.9:1.0 (n=1).

Chaetotaxy of maxilla (Fig. S3C). Cardo with one ventral seta (MX1). Inner face of stipes with a row of five stout setae (MX7–11); MX7 at base, MX8–9 on subbasal part, MX8 behind MX9, MX11 on anterior third, MX10 on midlength between MX9 and MX11. Pore-like sensilla MX2–3 situated ventrally on ca. posterior two fifths; MX2 on lateral part; MX3 on inner part. MX4–6 situated subapically on lateral face. Inner face bearing a row of sparsely arranged setae ventrally. Outer face bearing numerous short to moderately long setae. Ventral surface bearing a few short to minute setae. Dorsal surface of palpomere 1 with one rather short, stout seta (MX16) situated basally on inner face. Three sensilla (MX12–14) located laterally on distal part of sclerite; MX12 dorsal to MX13–14, MX13 between MX14 and MX12. Pore-like sensilla MX15 and MX17 on membrane behind inner appendage, MX17 dorsal, MX15 ventral. Inner appendage with one very long and a few short setae apically (gAPP). Palpomere 2 with two pore-like sensilla (MX18–19) and one minute seta (MX27); MX18 situated laterally on anterior margin of sclerite; MX27 behind MX18, situated laterally at basal margin of sclerite; MX19 on inner face of intersegmental membrane between palpomeres 2 and 3. Palpomere 3 with four sensilla (MX20–23, homology of MX20 and MX23 identified by comparison with *R. modestus*). MX22 located ventrally on subapical part of sclerite; MX20–21 and MX23 distal, on borderline between sclerite and intersegmental membrane; MX21 on inner face, MX23 lateroventral, MX20 laterodorsal. Palpomere 4 with one moderately long seta (MX24) on median part of inner surface,

and with digitiform (MX25) and pore-like (MX26) sensilla situated apically on outer face of sclerite; MX25 dorsal, MX26 ventral. Apical membranous area of palpomere 4 with several minute setae (gMX).

Labium (Fig. S3D) developed. Submentum fused to head capsule, transverse; submental sulcus indistinct. Mentum trapezoid, widest at base, with rounded anterior corners. Dorsal and lateral surface densely covered with small cuticular teeth, without bare areas. Prementum subquadrate, parallel sided, elongate, without cuticular teeth; ca. 1.7 times longer than wide. Ligula stout, partly sclerotised medially, rounded apically. Labial palpus moderately long, palpomere 1 slightly wider than palpomere 2; palpomere 2 long, distinctly longer than palpomere 1; intersegmental membrane between palpomere 1 and 2 bearing short hair-like cuticular projections dorsally.

Chaetotaxy of labium (Fig. S3D). Submentum with two pairs of sensilla (LA1–2); LA1 on lateral margin, LA2 short seta on anterolateral corner. Mentum with a group of numerous rather short spiniform setae on dorsal to lateral surface of anterior corners; ventral face of anterior corner bearing one long seta and two minute setae. LA4 on subapical part of anterior corner, LA3 lateral on midlength. Prementum and its anterior membranous area with five pairs of sensilla (LA5–9), and a pair of short setae on lateral face of prementum. LA5–7 on lateroventral surface of prementum, minute seta LA5 at base, long seta LA6 at midlength; pore-like sensillum LA7 located apically close to borderline between sclerite and membrane. LA8 situated subbasally on mesal part of dorsal surface of prementum. Sensillum LA9 situated laterally on anterior membranous area. Ligula with one pair of moderately long setae (LA10) and two pairs of pore-like sensilla (LA11–12); LA10 on basal margin of sclerite; LA12 at apex, LA11 ventrally on subbasal part. Palpomere 1 with two sensilla (LA13–14); LA13 minute seta, situated ventrally at base; LA14 pore-like, dorsally on intersegmental membrane between palpomeres 1 and 2. Palpomere 2 with one pore-like sensillum LA15 situated apically on outer face of sclerite; several minute setae of variable shape (gLA) on apical membranous area.

Figure S1 Mouthparts of *Rygmodus modestus*. A, Mandibles; B, labium; C, mentum; D, maxilla.

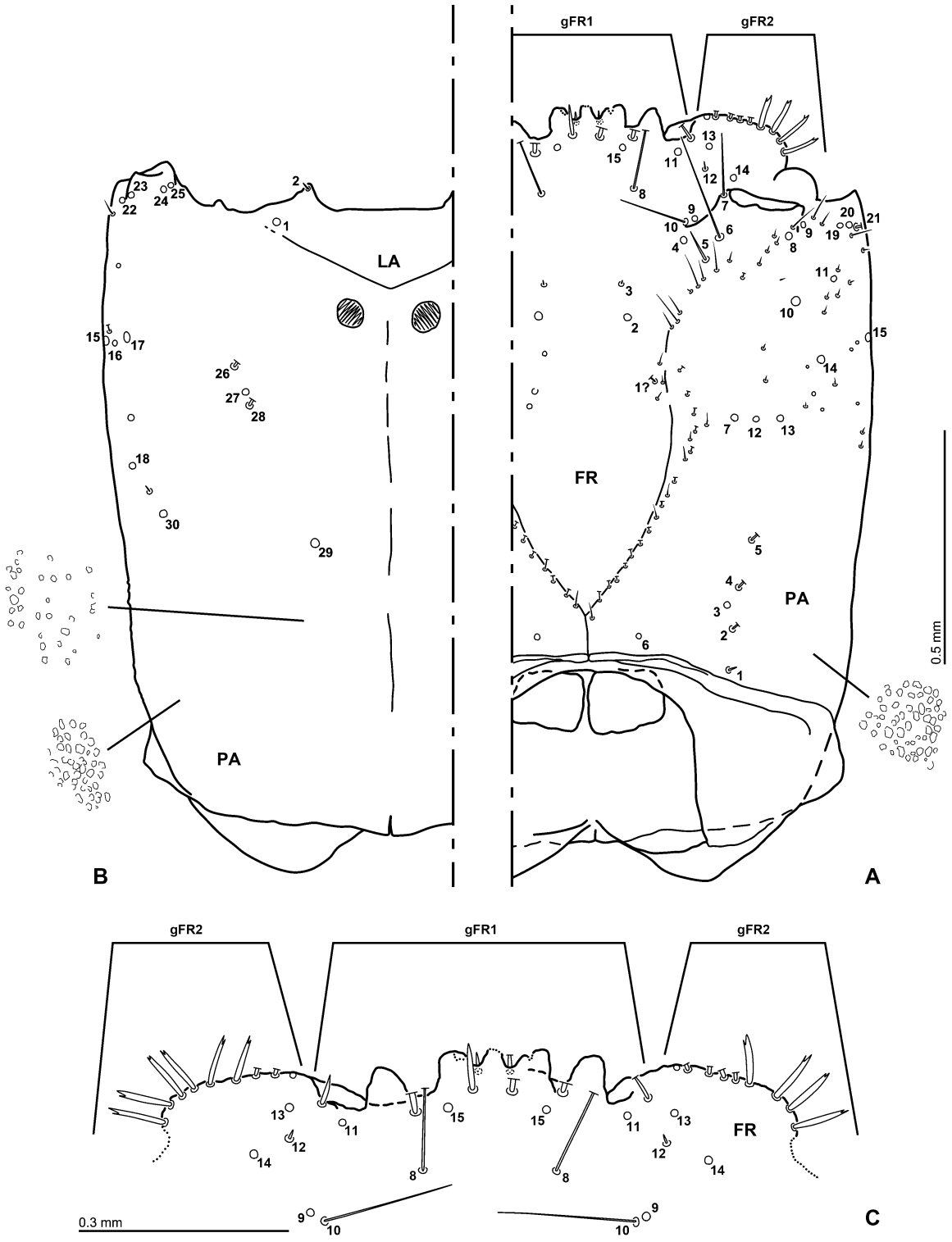

Figure S2 Head capsule of the third instar larva of *Rygmodus* sp. from Pelorus Bridge and its chaetotaxy. A, Dorsal view; B, ventral view; C, detail of clypeolabrum.

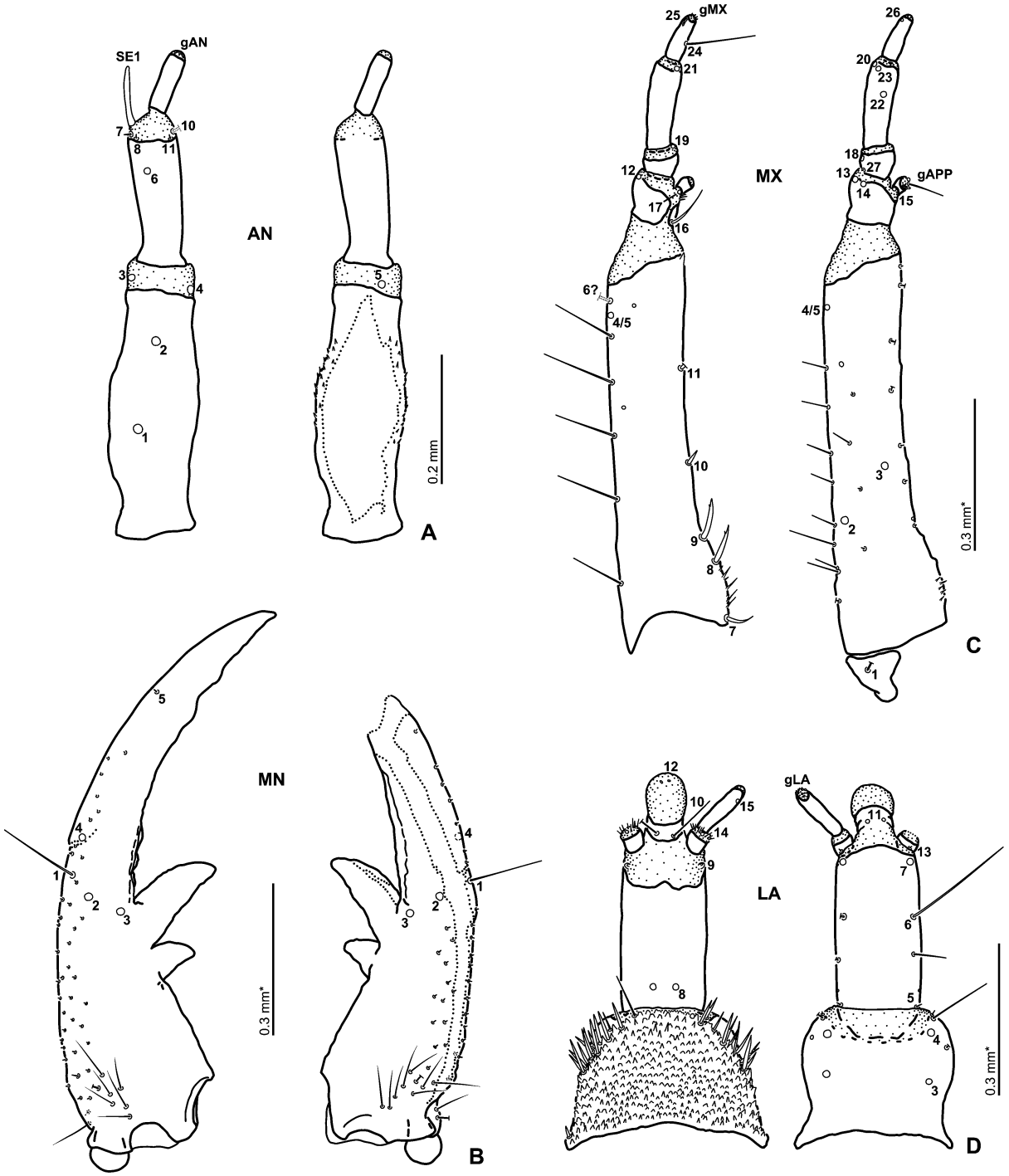

Figure S3 Head appendages of the third instar larva of *Rygmodus* sp. from Pelorus Bridge. A, Antenna, dorsal (left) and ventral (right) view; B, mandibles in dorsal view (right mandible broken at apex); C, maxilla, dorsal (left) and ventral (right) view; D, labium, dorsal (left) and ventral (right) view.

Table S1. List of specimens used for molecular analyses, along with GenBank accession numbers of their sequences. All vouchers are from New Zealand and are deposited in NMPC. List of abbreviated New Zealand areas: AK: Auckland; BR: Buller; CL: Coromandel; DN: Dunedin; FD: Fiordland; MB: Marlborough; NC: North Cartenbury; ND: Northland; SC: South Cartenbury; SL: Southland; WD: Westland; WO: Waikato (following Crosby *et al.* 1998, *New Zealand Journal of Zoology*, 25: 175–183).

Voucher #	Identification	Collecting data	GenBank Accession	
			cox1	H3
COL1794	*Rygmodus cyaneus* group	NC: Arthur's Pass Village, 42°56.32′S 171°33.71′E, ex *Hoheria*, 17.i.2011, R. Leschen (TB497)	MG920289	MG920309
COL1796	*Rygmodus modestus*	MB: Pelorus Bridge, 41°30.49′S 173°56.75′E, night collecting in waterfall splash zone, 29.xi.2010, Fikáček & Leschen (RL1509)	MG920290	–
COL1804	**Larva**	MB: Dead Horse Creek, S of Canvastown, 41°19.6′S 173°39.58′E, wet stones with algae and moss along stream, 30.xi.2010, Leschen & Fikáček (RL1511)	MG920291	MG920310
COL1818	*Rygmodus* sp. (*pedinoides / incretus*)	ND: Warawara State Forest, 35°22.01′S 173°16.7′E, ex *Cordyline banksii*, 13.xii.2008, Leschen & Buckley (RL1446)	MG920293	MG920312
COL1824	*Rygmodus femoralis*	WO: Mt Te Aroha, 37°32′S 175°44′E, ex *Cordyline indivisa*, 8.xii.2007, D. Seldon (RL1581)	–	MG920311
COL1826	*Rygmodus alienus*	BR: Klondyke spur, Victoria Range, 42°18.03′S 172°7.51′E, ex *Celmisia*, 11.i.2011, Leschen & Buckley (TB441)	MG920295	MG920297
COL1832	*Rygmodus cyaneus* group	WD: Kellys Creek, Otira, 42°48.12′S 171°34.3′E, beating *Hoheria*, 17.i.2011, Leschen & Buckley (TB490)	MG920287	MG920296
COL1841	*Rygmodus modestus*	CL: Tapu, Coroglen Track, 36°59′S 175°35′E, ex *Cordyline australis*, 16.xi.2009, D. Seldon (RL1580)	MG920292	MG920315
COL1842	*Rygmodus modestus*	same as COL1824	–	MG920307
COL1845	*Rygmodus tibialis*	WD: Cattle Walk Track, Waita River, 43°47.51′S 169°7.23′E, 7.xi.2007, Leschen & Carlton (RL1302)	MG920294	MG920300
COL1849	*Rygmodus cyaneus* group	NC: Temple Basin, Arthur's Pass, 42°54.58′S 171°34.69′E, ex *Hebe* and *Ranunculus*, 15.i.2011, Leschen & Buckley (TB478)	MG920288	MG920304
NZ155.2	*Rygmodus cyaneus* group	FD: Borland Rd., at stream just below Borland Saddle, 45°44.79'S 167°23.17'E; on *Hebe* bushes, 24.i.2016; Seidel, Sýkora & Fikáček (NZ022)	–	MG920298
SLE0129	*Rygmodus cyaneus* group	adopted from Short & Fikáček (2013)	KC935318	–
NZ46.1	*Adolopus* sp.	WO: Marokopa Falls, beating, 3.iii.2012, Gimmel & Leschen, 38°15.56'S, 174°50.926'E (RL1654)	–	MG920306
NZ73.1	*Hydrostygnus* sp.	ND: Puketi Forest, Manginangina Kauri Walk, brushing bark, 35°11.915'S 173°47.961'E, 18.iii. 2011, Leschen & Lord (RL1567)	–	MG920305
NZ82	*Saphydrus suffusus*	BR: Waterfall Creek Track, Maruia Springs, ex dead wood, 42°21.717'S 172°15.332'E, 10.i.2011, Leschen & Buckley (TB435)	–	MG920308
NZ125.1	*Enochrus* sp.	AK: Waitakere Ranges, Karekare - Whatipu reserve, 37°00′S 174°29′E; 2.i.2016, J.Hájek & P. Hlaváč lgt.	–	MG920299
NZ130.1	*Limnoxenus zealandicus*	AK: Waitakere Ranges, Karekare - Whatipu reserve, 37°00′S 174°29′E; 2.i.2016, J.Hájek & P. Hlaváč lgt.	–	MG920314

Table S1. (Continued)

Voucher #	Identification	Collecting data	GenBank Accession	
			cox1	H3
NZ131	*Limnoxenus zealandicus*	DN: 10 km N of Dunedin, Swampy Hill (open swamp), 45°47.7′S 170°28.9′E, 11.ii.2016, Hájek & Hlaváč lgt.	–	MG920303
NZ170.1	*Cyloma thomsonus*	SL: Catlins; McLean Falls Tk. at Tautuku River; 46°34.26'S169°20.98'E; 3-10.ii.2016; Seidel, Sýkora & Fikáček (2016-NZ051)	–	MG920313
NZ171	*Laccobius arrowi*	SL: Whitestone River at Hillside Manapouri Rd. 13.2 km S of Te Anau; 45°31.67'S 167°45.36'E, 28.i.2016, Seidel, Sýkora & Fikáček (2016-NZ035)	–	MG920302
NZ211.1	*Berosus pallidipennis*	SC: Peel Forest Reserve, 9.ii.2016, pasture pool, 43°53.9′S 171°13.8′E; 400 m, Hájek & Hlaváč	–	MG920301
NZ273.1	*Cylomissus glabratus*	AK: Nihotupu Stream at waterfall; 36°56.50'S 174°33.47'E; 6.iii.2016; Seidel & Leschen (2016-NZ-MS87)	–	MG920316

Table S2. Primers used for amplification of molecular data.

Gene fragment	Forward primer	Reverse primer
cox1	CAACATTTATTTTGATTTTTTGG	TCCAATGCACTAATCTGCCATATTA
H3	ATGGCTCGTACCAAGCAGACVGC	ATATCCTTRGGCATRATRGTGAC